CENTRALIZED AND DECENTRALIZED MAP UPDATING AND TERRAIN MASKING ANALYSIS

by

Martin Glen Bello

B.S. Cornell University
(1975)

M.S. Massachusetts Institute of Technology
(1977)

Submitted in Partial Fulfillment of the
Requirements of the Degree of

Doctor of Philosophy

at the

Massachusetts Institute of Technology

July, 1981

Signature of Author _____
Department of Electrical Engineering
and Computer Science
July 30, 1981

Certified by _____
Alan S. Willsky
Thesis Supervisor

Accepted by _____
Arthur C. Smith
Chairman, Departmental Graduate Committee

CENTRALIZED AND DECENTRALIZED MAP UPDATING
AND TERRAIN MASKING ANALYSIS

by

Martin Glen Bello

Submitted to the Department of Electrical Engineering
on July 30, 1981, in partial fulfillment of the
requirements for the Degree of Doctor of
Philosophy in Electrical Engineering

ABSTRACT

We focus on two problem areas involving multidimensional random processes, or random fields. The first area involves the formulation and solution of three types of spatial data assimilation problems, which we describe below, and that are motivated by the meteorological and geodetic application areas. In each of these application areas we have a variety of sensors that traverse some two-dimensional region, making measurements of some underlying random field, with the ultimate objective of forming a map, or a set of estimates of the field, over some global region of interest. The first problem, Centralized Map-Updating, is that of understanding how to incorporate measurements from new sensor surveys, into an existing field map, formed on the basis of old sensor surveys, and modelling of the field over the given global region. The second problem, Centralized Map-Combining, is directed at understanding how to merge several field maps, based on separate surveys and modelling of the field over the global region of interest, in order to obtain a final overall map. Finally, the third problem, Map-Centralization, is that of forming a map of the field over the given global region, by combining local maps of the field over subregions, that are formed on the basis of locally available survey data, and local field modelling. By using Hilbert space decomposition ideas, and by identifying maps with smoothed estimates of some state process that represents the field variables over the given region, we provide a simple, unified framework for the development of computationally efficient algorithms for the solution of the above problems. We present a specific spatial example that

demonstrates the applicability of our approach to mapping problems in the case of arbitrary survey geometries, through a stationary, discrete-space random field.

The second area of research consists of the development of analytical approaches for characterizing the effect of terrain, when modelled as a random field, in masking radar's observations. We consider both one- and two-dimensional masking geometries, and in each case analyze several measures of the masking effect, quantifying its variation with terrain statistics and radar siting elevation.

In a final chapter, providing a natural link between the above problem areas, we develop some analytical tools for assessing the impact of map errors in two specific applications that require the use of a terrain map.

Thesis Supervisor: Dr. Alan S. Willsky

Title: Associate Professor of Electrical Engineering

ACKNOWLEDGEMENTS

I gratefully acknowledge the invaluable technical guidance of my thesis supervisor, Professor Alan S. Willsky, whose energy and enthusiasm have helped to shape this thesis. I will always find unforgettable the constant encouragement and support with which he provided me.

I am thankful for the critcisms, and helpful suggestions, of each of my thesis readers: Dr. Bernard Levy, Dr. David Castanon, and Dr. George Verghese. Each contributed in different ways to making this a better thesis. I must especially thank Dr. Bernard Levy for making a truly exhaustive examination of the work, and in improving the presentation.

I must thank Mrs. Freda Zimmerman for her excellent work, through many arduous evenings and weekends in front of her typewriter, in preparing this manuscript. Thanks are also due to Mr. Arthur Giordani for his fine work in drawing the figures.

I also acknowledge my appreciation to Lincoln Laboratory for its financial support over the last several years, and especially to my supervisors there: Dr. John Delaney and Dr. Bob Francois.

Finally, I can never thank my parents, Edna and Phillip Bello, or my brother, Mike Bello, sufficiently, for a lifetime of caring, and in being there when I needed them, making it possible for me to realize this moment.

DEDICATED

TO

MY FAMILY

TABLE OF CONTENTS

TABLE OF CONTENTS (Continued)

TABLE OF CONTENTS (Continued)

TABLE OF CONTENTS (Continued)

TABLE OF CONTENTS (Continued)

TABLE OF CONTENTS (Continued)

LIST OF FIGURES

LIST OF FIGURES (Continued)

LIST OF FIGURES (Continued)

LIST OF FIGURES (Continued)

LIST OF FIGURES (Continued)

Chapter 1

Introduction

1.1 Overview

The study of the modelling and estimation of spatial random processes is a current area of vigorous research activity, with applications in image-processing, meteorology, and geophysical data processing, just to mention a few areas. In this thesis, we focus on two problem areas involving multidimensional random processes. The first area concerns the development of efficient algorithms for solving a wide class of spatial, data assimilation problems. We motivate and introduce these problems in Section 1.2. Our second problem area consists of the identification and development of analytical approaches for characterizing the masking effect produced by a terrain on a radars observations, when the terrain is modelled as a random field. We motivate this second problem area in Section 1.3, and suggest two subproblems connecting the two research areas, that we shall explore in Chapter 10.

1.2 Introduction to Mapping Problems

1.2.1 Centralized Map-Updating, Map-Combining, and Map-Centralization

The first part of this thesis focuses on a family of estimation problems directed at understanding how to combine efficiently information obtained from measurements of some spatial random process, in order to form maps, that is, estimates of the field over some area. We first give an abstract description of the type of problems we will consider, and then provide the specific motivation for these problems for both geodetic and meterorological applications [95] - [105].

In Fig. 1.1 we depict a given region R, that is crossed by a variety of sensors, making measurements of some underlying random field. For the sake of simplicity, we assume that these field measurements consist of two surveys over the subregions R_1 and R_2, which in general may either partially or completely overlap, or be completely separate. In many applications, the data from the various surveys will be delivered to some central computing facility, where based on some global model for the field quantities over the region R, we construct a map of the field over that region. We will call the map based on survey #1's data the global first-pass map. Then, the Centralized Map-Updating problem is defined as that of understanding how to combine, in a linear manner, the data from our second survey

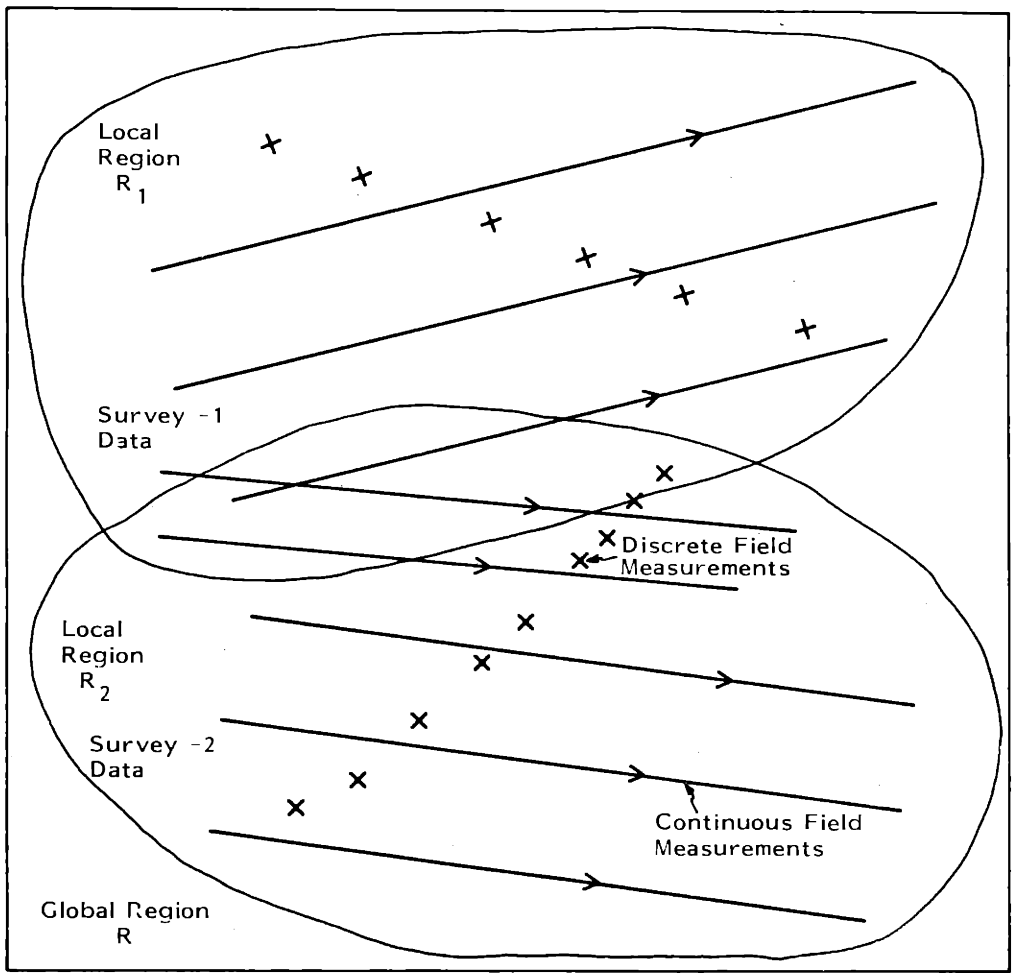

Fig. 1.1 Distribution of Measurements taken from Two Surveys of Some Underlying Random Field

with the first-pass map, in order to form an aggregate two-pass map based on all the available data. Similarly, the Centralized Map-Combining problem is defined by assuming that the data from each survey has been processed separately, based on some global model for the field quantities over R, in order to obtain two different maps. The problem is then that of understanding how to merge the two maps, in a linear manner, so as to obtain a final, aggregate two-pass map. Hence, the centralized map-updating and map-combining problems are directed at the efficient incorporation of either new data, or individual field maps, into an existing map of the field over some global region.

In the meteorological case, measurements of the vertical temperature profile of the earth's atmosphere are made and must be processed to obtain initial conditions to the equations of fluid mechanics used in numerical weather prediction [101]. In these equations, temperature is viewed as a function of atmospheric pressure rather than altitude (note that pressure and altitude are generally monotonic functions of one another). If we specify a discrete set of pressure levels, then we can model the temperature deviations from climatologically derived mean values, at those levels, as defining the value of a two-dimensional, vector random field, at each point on the earth's surface. For short periods of time relative to the atmospheric

dynamics, the vector of temperature deviations can be viewed as a static field.

Two of the main types of measurements that are employed to estimate the temperature field are radiosondes, which provide direct, but sparse, measurements of the temperatures at given pressure levels, and satellites, which take passive microwave or infrared radiation measurements at a set of frequencies, thus obtaining information related to the full temperature vs. pressure profile [103]. The satellite data may be viewed as providing spatially continuous measurements of the temperature field, while the radiosonde data consists of point measurements. In this setting there is a need for map-updating and map-combining procedures for incorporating new measurements into an existing map of the temperature field (from previous numerical weather predictions), or combining maps of the field constructed on the basis of different sets of data.

A second area motivating the estimation problems that we will study is that of geodetic data handling. Physical geodesy [96] is concerned with the study of the earth's gravitational field, and hence the objective of geodetic surveys is in mapping that field. Due to inhomogeneities in the distribution of the earth's mass, the gravitational field vector varies over the earth's surface. To a first approximation, the gravitational field vector is modelled as that produced by a homogenous

ellipsoidal mass. Several derived quantities, the gravitational anomalies, vertical deflections, and the undulation of the geoid, have been defined and are widely used to characterize the perturbation of the actual field from that produced by the reference ellipsoid. The gravitational anomalies essentially correspond to the difference between the actual and reference gravity fields, when each of the field values are evaluated at points which represent the same gravitational potential for the reference mass and the earth. The vertical deflections are defined as the differences in orientation of the actual and reference field vectors, defined at corresponding values of the gravitational potential. Finally, the undulation of the geoid is defined as the distance between the earth's equipotential surface closest to sea level (the geoid) and the reference ellipsoid. Each of these quantities has been modelled as a spatial random process, and the mathematics of geopotential theory [96] has been employed to derive statistical models for these quantities that are physically consistent [97]. Hence, we may think of the gravitational anomalies, the vertical deflections, and the undulation of the geoid, as together specifying a vector valued random field.

A multiplicity of measurement procedures are used to measure quantities such as those mentioned above that are related to the earth's gravitational field. For example, over a given ocean

region we may have ship measurements of the gravitational anomalies [95] and satellite measurements of ocean height, which essentially measures the undulation of the geoid [100]. Other recent studies [99] have examined the use of airborne measurements of the gradient of the gravity field. As in the meteorological application mentioned earlier, there is a need for map-updating and map-combining procedures for incorporating new data or combining individual gravity maps based on different sets of sensor data.

We have at this point motivated two types of data assimilation problems, centralized map-updating and map-combining, as defined relative to Fig. 1.1, where the information flow involved in the respective procedures is depicted in Figs. 1.2 - 1.3. In both Figs. 1.2 - 1.3, a global map based on the i-th survey data is defined as a map of the field over the global region R, constructed by using a model for the field quantities over that region, and the given survey data. In many applications, however, it is more reasonable to assume that the i-th survey data is processed on the basis of some local model for the field quantities over R_i, in order to derive a local field map. Such local models may represent a simplified model of the local field variables in R_i, neglecting some of the correlation structure present in the global model for the field over R. For example, in the geodetic case, local models for the field

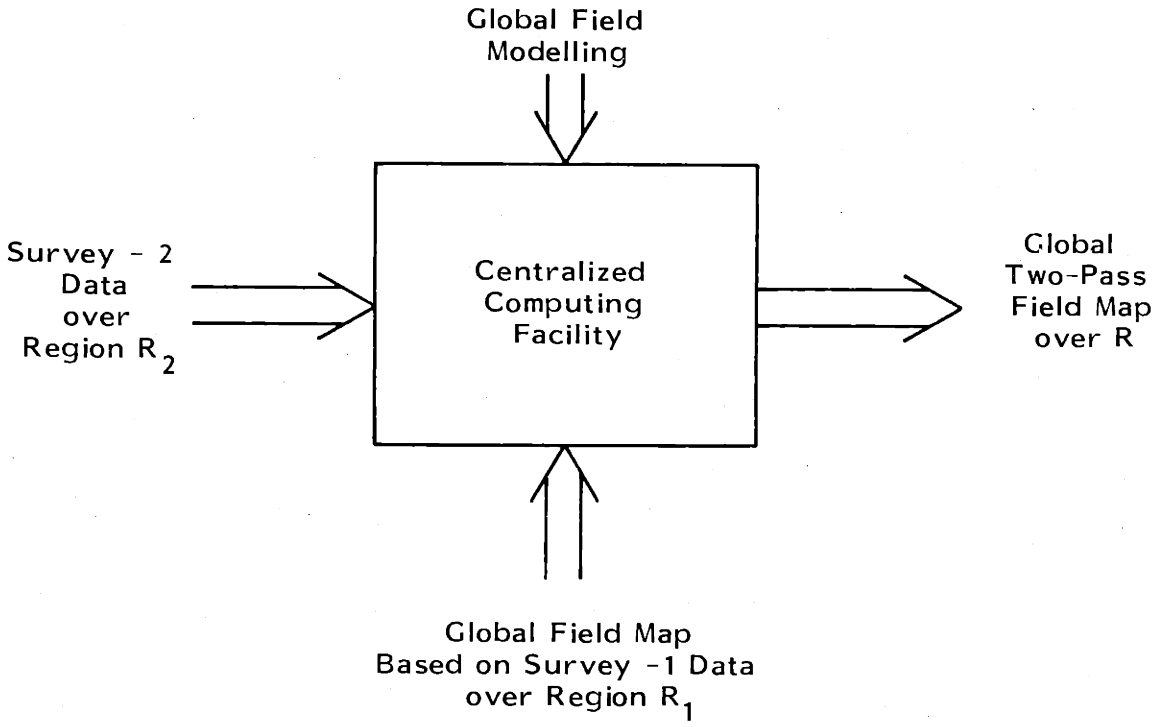

Fig. 1.2 Information Flow for the Centralized Map-Updating Problem

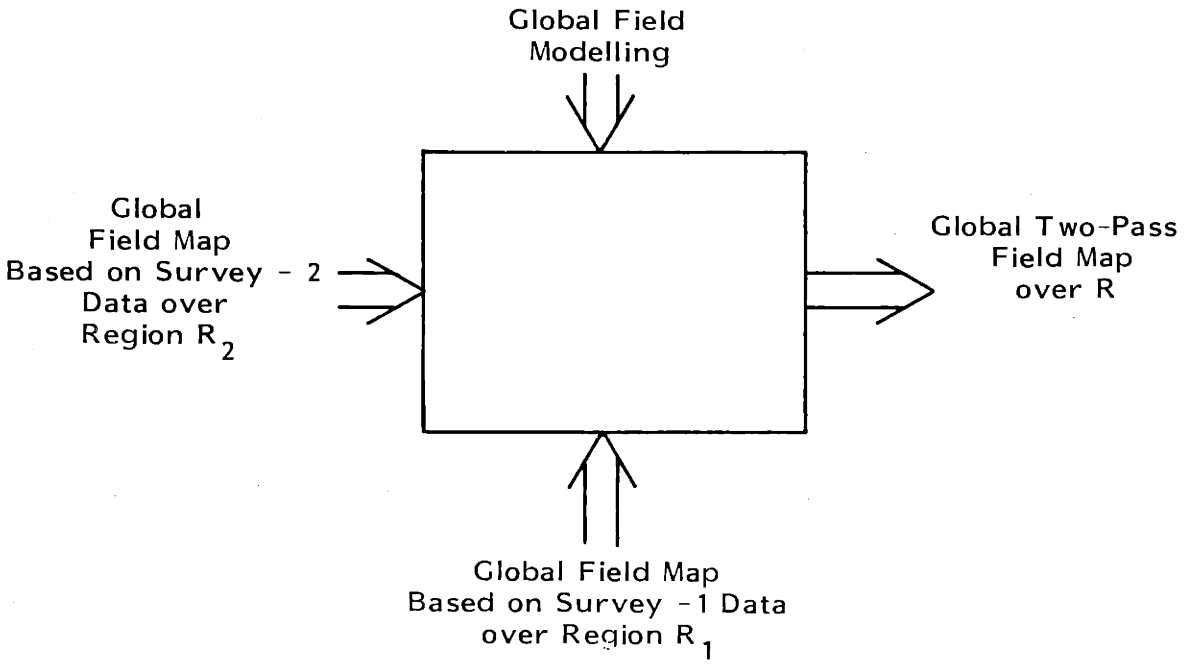

Fig. 1.3 Information Flow for the Centralized Map-Combining Problem

quantities over limited regions may be based on a flat earth assumption, while models for the field over extended areas may be consistent with a spherical earth assumption [98]. Alternatively, local models may represent exact lower dimensional representations of the restriction of the global field model to R_i. In the case when the i-th survey data is processed based on a local model for the field variables over R_i, to derive an i-th local map, we define the Map-Centralization problem as that of understanding when and how we may linearly combine the local maps over R_1 and R_2, in order to obtain the global two-pass map defined over R. We depict the information flow involved in the map-centralization problem in Fig. 1.4.

The map-centralization problem arises quite naturally in the context of our meteorological and geodetic applications. If we assume that each region R_i contains a collection of weather stations that pool their data, in order to compute local temperature vs. pressure profiles, then the map-centralization problem provides a framework for combining the local temperature maps over R_1 and R_2 in order to form a global map over R. In a geodetic setting, where we are continually increasing the size of our data base, i.e., such as in making more passes over an ocean region to measure gravitational anomalies, the map-centralization formulation allows us to combine a gravitational map obtained by using local modelling

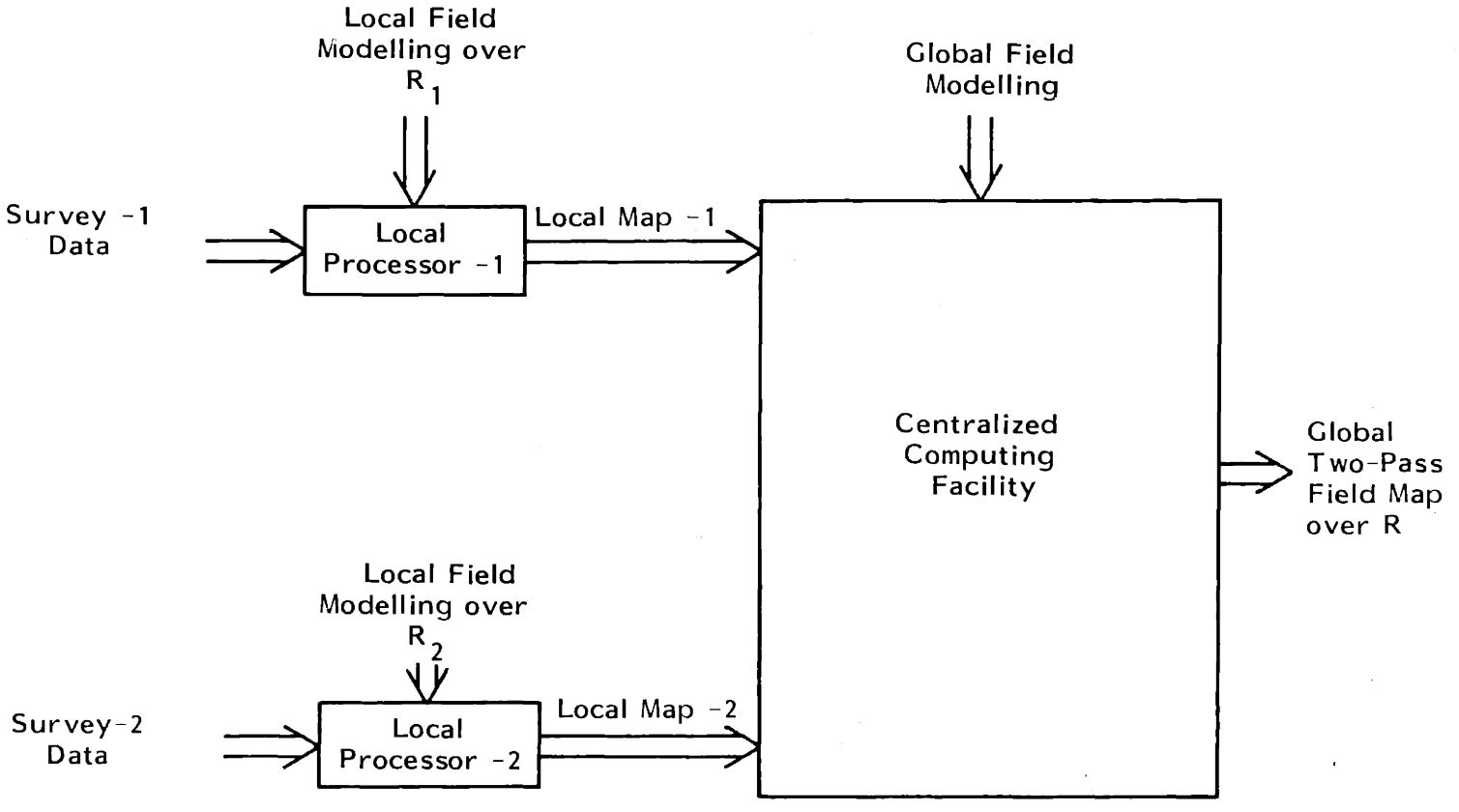

Fig. 1.4 Information Flow for the Map-Centralization Problem

and survey-1 data over some region R_1, with a second map obtained by employing local modelling and survey-2 data over R_2, when R_1 is contained in R_2.

We finally note that many current approaches to spatial estimation problems have been derived from work in the image processing area. Woods and Radewan [88], and Silverman [91], have formulated the image restoration problem as a one-dimensional linear estimation problem, where these authors use approximate finite dimensional Markov models for representing the image pixel intensities, line by line, that are derived by assuming a particular two-dimensional autoregressive representation for the image intensity field. Attasi [92] considered a special class of two-dimensional, vector autoregressive models and examined the solution of both filtering and smoothing problems. Then, working in a continuous-space setting, Wong has developed a two-dimensional stochastic calculus, and solved filtering and smoothing problems for fields modelled by a particular stochastic P.D.E. [93] - [94]. The above references represent a small fragment of the total amount of recent work involving spatial estimation problems, directed at image processing applications. A common thread that runs through much of this work, and will also appear here, is the formulation and solution of two-dimensional estimation

problems as one-dimensional problems. We expand on this point in the next section.

1.2.2 Centralized Map-Updating and Map-Combining in the Context of Two-Pass Smoothing

The preceding discussion has provided some motivation for the general features of three types of data assimilation problems: centralized map-updating, map-combining, and map-centralization. We will now explain more precisely what we mean by centralized map-updating and map-combining in the context of the parallel line measurement geometry in Fig. 1.5. In Fig. 1.5 the two solid lines represent the tracks over which survey-1 and survey-2 data have been obtained, and the dotted tracks represent lines on which we desire to map the field. In this case the problem is essentially one-dimensional, as we can think of the variable t parameterizing the distance along any of the tracks, as a one-dimensional variable used to index the aggregate field vector determined by sampling the field on a set of parallel tracks including those over which the survey is taken (and possibly including others if we want to do interpolation). In this setting, the survey-1 and survey-2 data can be modelled as linear measurements of the aggregate field vector process, with independent measurement noises, and we identify the i-th pass field map as the set of smoothed estimates of the aggregate field vector, based on the i-th survey data. Now, the

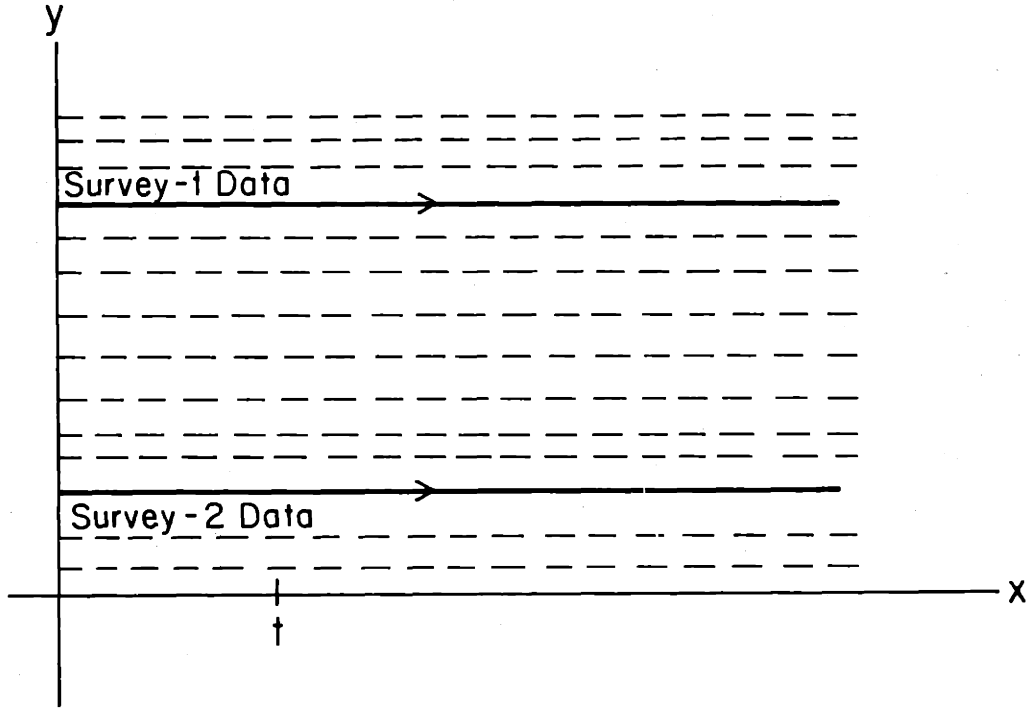

Fig. 1.5 Two Parallel Line Measurement Geometry

centralized map-updating problem is defined as that of computing the two-pass smoothed estimates (i.e., the estimates based on both surveys) of the aggregate field vector, as a linear functional of the survey-2 data, and of the old map, i.e., the smoothed estimates of the aggregate field vector based on survey-1 data. Similarly, the centralized map-combining problem is defined as that of computing the two-pass smoothed estimates of the aggregate field vector as a linear functional of individual smoothed estimates constructed from each separate survey. Hence, in the framework we have described, map-updating becomes smoothed estimate updating, and map-combining is equivalent to smoothed estimate combining. Consequently, the focus of much of our work will be on examining one-dimensional problems. Furthermore, we will also make one further assumption, which is that the aggregate field vector can be modelled as the output of a finite-dimensional linear system driven by white noise. While at first glance this may appear to be a crippling assumption, it is not. In fact, in Section 7.2 we present an example of the map-updating and map-combining problems, for the case of a parallel track measurement geometry through a scalar, stationary random field with a separable correlation function, in which case we may derive an exact finite-dimensional model for the aggregate field vector process. In Section 7.3 we also demonstrate that in a discrete space setting we can consider map-updating

problems for the case of more general measurement geometries, i.e., for non-parallel measurement tracks, through a general stationary random field. Finally, we observe that although we have restricted ourselves to finite-dimensional modelling of the field quantities of interest, the same techniques that we apply may be used to at least obtain representations of the solution to the map-updating and map-combining problems for the case of infinite-dimensional field models. That is, the results we will present expose all of the basic concepts that are needed in understanding mapping problems, and the only issues that remain are technical or algorithmic in nature.

From the above discussion, we have equated map formation with the solution of a linear, finite-dimensional, fixed interval smoothing problem. In fact, looking ahead, we will demonstrate that the solution of the centralized map-updating problem consists of adding together the old first-pass map, and a correction term that corresponds to an estimate for the first-pass map error. We will show that the appropriate correction term is in fact the smoothed estimate of the error in the first-pass smoothed estimate, based on the part of the second survey measurements not predictable from the first-pass data. Furthermore, we will show that the calculation of this correction term is of the same form as the original smoother, and this will follow from the fact that we may obtain finite-dimensional

Markovian realizations of the first-pass map error, or smoothing error, process [49],[83]. In addition, we will show that the solution of the centralized map-combining problem can be obtained directly from our results for map-updating. Hence, in our formulation, the operations of map-updating and map-combining are shown to be no more difficult than map-formation.

It is clear from the preceding discussion that the linear, fixed interval smoothing problem is of essential importance in our work. For this reason, in Chapter 2 we present a unified Hilbert space perspective on several especially relevant algorithms for solving the continuous-time, linear, fixed interval smoothing problem. This Hilbert space perspective will provide us with a systematic and simple framework for both obtaining a geometric understanding of how various solutions to the smoothing problem arise, and later for constructing solutions to the map-updating and map-combining problems, and in deriving representations for the smoothing error process.

In Chapter 3 we discuss the derivation of Markov models for the smoothing errors. The existence of such models is in some sense non-intuitive, since the smoothed estimate itself may not be generated by a single, causal, stochastic differential equation. The new derivation of these models presented here provides a clear, elementary understanding of the structure

of smoothing error realizations, and an intuitive feeling for why they exist at all.

Next, in Chapter 4, we formulate the centralized map-updating and map-combining problems in the context of two-pass smoothing for some continuous time, linear, finite-dimensional state process based on two sets of continuous measurements with independent observation noises. We employ some of the smoothing algorithms of Chapter 2, and the Markov models for the smoothing errors of Chapter 3, in order to derive the solution to these problems. We note that the algorithms that we obtain are of interest in themselves as providing solutions to the one-dimensional smoothed estimate updating, and smoothed estimate combining problems, as well as in solving spatial map-updating and map-combining problems of the type motivated by the parallel track measurement geometry of Fig. 1.5.

Then in Chapter 5, motivated by the meteorological application discussed earlier, where we have both discrete point measurements from radiosondes and spatially continuous measurements from satellites, we formulate and solve two variants of the centralized map-updating problem. We again consider map-updating in the context of the two-pass smoothing problem for a linear state process, given one continuous and one discrete measurement pass. When the first-pass measurements are

discrete, we consider separately the cases when we have as our first-pass map either the entire smoothed estimate history, or simply the smoothed estimates at the discrete measurement locations.

In Chapter 6 we turn to the precise mathematical formulation of the map-centralization problem depicted in Fig. 1.4, i.e., the problem of forming a global two-survey map as a linear functional of local maps constructed from data obtained over subregions R_1 and R_2, by using local field models over the respective regions. We solve the map-centralization problem for the special case where the local models over the subregions R_1 and R_2, essentially represent some restrictions of the global model to those regions.

Next, In Chapter 7, we conclude the first area of thesis research by demonstrating explicitly how we may solve some spatial examples of the centralized map-updating, centralized map-combining, and map-centralization problems by employing the one-dimensional framework of the preceding chapters. We present a continuous space example of all three problems for the case of an M-parallel line measurement geometry through a stationary, scalar random field with a separable correlation function. Then we present a discrete space example of the centralized map-updating problem for the case of two non-parallel measurement lines through a stationary, separable, scalar random field.

This last example demonstrates the applicability of our map-updating formalism to the case of arbitrary survey geometries through a general, stationary, discrete space random field. In order to consider the above discrete space map-updating problem, in Chapters 2 and 4 we present algorithms for discrete time smoothing, and centralized map-updating, in Appendices.

1.3 Introduction to Terrain Masking Analysis and Overview of Chapters 8 - 11

The motivation for the second major area of thesis research stems from the desire to characterize the effect of a terrain in masking radar's observations. Since we are interested in examining the masking effect for a typical, but generally unknown, radar location, sited at some specified elevation, in terrain of a given type, i.e., smooth, hilly, or mountainous, it is reasonable that we model the terrain as a spatial random process. We note in this respect that several authors [107] - [109], have reported successfully modelling terrain over limited areas as a stationary, Gaussian random field with an exponential correlation function. In our second area of work we use a statistical description of the terrain and analyze several statistical characterizations of terrain masking.

In Figs. 1.6 - 1.7 we depict profile views of two different masking geometries that may be thought of as corresponding to two different modes of radar operation. In each case, the lines emanating from the radar, i.e., the lines of sight, denote the paths along which, in our simplified view, all the electromagnetic energy from the radar propagates. The angle that the line of sight makes with respect to the horizontal direction is called the radar elevation angle, φ. In Fig. 1.6, we picture the case of a radar which we imagine as rotating around,

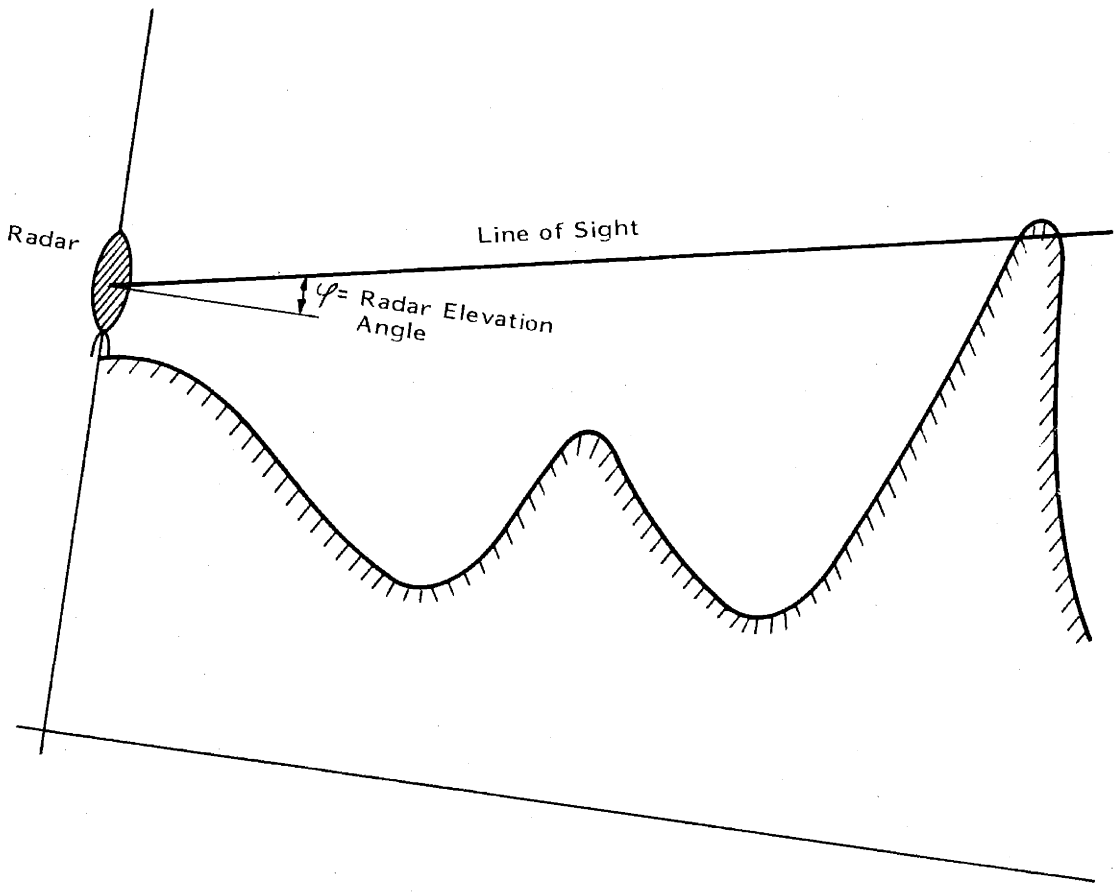

Fig. 1.6 Fixed Elevation Angle Geometry

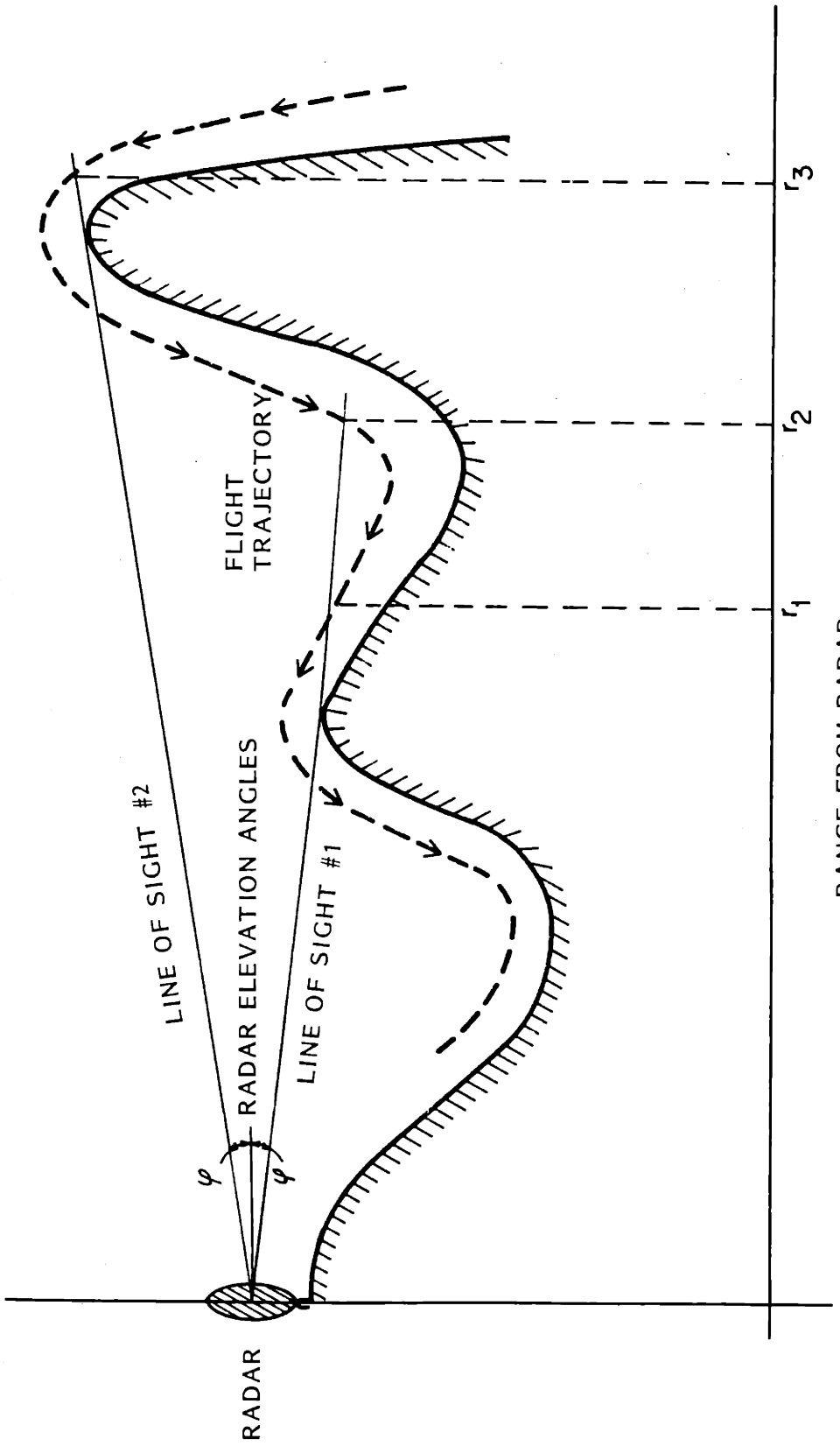

Fig. 1.7 Terrain-Following Geometry

maintaining a fixed elevation angle, and scanning the horizon for incoming objects. We will call this the search mode of radar operation. As depicted in Fig. 1.6, the terrain may block the fixed line-of-sight curve at some range, limiting the ability of the radar to detect objects.

In Fig. 1.7 we depict a masking geometry that corresponds to a tracking mode of radar operation, i.e., we imagine that the radar is tracking some object that is assumed to follow the terrain perfectly at some fixed, additional height. In the terrain-following geometry of Fig. 1.7, in direct contrast to the fixed elevation angle geometry of Fig. 1.6, the radar elevation angle becomes a random variable, which varies as a function of range, since the line of sight is constrained to pass through the radar and the terrain-following object. As the object approaches the radar it goes through successive periods of visibility and invisibility. Between ranges r_1 and r_2, and beyond r_3, we say that the object is masked with respect to the radar.

The objective of the work in Chapters 8 - 9 is to develop analytical approaches for quantifying the interplay between the likelihood of terrain blockages of the line of sight over a given range, radar siting height, and terrain statistics. For example, from our intuition we expect that the higher the radar is located, and the smoother the terrain, the farther a given

radar will be able to see. We note that the line-of-sight curve is defined differently in each of the masking formulations of Figs. 1.6 - 1.7. In the case of the fixed elevation angle geometry, we focus attention on a single line-of-sight curve. In the terrain-following geometry, the line of sight is determined by the terrain elevations, and the imagined terrain-following object's additional height.

We begin our analysis in Chapter 8 by identifying several computable measures of the masking effect for either of the two one-dimensional masking geometries defined in Figs. 1.6 - 1.7. In Chapter 9 we examine several analogous computable measures of the masking effect for a two-dimensional masking formulation that corresponds to the two-dimensional generalization of the one-dimensional fixed elevation angle geometry of Fig. 1.6, i.e., we imagine generating a line-of-sight cone by rotating the line-of-sight curve around the z axis, and consider various measures of the excursion set over which the terrain surface exceeds the line-of-sight cone, contained in a given disk about the radar.

In Chapter 8, to analyze the different measures of the masking effect that we will consider, we draw on work of Rice [114], and Leadbetter [118], on the frequencies of level and curve crossings for random processes. We also make use of the work of Fortet [122], Mehr and McFadden [123], and Dynkin [132],

on the theory of exit times, or first-passage times, for Markov processes. In Chapter 9 we employ work in the area of geometric characterizations of random fields, such as results of Longuet-Higgins [136] and Belyaev [137], on the average number density of maxima, minima, and saddle points of the field above a given level, and the attempts to generalize the notion of upcrossings to random fields of Adler [142] and Nosko [140]. Hence, the work of Chapters 8 - 9 provides a novel, yet practical application of work in the general area of geometric characterizations of both random processes and random fields.

In Chapter 10 we pose two problems, connecting the two major areas of thesis research. We note that the centralized map-updating and map-combining problem solutions provide the basis for continually improving maps based on new information. One question that naturally arises is: when do we have a map whose accuracy is adequate for a given application? In Chapter 10 we sketch the analysis of two different quantities by which to measure the adequacy or inadequacy of a terrain map intended for two separate applications. The first application we consider is the use of a terrain map by a terrain-following vehicle. The criteria that we use to assess map adequacy or inadequacy in this case are the steady state, average frequencies of crossings between the vehicle trajectory and the terrain curve (i.e., crashes), or the frequency of

crossings between the vehicle trajectory and some clearance level h_v, at which the probability of becoming visible to the radar can be shown to be unacceptably high, from the analysis of the masking effect. Since in any practical terrain-following vehicle, crossings between the vehicle trajectory and the terrain curve, or between the vehicle trajectory and the h_v clearance level, will be low probability events, we can think of the crossing frequencies that we compute as specifying upper bounds on the probability of these events occurring, per unit distance. The second application that we consider is the use of a terrain map to decide if an object at range r, and specified terrain-following height, is masked or unmasked with respect to the radar. In this case, the criterion we use to evaluate the utility of our map consists of an upper bound on the probability of making a wrong decision, as to object visibility, based on map information.

In the concluding Chapter 11 we summarize the contributions of this thesis, and identify some areas for continuing work. We feel that the work here represents a significant contribution to both the understanding and solution of mapping problems, and the analytical characterization of the effect of terrain in masking radar's observations.

Chapter 2

A Review of Some Solutions to the Linear Fixed-Interval Smoothing Problem from a Hilbert Space Perspective

2.1 Historical Review of Solutions to the Linear Fixed-Interval Smoothing Problem

In Chapter 1 we stated that we will identify maps of a given random field, with smoothed estimates of some underlying state process that represents the field. Looking ahead, we mentioned that the solution to the centralized map-updating problem based on two data passes assumes the form of the old map, plus a correction term that corresponds to an estimate for the first pass map error. We mentioned that the correction term is derived as the solution to a particular fixed-interval smoothing problem. Hence, the understanding of different approaches to the linear, fixed-interval smoothing problem[†] is fundamental to our work. Therefore, in this chapter we focus first on obtaining a historical perspective on the development of solutions to the fixed-interval smoothing problem, and later on making a unified presentation from a Hilbert

[†]By the linear fixed-interval smoothing problem we mean the construction of interpolated estimates of the state process, for linear state and observation equations, where the measurement noise is uncorrelated with the process noise.

space perspective, of several approaches to the smoothing problem that are especially relevant to our work.

In [9] - [10] H. E. Rauch derived the first algorithm for the fixed-interval smoothing problem for discrete-time state-space models, by employing a M.A.P. estimation approach. He obtained a backwards recursion for successive smoothed estimates, that employed the filtered estimates, and also the inverses of the filtering error covariance matrices. Later in [11], Rauch, Tung, and Striebel used formal limiting arguments to construct an analogous solution to the continuous time fixed-interval smoothing problem, i.e., a backwards differential equation satisfied by the smoothed estimates, that is driven by the filtered estimates. The initial condition for the backwards differential equation is obtained by noting that the filtered and smoothed estimates are the same at the final measurement time.

Bryson and Frazier [12] were the first authors to attack the continuous fixed-interval smoothing problem directly. They posed the determination of the smoothed estimates as the solution of an optimization problem with a quadratic objective function, imposing the state dynamics as constraints. Appealing to the calculus at variations, they obtained necessary conditions for the solution of the smoothing problem as a linear, two-point boundary-value problem. This boundary-value problem

is specified by what we will call the Hamiltonian equations for smoothing. Bryson and Frazier then employed a standard approach [56] for solving linear two-point boundary-value problems to represent the smoothed estimates by a closed form expression.

Cox [16] adopted a similar approach to Bryson and Frazier in discrete time, and derived analogous Hamiltonian equations, and an algorithm for computing the smoothed estimate as a correction to the filtered estimate, without requiring the inversion of filtering error covariance matrices.

The computational sequence embodied in both the Rauch-Tung-Striebel and the discrete Bryson-Frazier smoothing algorithms involves a forward sweep over the data to generate the filtered estimates, and then a backwards sweep to compute the smoothed estimates. In direct contrast, Mayne [17] introduced, in discrete time, the first two-filter form of the smoothed estimate. By a two-filter form, we mean an expression for the smoothed estimate as a linear combination of two estimates for the state at a given time; one estimate based on processing the past observations, and the second estimate based on the future observations. By employing a M.A.P. approach, dynamic programming techniques, and separating into two parts the optimizations involving the past and future observations, Mayne derived a formula for the smoothed estimate as a linear combination of the Kalman filtered estimate, and a second

estimate based on the future observations. Fraser [18] and later Fraser and Potter [19] derived a similar two-filter algorithm for both continuous and discrete-time problems, expressing the smoothed estimate as a linear combination of the standard Kalman filtered estimate and a particular backward filtered estimate that evolves in reverse time according to analogous equations. This backward filtered estimate has an associated error covariance matrix that is generated as the solution of a Ricatti equation, with an infinite initial condition at the final time. In [19], the authors obtained an alternative form of the algorithm, that avoids the problem of the infinite terminal error covariance matrix.

Next, Frost, Kailath and Geesy [22] - [24], drawing on the earlier work of Kolmogorov [8], Wold [15], and Wiener and Masani [13], applied the innovations approach to the study of filtering and smoothing problems. The innovations process represents a whitened version of the original observations. In addition, the innovations and measurements may each be obtained from the other by causal, linear operations, implying the statistical equivalence of the two processes. The whitening of the measurement process allowed the authors to appeal to results on estimation from orthogonal increments processes, in order to obtain representations for the filtered and smoothed estimates. In this setting, the smoothed estimate

is expressed as the filtered estimate plus a correction term computed from the future innovations.

In one case, a new approach to the linear fixed interval smoothing problem has stemmed from consideration of the non-linear smoothing problem. Laniotis [26] employed Bucy's representation theorem [27] to obtain an explicit form for the density of the state conditioned on the observations, and derived a new two-filter smoothing formula as a linear combination of the filtered estimate and a second quantity, where both terms are computed using a Kalman filtered estimate generated by assuming a zero initial condition, and a zero initial filtering error covariance matrix.

Techniques originally developed by physicists to characterize the transmission and reflection of waves propagating through a medium, under the heading of scattering theory [28], have been employed to obtain further insights into the smoothing problem. The scattering formalism essentially may be viewed as a signal flow diagram, in a ladder form, that represents the state estimates and adjoint variables of the Hamiltonian equations for smoothing. The manipulation of scattering diagrams provides a simple pictorial device for unifying derivations of smoothing formulae, and determining the effects of changing initial conditions on smoothed and filtered estimates. In [29] - [30], Ljung, Kailath, and

Friedlander introduced the scattering perspective on linear least squares estimation for both continuous and discrete-time problems. In [31], Verghese, Friedlander, and Kailath used scattering techniques to obtain a unified derivation of Laniotis' partitioned equations, the innovations, and Mayne-Fraser smoothing formulae. In [33], Ljung and Kailath employed the scattering approach to derive different methods for forming the smoothing error covariance, corresponding to different smoothing formulae, and through employing Zachrisson's [25] extended state formulation of the smoothing problem as a filtering problem, the authors obtained a framework for classifying all possible state-space smoothing formulae.

Work directed at obtaining backward state-space models, i.e., models for the state process that evolve backwards in time and correspond to a given forward model, have also resulted in new algorithms for smoothing. The first derivations of such backward models, for the continuous and discrete-time cases, followed from the use of the scattering formalism in [30],[33] by Kailath, Ljung, and Friedlander. In [36] Verghese and Kailath derived backward models that not only reproduce the same second order properties as the corresponding forward model, but retrace the same sample paths.

In [37], Sidhu and Desai employed backward models to derive a backwards analog of the Mayne-Fraser smoothing formula. In [38], Wall, Wilsky, and Sandell used backward models to construct a two-filter formula for the smoothed estimate as a linear combination of the forward filtered estimate and a reverse filtered estimate that corresponds to the conditional mean of the state given the future observations. These authors clarified the understanding of the Mayne-Fraser solution by identifying the backward filtered estimate that appears in that formula, as a maximum likelihood estimate for the state based on the future observations. The Mayne-Fraser backward filtered estimate uses the information contained in the future observations, without using a-priori state information, hence explaining the infinite error covariance at the final time. Since the reverse filtered estimate that appears in Wall's two-filter formula uses both a-priori state information, and the future observations, the Wall smoothing formula is symmetric with respect to the way it treats future and past observations. This symmetry is reflected in the fact that both forward and reverse filters are stable.

Other work in the area of stochastic realization theory has added a new perspective on the smoothing problem. Drawing on the earlier work of Faurre, Ruckebusch, and Lindquist and Picci in [72] - [82]; Badawi, Lindquist, and Pavon [83] were

able to interpret the Mayne-Fraser smoothing formula as a linear combination of state processes associated with certain stochastic realizations of the observations process, and show how it follows from orthogonal decompositions of the Hilbert space spanned by the data. In [84], Badawi developed an analogous theory for understanding the discrete-time smoothing problem. In addition, in [83], the authors derived the first backwards model for the smoothing error process.

Finally, in [49], Weinert and Desai, by employing Hilbert space ideas to construct a space that contains the part of the state process not predictable from the observations, derived a forward model for the smoothing error process. By subtracting this forward model for the smoothing errors, from the original state model, they obtained a pair of coupled differential equations which determine the solution of the smoothing problem. Their solution involves an initial reverse sweep over the data, and then a forward sweep to generate the smoothed estimates. The form of their equations is especially suitable for evaluating the effect of changes in the initial state covariance on the final estimates.

At this point, we have highlighted the historical development of solutions to the linear, fixed-interval smoothing problem. In this chapter, we will attempt to display how the structure of various solutions to the smoothing problem

follow from examining it in a Hilbert space setting. We have chosen to view smoothing formulae from a Hilbert space perspective, since the resulting geometric view of the estimation problem allows us to visualize, and understand on the most fundamental mathematical level, how the various solutions arise. We will show how different smoothing equations emerge either from different techniques of breaking up the Hilbert space spanned by the measurements, or from different procedures for realizing the projection defining the smoothed estimate in a recursive form, i.e., through a combination of forward and reverse processing of the data. Finally, we have adopted the Hilbert space point of view on smoothing, since we will use the same type of Hilbert space decomposition ideas in constructing the solution to the centralized map-updating and centralized map-combining problems, and even in the derivation of state models for the smoothing error process.

We next outline the contents of the chapter. In Section 2.2 we define the fixed-interval smoothing problem precisely in a Hilbert space setting for continuous and discrete-time state space models. In addition, we define some notation and state some mathematical results that are of critical importance to the presentation. At the end of Section 2.2 we summarize our unified perspective on where various solutions to the smoothing problem follow from in a

Hilbert space setting. Our presentation in the text is restricted to the continuous time smoothing problem. In Appendix 2A we consider parallel approaches to the discrete time smoothing problem. In Section 2.3 we derive the innovations form of the smoothing solution. In Section 2.4 we derive both the Hamiltonian and Rauch-Tung-Striebel smoothing formulae. In Section 2.5 we present the stochastic realization perspective on two-filter forms of the smoother, particularly the Mayne-Fraser and Wall smoothing formulae. Finally, in Section 2.6 we present the formulation of Weinert and Desai for solving the smoothing problem. The stochastic realization view of smoothing in [83],[84], and the approach of Weinert and Desai in [49] are especially of interest since they have led to a backward and forward model of the smoothing error process, respectively. Finally, we note that in Appendix 2C we present the scattering formalism for representing the Hamiltonian equations. Our coverage of this perspective on smoothing is brief, since we will only use it as a computational tool for making connections between the Hamiltonian equations and Weinert and Desai's formulation, and later for obtaining very quick alternative derivations of the solutions to the centralized map-updating and map-combining problems.

2.2 Formulation of the Smoothing Problem and Mathematical Preliminaries

In this section we define the linear fixed interval smoothing problem for continuous and discrete time state-space models, in a Hilbert space setting. In addition, we define some notation, and state some mathematical results for later use. In this chapter we consider continuous time state-space models of the form

$$dx(t) = A(t)\,x(t)\,dt + B(t)\,du(t) \quad , \tag{2.1}$$

$$dy(t) = H(t)\,x(t)\,dt + D(t)\,dv(t) \quad , \tag{2.2}$$

where

$$E[x(0)x'(0)] = \pi(0) \quad , \tag{2.3}$$

$$E[x(0)] = 0 \quad , \tag{2.4}$$

and

$$y(0) = 0 \quad , \tag{2.5}$$

and where $A(t)$ is $n \times n$, $B(t)$ is $n \times n_1$, $H(t)$ is $m \times n$, $D(t)$ is $m \times n_2$, and $n_1 + n_2 = p \geq m$. Here $u(\cdot)$ and $v(\cdot)$ are, respectively, some standard n_1 and n_2 dimensional independent Wiener processes. In addition, we assume that the observation noise is nonsingular, i.e.,

$$D(t)D'(t) = R(t) > 0 \quad . \tag{2.6}$$

We will let $\pi(\cdot)$ denote the state covariance matrix associated with the model (2.1), and will employ subscripted $\pi(\cdot)$'s in the future, whenever we need refer to a-priori state covariance matrices. We will also adopt subscripted $P(\cdot)$'s as standard notation to refer to error covariance matrices, associated with state estimates. We will think of the increments of the $y(\cdot)$ process, $dy(\cdot)$, as representing our fundamental observed variables. The Hilbert space spanned by these increments will be denoted as

$$Y = H(dy(\tau) \quad 0 \leq \tau \leq T) \triangleq H(y(\tau_1) - y(\tau_2);\ \tau_1,\tau_2 \in [0,T]) \ , \tag{2.7}$$

where the inner product between the zero-mean, finite second moment random variables x_1,x_2, $\langle x_1,x_2 \rangle$, is defined by

$$\langle x_1,x_2 \rangle = E[x_1x_2] \quad . \tag{2.8}$$

Then if $E[\cdot|L]$ denotes the projection onto the Hilbert space L, we define the smoothed estimate at σ based on the observation of $y(\cdot)$ over the interval $[0,T]$ by

$$\hat{x}_s(\sigma) \triangleq E[x(\sigma)|Y] \quad . \tag{2.9}$$

We will let $\tilde{x}_s(\sigma)$ denote the error in the smoothed estimate defined as

$$\tilde{x}(\sigma) \triangleq x(\sigma) - \hat{x}_s(\sigma) \quad . \tag{2.10}$$

In Appendix 2A, we will also consider the fixed interval smoothing problem for discrete state-space models of the form

$$x(t+1) = A(t)x(t) + B(t)u(t) \quad , \tag{2.11}$$

$$y(t) = H(t)x(t) + D(t)v(t) \quad , \tag{2.12}$$

where

$$E[x(0)x'(0)] = \pi(0) \quad , \tag{2.13}$$

$$E[x(0)] = 0 \quad , \tag{2.14}$$

and where $u(\cdot)$ and $v(\cdot)$ are some standard discrete white noise sequences. Letting the Hilbert space spanned by the observations $y(i)$ be given by

$$Y \triangleq H(y(i) \quad i = 1,\ldots,T) \quad , \tag{2.15}$$

the smoothed estimate $\hat{x}_s(i)$ is defined as

$$\hat{x}_s(i) \triangleq E[x(i)|Y] \quad . \tag{2.16}$$

We include the discussion in Appendix 2A of parallel approaches to the discrete-time smoothing problem, since in Chapter 7 we consider a specific discrete space example of the centralized map-updating problem.

We next state some mathematical results from the theory of quasi-martingales [46] that are essential to our presentation. We first note that throughout this work, since we assume that we are dealing with Gaussian random processes, we will use the same notation for projection and conditional expectation. By definition, a process f_t, measurable with respect to some increasing family of σ-fields, $\mathcal{J}_t$, is said to be a quasi-martingale if it may be represented in the form

Quasi-Martingale Decomposition

$$f_t = B_t + M_t \quad , \tag{2.17}$$

where B_t is a process with sample paths of bounded variation w.p.1, and M_t is a $\mathcal{J}_t$ martingale, i.e.,

$$E[M_s | \mathcal{J}_t] = M_t \quad \text{for} \quad s \geq t \quad . \tag{2.18}$$

The process B_t in relation (2.17) is constructed from its increments dB_t defined by

$$dB_t = E[df_t | \mathcal{J}_t] \quad . \tag{2.19}$$

Fisk [46] derives conditions on the process f_t such that a decomposition of the form in relation (2.17) exists.

We can appeal to the quasi-martingale decomposition result to obtain the rigorous meaning of a particular formal notation that we will frequently employ. Suppose that H_t denotes some increasing sequence of Hilbert spaces and that $d\eta_t$ denotes the increment of some second order random process η_t. Let $\mathcal{H}_t$ denote the σ-field spanned by the random variables contained in H_t, i.e.,

$$\mathcal{H}_t = \sigma\{H_t\} \quad , \tag{2.20}$$

then assuming that $E[\eta_t | \mathcal{H}_t]$ is a quasi-martingale, we may interpret $E[d\eta_t | H_t]$ as the increment of the bounded variation term in a decomposition of the form in (2.17).

A second result from the theory of quasi-martingales that we will employ repeatedly concerns a property of the martingale components of a process f_t, which is a quasi-martingale with respect to two different σ-fields, $\mathcal{J}_{1t}$ and $\mathcal{J}_{2t}$. Let us suppose that f_t has been decomposed as

$$f_t = B_{1t} + M_{1t} \quad , \tag{2.21}$$

or

$$f_t = B_{2t} + M_{2t} \quad , \tag{2.22}$$

with respect to $\mathcal{J}_{1t}$ and $\mathcal{J}_{2t}$, respectively. In order to state the desired result, we next define a process $\langle M,M\rangle_t$ that we can associate with a second order sample continuous martingale $(M_t,\mathcal{J}_t)$. By the Doob-Meyer decomposition theorem [48] we may decompose M_t^2 as

$$M_t^2 = m_t + \langle M,M\rangle_t \quad , \tag{2.23}$$

where m_t is a $\mathcal{J}_t$ martingale and $\langle M,M\rangle_t$ is a bounded variation, increasing process. Fisk [45] has shown that for a second order, sample continuous martingale M_t, $\langle M,M\rangle_t$ may be computed by the limit

$$\langle M,M\rangle_t = \lim_{n'\to\infty} \sum_{i=0}^{n'-1} \left[M_{t_{i+1}^{n'}} - M_{t_i^{n'}} \right]^2 \quad , \tag{2.24}$$

where $t_i^{n'}$ denotes some progressively finer partition of the interval $[0,t]$, as n' becomes infinite. The quantity on the right-hand side of relation (2.24) is termed the quadratic variation of M_t at time t. We can now state the desired result relating the different martingale components of a process f_t,

which is a quasi-martingale with respect to two σ-fields, $\mathcal{F}_{1t}$ and $\mathcal{F}_{2t}$, by asserting that in this case, the quadratic variation of M_{1t} and M_{2t} are the same, i.e.,

Equivalence of the Quadratic Variation of the Martingale Components of a Quasi-Martingale with respect to Two σ-Fields

$$\langle M_1, M_1 \rangle_t = \langle M_2, M_2 \rangle_t \quad . \tag{2.25}$$

The implications of relation (2.25) can only be appreciated by constructing $\langle M,M \rangle_t$ for a simple example. Let us suppose that M_t is given by the Wiener integral

$$M_t = \int_0^t a(s)\, dw(s) \quad , \tag{2.26}$$

where w(s) denotes a standard Brownian motion process. Then by employing the Ito-differential rule [48] we can show that M_t^2 may be expressed as

$$M_t^2 = 2 \int_0^t a(s) M_s dw(s) + \int_0^t a^2(t) dt \quad . \tag{2.27}$$

The first term in relation (2.27) is a stochastic integral corresponding to the martingale component m_t in relation (2.23), and so

$$\langle M,M\rangle_t = \int_0^t a^2(t)dt \quad . \tag{2.28}$$

Hence, for M_t defined by (2.26), we can identify $\langle M,M\rangle_t$ as the variance of the process. Therefore, in a somewhat more general setting, where we identify f_t with some vector Wiener process, equation (2.25) allows us to conclude that the martingale components of decompositions of f_t with respect to different σ-fields, with respect to which f_t is a quasi-martingale, are Wiener processes with the same statistics as the original process.

We next establish a notation for the past and future spaces spanned by the increments of a process, and then prove a simple result for estimation of a zero-mean random vector x based on the past values of a standard vector Wiener process. If we let $w(\cdot)$ denote our standard vector Wiener process with

$$E[w(t_1)w'(t_2)] = I \min\{t_1,t_2\} \quad , \tag{2.29}$$

then we define the past and future spaces at time t, relative to some fixed interval [0,T], as

$$W_t^+ = H(dw(\tau) \quad t \le \tau \le T) \triangleq H(w(\tau_1) - w(\tau_2);\ \tau_1,\tau_2 \in [t,T]) \ , \tag{2.30}$$

and

$$W_t^- = H(dw(\tau) \quad 0 \le \tau \le t) \triangleq H(w(\tau_1) - w(\tau_2);\ \tau_1,\tau_2 \in [0,t]) \ . \tag{2.31}$$

When we need to refer to the space spanned by the components of w(t) at time t, we will use the notation H(w(t)). We now note from [20] that $E[x|W_t^-]$ is given by

Estimation of a Random Vector x from the Observation of a Standard Wiener Process

$$E[x|W_t^-] = \int_0^t \frac{d}{ds} E[x\ w'(s)]dw(s) \quad . \tag{2.32}$$

The relation (2.32) follows from observing that for some matrix valued function $\varphi(s)$,

$$E[x|W_t^-] = \int_0^t \varphi(s)\ dw(s) \quad . \tag{2.33}$$

The orthogonality property of linear least squares estimates

$$E\left[\left[x - \int_0^t \varphi(s)\ dw(s)\right]\int_0^t \psi(s)\ dw(s)\right] = 0 \ , \tag{2.34}$$

for arbitrary square integrable $\psi(\cdot)$'s, allows us to deduce that

$$\varphi(s) = \frac{d}{ds} E[x\, w'(s)] \quad . \tag{2.35}$$

We conclude our presentation of the mathematical preliminaries that underly our work by establishing some standard notation for combining and taking orthogonal complements of Hilbert spaces. Let S_1, S_2, and S denote three Hilbert spaces. By the equation

$$S = S_1 \oplus S_2 \quad , \tag{2.36}$$

we will imply that S_1 and S_2 are orthogonal spaces, and that taken together they generate the space S. When more generally S_1 and S_2 are not orthogonal, we will use the notation $S_1 \vee S_2$ to denote

$$S_1 \vee S_2 \triangleq H(S_1, S_2) \quad , \tag{2.37}$$

i.e., the space generated by S_1 and S_2. In addition, when S_1 is a Hilbert sub-space of some larger standard space, i.e., such as the space of all zero-mean, finite second moment random variables, then we will use the notation $S_1^{\perp}$ to denote the Hilbert space generated by all elements in our standard space, orthogonal to S_1. Finally, if S_1 is contained in S, i.e., $S_1 \varepsilon S$, we will define the orthogonal complement of S_1 in S as

$$S \ominus S_1 \triangleq S \cap S_1^{\perp} \quad . \tag{2.38}$$

Hence, $S \ominus S_1$ denotes the Hilbert sub-space of S that is orthogonal to S_1, which taken together with S_1, generates S.

Now, before proceding to our presentation of the various smoothing formulae, we preview our unifying Hilbert space perspective on their origin. The various solutions to the fixed interval smoothing problem which we present correspond either to different ways of splitting up Y or to different approaches for realizing the conditional projection described in (2.9) and (2.16). We begin in Section 2.3 with the innovations approach [22], which arises in continuous time when we write Y as

$$Y = Y_t^- \oplus \boldsymbol{\nu}_t^+ \quad , \tag{2.39}$$

where Y_t^- and $\boldsymbol{\nu}_t^+$ denote, respectively, the Hilbert spaces generated by the past increments of $y(\cdot)$ at time t, and by the future increments of the innovations process $\nu(\cdot)$ defined by

$$d\nu(t) = dy(t) - E[dy(t)|Y_t^-] \quad . \tag{2.40}$$

Next, in Section 2.4, we discuss the Hamiltonian [31] and Rauch-Tung-Striebel [11] solutions to the smoothing problem,

which follow from taking $E[\cdot|Y]$ of both sides of the unconditional state dynamics (2.1), and then by using two different techniques for computing $E[du(t)|Y]$. Then, in Section 2.5, we use a stochastic realization point of view to interpret two-filter forms of the smoother. In this case the smoothed estimate, $\hat{x}_s(t)$, is expressed as a linear combination of two estimates, $\hat{x}_1(t)$ and $\hat{x}_2(t)$, where $\hat{x}_1(t)$ is obtained by processing the observation increments $dy(\tau)$ for $0 \leq \tau \leq t$ and $\hat{x}_2(t)$ is obtained by processing $dy(\tau)$ for $t \leq \tau \leq T$. Consequently, $\hat{x}_1(t)$ is often called a <u>forward</u> filtered estimate and $\hat{x}_2(t)$ is referred to as a <u>reverse</u> or <u>backward</u> filtered estimate. The fact that $\hat{x}_s(t)$ may be expressed in terms of $\hat{x}_1(t)$ and $\hat{x}_2(t)$ is reflected in the ability to decompose Y as

$$Y = H(\hat{x}_1(t),\hat{x}_2(t)) \oplus N_t \quad , \tag{2.41}$$

where N_t represents a Hilbert space orthogonal to the one spanned by the components of $x(t)$. Finally, in Section 2.6, we consider the approach of Weinert and Desai [49], which is the complement of the earlier approaches in the sense that instead of projecting $x(t)$ onto Y, we derive a procedure for computing $\hat{x}_s(\cdot)$ by subtracting from $x(t)$ the part that lies in $Y^{\perp}$ (the space of random variables orthogonal to Y).

2.3 The Innovations Approach to Smoothing

The innovations approach to linear least squares estimation was originally introduced by Kailath and Frost [22] - [23]. Letting $d\nu(t)$ be defined by relation (2.40), the significance of the innovations process stems from the following two properties:

$$Y_t^- = \boldsymbol{\nu}_t^- \quad , \tag{2.42}$$

proved by Meyer in [5], and the fact that

$$dw_*(s) = R^{-\frac{1}{2}}(s)d\nu(s), \tag{2.43}$$

is a standard Wiener process, proved by Kailath in [20]. Employing the fact that $\nu(\cdot)$ is an orthogonal increments process, and using relation (2.42), we can express the Hilbert space Y generated by the observations over a fixed interval as

$$Y = Y_t^- \oplus \boldsymbol{\nu}_t^+ \quad , \tag{2.44}$$

Hence, if we define the filtered estimate $\hat{x}_f(t)$ by

$$\hat{x}_f(t) \triangleq E[x(t)|Y_t^-] \quad , \tag{2.45}$$

we can employ relation (2.44) to compute $\hat{x}_s(t)$ as the sum of the projections of $x(t)$ onto the two orthogonal sub-spaces Y_t^- and $\mathcal{V}_t^+$, i.e.,

$$\hat{x}_s(t) = \hat{x}_f(t) + E\left[x(t)\,|\,\mathcal{V}_t^+\right] \quad . \tag{2.46}$$

To make relation (2.46) more explicit we need to compute the second term. In Appendix 2B we show how to employ our result (2.32) for estimation of a random vector based on the observation of a standard Wiener process to express the second term of relation (2.46) as

$$E\left[x(t)\,|\,\mathcal{V}_t^+\right] = P_f(t)\lambda(t|T) \quad , \tag{2.47}$$

where $P_f(\cdot)$ denotes the filtering error covariance matrix and $\lambda(t|T)$ is defined as

$$\lambda(t|T) = \int_{\tau=t}^{T} \Phi_{\Gamma}'(\tau,t)H'(\tau)R^{-1}(\tau)d\nu(\tau) \quad , \tag{2.48}$$

and where $\Phi_{\Gamma}(\cdot,\cdot)$ denotes the transition matrix corresponding to the filtering dynamics matrix $\Gamma(t)$ determined by

$$\Gamma(t) \triangleq A(t) - P_f(t)H'(t)R^{-1}(t)H(t) \quad . \tag{2.49}$$

Hence, by employing relation (2.47), the innovations solution to the continuous time fixed interval smoothing problem can be expressed as

Innovations Smoothing Formula

as
$$\hat{x}_s(t) = \hat{x}_f(t) + P_f(t)\lambda(t|T) \ . \tag{2.50}$$

In Appendix 2A we derive some analogs of relations (2.46) and (2.47) - (2.50) for discrete state-space models.

2.4 The Hamiltonian and Rauch-Tung-Striebel Approaches to Smoothing

The difference between the Hamiltonian and Rauch-Tung-Striebel approaches to smoothing lies not in the way Y is split between Y_t^- and $\mathcal{V}_t^+$, but in the way $E[du(t)|Y]$ is implemented when we condition the state-dynamics equation (2.1) with respect to Y. Hence, the starting point for our derivation of both algorithms is the relation

$$d\hat{x}_s(t) = A(t)\hat{x}_s(t)dt + B(t)\, E[du(t)|Y] \quad . \tag{2.51}$$

Now, by taking the decomposition (2.44) of Y into account, and by noting that du(t) is orthogonal to Y_t^-, we find that

$$E[du(t)|Y] = E\left[du(t)|\mathcal{V}_t^+\right] \quad . \tag{2.52}$$

We then use the fact that $R^{-\frac{1}{2}}(t)d\nu(t)$ is a standard Brownian motion process, and our result (2.32), in order to express the right-hand side of (2.52) as

$$E\left[du(t)|\mathcal{V}_t^+\right] = \int_{\tau=t}^{T} \frac{d}{d\tau} E[du(t)\ \nu'(\tau)]R^{-1}(\tau)d\nu(\tau) \quad . \tag{2.53}$$

Since $d\nu(\tau)$ may be expressed in terms of the filtering errors $\tilde{x}_f(\cdot)$ as

$$d\nu(\tau) = H(\tau)\tilde{x}_f(\tau)d\tau + D(\tau)d\nu(\tau) \quad , \tag{2.54}$$

the relation (2.53) may be written as

$$E\left[du(t)\,|\,\mathcal{V}_t^+\right] = \int_{\tau=t}^{T} E[du(t)\tilde{x}_f'(\tau)]H'(\tau)R^{-1}(\tau)d\nu(\tau) \quad . \tag{2.55}$$

Then by employing the equation for the evolution of the filtering error process, $\tilde{x}_f(\cdot)$, described in Appendix 2B, we can calculate $E[du(t)\tilde{x}_f'(\tau)]$. We find that

$$E\left[du(t)\,|\,\mathcal{V}_t^+\right] = B'(t)\lambda(t|T)dt \quad , \tag{2.56}$$

where $\lambda(t|T)$ is defined by (2.48).

The Hamiltonian and Rauch-Tung-Striebel solutions to the fixed interval smoothing problem now follow from two different ways of computing $\lambda(\cdot|T)$. Assuming the existence of $P_f^{-1}(\cdot)$, the Rauch-Tung-Striebel solution is determined by employing the innovations smoothing formulae (2.50) to express $\lambda(t|T)$ as

$$\lambda(t|T) = P_f^{-1}(t)(\hat{x}_s(t) - \hat{x}_f(t)) \quad . \tag{2.57}$$

Now, substituting relation (2.57) into (2.56), and using (2.52), we find that

$$E[du(t)|Y] = B'(t)P_f^{-1}(t)(\hat{x}_s(t) - \hat{x}_f(t))dt \quad . \tag{2.58}$$

If we use (2.58) in equation (2.51) we obtain the Rauch-Tung-Striebel smoothing formula that follows:

Rauch-Tung-Striebel Smoothing Formula

$$d\hat{x}_s(t) = A(t)\hat{x}_s(t)dt + B(t)B'(t)P_f^{-1}(t)(\hat{x}_s(t) - \hat{x}_f(t))dt \quad , \tag{2.59}$$

where $$\hat{x}_s(T) = \hat{x}_f(T) \quad . \tag{2.60}$$

We solve equation (2.59) in reverse time, after having generated the filtered estimates by a forward sweep over the data.

Alternatively, we can employ the definition of $\lambda(.|T)$, (2.48), to derive the backward differential equation

$$-d\lambda(t|T) = \Gamma'(t)\lambda(t|T)dt + H'(t)R^{-1}(t)d\nu(t) \quad , \tag{2.61}$$

where $$\lambda(T|T) = 0 \quad . \tag{2.62}$$

Using the definition of $d\nu(t)$, (2.40), as

$$d\nu(t) = dy(t) - H(t)\hat{x}_f(t)dt \quad , \tag{2.63}$$

and the fact that

$$\hat{x}_f(t) = \hat{x}_s(t) - P_f(t)\lambda(t|T) \quad , \tag{2.64}$$

we can obtain from (2.61) a second backward equation for $\lambda(\cdot|T)$, which taken together with the relation derived from substituting (2.56) into (2.51), results in the following Hamiltonian equations for smoothing:

Hamiltonian Equations for Smoothing

$$\begin{aligned} -d\lambda(t|T) &= A'(t)\lambda(t|T)dt - H'(t)R^{-1}(t)H(t)\hat{x}_s(t)dt \\ &\quad + H'(t)R^{-1}(t)dy(t) \quad , \end{aligned} \tag{2.65}$$

$$d\hat{x}_s(t) = A(t)\hat{x}_s(t)dt + B(t)B'(t)\lambda(t|T)dt \quad , \tag{2.66}$$

with the boundary conditions

$$\lambda(T|T) = 0 \quad , \tag{2.67}$$

and

$$\hat{x}_s(0) = P_f(0)\lambda(0|T) \quad . \tag{2.68}$$

The relation (2.68) is obtained by setting t=0 in the innovations smoothing formula (2.50).

From relations (2.65) - (2.68) we see that the Hamiltonian equations formulate the smoothing problem as the solution of a linear, two-point boundary value problem, and hence we may appeal to any of the techniques [56] for solving such boundary value problems, in order to obtain algorithms for computing the smoothed estimates. We mentioned earlier that scattering formalism provides a pictorial device, in the form of a type of ladder, signal-flow diagram, for displaying the Hamiltonian equations. We sketch this approach briefly in Appendix 2C, since we will only appeal to it as an auxiliary, computational tool.

2.5 The Stochastic Realization Theory View of Two-Filter Solutions to the Fixed Interval Smoothing Problem

Like the innovations approach, the two-filter forms of the smoothed estimate follow from some orthogonal decompositions of the observation space, Y, of the form

$$Y = H\left(\hat{x}_1(t), \hat{x}_2(t)\right) \oplus N_t \quad , \tag{2.69}$$

where $\hat{x}_1(t)$ and $\hat{x}_2(t)$ are computed by forward and reverse filtering operations, and $H(x(t))$ is orthogonal to the Hilbert space N_t. Hence, the decomposition (2.69) implies that $\hat{x}_s(t)$ may be obtained as a linear combination of $\hat{x}_1(t)$ and $\hat{x}_2(t)$. The derivation of smoothing solutions along the lines suggested by relation (2.69) is intimately related with stochastic realization theory. This section is devoted to presenting this approach.

In general, stochastic realization theory is concerned with the study of how and when a given process may be represented by a particular mathematical formalism. For example, the early work of Hida [57] and Cramer [58] focused on understanding representations of Gaussian processes as sums of Wiener integrals with respect to orthogonal increments processes. More recently, stochastic realization theory has focused on characterizing the family of minimal order state-space models that

may be employed to either represent exactly, or reproduce the same correlation properties, of a given process. Anderson [64] and Faurre [72] have studied the family of all stationary, discrete-time state models that will generate processes with a given rational power spectral density. Clerget [75] similarly studied the family of continuous time, nonstationary state models that generate a given finite-dimensionally, realizable correlation function. Akaike [71], and later Picci [77], drawing on Akaike's work and some ideas due to Mckean [60], have clarified the notion of exactly what should comprise a state-space for representing a stochastic system. Finally, Lindquist and Picci [78] - [82] and Ruckebusch [73] have studied the construction of state spaces, and the characterization of the family of state-space models that may be employed to exactly represent a given process.

Our presentation of the stochastic realization perspective on two-filter solutions to the smoothing problem is adapted from the work of Lindquist and Badawi [83] - [84], and the earlier papers of Lindquist and Picci [78] - [82]. We first define some terms and concepts that appear in their work. Relations (2.1) - (2.5) uniquely define the observations process $y(t)$ as the solution of a stochastic differential equation. We will define a proper stochastic realization of the observations $y(\cdot)$ as a set of matrices $F(t)$, $J(t)$, $C(t)$, and $E(t)$

together with some standard p-dimensional Wiener process $w(\cdot)$, such that for each time t

$$dy(t) = C(t)x(t)dt + E(t)dw(t) \quad , \tag{2.70}$$

where

$$dx(t) = F(t)x(t)dt + J(t)dw(t) \quad . \tag{2.71}$$

We note that relations (2.1) - (2.5) specify one proper stochastic realization of $y(\cdot)$ with

$$dw(t) \triangleq \left(\begin{array}{c|c} I & 0 \\ \hline 0 & I \end{array}\right) \left(\begin{array}{c} du(t) \\ \hline dv(t) \end{array}\right) \quad , \tag{2.72}$$

$$F(t) \triangleq A(t) \quad , \tag{2.73}$$

$$J(t) \triangleq \left(\begin{array}{c|c} B(t) & 0 \\ \hline 0 & 0 \end{array}\right) \quad , \tag{2.74}$$

$$C(t) = H(t) \quad , \tag{2.75}$$

and

$$E(t) = \left(\begin{array}{c|c} 0 & 0 \\ \hline 0 & D(t) \end{array}\right) \quad . \tag{2.76}$$

We will refer to the space generated by the state process as X, where

$$X \triangleq H(x(\tau) \cdot 0 \leq \tau \leq T) \quad . \tag{2.77}$$

We note here that $x(\cdot)$ is a Markov process, i.e., it satisfies the Markov property, which may be described in our Hilbert space setting as

$$E[X_t^+ | X_t^-] = E[X_t^+ | H(x(t))] \quad . \tag{2.78}$$

Relation (2.78) may be interpreted as saying that knowledge of the present value of the process is equivalent to knowledge of the entire past of the process, as far as predicting future values of the process. If the initial condition for $x(\cdot)$ is specified at $t=0$ with $H(dw(t))$ orthogonal to $x(0)$, then relations (2.70) - (2.71) specify a forward Markovian realization for the observations process $y(\cdot)$. Similarly, if we specify $x(T)$, and $H(dw(t))$ is orthogonal to $x(T)$, we say that relations (2.70) - (2.71) determine a backwards Markovian realization for the observations process $y(\cdot)$.

We classify proper stochastic realizations of the $y(\cdot)$ process on the basis of the Hilbert space, X, spanned by the associated state process $x(\cdot)$. A proper stochastic realization of the form specified by relations (2.70) - (2.71) is termed <u>internal</u> when

$$X \varepsilon Y \quad , \tag{2.79}$$

and external when

$$X \not\varepsilon Y \quad . \tag{2.80}$$

We note that the problem of computing the smoothed estimate for $x(t)$ given Y is nontrivial only when $x(\cdot)$ is the state process of an external realization. Hence, we expect that our original realization for the $y(\cdot)$ process, specified by relations (2.1) - (2.5), is an external realization.

The contribution of the stochastic realization theory perspective to understanding two-filter forms of the smoothed estimate lies in recognizing the processes $\hat{x}_1(\cdot)$ and $\hat{x}_2(\cdot)$, appearing in the orthogonal decomposition of relation (2.69), as state processes corresponding to proper, internal stochastic realizations of the observations process $y(\cdot)$. In the following section, we will first define three state processes corresponding to different internal realizations, $x_*(\cdot)$, $x^*(\cdot)$, and $\hat{x}_r(\cdot)$. The process $x_*(t)$ will correspond to the forward filtered estimate of $x(t)$, $x^*(t)$ will correspond to an estimate of $x(t)$ based on the future observations and identified with the Mayne-Fraser [19] backward filtered estimate, and $\hat{x}_r(t)$ will represent the reverse filtered estimate of $x(t)$ defined by

$$\hat{x}_r(t) = E[x(t) | Y_t^+] \quad . \tag{2.81}$$

We then show the role of $(x_*(t), x^*(t))$ and $(x_*(t), \hat{x}_r(t))$ in determining orthogonal decompositions of the observations space Y of the form (2.69), and ultimately in generating the Mayne-Fraser [19] and Wall [38] solutions of the smoothing problem. This approach provides a unified treatment of these two types of two-filter solutions to the smoothing problem.

Finally, we note that in Section 1.2 we motivated the importance of obtaining Markovian realizations of the smoothing error process for solving the centralized map-updating problem. The existence of such Markovian models for the smoothing errors is in some sense a surprising result, since the smoothed estimate itself may not be generated by a single causal, stochastic differential equation. The stochastic-realization framework provides an especially natural setting for examining the smoothing errors, which correspond, in imprecise terms, to the non-internal part of our original state process. Hence, we will show in Section 3.3 how the Bryson-Frazier form of the solution to the smoothing problem enables us to derive the first Markovian representation for the smoothing error process.

Construction of $x_*(\cdot)$

The idea of representing the observations process $y(\cdot)$ as the output of a model of the form (2.70) - (2.71), with an underlying state process that corresponds to a filtered estimate, appears in Kailath and Geesy's paper [24], and also the

work of Faurre [72] and Ruckebusch [73]. In notation originally due to Faurre, the Kalman filtered estimate, $x_*(\cdot)$, associated with the state-space model (2.1) - (2.5), is generated by the equation

$$dx_*(t) = A(t)x_*(t)dt + B_*(t)R^{-\frac{1}{2}}(t)(dy(t) - H(t)x_*(t)dt) \quad , \tag{2.82}$$

$$\text{with} \qquad x_*(0) = 0 \quad , \tag{2.83}$$

$$\text{where} \qquad B_*(t) = P_*(t)H(t)R^{-\frac{1}{2}}(t) \quad , \tag{2.84}$$

and $P_*(\cdot)$ corresponds to the filtering error covariance generated by the solution of the matrix Ricatti equation

$$\dot{P}_* = A(t)P_*(t) + P_*(t)A'(t) - P_*(t)H'(t)R^{-1}(t)H(t)P_*(t) + B(t)B'(t), \tag{2.85}$$

$$\text{with} \qquad P_*(0) = \pi(0) \quad . \tag{2.86}$$

If we define the normalized innovations process $dw_*(t)$ by

$$dw_*(t) = R^{-\frac{1}{2}}(t)(dy(t) - H(t)x_*(t)dt) \quad , \tag{2.87}$$

then from (2.82) and (2.87) we obtain the following internal realization for the $y(\cdot)$ process:

$$dx_*(t) = A(t)x_*(t)dt + B_*(t)dw_*(t) \quad , \tag{2.88}$$

with $$x_*(0) = 0 \quad , \tag{2.89}$$

and $$dy(t) = H(t)x_*(t)dt + R^{\frac{1}{2}}(t)dw_*(t) \quad . \tag{2.90}$$

We will let $\pi_*(\cdot)$ denote the state covariance associated with $x_*(\cdot)$. Hence, $\pi_*(\cdot)$ is generated by the equation

$$\dot{\pi}_*(t) = A(t)\pi_*(t) + \pi_*(t)A'(t) + B_*(t)B_*'(t) \quad , \tag{2.91}$$

with $$\pi_*(0) = 0 \quad . \tag{2.92}$$

Construction of $x^*(\cdot)$

At this point, we have shown that the Kalman filtered estimate, $x_*(\cdot)$, may be interpreted as the state process of a forward, internal realization of the observations process $y(\cdot)$. We next derive a second process, $x^*(t)$, that can be identified as an estimate of $x(t)$ based on future observations, and corresponds to the backward filtered estimate employed by Mayne and Fraser [19]. We will show that $x^*(\cdot)$, like $x_*(\cdot)$, may also be interpreted as the state process associated with a forward internal realization of the observations process $y(\cdot)$. To accomplish this, we will construct $x^*(\cdot)$ in a somewhat

indirect manner. Consider the collection of all forward, proper stochastic realizations of the observations process $y(\cdot)$ and imagine defining Kalman filtered estimates for each of these realizations. Then, we let $\mathcal{B}$ denote the class of all such forward stochastic realizations of $y(\cdot)$ that generate filtered estimates that reproduce the same sample paths as the estimate, $x_*(t)$, associated with our original model specified by relations (2.1) - (2.5). It can be shown [83] that the typical element in $\mathcal{B}$ assumes the following form:

$$dy(t) = H(t)x(t)dt + E(t)dw(t) \quad , \tag{2.93}$$

where

$$dx(t) = A(t)x(t)dt + J(t)dw(t) \quad , \tag{2.94}$$

and

$$E(t)E'(t) = R(t) \quad . \tag{2.95}$$

We note that $H(\cdot)$, $A(\cdot)$, and $R(\cdot)$ are invariant for realizations in $\mathcal{B}$, while $E(\cdot)$, $J(\cdot)$, and the input process $w(\cdot)$ vary. As in the case of our original model (2.1) - (2.5), we let $\pi(\cdot)$ denote the state covariance matrix associated with $x(\cdot)$. We note here that Faurre and Germain [72],[76], in the stationary case, and later Clerget [75], in the non-stationary case, have characterized the family of state-space models of the form specified by (2.93) - (2.95), that generate a $y(\cdot)$ process with

the same correlation properties as our original realization for for $y(\cdot)$ of (2.1) - (2.5). The realizations in the family $\mathcal{D}$ are proper realizations, i.e., they satisfy the stronger property of generating the same sample paths as the $y(\cdot)$ of (2.1) - (2.5). Faurre, Germain, and Clerget examined the structure of the set $\mathcal{P}$ of all state covariance matrices $\pi(\cdot)$ that result in a model (2.93) - (2.95) that represents a $y(\cdot)$ with the same second order properties as those determined by the original model (2.1) - (2.5). These authors show that in the space of $n \times n$ matrices, $\mathcal{P}$ is a closed and bounded convex set. Since the family of proper realizations of $y(\cdot)$ in $\mathcal{D}$ is contained in the larger family of realizations studied by Faurre, et al., it is not surprising that when realizations in $\mathcal{D}$ are ordered with respect to their state covariance matrices, we can determine a minimal and maximal covariance state process. We note that from the orthogonality property of filtering errors, the filtering error covariance matrix $P_*(t)$ associated with the realization (2.93) - (2.95) is given as

$$P_*(t) = \pi(t) - \pi_*(t) \quad , \tag{2.96}$$

and hence by imposing the non-negativity of $P_*(t)$, we find that

$$\pi(t) \geq \pi_*(t) \quad . \tag{2.97}$$

Thus, $x_*(\cdot)$ may be interpreted as the minimal covariance state process associated with realizations in $\mathcal{B}$. In what follows, we motivate the construction of $x^*(\cdot)$ as the maximal covariance state process associated with realizations in $\mathcal{B}$, i.e., for each state process $x(\cdot)$ associated with a realization in $\mathcal{B}$, we have

$$\pi(t) \leq \pi^*(t) \quad , \tag{2.98}$$

where $\pi^*(\cdot)$ denotes the state covariance associated with $x^*(\cdot)$.

Duality between $\mathcal{B}$ and $\overline{\mathcal{B}}$

The key to our construction of $x^*(\cdot)$ lies in the definition of an isomorphism between the set $\mathcal{B}$ of forward realizations and a corresponding set $\overline{\mathcal{B}}$ of backward realizations. In [72], for the stationary case, Faurre studied the family of backward Markovian realizations associated with representing the correlation properties of the time reversed process $y(-t)$, and the structure of the set $\overline{\mathcal{P}}$ made up of the corresponding state covariance matrices. He demonstrated a one-to-one correspondence between a state covariance $\pi(\cdot)$ in $\mathcal{P}$ and $\pi^{-1}(\cdot)$ in $\overline{\mathcal{P}}$. Hence, for the typical element in $\mathcal{B}$ specified by (2.93) - (2.95), we define its counterpart in $\overline{\mathcal{B}}$ as having a state process

$$\overline{x}(t) = \pi^{-1}(t)x(t) \quad , \tag{2.99}$$

assuming the invertibility of the state covariance matrix, $\pi(\cdot)$. Thus, the backward realization in $\bar{\mathcal{P}}$ has a state covariance matrix which is the inverse of that associated with its forward counterpart in $\mathcal{P}$. The correspondence between realizations in $\mathcal{P}$ and $\bar{\mathcal{P}}$ is determined from the relations (2.93) - (2.95), (2.99), and standard techniques [36] for specifying backward Markovian realizations from forward Markovian realizations. Hence, the backwards counterpart in $\bar{\mathcal{P}}$ of the realizations (2.93) - (2.95) is defined by the following relations:

Backward Markovian Realization with Inverse Covariance State Process

$$dy(t) = G'(t)\bar{x}(t)dt + E(t)d\bar{w}(t) \quad , \tag{2.100}$$

$$d\bar{x}(t) = -A'(t)\bar{x}(t)dt + \pi^{-1}(t)J(t)d\bar{w}(t) \quad , \tag{2.101}$$

with $$\bar{x}(T) = \pi^{-1}(T)x(T) \quad , \tag{2.102}$$

$$d\bar{w}(t) = dw(t) - J'(t)\bar{x}(t)dt \quad , \tag{2.103}$$

and $$G(t) \triangleq \pi(t)H'(t) + J(t)E'(t) \quad . \tag{2.104}$$

We note here that in [83] it is shown that the invariance of the Kalman filtered estimate, for realizations in $\mathcal{P}$, implies

the invariance of $G(\cdot)$ as well as of the backward Kalman filtered estimate, as defined for realizations in $\overline{\mathcal{B}}$. Finally, we remark that while (2.101) determines a backward Markovian realization for a normalized, $\pi^{-1}(\cdot)x(\cdot)$, version of the original state process, we will exhibit later a backwards Markovian realization for $x(\cdot)$ itself, obtained from the approach of Kailath and Verghese [36].

At this point, we have specified a one-to-one correspondence between the forward realization in $\mathcal{B}$ described by relations (2.93) - (2.95) and the backward realization in $\overline{\mathcal{B}}$ determined by (2.100) - (2.104). We can employ a completely analogous set of relations to (2.100) - (2.104) for defining the forward counterpart of a given realization in $\overline{\mathcal{B}}$. By using the fact that the state covariance associated with a given realization in $\mathcal{B}$ is the <u>inverse</u> of the state covariance associated with its backward counterpart in $\overline{\mathcal{B}}$, we may determine the forward realization in $\mathcal{B}$ whose state process $x^*(\cdot)$ has <u>maximal</u> state covariance, by identifying the realization in $\overline{\mathcal{B}}$ whose state process has <u>minimal</u> state covariance, and then taking its forward counterpart.

We identify now the realization in $\overline{\mathcal{B}}$ whose state process has minimal state covariance. Relations (2.100) - (2.104) allow us to determine the backward counterpart of our original realization specified by relations (2.1) - (2.5), with

associated state vector $\bar{x}(t)$, defined by

$$\bar{x}(t) = \pi^{-1}(t)x(t) \quad . \tag{2.105}$$

Hence, we can define the backward Kalman filtered estimate, $\bar{x}_*(t)$, as

$$\bar{x}_*(t) \triangleq E[\bar{x}(t)|Y_t^+] \quad . \tag{2.106}$$

Just as $x_*(\cdot)$ is the state process associated with the minimum state covariance realization in $\mathcal{R}$, $\bar{x}_*(\cdot)$ is the state process associated with the minimum state covariance realization in $\bar{\mathcal{R}}$. We will call the realization in $\bar{\mathcal{R}}$ with associated state vector $\bar{x}_*(\cdot)$, the backward filter realization. As we commented before, $\bar{x}_*(\cdot)$ will be the backward Kalman filtered estimate generated by each of the realizations in $\bar{\mathcal{R}}$. The relationships between the state processes $x_*(\cdot)$, $x(\cdot)$, $x^*(\cdot)$, $\bar{x}(\cdot)$, and $\bar{x}_*(\cdot)$ and the stochastic realizations of $y(\cdot)$ with which they are connected are depicted in Fig. 2.1.

We finally construct $x^*(\cdot)$ as the state process associated with the forward counterpart of the backward filter realization. Hence, $x^*(t)$ is defined as

$$x^*(t) = \bar{\pi}_*^{-1}(t)\bar{x}_*(t) \quad , \tag{2.107}$$

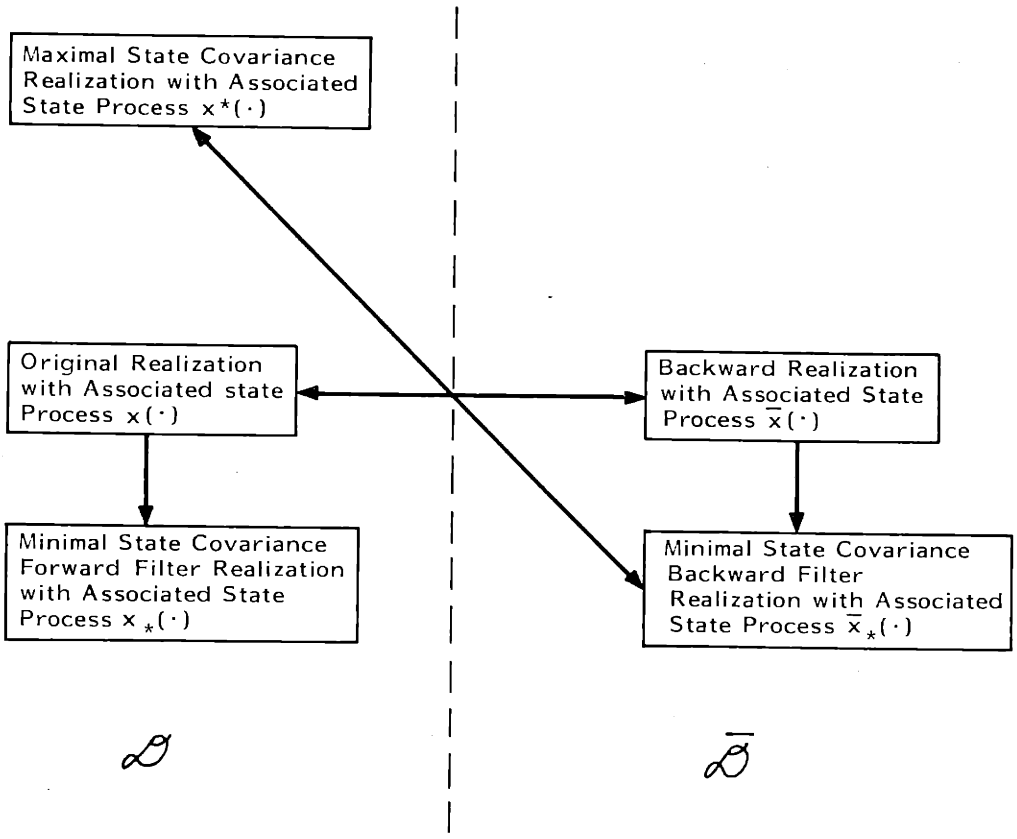

Fig. 2.1 Diagram Depicting the Relation between the State Processes $x(\cdot)$, $x_*(\cdot)$, $x^*(\cdot)$, $\bar{x}(\cdot)$, $\bar{x}_*(\cdot)$ and the Corresponding Stochastic Realizations of the Observations Process, $y(\cdot)$

where $\bar{\pi}_*(t)$ denotes the state covariance of $\bar{x}_*(t)$. From relation (2.107) the state covariance $\pi^*(t)$ associated with $x^*(t)$ is defined by

$$\pi^*(t) = \bar{\pi}_*^{-1}(t) \quad . \tag{2.108}$$

By employing equations for the evolution of $\bar{x}_*(t)$, and relation (2.107), we can show that $x^*(\cdot)$ evolves according to the equation:

Maximal Covariance State Process

$$dx^*(t) = A(t)x^*(t)dt - P^*(t)H'(t)R^{-1}(t)(dy(t) - H(t)x^*(t)dt) \ , \tag{2.109}$$

$$\text{with} \qquad x^*(0) = \bar{\pi}_*^{-1}(0)\bar{x}_*(0) \quad , \tag{2.110}$$

and where $P^*(t)$, defined as

$$P^*(t) = \pi^*(t) - \pi(t) \quad , \tag{2.111}$$

obeys the equation:

$$\dot{P}^*(t) = A(t)P^*(t) + P^*(t)A'(t) + P^*(t)H'(t)R^{-1}(t)P^*(t) - B(t)B'(t) \quad , \tag{2.112}$$

with $$P^*(0) = \bar{\pi}_*^{-1}(0) - \pi(0) \quad . \tag{2.113}$$

If we look at the time reversed versions of relations (2.109) and (2.112), we can recognize $x^*(\cdot)$ and $P^*(\cdot)$ as the Mayne-Fraser backward filtered estimate, and its corresponding filtering error covariance matrix. Wall [38] identified the Mayne-Fraser backward filtered estimate as a maximum likelihood estimate for the state based on the future observations. This is consistent with the fact that from relation (2.111) $P^*(T)$ is infinite; i.e., since at time T no observations are available, we have no information about $x(T)$.

Construction of $\hat{x}_r(\cdot)$

At this point we have identified the forward Kalman filtered estimate, $x_*(t)$, and the Mayne-Fraser backward filtered estimate, $x^*(t)$, as two processes associated with minimum and maximum state covariance internal realizations in $\mathcal{D}$, respectively. We next determine the reverse filtered estimate, $\hat{x}_r(t)$, defined by relation (2.81) and comment on its relation to $x^*(t)$. We first note that from Verghese and Kailath [36], the backwards Markovian realization of our original state process $x(\cdot)$, i.e., the backwards model for $x(\cdot)$ that retraces the same sample path in reverse time, is defined by

Some Sample Path-Backward State Realization

$$-dx(t) = -\left(A(t) + B(t)B'(t)\pi^{-1}(t)\right)x(t)dt - B(t)du_r(t), \quad (2.114)$$

where $u_r(\cdot)$ is a standard Wiener process defined by

$$du_r(t) = du(t) - B'(t)\pi^{-1}(t)x(t)dt \quad . \quad (2.115)$$

Therefore from the observation equation (2.5), and the definition (2.81), we can show that $\hat{x}_r(\cdot)$ is generated by

Backward Kalman Filtered Estimate

$$-d\hat{x}_r(t) = -\left(A(t) + B(t)B'(t)\pi^{-1}(t) + P_r(t)H'(t)R^{-1}(t)H(t)\right)\hat{x}_r(t)dt + P_r(t)H'(t)R^{-1}(t)dy(t) \quad , \quad (2.116)$$

$$\text{with} \qquad \hat{x}_r(\mathbf{T}) = 0 \qquad , \quad (2.117)$$

and where the filtering error covariance matrix $P_r(\cdot)$ obeys the relation

$$-\dot{P}_r(t) = -\left(A(t) + B(t)B'(t)\pi^{-1}(t)\right)P_r(t) - P_r(t)\left(A'(t) + \pi^{-1}(t)B(t)B'(t)\right) - P_r(t)H'(t)R^{-1}(t)H(t)P_r(t) + B(t)B'(t) \quad , \quad (2.118)$$

with $$P_r(T) = \pi(T) \ . \tag{2.119}$$

Finally, by employing relation (2.107) and (2.106) defining $x^*(t)$ and $\bar{x}_*(t)$, and by taking into account the relation (2.105) defining $\bar{x}(t)$, we see that $x^*(t)$ may be expressed as

$$x^*(t) = \pi^*(t)\pi^{-1}(t)\hat{x}_r(t) \ , \tag{2.120}$$

or alternatively that the reverse filtered estimate $\hat{x}_r(t)$ can be expressed as

$$\hat{x}_r(t) = \pi(t)\pi^{*-1}(t)x^*(t) \ . \tag{2.121}$$

We will now show that the smoothed estimate $E[x(t)|Y]$ may be computed as a linear combination of either $(x_*(t),x^*(t))$ or equivalently $(x_*(t),\hat{x}_r(t))$. We proceed, by first introducing an orthogonal decomposition of Y. In the case when the coefficient matrices associated with our original realization defined by relations (2.1) - (2.5) are analytic, and when the dimension of the state process $x(\cdot)$ is minimal, this orthogonal decomposition of Y will be shown to correspond directly to a decomposition of the form (2.69).

Our decomposition of Y is derived by noting that

$$Y = Y_t^- \vee Y_t^+ \quad . \tag{2.122}$$

We define the projections of Y_t^- onto Y_t^+ and Y_t^+ onto Y_t^- by

$$Y_t^{-|+} = H\left(E[\eta|Y_t^+] \;\forall\; \eta \in Y_t^-\right) \quad , \tag{2.123}$$

and

$$Y_t^{+|-} = H\left(E[\eta|Y_t^-] \;\forall\; \eta \in Y_t^+\right) \quad . \tag{2.124}$$

Then if we let

$$Y_t^{\square} \triangleq Y_t^{-|+} \vee Y_t^{+|-} \quad , \tag{2.125}$$

where we will call $Y_t^{\square}$ the frame space, and let N_t^+, N_t^- be determined by

$$Y_t^+ = Y_t^{-|+} \oplus N_t^+ \quad , \tag{2.126}$$

and

$$Y_t^- = Y_t^{+|-} \oplus N_t^- \quad , \tag{2.127}$$

We show (see Appendix 2D) that Y has the orthogonal decomposition

Frame Space Decomposition

$$Y = Y_t^{\square} \oplus N_t^+ \oplus N_t^- \quad . \tag{2.128}$$

The spaces $Y_t^{\square}$, $Y_t^{-|+}$, and $Y_t^{+|-}$ are each examples of what are called splitting subspaces [77]. We will define a splitting substance S_t as some Hilbert space contained in Y and satisfying either of the following two conditions:

$$E[\eta | Y_t^- \vee S_t] = E[\eta | S_t] \quad \forall \ \eta \in Y_t^+ \quad , \tag{2.129}$$

or

$$E[\eta | Y_t^+ \vee S_t] = E[\eta | S_t] \quad \forall \ \eta \in Y_t^- \quad . \tag{2.130}$$

Relation (2.129) may be interpreted as saying that S_t contains the same information as the entire past Y_t^-, as far as predicting the future, Y_t^+. Picci [77] noted that the properties satisfied by splitting subspaces coincide with our intuitive idea for what should constitute the state of a stochastic system, i.e., the minimal amount of information that allows us to predict the future. Lindquist and Picci [80] show that if we let S_t denote a minimal splitting subspace, i.e., we require that there is no proper subspace of S_t satisfying either (2.129) or (2.130), then

$$S_t \in Y_t^{\square} \quad . \tag{2.131}$$

The significance of relation (2.131) lies in the fact that if $x(t)$ denotes the state process of a minimal order, proper internal stochastic realization of $y(\cdot)$, then $H(x(t))$ defines a minimal splitting subspace. Hence, the frame space $Y_t^{\square}$ contains the state processes of all possible minimal order, proper internal stochastic realizations of $y(\cdot)$. In a stationary setting, these internal state processes are determined by specifying all the minimal square spectral factors of the matrix power spectral density associated with $y(\cdot)$ [86].

Our use for the decomposition (2.128) lies in the fact that we can verify, as in Appendix 2E, that when our coefficient matrices are analytic and our state space $x(\cdot)$ is of minimal dimension, we have

$$Y_t^{+|-} = H(x_*(t)) \quad , \tag{2.132}$$

and

$$Y_t^{-|+} = H(x^*(t)) = H(\hat{x}_r(t)) \quad . \tag{2.133}$$

In this case the decomposition of relation (2.128) becomes

$$Y = H(x_*(t); x^*(t)) \oplus N_t \quad , \tag{2.134}$$

where $N_t = N_t^+ \oplus N_t^-$, (2.135)

$N_t^+ = Y_t^+ \ominus H(x^*(t))$, (2.136)

and $N_t^- = Y_t^- \ominus H(x_*(t))$. (2.137)

To check that relation (2.134) represents an orthogonal decomposition of Y, of the type in relation (2.69), we verify that x(t) is orthogonal to N_t defined by relations (2.135) - (2.137). The orthogonality of x(t) to N_t^- and N_t^+ follows from expressing x(t) as

$$x(t) = (x(t) - x_*(t)) + x_*(t) \quad , \tag{2.138}$$

and $$x(t) = (x(t) - \hat{x}_r(t)) + \hat{x}_r(t) \quad , \tag{2.139}$$

respectively. From relation (2.137), $x_*(t)$ is orthogonal to N_t^- and $x(t)-x_*(t)$ is orthogonal to Y_t^-, which contains N_t^-. This implies from relation (2.138) that x(t) is orthogonal to N_t^-. We show similarly that x(t) is orthogonal to N_t^+.

The orthogonal decomposition of Y in (2.134) allows us to conclude that $\hat{x}_s(t)$ may be expressed as

$$\hat{x}_s(t) = K_*(t)x_*(t) + K^*(t)x^*(t) \quad . \tag{2.140}$$

To calculate $K_*(t), K^*(t)$ we use the orthogonality conditions

$$E[(x(t) - K_*(t)x_*(t) - K^*(t)x^*(t))x_*'(t)] = 0 \ , \quad (2.141)$$

and $$E[(x(t) - K_*(t)x_*(t) - K^*(t)x^*(t))x^{*'}(t)] = 0 \ . \quad (2.142)$$

From the following correlation properties between $x(\cdot)$, $x_*(\cdot)$, and $x^*(\cdot)$, which are verified in Appendix 2F:

$$E[x(t)x_*'(t)] = \pi_*(t) \ , \quad (2.143)$$

$$E[x(t)x^{*'}(t)] = \pi(t) \ , \quad (2.144)$$

and $$E[x_*(t)x^{*'}(t)] = \pi_*(t) \ , \quad (2.145)$$

and by using (2.141) - (2.142), Lindquist and Badawi [83] were able to show that $\hat{x}_s(t)$ is determined by

Mayne-Fraser Two-Filter Smoothing Formula

$$\hat{x}_s(t) = P_s(t)\left\{P_*^{-1}(t)x_*(t) + P^{*-1}(t)x^*(t)\right\} \ , \quad (2.146)$$

where $$P_s^{-1}(t) = P_*^{-1}(t) + P^{*-1}(t) \ , \quad (2.147)$$

and $P_s(t)$ is the smoothing error covariance matrix. The form

of the Mayne-Fraser smoothing formula (2.146) is a consequence of the fact, which may be proved from the correlation properties (2.143) - (2.145), that the errors in the estimates $x_*(t)$ and $x^*(t)$ are orthogonal.

We finally employ relation (2.146) to verify the Wall [38] two-filter form of the smoothed estimate. By using relation (2.121) to relate $x^*(\cdot)$ and $\hat{x}_r(\cdot)$, equation (2.146) may be written as

$$\hat{x}_s(t) = P_s(t)\left\{P_*^{-1}(t)x_*(t) + P^{*-1}(t)\pi^*(t)\pi^{-1}(t)\hat{x}_r(t)\right\} . \quad (2.148)$$

By using the definition (2.111) for $P^*(\cdot)$, and the matrix identity

$$\left[M_1^{-1} - M_2'M_3^{-1}M_2\right]^{-1} = M_1 - M_1M_2'(M_2M_1M_2' - M_3)^{-1}M_2M_1 , \quad (2.149)$$

$P^{*-1}(\cdot)$ may be expressed as

$$P^{*-1}(t) = \left(\pi^{-1}(t) + P^{*-1}(t)\right)\pi(t)\pi^{*-1}(t) . \quad (2.150)$$

We will show in what follows that

$$P_r^{-1}(t) = \pi^{-1}(t) + P^{*-1}(t) , \quad (2.151)$$

so that by using (2.150) and (2.151) in (2.148), we can express $\hat{x}_s(t)$ as

Wall Two-Filter Smoothing Formula

$$\hat{x}_s(t) = P_s(t)\left\{P_*^{-1}(t)x_*(t) + P_r^{-1}(t)\hat{x}_r(t)\right\} , \qquad (2.152)$$

where $$P_s^{-1}(t) = P_*^{-1}(t) + P_r^{-1}(t) - \pi^{-1}(t) \quad . \qquad (2.153)$$

Relation (2.152) represents the Wall two-filter form of the smoothed estimate. We prove relation (2.151) by observing that from equation (2.121) for $\hat{x}_r(\cdot)$, $P_r(t)$ can be expressed as

$$P_r(t) = E\left[(x(t) - \pi(t)\pi^{*-1}(t)x^*(t))(x(t) - \pi(t)\pi^{*-1}(t)x^*(t))'\right]. \qquad (2.154)$$

Hence, by employing (2.154), $P_r(t)$ may be written as

$$P_r(t) = \pi(t) - \pi(t)\pi^{*-1}(t)\pi(t) \quad , \qquad (2.155)$$

and by the use of (2.149), P_r^{-1} may be written in the form that appears in equation (2.151).

Finally, we note that in direct contrast to the Mayne-Fraser smoothing formula (2.146), equation (2.152) does not

represent the combining of two estimates with orthogonal errors. The correlation between the estimation errors is derived from the fact that the initial forward and reverse filtering errors are x(0) and x(T), respectively. The correlation between x(T) and x(0) follows from our a-priori statistics for x(0), and the state model (2.1). The subtraction that occurs in the smoothing error covariance equation (2.153) is a reflection of the fact that both estimates, $x_*(\cdot)$ and $\hat{x}_r(\cdot)$, use a-priori state information.

At this point we have succeeded in motivating the Mayne-Fraser and Wall two-filter solutions to the continuous time fixed interval smoothing problem by using a stochastic realization theory point of view. Badawi, in his thesis [84], develops a similar perspective on solutions of the discrete fixed interval smoothing problem, which we sketch in Appendix 2A.

2.6 The Smoothing Method of Weinert and Desai

While the preceding approaches to the fixed interval smoothing problem have relied on alternative ways of expressing or decomposing Y, in the final approach, due to Weinert and Desai [49], a recursive algorithm for computing $\hat{x}_s(t)$ is derived starting from the identity

$$\hat{x}_s(t) = x(t) - \tilde{x}_s(t) \quad , \tag{2.156}$$

where $\tilde{x}_s(t)$ denotes the smoothing error. These authors derive a forward Markovian realization for $\tilde{x}_s(\cdot)$, which when combined with the unconditional state dynamics (2.1) yields a set of stochastic differential equations for computing $\hat{x}_s(\cdot)$. In what follows, we present the method of Weinert and Desai for deriving a forward Markovian model for $\tilde{x}_s(\cdot)$ and the resulting algorithm for $\hat{x}_s(\cdot)$ that follows from relation (2.156). In Appendix 3B we will use an analogous formulation in discrete time for deriving forward models for $\tilde{x}_s(\cdot)$.

We first modify our original state space model to correspond to that considered in [49]. We note that without loss of generality, since the observations process $y(\cdot)$ may be scaled, we can regard our measurements as being modelled by

$$dy(t) = \bar{H}(t)x(t)dt + d\bar{v}(t) \quad , \tag{2.157}$$

where $\bar{H}(t) = R^{-\frac{1}{2}}(t)H(t)$, (2.158)

and $\bar{v}(\cdot)$ is a standard Brownian motion process defined by

$$d\bar{v}(t) = R^{-\frac{1}{2}}(t)D(t)dv(t) \quad . \tag{2.159}$$

We suppose that the initial state covariance $\pi(0)$ has been factorized as

$$\pi(0) = MM' \quad , \tag{2.160}$$

where M is n x q and rank $\{\pi(0)\} = q$. Then we can model x(0) as

$$x(0) = M\delta \quad , \tag{2.161}$$

where δ represents a vector of q orthonormal random variables.

We now construct a complementary subspace for Y, Y_c, that will allow us to express $\tilde{x}_s(t)$ as a projection. First, we define a space S which contains X and Y by

$$S = H(\delta, du(\tau), d\bar{v}(\tau) \quad 0 \le \tau \le T) \quad . \tag{2.162}$$

We then define the subspace Y_c by requiring that

$$S = Y \oplus Y_c \quad . \tag{2.163}$$

Since $x(t) \in S$ and $E[x(t)|Y] = \hat{x}_s(t)$, from relation (2.163) we must be able to express $\tilde{x}_s(t)$ as

$$\tilde{x}_s(t) = E[x(t)|Y_c] \quad . \tag{2.164}$$

Hence, the space Y_c contains all the information about $x(t)$ that is lost, given that we observe Y.

Our next step is to identify a basis for Y_c that allows us to compute the projection in relation (2.164). We first note that our observations process may be expressed by representing $x(t)$ as the solution of the stochastic differential equation (2.1):

$$dy(t) = [\bar{H}(t)\Phi_A(t,0)M\delta]\,dt + \left[\int_0^t \bar{H}(t)\Phi_A(t,\tau)B(\tau)du(\tau)\right]dt + d\bar{v}(t). \tag{2.165}$$

We next define the linear operator L as mapping an element in R^q, e, into the space of m-vector square integrable functions on $[0,T]$, $L_2^{(m)}[0,T]$, i.e., we specify L as sending

$$e \quad \text{into} \quad \bar{H}(\cdot)\Phi_A(\cdot,0)Me \quad . \tag{2.166}$$

We similarly define the linear operator G, mapping $L_2^{(n_1)}[0,T]$ into $L_2^{(m)}[0,T]$, as sending

$$\psi(\cdot) \quad \text{into} \quad \int_0^{\bullet} \bar{H}(\cdot)\Phi_A(\cdot,\tau)B(\tau)\psi(\tau)d\tau \ . \tag{2.167}$$

Then, letting our inner product be defined in the standard manner on R^q, and as

$$\langle \psi_1(\cdot),\psi_2(\cdot)\rangle = \int_0^T \psi_1'(\tau)\psi_2(\tau)d\tau \quad , \tag{2.168}$$

on $L_2^{(m)}[0,T]$, we can determine the adjoint operators L^* and G^*, which map $L_2^{(m)}[0,T]$ into R^q and $L_2^{(m)}[0,T]$ into $L_2^{(n_1)}[0,T]$, respectively. Noting that L^* and G^* are specified as integrals of a given function $\psi(\cdot)$ weighted by some kernel $K(t,\tau)$, i.e., as

$$\int_0^T K(t,\tau)\psi(\tau)d\tau \quad , \tag{2.169}$$

we will imagine the kernel $K(\cdot,\cdot)$ as determining the Wiener integral

$$\int_0^T K(t,\tau)dw(\tau) \quad , \tag{2.170}$$

for some m-vector standard Brownian motion process. Hence, we will use the notations $L^*(dw)$ or $G^*(dw)$ to denote Wiener integrals defined in the manner suggested by equation (2.169) - (2.170). Finally, we will show in what follows that by

constructing the new quantities

$$dz(t) = du(t) - G^*(d\bar{v})dt \quad , \tag{2.171}$$

and

$$\theta = \delta - L^*(d\bar{v}) \quad , \tag{2.172}$$

or written out explicitly

$$dz(t) = du(t) - \left[\int_{\tau=t}^{T} B'(t)\Phi_A'(\tau,t)\bar{H}'(\tau)d\bar{v}(\tau)\right]dt, \tag{2.173}$$

and

$$\theta = \delta - \left[\int_{\tau=0}^{T} M'\Phi_A'(\tau,0)\bar{H}'(\tau)d\bar{v}(\tau)\right] \quad , \tag{2.174}$$

our basis for Y_c may be obtained as

Basis for Complementary Space, Y_c

$$Y_c = H(\theta) \vee Z \quad , \tag{2.175}$$

where

$$Z \triangleq H(dz(\tau) \quad 0 \leq \tau \leq T) \quad . \tag{2.176}$$

Verification of Basis for Y_c

We now prove relation (2.175) by demonstrating first that $H(\theta) \vee Z$ is orthogonal to Y and then that $S \in H(\theta, dz(\tau), dy(\tau)\ 0 \le \tau \le T)$. Since from the definitions of dy(t), dz(t), and θ, $H(\theta, dz(\tau), dy(\tau)\ \ 0 \le \tau \le T) \in \mathbf{S}$, we will then have validated (2.175). The orthogonality of $(\theta, dz(t_2))$ and $dy(t_1)$ follows by expressing $dy(t_1)$ from (2.165), employing relations (2.173) - (2.174) to express $(\theta, dz(t_2))$, and checking that

$$E[\theta\, y'(t_1)] = 0 \quad , \tag{2.177}$$

and

$$E[z(t_2)y'(t_1)] = 0 \quad . \tag{2.178}$$

We next show that $S \in H(\theta, dz(\tau), dy(\tau)\ \ 0 \le \tau \le T)$. By defining $\gamma(t)$ as

$$\gamma(t) \triangleq \int_{\tau=t}^{T} \Phi_A'(\tau, t)\bar{H}'(\tau)d\bar{v}(\tau) \quad , \tag{2.179}$$

we can express relations (2.173) - (2.174) as

$$dz(t) = -B'(t)\gamma(t)dt + du(t) \quad , \tag{2.180}$$

and

$$\theta = \delta - M'\gamma(0) \quad , \tag{2.181}$$

where $\gamma(\cdot)$ satisfies

$$d\gamma(t) = -A'(t)\gamma(t)dt - \bar{H}'(t)d\bar{v}(t) \quad , \tag{2.182}$$

with $$\gamma(T) = 0 \quad . \tag{2.183}$$

Hence, by employing relations (2.157), (2.180), and (2.181), $d\bar{v}(t)$, $du(t)$, and δ may be expressed as

$$d\bar{v}(t) = dy(t) - \bar{H}(t)x(t)dt \quad , \tag{2.184}$$

$$du(t) = dz(t) + B'(t)\gamma(t)dt \quad , \tag{2.185}$$

and $$\delta = M'\gamma(0) + \theta \quad . \tag{2.186}$$

We now show that $x(\cdot)$ and $\gamma(\cdot)$ can be recovered given θ, $dy(\cdot)$, $dz(\cdot)$, yielding the result that $S \in H(\theta, dy(\tau), dz(\tau) \quad 0 \leq \tau \leq T)$ from relations (2.184) - (2.186). We may substitute relations (2.184) and (2.185) into the $x(\cdot)$ and $\gamma(\cdot)$ dynamical equations to obtain the following coupled equations for $x(\cdot)$ and $\gamma(\cdot)$:

$$dx(t) = A(t)x(t)dt + B(t)[dz(t) + B'(t)\gamma(t)dt] \quad , \tag{2.187}$$

and $$d\gamma(t) = -A'(t)\gamma(t)dt - \bar{H}'(t)[dy(t) - \bar{H}(t)x(t)dt] \quad . \tag{2.188}$$

Relations (2.187) - (2.188) together with the conditions

$$\gamma(T) = 0 \quad , \tag{2.189}$$

and

$$x(0) = M[M'\gamma(0) + \theta] \quad , \tag{2.190}$$

determine $x(\cdot)$ and $\gamma(\cdot)$ as the solution of a two-point boundary value problem. Therefore, we have demonstrated that knowledge of θ, $dz(\cdot)$, and $dy(\cdot)$ allow us to reconstruct all the elements in S, finally verifying our basis for Y_c.

At this point, we can equivalently form a basis for Y_c from the quantities $\tilde{\theta}$ and $d\alpha(\cdot)$ defined by

$$\tilde{\theta} = \theta - E[\theta|Z] \quad , \tag{2.191}$$

and

$$d\alpha(\tau) = dz(\tau) - E[dz(\tau)|Z_\tau^+] \quad . \tag{2.192}$$

The process $d\alpha(\cdot)$ corresponds to the innovations of the $dz(\cdot)$'s, and therefore $Z = \boldsymbol{\alpha}$. The random vector $\tilde{\theta}$ corresponds to the part of θ orthogonal to Z. Hence, Y_c has the orthogonal decomposition

$$Y_c = H(\tilde{\theta}) \oplus \boldsymbol{\alpha} \quad . \tag{2.193}$$

Derivation of Forward Model for $\tilde{x}_s(\cdot)$

By employing the decomposition (2.193) and our earlier result (2.32) for estimation from an orthogonal increments process, we may compute $\tilde{x}_s(t) = E[x(t)|Y_c]$ as

$$\tilde{x}_s(t) = E[x(t)\tilde{\theta}']E[\tilde{\theta}\tilde{\theta}']^{-1}\tilde{\theta} + \int_{\tau=0}^{T} - \frac{d}{d\tau} E[x(t)\alpha'(\tau)]d\alpha(\tau) \quad . \tag{2.194}$$

We now employ expressions for $\tilde{\theta}$ and $d\alpha(\cdot)$ to evaluate the expectations that appear in relation (2.194). We define the reverse-time filtered estimate $\hat{\gamma}_r(t)$ as

$$\hat{\gamma}_r(t) = E[\gamma(t)|Z_t^+] \quad , \tag{2.195}$$

and let $\tilde{\gamma}_r(t)$ denote the filtering error associated with $\hat{\gamma}_r(t)$. Hence, by using the definition of $d\alpha(\cdot)$ in relation (2.192), and relation (2.180) defining $dz(\cdot)$, we can express $d\alpha(t)$ as

$$d\alpha(t) = du(t) - B'(t)\tilde{\gamma}_r(t)dt \quad . \tag{2.196}$$

Similarly, by using the definitions of θ in (2.181) and $\tilde{\theta}$ in (2.191), we can express $\tilde{\theta}$ as

$$\tilde{\theta} = \delta - M'\tilde{\gamma}_r(0) \quad . \tag{2.197}$$

The reverse time filtered estimate of $\gamma(t)$, $\hat{\gamma}_r(t)$, is generated by the backward Kalman filtering equations

$$-d\hat{\gamma}_r(t) = \Gamma_b'(t)\hat{\gamma}_r(t)dt - P_b(t)B(t)dz(t) \quad , \tag{2.198}$$

$$\text{with} \qquad \hat{\gamma}_r(T) = 0 \quad , \tag{2.199}$$

$$\text{where} \qquad \Gamma_b(t) = A(t) - B(t)B'(t)P_b(t) \quad , \tag{2.200}$$

and $P_b(\cdot)$ is the filtering error covariance matrix generated by

$$-\dot{P}_b(t) = A'(t)P_b(t) + P_b(t)A(t) + \bar{H}'(t)\bar{H}(t) - P_b(t)B(t)B'(t)P_b(t) \quad , \tag{2.201}$$

$$\text{with} \qquad P_b(T) = 0 \quad . \tag{2.202}$$

Hence, the filtering error, $\tilde{\gamma}_r(\cdot)$, obeys the stochastic differntial equation

$$-d\tilde{\gamma}_r(t) = \Gamma_b(t)\tilde{\gamma}_r(t)dt + P_b(t)B(t)du(t) + \bar{H}'(t)d\bar{v}(t), \tag{2.203}$$

$$\text{with} \qquad \tilde{\gamma}_r(T) = 0 \quad . \tag{2.204}$$

We may now use equation (2.196) and the fact that $x(t)$ and $\tilde{\gamma}_r(\tau)$ may be expressed as

$$x(t) = \Phi_A(t,0)M\delta + \int_{s_1=0}^{t} \Phi_A(t,s_1)B(s_1)du(s_1) \ , \qquad (2.205)$$

and

$$\tilde{\gamma}_r(\tau) = \int_{s_2=\tau}^{T} \Phi'_{\Gamma_b}(s_2,\tau)[P_b(s_2)B(s_2)du(s_2) + \bar{H}'(s_2)d\bar{v}(s_2)] \ , \qquad (2.206)$$

where $\Phi_{\Gamma_b}(\cdot,\cdot)$ denotes the transition matrix associated with $\Gamma_b(\cdot)$, to show that

$$-\frac{d}{d\tau} E[x(t)\alpha'(\tau)] = \begin{cases} 0 & \tau > t \\ \Phi_{\Gamma_b}(t,\tau)B(\tau) & \tau \leq t \end{cases} \ , \qquad (2.207)$$

and

$$E[x(t)\tilde{\theta}'] = \Phi_{\Gamma_b}(t,0)M \ . \qquad (2.208)$$

Hence, by substituing relations (2.207) - (2.208) into (2.194) we can derive the following forward stochastic differential equation for $\tilde{x}_s(\cdot)$:

Weinert and Desai's Forward Model for $\tilde{x}_s(\cdot)$

$$d\tilde{x}_s(t) = \Gamma_b(t)\tilde{x}_s(t)dt + B(t)d\alpha(t) \quad , \qquad (2.209)$$

where $$\tilde{x}_s(0) = M(I + M'P_b(0)M)^{-1}\tilde{\theta} \quad , \qquad (2.210)$$

and hence $$E[\tilde{x}_s(0)\tilde{x}_s'(0)] = M(I + M'P_b(0)M)^{-1}M' \quad . \qquad (2.211)$$

Since $\pi(0) = MM'$, relation (2.211) may also be expressed as

$$E[\tilde{x}_s(0)\tilde{x}_s'(0)] = \pi(0)(I + P_b(0)\pi(0))^{-1} \quad . \qquad (2.212)$$

Derivation of Smoothing Equations of Weinert and Desai

We may finally employ the unconditional $x(\cdot)$ dynamics and the $\tilde{x}_s(\cdot)$ dynamics expressed by relation (2.209) to derive stochastic differential equations for generating $\hat{x}_s(\cdot)$. By forming $d\hat{x}_s(\cdot)$ from relation (2.156) as

$$d\hat{x}_s(t) = dx(t) - d\tilde{x}_s(t) \quad , \qquad (2.213)$$

we will show that we obtain the following pair of equations:

Weinert and Desai's Smoothing Algorithm

$$d\hat{x}_s(t) = \Gamma_b(t)\hat{x}_s(t)dt + B(t)B'(t)\rho(t)dt \quad , \qquad (2.214)$$

$$-d\rho(t) = -\Gamma_b'(t)\rho(t)dt + \bar{H}'(t)dy(t) \quad , \tag{2.215}$$

with $$\hat{x}_s(0) = \pi(0)(I + P_b(0)\pi(0))^{-1}\rho(0) \quad , \tag{2.216}$$

and $$\rho(T) = 0 \quad . \tag{2.217}$$

We obtain (2.214) by using (2.213), replacing $\tilde{x}_s(t)$ by $x(t)-\hat{x}_s(t)$, expressing $d\alpha(t)$ by (2.196), and identifying $\rho(t)$ as

$$\rho(t) = \tilde{\gamma}_r(t) + P_b(t)x(t) \quad . \tag{2.218}$$

By employing the $x(\cdot)$ and $\tilde{\gamma}_r(\cdot)$ dynamics we can verify relations (2.215) and (2.217) for the evolution of $\rho(\cdot)$. Finally, by forming $\hat{x}_s(0)$ as $x(0)-\tilde{x}_s(0)$, using $M\mathcal{S}$ to represent $x(0)$ and relation (2.210) for $\tilde{x}_s(0)$, we can check (2.216).

To conclude our discussion of Weinert and Desai's approach to smoothing, we note that the algorithm involves a reverse sweep over the data to generate $\rho(\cdot)$, and then a forward sweep to compute $\hat{x}_s(\cdot)$, through (2.214). In Appendix 2G we derive the smoothing equations (2.214) - (2.217) by employing the scattering formalism, and in the process interpret the input noise $d\alpha(t)$, connected with the forward smoothing error

realization (2.209), in terms of familiar quantities such as the original process noise, filtering errors, and smoothing errors.

2.7 Conclusion

The approaches to the fixed-interval smoothing problem in this chapter emerge from either different techniques for splitting up the observation space Y, or from different procedures for realizing the projection $E[x(t)|Y]$ as the solution to a set of stochastic differential equations. In Section 2.3, from a decomposition of Y given by (2.44), the solution to the smoothing problem was derived as the filtered estimate plus some correction term that corresponds to an estimate for the filtering error given the future innovations. In Section 2.5, by employing the framework of stochastic realization theory, we gave a unified presentation of the Mayne-Fraser and Wall two-filter forms of the smoothed estimate, which follow from splitting up Y as in relation (2.134). In Sections 2.4 and 2.6 we presented three different approaches for computing the smoothed estimate as the solution to a set of stochastic differential equations. In Section 2.4, the Rauch-Tung-Striebel and Hamiltonian equations for smoothing were derived from projecting the dynamics of the state $x(\cdot)$ onto Y, and employing two different techniques for forming $E[du(t)|Y]$. In Section 2.6, in the approach of Weinert and Desai, an algorithm for computing the smoothed estimate was obtained by subtracting the forward smoothing error dynamics from the original state

dynamics. In Appendix 2G we employed the scattering formalism to connect the Hamiltonian equations with those of Weinert and Desai.

Appendix 2A

Approaches to the Discrete-Time Fixed Interval Smoothing Problem

In this Appendix we consider, in a discrete-time setting, some of the same algorithms for solving the fixed interval smoothing problem that we presented in Chapter 2. In Section 2A.1 we describe the innovations solution to the discrete-time smoothing problem. Then in Section 2A.2 we present the discrete-time Hamiltonian equations and a discrete analog of the Rauch-Tung-Striebel smoothing formula. Finally, in Section 2A.3, we briefly sketch the stochastic realization perspective on two-filter solutions developed by Badawi in [84], in order to motivate analogs of the Mayne-Fraser and Wall smoothing formulae. We do not present the discrete counterpart of Weinert and Desai's approach to smoothing, since we introduce it in Appendix 3B, in order to obtain a forward Markovian realization of the smoothing error process.

2A.1 The Innovations Approach to the Discrete-Time Fixed Interval Smoothing Problem

The discrete-time innovations solution to the smoothing problem is based on a decomposition of Y similar to that discussed in Section 2.3. If we let Y_t^- and Y_t^+ be defined as

$$Y_t^- = H(y(i) \quad i = 1,\ldots,t-1) \quad , \tag{A.1}$$

and

$$Y_t^+ = H(y(i) \quad i = t,\ldots,T) \quad , \tag{A.2}$$

we can decompose Y in the following way:

$$Y = Y_t^- \oplus \boldsymbol{\nu}_t^+ \quad , \tag{A.3}$$

where

$$\nu(i) \triangleq y(i) - E[y(i)|Y_i^-] \quad . \tag{A.4}$$

We now define two types of estimates of x(i): a filtered estimate $\hat{x}_f(i)$ determined as

$$\hat{x}_f(i) = E[x(i)|Y_{i+1}^-] \quad , \tag{A.5}$$

and the one step ahead predicted estimate $\hat{x}_{fp}(i)$ given as

$$\hat{x}_{fp}(i) = E[x(i)|Y_i^-] \quad . \tag{A.6}$$

We let $\tilde{x}_f(i)$ and $\tilde{x}_{fp}(i)$ denote the filtering and one-step prediction errors, respectively, and $P_f(i)$, $P_{fp}(i)$ denote the corresponding covariance matrices. Then the innovations $\nu(i)$, defined by relation (A.4), may be expressed as

$$\nu(i) = H(i)\tilde{x}_{fp}(i) + D(i)v(i) \quad . \tag{A.7}$$

Now by employing the decompositions of Y determined by setting t=i and t=i+1 in (A.3), and by noting that $\nu(i)$ is a discrete white noise sequence with covariance $P_\nu(i)$ given by

$$P_\nu(i) = H(i)P_{fp}(i)H'(i) + R(i) \quad , \tag{A.8}$$

we obtain the following two forms of the smoothed estimate:

$$\hat{x}_s(i) = \hat{x}_{fp}(i) + \sum_{j=i}^{T} E[x(i)\nu'(j)]P_\nu^{-1}(j)\nu(j) \quad , \tag{A.9}$$

and $$\hat{x}_s(i) = \hat{x}_f(i) + \sum_{j=i+1}^{T} E[x(i)\nu'(j)]P_\nu^{-1}(j)\nu(j) \quad , \tag{A.10}$$

which may be rewritten by using relation (A.7) for $\nu(i)$ and the orthogonality property satisfied by $\hat{x}_{fp}(\cdot)$ as

$$\hat{x}_s(i) = \hat{x}_{fp}(i) + \sum_{j=i}^{T} E[\tilde{x}_{fp}(i)\tilde{x}'_{fp}(j)]H'(j)P_\nu^{-1}(j)\nu(j) \quad , \tag{A.11}$$

and

$$\hat{x}_s(i) = \hat{x}_f(i) + \sum_{j=i+1}^{T} E[\tilde{x}_{fp}(i)\tilde{x}'_{fp}(j)]H'(j)P_\nu^{-1}(j)\nu(j) \quad . \qquad (A.12)$$

The second term in equations (A.11) - (A.12) represent $E\left[x(i)\,|\,\boldsymbol{\mathcal{V}}_i^+\right]$ and $E\left[x(i)\,|\,\boldsymbol{\mathcal{V}}_{i+1}^+\right]$, respectively. Since the one-step predicted estimates are generated by

$$\hat{x}_{fp}(i+1) = A(i)(I - P_f(i)H'(i)R^{-1}(i)H(i))\hat{x}_{fp}(i) + A(i)P_f(i)H'(i)R^{-1}(i)y(i), \qquad (A.13)$$

the one-step prediction error dynamics are given by

$$\tilde{x}_{fp}(i+1) = A(i)(I - P_f(i)H'(i)R^{-1}(i)H(i))\tilde{x}_{fp}(i) + B(i)u(i) - A(i)P_f(i)H'(i)R^{-1}(i)(D(i)v(i)) \quad . \qquad (A.14)$$

Then if we define the discrete-time transition matrix Γ_{ij} by

$$\Gamma_{ij} \triangleq \begin{cases} I & i = j \\ \prod_{\ell=i}^{j-1} A(\ell)(I - P_f(\ell)H'(\ell)R^{-1}(\ell)H(\ell)) & j > i \end{cases} , \qquad (A.15)$$

we can compute $E[\tilde{x}_{fp}(i)\tilde{x}'_{fp}(j)]$ as

$$E[\tilde{x}_{fp}(i)\tilde{x}'_{fp}(j)] = P_{fp}(i)\Gamma'_{ij} \quad . \tag{A.16}$$

This identity can be combined with relations (A.11) and (A.12) so that we obtain the following two expressions for $\hat{x}_s(i)$:

Innovations Smoothing Formulae

$$\hat{x}_s(i) = \hat{x}_{fp}(i) + P_{fp}(i)\left\{\sum_{j=i}^{T} \Gamma'_{ij}H'(j)P_\nu^{-1}(j)\nu(j)\right\} , \tag{A.17}$$

$$\text{and} \quad \hat{x}_s(i) = \hat{x}_f(i) + P_{fp}(i)\left\{\sum_{j=i+1}^{T} \Gamma'_{ij}H'(j)P_\nu^{-1}(j)\nu(j)\right\}. \tag{A.18}$$

These equations constitute the innovations solution of the discrete-time smoothing problem [23].

2A.2 The Discrete-Time Hamiltonian and Rauch-Tung-Striebel Smoothing Equations

We next derive the Hamiltonian and Rauch-Tung-Striebel smoothing formulae by conditioning with respect to Y the equation for the evolution of $x(\cdot)$, to obtain

$$\hat{x}_s(i+1) = A(i)\hat{x}_s(i) + B(i)\, E[u(i)|Y] \quad , \tag{A.19}$$

and implementing the computation of $E[u(i)|Y]$ by two different methods. Employing the decomposition

$$Y = Y_{i+1}^{-} \oplus \boldsymbol{\nu}_{i+1}^{+} \quad , \tag{A.20}$$

and noting that $u(i)$ is orthogonal to Y_{i+1}^{-}, we find that

$$E[u(i)|Y] = E\left[u(i)|\boldsymbol{\nu}_{i+1}^{+}\right] \quad . \tag{A.21}$$

Also, since the $\nu(i)$'s are white, with covariance $P_\nu(i)$, and may be expressed by (A.7), the projection (A.21) can be computed as

$$E\left[u(i)|\boldsymbol{\nu}_{i+1}^{+}\right] = \sum_{j=i+1}^{T} E[u(i)\tilde{x}'_{fp}(j)]H'(j)P_\nu^{-1}(j)\nu(j). \tag{A.22}$$

Now, if we use the one-step ahead prediction error dynamics of relation (A.14), equation (A.22) becomes

$$E\left[u(i)\,|\,\boldsymbol{\nu}_{i+1}^{+}\right] = B'(i)\left[\sum_{j=i+1}^{T} \Gamma'_{i+1,j} H'(j) P_{\nu}^{-1}(j)\nu(j)\right], \quad \text{(A.23)}$$

where Γ_{ij} is defined by (A.15). Therefore, if we define $\lambda(i+1|T)$ by

$$\lambda(i+1|T) \triangleq \sum_{j=i+1}^{T} \Gamma'_{i+1,j} H'(j) P_{\nu}^{-1}(j)\nu(j), \quad \text{(A.24)}$$

then (A.23) may be expressed as

$$E\left[u(i)\,|\,\boldsymbol{\nu}_{i+1}^{+}\right] = B'(i)\lambda(i+1|T) \quad . \quad \text{(A.25)}$$

We now show that the Hamiltonian and Rauch-Tung-Striebel smoothing equations follow from two different approaches for computing $\lambda(\cdot|T)$, and the substitution of (A.25) into equation (A.19). We note first that the expression (A.24) implies that the $\lambda(j|T)$'s satisfy the following backward equation:

$$\lambda(i|T) = H'(i)P_{\nu}^{-1}(i)\nu(i) + [A(i)(I - P_f(i)H'(i)R^{-1}(i)H(i))]' \cdot \lambda(i+1|T) \ , \quad \text{(A.26)}$$

where $\lambda(T+1|T) = 0$. (A.27)

Using the definition of $\nu(i)$ as

$$\nu(i) = y(i) - H(i)\hat{x}_{fp}(i) \quad , \tag{A.28}$$

and the following relation for $\hat{x}_{fp}(i)$:

$$\hat{x}_{fp}(i) = \hat{x}_s(i) - P_{fp}(i)\lambda(i|T) \quad , \tag{A.29}$$

which follows from the innovations form of the smoothed estimate (A.17), we obtain from relation (A.26) a new backward equation for the $\lambda(\cdot|T)$'s which together with (A.19) and (A.25), determine the following Hamiltonian equations [31] for smoothing:

Hamiltonian Equations for Smoothing

$$\lambda(i|T) = H'(i)R^{-1}(i)y(i) - H'(i)R^{-1}(i)H(i)\hat{x}_s(i) + A'(i)\lambda(i+1|T), \tag{A.30}$$

$$\hat{x}_s(i+1) = A(i)\hat{x}_s(i) + B(i)B'(i)\lambda(i+1|T) \quad , \tag{A.31}$$

where $\lambda(T+1|T) = 0$, (A.32)

and $\hat{x}_s(0) = P_{fp}(0)\lambda(0|T)$. (A.33)

Finally, by assuming the invertibility of the matrices A(i), we can derive a Rauch-Tung-Striebel type algorithm for computing the $\hat{x}_s(\cdot)$'s. Solving for $\hat{x}_s(i)$ in relation (A.31) we obtain

$$\hat{x}_s(i) = A^{-1}(i)\ (\hat{x}_s(i+1) - B(i)B'(i)\lambda(i+1|T)) \quad . \tag{A.34}$$

Now, using an expression for $\lambda(i+1|T)$ derived from relation (A.29), and expressing $\hat{x}_{fp}(i+1)$ in terms of $\hat{x}_f(i)$, equation (A.34) yields the following Rauch-Tung-Striebel smoothing algorithm [10]:

Rauch-Tung-Striebel Smoothing Algorithm

$$\begin{aligned}\hat{x}_s(i) &= A^{-1}(i)(I - B(i)B'(i)P_{fp}^{-1}(i+1))\hat{x}_s(i+1) \\ &\quad + A^{-1}(i)B(i)B'(i)P_{fp}^{-1}(i+1)A(i)\hat{x}_f(i) \quad ,\end{aligned} \tag{A.35}$$

with initial condition

$$\hat{x}_s(T) = \hat{x}_f(T) \quad . \tag{A.36}$$

2A.3 The Stochastic Realization Theory View of Two-Filter Solutions for the Discrete Fixed Interval Smoothing Problem

As in the case of solutions to the continuous time smoothing problem, both the discrete innovations smoothing formulae and discrete two-filter smoothing formulae follow from different ways of splitting the observations space, Y. In this section we outline the stochastic realization theory perspective on two-filter solutions of the discrete, fixed interval smoothing problem. We again define proper stochastic realizations of the observations process $y(\cdot)$ as being determined by a set of matrices $F(\cdot)$, $C(\cdot)$, $J(\cdot)$, and $E(\cdot)$ and a standard $p \geq m$ dimensional discrete white noise process $w(\cdot)$, such that

$$y(t) = C(t)x(t) + E(t)w(t) \quad , \tag{A.37}$$

with

$$x(t+1) = F(t)x(t) + J(t)w(t) \quad . \tag{A.38}$$

The relations (A.37) - (A.38) represent a forward Markovian realization of $y(\cdot)$ when $H(w(\tau))$ is orthogonal to $H(x(0))$. For a backward Markovian realization, (A.38) would be replaced by

$$x(t-1) = F(t)x(t) + J(t)w(t) \quad , \tag{A.39}$$

and we would require $H(w(\tau))$ to be orthogonal to $H(x(T))$. We classify realizations as being internal or external according to whether the space X generated by the state process satisfies either

$$X \varepsilon Y \quad , \tag{A.40}$$

or $$X \not\varepsilon Y \quad , \tag{A.41}$$

respectively.

Two-filter solutions to discrete fixed interval smoothing problems again follow from the frame space decomposition

$$Y = [Y_t^{+|-} \vee Y_t^{-|+}] \oplus N_t^+ \oplus N_t^- \quad , \tag{A.42}$$

where $$N_t^+ = Y_t^+ \ominus Y_t^{-|+} \quad , \tag{A.43}$$

and $$N_t^- = Y_t^- \ominus Y_t^{+|-} \quad . \tag{A.44}$$

Let us supposed that $\hat{x}_1(\cdot)$ and $\hat{x}_2(\cdot)$ correspond to some forward and reverse filtered estimates of x(t) and may be identified as minimal order state processes associated with some internal, proper forward and reverse Markovian realizations of the $y(\cdot)$ process, respectively. Then we argue that

$$H(\hat{x}_1(t)) \varepsilon Y_t^{+|-} \quad , \tag{A.45}$$

and $$H(\hat{x}_2(t)) \varepsilon Y_t^{-|+} \quad , \tag{A.46}$$

since $Y_t^{+|-}$ and $Y_t^{-|+}$ are splitting subspaces (see definitions (2.129) - (2.130)) that contain all the state processes associated with minimal order, internal, forward and reverse Markovian realizations of $y(\cdot)$ [79], respectively. Hence, if we can show that

$$Y_t^{+|-} \varepsilon H(\hat{x}_1(t)) \ , \tag{A.47}$$

and $$Y_t^{-|+} \varepsilon H(\hat{x}_2(t)) \ , \tag{A.48}$$

(A.42) reduces to a decomposition of the form

$$Y = H(\hat{x}_1(t),\hat{x}_2(t)) \oplus N_t^+ \oplus N_t^- \quad , \tag{A.49}$$

where $$N_t^+ = Y_t^+ \ominus H(\hat{x}_2(t)) \quad , \tag{A.50}$$

and $$N_t^- = Y_t^- \ominus H(\hat{x}_1(t)) \quad . \tag{A.51}$$

We then need only verify, using orthogonality properties of the errors in $\hat{x}_1(\cdot)$ and $\hat{x}_2(\cdot)$, that $H(x(t))$ is orthogonal to N_t^+ and

N_t^-, in order to motivate the computation of $\hat{x}_s(t)$ as a linear combination of $\hat{x}_1(t)$ and $\hat{x}_2(t)$.

We proceed to identify several choices for $\hat{x}_1(\cdot)$ and $\hat{x}_2(\cdot)$, determining decompositions of Y of the form in (A.49). First we display discrete analogs of the continuous time processes $x_*(t)$ and $x^*(t)$, and motivate a discrete Mayne-Fraser type solution to the smoothing problem [84]. We then conclude this section by identifying two Wall two-filter solutions to the smoothing problem.

We define $x_*(t)$ as the one step ahead predicted estimate of x(t), determined from our original realization of relations (2.11) - (2.14), as

$$x_*(t) = E[x(t)|Y_t^-] \quad . \tag{A.52}$$

As in continuous time, we let $\mathcal{D}$ denote the family of proper forward realizations of $y(\cdot)$ that generate the same one-step predicted estimates, $x_*(\cdot)$, and note that the typical realization in $\mathcal{D}$ assumes the form:

$$y(t) = H(t)x(t) + E(t)w(t) \quad , \tag{A.53}$$

with

$$x(t+1) = A(t)x(t) + J(t)w(t) \quad . \tag{A.54}$$

We let $\pi(t)$ denote the covariance matrix associated with $x(t)$. Unlike in continuous time,

$$\bar{R}(t) \triangleq E(t)E'(t) \quad , \tag{A.55}$$

is not invariant over $\mathcal{B}$, and is not equal to our original measurement noise covariance, $R(t)$. As an example of this fact, consider the internal realization in $\mathcal{B}$ with state vector $x_*(t)$. For this realization, $E_*(t)$ will correspond to the square root of the discrete-time innovations covariance matrix at time t.

We next define a correspondence between forward realizations in $\mathcal{B}$ and a family of backward realizations, that will allow us to express $x^*(t)$ as the state process associated with the forward counterpart of a particular internal, backward realization. The backwards counterpart of a realization in $\mathcal{B}$ specified by relations (A.53) - (A.54) is determined by constructing a backwards Markovian realization with associated state process

$$\bar{x}(t) = \pi^{-1}(t+1)x(t+1) \quad , \tag{A.56}$$

when $\pi(\cdot)$ is invertible, or more generally

$$\bar{x}(t) = \pi^{\#}(t+1)x(t+1) \quad , \tag{A.57}$$

where # denotes the Moore-Penrose pseudo-inverse. Badawi [84] presents the details of constructing backward realizations when either (A.56) or more generally (A.57), holds. Now, assuming that our original realization for $x(\cdot)$ has an associated state covariance $\pi(\cdot) > 0$, we can define a backwards counterpart with an associated state vector $\bar{x}(t)$ specified in (A.56), and hence we can determine the backward filtered estimate

$$\bar{x}_*(t) = E[\bar{x}(t) | Y_{t+1}^{+}] \quad . \tag{A.58}$$

The estimate $\bar{x}_*(\cdot)$ will then be the state process, with state covariance $\bar{\pi}_*(\cdot)$, associated with a backward, internal realization. At this point, we can define $x^*(t)$ as the state process associated with the forward counterpart of the backward filter realization, so that

$$x^*(t) = \bar{\pi}_*^{\#}(t-1)\bar{x}_*(t-1) \quad . \tag{A.59}$$

Employing the definitions of $x_*(t)$ and $x^*(t)$, we can verify that

$$Y_t^{+|-} \in H(x_*(t)) \quad , \tag{A.60}$$

and $$Y_t^{-|+} \in H(x^*(t)) \quad , \tag{A.61}$$

motivating an orthogonal decomposition for Y of the form (A.49), and ultimately determining a discrete analog of the Mayne-Fraser two-filter solution to the smoothing problem. The details of this approach are contained in Badawi's thesis [84].

We finally present two forms of Wall's [38] solution to the discrete-time smoothing problem. Let us define the following forward and reverse filtered estimates, $\hat{x}_f(t)$, $\hat{x}_r(t)$, and $\hat{x}_{rp}(t)$, by

$$\hat{x}_f(t) = E[x(t)|Y_{t+1}^-] \quad , \tag{A.62}$$

$$\hat{x}_r(t) = E[x(t)|Y_t^+] \quad , \tag{A.63}$$

and $$\hat{x}_{rp}(t) = E[x(t)|Y_{t+1}^+] \quad . \tag{A.64}$$

Then, we can verify that since

$$Y_t^{+|-} \in H(x_*(t)) \quad , \tag{A.65}$$

$$Y_t^{-|+} \in H(\hat{x}_r(t)) \quad , \tag{A.66}$$

and $$Y_{t+1}^{+|-} \in H(\hat{x}_f(t)) \quad , \tag{A.67}$$

$$Y_{t+1}^{-|+} \in H(\hat{x}_{rp}(t)) \quad , \tag{A.68}$$

we can make orthogonal decompositions of Y of the form in (A.49). Hence, the preceding argument motivates the following two-filter solutions to the discrete-time smoothing problem that appear in [38]:

$$\hat{x}_s(t) = P_s(t)\left\{P_*^{-1}(t)x_*(t) + P_r^{-1}(t)\hat{x}_r(t)\right\} \quad , \tag{A.69}$$

where $$P_s^{-1}(t) = P_*^{-1}(t) + P_r^{-1}(t) - \pi^{-1}(t) \quad , \tag{A.70}$$

and $$\hat{x}_s(t) = P_s(t)\left\{P_f^{-1}(t)\hat{x}_f(t) + P_{rp}^{-1}(t)\hat{x}_{rp}(t)\right\} \quad , \tag{A.71}$$

where $$P_s^{-1}(t) = P_f^{-1}(t) + P_{rp}^{-1}(t) - \pi^{-1}(t) \quad , \tag{A.72}$$

and $P_*(\cdot)$, $P_r(\cdot)$, $P_{rp}(\cdot)$, $P_f(\cdot)$ denote the filtering error covariance matrices associated with the estimates $x_*(\cdot)$, $\hat{x}_r(\cdot)$ $\hat{x}_{rp}(\cdot)$, and $\hat{x}_f(\cdot)$, respectively.

Appendix 2B

Proof that $E\left[x(t)\,|\,\boldsymbol{\nu}_t^+\right] = P_f(t)\lambda(t|T)$

By employing relation (2.32), and the fact that $R^{-\frac{1}{2}}(s)d\nu(s)$ determines a standard Wiener process, we can form the projection of $x(t)$ onto the future innovations $\boldsymbol{\nu}_t^+$ as

$$E\left[x(t)\,|\,\boldsymbol{\nu}_t^+\right] = \int_{\tau=t}^{T} \frac{d}{d\tau} E[x(t)\nu'(\tau)]R^{-1}(\tau)d\nu(\tau). \qquad (B.1)$$

Since $d\nu(\tau)$ may be expressed as

$$d\nu(\tau) = H(\tau)\tilde{x}_f(\tau)d\tau + D(\tau)dv(\tau)\ , \qquad (B.2)$$

where $$\tilde{x}_f(\tau) = x(\tau) - \hat{x}_f(\tau)\ , \qquad (B.3)$$

and since $\nu(\tau)$ is orthogonal to $\hat{x}_f(t)$ for $\tau > t$, the relation (B.1) becomes

$$E\left[x(t)\,|\,\boldsymbol{\nu}_t^+\right] = \int_{\tau=t}^{T} E[\tilde{x}_f(t)\tilde{x}_f'(\tau)]H'(\tau)R^{-1}(\tau)d\nu(\tau)\ . \qquad (B.4)$$

Noting that the standard Kalman filtering equations for $\hat{x}_f(\cdot)$ are specified by

$$d\hat{x}_f(t) = \left(A(t) - P_f(t)H'(t)R^{-1}(t)H(t)\right)\hat{x}_f(t)dt$$
$$+ P_f(t)H'(t)R^{-1}(t)dy(t) \quad , \tag{B.5}$$

where the filtering error covariance matrix $P_f(\cdot)$ satisfies

$$\dot{P}_f(t) = A(t)P_f(t) + P_f(t)A'(t) + B(t)B'(t)$$
$$- P_f(t)H'(t)R^{-1}(t)H(t)P_f(t) \quad , \tag{B.6}$$

with $$P_f(0) = \pi(0) \quad , \tag{B.7}$$

the dynamics of $\tilde{x}_f(t)$ are given by

$$d\tilde{x}_f(t) = \left(A(t) - P_f(t)H'(t)R^{-1}(t)H(t)\right)\tilde{x}_f(t)dt + B(t)du(t)$$
$$- P_f(t)H'(t)R^{-1}(t)D(t)dv(t) \quad . \tag{B.8}$$

Hence, if we denote

$$\Gamma(t) \triangleq A(t) - P_f(t)H'(t)R^{-1}(t)H(t) \quad , \tag{B.9}$$

and if $\Phi_\Gamma(t,\tau)$ is the corresponding transition matrix, we can express $E[\tilde{x}_f(t)\tilde{x}_f'(\tau)]$ for $\tau \geq t$ as

$$E[\tilde{x}_f(t)\tilde{x}_f'(\tau)] = P_f(t)\underline{\Phi}_T'(\tau,t) \quad . \tag{B.10}$$

Finally, if we define $\lambda(t|T)$ as

$$\lambda(t|T) \triangleq \int_{\tau=t}^{T} \underline{\Phi}_T'(\tau,t)H'(\tau)R^{-1}(\tau)d\nu(\tau) \quad , \tag{B.11}$$

by substituting (B.11) and (B.10) into (B.4), we obtain the relation

$$E\left[\underline{x}(t)\,|\,\boldsymbol{\nu}_t^+\right] = P_f(t)\lambda(t|T) \quad . \tag{B.12}$$

Appendix 2C

The Scattering Formalism for Picturing the Hamiltonian Equations

We now sketch the scattering theory framework for representing the Hamiltonian equations for smoothing [29] - [31]. Scattering theory is concerned with the analysis of waves propagating forward and backward through a medium, from the knowledge of the transmission and reflection properties of that medium. Let $u_+(s)$ and $u_-(s)$ denote a forward and reverse wave at location s, $u_+(t)$ and $u_-(t)$ denote the corresponding quantities at location t, where $t > s$, then the effect of the intervening medium may be modelled by the following matrix equation:

$$\begin{pmatrix} u_+(t) \\ u_-(t) \end{pmatrix} = \begin{pmatrix} a_0(s,t) & \rho_0(s,t) \\ r_0(s,t) & \alpha_0(s,t) \end{pmatrix} \begin{pmatrix} u_+(s) \\ u_-(t) \end{pmatrix} + \begin{pmatrix} q^+(s,t) \\ q^-(s,t) \end{pmatrix}, \qquad (C.1)$$

where $a_0(s,t)$ and $\alpha_0(s,t)$ are the forward and reverse transmission coefficients, $\rho_0(s,t)$ and $r_0(s,t)$ are the right and left-hand reflection coefficients, and $q^+(s,t)$ and $q^-(s,t)$ denote the internal source contributions. The matrix of reflection and transmission coefficients is termed the

scattering matrix, $S(s,t)$. The relation (C.1) may be represented by the signal flow diagram of Fig. C.1.

We can now conceive of cascading two sections of medium from τ_1 to s and s to τ_2, as pictured in Fig. C.2. By employing matrix equations of the same form as relation (C.1) for each medium, or the use of flow graph composition rules [34], we can arrive at scattering parameters for the aggregate medium from τ_1 to τ_2. If $S(\tau_1,s)$ and $S(s,\tau_2)$ denote the scattering matrices associated with the first and second media, respectively, then we define the aggregate scattering matrix $S(\tau_1,\tau_2)$ by

$$S(\tau_1,\tau_2) = S(\tau_1,s) * S(s,\tau_2) ,$$

where * denotes the Redheffer star product defined by

$$S(\tau_1,\tau_2) \triangleq \begin{pmatrix} a_2[I - \rho_1 r_2]^{-1} \alpha_1 & \rho_2 + a_2\rho_1[I - r_2\rho_1]^{-1} \alpha_2 \\ r_1 + \alpha_1 r_2[I - \rho_1 r_2]^{-1} a_1 & \alpha_1[I - r_2\rho_1]^{-1} \alpha_2 \end{pmatrix} . \tag{C.2}$$

Similarly, we find an aggregate internal source vector defined by

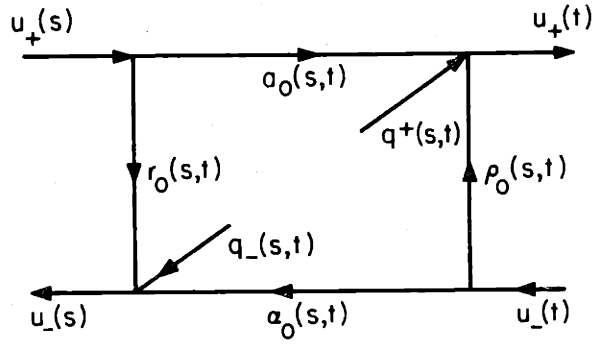

Fig. C.1 Signal Flow Diagram Associated with Relation C.1

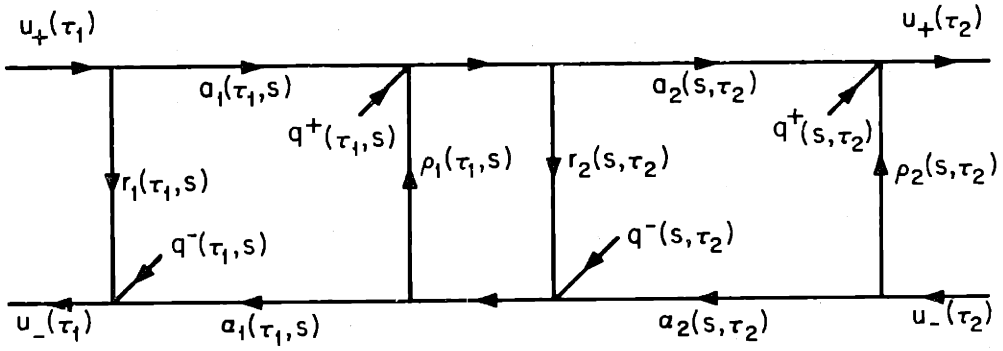

Fig. C.2 Signal Flow Diagram for the Cascade of Two Media

$$\begin{pmatrix} q^{+}(\tau_1,\tau_2) \\ \hline q^{-}(\tau_1,\tau_2) \end{pmatrix} \triangleq \begin{pmatrix} q^{+}(s,\tau_2) + a_2[I-\rho_1 r_2]^{-1}[q^{+}(\tau_1,s) + \rho_1 q^{-}(s,\tau_2)] \\ q^{-}(\tau_1,s) + \alpha_1[I-r_2\rho_1]^{-1}[q^{-}(s,\tau_2) + r_2 q^{+}(\tau_1,s)] \end{pmatrix} . \tag{C.3}$$

Having determined the effect of cascading two media of the form given in Fig. C.1, the scattering diagram associated with the discrete time fixed-interval smoothing problem is presented in Fig. C.3, where we note that $\hat{x}_{fp}(T+1)$ denotes the one-step ahead predicted estimate at time T+1. The smoothed estimates, $\hat{x}_s(\cdot)$, and adjoint variables, $\lambda(\cdot|T)$, defined in Appendix 2A, are identified with forward and reverse waves in the scattering formalism. We can construct an analogous diagram in continuous time by discretizing the Hamiltonian system of Section 2.4 and replacing the discrete time scattering sections, with incremental sections of the form given in Fig. C.4. By breaking the scattering diagram at some intermediate time, $t \in [0,T]$, and by using the formulae (C.2) and (C.3) to compute the equivalent scattering parameters for the aggregated sections [0,t] and [t,T], we can derive numerous forms of the solution to the smoothing problem [31]. We refer the interested reader to [29] - [31] for a derivation of the aggregate scattering parameters and internal source contributions, associated with the intervals [0,t] and [t,T], respectively.

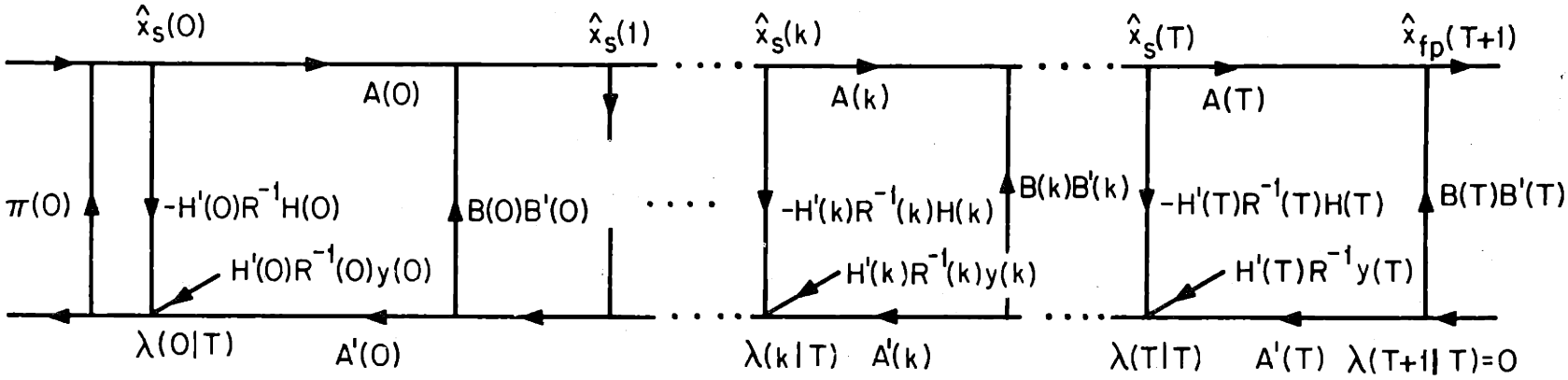

Fig. C.3 Scattering Diagram for Discrete-Time Fixed Interval Smoothing

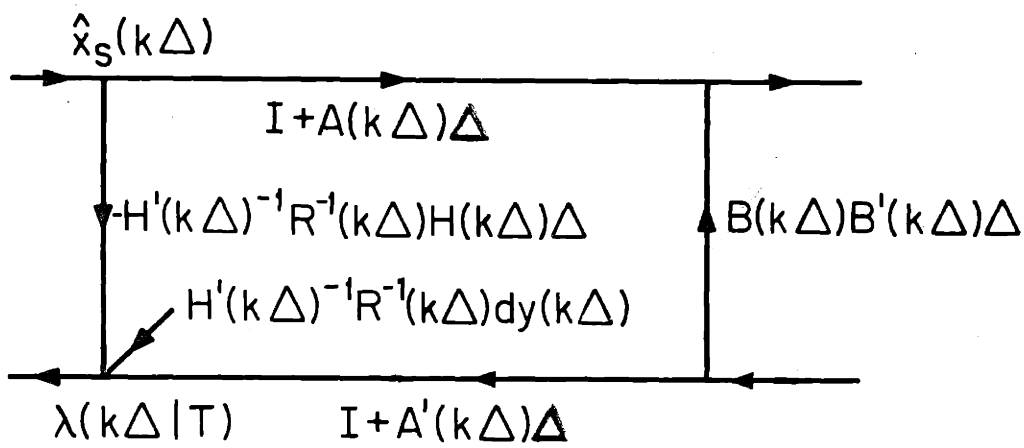

Fig. C.4 Incremental Sections for the Continuous Time Scattering Diagram

Appendix 2D

Proof of the Frame Space Decomposition of Y

In this Appendix we prove the following orthogonal decomposition of Y [80]:

$$Y = Y_t^{\square} \oplus N_t^{+} \oplus N_t^{-} \quad , \tag{D.1}$$

where $$Y_t^{\square} \triangleq Y_t^{-|+} \vee Y_t^{+|-} \quad , \tag{D.2}$$

is termed the frame space,

$$N_t^{+} \triangleq Y_t^{+} \ominus Y_t^{-|+} \quad , \tag{D.3}$$

and $$N_t^{-} \triangleq Y_t^{-} \ominus Y_t^{+|-} \quad . \tag{D.4}$$

From the fact that $Y \in Y_t^{-} \vee Y_t^{+}$, in order to prove (D.1) we need only verify the mutual orthogonality of $Y_t^{\square}$, N_t^{+}, and N_t^{-}. This mutual orthogonality follows from the fact, to be verified in what follows, that we can represent N_t^{+} and N_t^{-} as

$$N_t^{+} = Y_t^{+} \cap \left(Y_t^{-}\right)^{\perp} \quad , \tag{D.5}$$

and $$N_t^- = Y_t^- \cap \left(Y_t^+\right)^{\perp} \quad . \tag{D.6}$$

We can show $N_t^+ \perp N_t^-$ because from (D.5), $N_t^+ \varepsilon Y_t^+$, and from (D.6) $N_t^- \varepsilon \left(Y_t^+\right)^{\perp}$. In addition, by construction from relation (D.3) $N_t^+ \perp Y_t^{-|+}$. But since from (D.5), $N_t^+ \varepsilon \left(Y_t^-\right)^{\perp}$ and $Y_t^{+|-} \varepsilon Y_t^-$, we also have $N_t^+ \perp Y_t^{+|-}$. Similarly, we can argue that $N_t^- \perp Y_t^{+|-}$ and $N_t^- \perp Y_t^{-|+}$. Hence, since $Y_t^{\square}$ is defined by (D.3), we have established the mutual orthogonality of all three spaces in (D.1).

We now verify relation (D.5) by showing that both $N_t^+ \varepsilon Y_t^+ \cap \left(Y_t^-\right)^{\perp}$ and $Y_t^+ \cap \left(Y_t^-\right)^{\perp} \varepsilon N_t^+$. The proof of relation (D.6) proceeds in an analogous manner, and hence is not included. Suppose that v is a random variable in N_t^+. By relation (D.3) defining N_t^+, we know that $v \epsilon Y_t^+$. We next express $E[v\,z]$ for $z \epsilon Y_t^-$ as an iterated expectation of the form

$$E[v\,z] = E\left[E[v\,z\,|Y_t^+]\right] \quad . \tag{D.7}$$

Now, using the fact that $v \epsilon Y_t^+$, relation (D.7) becomes

$$E[v\,z] = E\left[v\,E[z|Y_t^+]\right] \quad . \tag{D.8}$$

But $E[z|Y_t^+] \epsilon Y_t^{-|+}$, and since by construction we have $v \epsilon N_t^+ \perp Y_t^{-|+}$, we must have $E[v\,z] = 0$, so that $v \epsilon \left(Y_t^-\right)^{\perp}$. This

completes the proof that $N_t^+ \in Y_t^+ \cap \left(Y_t^-\right)^\perp$. Now we suppose that v is a random variable in $Y_t^+ \cap \left(Y_t^-\right)^\perp$. Hence, $v \in Y_t^+$ and $v \in \left(Y_t^-\right)^\perp$. We must show that $E[v\,\eta] = 0$ for all η in $Y_t^{+|-}$, and hence that $v \in \left(Y_t^{-|+}\right)^\perp$, and thus by definition $v \in N_t^+$. This follows from the fact that any $\eta \in Y_t^{-|+}$ can be approximated arbitrarily closely in the sense of mean square convergence by a sum of the form

$$\sum_{k=1}^{n} c_{n,k}\, E[z_k | Y_t^+] \quad , \tag{D.9}$$

from some z_k's $\in Y_t^-$. Hence,

$$E[v\,\eta] = \lim_{n\to\infty} \left\{ \sum_{k=1}^{n} c_{n,k}\, E\left[v\, E[z_k | Y_t^+]\right] \right\} \quad , \tag{D.10}$$

and, therefore,

$$E[v\,\eta] = \lim_{n\to\infty} \left\{ \sum_{k=1}^{n} c_{n,k}\, E[v\, z_k] \right\} \quad . \tag{D.11}$$

Now we use the fact that $v \in \left(Y_t^-\right)^\perp$ to show that $E[v\,\eta] = 0$.

Appendix 2E

Proof that $Y_t^{+|-} = H(x_*(t))$ and $Y_t^{-|+} = H(x^*(t))$

In this Appendix we will verify that in general

$$Y_t^{+|-} \varepsilon H(x_*(t)) \quad , \tag{E.1}$$

and

$$Y_t^{-|+} \varepsilon H(x^*(t)) = H(\hat{x}_r(t)) \quad , \tag{E.2}$$

The above inclusions become equalities when the state-space realizations in $\mathcal{S}$ are of minimal dimension, i.e., if those realizations are controllable and observable. We verify relation (E.1) by noting that Y_t^+ may be characterized as

$$Y_t^+ = H\left(\int_{\tau=t}^{T} \psi'(\tau)dy(\tau) \;\forall\; \psi'(\cdot) = (\psi_1(\cdot),\ldots,\psi_m(\cdot)),\psi_i(\cdot) \in L_2(t,T) \right), \tag{E.3}$$

where $L_2(t,T)$ denotes the class of square integrable functions on (t,T). Hence if we recall the definition of $Y_t^{+|-}$, $Y_t^{+|-}$ may be expressed as

$$Y_t^{+|-} = H\left(\int_{\tau=t}^{T} \psi'(\tau)\, E[dy(\tau)|Y_t^-] \right) \quad . \tag{E.4}$$

Now, by using the fact that for a given realization in $\mathcal{P}$ $dy(\tau) = H(\tau)x(\tau)d\tau + E(\tau)dw(\tau)$, and noting that $dw(\tau) \perp Y_t^-$ for $\tau \geq t$, and $E[x(\tau)|Y_t^-]$ is given as

$$E[x(\tau)|Y_t^-] = \Phi_A(\tau,t)x_*(t) \quad , \tag{E.5}$$

where $\Phi_A(\cdot,\cdot)$ denotes the transition matrix associated with $A(\cdot)$, we can show that $Y_t^{+|-}$ may be written as

$$Y_t^{+|-} = H\left(\left[\int_{\tau=t}^{T} \Phi_A'(\tau,t)H'(\tau)\psi(\tau)d\tau\right]' x_*(t)\right) \quad . \tag{E.6}$$

The relation (E.6) implies that $Y_t^{+|-} \in H(x_*(t))$. In the case where the state space $x(\cdot)$ is of minimal dimension, the assumed analyticity of the coefficient matrices $A(\cdot),H(\cdot)$, implies the differential observability of the system, and hence the differentiable controllability of the adjoint system [42]. By differential controllability and differential observability we mean that the system is controllable or observable over an infinitesimal period of time. Therefore, by varying the choice of $\psi(\cdot)$ on the right-hand side of (E.6), we can generate all possible linear combinations of the components of $x_*(t)$. Consequently, $Y_t^{+|-} = H(x_*(t))$.

To verify relation (E.2) we proceed similarly. We use the equation

$$dy(\tau) = G'(\tau)\bar{x}(\tau)d\tau + E(\tau)d\bar{w}(\tau) \quad , \tag{E.7}$$

for $dy(\cdot)$ associated with the corresponding backward realization in $\bar{\mathcal{B}}$. We can show that $Y_t^{-|+}$ may be represented as

$$Y_t^{-|+} = H\left(\left[\int_0^t \Phi_A(t,\tau)G(\tau)\psi(\tau)d\tau\right]' \bar{x}_*(t)\right) \quad . \tag{E.8}$$

From the definition of $x^*(\cdot)$, we can rewrite (E.8) as

$$Y_t^{-|+} = H\left(\left\{\left[\int_0^t \Phi_A(t,\tau)G(\tau)\psi(\tau)d\tau\right]' \pi^{*-1}(t)\right\}x^*(t)\right) \quad , \tag{E.9}$$

so that $Y_t^{-|+} \varepsilon H(x^*(t))$. From the relation connecting $\hat{x}_r(\cdot)$ and $x^*(\cdot)$, we have $H(\hat{x}_r(t)) = H(x^*(t))$. Assuming that realizations in $\mathcal{B}$ have state processes of minimal dimension, the corresponding realization in $\bar{\mathcal{B}}$ with state process $\bar{x}(\cdot)$ must be of minimal dimension. Hence, (A',G') must be an observable pair and therefore (A,G) is a controllable pair. In this way, we argue that by varying $\psi(\cdot)$ on the right-hand side of (E.9), we can generate all possible linear combinations of the components of $x^*(t)$. Hence, $H(x^*(t)) \varepsilon Y_t^{-|+}$, proving that $Y_t^{-|+} = H(x^*(t))$.

Appendix 2F

Verification of Correlation Properties between $x(\cdot)$, $x_*(\cdot)$, and $x^*(\cdot)$

In this Appendix we prove that

$$E[x(t)x_*'(t)] = \pi_*(t) \quad , \tag{F.1}$$

$$E[x(t)x^{*'}(t)] = \pi(t) \quad , \tag{F.2}$$

and

$$E[x_*(t)x^{*'}(t)] = \pi_*(t) \quad . \tag{F.3}$$

Relations (F.1) - (F.2) follow from orthogonality properties satisfied by the errors associated with the estimates $x_*(\cdot)$ and $\bar{x}_*(\cdot)$, respectively. Hence, if we represent $x(t)$ as

$$x(t) = [x(t) - x_*(t)] + x_*(t) \quad , \tag{F.4}$$

and form $E[x(t)x_*'(t)]$, we obtain (F.1). We next represent $x^*(t)$ as

$$x^*(t) = \bar{\pi}_*^{-1}(t)\bar{x}_*(t) \quad , \tag{F.5}$$

and $x(t)$ as

$$x(t) = \pi(t)\bar{x}(t) \quad , \tag{F.6}$$

in order to compute $E[x(t)x^{*'}(t)]$ as

$$E[x(t)x^{*'}(t)] = \pi(t)E[\bar{x}(t)\bar{x}_{*}'(t)]\bar{\pi}_{*}^{-1}(t) \quad . \tag{F.7}$$

But by representing $\bar{x}(t)$ as

$$\bar{x}(t) = [\bar{x}(t) - \bar{x}_{*}(t)] + \bar{x}_{*}(t) \quad , \tag{F.8}$$

we can show that

$$E[\bar{x}(t)\bar{x}_{*}'(t)] = \bar{\pi}_{*}(t) \quad . \tag{F.9}$$

Substituting (F.9) into (F.7) we obtain relation (F.2).

Relation (F.3) follows from the fact that $x^{*}(t)$ can be represented as

$$x^{*}(t) = E[x^{*}(t)|Y_{t}^{-}] + \tilde{x}^{*}(t) \quad , \tag{F.10}$$

where $\tilde{x}^{*}(t) \perp Y_{t}^{-}$. Now, since $x^{*}(\cdot)$ is a state process associated with a realization in $\mathcal{B}$, we must have

$$x_*(t) = E[x^*(t)|Y_t^-] \quad . \tag{F.11}$$

Hence, by substituting relation (F.11) into (F.10) and forming $E[x_*(t)x^{*'}(t)]$, we obtain relation (F.3).

Appendix 2G

Connection between Weinert and Desai's Approach to Smoothing and the Scattering Formalism

In this Appendix we connect Weinert and Desai's smoothing algorithm with an identical procedure that follows from the scattering formalism of Appendix 2C, for the purpose of interpreting the noise $d\alpha(\cdot)$ that drives the smoothing error dynamics (2.209).

If we break the scattering diagram for the smoothing problem at a time instant $0<\tau<T$, it is shown in [31], by using the relations of Appendix 2C to derive formulae for the evolution of aggregate scattering parameters and internal source contributions for the sections $[0,\tau]$ and $[\tau,T]$, that the scattering picture may be represented as in Fig. G.1, where $O_0(\cdot,T)$ and $\lambda_0(\cdot|T)$ are generated by

$$-\frac{\partial O_0(\sigma,T)}{\partial\sigma} = A'(\sigma)O_0(\sigma,T) + O_0(\sigma,T)A(\sigma) + \bar{H}'(\sigma)\bar{H}(\sigma) - O_0(\sigma,T)B(\sigma)B'(\sigma)O_0(\sigma,T) \quad , \tag{G.1}$$

with $$O_0(T,T) = 0 \quad , \tag{G.2}$$

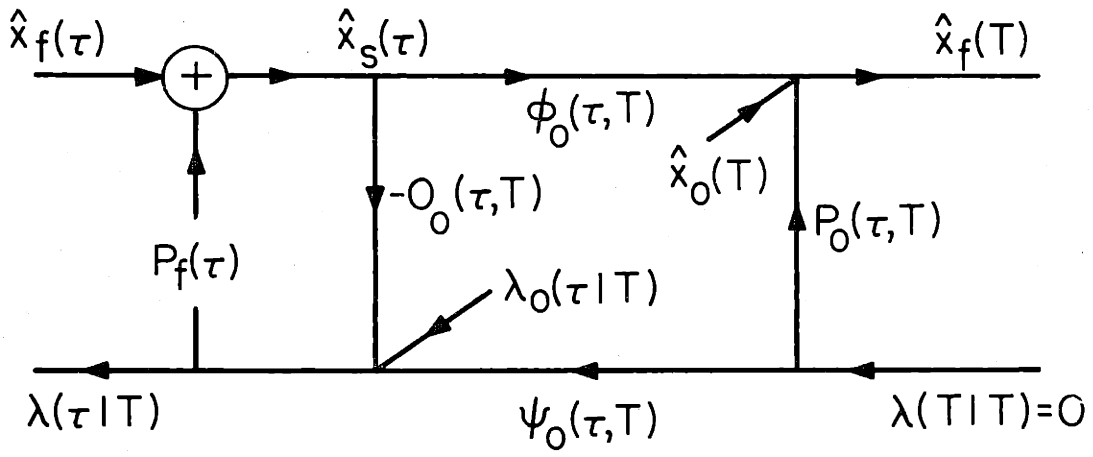

Fig. G.1 Equivalent Scattering Diagram Breaking the Medium at Time $t=\tau$

and

$$-d\lambda_0(\sigma|T) = [A(\sigma) - B(\sigma)B'(\sigma)O_0(\sigma,T)]'\lambda_0(\sigma|T)d\sigma + \bar{H}'(\sigma)dy(\sigma) \quad , \tag{G.3}$$

with $$\lambda_0(T|T) = 0 \quad . \tag{G.4}$$

From Fig. G.1, we can compute $\lambda(\tau|T)$ as

$$\lambda(\tau|T) = \lambda_0(\tau|T) - O_0(\tau,T)\hat{x}_s(\tau) \quad . \tag{G.5}$$

By substituting relation (G.5) into the forward equation for the evolution of $\hat{x}_s(\cdot)$ in the Hamiltonian formulation of smoothing, we obtain the following equation for the evolution of $\hat{x}_s(\cdot)$:

$$d\hat{x}_s(\tau) = [A(\tau) - B(\tau)B'(\tau)O_0(\tau,T)]\hat{x}_s(\tau)d\tau + B(\tau)B'(\tau)\lambda_0(\tau|T)d\tau \quad . \tag{G.6}$$

Specializing (G.5) for $\tau = 0$, and substituting the result into the innovations formula for $\hat{x}_s(0)$, we can solve for $\hat{x}_s(0)$ as

$$\hat{x}_s(0) = \pi(0)(I + O_0(0,T)\pi(0))^{-1}\lambda_0(0|T) \quad . \tag{G.7}$$

Hence, comparing the equations for the evolution of $\rho(\cdot)$, $\lambda_0(\cdot|T)$, and for $O_0(\cdot,T), P_b(\cdot)$ we recognize that

$$O_0(t,T) = P_b(t) \quad , \tag{G.8}$$

and $$\lambda_0(t|T) = \rho(t) \quad . \tag{G.9}$$

Now, by using the definition of $\rho(t)$ as

$$\rho(t) = \tilde{\gamma}_r(t) + P_b(t)x(t) \quad , \tag{G.10}$$

and relation (G.5) to solve for $\lambda_0(t|T)$, we can express $\tilde{\gamma}_r(t)$ as

$$\tilde{\gamma}_r(t) = \lambda(t|T) + O_0(t,T)(\hat{x}_s(t) - x(t)) \quad . \tag{G.11}$$

Also, we note that by identifying $P_*^{-1}(t)$ as $P_f^{-1}(t)$ and $P^{*-1}(t)$ as $O_0(t,T)$ in our expression for the inverse smoothing error covariance associated with the Mayne-Fraser smoothed estimate, we find that

$$P_s^{-1}(t) = P_f^{-1}(t) + O_0(t,T) \quad . \tag{G.12}$$

Hence, by expressing $\lambda(t|T)$ as

$$\lambda(t|T) = P_f^{-1}(t)(\hat{x}_s(t) - \hat{x}_f(t)) \quad , \tag{G.13}$$

we can rewrite relation (G.11) as

$$\tilde{\gamma}_r(t) = - P_s^{-1}(t)\tilde{x}_s(t) + P_f^{-1}(t)\tilde{x}_f(t) \quad . \tag{G.14}$$

Finally, by employing (G.14) in the relation

$$d\alpha(t) = du(t) - B'(t)\tilde{\gamma}_r(t)dt \quad , \tag{G.15}$$

we can express $d\alpha(t)$ as

$$\underline{\text{Input Noise to Weinert and Desai's Forward Model for } \tilde{x}_s(\cdot)}$$

$$d\alpha(t) = du(t) - B'(t)\left[P_f^{-1}(t)\tilde{x}_f(t) - P_s^{-1}(t)\tilde{x}_s(t)\right]dt \quad . \tag{G.16}$$

Chapter 3

Smoothing Error Models

3.1 Introduction

In Section 1.2 we motivated the importance of obtaining Markovian realizations of the smoothing error process in order to solve the centralized map-updating problem. In this chapter we unify several different approaches for deriving forward and reverse Markovian representations of the smoothing errors. The main thrust of our presentation is in Section 3.2, where we present an original derivation of forward and reverse models for $\tilde{x}_s(\cdot)$ by employing martingale decompositions of the process noise, du(t). This martingale decomposition approach essentially corresponds to Markovianizing a simple relation for the evolution of $\tilde{x}_s(\cdot)$ obtained by subtracting from the unconditional dynamics, $x(\cdot)$, an equation for generating $\hat{x}_s(\cdot)$ that we used as the starting point for the derivation of the Hamiltonian and Rauch-Tung-Striebel equations for smoothing. The appeal of our martingale decomposition approach to deriving smoothing error realizations lies in its simplicity, and in the fact that it displays clearly the interpretation of each term appearing in those realizations. The consistency of the forward model for $\tilde{x}_s(\cdot)$ that we obtain is then checked by comparing it

with that of Weinert and Desai. In Section 3.3 we present a second original derivation for a backward model of the smoothing errors. We show how such a model follows simply from a representation of the smoothing errors derived from the innovations form of the smoothed estimate. Our derivation of Section 3.3 illustrates how the backward model for the smoothing error process follows from the structure of the backward realization for the filtering errors, alone, thus demonstrating why it is reasonable that n-dimensional, state-space, Markovian realizations for the smoothing error process exist at all. Finally, in Section 3.4 we sketch and interpret the original approach of Lindquist and Badawi [83], using stochastic realization concepts, to derive a related backward Markovian representation for the smoothing errors.

3.2 Derivation of Forward and Reverse Markovian Realizations for the Smoothing Error Process by Employing Martingale Decompositions of the Process Noise

We first introduce some definitions, and then derive an equation for the evolution of the smoothing error process, which is the starting point for the construction of forward and reverse Markovian realizations. We note that the state dynamics (2.1) may be written as

$$dx(t) = A(t)x(t)dt + d\xi(t) \quad , \tag{3.1}$$

where $d\xi(t)$ is defined by

$$d\xi(t) \triangleq B(t)du(t) \quad . \tag{3.2}$$

We define the σ-field $\mathbf{y}$ as that generated by the fixed interval of observations, i.e.,

$$\mathbf{y} \triangleq \sigma\{y(\tau) \quad 0 \leq \tau \leq T\} \quad . \tag{3.3}$$

Hence, the smoothed estimate $\hat{x}_s(t)$ is defined by

$$\hat{x}_s(t) = E[x(t)|\mathbf{y}] \quad . \tag{3.4}$$

If we take the conditional expectation $E[\cdot|\mathbf{y}]$ on both sides of (3.1) we obtain an equation for the evolution of $\hat{x}_s(\cdot)$, which when subtracted from (3.1) yields the following evolution equation for $\tilde{x}_s(\cdot)$:

$$d\tilde{x}_s(t) = A(t)\tilde{x}_s(t)dt + d\tilde{\xi}(t) \quad , \tag{3.5}$$

where $$d\tilde{\xi}(t) \triangleq d\xi(t) - E[d\xi(t)|\mathbf{y}] \quad . \tag{3.6}$$

The relation (3.5) does not represent a Markovian realization of the smoothing error process since $\tilde{\xi}(\cdot)$ is not a Wiener process, and since $\tilde{\xi}(\cdot)$ is not independent of the initial condition of $\tilde{x}_s(\cdot)$, i.e., $\sigma\{d\tilde{\xi}(\tau) \quad 0 \le \tau \le T\}$ is not independent of either $\sigma\{\tilde{x}_s(0)\}$ or $\sigma\{\tilde{x}_s(T)\}$. Our first method for deriving forward and reverse Markovian realizations of the smoothing error process is to Markovianize relation (3.5), by decomposing $d\xi(t)$ with respect to some σ-fields that we now specify. Let us define σ-fields associated with the future and past values of the smoothing error process by

$$\tilde{\mathcal{X}}_t^+ = \sigma\{\tilde{x}_s(\tau) \quad t \le \tau \le T\} \quad , \tag{3.7}$$

and $$\tilde{\mathcal{X}}_t^- = \sigma\{x_s(\tau) \quad 0 \le \tau \le t\} \quad . \tag{3.8}$$

Now, we define two σ-fields, $\mathcal{I}_t$ and $\mathcal{J}_t$, by

$$\mathcal{I}_t = \sigma\{\tilde{x}_t^+, \mathbf{y}\} \quad , \tag{3.9}$$

and

$$\mathcal{J}_t = \sigma\{\tilde{x}_t^-, \mathbf{y}\} \quad . \tag{3.10}$$

We may verify† that

$$\xi(t) = \int_{\tau=0}^{t} d\xi(\tau) \quad , \tag{3.11}$$

and

$$\xi_r(t) \triangleq \int_{\tau=t}^{T} d\xi(\tau) \quad , \tag{3.12}$$

are some quasi-martingales with respect to the σ-fields $\mathcal{J}_t$ and $\mathcal{I}_t$, respectively. Therefore, we can decompose $d\xi(t)$ as follows:

$$d\xi(t) = E[d\xi(t)|\mathcal{I}_t] + d\tilde{\xi}_r(t) \quad , \tag{3.13}$$

---

†According to [46], to verify that $\xi(\cdot)$ and $\xi_r(\cdot)$ are some quasi-martingales with respect to the σ-fields $\mathcal{J}_t$ and $\mathcal{I}_t$, we need only check that they are adapted to these σ-fields. This is guaranteed if we note that

$$d\xi(t) = d\tilde{x}_s(t) - A(t)\tilde{x}_s(t)dt + E[d\xi(t)|\mathbf{y}] \, ,$$

since this shows that $\xi(t)$ and $\xi_r(t)$ depend only on either $\tilde{x}_t^-, \mathbf{y}$ or $\tilde{x}_t^+, \mathbf{y}$, respectively, i.e., $\xi(t)$ is adapted to $\mathcal{J}_t$ and $\xi_r(t)$ is adapted to $\mathcal{I}_t$, respectively.

and $$d\xi(t) = E[d\xi(t)|\mathcal{Y}_t] + d\tilde{\xi}_f(t) \quad . \tag{3.14}$$

We will show that by using the relations (3.13) - (3.14) to represent the process $d\tilde{\xi}(t)$ (defined in (3.6)) in equation (3.5), we obtain some reverse and forward Markovian realizations for the smoothing error process. The motivation for decomposing the process noise, $d\xi(\cdot)$, as in (3.13) - (3.14), is that ultimately $\tilde{\xi}_r(\cdot)$ and $\tilde{\xi}_f(\cdot)$ will function as input Wiener processes for the reverse and forward realizations of $\tilde{x}_s(\cdot)$. We note also that these noises will be independent, respectively, of $\tilde{x}_s(T)$ and $\tilde{x}_s(0)$, so that the models that we shall obtain will be some Markovian realizations of $\tilde{x}_s(\cdot)$.

Now, since $\mathbf{y}$ and either $\tilde{x}_t^+$ or $\tilde{x}_t^-$ are independent, the identities (3.13) - (3.14) may be expressed as

$$d\xi(t) = E[d\xi(t)|\tilde{x}_t^+] + E[d\xi(t)|\mathbf{y}] + d\tilde{\xi}_r(t) \quad , \tag{3.15}$$

and $$d\xi(t) = E[d\xi(t)|\tilde{x}_t^-] + E[d\xi(t)|\mathbf{y}] + d\tilde{\xi}_f(t) \quad . \tag{3.16}$$

Noting from our earlier result (2.25) that the martingale parts of a given quasi-martingale decomposed with respect to different σ-fields have the same quadratic variation, we can conclude that $d\tilde{\xi}_r(t)$ and $d\tilde{\xi}_f(t)$ can be represented as

$$d\tilde{\xi}_r(t) = B(t)d\tilde{u}_r(t) \quad , \tag{3.17}$$

and $$d\tilde{\xi}_f(t) = B(t)d\tilde{u}_f(t) \quad , \tag{3.18}$$

where $\tilde{u}_r(\cdot)$ and $\tilde{u}_f(\cdot)$ are some standard Wiener processes. Therefore, if we use relations (3.15) - (3.16) to define $d\tilde{\xi}(t)$ in (3.5), we obtain the following equations for the evolution of the smoothing error process:

$$d\tilde{x}_s(t) = A(t)\tilde{x}_s(t)dt + B(t)E[du(t)|\tilde{\mathcal{X}}_t^-] + B(t)d\tilde{u}_f(t) \ , \tag{3.19}$$

and

$$d\tilde{x}_s(t) = A(t)\tilde{x}_s(t)dt + B(t)E[du(t)|\tilde{\mathcal{X}}_t^+] + B(t)d\tilde{u}_r(t) \ , \tag{3.20}$$

where

$$d\tilde{u}_f(t) = du(t) - E[du(t)|\tilde{\mathcal{X}}_t^-] - E[du(t)|\mathbf{y}] \ , \tag{3.21}$$

and

$$d\tilde{u}_r(t) = du(t) - E[du(t)|\tilde{\mathcal{X}}_t^+] - E[du(t)|\mathbf{y}] \ . \tag{3.22}$$

In Appendix 3A we employ an explicit representation of the smoothing error process arising from the innovations solution to the smoothing problem to verify that

$$E[du(t)|\tilde{\mathcal{X}}_t^+] = B'(t)P_f^{-1}(t)\tilde{x}_s(t)dt \quad , \tag{3.23}$$

and

$$E[du(t)|\tilde{\mathcal{X}}_t^-] = B'(t)\left(P_f^{-1}(t) - P_s^{-1}(t)\right)\tilde{x}_s(t)dt \quad , \tag{3.24}$$

where $P_f(\cdot)$ and $P_s(\cdot)$ denote the filtering and smoothing error covariance matrices, respectively. Therefore, by substituting (3.23) and (3.24) in (3.19) and (3.20) we obtain the following forward and reverse Markovian realizations of the smoothing error process:

$$d\tilde{x}_s(t) = \left[A(t) + B(t)B'(t)\left(P_f^{-1}(t) - P_s^{-1}(t)\right)\right]\tilde{x}_s(t)dt + B(t)d\tilde{u}_f(t), \tag{3.25}$$

and

$$d\tilde{x}_s(t) = \left[A(t) + B(t)B'(t)P_f^{-1}(t)\right]\tilde{x}_s(t)dt + B(t)d\tilde{u}_r(t) \quad . \tag{3.26}$$

At this point, we note that through equations (3.25) - (3.26) we have achieved the major objective of this chapter. The reader who is not interested in understanding the connection between the forward model (3.25), and the one of Weinert

and Desai, or in looking into two alternative perspectives for obtaining backward models of $\tilde{x}_s(\cdot)$ in Sections 3.3 and 3.4, should proceed to Chapter 4.

We now connect the forward realization given by (3.25) with the one of Weinert and Desai, which is given by equation (2.209). In Appendix 2G we effectively showed that

$$P_b(t) = -\left(P_f^{-1}(t) - P_s^{-1}(t)\right) \quad , \tag{3.27}$$

and hence to prove that (2.209) and (3.25) represent the same equation for the evolution of $\tilde{x}_s(\cdot)$, we need only to show that

$$d\alpha(t) = d\tilde{u}_f(t) \quad . \tag{3.28}$$

If we use (3.24) to express $E[du(t)|\tilde{\mathcal{Y}}_t^-]$ as

$$E[du(t)|\tilde{\mathcal{Y}}_t^-] = B'(t)\left(P_f^{-1}(t) - P_s^{-1}(t)\right)\left(x(t) - \hat{x}_s(t)\right)dt \quad , \tag{3.29}$$

and we compute $E[du(t)|\mathbf{y}]$ from (2.58) in the form

$$E[du(t)|\mathbf{y}] = B'(t)P_f^{-1}(t)\left(\hat{x}_s(t) - \hat{x}_f(t)\right)dt, \tag{3.30}$$

then we obtain from (3.21) the following representation for $d\tilde{u}_f(t)$:

$$d\tilde{u}_f(t) = du(t) - B'(t)P_f^{-1}(t)\tilde{x}_f(t)dt + B'(t)P_s^{-1}(t)\tilde{x}_s(t)dt \ . \tag{3.31}$$

In Appendix 2G we show that $d\alpha(t)$ may also be expressed as in (3.31), verifying equation (3.28).

3.3 The Derivation of a Backward Model for $\tilde{x}_s(\cdot)$ from a Representation for $\tilde{x}_s(t)$ following from the Innovations Form of the Smoothed Estimate

The derivation of a backward model for $\tilde{x}_s(\cdot)$, consistent with (3.26) follows from noting that the innovations smoothing formula may be expressed as

$$\hat{x}_s(t) = \hat{x}_f(t) + E\left[\tilde{x}_f(t) \mid \boldsymbol{\nu}_t^+\right] , \tag{3.32}$$

and hence

$$\tilde{x}_s(t) = \tilde{x}_f(t) - E\left[\tilde{x}_f(t) \mid \boldsymbol{\nu}_t^+\right] . \tag{3.33}$$

We will exploit the representation of relation (3.33) to obtain a reverse time model for $\tilde{x}_s(\cdot)$. We first form a reversed time realization of $\tilde{x}_f(\cdot)$ from the forward realization

$$\begin{aligned} d\tilde{x}_f(t) = &\left(A(t) - P_f(t)H'(t)R^{-1}(t)H(t)\right)\tilde{x}_f(t)dt \\ &+ B(t)du(t) - P_f(t)H'(t)R^{-1}(t)D(t)dv(t), \end{aligned} \tag{3.34}$$

by decomposing the input noises du(t) and dv(t) with respect to $\sigma\left\{\tilde{x}_f(\tau) \quad t \le \tau \le T\right\}$ as

$$du(t) = B'(t)P_f^{-1}(t)\tilde{x}_f(t)dt + d\tilde{u}_b(t) , \tag{3.35}$$

and

$$dv(t) = -D'(t)R^{-1}(t)H(t)\tilde{x}_f(t)dt + d\tilde{v}_r(t) \quad . \tag{3.36}$$

By employing relations (3.35) and (3.36), and recognizing that $D(t)d\tilde{v}_r(t) = d\nu(t)$, we obtain the following backward realization for $\tilde{x}_f(\cdot)$:

$$-d\tilde{x}_f(t) = -\left[A(t) + B(t)B'(t)P_f^{-1}(t)\right]\tilde{x}_f(t)dt - B(t)d\tilde{u}_b(t) + P_f(t)H'(t)R^{-1}(t)d\nu(t) \quad . \tag{3.37}$$

We next show that the input process, $d\tilde{u}_r(t)$, of the reverse time model (3.26) is identical to $d\tilde{u}_b(t)$, where

$$d\tilde{u}_b(t) = du(t) - B'(t)P_f^{-1}(t)\tilde{x}_f(t)dt \quad . \tag{3.38}$$

If we express $E[du(t)|\tilde{X}_t^+]$ from relation (3.25) as

$$E[du(t)|\tilde{X}_t^+] = B'(t)P_f^{-1}(t)(x(t) - \hat{x}_s(t))dt \ , \tag{3.39}$$

and compute $E[du(t)|\mathbf{y}]$ by relation (3.30), by using (3.22) we can express $d\tilde{u}_r(t)$ as

$$d\tilde{u}_r(t) = du(t) - B'(t)P_f^{-1}(t)\tilde{x}_f(t)dt \quad . \tag{3.40}$$

Then, since $d\tilde{u}_b(t) = d\tilde{u}_r(t)$, we know that $d\tilde{u}_b(t) \perp Y$ and hence $d\tilde{u}_b(\tau) \perp \mathcal{V}_t^+$ for all τ, t. Therefore, if we define $\varphi(t)$ as

$$\varphi(t) = E\left[\tilde{x}_f(t) \mid \mathcal{V}_t^+\right] \quad , \tag{3.41}$$

by formally taking $E\left[\cdot \mid \mathcal{V}_t^+\right]$ of both sides of relation (3.37) we obtain the backward model

$$-d\varphi(t) = -\left(A(t) + B(t)B'(t)P_f^{-1}(t)\right)\varphi(t)dt + P_f(t)H'(t)R^{-1}(t)d\nu(t), \tag{3.42}$$

with $$\varphi(T) = 0 \quad . \tag{3.43}$$

Then, from relation (3.33) we obtain the backward model (3.26) for the smoothing error by forming $d\tilde{x}_s(t)$ as

$$d\tilde{x}_s(t) = d\tilde{x}_f(t) - d\varphi(t) \quad , \tag{3.44}$$

and substituting the expressions for $d\tilde{x}_f(t)$ and $d\varphi(t)$, respectively. We finally note that $\varphi(t)$, in equation (3.41), represents the error reduction in smoothing, over filtering. The derivation of this section, through equations (3.37), (3.41), and (3.44), demonstrates how the existence and structure of the

backward realization for the smoothing errors, follows from the structure of the backward model for the filtering errors alone.

3.4 The Stochastic Realization Perspective on Obtaining a Backwards Markovian Representation for $\tilde{x}_s(\cdot)$

We finally outline briefly the stochastic realization approach of Lindquist and Badawi in [83] for obtaining a related backwards Markovian representation of the smoothing error process. We will show that our derivation of the backward model in Section 3.3 is actually closely related to the method of Lindquist and Badawi in [83]. We first derive a restatement of the innovations smoothing formula, in a stochastic realization setting. From the correlation relation (2.145), we can show that

$$E[x^*(t)|H(x_*(t))] = x_*(t) \quad , \tag{3.45}$$

and thus defining $q(t)$ as

$$q(t) \triangleq x^*(t) - E[x^*(t)|H(x_*(t))] \equiv x^*(t) - x_*(t) \ , \tag{3.46}$$

we can motivate the orthogonal decomposition

$$H(x_*(t),x^*(t)) = H(x_*(t)) \oplus H(q(t)) \ . \tag{3.47}$$

The decomposition (3.47) results in the following formula for the smoothed estimate:

$$\hat{x}_s(t) = x_*(t) + P_*(t)\pi_d^{-1}(t)q(t) \quad , \tag{3.48}$$

where $$\pi_d(t) \triangleq \pi^*(t) - \pi_*(t) \quad . \tag{3.49}$$

Relation (3.48) is the same as the innovations smoothing formula, and hence if $\tilde{x}_*(t)$ denotes the filtering error process, by comparison with (2.32) we find that

$$E\left[\tilde{x}_*(t) \mid \mathcal{V}_t^+\right] = P_*(t)\pi_d^{-1}(t)q(t) \quad . \tag{3.50}$$

Now, if we define

$$\bar{q}(t) = \pi_d^{-1}(t)q(t) \quad , \tag{3.51}$$

and $$g(t) = P_*^{-1}(t)\tilde{x}_*(t) \quad , \tag{3.52}$$

we obtain from (3.48) the following representation for $\tilde{x}_s(t)$:

$$\tilde{x}_s(t) = P_*(t)\delta(t) \quad , \tag{3.53}$$

where $\delta(t) \triangleq g(t) - \bar{q}(t)$. (3.54)

Taking into account equation (3.50), we may interpret $\delta(t)$ as

$$\delta(t) = g(t) - E\left[g(t) \mid \boldsymbol{\nu}_t^+\right] . \tag{3.55}$$

Hence, by comparing the representations for the smoothing errors of (3.53) and (3.32), the difference lies in the fact that the former uses the normalized filtering errors, $g(t)$, and the latter employs the actual filtering errors, $\tilde{x}_*(t)$.

The approach in [83] to obtaining a backwards Markovian representation for $\tilde{x}_s(t)$, the complete details of which we will not reproduce here, consists of using relation (3.53), and deriving a backwards Markovian realization for the process $\delta(\cdot)$. The backward model for $\delta(\cdot)$ is obtained by first determining forward models for $\tilde{x}_*(t)$ and $q(t)$, then using relations (2.101)-(2.103) to determine backward models for their inverse covariance counterparts $g(t)$ and $\bar{q}(t)$, and finally using the definition of $\delta(\cdot)$ to derive its backward model.

3.5 Conclusion

In this Chapter we have connected two existing approaches for deriving Markovian realizations of the smoothing error process, the approach of Weinert and Desai [49] and the stochastic realization perspective [83], with two new techniques, the process noise, martingale decomposition approach of Section 3.2 and finally in Section 3.3 the use of the representation of $\tilde{x}_s(t)$ in relation (3.33) to obtained a backward model for $\tilde{x}_s(\cdot)$. Of all four approaches for obtaining dynamical equations satisfied by the smoothing error process, the martingale decomposition approach offers the clearest insight into the meaning of each of the terms that appear in the forward and reverse Markovian realizations of $\tilde{x}_s(\cdot)$.

The stochastic realization perspective [83] on obtaining a backwards Markovian representation for the smoothing error process is based on an expression (3.53) for $\tilde{x}_s(t)$ closely related to that in equation (3.33). However, the derivation stemming from relation (3.33) is clearer, since we show how the existence of a backward realization for the smoothing error process follows from the structure of the backward realization of the filtering error process alone.

Appendix 3A

Proof of Expressions for the Projections of the Increments of the Process Noise onto the Hilbert Spaces Generated by the Future and Past Values of the Smoothing Errors, Respectively

In this Appendix we verify that

$$E[du(t)\,|\,\tilde{\chi}_t^+] = B'(t)P_f^{-1}(t)\tilde{x}_s(t)dt \quad , \tag{A.1}$$

and that

$$E[du(t)\,|\,\tilde{\chi}_t^-] = B'(t)\left(P_f^{-1}(t) - P_s^{-1}(t)\right)\tilde{x}_s(t)dt \quad , \tag{A.2}$$

by checking the orthogonality conditions

$$E\left[[du(t) - B'(t)P_f^{-1}(t)x_s(t)dt]\tilde{x}_s'(\tau)\right] = 0 \quad \text{for } \tau \geq t, \tag{A.3}$$

and $$E\left[[du(t) - B'(t)\left(P_f^{-1}(t) - P_s^{-1}(t)\right)\tilde{x}_s(t)dt]\tilde{x}_s'(\tau)\right] = 0$$

$$\text{for } \tau \leq t. \tag{A.4}$$

To check the relations (A.3) - (A.4) we employ the following representation for $\tilde{x}_s(t)$, derived from the innovations solution (see Section 2.2) to the smoothing problem:

$$\tilde{x}_s(t) = \tilde{x}_f(t) - P_f(t) \int_{s=t}^{T} \Phi'_\Gamma(s,t)H'(s)R^{-1}(s)d\nu(s) \quad , \quad (A.5)$$

where $\Phi_\Gamma(\cdot,\cdot)$ denotes the transition matrix associated with the filtering dynamics matrix $\Gamma(t)$, defined by

$$\Gamma(t) \triangleq A(t) - P_f(t)H'(t)R^{-1}(t)H(t) \quad . \quad (A.6)$$

We being by verifying relation (A.3). Since we may express $\tilde{x}_s(t)$ as

$$\tilde{x}_s(t) = x(t) - \hat{x}_s(t) \quad , \quad (A.7)$$

and $\tilde{x}_s(\tau) \perp \hat{x}_s(t)$, we can compute $E[\tilde{x}_s(t)\tilde{x}'_s(\tau)]$ as

$$E[\tilde{x}_s(t)\tilde{x}'_s(\tau)] = E[x(t)\tilde{x}'_s(\tau)] \quad . \quad (A.8)$$

We note also that

$$d\nu(s) = H(s)\tilde{x}_f(s) + D(s)dv(s) \quad , \quad (A.9)$$

and from the orthogonality property satisfied by the filtered estimates, and the filtering error dynamics, we also have for $s \geq t$

$$E[x(t)\tilde{x}_f'(s)] = E[\tilde{x}_f(t)\tilde{x}_f'(s)] = P_f(t)\Phi_T'(s,t) \quad . \tag{A.10}$$

Then, by employing relations (A.8) and (A.10) we can express $E[\tilde{x}_s(t)\tilde{x}_s'(\tau)]$ for $\tau \geq t$ as

$$E[\tilde{x}_s(t)\tilde{x}_s'(\tau)] = P_f(t)\Phi_T'(\tau,t) - P_f(t)\left[\int_{s=\tau}^{T} \Phi_T'(s,t)H'(s)R^{-1}(s)H(s)\Phi_T(s,\tau)ds\right]P_f(\tau). \tag{A.11}$$

In a similar manner, we compute $E[du(t)\tilde{x}_s'(\tau)]$ for $\tau \geq t$, by employing (A.5),(A.9) and by taking into account the fact that from the filtering error dynamics, $E[du(t)\tilde{x}_f'(s)]$ for $s \geq t$ may be expressed as

$$E[du(t)\tilde{x}_f'(s)] = B'(t)\Phi_T'(s,t) \quad . \tag{A.12}$$

We thus find that $E[du(t)\tilde{x}_s'(\tau)]$ may be computed as

$$E[du(t)\tilde{x}_s'(\tau)] = B'(t)\left\{\Phi_T'(\tau,t) - \left[\int_{s=\tau}^{T} \Phi_T'(s,t)H'(s)R^{-1}(s) \cdot H(s)\Phi_T(s,\tau)ds\right]P_f(\tau)\right\}, \tag{A.13}$$

so that by combining relations (A.11) and (A.13) the orthogonality condition (A.3) is verified.

We finally observe from relations (A.11) and (A.13) that the projection of du(t) onto $\tilde{\chi}_t^+$ is equivalent to its conditional mean given $\tilde{x}_s(t)$ alone. Hence, we have demonstrated through relation (A.3) that the error in the estimation of du(t) from $\tilde{x}_s(t)$ is not only orthogonal to $\tilde{x}_s(t)$, but to the entire future space of smoothing errors, $\tilde{\chi}_t^+$.

We verify similarly the relation (A.4). We note first that $du(t) \perp \tilde{x}_f(\tau)$ for $\tau < t$. Hence, by using (A.5) and (A.12) we can compute $E[du(t)\tilde{x}_s'(\tau)]$ for $\tau \leq t$ as

$$E[du(t)\tilde{x}_s'(\tau)] = -B'(t)\left[\int_{s=t}^{T} \Phi_T'(s,t)H'(s)R^{-1}(s)H(s)\Phi_T(s,\tau)ds\right]P_f(\tau). \tag{A.14}$$

Now, by using the fact that

$$E[\tilde{x}_s(t)\tilde{x}_s'(\tau)] = E[\tilde{x}_s(t)x'(\tau)] \quad , \tag{A.15}$$

and reasoning as in (A.10) that

$$E[\tilde{x}_f(s)x'(\tau)] = \Phi_T(s,\tau)P_f(\tau) \quad , \tag{A.16}$$

we can compute $E[\tilde{x}_s(t)\tilde{x}_s'(\tau)]$ for $\tau \leq t$ as

$$E[\tilde{x}_s(t)\tilde{x}_s'(\tau)] = \Phi_T(t,\tau)P_f(\tau) - P_f(t)\left[\int_{s=t}^{T}\Phi_T'(s,t)H'(s) \cdot R^{-1}(s)H(s)\Phi_T(s,\tau)ds\right]P_f(\tau). \quad (A.17)$$

By substituting relations (A.14) and (A.17) into (A.4), we can show that to verify the desired orthogonality condition one needs to prove an identity of the form

$$P_s^{-1}(t) - P_f^{-1}(t) = P_s^{-1}(t)P_f(t)\int_{s=t}^{T}\Phi_T'(s,t)H'(s)R^{-1}(s)H(s)\Phi_T(s,t)ds. \quad (A.18)$$

We can prove relation (A.18) by observing that $P_s(t)$ can be expressed from (A.17) as

$$P_s(t) = P_f(t) - P_f(t)\left[\int_{s=t}^{T}\Phi_T'(s,t)H'(s)R^{-1}(s)H(s)\Phi_T(s,t)ds\right]P_f(t). \quad (A.19)$$

Appendix 3B

Dynamical Equations for the Smoothing Error Process in Discrete Time

In this Appendix we proceed to derive Markovian realizations for the smoothing error process associated with the discrete-time smoothing problem. We begin by presenting the process noise decomposition approach, employed in continuous time. We use the decomposition approach to derive a backward model for $\tilde{x}_s(\cdot)$, and then demonstrate the consistency of that method with a second technique analogous to that of Section 3.3. Next, we employ the discrete version of the approach of Weinert and Desai, to identify a forward realization for $\tilde{x}_s(\cdot)$. We finally show that the structure of the forward model that we obtain is consistent with that predicted by the noise decomposition procedure.

In discrete time, there is a sharper distinction between the derivation of backward and forward realizations of the smoothing error process. Let us define the σ-field, $\mathbf{y}$, spanned by the discrete observations $y(i)$ by

$$\mathbf{y} \triangleq \sigma\{y(1),\ldots,y(T)\} \ , \tag{B.1}$$

and let the state evolution equation be expressed as

$$x(t+1) = A(t)x(t) + \xi(t) \quad , \tag{B.2}$$

where $\xi(\cdot)$ is a discrete white noise sequence defined by

$$\xi(t) = B(t)u(t) \quad . \tag{B.3}$$

Then, to derive a backwards equation for $\tilde{x}_s(\cdot)$, we must start with the assumption that the dynamics matrix A(t) is invertible, so we may use the following deterministically reversed version of relation (B.2):

$$x(t) = A^{-1}(t)x(t+1) - A^{-1}(t)\xi(t) \quad . \tag{B.4}$$

Conditioning both sides of (B.4) with respect to $\mathbf{y}$, and subtracting the resulting relation from (B.4), we obtain

$$\tilde{x}_s(t) = A^{-1}(t)\tilde{x}_s(t+1) - A^{-1}(t)\tilde{\xi}(t) \quad , \tag{B.5}$$

where $$\tilde{\xi}(t) = \xi(t) - E[\xi(t)|\mathbf{y}] \quad . \tag{B.6}$$

To similarly derive a forward equation for $\tilde{x}_s(\cdot)$, we condition both sides of (B.2) with respect to $\mathbf{y}$, and subtract the resulting

relation from (B.2) to obtain

$$\tilde{x}_s(t+1) = A(t)\tilde{x}_s(t) + \tilde{\xi}(t) \quad . \tag{B.7}$$

The relations (B.5) and (B.7) do not represent Markovian realizations for $\tilde{x}_s(\cdot)$ since $\tilde{\xi}(\cdot)$ is not a white noise sequence, and is correlated with both $\tilde{x}_s(0)$ and $\tilde{x}_s(T)$. As in the continuous time problem, forward and reverse Markovian models for $\tilde{x}_s(\cdot)$ follow from employing appropriate decompositions of $\xi(t)$ in relations (B.5) and (B.7), respectively. Let us define the σ-fields $\tilde{X}_t^+$ and $\tilde{X}_t^-$ corresponding to future and past values of $\tilde{x}_s(\cdot)$ by

$$\tilde{X}_t^+ \triangleq \sigma\left\{\tilde{x}_s(t), \tilde{x}_s(t+1), \ldots, \tilde{x}_s(T)\right\} \quad , \tag{B.8}$$

and

$$\tilde{X}_t^- \triangleq \sigma\left\{\tilde{x}_s(0), \quad \ldots \quad , \tilde{x}_s(t-1)\right\} \quad . \tag{B.9}$$

Next, we define the two σ-fields $\mathcal{F}_t$ and $\mathcal{L}_t$ by

$$\mathcal{F}_t = \sigma\left\{\tilde{X}_{t+1}^+, \mathbf{y}\right\} \quad , \tag{B.10}$$

and

$$\mathcal{L}_t = \sigma\left\{\tilde{X}_{t+1}^-, \mathbf{y}\right\} \quad . \tag{B.11}$$

If we now decompose $\xi(t)$ with respect to $\mathcal{T}_t$ and $\mathcal{J}_t$ as

$$\xi(t) = E[\xi(t)|\mathcal{T}_t] + \tilde{\xi}_r(t) \quad , \tag{B.12}$$

and $$\xi(t) = E[\xi(t)|\mathcal{J}_t] + \tilde{\xi}_f(t) \quad , \tag{B.13}$$

by substituting relations (B.12) and (B.13) into relations (B.5) and (B.7) we obtain the following reverse and forward equations for the evolution of the smoothing error process:

$$\tilde{x}_s(t) = A^{-1}(t)\tilde{x}_s(t+1) - A^{-1}(t)E\left[\xi(t)|\tilde{X}^+_{t+1}\right] - A^{-1}(t)\tilde{\xi}_r(t), \tag{B.14}$$

and $$\tilde{x}_s(t+1) = A(t)\tilde{x}_s(t) + E\left[\xi(t)|\tilde{X}^-_{t+1}\right] + \tilde{\xi}_f(t) \quad . \tag{B.15}$$

From relations (B.12)- (B.15) we can show that $\tilde{\xi}_f(t)$ and $\tilde{\xi}_r(t)$ represent forward and reverse martingale difference sequences with respect to the σ-fields $\mathcal{J}_{t+1}$ and $\mathcal{T}_{t-1}$, respectively, i.e., $\tilde{\xi}_f(t)$ is adapted to $\mathcal{J}_{t+1}$, $\tilde{\xi}_r(t)$ is adapted to $\mathcal{T}_{t-1}$, and we have both

$$E[\tilde{\xi}_f(t)|\mathcal{J}_t] = 0 \quad , \tag{B.16}$$

and $$E[\tilde{\xi}_r(t)|\mathcal{T}_t] = 0 \quad . \tag{B.17}$$

This martingale difference property [47] implies that $\tilde{\xi}_f(\cdot)$ and $\tilde{\xi}_r(\cdot)$ represent discrete white noise sequences associated with forward and reverse Markovian realizations of the smoothing error process specified by relations (B.14) - (B.15).

Employing the definition of $\xi(t)$ in relation (B.3), and letting

$$\tilde{\xi}_r(t) = B(t)\tilde{u}_r(t) \quad , \tag{B.18}$$

and $$\tilde{\xi}_f(t) = B(t)\tilde{u}_f(t) \quad , \tag{B.19}$$

relations (B.12) - (B.15) imply the following reverse and forward Markovian realizations of the smoothing error process:

$$\tilde{x}_s(t) = A^{-1}(t)\tilde{x}_s(t+1) - A^{-1}(t)B(t)E[u(t)|\tilde{X}^+_{t+1}] - A^{-1}(t)B(t)\tilde{u}_r(t), \tag{B.20}$$

and $$\tilde{x}_s(t+1) = A(t)\tilde{x}_s(t) + B(t)E[u(t)|\tilde{X}^-_{t+1}] + B(t)\tilde{u}_f(t), \tag{B.21}$$

where

$$\tilde{u}_r(t) = u(t) - E[u(t)|\tilde{X}^+_{t+1}] - E[u(t)|\mathbf{y}] \quad , \tag{B.22}$$

and $$\tilde{u}_f(t) = u(t) - E[u(t)|\tilde{X}^-_{t+1}] - E[u(t)|\mathbf{y}] \quad . \tag{B.23}$$

We note here that unlike in continuous time, $\tilde{u}_r(\cdot)$ and $\tilde{u}_f(\cdot)$ are not standard discrete white noise sequences, i.e., their covariances must be determined from relations (B.22) - (B.23).

To complete the specification of the reverse and forward realizations of $\tilde{x}_s(\cdot)$, we need to compute $E[u(t)|\tilde{X}^+_{t+1}]$ and $E[u(t)|\tilde{X}^-_{t+1}]$. In what follows, we first verify directly the calculation of $E[u(t)|\tilde{X}^+_{t+1}]$, by employing an explicit representation for the smoothing errors derived from the innovations form of the smoothed estimate. We then approach the calculation of $E[u(t)|\tilde{X}^-_{t+1}]$ indirectly, by using Weinert and Desai's formulation to derive a forward model for the smoothing errors, and then identifying both $E[u(t)|\tilde{X}^-_{t+1}]$ and $\tilde{u}_f(t)$ in this setting.

We will now show that

$$E[u(t)|\tilde{X}^+_{t+1}] = B'(t)P^{-1}_{fp}(t+1)\tilde{x}_s(t+1) = E[u(t)|\tilde{x}_s(t+1)], \tag{B.24}$$

where $P_{fp}(t+1)$ denotes the one-step ahead, prediction error covariance matrix at time t+1. We prove (B.24) by verifying the orthogonality condition

$$E\left[\left(u(t) - B'(t)P^{-1}_{fp}(t+1)\tilde{x}_s(t+1)\right)\tilde{x}'_s(t+\ell)\right] = 0 , \tag{B.25}$$

for $\ell \geq 1$. We employ the following representation of $\tilde{x}_s(t)$, which follows from the innovations solution to the discrete time smoothing problem (see Appendix 2A):

$$\tilde{x}_s(t) = \tilde{x}_{fp}(t) - P_{fp}(t) \sum_{j=t}^{T} \Gamma'_{t,j} H'(j) P_\nu^{-1}(j) \nu(j) , \qquad (B.26)$$

where $\tilde{x}_{fp}(t)$ denotes the one-step ahead prediction error at time t, $\Gamma_{t,j}$ corresponds to the discrete transition matrix associated with the evolution of the $\hat{x}_{fp}(\cdot)$'s, and $\nu(j)$ denotes the discrete innovations process. Using equations for the evolution of $\tilde{x}_{fp}(\cdot)$ (see Appendix 2A) we compute the correlation matrices $E[u(t)\tilde{x}'_s(t+\ell)]$ and $E[\tilde{x}_s(t+1)\tilde{x}'_s(t+\ell)]$ as

$$E[u(t)\tilde{x}'_s(t+\ell)] = B'(t)\Gamma'_{t+1,t+\ell} - \left[\sum_{j=t+\ell}^{T} B'(t)\Gamma'_{t+1,j} H'(j) P_\nu^{-1}(j) H(j) \Gamma_{t+\ell,j} \right] P_{fp}(t+\ell), \qquad (B.27)$$

and

$$E[\tilde{x}_s(t+1)\tilde{x}'_s(t+\ell)] = P_{fp}(t+1)\Gamma'_{t+1,t+\ell} - P_{fp}(t+1)\left[\sum_{j=t+\ell}^{T} \Gamma'_{t+1,j} H'(j) P_\nu^{-1}(j) H(j) \Gamma_{t+\ell,j} \right] P_{fp}(t+\ell). \qquad (B.28)$$

Substitution of relations (B.27) - (B.28) into (B.25) results in the validation of the desired orthogonality condition. Finally, we can check the second equality of relation (B.24) by forming $E[u(t)|\tilde{x}_s(t+1)]$ as

$$E[u(t)|\tilde{x}_s(t+1)] = E[u(t)\tilde{x}_s'(t+1)]\left[E[\tilde{x}_s(t+1)\tilde{x}_s'(t+1)]\right]^{-1}\tilde{x}_s(t+1), \tag{B.29}$$

and using relations (B.27) - (B.28) to compute the required correlation matrices.

By substituting relation (B.24) into (B.20) we obtain the following backward model for $\tilde{x}_s(\cdot)$:

$$\boxed{\tilde{x}_s(t) = A^{-1}(t)\left(I - B(t)B'(t)P_{fp}^{-1}(t+1)\right)\tilde{x}_s(t+1) - A^{-1}(t)B(t)\tilde{u}_r(t).} \tag{B.30}$$

By using relations derived in the discussion of the discrete Hamiltonian and Rauch-Tung-Striebel smoothing formulae of Appendix 2A, we may show that

$$E[u(t)|\mathbf{y}] = B'(t)P_{fp}^{-1}(t+1)\left(\hat{x}_s(t+1) - \hat{x}_{fp}(t+1)\right). \tag{B.31}$$

Therefore, by substituting (B.24) and (B.31) into our expression (B.22) for $\tilde{u}_r(t)$, we obtain the simpler relation

$$\tilde{u}_r(t) = u(t) - B'(t)P_{fp}^{-1}(t+1)\tilde{x}_{fp}(t+1) \ . \qquad (B.32)$$

By employing relation (B.32), we compute the covariance of the noise $\tilde{u}_r(t)$ as

$$E[\tilde{u}_r(t)\tilde{u}_r'(t)] = I - B'(t)P_{fp}^{-1}(t+1)B(t) \ . \qquad (B.33)$$

The backward realization for $\tilde{x}_s(\cdot)$ determined by relations (B.30), (B.32) falls directly out of the discrete time version of the approach in Section 3.3, which is suggested in Badawi's thesis [84]. This second approach for deriving the same backward model for $\tilde{x}_s(\cdot)$ illustrates the point that the structure of that model is completely determined by the structure of the backward realization for the one-step ahead prediction errors. We first note that the innovations smoothing formula can be written as

$$\hat{x}_s(t) = \hat{x}_{fp}(t) + E\left[x(t) \mid \boldsymbol{\nu}_t^+\right] \ . \qquad (B.34)$$

Hence, by representing $x(t)$ in (B.34) as $\hat{x}_{fp}(t) + \tilde{x}_{fp}(t)$, observing that $\hat{x}_{fp}(t) \perp \boldsymbol{\nu}_t^+$, and using (B.34) to form $\tilde{x}_s(t)$, we find

that

$$\tilde{x}_s(t) = \tilde{x}_{fp}(t) - E\left[\tilde{x}_{fp}(t) \mid \boldsymbol{\nu}_t^+\right] \quad . \tag{B.35}$$

We now note that the equations in Appendix 2A for the evolution of $\tilde{x}_{fp}(i)$ may be rewritten as

$$\tilde{x}_{fp}(i+1) = A(i)\tilde{x}_{fp}(i) + B(i)u(i) - A(i)P_f(i)H'(i)R^{-1}(i)\nu(i) \quad . \tag{B.36}$$

Assuming that A(i) is invertible, in order to effect a deterministic reversal of relation (B.36), and decomposing u(i) with respect to $\sigma\{\tilde{x}_{fp}(j+1) \quad j \geq i\}$ as

$$u(i) = B'(i)P_{fp}^{-1}(i+1)\tilde{x}_{fp}(i+1) + \tilde{u}_r(i) \quad , \tag{B.37}$$

where from (B.32) we note that $\tilde{u}_r(i)$ is the input to our backward model for $\tilde{x}_s(\cdot)$, we obtain from relation (B.36) the following backward model for $\tilde{x}_{fp}(\cdot)$:

$$\begin{aligned}\tilde{x}_{fp}(i) = {} & A^{-1}(i)\left(I - B(i)B'(i)P_{fp}^{-1}(i+1)\right)\tilde{x}_{fp}(i+1) \\ & - A^{-1}(i)B(i)\tilde{u}_r(i) + P_f(i)H'(i)R^{-1}(i)\nu(i) \quad . \end{aligned} \tag{B.38}$$

As a consequence of equation (B.35), the backward model for $\tilde{x}_s(\cdot)$ of relations (B.30), (B.32) is immediately determined from (B.38). This follows from the fact that we can condition both sides of (B.38) with respect to $\mathbf{y}$ to obtain a backward equation for the evolution of $E\left[\tilde{x}_{fp}(i) \mid \boldsymbol{\nu}_i^+\right]$, so as to perform the subtraction in relation (B.35), and derive the desired backward model for $\tilde{x}_s(\cdot)$.

We now introduce the discrete time version of the formulation of Weinert and Desai, in order to derive a forward Markovian realization for the smoothing error process. We will then make the connection between the realization that we obtain, and the form predicted by relations (B.21), (B.23). As in continuous time, we assume that the observations $y(\cdot)$ are scaled, i.e., we let

$$y(t) = \bar{H}(t)x(t) + \bar{v}(t) \ , \tag{B.39}$$

where $$\bar{H}(t) = R^{-1/2}(t)H(t) \ , \tag{B.40}$$

$$\bar{v}(t) = R^{-1/2}(t)\, D(t)\, v(t) \ , \tag{B.41}$$

and $\bar{v}(\cdot)$ is now a standard discrete white noise sequence. In addition, we model $x(0)$ as

$$x(0) = M\delta \quad , \tag{B.42}$$

where M is a matrix of rank $q \leq n$ such that

$$\pi(0) = MM' \quad , \tag{B.43}$$

and δ represents a vector of q orthonormal random variables.

Retracing the steps of the continuous time derivation for the forward realization of $\tilde{x}_s(\cdot)$, we define the space S containing both the state and measurement processes as

$$S \triangleq H(\delta, u(i), \bar{v}(i+1) \quad i = 0, \ldots, T-1) \quad , \tag{B.44}$$

and the complementary space Y_c by requiring that

$$S = Y \oplus Y_c \quad . \tag{B.45}$$

Hence, since $x(t) \in S$ and $\hat{x}_s(t) = E[x(t)|Y]$, from relation (B.45) we may compute $\tilde{x}_s(t)$ as

$$\tilde{x}_s(t) = E[x(t)|Y_c] \quad . \tag{B.46}$$

We now identify a basis for Y_c that allows us to represent $\tilde{x}_s(t)$ by employing relation (B.46). To determine our basis for Y_c, we write out the observation equation (B.39) more explicitly as

$$y(i) = \bar{H}(i)\Phi_{i,0}M\mathcal{E} + \sum_{j=0}^{i-1} \bar{H}(i)\Phi_{i,j+1}B(j)u(j) + \bar{v}(i), \qquad (B.47)$$

where $\Phi_{\cdot,\cdot}$ denotes the discrete transition matrix defined by

$$\Phi_{\ell_1,\ell_2} = \begin{cases} I & \ell_1 = \ell_2 \\ \prod_{j=\ell_2}^{\ell_1-1} A(j) & \ell_1 \geq \ell_2+1 \end{cases} . \qquad (B.48)$$

Then, we identify the operators L and G as mapping the vector e, in R^q, and the p-vector sequence $\psi(\cdot)$, as

$$e \quad \text{into} \quad \bar{H}(\cdot)\Phi_{\cdot,0}\, M\, e \quad , \qquad (B.49)$$

$$\text{and} \qquad \psi(\cdot) \text{ into } \sum_{j=0}^{\cdot-1} \bar{H}(\cdot)\Phi_{\cdot,j+1}B(j)\psi(j) \quad , \qquad (B.50)$$

repectively. Assuming that the inner product on R^q is the dot product of two q-vectors, and the inner product on the space of p-vector valued functions on [0,T] is defined as

$$\langle \psi_1(\cdot), \psi_2(\cdot) \rangle \triangleq \sum_{i=0}^{T} \psi_1'(i)\psi_2(i) \ , \tag{B.51}$$

the adjoint operators L* and G* may be determined. At this point we define the new quantities

$$z(\cdot) \triangleq u(\cdot) - G^*(\bar{v}(\cdot)) \ , \tag{B.52}$$

and

$$\theta \triangleq \delta - L^*(\bar{v}(\cdot)) \ . \tag{B.53}$$

Letting Z denote the space spanned by the $z(\cdot)$'s, we show in what follows, that we may express the complementary space Y_c as

$$Y_c = Z \vee H(\theta) \ . \tag{B.54}$$

The proof of (B.54) proceeds in the same manner as for the continuous smoothing problem. We will sketch the details more briefly here. We first note that $G^*(\bar{v}(\cdot))$ and $L^*(\bar{v}(\cdot))$ may be expressed as

$$G^*(\bar{v}(\cdot)) = B'(\cdot) \sum_{i=\cdot+1}^{T} \Phi_{i,\cdot+1}' \bar{H}'(i)\bar{v}(i) \ , \tag{B.55}$$

and

$$L^*(\bar{v}(\cdot)) = M' \sum_{i=1}^{T} \Phi_{i,0}' \bar{H}'(i)\bar{v}(i) \ . \tag{B.56}$$

By substituting (B.55) and (B.56) into (B.52) and (B.53), and employing relation (B.47) for $y(i)$, we can show that $Z \vee H(\theta) \perp Y$. Now, since from the definitions of $y(i)$, θ, $z(i)$, $Y \oplus (Z \vee H(\theta)) \in S$, we need only prove the reverse inclusion, $S \in Y \oplus (Z \vee H(\theta))$, in order to validate relation (B.54).

To later facilitate our construction of $E[x(t)|Y_c]$, and in order to prove that $S \in Y \oplus (Z \vee H(\theta))$, we define the process $\gamma(\cdot)$ by

$$\gamma(j) \triangleq \sum_{i=j+1}^{T} \Phi'_{i,j+1} \bar{H}'(i)\bar{v}(i) \quad . \tag{B.57}$$

From relation (B.57) we can show that $\gamma(\cdot)$ evolves according to the backward equations

$$\gamma(j) = A'(j+1)\gamma(j+1) + \bar{H}'(j+1)\bar{v}(j+1) \quad , \tag{B.58}$$

with $$\gamma(T) = 0 \quad . \tag{B.59}$$

By employing relation (B.57), the equations (B.52) and (B.53) may be expressed as

$$z(i) = -B'(i)\gamma(i) + u(i) \quad , \tag{B.60}$$

and $$\theta = \delta - M'A'(0)\gamma(0) \quad . \tag{B.61}$$

Now, by rearranging relations (B.39), (B.60), and (B.61) we can show that $\bar{v}(\cdot)$, $u(\cdot)$, and δ are determined by knowledge of $\gamma(\cdot)$, $x(\cdot)$. Finally, in a manner exactly analogous to the continuous time case, we can show that given θ, $y(\cdot)$, and $z(\cdot)$, $x(\cdot)$ and $\gamma(\cdot)$ are determined as the solution of an appropriate two-point boundary value problem. Therefore, we can show that $S \varepsilon Y \oplus (Z \vee H(\theta))$, completing the verification of relation (B.54).

Having shown that θ, $z(\cdot)$ form a basis for Y_c, we can equivalently form a basis for Y_c from $\tilde{\theta}$, $\alpha(\cdot)$ where

$$\tilde{\theta} = \theta - E[\theta|Z] \quad , \tag{B.62}$$

and

$$\alpha(i) = z(i) - E[z(i)|Z_{i+1}^{+}] \quad . \tag{B.63}$$

From relations (B.62) and (B.63) we observe that $\alpha(\cdot)$ represents the discrete innovations sequence corresponding to $z(\cdot)$, and $\tilde{\theta} \perp \alpha(\cdot)$, motivating the following orthogonal decomposition of Y_c:

$$Y_c = H(\tilde{\theta}) \oplus \boldsymbol{\alpha} \, . \tag{B.64}$$

We finally obtain a forward Markovian realization for $\tilde{x}_s(t)$ by using the decomposition of Y_c in relation (B.64) in order to form $E[x(t)|Y_c]$ as

$$\tilde{x}_s(t) = E[x(t)\tilde{\theta}']E[\tilde{\theta}\,\tilde{\theta}']^{-1}\tilde{\theta}$$

$$+ \sum_{i=0}^{T-1} E[x(t)\alpha'(i)]E[\alpha(i)\alpha'(i)]^{-1}\alpha(i) \quad . \tag{B.65}$$

By employing relations (B.58) - (B.60) to define the reverse filtered and predicted estimates $\hat{\gamma}_r(t)$ and $\hat{\gamma}_{rp}(t)$ as

$$\hat{\gamma}_r(t) \triangleq E[\gamma(t)|Z_t^+] \quad , \tag{B.66}$$

and

$$\hat{\gamma}_{rp}(t) \triangleq E[\gamma(t)|Z_{t+1}^+] \quad , \tag{B.67}$$

with $\tilde{\gamma}_r(t)$ and $\tilde{\gamma}_{rp}(t)$ denoting the corresponding reverse filtering and prediction errors, we can express $\tilde{\theta}$ and $\alpha(t)$ as

$$\tilde{\theta} = \delta - M'A'(0)\tilde{\gamma}_r(0) \quad , \tag{B.68}$$

and

$$\alpha(t) = u(t) - B'(t)\tilde{\gamma}_{rp}(t) \quad . \tag{B.69}$$

We will let $P_b(\cdot)$ and $P_{bp}(\cdot)$ denote the filtering and prediction error covariance matrices associated with the estimates $\hat{\gamma}_r(\cdot)$ and $\hat{\gamma}_{rp}(\cdot)$, respectively.

We now employ relations (B.68) - (B.69) to motivate the calculation of the correlation matrices that appear in relation

(B.65). By using standard discrete time Kalman filtering equations to obtain backward recursions for $\hat{\gamma}_r(\cdot)$ and $\hat{\gamma}_{rp}(t)$, we can derive the following backward equations for the evolution of $\tilde{\gamma}_{rp}(\cdot)$ and $\tilde{\gamma}_r(\cdot)$:

$$\tilde{\gamma}_{rp}(j) = A'(j+1)\left(I - P_b(j+1)B(j+1)B'(j+1)\right)\tilde{\gamma}_{rp}(j+1)$$
$$+ A'(j+1)P_b(j+1)B(j+1)u(j+1) + \bar{H}'(j+1)\bar{v}(j+1), \quad (B.70)$$

with $$\tilde{\gamma}_{rp}(T-1) = \bar{H}'(T)\bar{v}(T) \ , \quad (B.71)$$

and $$\tilde{\gamma}_r(j) = \left(I - P_b(j)B(j)B'(j)\right)A'(j+1)\tilde{\gamma}_r(j+1)$$
$$+ \left(I - P_b(j)B(j)B'(j)\right)\bar{H}'(j+1)\bar{v}(j+1) + P_b(j)B(j)u(j) \ , \quad (B.72)$$

with $$\tilde{\gamma}_r(T) = 0 \ . \quad (B.73)$$

Now by using relations (B.70) - (B.73) to obtain explicit formulae for $\tilde{\gamma}_{rp}(t)$ and $\tilde{\gamma}_r(0)$, and substituting the resulting expressions into (B.69) and (B.68), we can obtain the following expressions for $E[x(t)\tilde{\theta}']$ and $E[x(t)\alpha'(t')]$:

$$E[x(t)\tilde{\theta}'] = \Phi^*_{t,0} M \ , \quad (B.74)$$

and

$$E[x(t)\alpha'(t')] = \begin{cases} 0 & t' \geq t \\ \Phi^*_{t,t'+1} B(t') & t' < t \end{cases} , \qquad (B.75)$$

where $\Phi^*_{i_2,i_1}$ is defined by

$$\Phi^*_{i_2,i_1} \triangleq \begin{cases} I & i_2 = i_1 \\ \prod_{\ell=i_1}^{i_2-1} \left(I - B(\ell)B'(\ell)P_b(\ell)\right)A(\ell) & i_2 \geq i_1+1 \end{cases} . \qquad (B.76)$$

Finally, we note from (B.68), (B.69) that $E[\tilde{\theta}\,\tilde{\theta}']$ and $E[\alpha(t)\alpha'(t)]$ are given by

$$E[\tilde{\theta}\,\tilde{\theta}'] = I + M'A'(0)P_b(0)A(0)M , \qquad (B.77)$$

and $$E[\alpha(t)\alpha'(t)] = I + B'(t)P_{bp}(t)B(t) . \qquad (B.78)$$

Thus, by using relations (B.74) - (B.78) in relation (B.65), we obtain the following forward model for $\tilde{x}_s(\cdot)$:

Forward Model for the Smoothing Errors following from Weinert and Desai's Formulation

$$\tilde{x}_s(t+1) = \left(I - B(t)B'(t)P_b(t)\right)A(t)\tilde{x}_s(t) + B(t)\left(I + B'(t)P_{bp}(t)B(t)\right)^{-1}\alpha(t) \quad , \tag{B.79}$$

where $$\tilde{x}_s(0) = M\left(I + M'A'(0)P_b(0)A(0)M\right)^{-1}\tilde{\theta} \quad . \tag{B.80}$$

If we compare relation (B.79) with the model for $\tilde{x}_s(\cdot)$ of (B.21), obtained by the noise decomposition approach, we are tempted to identify $E[u(t)|\tilde{X}^-_{t+1}]$ and $\tilde{u}_f(t)$ as

$$E[u(t)|\tilde{X}^-_{t+1}] = -B'(t)P_b(t)A(t)\tilde{x}_s(t) \quad , \tag{B.81}$$

and $$\tilde{u}_f(t) = \left(I + B'(t)P_{bp}(t)B(t)\right)^{-1}\alpha(t) \quad . \tag{B.82}$$

We will conclude this Appendix by verifying relations (B.81) - (B.82).

We first check relation (B.81), by validating the orthogonality condition

$$E\left[\left(u(t) + B'(t)P_b(t)A(t)\tilde{x}_s(t)\right)\tilde{x}'_s(\ell)\right] = 0 \quad , \tag{B.83}$$

for $\ell = 0,\ldots,t$. To compute the correlation matrices that appear in relation (B.83), we use the representation for $\tilde{x}_s(t)$

in (B.65), i.e.,

$$\tilde{x}_s(t) = \Phi^*_{t,0} M\left(I + M'A'(0)P_b(0)A(0)M\right)^{-1}\tilde{\theta}$$

$$+ \sum_{t'=0}^{t-1} \Phi^*_{t,t'+1} B(t')\left(I + B'(t')P_{bp}(t')B(t')\right)^{-1}\alpha(t') \quad . \quad (B.84)$$

By employing relation (B.84) and the mutual orthogonality of $\tilde{\theta}$, $\alpha(\cdot)$, we compute $E[\tilde{x}_s(t)\tilde{x}'_s(\ell)]$ as

$$E[\tilde{x}_s(t)\tilde{x}'_s(\ell)] = \Phi^*_{t,0} M\left(I + M'A'(0)P_b(0)A(0)M\right)^{-1} M'\Phi^{*\prime}_{\ell,0}$$

$$+ \sum_{t'=0}^{\ell-1} \Phi^*_{t,t'+1} B(t')\left(I + B'(t')P_{bp}(t')B(t')\right)^{-1}$$

$$\cdot\, B'(t')\Phi^{*\prime}_{\ell,t'+1} \quad . \quad (B.85)$$

Finally, using relations (B.68) - (B.69) to express $\tilde{\theta}$ and $\alpha(t')$, and employing the $\tilde{\gamma}_{rp}(\cdot)$ and $\tilde{\gamma}_r(\cdot)$ dynamics given by relations (B.70) and (B.72), we can establish the following string of identities:

$$E[u(t)\tilde{\theta}'] = - E[u(t)\tilde{\gamma}'_r(0)]A(0)M = - B'(t)P_b(t)A(t)\Phi^*_{t,0}M \quad , \quad (B.86)$$

and

$$E[u(t)\alpha'(t')] = - E[u(t)\tilde{\gamma}'_{rp}(t')]B(t')$$

$$= - B'(t)P_b(t)A(t)\Phi^*_{t,t'+1}B(t') \ , \qquad (B.87)$$

for $t' = 0,\ldots,\ell-1$, $\ell-1 < t$. Now, by using relation (B.86) and (B.87) we can show that $E[u(t)\tilde{x}'_s(\ell)]$, for $\ell = 0,\ldots,t$, may be expressed as

$$E[u(t)\tilde{x}'_s(\ell)] = - B'(t)P_b(t)A(t)\Phi^*_{t,0}M\left(I + M'A'(0)P_b(0)A(0)M\right)^{-1}M'\Phi^{*\prime}_{\ell,0}$$

$$+ \sum_{t'=0}^{\ell-1} - B'(t)P_b(t)A(t)\Phi^*_{t,t'+1}$$

$$\cdot\ B(t')\left(I + B'(t')P_{bp}(t')B(t')\right)^{-1}B'(t')\Phi^{*\prime}_{\ell,t'+1} \ . \qquad (B.88)$$

Substituting relations (B.85) and (B.88) into relation (B.83), we can verify the desired orthogonality condition.

We finally sketch the proof of relation (B.82) relating the input noise to the forward smoothing error model derived from a process noise decomposition approach, with the input noise appearing in the forward model derived from Weinert and Desai's formulation. We verify (B.82) as a consequence of

connecting the discrete Hamiltonian equation for generating $\hat{x}_s(\cdot)$ with the forward recursion for $\hat{x}_s(\cdot)$ that follows from using our state dynamics $x(\cdot)$, and forward smoothing error model (B.79), to form

$$\hat{x}_s(i) = x(i) - \tilde{x}_s(i) \quad . \tag{B.89}$$

By using the above relation as described we obtain the following forward recursion for $\hat{x}_s(\cdot)$:

$$\hat{x}_s(t+1) = A(t)\hat{x}_s(t)$$

$$+ B(t)B'(t)\left[\tilde{\gamma}_{rp}(t) + P_b(t)(A(t)\tilde{x}_s(t) + B(t)\alpha(t))\right] . \tag{B.90}$$

Motivated by the comparison of (B.90) with the forward equation for $\hat{x}_s(\cdot)$ appearing in the discrete Hamiltonian equations for smoothing, we can prove that the adjoint variables $\lambda(t+1|T)$ can be expressed as

$$\lambda(t+1|T) = \tilde{\gamma}_{rp}(t) + P_b(t)\Big(A(t)\tilde{x}_s(t) + B(t)\alpha(t)\Big) \quad . \tag{B.91}$$

The proof of (B.91) consists of verifying that both sides satisfy the same backward equation with identical end conditions. Given relation (B.91) we can solve for $\tilde{\gamma}_{rp}(t)$, and

substitute the result into (B.69) for $\alpha(t)$ to find that

$$\alpha(t) = u(t) - B'(t)[\lambda(t+1|T) - P_b(t)A(t)\tilde{x}_s(t) - P_b(t)B(t)\alpha(t)]. \tag{B.92}$$

By rearranging equation (B.92), and employing the identity

$$\left(I + B'(t)P_{bp}(t)B(t)\right)^{-1} = I - B'(t)P_b(t)B(t) , \tag{B.93}$$

we obtain the following relation:

$$\left(I + B'(t)P_{bp}(t)B(t)\right)^{-1}\alpha(t) = u(t) - B'(t)\lambda(t+1|T) + B'(t)P_b(t)A(t)\tilde{x}_s(t) . \tag{B.94}$$

But now, noting from Appendix 2A that

$$E[u(t)|\mathbf{y}] = B'(t)\lambda(t+1|T) , \tag{B.95}$$

and by taking account of relation (B.81), we can recognize the right-hand side of (B.94) to be $\tilde{u}_f(t)$, as defined in relation (B.23). Finally, having proved (B.82), we may use it in conjunction with (B.93) to compute the covariance of $\tilde{u}_f(t)$ as

$$E[\tilde{u}_f(t)\tilde{u}_f'(t)] = I - B'(t)P_b(t)B(t) \ . \qquad \text{(B.96)}$$

Chapter 4

Centralized Map-Updating and Map-Combining

4.1 Introduction

In Chapter 1 we motivated the centralized map-updating and map-combining problems, in the context of meteorological and geodetic data processing, as spatial data assimilation problems which provide a mathematical framework for combining a map of some underlying random field, based on old sensor surveys, with current data, or merging maps based on separate sensor surveys, respectively. We then defined the centralized map-updating and map-combining problems for the case of two-measurement passes over some one-dimensional tracks, along which the underlying process may be represented by some finite dimensional state-space model. In this setting the centralized map-updating problem is defined as that of computing the two-data pass smoothed state estimates as a linear functional of the first-pass smoothed estimate history, and the second-pass data. Similarly, the centralized map-combining problem was defined as that of computing the two-data pass smoothed state estimates as a linear functional of the individual smoothed estimate histories derived from each data pass separately. In Sections 4.2 and 4.3 we will solve these essentially one-

dimensional, two-data pass versions of the centralized map-updating and map-combining problems, respectively. Our solution technique will make use of Hilbert space decompositions of the two-data pass space, as well as results on Markovian realizations of the smoothing error process, which we derived in Chapter 3. In Appendix 4E we present the analogous solution of the discrete-time centralized map-updating problem, which we use in Chapter 7 to solve a discrete space map-updating problem.

In Appendices 4B - 4D we present several alternative approaches for solving the centralized map-updating problem. In Appendix 4B we present a M.A.P. approach, which results in some heuristic insights into the simplicity of the solution. In Appendix 4C we present a method of solution that involves algebraic manipulation of filtering and smoothing equations, and illustrates an approach that we apply later to derive solutions of map-centralization problems. Then in Appendix 4D, we demonstrate the power of the scattering formalism in facilitating a very quick solution to both the centralized map-updating and map-combining problems.

We finally note that the centralized map-updating and map-combining problems of this chapter may be useful in a general distributed processing setting. Let us imagine some network of processors which can communicate with each other,

and where each processor makes measurements of the same underlying phenomena. Then, the centralized map-updating and map-combining problem formulations provide a mathematical framework for individual processors to combine their own estimates with either data or estimates obtained from other processors.

4.2 Centralized Map-Updating

In this section we derive three two-filter algorithms for solving the two-measurement pass version of the centralized map-updating problem, as defined below. The first procedure, which we will call the Smoothing Error Filter Algorithm, will follow directly from using Hilbert space decompositions of the two-data pass space, and the smoothing error models of Chapter 3. The second and third forms of the centralized map-updating solution, which we will call the Information Filter Algorithm and the Symmetric Filter Algorithm, respectively, are each derived from the Smoothing Error Filter Algorithm, and ultimately serve to facilitate the derivation of the solution to the centralized map-combining problem in Section 4.3.

We now proceed to define the centralized map-updating problem considered in this section. We assume that we have some underlying state process $x(\cdot)$ modelled as

$$dx(t) = A\,x(t)\,dt + B\,du(t) \quad , \tag{4.1}$$

with an associated state covariance π defined as the solution to

$$\dot{\pi} = A\pi + \pi A' + BB' \quad .^{\dagger} \tag{4.2}$$

We assume that two-measurement passes have been made, with mutually independent measurement noises, and are modelled by

$$dy_1(t) = H_1 x(t)dt + D_1 dv_1(t) \quad , \tag{4.3}$$

and

$$dy_2(t) = H_2 x(t)dt + D_2 dv_2(t) \quad , \tag{4.4}$$

where

$$D_1 D_1' = R_1 > 0 \quad , \tag{4.5}$$

and

$$D_2 D_2' = R_2 > 0 \quad . \tag{4.6}$$

Then, letting Y_i be defined as the Hilbert spaces spanned by the individual measurement passes, i.e.,

$$Y_i \triangleq H(dy_i(\tau) \quad 0 \leq \tau \leq T) \quad , \tag{4.7}$$

and Y denote the space spanned by both data passes, i.e.,

$$Y \triangleq Y_1 \vee Y_2 \quad , \tag{4.8}$$

---

†We will suppress the time dependence of system matrices, state covariance matrices, and error covariance matrices, for the sake of notational simplicity.

we can define the smoothed estimates $\hat{x}_{is}(t)$ corresponding to the maps derived from each data pass separately as

$$\hat{x}_{is}(t) = E[x(t)|Y_i] \quad , \tag{4.9}$$

and the smoothed estimate $\hat{x}_s(t)$ corresponding to the aggregate, two data pass map as

$$\hat{x}_s(t) = E[x(t)|Y] \quad . \tag{4.10}$$

We will let $\tilde{x}_{is}(t)$ and $\tilde{x}_s(t)$ denote the smoothing errors corresponding to the estimates (4.9) and (4.10), and P_{is},P_s denote the corresponding smoothing error covariance matrices. When we need to refer to the filtering error covariances associated with the estimation of $x(t)$ from either Y_{it}^- or Y_{it}^+, we will use the notations P_{if} and P_{ir}, respectively. In this context, the centralized map-updating problem is specified as that of computing $\hat{x}_s(\cdot)$ as a linear functional of $\hat{x}_{is}(\cdot)$ and the second pass data, $y_2(\cdot)$.

We next show how the solution to the centralized map-updating problem follows from the following orthogonal decomposition of the two data pass Hilbert space Y:

$$Y = Y_1 \oplus \tilde{Y}_2 \quad , \tag{4.11}$$

where $$\tilde{Y}_2 \triangleq H(d\tilde{y}_2(\tau) \quad 0 \le \tau \le T) \quad , \tag{4.12}$$

and $$d\tilde{y}_2(\tau) = dy_2(\tau) - E[dy_2(\tau)|Y_1] \quad . \tag{4.13}$$

The space $\tilde{Y}_2$ denotes the part of the second-pass data space Y_2 that is not predictable from the first-pass data, Y_1. By using the independence of the measurement noises, we can express $d\tilde{y}_2(\tau)$ as

$$d\tilde{y}_2(\tau) = dy_2(\tau) - H_2\hat{x}_{1s}(\tau)d\tau \quad , \tag{4.14}$$

or alternatively as

$$d\tilde{y}_2(\tau) = H_2\tilde{x}_{1s}(\tau)d\tau + D_2dv_2(\tau) \quad . \tag{4.15}$$

By projecting x(t) onto both sides of relation (4.11), and using the orthogonality property satisfied by first-pass smoothing errors, we find that

$$\hat{x}_s(t) = \hat{x}_{1s}(t) + E[\tilde{x}_{1s}(t)|\tilde{Y}_2] \quad . \tag{4.16}$$

Relation (4.16) represents the two-pass map as the sum of the first-pass map plus a correction term corresponding to an estimate for the first-pass map error. If we use (4.14) to define $d\tilde{y}_2(\cdot)$, we can see that the second term in (4.16) can be expressed as a linear functional of $\hat{x}_{1s}(\cdot)$ and $dy_2(\cdot)$, and hence equation (4.16) represents the solution to the centralized map-updating problem.

Therefore, the problem of deriving algorithms for map-updating reduces to the computation of the mean of $\tilde{x}_{1s}(t)$, conditioned on $\tilde{Y}_2$. From relation (4.15) we can see that the calculation of $E[\tilde{x}_{1s}(t)|\tilde{Y}_2]$ is essentially a fixed-interval smoothing problem, with the first-pass smoothing errors as the fundamental observed variables. Given (see Chapter 3) the following forward and reverse Markovian realizations of the first-pass smoothing errors:

$$d\tilde{x}_{1s}(t) = \left[A + Q(P_{1f}^{-1} - P_{1s}^{-1})\right]\tilde{x}_{1s}(t)dt + B\, d\tilde{u}_{1f}(t), \quad (4.17)$$

and

$$d\tilde{x}_{1s}(t) = \left[A + Q\, P_{1f}^{-1}\right]\tilde{x}_{1s}(t)dt + B\, d\tilde{u}_{1r}(t) \quad , \quad (4.18)$$

where $\tilde{u}_{1f}(\cdot)$ and $\tilde{u}_{1r}(\cdot)$ are standard Wiener processes, and

$$Q \triangleq BB' \quad , \quad (4.19)$$

the problem of computing $E[\tilde{x}_{1s}(t)|\tilde{Y}_2]$ may be solved by any of the approaches of Chapter 2.

In what follows, we first employ the Wall two-filter form of the smoother to compute $E[\tilde{x}_{1s}(t)|\tilde{Y}_2]$, and derive the Smoothing Error Filter Algorithm for solving the centralized map-updating problem. The remaining two procedures, the Information Filter Algorithm and the Symmetric Filter Algorithm for map-updating, will follow from different methods of forming $E[\tilde{x}_{1s}(t)|\tilde{Y}_2]$. In each case, we will display the relevant on-line equations defining the algorithms inside boxes.

4.2.1 The Smoothing Error Filter Algorithm for Map-Updating

We now define the following forward and reverse filtered estimates of $\tilde{x}_{1s}(t)$:

$$\hat{\tilde{x}}_f(t) \triangleq E[\tilde{x}_{1s}(t) | \tilde{Y}_{2t}^-] \quad , \tag{4.20}$$

and

$$\hat{\tilde{x}}_r(t) = E[\tilde{x}_{1s}(t) | \tilde{Y}_{2t}^+] \quad . \tag{4.21}$$

We will let P_{fs} and P_{rs} denote the filtering error covariance matrices corresponding to the estimates (4.20) and (4.21), respectively. Then, by using standard Kalman filtering results applied to the forward and reverse models for $\tilde{x}_{1s}(\cdot)$ specified by relations (4.17) and (4.18), and the observation equation (4.15), we obtain the following equations for the evolution of $\hat{\tilde{x}}_f(\cdot)$, P_{fs}, $\hat{\tilde{x}}_r(\cdot)$, and P_{rs}:

$$\boxed{d\hat{\tilde{x}}_f(t) = \left(A + Q(P_{1f}^{-1} - P_{1s}^{-1}) - P_{fs}H_2'R_2^{-1}H_2\right)\hat{\tilde{x}}_f(t)dt + P_{fs}H_2'R_2^{-1}d\tilde{y}_2(t),} \tag{4.22}$$

with

$$\boxed{\hat{\tilde{x}}_f(0) = 0 \ ,} \tag{4.23}$$

$$\dot{P}_{fs} = \left[A + Q(P_{1f}^{-1} - P_{1s}^{-1})\right]P_{fs} + P_{fs}\left[A + Q(P_{1f}^{-1} - P_{1s}^{-1})\right]' + Q - P_{fs}H_2'R_2^{-1}H_2P_{fs} \quad , \tag{4.24}$$

with $$P_{fs}(0) = P_{1s}(0) \quad , \tag{4.25}$$

$$\boxed{-d\hat{\tilde{x}}_r(t) = (-A - QP_{1f}^{-1} - P_{rs}H_2'R_2^{-1}H_2)\hat{\tilde{x}}_r(t)dt + P_{rs}H_2'R_2^{-1}d\tilde{y}_2(t) \quad ,} \tag{4.26}$$

with $$\boxed{\tilde{x}_r(T) = 0 \quad ,} \tag{4.27}$$

and

$$-\dot{P}_{rs} = (-A - QP_{1f}^{-1})P_{rs} + P_{rs}(-A - QP_{1f}^{-1})' + Q - P_{rs}H_2'R_2^{-1}H_2P_{rs} \quad , \tag{4.28}$$

with $$P_{rs}(T) = P_{1s}(T) \quad . \tag{4.29}$$

By using the relation (4.16), the two-pass smoothing error $\tilde{x}_s(t)$ may be expressed as

$$\tilde{x}_s(t) = \tilde{x}_{1s}(t) - E[\tilde{x}_{1s}(t)|\tilde{Y}_2] \quad , \tag{4.30}$$

and by applying Wall's formula for the two-pass smoothing error covariance matrix (see Chapter 2), we can express P_s^{-1} as

$$P_s^{-1} = P_{fs}^{-1} + P_{rs}^{-1} - P_{ls}^{-1} \quad , \tag{4.31}$$

and $E[\tilde{x}_{ls}(t)|\tilde{Y}_2]$ is given by the two filter formula

$$\boxed{E[\tilde{x}_{ls}(t)|\tilde{Y}_2] = P_s\left\{P_{fs}^{-1}\hat{\tilde{x}}_f(t) + P_{rs}^{-1}\hat{\tilde{x}}_r(t)\right\} \quad .} \tag{4.32}$$

Hence, our first procedure for map updating is obtained by substituting (4.32) into (4.16), and using (4.22) - (4.23) and (4.26) - (4.27) to compute $\hat{\tilde{x}}_f(\cdot)$ and $\hat{\tilde{x}}_r(\cdot)$, respectively. The error covariances P_{fs}, P_{rs} are computed off-line by the equations (4.24) - (4.25) and (4.28) - (4.29), respectively.

4.2.2 Information Filter Algorithm for Map-Updating

In what follows we will identify two alternative forms of relation (4.32) that will aid us in connecting the solution to the map-updating problem described above, with a similar algorithm obtained from the scattering perspective. The first alternative form of relation (4.32) is obtained by defining $\gamma_f(t)$ and $\gamma_r(t)$ as

$$\gamma_f(t) = P_{fs}^{-1} \hat{\tilde{x}}_f(t) \quad , \tag{4.33}$$

and

$$\gamma_r(t) = P_{rs}^{-1} \hat{\tilde{x}}_r(t) \quad . \tag{4.34}$$

By using the relations (4.22) - (4.34) we can derive the following stochastic differential equations for the evolution of $\gamma_f(\cdot)$ and $\gamma_r(\cdot)$:

$$\boxed{d\gamma_f(t) = \left[-A' - \left\{P_{1f}^{-1} + P_{fs}^{-1} - P_{1s}^{-1}\right\}Q\right]\gamma_f(t)dt + H_2'R_2^{-1}d\tilde{y}_2(t),} \tag{4.35}$$

with $$\boxed{\gamma_f(0) = 0 \ ,} \tag{4.36}$$

and

$$\boxed{-d\gamma_r(t) = \left[A' + \left\{P_{1f}^{-1} - P_{rs}^{-1}\right\}Q\right]\gamma_r(t)dt + H_2'R_2^{-1}d\tilde{y}_2(t) \ ,} \tag{4.37}$$

with $\boxed{\gamma_r(T) = 0 \quad .}$ (4.38)

Then by substituting (4.33) - (4.34) into (4.32) we derive the following relation:

$$\boxed{E[\tilde{x}_{1s}(t)|\tilde{Y}_2] = P_s\{\gamma_f(t) + \gamma_r(t)\} \quad .} \tag{4.39}$$

We next derive alternative forms of equations (4.35) and (4.37) that will lead to a final technique for calculating $E[\tilde{x}_{1s}(t)|\tilde{Y}_2]$ in Section 4.2.3. Our alternative forms for (4.35) and (4.37) are obtained by expressing the bracketed terms in those relations in terms of quantities related to the forward and reverse two-pass filtering error covariance matrices, which we will now define.

We let P_f denote the two-pass filtering error covariance matrix associated with the forward two-pass filtered estimate, $\hat{x}_f(t)$, defined by

$$\hat{x}_f(t) = E[x(t)|Y_t^-] \quad , \tag{4.40}$$

where $$Y_t^- = Y_{1t}^- \vee Y_{2t}^- \quad . \tag{4.41}$$

Similarly, we let P_r denote the two-pass filtering error covariance matrix associated with the reverse two-pass filtered estimate, $\hat{x}_r(t)$, defined by

$$\hat{x}_r(t) = E[x(t)|Y_t^+] \quad , \tag{4.42}$$

where $$Y_t^+ = Y_{1t}^+ \vee Y_{2t}^+ \quad . \tag{4.43}$$

Finally, we define the quantities O_{01} and O_0 by requiring that

$$P_{1s}^{-1} = P_{1f}^{-1} + O_{01} \quad , \tag{4.44}$$

and $$P_s^{-1} = P_f^{-1} + O_0 \quad , \tag{4.45}$$

so that by comparing (4.44) - (4.45) with the corresponding expressions for P_{1s}^{-1} and P_s^{-1} associated with the Wall two-filter formulae for $\hat{x}_{1s}(\cdot)$ and $\hat{x}_s(\cdot)$, we find that

$$O_{01} = P_{1r}^{-1} - \pi^{-1} \quad , \tag{4.46}$$

and $$O_0 = P_r^{-1} - \pi^{-1} \quad . \tag{4.47}$$

If we think of the inverse of an error covariance matrix, associated with a given estimate, as conveying the amount of

information contained in that estimate, then relations (4.46) - (4.47) signify that O_{01} and O_0 are obtained by subtracting the a-priori information from the information contained in the appropriate backwards filtered estimate. Hence, we can think of O_{01} and O_0 as representing the information on x(t) contained in the future observations alone, not using a-priori knowledge. In fact, we can show that O_{01} and O_0 are the inverses of the error covariance matrices P_{1B} and P_B, respectively, associated with the backwards filtered estimates appearing the the Mayne-Fraser solution to the first- and two-pass smoothing problems, respectively.

Having defined the two-pass forward and reverse filtering error covariance matrices P_f and P_r, and specified and interpreted O_0 and O_{01}, we are ready to motivate the following two identities, which result in alternative forms for relations (4.35) and (4.37), and are proved formally in Appendix 4A:

$$P_f^{-1} = P_{1f}^{-1} + P_{fs}^{-1} - P_{1s}^{-1} \quad , \tag{4.48}$$

and

$$O_0 = P_{rs}^{-1} - P_{1f}^{-1} \quad . \tag{4.49}$$

We can motivate relation (4.48) in terms of combining information on x(t) contained in Y_t^- and Y_{1t}^+ by rearranging it in the form:

$$P_{fs}^{-1} = P_{f}^{-1} + O_{01} \quad . \tag{4.50}$$

In Appendix 4A we show that the error covariance matrix P_{fs} is equivalent to that associated with an estimate, $\hat{x}_{fs}(t)$, for $x(t)$, based on Y_t^- and Y_{1t}^+. Since O_{01} represents the new information contained in the future observations Y_{1t}^+, we obtain equation (4.50). Similarly, we may motivate the relation (4.49) by rewriting it as

$$P_{rs}^{-1} = P_{1f}^{-1} + O_0 \quad . \tag{4.51}$$

If we let $\hat{x}_{rs}(t)$ denote an estimate for $x(t)$ based on Y_t^+ and Y_{1t}^-, then it can be shown that the error covariance matrix associated with $\hat{x}_{rs}(t)$ is identical to P_{rs}. Since O_0 represents the new information contained in Y_t^+, we obtain equation (4.51).

Hence, by employing relations (4.48) and (4.49), the equations (4.35) and (4.37) for generating $\gamma_f(\cdot)$ and $\gamma_r(\cdot)$ can be rewritten as follows:

$$d\gamma_f(t) = (-A' - P_f^{-1}Q)\gamma_f(t)dt + H_2'R_2^{-1}d\tilde{y}_2(t) \ , \tag{4.52}$$

and

$$-d\gamma_r(t) = (A' - O_0Q)\gamma_r(t)dt + H_2'R_2^{-1}d\tilde{y}_2(t) \quad . \tag{4.53}$$

Therefore, the Information Filter Algorithm for map-updating is specified by using relations (4.52) - (4.53) to form $E[\tilde{x}_{1s}(t)|\tilde{Y}_2]$, in equation (4.39), and substituting the result into (4.16). The quantities P_f and O_0 are computed offline by using standard equations for the evolution of filtering covariance matrices, and relation (4.47), respectively. In Appendix 4B we show how an algorithm for computing $E[\tilde{x}_{1s}(t)|\tilde{Y}_2]$ of the form in relation (4.39), where $\gamma_f(\cdot)$ and $\gamma_r(\cdot)$ are generated by equations (4.52) - (4.53), follows from the solution to a quadratic optimization problem, motivated by a M.A.P. estimation approach applied to a discrete-time map-updating problem. The M.A.P. approach offers some interesting, as yet only heuristic, insights into the map-updating problem, which are stated in Appendix 4B and Section 4.3.

4.2.3 Symmetric Filter Algorithm for Map-Updating

We now present a third algorithm for computing $E[\tilde{x}_{1s}(t)|\tilde{Y}_2]$. Let us define $q_f(t)$ and $q_r(t)$ by

$$q_f(t) \triangleq P_f \gamma_f(t) \quad , \tag{4.54}$$

and

$$q_r(t) \triangleq P_r \gamma_r(t) \quad . \tag{4.55}$$

Then, by employing (4.54) - (4.55) we can rewrite relation (4.39) as

$$\boxed{E[\tilde{x}_{1s}(t)|\tilde{Y}_2] = P_s\left\{P_f^{-1}q_f(\sigma) + P_r^{-1}q_r(\sigma)\right\} \quad .} \tag{4.56}$$

But since P_f and P_r denote the error covariance matrices associated with the forward and reverse two-pass filtered estimates defined by relations (4.40) and (4.42), respectively, by applying standard Kalman filtering results to the forward model (2.1) and the reverse model (2.114) we can show that P_f and P_r are generated by the equations:

$$\dot{P}_f = A P_f + P_f A' + Q - P_f(H_1' R_1^{-1} H_1 + H_2' R_2^{-1} H_2)P_f \quad , \tag{4.57}$$

with $$P_f(0) = \pi(0) \quad , \tag{4.58}$$

and $$-\dot{P}_r = (-A - Q\pi^{-1})P_r + P_r(-A - Q\pi^{-1})' + Q$$
$$- P_r(H_1' R_1^{-1} H_1 + H_2' R_2^{-1} H_2)P_r \quad , \tag{4.59}$$

with $$P_r(T) = \pi(T) \quad . \tag{4.60}$$

Now, by employing relations (4.54) - (4.55), (4.52) - (4.53), and (4.57) - (4.60), noting that O_0 may be expressed as in relation (4.47), we derive the following equations for the evolution of $q_f(t)$ and $q_r(t)$:

$$dq_f(t) = \left(A - P_f(H_1' R_1^{-1} H_1 + H_2' R_2^{-1} H_2)\right) q_f(t)dt + P_f H_2' R_2^{-1}\, d\tilde{y}_2(t) \quad , \tag{4.61}$$

with $$q_f(0) = 0 \quad , \tag{4.62}$$

and $$-dq_r(t) = \left(-A - Q\pi^{-1} - P_r(H_1' R_1^{-1} H_1 + H_2' R_2^{-1} H_2)\right) q_r(t)dt + P_r H_2' R_2^{-1}\, d\tilde{y}_2(t) \quad , \tag{4.63}$$

with $$q_r(T) = 0 \quad . \tag{4.64}$$

Therefore, the Symmetric Filter Algorithm for map-updating is defined by using (4.56) and (4.61) - (4.64) to compute $E[\tilde{x}_{1s}(t)|\tilde{Y}_2]$ in relation (4.16), where the two-pass filtering

error covariance matrices P_f and P_r are computed off-line by the equations (4.57) - (4.58) and (4.59) - (4.60), respectively. The above algorithm for map-updating is identical to a procedure originally obtained by algebraic manipulations of one- and two-pass smoothing and filtering equations. This algebraic approach to deriving the Symmetric Filter Algorithm is outlined in Appendix 4C. In addition, in Section 4.3 we draw attention to the close connection between the algorithm for computing $E[\tilde{x}_{1s}(t)|\tilde{Y}_2]$ of relation (4.56), and the form of the solution to the two-pass smoothing problem, facilitating the solution of the map-combining problem.

Finally, in Appendix 4D we show that an algorithm for map-updating that follows from the scattering perspective is given by

$$\hat{x}_s(t) = \hat{x}_{1s}(t) + P_s\left\{P_f^{-1}q_f(t) + P_B^{-1}q_B(t)\right\} , \qquad (4.65)$$

where P_B is the filtering error covariance matrix that is associated with the backwards filtered estimate appearing in the Mayne-Fraser form of the two-pass smoothed estimate. Hence, P_B obeys the backward equation

$$-\dot{P}_B = -A P_B - P_B A' + Q - P_B(H_1' R_1' H_1 + H_2' R_2^{-1} H_2) , \qquad (4.66)$$

with $$P_B^{-1}(T) = 0 \quad . \tag{4.67}$$

In addition, $q_B(\cdot)$ obeys the backward equation

$$-dq_B(t) = -\left(A + P_B(H_1' R_1^{-1} H_1 + H_2' R_2^{-1} H_2)\right) q_B(t)dt + P_B H_2' R_2^{-1} d\tilde{y}_2(t), \tag{4.68}$$

with $$P_B^{-1}(T)q_B(T) = 0 \quad . \tag{4.69}$$

We can show that $P_B^{-1}q_B(\cdot)$ evolves according to the same backward equation as $\gamma_r(\cdot)$ in (4.53).

4.3 Centralized Map-Combining

In Section 4.2 we showed how some algorithms for centralized map-updating followed from an orthogonal decomposition of the two-data pass space Y, and the use of the smoothing error models obtained in Chapter 3. In the current section, we will use the results of the preceding section to derive some solutions to the centralized map-combining problem - the problem of forming the two-pass smoothed estimate $\hat{x}_s(t)$ as a linear functional of the smoothed estimates corresponding to each data pass, $\hat{x}_{1s}(\cdot)$ and $\hat{x}_{2s}(\cdot)$. In what follows, we will again display inside boxes, the essential relations defining the centralized map-combining procedure.

We will first show how centralized map-combining algorithms follow from an identity obtained by using map-updating results. Relation (4.16), which yields the solution to the map-updating problem, follows from decomposing Y as

$$Y = Y_1 \oplus \tilde{Y}_2 \quad . \tag{4.70}$$

We could similarly imagine decomposing Y as

$$Y = Y_2 \oplus \tilde{Y}_1 \quad , \tag{4.71}$$

where $$\tilde{Y}_1 \triangleq H(d\tilde{y}_1(\tau) \quad 0 \le \tau \le T) \quad , \tag{4.72}$$

and $$d\tilde{y}_1(t) = dy_1(t) - H_1\hat{x}_{2s}(t)dt$$

$$\equiv H_1\tilde{x}_{2s}(t)dt + D_1dv_1(t) \quad . \tag{4.73}$$

Hence, by employing the decomposition expressed by relation (4.71), we can derive the following formula for $\hat{x}_s(t)$, analogous to relation (4.16):

$$\hat{x}_s(t) = \hat{x}_{2s}(t) + E[\tilde{x}_{2s}(t)|\tilde{Y}_1] \quad . \tag{4.74}$$

By adding (4.74) and (4.16), and by subtracting $\hat{x}_s(t)$ from both sides of the resulting identity, we obtain the following relation:

$$\boxed{\hat{x}_s(t) = \hat{x}_{1s}(t) + \hat{x}_{2s}(t) + \left[E[\tilde{x}_{1s}(\sigma)|\tilde{Y}_2] + E[\tilde{x}_{2s}(t)|\tilde{Y}_1] - \hat{x}_s(t)\right].} \tag{4.75}$$

We will demonstrate in what follows that algorithms for centralized map-combining follow from this relation.

We next show, first informally through the use of block diagrams, and then formally by writing out the relevant equations, that relation (4.75) represents the solution to the

the centralized map-combining problem. In Fig. 4.1 we depict the solution of the two-pass smoothing problem. The system block with the notation, TPS, denotes the forward and reverse processing of observations $dy_1(\tau)$ and $dy_2(\tau)$, for $0 \leq \tau \leq T$, embedded in the Wall two-filter solution to the smoothing problem. In a similar manner, the solution of our original map-updating problem determined by relations (4.16), (4.56) and (4.61) - (4.64) may be represented as in Fig. 4.2.1.

The block diagram of Fig. 4.2.1 suggests that the computation of $E[\tilde{x}_{1s}(t)|\tilde{Y}_2]$ is equivalent to a two-pass smoothing problem where we imagine that the smoothing errors $\tilde{x}_{1s}(\cdot)$ evolve according to an equation of the same form as the unconditional state dynamics (4.1), and we have the two sets of measurements with independent measurement noises

$$0 = H_1\tilde{x}_{1s}(\tau)d\tau + D_1 d\tilde{v}_1(\tau) \quad , \tag{4.76}$$

and

$$d\tilde{y}_2(\tau) = H_2\tilde{x}_{1s}(\tau)d\tau + D_2 dv_2(\tau) \quad . \tag{4.77}$$

The above observation essentially represents our heuristic understanding for the simplicity of the algorithm for computing $E[\tilde{x}_{1s}(t)|\tilde{Y}_2]$. This observation emerges most clearly in an intermediate step of the M.A.P. approach to map-updating of Appendix 4B.

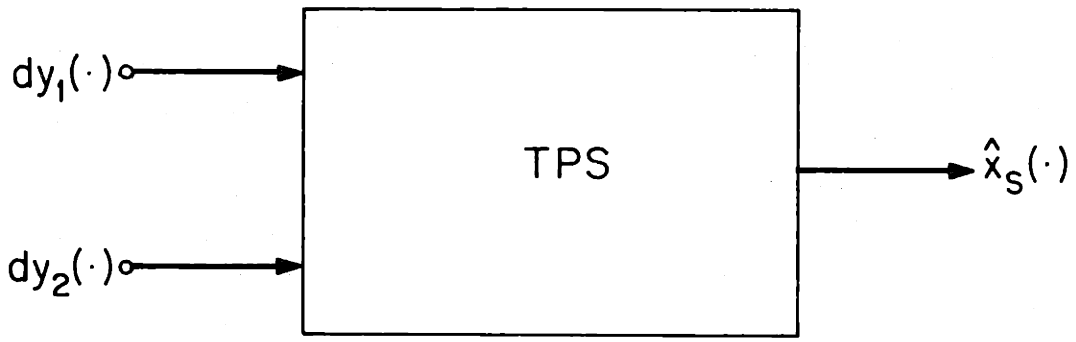

Fig. 4.1 Solution to the Two-Pass Smoothing Problem

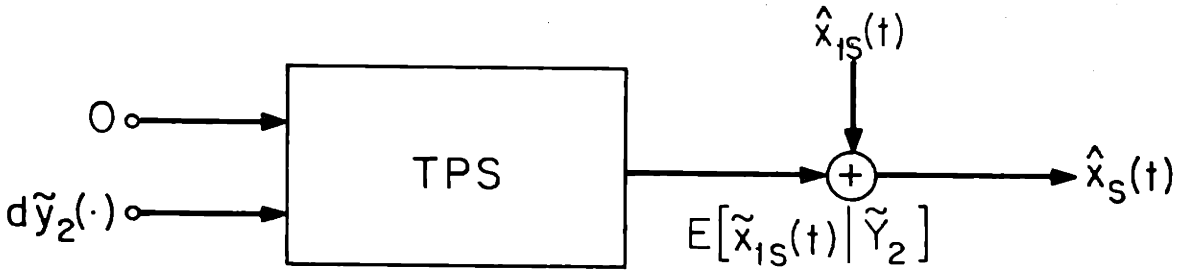

Fig. 4.2.1 Solution to Original Map-Updating Problem

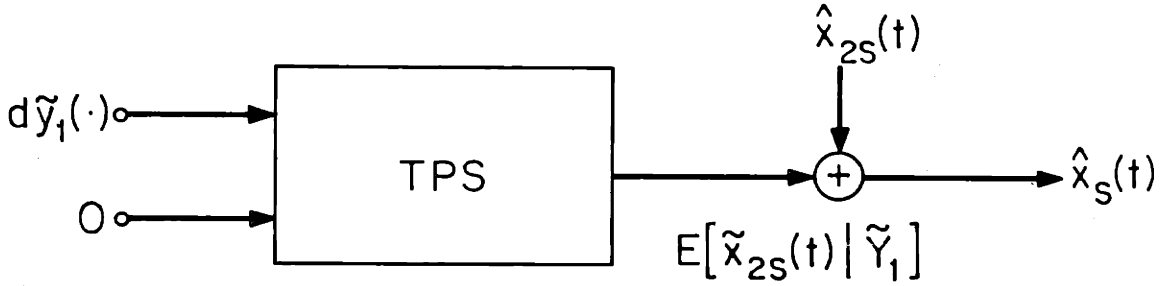

Fig. 4.2.2 Solution to a Variant of the Map-Updating Problem where the Order of Processing is Interchanged

In Fig. 4.2.2 we diagram the solution to a map-updating problem obtained by reversing the order of processing of the two sets of observations, and described by equation (4.74). By adding the block diagrams of relations (4.2.1),(4.2.2) and subtracting the two-pass smoothing block diagram of Fig. 4.1, employing the linearity of the system TPS, and using the definitions of $d\tilde{y}_1(\cdot), d\tilde{y}_2(\cdot)$, we obtain the final block diagram of Fig. 4.3. The diagram in Fig. 4.3 displays clearly how equation (4.75) expresses the two-pass smoothed estimate as a linear functional of the individual smoothed estimates, $\hat{x}_{1s}(\cdot)$ and $\hat{x}_{2s}(\cdot)$.

Having informally verified that relation (4.75) solves the centralized map-combining problem, we now present the details for forming the term inside the brackets. Let us define the forward and reverse two-pass filtering dynamics matrices, Γ_f and Γ_r, by

$$\Gamma_f \triangleq A - P_f(H_1' R_1^{-1} H_1 + H_2' R_2^{-1} H_2) \quad , \tag{4.78}$$

$$\text{and} \quad \Gamma_r = -A - Q\pi^{-1} - P_r(H_1' R_1^{-1} H_1 + H_2' R_2^{-1} H_2) \quad . \tag{4.79}$$

Then from relations (4.56), (4.61) - (4.64), $E[\tilde{x}_{1s}(t)|\tilde{Y}_2]$ may be computed as

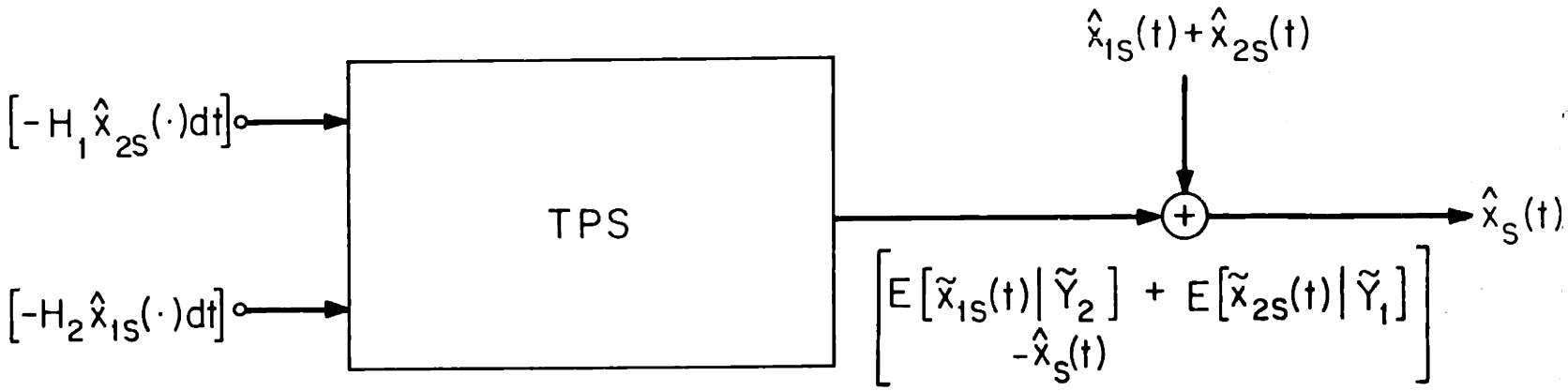

Fig. 4.3 Solution to the Centralized Map-Combining Problem

$$E[\tilde{x}_{1s}(t)|\tilde{Y}_2] = P_s\left\{P_f^{-1}q_{1f}(t) + P_r^{-1}q_{1r}(t)\right\} , \qquad (4.80)$$

where

$$dq_{1f}(t) = \Gamma_f q_{1f}(t)dt + P_f H_2' R_2^{-1}[dy_2(t) - H_2\hat{x}_{1s}(t)dt], \qquad (4.81)$$

and

$$-dq_{1r}(t) = \Gamma_r q_{1r}(t)dt + P_r H_2' R_2^{-1}[dy_2(t) - H_2\hat{x}_{1s}(t)dt], \qquad (4.82)$$

with $$q_{1f}(0) = q_{1r}(T) = 0 . \qquad (4.83)$$

In a completely analogous manner, $E[\tilde{x}_{2s}(t)|\tilde{Y}_1]$ may be computed as

$$E[\tilde{x}_{2s}(t)|\tilde{Y}_1] = P_s\left\{P_f^{-1}q_{2f}(t) + P_r^{-1}q_{2r}(t)\right\} , \qquad (4.84)$$

where

$$dq_{2f}(t) = \Gamma_f q_{2f}(t)dt + P_f H_1' R_1^{-1}[dy_1(t) - H_1\hat{x}_{2s}(t)dt], \qquad (4.85)$$

and

$$-dq_{2r}(t) = \Gamma_r q_{2r}(t)dt + P_r H_1' R_1^{-1}[dy_1(t) - H_1\hat{x}_{2s}(t)dt], \qquad (4.86)$$

with $$q_{2f}(0) = q_{2r}(T) = 0 \quad . \tag{4.87}$$

Finally, we note that Wall's two-filter formula for computing $\hat{x}_s(t)$ is given by

$$\hat{x}_s(t) = P_s\left\{P_f^{-1}\hat{x}_f(t) + P_r^{-1}\hat{x}_r(t)\right\} \quad , \tag{4.88}$$

where $$d\hat{x}_f(t) = \Gamma_f\hat{x}_f(t)dt + P_f[H_1'R_1^{-1}dy_1(t) + H_2'R_2^{-1}dy_2(t)], \tag{4.89}$$

and $$-d\hat{x}_r(t) = \Gamma_r\hat{x}_r(t)dt + P_r[H_1'R_1^{-1}dy_1(t) + H_2'R_2^{-1}dy_2(t)], \tag{4.90}$$

with $$\hat{x}_f(0) = \hat{x}_r(T) = 0 \quad . \tag{4.91}$$

Hence, by defining $\theta_f(t)$ and $\theta_r(t)$ as

$$\theta_f(t) \triangleq q_{1f}(t) + q_{2f}(t) - \hat{x}_f(t) \quad , \tag{4.92}$$

and $$\theta_r(t) \triangleq q_{1r}(t) + q_{2r}(t) - \hat{x}_r(t) \quad , \tag{4.93}$$

and employing relations (4.80) - (4.91), we can show that

$$\left[E[\tilde{x}_{1s}(t)|\tilde{Y}_2] + E[\tilde{x}_{2s}(t)|\tilde{Y}_1] - \hat{x}_s(t)\right] = P_s\left\{P_f^{-1}\theta_f(t) + P_r^{-1}\theta_r(t)\right\}, \tag{4.94}$$

where $\theta_f(\cdot)$ and $\theta_r(\cdot)$ satisfy the equations

$$d\theta_f(t) = \Gamma_f\theta_f(t)dt - P_f[H_2'R_2^{-1}H_2\hat{x}_{1s}(t)dt + H_1'R_1^{-1}H_1\hat{x}_{2s}(t)dt], \tag{4.95}$$

and

$$-d\theta_r(t) = \Gamma_r\theta_r(t)dt - P_r[H_2'R_2^{-1}H_2\hat{x}_{1s}(t)dt + H_1'R_1^{-1}H_1\hat{x}_{2s}(t)dt], \tag{4.96}$$

with

$$\theta_f(0) = \theta_r(T) = 0 \quad . \tag{4.97}$$

Therefore, by substituting relation (4.94) into (4.75), we obtain the following centralized map-combining algorithm:

Centralized Map-Combining Algorithm

$$\hat{x}_s(t) = \hat{x}_{1s}(t) + \hat{x}_{2s}(t) + P_s\left\{P_f^{-1}\theta_f(t) + P_r^{-1}\theta_r(t)\right\} \quad . \tag{4.98}$$

Hence, relation (4.94) together with equations (4.95) - (4.97) specify the desired algorithm for centralized map-combining, where the two-pass filtering error covariance matrices are computed offline by the equations (4.57) - (4.60).

We finally note from the form of relation (4.98), that the presence of the term involving $\theta_f(t), \theta_r(t)$ is a reflection of the fact that in general Y_1 and Y_2 are not orthogonal measurement spaces, i.e., they both result from observing some underlying state process with the same initial condition and generating process noise. Hence, the second term in relation (4.98) effects a subtraction that compensates for the non-orthogonality of Y_1 and Y_2. As a simple example for which Y_1 and Y_2 are orthogonal, consider the two-dimensional state model

$$\begin{pmatrix} d\Delta_1(t) \\ d\Delta_2(t) \end{pmatrix} = \begin{pmatrix} a_1 & 0 \\ 0 & a_2 \end{pmatrix} \begin{pmatrix} \Delta_1(t) \\ \Delta_2(t) \end{pmatrix} dt + \begin{pmatrix} b_1 du_1(t) \\ b_2 du_2(t) \end{pmatrix} , \qquad (4.99)$$

where we have measurements

$$dy_1(t) = (1 \quad 0) \begin{pmatrix} \Delta_1(t) \\ \Delta_2(t) \end{pmatrix} dt + d_1 dv_1(t) , \qquad (4.100)$$

$$\text{and} \quad dy_2(t) = (0 \quad 1) \begin{pmatrix} \Delta_1(t) \\ \Delta_2(t) \end{pmatrix} dt + d_2 dv_2(t) \quad , \tag{4.101}$$

and where

$$\pi(0) = \begin{pmatrix} \pi_1(0) & 0 \\ 0 & \pi_2(0) \end{pmatrix} . \tag{4.102}$$

In this case $\Delta_1(\cdot)$ and $\Delta_2(\cdot)$ are independent, and observed separately through the measurements $y_1(\cdot)$ and $y_2(\cdot)$, so that

$$\hat{x}_{1s}(t) = \begin{pmatrix} \hat{\Delta}_{1s}(t) \\ 0 \end{pmatrix} , \tag{4.103}$$

$$\text{and} \qquad \hat{x}_{2s}(t) = \begin{pmatrix} 0 \\ \hat{\Delta}_{2s}(t) \end{pmatrix} , \tag{4.104}$$

$$\text{where} \qquad \hat{\Delta}_{is}(t) \triangleq E[\Delta_i(t) | Y_i] . \tag{4.105}$$

By examining relations (4.95) - (4.96) for the generation of $\theta_f(\cdot)$ and $\theta_r(\cdot)$, and noting (4.103) - (4.104), we can verify that in the above case these quantities vanish.

4.4 Conclusion

In Section 4.2 we employed forward and reverse Markovian realizations of the smoothing error process, as well as an orthogonal decomposition of the two-data pass space Y, to derive two-filter algorithms for solving the centralized map-updating problem. We note here that while we used the Wall two-filter smoothing formula, for computing the correction to the first pass map, $E[\tilde{x}_{1s}(t)|\tilde{Y}_2]$, a multiplicity of approaches are conceivable for computing this term, corresponding to all the fixed-interval smoothing algorithms of Chapter 2, as well as others. A major conclusion derived from considering any of the algorithms presented, is that the operation of map-updating is no more difficult, computationally, than the operation of map formation, i.e., the calculation of a smoothed estimate. We view this as a fact that has potentially significant implications for problems involving the continual assimilation of data, as in meteorology.

In Section 4.3, pictorially through Figs. 4.1 - 4.3, we demonstrated the essential significance of the centralized map-updating problem solution, in solving the centralized map-combining problem. As in the case of map-updating, the operation of map-combining is no more difficult that that of map formation.

We finally comment on a variant of the centralized map-updating and map-combining problems of this chapter, that is of interest in a distributed processing setting. In this case we imagine that processor #1 employs the measurements $dy_1(\cdot)$, but in addition obtains either the state estimates $\hat{x}_{2s}(\cdot)$ computed by processor #2, on the basis of $dy_2(\cdot)$, or alternatively, the data $dy_2(\cdot)$ itself, in order to form the final two-pass smoothed estimates, $\hat{x}_s(\cdot)$. The difference between the above problems, and the map-updating and map-combining problems of the preceding chapter, arises when we assume that the processors use different a-priori information in forming their estimates, $\hat{x}_{is}(\cdot)$. We can equivalently describe this situation by assuming that both processors assume a state model of the form (4.1), with $\pi^{-1}(0) = 0$, and with the additional discrete measurement y_{id} defined by

$$y_{id} = x(0) + n_{id} \ , \tag{4.106}$$

where $$E[n_{id}n_{id}'] = R_{id} \ . \tag{4.107}$$

In this case, by defining

$$Y_i = H(y_{id}, dy_i(\tau) \quad 0 \leq \tau \leq T) \ , \tag{4.108}$$

and by using the same type of Hilbert space decompositions of $Y_1 \vee Y_2$, as we did to derive solutions of the map-updating and map-combining problems of this chapter, one should be able to derive analogous algorithms for the solution of the above problems.

Appendix 4A

Proof of Identities Connecting Forward and Reverse Filtering Error Covariance Matrices Associated with the Estimation of Smoothing Errors, and Two-Pass Filtering Error Covariance Quantities

In this Appendix we prove the identities

$$P_f^{-1} = P_{1f}^{-1} + P_{fs}^{-1} - P_{1s}^{-1} \quad , \tag{A.1}$$

and

$$O_0 = P_{rs}^{-1} - P_{1f}^{-1} \quad , \tag{A.2}$$

which may be rewritten as

$$P_{fs}^{-1} = O_{01} + \bar{P}_f^1 \quad , \tag{A.3}$$

and

$$P_{rs}^{-1} = P_{1f}^{-1} + O_0 \quad , \tag{A.4}$$

respectively. Our proof proceeds by identifying P_{fs} and P_{rs} as error covariance matrices associated with some estimates of $x(t)$. Let us define $\hat{x}_{fs}(t)$ and $\hat{x}_{rs}(t)$ by

$$\hat{x}_{fs}(t) \stackrel{\Delta}{=} E[x(t) | Y_1 \vee Y_{2t}^-] \quad , \tag{A.5}$$

and $$\hat{x}_{rs}(t) \triangleq E[x(t)|Y_1 \vee Y_{2t}^{+}] \quad . \tag{A.6}$$

Then by employing the orthogonal decompositions

$$Y_1 \vee Y_{2t}^{-} = Y_1 \oplus \tilde{Y}_{2t}^{-} \quad , \tag{A.7}$$

and $$Y_1 \vee Y_{2t}^{+} = Y_1 \oplus \tilde{Y}_{2t}^{+} \quad , \tag{A.8}$$

where $$\tilde{Y}_2 \triangleq H(d\tilde{y}_2(\tau) \quad 0 \leq \tau \leq T) \quad , \tag{A.9}$$

and $$d\tilde{y}_2(\tau) = H_2\tilde{x}_{1s}(\tau)d\tau + D_2 dv_2(\tau)$$

$$\equiv dy_2(\tau) - H_2\hat{x}_{1s}(\tau)d\tau \quad , \tag{A.10}$$

we may express $\hat{x}_{fs}(t)$ and $\hat{x}_{rs}(t)$ of (A.5) - (A.6) as

$$\hat{x}_{fs}(t) = \hat{x}_{1s}(t) + E[\tilde{x}_{1s}(t)|\tilde{Y}_{2t}^{-}] \quad , \tag{A.11}$$

and $$\hat{x}_{rs}(t) = \hat{x}_{1s}(t) + E[\tilde{x}_{1s}(t)|\tilde{Y}_{2t}^{+}] \quad . \tag{A.12}$$

The relations (A.11) - (A.12) imply the following expressions for the estimate errors $\tilde{x}_{fs}(t)$ and $\tilde{x}_{rs}(t)$:

$$\tilde{x}_{fs}(t) = \tilde{x}_{1s}(t) - E[\tilde{x}_{1s}(t)|\tilde{Y}_{2t}^{-}] \quad , \tag{A.13}$$

and $$\tilde{x}_{rs}(t) = \tilde{x}_{ls}(t) - E[\tilde{x}_{ls}(t) | \tilde{Y}^{+}_{2t}] \quad . \tag{A.14}$$

These equations demonstrate that P_{fs} and P_{rs}, which by definition are covariance matrices associated with the right-hand sides of (A.13) - (A.14), may also be interpreted as error covariance matrices associated with the estimates $\hat{x}_{fs}(t)$ and $\hat{x}_{rs}(t)$, respectively. The relations (A.3) - (A.4) now follow by noting that

$$Y_1 \vee Y^{-}_{2t} = Y^{-}_{t} \vee Y^{+}_{1t} \quad , \tag{A.15}$$

$$Y_1 \vee Y^{+}_{2t} = Y^{+}_{t} \vee Y^{-}_{1t} \quad , \tag{A.16}$$

and using the Mayne-Fraser smoothing formula for the smoothing error covariance.

Appendix 4B

The M.A.P. Approach to Centralized Map-Updating

The M.A.P. approach [1] to the estimation of a random vector X given some observation vector Z is defined by requiring that

$$p_c\left(\hat{X}_{M.A.P.}|Z\right) = \max\left\{p_c(\cdot|Z)\right\} \quad , \tag{B.1}$$

where $p_c(\cdot|\cdot)$ denotes the conditional density for X given Z. In the case when X and Z are jointly Gaussian random vectors, $\hat{X}_{M.A.P.}$ coincides with the conditional mean, and the best linear estimate for X given Z. In this Appendix, we use the M.A.P. approach to formulate the solution to a particular class of discrete-time centralized map-updating problems. We then use the insight that we obtain to calculate the solution to a white noise version of the continuous-time map-updating problem, as the result of optimizing a particular quadratic functional. The map-updating procedure which we derive here is closely related to the Information-Filter Algorithm for map-updating of Section 4.2.2. In addition, the details of the M.A.P. approach suggest some heuristic reasons for the

simplicity of the algorithm for computing the correction term to the first-pass smoothed estimates, that is embedded in the map-updating procedure.

We consider first the M.A.P. approach to the solution of a discrete-time map-updating problem for which the zero-mean state process $x(\cdot)$ can be described by the forward and reverse Markovian realizations:

$$x(i+1) = F(i)x(i) + G(i)w(i) \ , \tag{B.2}$$

and

$$x(i) = \overline{F}(i+1)x(i+1) + \overline{G}(i+1)\overline{w}(i+1) \ , \tag{B.3}$$

where $w(\cdot),\overline{w}(\cdot)$ denote standard discrete white noise processes. We will let $\pi(k)$ denote the state covariance associated with $x(k)$, and define

$$Q(i) \triangleq G(i)G'(i) \ , \tag{B.4}$$

and

$$\overline{Q}(i) \triangleq \overline{G}(i)\overline{G}'(i) \ . \tag{B.5}$$

The analysis that follows assumes the invertibility of the $F(i)$'s, $Q(i)$'s, $\overline{F}(i)$'s, and $\overline{Q}(i)$'s. By employing the results of Kailath and Verghese [36] on backward models, we can let

$$\bar{F}(i+1) \triangleq F^{-1}(i)\left(I - Q(i)\pi^{-1}(i+1)\right) , \tag{B.6}$$

and $$\bar{Q}(i+1) \triangleq F^{-1}(i)\left(Q(i) - Q(i)\pi^{-1}(i+1)Q(i)\right)F'^{-1}(i). \tag{B.7}$$

We next assume we have made two measurement passes over the interval [0,T], which are modelled by

$$y_i(j) = H_i(j)x(j) + n_i(j), \quad \text{for } i = 1,2 , \tag{B.8}$$

where the $n_i(\cdot)$, $i = 1,2$, are mutually independent white noise processes with

$$E[n_i(j)n_i'(j)] = R_i(j) . \tag{B.9}$$

We introduce the following notation for aggregate measurement and state vectors:

$$Z_1 \triangleq (y_1(0), \ldots, y_1(T)) , \tag{B.10}$$

$$Z_2 \triangleq (y_2(0), \ldots, y_2(T)) , \tag{B.11}$$

$$\tilde{Z}_2 \triangleq (\tilde{y}_2(0), \ldots, \tilde{y}_2(T)) , \tag{B.12}$$

where $$\tilde{y}_2(k) \triangleq y_2(k) - H_2(k)\hat{x}_{1s}(k) \ , \tag{B.13}$$

and $$X \triangleq (x(0), \ldots, x(T)) \ . \tag{B.14}$$

In addition, we let Y denote the Hilbert space spanned by the two measurement passes, Y_1 and Y_2 correspond to the Hilbert spaces spanned by each separate measurement pass, and $\tilde{Y}_2$ denotes the Hilbert space spanned by the component vectors of $\tilde{Z}_2$.

The centralized map-updating problem is defined as that of computing the conditional mean of the $x(\cdot)$'s given Y, as a linear functional of the first-pass smoothed estimates, $\hat{x}_{1s}(\cdot)$, and the second-pass data, $y_2(\cdot)$. If we let $\hat{X}_{1s}$, $\tilde{X}_{1s}$, and $\hat{X}_s$ denote the aggregate first pass smoothed estimates, first-pass smoothing errors, and the two-pass smoothed estimates, respectively, then the Hilbert space decomposition

$$Y = Y_1 \oplus \tilde{Y}_2 \ , \tag{B.15}$$

implies that

$$\hat{X}_s = \hat{X}_{1s} + E[\tilde{X}_{1s} | \tilde{Y}_2] \ . \tag{B.16}$$

In order to make (B.16) more explicit, we consider the M.A.P. approach for computing $E[\tilde{X}_{1s}|\tilde{Y}_2]$. Letting $\tilde{p}_{12}(\cdot|\cdot)$ denote the conditional density for $\tilde{X}_{1s}$ given $\tilde{Z}_2$, $\tilde{p}_{21}(\cdot|\cdot)$ denote the conditional density for $\tilde{Z}_2$ given $\tilde{X}_{1s}$, $\tilde{p}(\cdot)$ denote the density for $\tilde{X}_{1s}$, and $\tilde{\mu}_2(\cdot)$ denote the density for $\tilde{Z}_2$, we can use Bayes rule to express $\tilde{p}_{12}(\tilde{X}_{1s}|\tilde{Z}_2)$ as

$$p_{12}(\tilde{X}_{1s}|\tilde{Z}_2) = \frac{\tilde{p}_{21}(\tilde{Z}_2|\tilde{X}_{1s})\tilde{p}(\tilde{X}_{1s})}{\tilde{\mu}_2(\tilde{Z}_2)} \quad . \tag{B.17}$$

Hence, the optimization of (B.17), as a function of $\tilde{X}_{1s}$, defines the M.A.P. estimate for $\tilde{X}_{1s}$ given $\tilde{Z}_2$, and thus $E[\tilde{X}_{1s}|\tilde{Y}_2]$.

We proceed to form the exponent of $p_{12}(\tilde{X}_{1s}|\tilde{Z}_2)$ through the use of (B.17), by identifying the exponents of $\tilde{p}_{21}(\tilde{Z}_2|\tilde{X}_{1s})$ and $\tilde{p}(\tilde{X}_{1s})$. Then, we formulate the calculation of the component vectors in $E[\tilde{X}_{1s}|\tilde{Y}_2]$ as the solution of a quadratic optimization problem. From the fact that $\tilde{Z}_2$ is composed of the $\tilde{y}_2(i)$'s defined by

$$\tilde{y}_2(i) = H_2(i)\tilde{x}_{1s}(i) + n_2(i) \quad , \tag{B.18}$$

and the $n_2(\cdot)$'s represent a white noise sequence, and by using $q(i)$ as a simplified notation for $\tilde{x}_{1s}(i)$, we can show that the exponent of the conditional density for $\tilde{Z}_2$ given $\tilde{X}_{1s}$ is

specified by

$$\mathrm{Ln}\left\{\tilde{p}_{21}(\tilde{Z}_2|\tilde{X}_{1s})\right\} = -\frac{1}{2}\sum_{i=0}^{T}\left(\tilde{y}_2(i) - H_2(i)q(i)\right)' R_2^{-1}(i)\left(\tilde{y}_2(i) - H_2(i)q(i)\right)$$

$$+ \text{constant} . \qquad \text{(B.19)}$$

We form the exponent of $\tilde{p}(\tilde{X}_{1s})$ by relating this density to the conditional density for X given Z_1, $p_{so}(\cdot|\cdot)$. By recognizing that

$$X = \hat{X}_{1s} + \tilde{X}_{1s} , \qquad \text{(B.20)}$$

we claim that

$$\tilde{p}(\tilde{X}_{1s}) = p_{so}(\hat{X}_{1s} + \tilde{X}_{1s}|Z_1) . \qquad \text{(B.21)}$$

We next define the conditional density for Z_1 given X as $p_{os}(\cdot|\cdot)$, let $p(\cdot)$ denote the density for the aggregate state X, and let $\mu_1(\cdot)$ denote the density for Z_1. Then, by using Bayes rule we express $p_{so}(X|Z_1)$ as

$$p_{so}(X|Z_1) = \frac{p_{os}(Z_1|X)p(X)}{\mu_1(Z_1)} . \qquad \text{(B.22)}$$

Therefore, by employing (B.21), we may express the density for

the aggregate smoothing errors by

$$\tilde{p}(\tilde{X}_{1s}) = \frac{p_{os}(Z_1|\hat{X}_{1s}+\tilde{X}_{1s})p(\hat{X}_{1s}+\tilde{X}_{1s})}{\mu_1(Z_1)} \quad . \tag{B.23}$$

Careful interpretation of relation (B.23) allows us to form the exponent of $\tilde{p}(\tilde{X}_{1s})$. We note that since the $\tilde{x}_{1s}(i)$'s are zero-mean, the exponent of the density on the left-hand side of (B.23) is a quadratic form in the $\tilde{x}_{1s}(i)$ variables, with no linear terms in $\tilde{x}_{1s}(i)$. This implies that in forming the exponent of the right-hand side of (B.23), we may ignore all terms linear in $\tilde{x}_{1s}(i)$. We proceed to identify the exponents of $p_{os}(Z_1|X)$ and $p(X)$, so as to ultimately use (B.23) to identify the exponent for $\tilde{p}(\tilde{X}_{1s})$.

The exponent of $p_{os}(Z_1|X)$ follows from the definition (B.8) for $y_1(j)$, and the fact that $n_1(\cdot)$ represents a discrete white noise sequence, as

$$\text{Ln}\left\{p_{os}(Z_1|X)\right\} = -\frac{1}{2}\sum_{i=0}^{T}\left(y_1(i) - H_1(i)x(i)\right)' R_1^{-1}(i)\left(y_1(i) - H_1(i)x(i)\right) + \text{constant}. \tag{B.24}$$

We next compute the exponent for the aggregate state density, $p(X)$. For the later purpose of obtaining symmetric, two-filter algorithms for computing the component vectors in

$E[\tilde{X}_{1s}|\tilde{Z}_2]$, we form p(X) in a manner which places a-priori information at both endpoints x(0) and x(T). If we let $p_{ft}(\cdot|\cdot)$ denote the transition density for x(t) conditioned on x(t-1), $p_{bt}(\cdot|\cdot)$ denote the transition density for x(t) conditioned on x(t+1), and $p_t(\cdot)$ denote the density for x(t), then we can show that

$$p(X) = \frac{\left[p_0(x(0)) \prod_{i=1}^{t} p_{fi}(x(i)|x(i-1))\right]\left[p_T(x(T)) \prod_{i=t}^{T-1} p_{bi}(x(i)|x(i+1))\right]}{p_t(x(t))} \tag{B.25}$$

By using the forward Markov model (B.2) to form the $p_{fi}(\cdot|\cdot)$'s, and the backward model (B.3) to form the $p_{bi}(\cdot|\cdot)$'s, we can identify from (B.25) the following exponent for p(X):

$$\begin{aligned}
\mathrm{Ln}\{p(X)\} = & -\frac{1}{2}x'(0)\pi^{-1}(0)x(0) \\
& -\frac{1}{2}\sum_{i=0}^{t-1}\Big(x(i+1) - F(i)x(i)\Big)' Q^{-1}(i)\Big(x(i+1) - F(i)x(i)\Big) \\
& -\frac{1}{2}x'(T)\pi^{-1}(T)x(T) \\
& -\frac{1}{2}\sum_{i=t}^{T-1}\Big(x(i) - \overline{F}(i+1)x(i+1)\Big)' \overline{Q}^{-1}(i+1)\Big(x(i) - \overline{F}(i+1)x(i+1)\Big) \\
& +\frac{1}{2}x'(t)\pi^{-1}(t)x(t) + \text{constant} .
\end{aligned} \tag{B.26}$$

Now, by employing (B.26) and (B.24) in (B.23) to collect the quadratic terms in the exponent of $\tilde{p}(\tilde{X}_{ls})$, we find that

$$\begin{aligned}
\mathrm{Ln}\left\{\tilde{p}(\tilde{X}_{ls})\right\} = & -\frac{1}{2}q'(0)\pi^{-1}(0)q(0) \\
& -\frac{1}{2}\sum_{i=0}^{t-1}\Big(q(i+1) - F(i)q(i)\Big)' Q^{-1}(i)\Big(q(i+1) - F(i)q(i)\Big) \\
& -\frac{1}{2}q'(T)\pi^{-1}(T)q(T) \\
& -\frac{1}{2}\sum_{i=t}^{T-1}\Big(q(i) - \overline{F}(i+1)q(i+1)\Big)' \overline{Q}^{-1}(i+1)\Big(q(i) - \overline{F}(i+1)q(i+1)\Big) \\
& +\frac{1}{2}q'(t)\pi^{-1}(t)q(t) \\
& -\frac{1}{2}\sum_{i=0}^{T} q'(i)H_1'(i)R_1^{-1}(i)H_1(i)q(i) + \text{constant.} \qquad \text{(B.27)}
\end{aligned}$$

Relation (B.27) may be interpreted as saying that the correlation structure of the $\tilde{x}_{ls}(i)$'s is equivalent to that generated by assuming that the $q(\cdot)$'s obey the forward and reverse equations

$$q(i+1) = F(i)q(i) + G(i)\tilde{w}(i) \quad , \qquad \text{(B.28)}$$

and

$$q(i) = \overline{F}(i+1)q(i+1) + \overline{G}(i+1)\tilde{\overline{w}}(i+1) \quad , \qquad \text{(B.29)}$$

for some standard white noise processes $\tilde{w}(\cdot)$, $\tilde{\tilde{w}}(\cdot)$, together with the constraint equation

$$0 = H_1(i)q(i) + \tilde{n}_1(i) \quad , \tag{B.30}$$

where $\tilde{n}_1(\cdot)$ is a white noise sequence with covariance $R_1(\cdot)$.

Finally, when we form the exponent for the conditional density of $\tilde{X}_{1s}$ given $\tilde{Z}_2$ by using (B.17), (B.19), and (B.27), we effectively add the term

$$-\frac{1}{2}\sum_{i=0}^{T}\left(\tilde{y}_2(i) - H_2(i)q(i)\right)' R_2^{-1}(i)\left(\tilde{y}_2(i) - H_2(i)q(i)\right) \tag{B.31}$$

to equation (B.27), and thus the correlation structure for $\tilde{X}_{1s}$ conditioned on $\tilde{Z}_2$ is equivalent to assuming the $q(\cdot)$'s evolve according to equations of the same form as the unconditional state dynamics, together with the constraint (B.30), and the observations

$$\tilde{y}_2(i) = H_2(i)q(i) + n_2(i) \quad , \tag{B.32}$$

where $n_2(\cdot)$ and $\tilde{n}_1(\cdot)$ are uncorrelated. Hence, it is not surprising that the algorithm for computing $E[\tilde{X}_{1s}(t)|\tilde{Y}_2]$ resembles the solution of a two-pass smoothing problem for which

the $q(\cdot)$'s evolve in the same manner as the $x(\cdot)$'s, and we have measurements (B.30), (B.32).

At this point we are in a position to formulate the calculation of the M.A.P. estimate for $\tilde{X}_{1s}$ given $\tilde{Z}_2$ as the solution to a quadratic optimization problem. From (B.17), (B.19), and (B.27) we can express the negative of the exponent of $\tilde{p}_{12}(\tilde{X}_{1s}|\tilde{Z}_2)$ as

$$-\text{Ln}\left\{\tilde{p}_{12}(\tilde{X}_{1s}|\tilde{Z}_2)\right\} = J\Big(q(0), \ldots, q(T)\Big) + \text{constant} , \qquad \text{(B.33)}$$

where

$$J\Big(q(0), \ldots, q(T)\Big) = J_{0,t}\Big(q(0), \ldots, q(t)\Big) + J_{t,T}\Big(q(t), \ldots, q(T)\Big) - \frac{1}{2}q'(t)\pi^{-1}(t)q(t), \qquad \text{(B.34)}$$

and $J_{0,t}(\cdot)$, $J_{t,T}(\cdot)$ are defined by

$$J_{0,t}\big(q(0), \ldots, q(t)\big) =$$

$$\frac{1}{2}\sum_{i=0}^{t-1}\big(\tilde{y}_2(i) - H_2(i)q(i)\big)' R_2^{-1}(i)\big(\tilde{y}_2(i) - H_2(i)q(i)\big)$$

$$+ \frac{1}{2}\sum_{i=0}^{t-1} q'(i)H_1'(i)R_1^{-1}(i)H_1(i)q(i)$$

$$+ \frac{1}{2}\, q'(0)\pi^{-1}(0)q(0)$$

$$+ \frac{1}{2}\sum_{i=0}^{t-1}\big(q(i+1) - F(i)q(i)\big)' Q^{-1}(i)\big(q(i+1) - F(i)q(i)\big), \qquad \text{(B.35)}$$

and

$$J_{t,T}\big(q(t), \ldots, q(T)\big) =$$

$$\frac{1}{2}\sum_{i=t}^{T}\big(\tilde{y}_2(i) - H_2(i)q(i)\big)' R_2^{-1}(i)\big(\tilde{y}_2(i) - H_2(i)q(i)\big)$$

$$+ \frac{1}{2}\sum_{i=t}^{T} q'(i)H_1'(i)R_1^{-1}(i)H_1(i)q(i)$$

$$+ \frac{1}{2}\, q'(T)\pi^{-1}(T)q(T)$$

$$+ \frac{1}{2}\sum_{i=t}^{T-1}\big(q(i) - \bar{F}(i+1)q(i+1)\big)' \bar{Q}^{-1}(i+1)\big(q(i) - \bar{F}(i+1)\bar{q}(i+1)\big). \qquad \text{(B.36)}$$

Following the approach of Mayne [17] to the solution of the ordinary fixed interval smoothing problem, we compute $\hat{q}_s(t)$, defined by

$$\hat{q}_s(t) \triangleq E[\tilde{x}_{1s}(t)|\tilde{Y}_2] \ , \qquad (B.37)$$

by performing the following minimization:

$$\min_{\substack{q(0),\ldots,q(t-1)\\ q(t+1),\ldots,q(T)}} J\big(q(0),\ldots,q(T)\big) = \frac{1}{2}\big(q(t) - \hat{q}_s(t)\big)' P_s^{-1}(t)\big(q(t) - \hat{q}_s(t)\big) + \text{constant} \ , \qquad (B.38)$$

where $P_s(t)$ denotes the error covariance matrix associated with $\hat{q}_s(t)$, or equivalently, the two-pass smoothing error covariance matrix.

Two-filter formulae for computing $\hat{q}_s(t)$ follow from breaking up the minimization expressed by (B.38) into two separate minimizations of $J_{0,t}\big(q(0),\ldots,q(t)\big)$ and $J_{t,T}\big(q(t),\ldots,q(T)\big)$, over $\big(q(0),\ldots,q(t-1)\big)$ and $\big(q(t+1),\ldots,q(T)\big)$, respectively. By using relations (B.28) - (B.29), the invertibility of the G(i)'s, $\bar{G}$(i)'s and their relation to Q(i), $\bar{Q}$(i), we can reformulate the minimization of $J_{0,t}\big(q(0),\ldots,q(t)\big)$ and $J_{t,T}\big(q(t),\ldots,q(T)\big)$ as dynamic programming problems in the following manner:

$$\min_{(q(0),\ldots,q(t-1))} \left\{ J\left(q(0),\ldots,q(t)\right) \right\} = V_f(t,q(t)) \equiv$$

$$\min_{\substack{\tilde{w}(i),\ i=0,\ldots,t-1 \\ q(i+1)=F(i)q(i)+G(i)\tilde{w}(i)}}$$

$$\left[\begin{array}{l} \frac{1}{2} \sum_{i=0}^{t-1} \left(\tilde{y}_2(i) - H_2(i)q(i)\right)' R_2^{-1}(i) \left(\tilde{y}_2(i) - H_2(i)q(i)\right) \\ + \frac{1}{2} \sum_{i=0}^{t-1} q'(i)H_1'(i)R_1^{-1}(i)H_1(i)q(i) \\ + \frac{1}{2} q'(0)\pi^{-1}(0)q(0) + \frac{1}{2} \sum_{i=0}^{t-1} \tilde{w}'(i)\tilde{w}(i) \end{array} \right], \tag{B.39}$$

and

$$\min_{q(t+1),\ldots,q(T)} \left\{ J_{t,T}\left(q(t),\ldots,q(T)\right) \right\} = V_b(t,q(t)) \equiv$$

$$\min_{\substack{\simeq \\ w(i),\ i=t+1,\ldots,T \\ q(i)=\bar{F}(i+1)q(i+1)+\bar{G}(i+1)\tilde{\tilde{w}}(i+1)}}$$

$$\left[\begin{array}{l} \frac{1}{2} \sum_{i=t}^{T} \left(\tilde{y}_2(i) - H_2(i)q(i)\right)' R_2^{-1}(i) \left(\tilde{y}_2(i) - H_2(i)q(i)\right) \\ + \frac{1}{2} \sum_{i=t}^{T} q'(i)H_1'(i)R_1^{-1}(i)H_1(i)q(i) \\ + \frac{1}{2} q(T)\pi^{-1}(T)q(T) + \frac{1}{2} \sum_{i=t+1}^{T} \tilde{\tilde{w}}'(i)\tilde{\tilde{w}}(i) \end{array} \right]. \tag{B.40}$$

We note now that by using the principle of optimality [39] to derive equations satisfied by $V_f(t,q(t))$ and $V_b(t,q(t))$, assuming quadratic forms for these quantities, and taking into account (B.34) and (B.38), we can obtain a two-filter formula for $\hat{q}_s(t)$. Rather than doing this, we will use the preceding results to motivate the formulation and solution of a white noise version of the continuous-time centralized map-updating problem, as the problem of optimizing a quadratic functional.

We next define the white noise version of the map-updating problem which we will solve. We assume that we have some continuous state process modelled by

$$\frac{dx}{dt} = A\,x(t) + B\,w(t) \quad , \tag{B.41}$$

where $$E[w(t_1)w'(t_2)] = I\,\delta(t_1 - t_2) \quad . \tag{B.42}$$

Letting $$Q \triangleq B\,B' \quad , \tag{B.43}$$

and π denote the state covariance associated with $x(\cdot)$, we note from Kailath and Verghese [36] that $x(\cdot)$ satisfies the backward model

$$-\frac{dx}{dt} = -(A + Q\pi^{-1})x(t) - B\bar{w}(t) \quad , \tag{B.44}$$

where $\bar{w}(\cdot)$ is a standard white noise process. In addition, we assume that we have two measurement passes

$$m_1(t) = H_1 x(t) + n_1(t) \quad , \tag{B.45}$$

$$m_2(t) = H_2 x(t) + n_2(t) \quad , \tag{B.46}$$

where the $n_i(\cdot)$, $i = 1,2$, are independent white noise processes with respective intensities, $R_i(\cdot)$, $i = 1,2$. We can think of (B.41) and (B.45) - (B.46) as being derived from the differential formulation of Section 4.2 by letting

$$\left.\begin{aligned} & du(t) = w(t)dt \quad , \\ \text{and} \quad & dy_i(t) = m_i(t)dt \quad , \\ \text{with} \quad & D_i(t)dv_i(t) = n_i(t)dt \quad . \end{aligned}\right\} \tag{B.47}$$

We now use the fact that by discretizing the continuous-time, white noise formulation of the centralized map-updating problem, we obtain a discrete measurement map-updating problem of the exact type discussed earlier, so that by noting (B.47), we can argue that the solution of the continuous-time problem may be stated as follows. Let us define $\tilde{m}_2(t)$ as

$$\tilde{m}_2(t) \triangleq m_2(t) - H_2\hat{x}_{1s}(t) \quad , \tag{B.48}$$

then $$\hat{x}_s(t) = \hat{x}_{1s}(t) + \hat{q}_s(t) \quad , \tag{B.49}$$

where $\hat{q}_s(t)$ is determined by

$$\min_{\left(q(\tau)\ \tau\neq t\right)} \{J\} = \left(q(t) - \hat{q}_s(t)\right)' P_s^{-1}(t)\left(q(t) - \hat{q}_s(t)\right) + \text{constant} \quad , \tag{B.50}$$

where

$$J \triangleq J_{0,t} + J_{t,T} - \tfrac{1}{2}q'(t)\pi^{-1}(t)q(t) \quad , \tag{B.51}$$

and

$$\begin{aligned} J_{0,t} \triangleq\ & \tfrac{1}{2}q'(0)\pi^{-1}(0)q(0) + \tfrac{1}{2}\int_0^t \tilde{w}'(\tau)\tilde{w}(\tau)\,d\tau \\ & + \tfrac{1}{2}\int_0^t q'(\tau)H_1'R_1^{-1}H_1\,q(\tau)\,d\tau \\ & + \tfrac{1}{2}\int_0^t \left(\tilde{m}_2(\tau) - H_2q(\tau)\right)' R_2^{-1}\left(\tilde{m}_2(\tau) - H_2q(\tau)\right)d\tau \quad , \end{aligned} \tag{B.52}$$

with $$\dot{q}(\tau) = A\,q(\tau) + B\tilde{w}(\tau) \quad , \tag{B.53}$$

and

$$J_{t,T} \triangleq \frac{1}{2}q'(T)\pi^{-1}(T)q(T) + \frac{1}{2}\int_t^T \tilde{\tilde{w}}'(\tau)\tilde{\tilde{w}}(\tau)d\tau$$

$$+ \frac{1}{2}\int_t^T q'(\tau)H_1'R_1^{-1}H_1 q(\tau)d\tau$$

$$+ \frac{1}{2}\int_t^T \left(\tilde{m}_2(\tau) - H_2 q(\tau)\right)' R_2^{-1}\left(\tilde{m}_2(\tau) - H_2 q(\tau)\right)d\tau \ , \qquad (B.54)$$

with $$-\dot{q}(\tau) = -(A+Q\pi^{-1})q(\tau) - B\tilde{\tilde{w}}(\tau) \ . \qquad (B.55)$$

We finally outline the use of dynamic programming techniques to perform the optimizations defined by equations (B.50) - (B.55). If we define

$$V_f(t,q(t)) \triangleq \min_{\substack{\tilde{w}(\tau),\ 0\le\tau\le t \\ \dot{q}(\tau)=Aq(\tau)+B\tilde{w}(\tau)}} \{J_{0,t}\} \ , \qquad (B.56)$$

and

$$V_b(t,q(t)) \triangleq \min_{\substack{\simeq \\ w(\tau),\ t\le\tau\le T \\ -\dot{q}(\tau)=-(A+Q\pi^{-1})q(\tau)-B\tilde{\tilde{w}}(\tau)}} \{J_{t,T}\} \ , \qquad (B.57)$$

then by using the principle of optimality [39] we can obtain the Hamilton-Jacobi-Bellman equations satisfied by these quantities. Letting $V_{f,t}(t,q(t))$, $V_{b,t}(t,q(t))$ and

$V_{f,q}(t,q(t))$, $V_{b,q}(t,q(t))$ denote the partial derivatives of $V_f(t,q(t))$, $V_b(t,q(t))$, with respect to t, and the gradient, as a row vector, with respect to the variables in q(t), respectively, then we obtain the relations

$$V_{f,t}(t,q(t)) = -\frac{1}{2}V_{f,q}(t,q(t))QV'_{f,q}(t,q(t)) - V_{f,q}(t,q(t))Aq(t) + \frac{1}{2}q'(t)H_1'R_1^{-1}H_1q(t) + \frac{1}{2}\left(\tilde{m}_2(t) - H_2q(t)\right)'R_2^{-1}\left(\tilde{m}_2(t) - H_2q(t)\right) \quad , \quad (B.58)$$

with $$V_{f,0}(0,q(0)) = \frac{1}{2}q'(0)\pi^{-1}(0)q(0) \quad , \quad (B.59)$$

and $$-V_{b,t}(t,q(t)) = -\frac{1}{2}V_{b,q}(t,q(t))QV'_{b,q}(t,q(t)) + V_{b,q}(t,q(t))(A+Q\pi^{-1})q(t) + \frac{1}{2}q'(t)H_1'R_1^{-1}H_1q(t) + \frac{1}{2}\left(\tilde{m}_2(t) - H_2q(t)\right)R_2^{-1}\left(\tilde{m}_2(t) - H_2q(t)\right) , \quad (B.60)$$

with $$V_{b,T}(T,q(T)) = \frac{1}{2}q'(T)\pi^{-1}(T)q(T) \quad . \quad (B.61)$$

If we now assume that

$$V_{f,t}(t,q(t)) = \frac{1}{2}q'(t)P_f^{-1}(t)q(t) + \xi_f'(t)q(t) + c_f(t), \quad (B.62)$$

$$V_{b,t}(t,q(t)) = \frac{1}{2}q'(t)P_r^{-1}(t)q(t) + \xi_r'(t)q(t) + c_b(t), \quad \text{(B.63)}$$

and use (B.58) - (B.61) and (B.50) - (B.51), we can show that

$$\hat{q}_s(t) = - P_s^{-1}(t)\left\{\xi_f(t) + \xi_r(t)\right\} , \quad \text{(B.64)}$$

where $$P_s^{-1}(t) = P_f^{-1}(t) + P_r^{-1}(t) - \pi^{-1}(t) , \quad \text{(B.65)}$$

$$\dot{\xi}_f(t) = (-A' - P_f^{-1}Q)\xi_f(t) - H'_2R_2^{-1}\tilde{m}_2(t) , \quad \text{(B.66)}$$

$$-\dot{\xi}_r(t) = \left(A' + (\pi^{-1} - P_r^{-1})Q\right)\xi_r(t) - H_2'R_2^{-1}\tilde{m}_2(t) , \quad \text{(B.67)}$$

and $$\xi_f(0) = \xi_r(T) = 0 . \quad \text{(B.68)}$$

The quantities P_f^{-1} and P_r^{-1} correspond to the inverses of the two-data pass, forward and reverse filtering error covariance matrices, respectively, and evolve as

$$\frac{d}{dt}(P_f^{-1}) = H_2'R_2^{-1}H_2 + H_1'R_1^{-1}H_1 - P_f^{-1}QP_f^{-1} - A'P_f^{-1} - P_f^{-1}A , \quad \text{(B.69)}$$

with $$P_f^{-1}(0) = \pi^{-1}(0) , \quad \text{(B.70)}$$

and

$$-\frac{d}{dt}(P_r^{-1}) = H_2'R_2^{-1}H_2 + H_1'R_1^{-1}H_1 - P_r^{-1}QP_r^{-1} + (A' + \pi^{-1}Q)P_r^{-1} + P_r^{-1}(A + Q\pi^{-1}) \quad , \tag{B.71}$$

with $$P_f^{-1}(T) = \pi^{-1}(T) \quad . \tag{B.72}$$

In conclusion, we note that the formula for map-updating obtained by substituting equation (B.64) for $\hat{q}_s(t)$ into (B.49), is essentially the Information Filter Algorithm of Section 4.2.2, when we identify $\gamma_f(\cdot)$ and $\gamma_r(\cdot)$ with $-\xi_f(\cdot)$ and $-\xi_r(\cdot)$, respectively. From the form of the correlation structure for $\tilde{x}_{1s}$ conditioned on $\tilde{Z}_2$, derived from our earlier analysis of the discrete-time map-updating problem, we can see why the algorithm for computing $\hat{q}_s(t)$ of (B.64) - (B.72) resembles the solution of a two-pass smoothing problem, where the q(·)'s evolve according to equations of the same form as the unconditional state dynamics, and the two measurement passes are described by

$$0 = H_1 q(\tau) + \tilde{n}_1(\tau) \quad , \tag{B.73}$$

and $$\tilde{m}_2(\tau) = H_2 q(\tau) + n_2(\tau) \quad , \tag{B.74}$$

(where $\tilde{n}_1(\cdot)$, $n_2(\cdot)$ are independent white noise processes with intensities $R_1(\cdot)$, $R_2(\cdot)$, respectively).

Appendix 4C

An Algebraic Approach to Centralized Map-Updating

In this Appendix we demonstrate how the centralized map-updating algorithm obtain in Section 4.2.3 may be derived by starting from the Wall two-filter solution to the two-pass smoothing problem. We note first that we can represent the two-pass forward filtered estimate, $\hat{x}_f(t)$, as the output of a system with time-varying impulse response, $\Phi_{\bar{\Gamma}_f}(t,\tau)$, corresponding to the transition matrix associated with the two-pass filter dynamics matrix, $\bar{\Gamma}_f$, and with the inputs $P_f H_1' R_1^{-1} dy_1(\cdot)$ and $P_f H_2' R_2^{-1} dy_2(\cdot)$. This observation is depicted in Fig. C.1. By working with the block diagram representation of $\hat{x}_f(t)$ in Fig. C.1, and employing both first-pass filtering equations and the relationship between first-pass smoothed and filtered estimates, we will ultimately express $\hat{x}_f(t)$ as a linear functional of $\hat{x}_{1f}(t)$, $dy_2(\cdot)$, and $\hat{x}_{1s}(\cdot)$. Using the same technique we can express $\hat{x}_r(t)$ as a functional of $\hat{x}_{1r}(t)$, $dy_2(\cdot)$, and $\hat{x}_{1s}(\cdot)$. Substitution of the resulting relations for $\hat{x}_f(t)$ and $\hat{x}_r(t)$ into the Wall two-pass smoothing formula will yield the desired centralized map-updating algorithm.

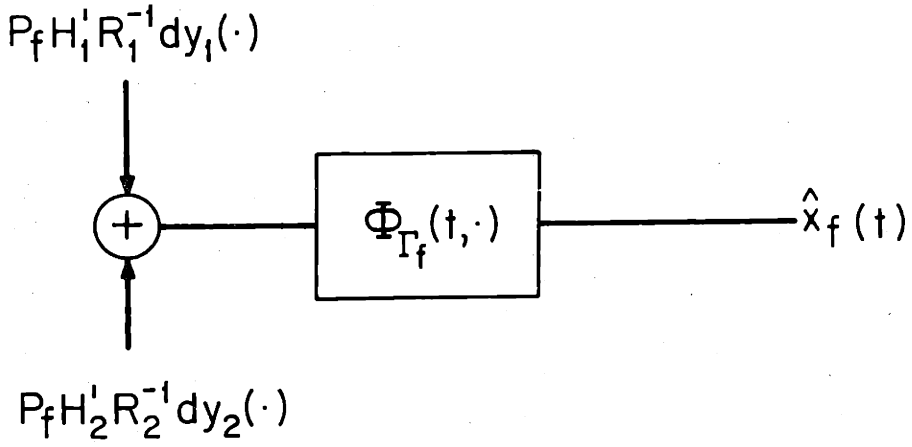

Fig. C.1 Two-Pass Forward Filtering Block Diagram

We first observe that the first-pass filtering equations are specified by

$$d\hat{x}_{1f}(t) = (A - P_{1f}H_1'R_1^{-1}H_1)\hat{x}_{1f}(t)dt + P_{1f}H_1'R_1^{-1}dy_1(t) \quad , \qquad (C.1)$$

where $$\dot{P}_{1f} = A P_{1f} + P_{1f}A' + Q - P_{1f}H_1'R_1^{-1}H_1P_{1f} \quad , \qquad (C.2)$$

and $$P_{1f}(0) = \pi(0) \quad . \qquad (C.3)$$

Assuming our state equations for $x(\cdot)$ are controllable from the noise, $du(\cdot)$, $P_{1f}(t)$ will be nonsingular, and we may use relation (C.1) to express $H_1'R_1^{-1}dy_1(t)$ as

$$H_1'R_1^{-1}dy_1(t) = P_{1f}^{-1}\left\{ d\hat{x}_{1f}(t) - (A - P_{1f}H_1'R_1^{-1}H_1)\hat{x}_{1f}(t)dt \right\} , \qquad (C.4)$$

Hence, we can conceive of replacing $H_1'R_1^{-1}dy_1(t)$ in the block diagram of Fig. C.1 by the right-hand side of relation (C.4). Now, as an aside, consider the two systems pictured in Fig. C.2. Assuming that $\Phi_F(t,\tau)$ is a transition matrix associated with dynamics matrix $F(\cdot)$, and that $W(0)\alpha(0)$ is zero, we can show from integration by parts that both systems are equivalent. Therefore, replacing $H_1'R_1^{-1}dy_1(\cdot)$ in Fig. C.1 by the right-hand side of relation (C.4) and identifying $\dot{\alpha}(\cdot)$ with

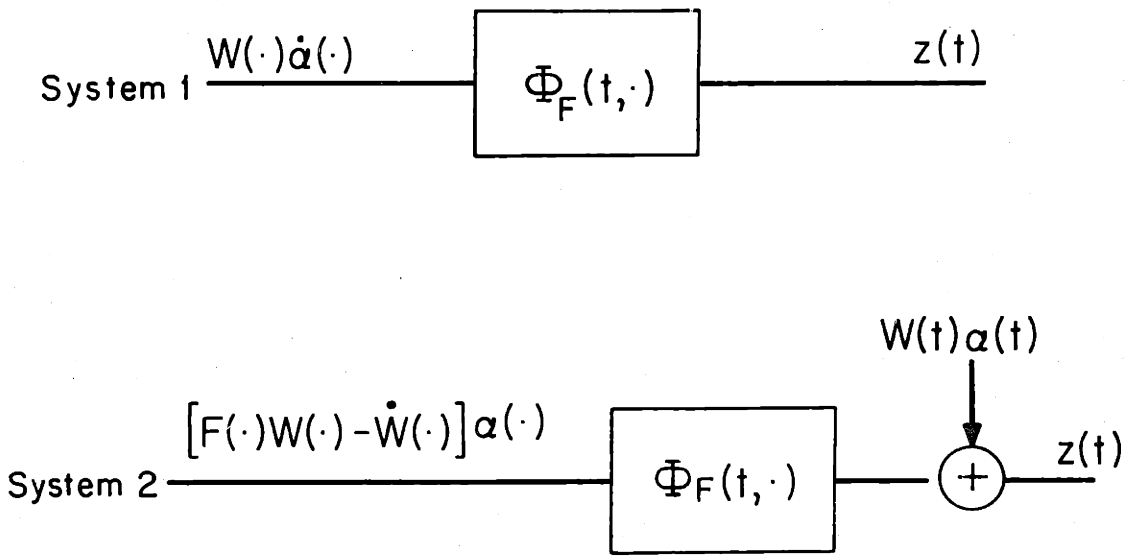

Fig. C.2 Two Equivalent Block Diagrams Given that $W(t)\alpha(t)\big|_{t=0} = 0$ and that $\Phi_F(\cdot,\cdot)$ is the Transition Matrix Associated with the Dynamics Matrix $F(\cdot)$

$d\hat{x}_{1f}(t) \equiv \dot{\hat{x}}_{1f}(t)dt$, we may use the rule expressed by Fig. C.2, superposition, and some algebraic manipulations to derive the new two-pass filtering block diagram depicted in Fig. C.3.

Thus far, in Fig. C.3 we have expressed the two-pass filtered estimate, $\hat{x}_f(t)$, as a linear functional of the first-pass filtered estimate, $\hat{x}_{1f}(t)$, and second-pass data, $dy_2(\cdot)$. We now note from Fig. C.3 that if $(Q\,P_{1f}^{-1}\hat{x}_{1f}(\cdot))dt$ may be expressed as a linear functional of $\hat{x}_{1s}(\cdot)$, we can then attain our goal of forming the two-pass filtered estimate, $\hat{x}_f(t)$, from the first-pass smoothed estimates, $\hat{x}_{1s}(\cdot)$,$\hat{x}_{1f}(t)$, and the new data, $dy_2(\cdot)$. Rewriting the Wall two-filter solution to the first-pass smoothing problem as

$$P_{1s}^{-1}\hat{x}_{1s}(t) = P_{1f}^{-1}\hat{x}_{1f}(t) + P_{1r}^{-1}\hat{x}_{1r}(t) \quad , \tag{C.5}$$

taking the differential of the above equation, and using the first-pass forward and reverse filtering equations to form $d\hat{x}_{1f}(t)$ and $d\hat{x}_{1r}(t)$, we may obtain the following expression for $(Q\,P_{1f}^{-1}\hat{x}_{1f}(t))dt$:

$$(Q\,P_{1f}^{-1}\hat{x}_{1f}(t))dt = P_{1s}(t)\Big\{(-A' - \pi^{-1}Q + P_{1r}^{-1}Q)P_{1s}^{-1}\hat{x}_{1s}(t)dt - P_{1s}^{-1}(t)d\hat{x}_{1s}(t) + P_{1s}^{-1\cdot}P_{1s}P_{1s}^{-1}\hat{x}_{1s}(t)dt\Big\}. \tag{C.6}$$

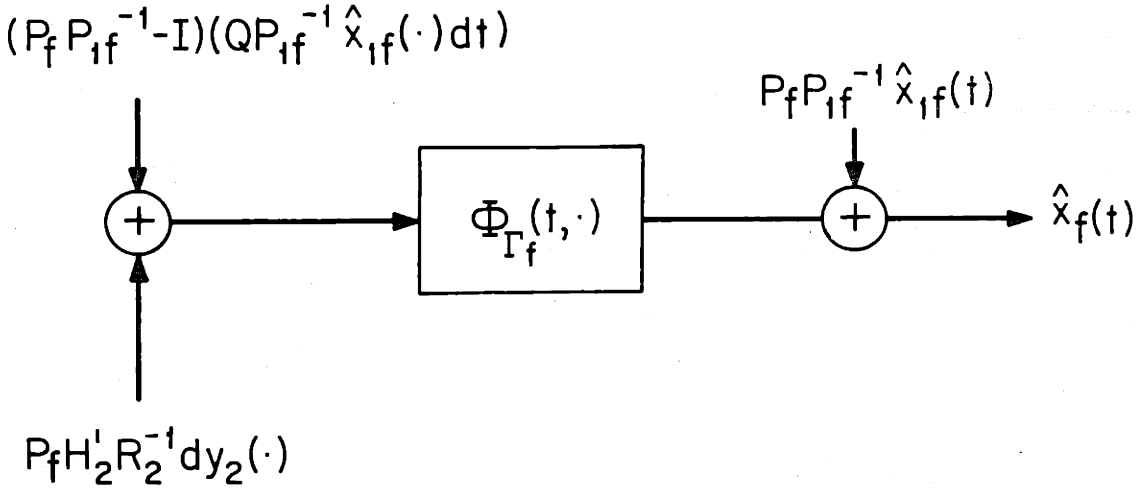

Fig. C.3 New Two-Pass Forward Filtering Block Diagram

Now, by substituting the above relation for $(Q\,P_{1f}^{-1}\hat{x}_{1f}(t))dt$ into the block diagram representation for $\hat{x}_f(t)$ in Fig. C.3 and employing the block diagram equivalence of Fig. C.2 for eliminating the derivative term, $d\hat{x}_{1s}(t) \equiv \dot{\hat{x}}_{1s}(t)dt$, with some additional algebra we obtain the final diagram of Fig. C.4 representing the two-pass filtered estimate as a functional of $\hat{x}_{1f}(t)$, $\hat{x}_{1s}(\cdot)$, and $dy_2(\cdot)$. Letting the output of the two-pass filtering dynamics block be denoted as $q_f(t)$, we can express $\hat{x}_f(t)$ by

$$\hat{x}_f(t) = P_f P_{1f}^{-1}\hat{x}_{1f}(t) - (P_f P_{1f}^{-1} - I)\hat{x}_{1s}(t) + q_f(t) \quad , \qquad (C.7)$$

where $q_f(t)$ satisfies the stochastic differential equation

$$dq_f(t) = \Gamma_f q_f(t)dt + P_f H_2' R_2^{-1}(dy_2(t) - H_2(t)\hat{x}_{1s}(t)dt), \qquad (C.8)$$

with $$q_f(0) = 0 \quad . \qquad (C.9)$$

Hence, in Fig. C.4, with the exception of the additive term, $\hat{x}_{1f}(t)$, we have very nearly obtained the desired map-updating structure for computing the quantities defining $\hat{x}_s(t)$ as a linear functional of the new data, $dy_2(\cdot)$, and the old

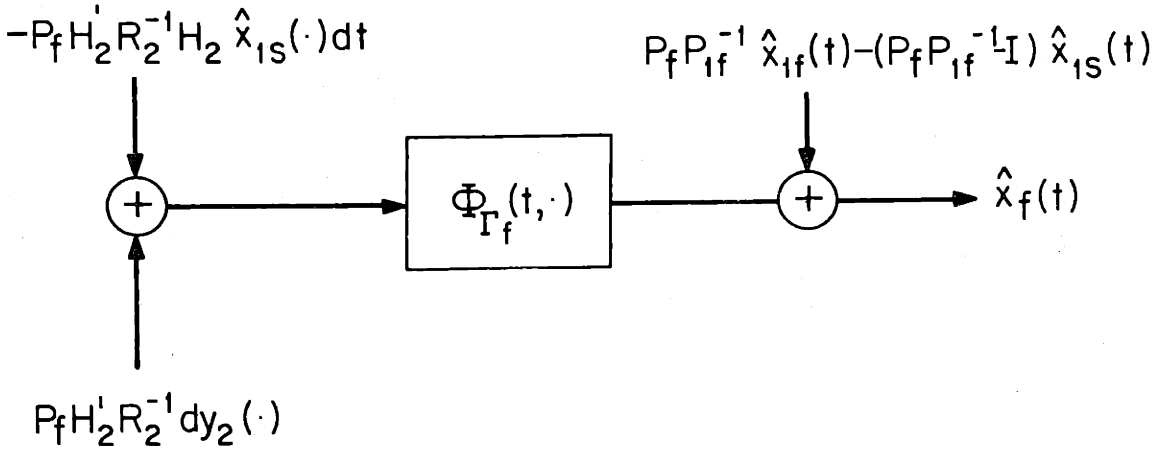

Fig. C.4 Final Two-Pass Forward Filtering Block Diagram

map, $\hat{x}_{1s}(\cdot)$. The input process to the two-pass filtering dynamics block, $[dy_2(\cdot) - H_2\hat{x}_{1s}(\cdot)dt]$, represents the new information contained in the second-pass data, i.e., the part not predictable from the entire first-pass measurements.

By an analogous series of operations on the block diagram representation for the two-pass reverse filtered estimate, $\hat{x}_r(t)$, we arrive at the following relations which are similar to (C.7) - (C.9):

$$\hat{x}_r(t) = P_r P_{1r}^{-1}\hat{x}_{1r}(t) - (P_r P_{1r}^{-1} - I)\hat{x}_{1s}(t) + q_r(t) \ , \qquad (C.10)$$

where $q_r(\cdot)$ satisfies the following differential equation evolving backwards in time:

$$-dq_r(t) = \Gamma_r q_r(t)dt + P_r H_2' R_2^{-1}(dy_2(t) - H_2\hat{x}_{1s}(t)dt), \qquad (C.11)$$

with $$q_r(T) = 0 \ . \qquad (C.12)$$

Finally, by substituting relations (C.7) and (C.10) into Wall's solution for the two-pass smoothed estimate, we obtain the following relation:

$$\hat{x}_s(t) = P_s\left\{P_f^{-1}q_f(t) + P_r^{-1}q_r(t)\right\} + \hat{x}_{1s}(t) \ .$$

Hence, by algebraic manipulations of one- and two-pass filtering and smoothing equations we have obtained the symmetric filter map-updating algorithm of Section 4.2.3.

Appendix 4D

The Scattering Approach to Centralized Map-Updating and Map-Combining

In this Appendix we use the scattering formalism of Appendix 2G in order to construct scattering diagrams that represent the solution to both the centralized map-updating and map-combining problems. We first note that different scattering mediums are employed to represent the calculation of either $\hat{x}_{1s}(\cdot)$, $\hat{x}_{2s}(\cdot)$, or $\hat{x}_s(\cdot)$. Our technique for constructing solutions to the map-updating or map-combining problems will be to first manipulate the scattering diagrams associated with either $\hat{x}_{1s}(\cdot)$ or $\hat{x}_{2s}(\cdot)$, so that they correspond to the same medium as that associated with the two-pass smoothed estimate, $\hat{x}_s(\cdot)$. Once we have represented $\hat{x}_s(\cdot)$, $\hat{x}_{1s}(\cdot)$, and $\hat{x}_{2s}(\cdot)$ by the same scattering medium, we can use the linearity of that medium to apply the principle of superposition, i.e., we can effectively add or subtract scattering diagrams.

We depict the incremental layers that make up the scattering medium for representing $\hat{x}_{1s}(\cdot)$, $\hat{x}_{2s}(\cdot)$, and $\hat{x}_s(\cdot)$ in Fig. D.1. We note that in the formulation we present, scattering diagrams are essentially flow graphs, and the quantities that appear along the edges of those graphs are gains. Hence, by employing

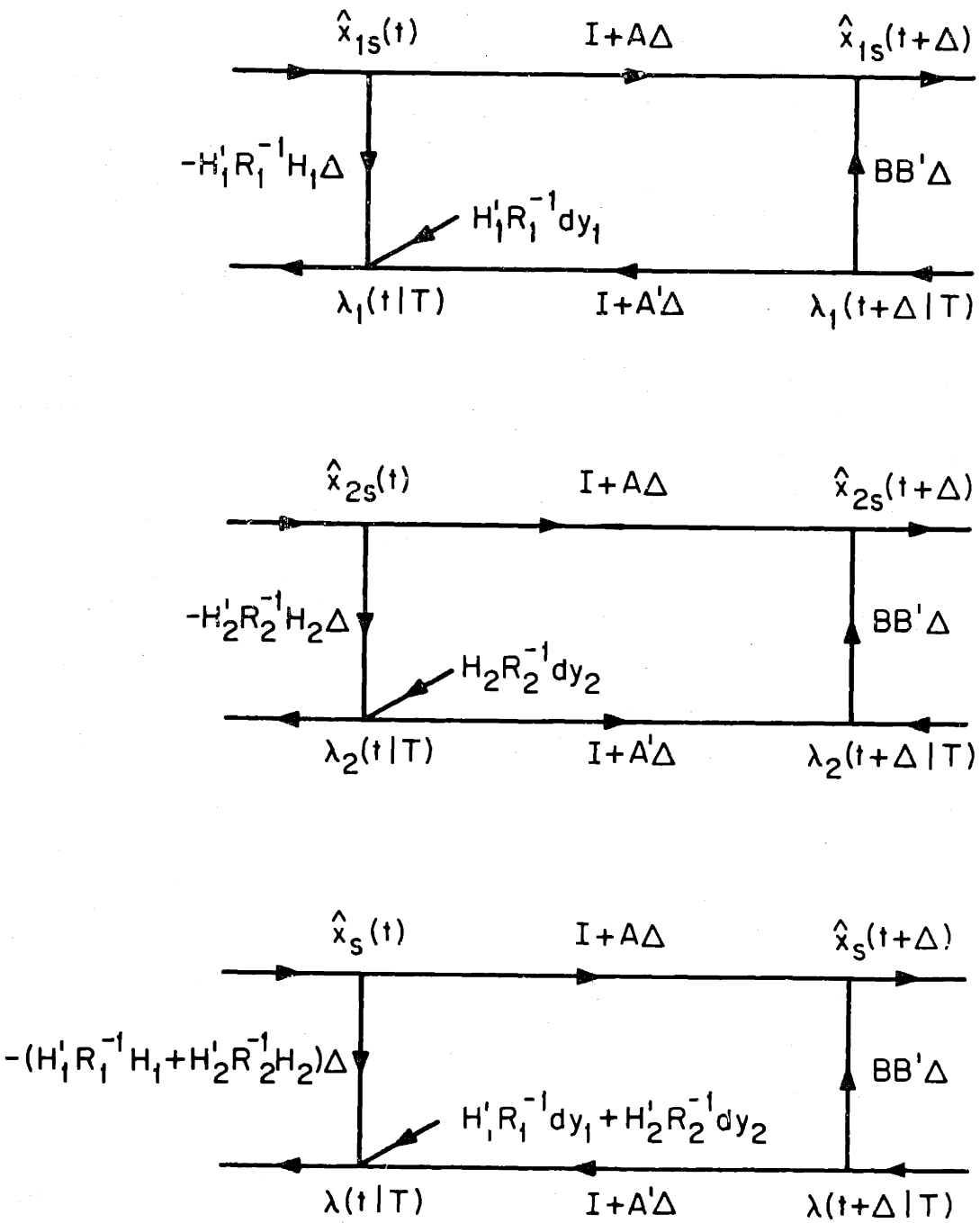

Fig. D.1 Incremental Scattering Sections Associated with $\hat{x}_{1s}(\cdot)$, $\hat{x}_{2s}(\cdot)$, and $\hat{x}_s(\cdot)$

flow graph manipulation rules to essentially add and subtract the same term, we can obtain the equivalent incremental scattering layers of Fig. D.2 for representing $\hat{x}_{1s}(\cdot)$ and $\hat{x}_{2s}(\cdot)$.

In Fig. D.2 we have represented both $\hat{x}_{1s}(\cdot)$ and $\hat{x}_{2s}(\cdot)$ by the same scattering medium as that associated with the two-pass smoothed estimate, $\hat{x}_s(\cdot)$. Therefore, we can now apply the principle of superposition to add and subtract scattering diagrams associated with either $\hat{x}_{1s}(\cdot)$, $\hat{x}_{2s}(\cdot)$, or $\hat{x}_s(\cdot)$. Subtracting the diagram of Fig. D.2 representing $\hat{x}_{1s}(\cdot)$, from the scattering picture for $\hat{x}_s(\cdot)$ of Fig. D.1, we obtain the map-updating scattering picture of Fig. D.3. We can now use any technique for solving scattering problems to obtain a multiplicity of possible methods for computing $\hat{x}_s(t) - \hat{x}_{1s}(t)$. In particular, we can obtain a Mayne-Fraser type two-filter algorithm for computing this term as follows:

$$\hat{x}_s(t) - \hat{x}_{1s}(t) = P_s\left\{P_f^{-1}q_f(t) + P_B^{-1}q_B(t)\right\}, \qquad (D.1)$$

where

$$dq_f(t) = \left(A - P_f(H_1'R_1^{-1}H_1 + H_2'R_2^{-1}H_2)\right)q_f(t)dt + P_fH_2'R_2^{-1}d\tilde{y}_2(t), \qquad (D.2)$$

with $$q_f(0) = 0 \quad , \qquad (D.3)$$

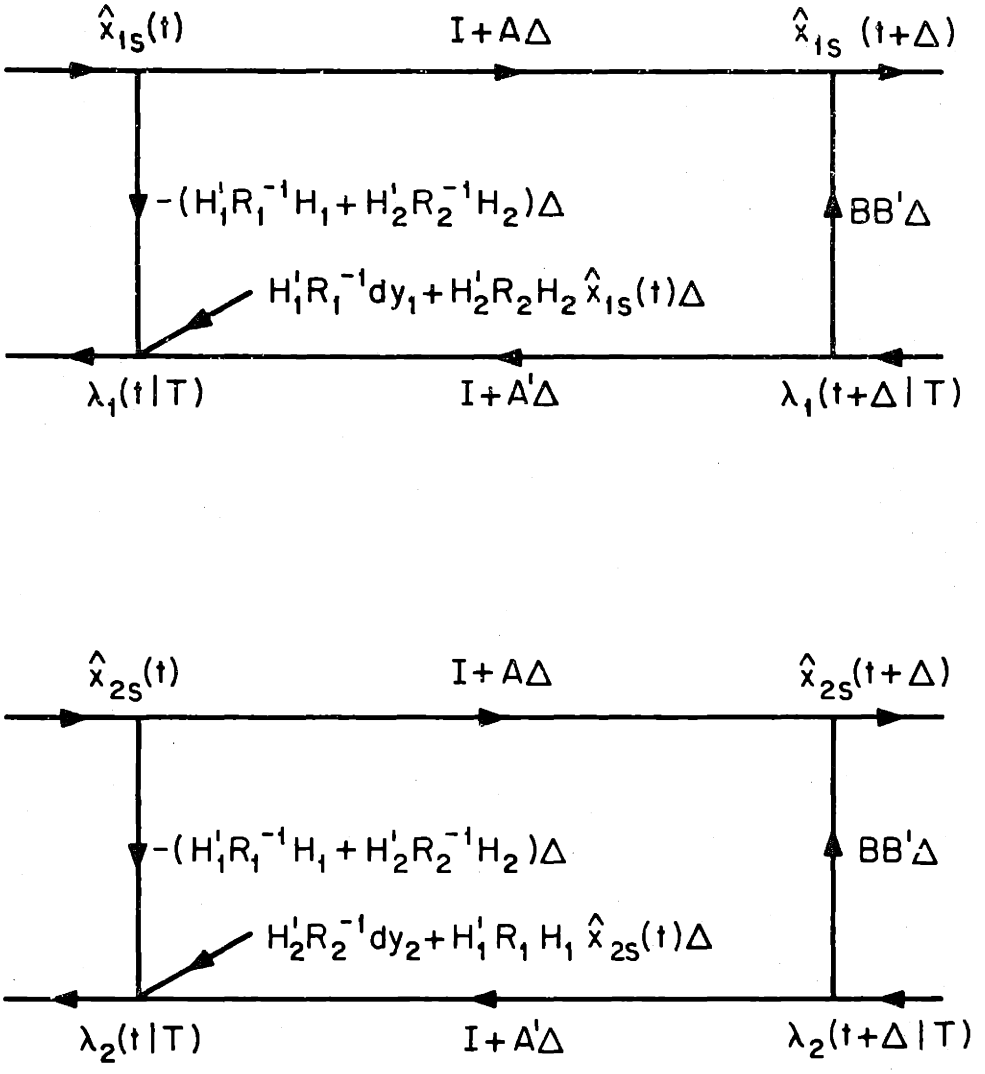

Fig. D.2 Equivalent Representation for the Incremental Scattering Sections Associated with $\hat{x}_{1s}(\cdot)$ and $\hat{x}_{2s}(\cdot)$

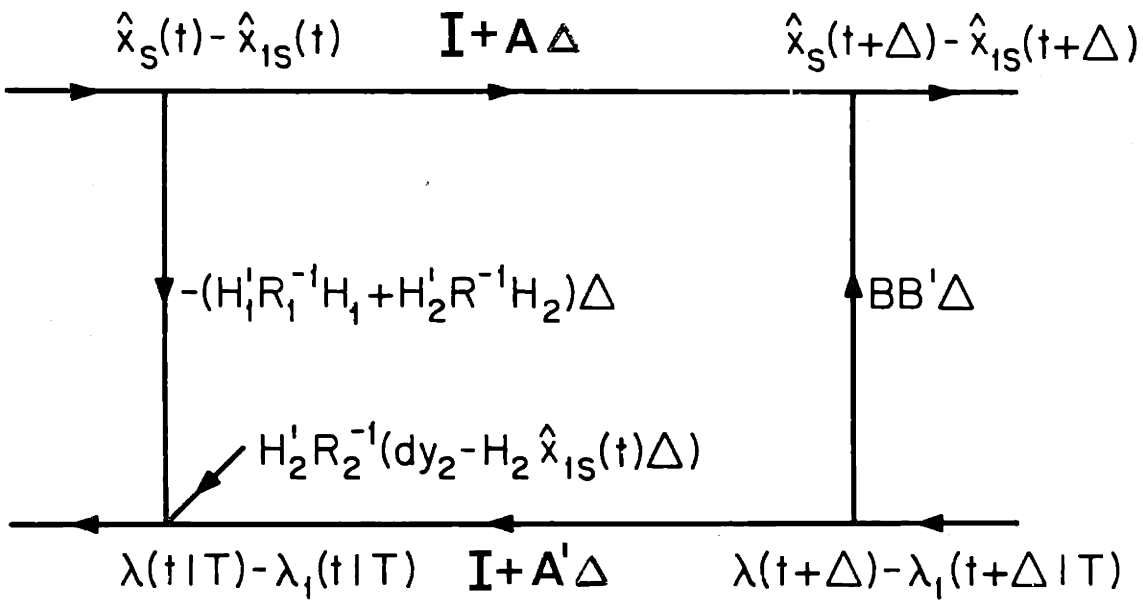

Fig. D.3 Incremental Scattering Sections Associated with the Centralized Map-Updating Problem

and P_f evolves as

$$\dot{P}_f = A P_f + P_f A' + BB' - P_f(H_1'R_1^{-1}H_1 + H_2'R_2^{-1}H_2)P_f \ , \qquad (D.4)$$

with $$P_f(0) = \pi(0) \quad . \qquad (D.5)$$

In addition, $q_B(\cdot)$ satisfies the backward equation

$$-dq_B(t) = \left(-A - P_B(H_1'R_1^{-1}H_1 + H_2'R_2^{-1}H_2)\right) q_B(t)dt + P_B H_2'R_2^{-1} d\tilde{y}_2(t), \qquad (D.6)$$

with $$P_B^{-1}(T)q_B(T) = 0 \ , \qquad (D.7)$$

and P_B evolves as

$$-\dot{P}_B = -A P_B - P_B A' + BB' - P_B(H_1'R_1^{-1}H_1 + H_2'R_2^{-1}H_2)P_B, \qquad (D.8)$$

with $$P_B^{-1}(T) = 0 \quad . \qquad (D.9)$$

To solve the centralized map-combining problem, we similarly subtract the sum of the scattering diagrams for $\hat{x}_{1s}(\cdot)$ and $\hat{x}_{2s}(\cdot)$ in Fig. D.2, from the scattering picture associated with the two-pass smoothed estimate, $\hat{x}_s(\cdot)$, to obtain the resulting diagram of Fig. D.4. Hence, Fig. D.4 results in the

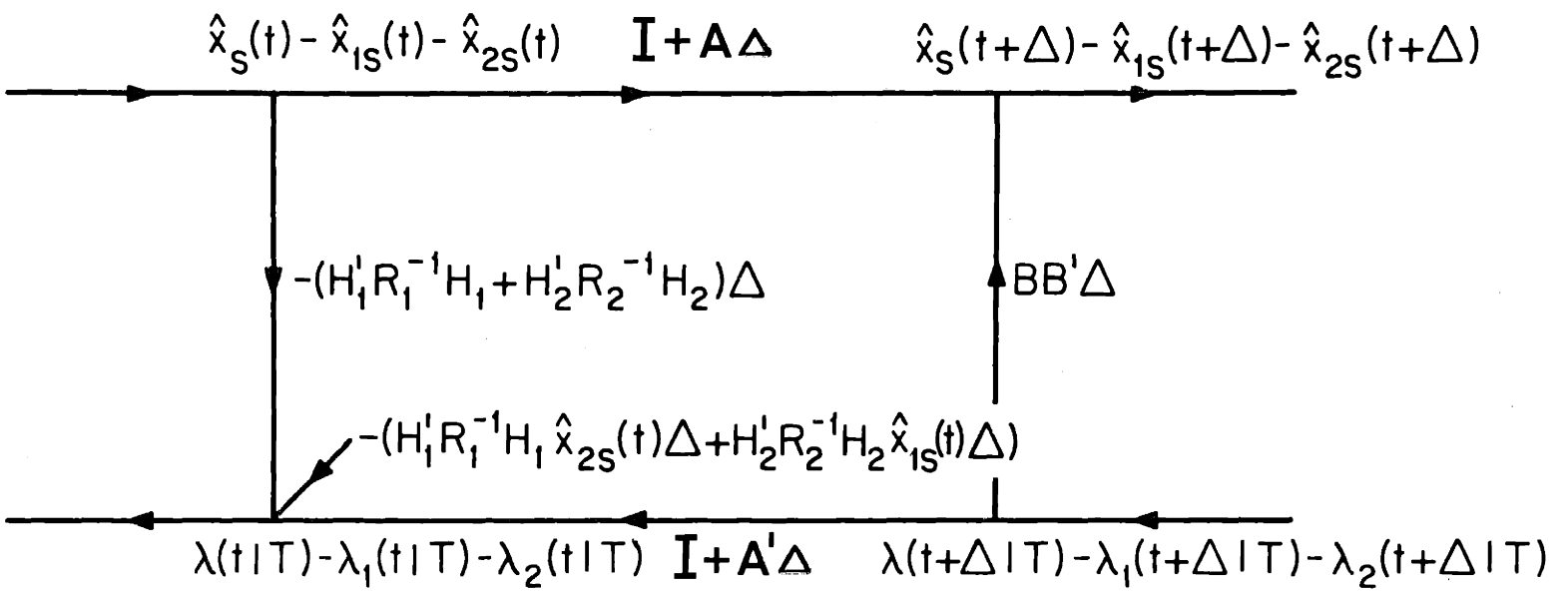

Fig. D.4 Incremental Scattering Sections Associated with the Centralized Map-Combining Problem

following two-filter algorithm, analogous to that of (D.1) - (D.9), but for computing $\hat{x}_s(t) - \hat{x}_{1s}(t) - \hat{x}_{2s}(t)$:

$$\hat{x}_s(t) - \hat{x}_{1s}(t) - \hat{x}_{2s}(t) = P_s\left\{P_f^{-1}\theta_f(t) + P_B^{-1}\theta_B(t)\right\} , \qquad (D.10)$$

where

$$d\theta_f(t) = \left(A - P_f(H_1'R_1^{-1}H_1 + H_2'R_2^{-1}H_2)\right)\theta_f(t)dt$$
$$- P_f(H_1'R_1^{-1}H_1\hat{x}_{2s}(t)dt + H_2'R_2^{-1}H_2\hat{x}_{1s}(t)dt) , \qquad (D.11)$$

with $$\theta_f(0) = 0 , \qquad (D.12)$$

and

$$-d\theta_B(t) = \left(-A - P_B(H_1'R_1^{-1}H_1 + H_2'R_2^{-1}H_2)\right)\theta_B(t)dt$$
$$- P_B(H_1'R_1^{-1}H_1\hat{x}_{2s}(t)dt + H_2'R_2^{-1}H_2\hat{x}_{1s}(t)dt) , \qquad (D.13)$$

with $$P_B^{-1}(T)\theta_B(T) = 0 . \qquad (D.14)$$

In conclusion, through Fig. D.3 and Fig. D.4 we have demonstrated the power and simplicity of the use of the scattering formalism for deriving solutions to both the centralized map-updating and map-combining problems.

Appendix 4E

Solution to the Centralized Discrete Map-Updating Problem

In this Appendix we pose and solve the discrete version of the centralized map-updating problem. We assume that $x(t)$ represents some discrete time state process that evolves as

$$x(t+1) = A(t)x(t) + B(t)u(t) \ , \tag{E.1}$$

with $$E[x(0)x'(0)] = \pi(0) \ , \tag{E.2}$$

and where $u(\cdot)$ represents a standard discrete white noise process. We suppose that we have two-measurement passes modelled by

$$y_1(t) = H_1(t)x(t) + D_1(t)v_1(t) \quad \text{for } t = 1,\ldots,T, \tag{E.3}$$

and $$y_2(t) = H_2(t)x(t) + D_2(t)v_2(t) \quad \text{for } t = 1,\ldots,T, \tag{E.4}$$

where $$D_1(t)D_1'(t) \triangleq R_1(t) > 0 \ , \tag{E.5}$$

$$D_2(t)D_2'(t) \triangleq R_2(t) > 0 \ , \tag{E.6}$$

and where $v_1(\cdot)$, $v_2(\cdot)$ represent two independent, standard white noise processes, uncorrelated with the process noise $u(\cdot)$. We will let Y_1 and Y_2 denote the Hilbert spaces spanned by the first and second pass data, respectively. The centralized map-updating problem is then defined as that of computing the two-pass smoothed estimate, $\hat{x}_s(t)$, defined by

$$\hat{x}_s(t) = E[x(t)|Y] \ , \tag{E.7}$$

where $$Y = Y_1 \vee Y_2 \ , \tag{E.8}$$

as a linear functional of the first-pass smoothed estimates, $\hat{x}_{1s}(\cdot)$, determined by

$$\hat{x}_{1s}(t) = E[x(t)|Y_1] \ , \tag{E.9}$$

and the second-pass measurements, $y_2(\cdot)$.

The solution to the discrete time centralized map-updating problem follows from decomposing Y as

$$Y = Y_1 \oplus \tilde{Y}_2 \ , \tag{E.10}$$

where $$\tilde{y}_2(t) \triangleq y_2(t) - E[y_2(t)|Y_1] \ , \tag{E.11}$$

or equivalently

$$\tilde{y}_2(t) = y_2(t) - H_2(t)\hat{x}_{1s}(t) \equiv H_2(t)\tilde{x}_{1s}(t) + D_2(t)v_2(t). \tag{E.12}$$

By employing the orthogonal decomposition in relation (E.10) we obtain the following discrete time expression which constitutes the analog of relation (4.16):

$$\hat{x}_s(t) = \hat{x}_{1s}(t) + E[\tilde{x}_{1s}(t)|\tilde{Y}_2] \ . \tag{E.13}$$

We next employ the Wall two-filter form of the smoother of Appendix 2A for computing $E[\tilde{x}_{1s}(t)|\tilde{Y}_2]$. To evaluate the second term in relation (E.13), we use the forward and reverse Markovian realizations of the first-pass smoothing error process obtained in Appendix 3B. The forward Markovian realization of $\tilde{x}_{1s}(\cdot)$ is determined by the relation

$$\tilde{x}_{1s}(t+1) = \Big(I - B(t)B'(t)P_{1b}(t)\Big)A(t)\tilde{x}_{1s}(t) + B(t)\tilde{u}_{1f}(t), \tag{E.14}$$

where $\tilde{u}_{1f}(\cdot)$ is a discrete, vector white noise sequence with

$$E[\tilde{u}_{1f}(t)\tilde{u}'_{1f}(t)] = I - B'(t)P_{1b}(t)B(t) \ , \tag{E.15}$$

and $P_{1b}(\cdot)$ and $P_{1bp}(\cdot)$ are interpreted as the reverse filtered and reverse predicted error covariance matrices associated with reverse filtered and predicted estimates of the adjoint state process $\gamma(\cdot)$ defined in Appendix 3B. The quantities $P_{1b}(\cdot)$ and $P_{1bp}(\cdot)$ satisfy the backward relations:

$$P_{1bp}(t) = A'(t+1)P_{1b}(t+1)A(t+1) + H_1'(t+1)R_1^{-1}(t+1)H_1(t+1), \quad \text{(E.16)}$$

$$P_{1b}(t) = P_{1bp}(t) - P_{1bp}(t)B(t)\left[B'(t)P_{1bp}(t)B(t) + I\right]^{-1} B'(t)P_{1bp}(t), \quad \text{(E.17)}$$

with $$P_{1b}(T) = 0 \ . \quad \text{(E.18)}$$

The forward Markovian realization of the smoothing error process specified by relations (E.14) - (E.15) is valid for arbitrary process dynamics matrices, $A(\cdot)$. When $A(t)$ is invertible, by using the results of Appendix 3B, we obtain the following backward Markovian realization of the smoothing error process:

$$\tilde{x}_{1s}(t) = A^{-1}(t)\left(I - B(t)B'(t)P_{1fp}^{-1}(t+1)\right)\tilde{x}_{1s}(t+1) - A^{-1}(t)B(t)\tilde{u}_{1r}(t), \quad \text{(E.19)}$$

where $\tilde{u}_{1r}(t)$ is a vector, discrete white noise sequence with

$$E[\tilde{u}_{1r}(t)\tilde{u}'_{1r}(t)] = I - B'(t)P^{-1}_{1fp}(t+1)B(t), \qquad (E.20)$$

and where $P_{1fp}(t)$ denotes the error covariance matrix associated with the forward, first-pass one-step ahead predicted estimate, $\hat{x}_{1fp}(t)$. Letting $P_{1f}(t)$ denote the error covariance matrix associated with the forward first-pass filtered estimate, $\hat{x}_{1f}(t)$, we obtain from standard discrete time Kalman filtering results the following equations for the evolution of $P_{1f}(\cdot)$ and $P_{1fp}(\cdot)$:

$$P_{1fp}(t+1) = A(t)P_{1f}(t)A'(t) + B(t)B'(t) , \qquad (E.21)$$

$$P_{1f}(t) = P_{1fp}(t) - P_{1fp}(t)H'_1(t)\left[H_1(t)P_{1fp}(t)H'_1(t) + R_1(t)\right]^{-1}H_1(t)P_{1fp}(t), \qquad (E.22)$$

with $$P_{1f}(0) = \pi(0) . \qquad (E.23)$$

Having specified the forward and reverse Markovian realizations of the smoothing error process, we now proceed to compute $E[\tilde{x}_{1s}(t)|\tilde{Y}_2]$. As in Section 4.2, we define the

following forward and reverse filtered estimates of the first-pass smoothing errors:

$$\hat{\tilde{x}}_f(t) = E[\tilde{x}_{ls}(t)|\tilde{Y}^-_{2,t+1}] \ , \tag{E.24}$$

$$\hat{\tilde{x}}_{fp}(t) = E[\tilde{x}_{ls}(t)|\tilde{Y}^-_{2,t}] \ , \tag{E.25}$$

$$\hat{\tilde{x}}_r(t) = E[\tilde{x}_{ls}(t)|\tilde{Y}^+_{2,t}] \ , \tag{E.26}$$

and

$$\hat{\tilde{x}}_{rp}(t) = E[\tilde{x}_{ls}(t)|\tilde{Y}^+_{2,t+1}], \tag{E.27}$$

where $P_{fs}(t)$, $P_{fps}(t)$, $P_{rs}(t)$, and $P_{rps}(t)$ denote the corresponding error covariance matrices. Then, by employing Wall's solution to the smoothing problem of Appendix 2A, we form $E[\tilde{x}_{ls}(t)|\tilde{Y}_2]$ as

$$E[\tilde{x}_{ls}(t)|\tilde{Y}_2] = P_s(t)\left\{P^{-1}_{fs}(t)\hat{\tilde{x}}_f(t) + P^{-1}_{rps}(t)\hat{\tilde{x}}_{rp}(t)\right\} \ , \tag{E.28}$$

where

$$P^{-1}_s(t) = P^{-1}_{fs}(t) + P^{-1}_{rps}(t) - P^{-1}_{ls}(t) \ . \tag{E.29}$$

Hence, we may now employ relations (E.14) - (E.15) to specify the forward model for $\tilde{x}_{ls}(\cdot)$, (E.12) to define $\tilde{y}_2(\cdot)$, and standard discrete time Kalman filtering equations to

obtain the following relations for the evolution of $\hat{x}_f(t)$, $P_{fs}(t)$, and $P_{fps}(t)$:

$$\hat{x}_f(t) = \left(I - P_{fs}(t)H_2'(t)R_2^{-1}(t)H_2(t)\right)\left(I - B(t-1)B'(t-1)P_{1b}(t-1)\right) \cdot A(t-1)\hat{x}_f(t-1) + P_{fs}(t)H_2'(t)R_2^{-1}(t)\tilde{y}_2(t) , \tag{E.30}$$

$$P_{fps}(t) = \left(I - B(t-1)B'(t-1)P_{1b}(t-1)\right)A(t-1)P_{fs}(t-1)A'(t-1) \cdot \left(I - B(t-1)B'(t-1)P_{1b}(t-1)\right)' + B(t-1)\left(I - B'(t-1)P_{1b}(t-1)B(t-1)\right)B'(t-1) , \tag{E.31}$$

$$P_{fs}(t) = P_{fps}(t) - P_{fps}(t)H_2'(t)[H_2(t)P_{fps}(t)H_2'(t) + R_2(t)]^{-1}H_2(t)P_{fps}(t), \tag{E.32}$$

with $$P_{fs}(0) = P_{1s}(0) . \tag{E.33}$$

Similarly, we use relations (E.19) - (E.20) to specify the backward model for $\tilde{x}_{1s}(\cdot)$, and apply standard discrete time Kalman filtering formulae to derive the following relations

for the backward evolution of $\hat{x}_{rp}(t)$, $P_{rs}(t)$, and $P_{rps}(t)$:

$$\hat{x}_{rp}(t) = A^{-1}(t)\left(I - B(t)B'(t)P_{1fp}^{-1}(t+1)\right)$$
$$\cdot\left\{\left(I - P_{rs}(t+1)H_2'(t+1)R_2^{-1}(t+1)H_2(t+1)\right)\hat{x}_{rp}(t+1)\right.$$
$$\left. + P_{rs}(t+1)H_2'(t+1)R_2^{-1}(t+1)y_2(t+1)\right\}, \quad (E.34)$$

$$P_{rps}(t) = \left[A^{-1}(t)\left(I - B(t)B'(t)P_{1fp}^{-1}(t+1)\right)\right]P_{rs}(t+1)$$
$$\cdot\left[A^{-1}(t)\left(I - B(t)B'(t)P_{1fp}^{-1}(t+1)\right)\right]'$$
$$+ A^{-1}(t)B(t)\left(I - B'(t)P_{1fp}^{-1}(t+1)B(t)\right)B'(t)A'^{-1}(t),$$
$$(E.35)$$

$$P_{rs}(t+1) = P_{rps}(t+1) - P_{rps}(t+1)H_2'(t+1)\left[H_2(t+1)P_{rps}(t+1)H_2'(t+1)\right.$$
$$\left. + R_2(t+1)\right]^{-1}H_2(t+1)P_{rps}(t+1),$$
$$(E.36)$$

with $$P_{rps}(T) = P_{ls}(T) . \quad (E.37)$$

Relations (E.13) and (E.28) - (E.37) define the desired solution of the discrete centralized map-updating problem. To conclude this Appendix, we note a connection that can be

made between the first-pass smoothing error covariance matrices, $P_{1s}(\cdot)$, the adjoint variable reverse predicted error covariance matrices, $P_{1bp}(\cdot)$, and the one-step ahead prediction error covariance matrices, $P_{1fp}(\cdot)$. By breaking the scattering diagram associated with the first-pass smoothing problem into the sections [0,t] and [t+1,T], and employing relations of Appendix 2C to identify aggregate scattering parameters and internal source contributions, we can obtain the equivalent scattering picture of Fig. E.1. By comparing the expression for $\hat{x}_{1s}(t+1)$ that follows from Fig. E.1 with other two-filter forms of the smoothed estimate, we obtain the following identity for $P_{1s}^{-1}(t+1)$:

$$P_{1s}^{-1}(t+1) = P_{1fp}^{-1}(t+1) + P_{1bp}(t) \quad . \tag{E.38}$$

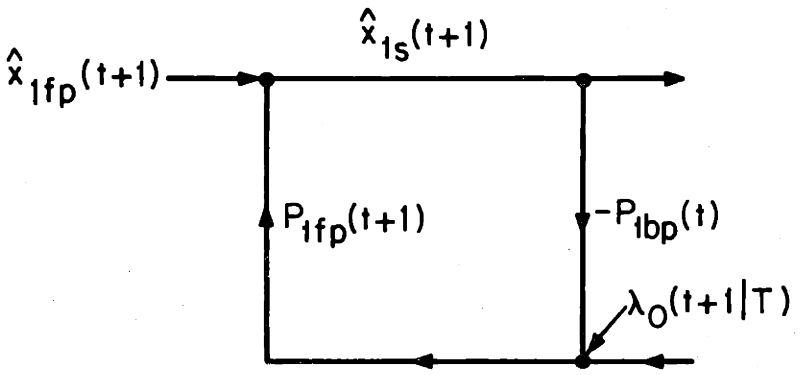

Fig. E.1 Equivalent Scattering Diagram Breaking the Medium into the Sections [0,t] and [t+1,T]

Chapter 5

Continuous Discrete Map-Updating Problems

5.1 Introduction

In Chapter 4 we used some Markovian realizations of the first-pass smoothing error process to derive solutions to the centralized map-updating and map-combining problems in the case where both the first- and second-pass data are modelled as continuous measurements. In the present chapter, we use a similar approach to derive algorithms for solving two variants of the map-updating problem. The first variant that we consider is the case when the first-pass data are discrete measurements, and the second-pass data are continuous, and modelled in the same manner as in Chapter 4. For this problem we distinguish two special cases. In Section 5.2 we consider the situation when we have as our first-pass map the entire first-pass smoothed estimate history, $\hat{x}_{ls}(\cdot)$. In Section 5.3 we examine the case when we only have the estimates $\hat{x}_{ls}(t_i)$ at the discrete measurement times. In each case, the map-updating problem is defined as that of expressing the two-pass smoothed estimate as a linear functional of the second-pass continuous measurements and the old map. Again, we display inside boxes the equations defining the processing algorithm involved in

map-updating. Finally, in Appendix 5E we consider a second variant of the map-updating problem, for which the first-pass data is continuous, and the second-pass data discrete. We note that the problems of this chapter are especially motivated by meteorological data assimilation problems where we may have discrete measurements from radiosondes, and continuous measurements via satellites, of the temperatures vs. pressure profile.

5.2 Centralized Map-Updating when the First-Pass Data is Discrete, the Second-Pass Data is Continuous, and $\hat{x}_{1s}(\cdot)$ is Available

In this section, we will show that the solution to the centralized map-updating problem, in the case when the first-pass data is discrete and the second-pass data is continuous, can again be represented as in relation (4.16) by

$$\boxed{\hat{x}_s(t) = \hat{x}_{1s}(t) + E[\tilde{x}_{1s}(t)|\tilde{Y}_2] \ ,} \tag{5.1}$$

where $E[\tilde{x}_{1s}(t)|\tilde{Y}_2]$ may be computed as in equation (4.39) by

$$\boxed{E[\tilde{x}_{1s}(t)|\tilde{Y}_2] = P_s\{\gamma_f(t) + \gamma_r(t)\} \ ,} \tag{5.2}$$

and the quantities $\gamma_f(\cdot),\gamma_r(\cdot)$ evolve as in equations (4.52) - (4.53) as

$$\boxed{d\gamma_f(t) = (-A' - P_f^{-1}Q)\gamma_f(t)dt + H_2'R_2^{-1}d\tilde{y}_2(t) \ ,} \tag{5.3}$$

$$\boxed{-d\gamma_r(t) = (A' - O_0Q)\gamma_r(t)dt + H_2'R_2^{-1}d\tilde{y}_2(t) \ ,} \tag{5.4}$$

with

$$\boxed{\gamma_f(0) = \gamma_r(T) = 0 \ ,} \tag{5.5}$$

and with P_f and O_0 defined appropriately. The validity of relation (4.16), for our current problem, will again be shown to be a consequence of an orthogonal decomposition of the Hilbert space spanned by the two data passes. We finally show that the use of relations (4.39) and (4.52) - (4.53) to compute $E[\tilde{x}_{1s}(t)|\tilde{Y}_2]$ follows from the fact that the first-pass smoothing error dynamics obey identical reverse and forward stochastic differential equations to those of Chapter 3, with P_{1f} calculated appropriately. Hence, we ultimately show that the map-updating algorithm may be defined by the relations (5.1) - (5.5), where we will later indicate the appropriate off-line equations for computing P_f and O_0.

We begin by defining the first-pass smoothed estimates, $\hat{x}_{1s}(\cdot)$, the two-pass smoothed estimates, $\hat{x}_s(\cdot)$, and some related quantities required in their computation. We assume that the first-pass measurements are modelled by

$$y_1(i) = H_1 x(t_i) + D_1 v_1(i) \quad , \tag{5.6}$$

for $i = 1,\ldots,N$, where the t_i's denote the discrete measurement times in the interval $[0,T]$, and the $v_1(i)$'s represent a standard discrete white noise process with

$$D_1 D_1' \triangleq R_1 > 0 \quad . \tag{5.7}$$

If we define the Hilbert space spanned by the first-pass measurements, Y_1, as

$$Y_1 = H(y_1(i) \quad i = 1,\ldots,N) \quad , \tag{5.8}$$

then $\hat{x}_{1s}(t)$ is defined as

$$\hat{x}_{1s}(t) = E[x(t)|Y_1] \quad . \tag{5.9}$$

By employing Wall's two-filter smoothing solution, we can express $\hat{x}_{1s}(t)$ for $t_\ell < t < t_{\ell+1}$ as

$$\hat{x}_{1s}(t) = P_{1s}\left\{P_{1f}^{-1}\hat{x}_{1f}(t) + P_{1r}^{-1}\hat{x}_{1r}(t)\right\} \quad , \tag{5.10}$$

where $$P_{1s}^{-1} = P_{1f}^{-1} + P_{1r}^{-1} - \pi^{-1} \quad , \tag{5.11}$$

$$\hat{x}_{1f}(t) = E[x(t)|Y_{1,\ell+1}^{-}] \quad , \tag{5.12}$$

$$\hat{x}_{1r}(t) = E[x(t)|Y_{1,\ell+1}^{+}] \quad , \tag{5.13}$$

π denotes the a-priori state covariance matrix, and P_{1f}, P_{1r} denote the filtering error covariance matrices associated with the estimates defined by relations (5.12) - (5.13), respectively.

Let us also define O_{01} as

$$O_{01} = P_{1r}^{-1} - \pi^{-1} \quad , \tag{5.14}$$

so that from relation (5.11)

$$P_{1s}^{-1} = P_{1f}^{-1} + O_{01} \quad . \tag{5.15}$$

In Appendix 5A we derive equations for the evolution of the first-pass forward and reverse filtered estimates, $\hat{x}_{1f}(\cdot)$ and $\hat{x}_{1r}(\cdot)$, and their corresponding error covariance matrices, P_{1f} and P_{1r}. Between measurement times, the estimates $\hat{x}_{1f}(\cdot)$ and $\hat{x}_{1r}(\cdot)$ correspond to predicted estimates based on the past or future observations, respectively, and hence we obtain the following relations for $t \in (t_\ell, t_{\ell+1})$:

$$d\hat{x}_{1f}(t) = A\hat{x}_{1f}(t)dt \quad , \tag{5.16}$$

with $$\dot{P}_{1f} = A P_{1f} + P_{1f} A' + Q \quad , \tag{5.17}$$

and $$-d\hat{x}_{1r}(t) = (-A - Q\pi^{-1})\hat{x}_{1r}(t)dt \quad , \tag{5.18}$$

with $$-\dot{P}_{1r} = (-A - Q\pi^{-1})P_{1r} + P_{1r}\left(-A - Q\pi^{-1}\right)' + Q \quad . \tag{5.19}$$

Next, we note that from the $x(\cdot)$ dynamics we can derive a discrete Markov model for the evolution of the $x(t_i)$'s, which taken together with the measurement relation (5.6), allows us to identify the estimates $\hat{x}_{1f}(t_\ell-)$ and $\hat{x}_{1f}(t_\ell+)$ as the one step ahead predicted estimate, and the filtered estimate, respectively. Hence, we can use standard discrete-time Kalman filtering relations to obtain the following measurement update relations for $\hat{x}_{1f}(\cdot)$, $P_{1f}(\cdot)$, at $t = t_\ell$, and for $\hat{x}_{1r}(\cdot)$, $P_{1r}(\cdot)$ at $t = t_{\ell+1}$:

$$\hat{x}_{1f}(t_\ell+) = (I - P_{1f}(t_\ell+)H_1'R_1^{-1}H_1)\hat{x}_{1f}(t_\ell-) + P_{1f}(t_\ell+)H_1'R^{-1}y_1(\ell), \tag{5.20}$$

$$\text{with} \qquad P_{1f}^{-1}(t_\ell+) = P_{1f}^{-1}(t_\ell-) + H_1'R_1^{-1}H_1 \quad , \tag{5.21}$$

$$\text{and} \quad \hat{x}_{1r}(t_{\ell+1}-) = (I - P_{1r}(t_{\ell+1}-)H_1'R_1^{-1}H_1)\hat{x}_{1r}(t_{\ell+1}+) + P_{1r}(t_{\ell+1}-)H_1'R_1^{-1}y_1(\ell+1) \quad , \tag{5.22}$$

$$\text{with} \qquad P_{1r}^{-1}(t_{\ell+1}-) = P_{1r}^{-1}(t_{\ell+1}+) + H_1'R_1^{-1}H_1 \ . \tag{5.23}$$

Finally, we note that in Appendix 5A we use relations (5.10) - (5.11), and the measurement and error covariance update equations (5.20) - (5.23), to show that the first-pass smoothed

estimates, $\hat{x}_{1s}(\cdot)$, and their associated error covariance matrices, $P_{1s}(\cdot)$, are both continuous functions of time. The continuity of $\hat{x}_{1s}(\cdot)$ and $P_{1s}(\cdot)$ is not entirely obvious, since both forward and reverse filtered estimates, and their corresponding error covariance matrices, are discontinuous at the discrete measurement times.

Having determined the first-pass smoothed estimates, $\hat{x}_{1s}(\cdot)$, and the first-pass smoothing error covariance matrices, $P_{1s}(\cdot)$, we now proceed to detail the construction of the two-pass smoothed estimates, $\hat{x}_s(\cdot)$, the two-pass smoothing error covariance matrices, $P_s(\cdot)$, and the related quantities, P_f and O_0. For $t_\ell < t < t_{\ell+1}$ we can construct the two-pass smoothed estimate, $\hat{x}_s(t)$, defined by

$$\hat{x}_s(t) \stackrel{\Delta}{=} E[x(t) | Y_1 \vee Y_2] \quad , \tag{5.24}$$

in an analogous manner to the first-pass smoothed estimate determined by relations (5.10) - (5.13), as

$$\hat{x}_s(t) = P_s\left\{P_f^{-1}\hat{x}_f(t) + P_r^{-1}\hat{x}_r(t)\right\} \quad , \tag{5.25}$$

where $$P_s^{-1} = P_f^{-1} + P_r^{-1} - \pi^{-1} \quad , \tag{5.26}$$

$$\hat{x}_f(t) = E[x(t) | Y_{1,\ell+1}^{-} \vee Y_{2t}^{-}] \quad , \tag{5.27}$$

and $$\hat{x}_r(t) = E[x(t) | Y_{1,\ell+1}^{+} \vee Y_{2t}^{+}] \quad , \tag{5.28}$$

with P_f and P_r denoting error covariance matrices associated with the estimates $\hat{x}_f(t)$ and $\hat{x}_r(t)$, respectively. Following relation (5.14), we define O_0 as

$$O_0 = P_r^{-1} - \pi^{-1} \quad , \tag{5.29}$$

so that from relation (5.26)

$$P_s^{-1} = P_f^{-1} + O_0 \quad . \tag{5.30}$$

In Appendix 5B we derive equations for the evolution of the two-pass forward and reverse filtered estimates, $\hat{x}_f(\cdot)$ and $\hat{x}_r(\cdot)$, and the two-pass forward and reverse filtering error covariance matrices, $P_f(\cdot)$ and $P_r(\cdot)$. While in the case of the first-pass filtered estimates, the filtered estimates between first-pass measurement times essentially correspond to predicted estimates based on the unconditional state dynamics, the two-pass filtered estimates between first-pass measurement times are constructed by standard Kalman filtering equations applied to the second-pass measurements. Hence, for $t \in (t_\ell, t_{\ell+1})$ we find that

$$d\hat{x}_f(t) = (A - P_f H_2' R_2^{-1} H_2)\hat{x}_f(t)dt + P_f H_2' R_2^{-1} dy_2 \quad , \tag{5.31}$$

with $$\dot{P}_f = A P_f + P_f A' + Q - P_f H_2' R_2^{-1} H_2 P_f \ , \tag{5.32}$$

and $$-d\hat{x}_r(t) = (-A - Q\pi^{-1} - P_r H_2' R_2^{-1} H_2)\hat{x}_r(t)dt + P_r H_2' R_2^{-1} dy_2 \ , \tag{5.33}$$

with $$-\dot{P}_r = (-A - Q\pi^{-1})P_r + P_r\left(-A - Q\pi^{-1}\right)' + Q - P_r H_2' R_2^{-1} H_2 P_r \ . \tag{5.34}$$

Finally, in Appendix 5B we verify that the two-pass forward and reverse filtered estimates, and their associated error covariance matrices, satisfy measurement update relations of the same form as equations (5.20) - (5.23) for the corresponding first-pass quantities.

Having sketched the construction of $\hat{x}_{1s}(\cdot)$, $\hat{x}_s(\cdot)$, and of the related error covariance matrices, we can now proceed to show that the solution to the map-updating problem for the present case assumes the same form as in the two-continuous data pass case treated in Section 4.2. We first note that the Hilbert space spanned by the two measurement passes has the orthogonal decomposition

$$Y_1 \vee Y_2 = Y_1 \oplus \tilde{Y}_2 \ , \tag{5.35}$$

where $$d\tilde{y}_2(t) = dy_2(t) - H_2(t)\hat{x}_{1s}(t)dt \quad . \tag{5.36}$$

From the decomposition expresssed by relation (5.36) we obtain the expression for $\hat{x}_s(t)$ of (5.1).

We next verify that we can use relations (5.2) and (5.3) - (5.5) to compute $E[\tilde{x}_{1s}(t)|\tilde{Y}_2]$ by showing that the first-pass smoothing error dynamics obey identical reverse and forward stochastic differential equations to those of Chapter 3, and also by demonstrating that the identities

$$P_f^{-1} = P_{1f}^{-1} + P_{fs}^{-1} - P_{1s}^{-1} \quad , \tag{5.37}$$

and $$0_0 = P_{rs}^{-1} - P_{1f}^{-1} \quad , \tag{5.38}$$

are again valid, where P_{fs}, P_{rs} denote the forward and reverse filtering error covariance matrices associated with the estimation of $\tilde{x}_{1s}(t)$ from $\tilde{Y}_{2t}^-$ and $\tilde{Y}_{2t}^+$, respectively.

Letting the σ-field $\mathbf{y}_1$ generated by the first-pass measurements be defined as

$$\mathbf{y}_1 = \sigma\{y_1(i) \quad i = 1,\ldots,N\} \quad , \tag{5.39}$$

letting $\tilde{\mathbf{x}}_{1t}^+$ denote the σ-field spanned by future values of the first-pass smoothing errors, and retracing the steps of

Section 3.2, we derive the following backward model for $\tilde{x}_{1s}(\cdot)$:

$$-d\tilde{x}_{1s}(t) = -A\tilde{x}_{1s}(t)dt - B\,E[du(t)|\tilde{\chi}^{+}_{1t}] - B\,d\tilde{u}_{1r}(t), \quad (5.40)$$

where $$d\tilde{u}_{1r}(t) = du(t) - E[du(t)|\tilde{\chi}^{+}_{1t}] - E[du(t)|\mathbf{y}_1] \ . \quad (5.41)$$

In Appendix 5C we derive an explicit representation for the smoothing error process from an innovations form of the smoothed estimate, that we employ in Appendix 5D to verify that

$$E[du(t)|\tilde{\chi}^{+}_{1t}] = B'P^{-1}_{1f}(t-)\tilde{x}_{1s}(t)dt. \quad (5.42)$$

Hence, by verifying relation (5.42), we have demonstrated that the smoothing error process, $\tilde{x}_{1s}(\cdot)$, has a backward Markovian realization of the same form as that in Chapter 3, with $P_{1f}(\cdot)$ computed by relations (5.17) and (5.21). By using the continuity of the smoothing error process proved in Appendix 5A to justify decomposing $Bd\tilde{u}_{1r}(t)$ with respect to $\tilde{\chi}^{-}_{1t}$ as

$$Bd\tilde{u}_{1r}(t) = BB'P^{-1}_{1s}\tilde{x}_{1s}(t)dt + Bd\tilde{u}_{1f}(t) \ , \quad (5.43)$$

and substituting relation (5.43) into equation (5.40), we obtain a forward Markovian realization for $\tilde{x}_{1s}(\cdot)$ of the same form as in Chapter 3.

Given that the smoothing error process evolves according to forward and backward equations of the same form as relations (3.25) - (3.26), we can again compute $E[\tilde{x}_{1s}(t)|\tilde{Y}_2]$ as

$$E[\tilde{x}_{1s}(t)|\tilde{Y}_2] = P_s\left\{P_{fs}^{-1}\hat{\tilde{x}}_f(t) + P_{rs}^{-1}\hat{\tilde{x}}_r(t)\right\} \quad , \tag{5.44}$$

where $\hat{\tilde{x}}_f(t), \hat{\tilde{x}}_r(t)$ denote forward and reverse filtered estimates of $\tilde{x}_{1s}(t)$ based on $\tilde{Y}_{2t}^-, \tilde{Y}_{2t}^+$, respectively, and P_{fs}, P_{rs} denote their corresponding error covariance matrices, and all these quantities satisfy equations of the same form as those of Section 4.2.1.

If we next define $\gamma_f(t)$ and $\gamma_r(t)$ as

$$\gamma_f(t) \triangleq P_{fs}^{-1}\hat{\tilde{x}}_f(t) \quad , \tag{5.45}$$

and

$$\gamma_r(t) \triangleq P_{rs}^{-1}\hat{\tilde{x}}_r(t) \quad , \tag{5.46}$$

we can substitute (5.45) - (5.46) into (5.44) to obtain relation (5.2), where relations (5.3) - (5.4) for the evolution of $\gamma_f(\cdot), \gamma_r(\cdot)$ follow from using the relations of Chapter 4 for the evolution of P_{fs}, $\hat{\tilde{x}}_f(\cdot)$, P_{rs}, and $\hat{\tilde{x}}_r(\cdot)$, and also from employing the identifies (5.37) - (5.38).

We motivate the identities (5.37) - (5.38) in the same way as in Section 4.2.2, by rewriting them as

$$P_{fs}^{-1} = P_{f}^{-1} + O_{01} \quad , \tag{5.47}$$

and

$$P_{rs}^{-1} = P_{1f}^{-1} + O_{0} \quad . \tag{5.48}$$

By the same argument as in Appendix 4A, P_{fs} and P_{rs} may be identified as error covariance matrices associated with some estimates of $x(t)$, $\hat{x}_{fs}(t)$, and $\hat{x}_{rs}(t)$, based on $Y_1 \vee Y_{2t}^{-}$ and $Y_1 \vee Y_{2t}^{+}$, respectively. In this context, relations (5.47) - (5.48) follow from noting that for $t \in (t_{\ell}, t_{\ell+1})$

$$Y_1 \vee Y_{2t}^{-} = \left(Y_{1,\ell+1}^{-} \vee Y_{2t}^{-}\right) \vee Y_{1,\ell+1}^{+} \quad , \tag{5.49}$$

$$Y_1 \vee Y_{2t}^{+} = Y_{1,\ell+1}^{-} \vee \left(Y_{1,\ell+1}^{+} \vee Y_{2t}^{+}\right) \quad , \tag{5.50}$$

and using the definitions of O_{01}, O_0 in (5.14) and (5.29), and formulae for the inverses of smoothing error covariance matrices.

We finally summarize the equations for the evolution of the off-line quantities that appear in equations (5.3) - (5.4). From our earlier discussion of the construction of forward and reverse two-pass filtered estimates and their associated error

covariance matrices, and the use of the definition (5.29) for O_0, we find that on the interior of first-pass measurement intervals, P_f and O_0 satisfy

$$\dot{P}_f = A P_f + P_f A' + Q - P_f H_2' R_2^{-1} H_2 P_f \ , \tag{5.51}$$

and

$$-\dot{O}_0 = A' O_0 + O_0 A + H_2' R_2^{-1} H_2 - O_0 Q O_0 \ . \tag{5.52}$$

At first-pass measurements times, P_f and O_0 obey the update equations:

$$P_f^{-1}(t_i+) = P_f^{-1}(t_i-) + H_1' R_1^{-1} H_1 \ , \tag{5.53}$$

and

$$O_0(t_i-) = O_0(t_i+) + H_1' R_1^{-1} H_1 \ . \tag{5.54}$$

The initial conditions for both quantities are given by

$$P_f(0) = \pi(0) \ , \tag{5.55}$$

and

$$O_0(T) = 0 \ . \tag{5.56}$$

5.3 Centralized Map-Updating when the First-Pass Data is Discrete, the Second-Pass Data is Continuous, and only the $\hat{x}_{1s}(t_j)$'s are Available

In Section 5.2 we demonstrated that the solution to the centralized map-updating problem when the first-pass data was discrete, the second-pass data continuous, and the complete record of $\hat{x}_{1s}(\cdot)$ is available, can be computed using the same algorithm as for the two-continuous data pass problem. In this section, we show that in general, the two-pass smoothed estimate coincides with the best linear estimate of the state process given the first-pass smoothed estimates calculated at the discrete measurement times, and the continuous second-pass measurements, $dy_2(\cdot)$. We present a special case for which we show explicitly how the entire first-pass smoothed estimate history, $\hat{x}_{1s}(\cdot)$, is computable as a linear functional of the $\hat{x}_{1s}(t_i)$'s, and where the desired map-updating algorithm then follows from applying the results of Section 5.2.

We begin by noting that the condition that the best linear estimate for x(t) given the first-pass smoothed estimates at the discrete measurement times be equal to the first-pass smoothed estimate is equivalent to having

$$E[x(t)|H(\hat{x}_{1s}(t_j) \quad j=1,\ldots,N)] = E[x(t)|Y_1] \ . \tag{5.57}$$

We now will argue that (5.57) implies that the best linear estimate for $x(t)$ given the $\hat{x}_{1s}(t_j)$'s and the second-pass measurements coincides with the two-pass smoothed estimate, i.e.,

$$E[x(t)|H(\hat{x}_{1s}(t_j) \quad j=1,\ldots,N) \vee Y_2] = \hat{x}_s(t) \ . \qquad (5.58)$$

The relation (5.57) suggests that we may express $\hat{x}_{1s}(t)$ as a linear combination of the $\hat{x}_{1s}(t_j)$'s, and hence that we may use the results of Section 5.2 to express the two-pass smoothed estimate as a linear functional of the $\hat{x}_{1s}(t_j)$'s and the second-pass data, $dy_2(\cdot)$, implying equation (5.58)

We now prove that, in fact, relation (5.57) is true in general. Let us define the Hilbert space spanned by the state values at the discrete measurement times, X_D, by

$$X_D \triangleq H(x(t_j) \quad j=1,\ldots,N) \ . \qquad (5.59)$$

Then, we may represent $x(t)$ as

$$x(t) = E[x(t)|X_D] + \tilde{x}_D(t) \quad , \qquad (5.60)$$

where $H(\tilde{x}_D(t))$ is orthogonal to X_D. But from relation (5.6) defining the $y_1(j)$'s, we can show that $\tilde{x}_D(t)$ is uncorrelated

with $y_1(j)$. Hence, by projecting both sides of relation (5.60) onto Y_1 we can obtain the following relation:

$$E[x(t)|Y_1] = E\left[E[x(t)|X_D]|Y_1\right] \quad . \tag{5.61}$$

Now, since we may express $E[x(t)|X_D]$ as a linear combination of the $x(t_j)$'s, the quantity on the right-hand side of equation (5.61) may be expressed as a linear combination of the $\hat{x}_{1s}(t_j)$'s, proving relation (5.57).

We now identify an important special case for which we show explicitly how to compute $\hat{x}_{1s}(\cdot)$, given the $\hat{x}_{1s}(t_j)$'s. We first note that we can imagine generating the $\hat{x}_{1s}(t_j)$'s by employing the following equations for the evolution of the state at the discrete measurement times:

$$x(t_{\ell+1}) = \Phi_A(t_{\ell+1},t_\ell)x(t_\ell) + w_\ell \ , \tag{5.62}$$

with

$$w_\ell = \int_{\tau=t_\ell}^{t_{\ell+1}} \Phi_A(t_{\ell+1},\tau)B(\tau)du(\tau) \ , \tag{5.63}$$

and using the observation equation (5.6). Hence, by applying the discrete-time version of the Rauch-Tung-Striebel solution to the smoothing problem represented in Appendix 2A as

$$\hat{x}_s(i) = A^{-1}(i)\left(I - B(i)B'(i)P_{fp}^{-1}(i+1)\right)\hat{x}_s(i+1)$$
$$+ A^{-1}(i)[B(i)B'(i)]P_{fp}^{-1}(i+1)A(i)\hat{x}_f(i) \quad , \qquad (5.64)$$

and making the following identifications to our current problem:

$$\left.\begin{aligned} A(i) &\equiv \Phi_A(t_{i+1},t_i) \quad , \\ P_{fp}(i+1) &\equiv P_{1f}(t_{i+1}-) \quad , \\ \hat{x}_f(i) &\equiv \hat{x}_{1f}(t_i+) \quad , \\ \text{and} \qquad B(i)B'(i) &\equiv Q_D(i) \quad , \end{aligned}\right\} \qquad (5.65)$$

where

$$Q_D(i) \triangleq \int_{\tau=t_i}^{t_{i+1}} \Phi_A(t_{i+1},\tau)B(\tau)B'(\tau)\Phi_A'(t_{i+1},\tau)\,d\tau \quad , \qquad (5.66)$$

we may obtain the following backward recursion for generating the $\hat{x}_{1s}(t_i)$'s from the $\hat{x}_{1f}(t_i+)$'s:

$$\hat{x}_{1s}(t_i) = \Phi_A^{-1}(t_{i+1},t_i)\left(I - Q_D(i)P_{1f}^{-1}(t_{i+1}-)\right)\hat{x}_{1s}(t_{i+1})$$
$$+ \Phi_A^{-1}(t_{i+1},t_i)Q_D(i)P_{1f}^{-1}(t_{i+1}-)\Phi_A(t_{i+1},t_i)\hat{x}_{1f}(t_i+), \qquad (5.67)$$

with $\hat{x}_{1s}(t_N) = \hat{x}_{1f}(t_N+)$. (5.68)

The special case that we consider, for which we will show explicitly how the continuous first-pass smoothed estimates, $\hat{x}_{1s}(\cdot)$, are computable as a linear function of the $\hat{x}_{1s}(t_i)$'s, is defined by requiring that

$$Q_D(i) > 0 \quad , \tag{5.69}$$

for $i = 1,\ldots,N-1$. From relation (5.66), we can see that this is equivalent to requiring that our original continuous-time state-space model be controllable from the noise, $du(\cdot)$, over each of the intervals between measurements. The assumption (5.69) allows us to use equation (5.67) to compute the forward filtered estimates, $\hat{x}_{1f}(t_i+)$, as a linear functional of the $\hat{x}_{1s}(t_i)$'s. Then by using the expression (5.10) for $\hat{x}_{1s}(t_i)$, and given our knowledge of the filtered estimates, $\hat{x}_{1f}(t_i+)$, and the smoothed estimates, $\hat{x}_{1s}(t_i)$, we may compute the reverse filtered estimates, $\hat{x}_{1r}(t_i-)$. At this point, given knowledge of the $\hat{x}_{1f}(t_i+)$'s and $\hat{x}_{1r}(t_i-)$'s, we can compute $\hat{x}_{1s}(t)$ at any point $t \in [0,T]$, by employing (5.10).

We finally show explicitly how to reconstruct $\hat{x}_{1s}(t)$, given knowledge of the $\hat{x}_{1s}(t_i)$'s, when the $Q_D(i)$'s are positive

definite. From equations (5.67) - (5.68) we obtain the following relation for generating the $\hat{x}_{1f}(t_i+)$'s from the $\hat{x}_{1s}(t_i)$'s:

$$\hat{x}_{1f}(t_i+) = \left[\Phi_A^{-1}(t_{i+1},t_i)Q_D(i)P_{1f}^{-1}(t_{i+1}-)\Phi_A(t_{i+1},t_i)\right]^{-1} \cdot \left\{\hat{x}_{1s}(t_i) - \Phi_A^{-1}(t_{i+1},t_i)\left(I - Q_D(i)P_{1f}^{-1}(t_{i+1}-)\right)\hat{x}_{1s}(t_{i+1})\right\}, \tag{5.70}$$

for $i = N-1,\ldots,1$,

with $$\hat{x}_{1f}(t_N+) = \hat{x}_{1s}(t_N) \quad . \tag{5.71}$$

Then, we note that by specializing relation (5.10) for $t = t_i-$, and solving for $\hat{x}_{1r}(t_i-)$, we obtain the following equation:

$$\hat{x}_{1r}(t_i-) = \left[P_{1s}(t_i)P_{1r}^{-1}(t_i-)\right]^{-1}\left\{\hat{x}_{1s}(t_i) - P_{1s}(t_i)P_{1f}^{-1}(t_i-) \cdot \Phi_A(t_i,t_{i-1})\hat{x}_{1f}(t_{i-1}+)\right\}, \tag{5.72}$$

for $i = 2,\ldots,N$, with

$$\hat{x}_{1r}(t_1-) = \hat{x}_{1s}(t_1). \tag{5.73}$$

At this point, given the $\hat{x}_{1f}(t_i+)$'s and $\hat{x}_{1r}(t_i-)$'s we can form $\hat{x}_{1s}(t)$ for any $t \in [0,T]$, by using (5.10). Let us define the

transition matrix $\psi(\cdot,\cdot)$ associated with the reverse time Markovian realization for $x(\cdot)$ in (2.114) by

$$\frac{d}{dt}\psi'(t,\tau) = \left[-A - Q\pi^{-1}\right]' \psi'(t,\tau) \quad , \tag{5.74}$$

with $$\psi(\tau,\tau) = I \quad . \tag{5.75}$$

Then, we can express $\hat{x}_{ls}(t)$ for $t_i < t < t_{i+1}$, $i = 1,\ldots,N-1$, by

$$\hat{x}_{ls}(t) = P_{ls}\left\{P_{lf}^{-1}\Phi_A(t,t_i)\hat{x}_{lf}(t_i+) + P_{lr}^{-1}\psi(t_{i+1},t)\hat{x}_{lr}(t_{i+1}-)\right\}. \tag{5.76}$$

Similarly, for $t < t_1$ and $t > t_N$ we obtain the following two relations for $\hat{x}_{ls}(t)$:

$$\hat{x}_{ls}(t) = \psi(t_1,t)\hat{x}_{ls}(t_1) \quad , \tag{5.77}$$

and $$\hat{x}_{ls}(t) = \Phi_A(t,t_N)\hat{x}_{ls}(t_N) \quad , \tag{5.78}$$

respectively. Therefore, we have shown that the entire map $\hat{x}_{ls}(\cdot)$ can be reconstructed from its values at the discrete measurement times.

5.4 Conclusion

In Section 5.2 we demonstrated that the solution to the centralized map-updating problem when the first-pass data consists of discrete measurements and the second-pass data is continuous, assumes the same form as for the two continuous data pass case of Section 4.2. This was shown to be a product of the fact that first-pass smoothing errors have forward and reverse Markovian realizations of the same form as those obtained in Chapter 3, and by using a Hilbert space decomposition of the aggregate, two-pass data space similar to the one discussed in Chapter 4.

In Section 5.3 we showed that the fact that the first-pass smoothed estimate for $x(t)$ is equal to the best linear estimate for $x(t)$ given the first-pass smoothed estimates at the discrete measurement times, implies that the two-pass smoothed estimate coincides with the best linear estimate for $x(t)$ given the $\hat{x}_{1s}(t_j)$'s and the second-pass data. Hence, to solve the map-updating problem given only the values of the first-pass map at the discrete measurement times, we first reconstruct $\hat{x}_{1s}(\cdot)$ from the $\hat{x}_{1s}(t_i)$'s, and then use the algorithm of Section 5.2. We finally derived an explicit procedure for computing $\hat{x}_{1s}(t)$ as a functional of the $\hat{x}_{1s}(t_j)$'s, in the special case where the state is controllable from the process noise over measurement subintervals.

Appendix 5A

Derivation of Equations for the Evolution of $\hat{x}_{1f}(\cdot)$, $\hat{x}_{1r}(\cdot)$, $P_{1f}(\cdot)$, $P_{1r}(\cdot)$ and Proof of the Continuity of $\hat{x}_{1s}(\cdot)$ and $P_{1s}(\cdot)$

In this Appendix we obtain equations for the evolution of the first-pass forward and reverse filtered estimates, and their corresponding error covariance matrices, given that the first-pass measurements are discrete, and the state model is continuous. We finally prove that the resulting first-pass smoothed estimates, and their error covariance matrices, are continuous functions of time.

By relating $x(t_{\ell+1})$ and $x(t_\ell)$ through the state dynamics as

$$x(t_{\ell+1}) = \Phi_A(t_{\ell+1},t_\ell)x(t_\ell) + w_\ell \quad , \tag{A.1}$$

where $$w_\ell = \int_{\tau=t_\ell}^{t_{\ell+1}} \Phi_A(t_{\ell+1},\tau)Bdu(\tau) \quad , \tag{A.2}$$

we can employ the model (A.1), together with the observation equation

$$y_1(\ell) = H_1x(t_\ell) + D_1v_1(\ell) \quad , \tag{A.3}$$

to derive equations for the evolution of the filtered estimates of the $x(t_i)$'s. Hence, $\hat{x}_{1f}(t_\ell -)$ may be identified as a one-step ahead predicted estimate of $x(t_\ell)$, and $\hat{x}_{1f}(t_\ell +)$ as the filtered estimate of $x(t_\ell)$. Therefore, by employing standard discrete time Kalman filtering results [2] we can write the measurement update relations:

$$\hat{x}_{1f}(t_\ell +) = (I - P_{1f}(t_\ell +)H_1' R_1^{-1} H_1)\hat{x}_{1f}(t_\ell -) + P_{1f}(t_\ell +)H_1' R_1^{-1} y_2(\ell), \tag{A.4}$$

and $$P_{1f}^{-1}(t_\ell +) = P_{1f}^{-1}(t_\ell -) + H_1' R_1^{-1} H_1 \quad . \tag{A.5}$$

In the interior of the interval $[t_\ell, t_{\ell+1}]$, we have no additional measurements, and hence $\hat{x}_{1f}(t)$ corresponds to a predicted estimate, with P_{1f} being its associated error covariance matrix, and where both quantities evolve as

$$d\hat{x}_{1f}(t) = A\hat{x}_{1f}(t)dt \quad , \tag{A.6}$$

and $$\dot{P}_{1f} = A P_{1f} + P_{1f} A' + Q \quad . \tag{A.7}$$

The initial conditions for $\hat{x}_{1f}(0)$ and $P_{1f}(0)$ are given by 0 and $\pi(0)$, respectively.

We can similarly obtain backward equations for the evolution of $\hat{x}_{1r}(\cdot)$ and P_{1r}. Corresponding to equations (A.4) - (A.5) we determine the backward relations

$$\hat{x}_{1r}(t_{\ell+1}-) = (I - P_{1r}(t_{\ell+1}-)H_1'R_1^{-1}H_1)\hat{x}_{1r}(t_{\ell+1}+) + P_{1r}(t_{\ell+1}-)H_1'R_1^{-1}y_1(\ell+1) \quad , \tag{A.8}$$

and

$$P_{1r}^{-1}(t_{\ell+1}-) = P_{1r}^{-1}(t_{\ell+1}+) + H_1'R_1^{-1}H_1 \quad . \tag{A.9}$$

By employing the backward Markovian realization (2.114) for the state process $x(\cdot)$, we obtain the following equations, analogous to (A.6) - (A.7), for the evolution of $\hat{x}_{1r}(\cdot)$ and P_{1r} in the interior of the interval $[t_\ell, t_{\ell+1}]$:

$$-d\hat{x}_{1r}(t) = (-A - Q\pi^{-1})\hat{x}_{1r}(t)dt \quad , \tag{A.10}$$

and

$$-\dot{P}_{1r} = (-A - Q\pi^{-1})P_{1r} + P_{1r}\left(-A - Q\pi^{-1}\right)' + Q \quad , \tag{A.11}$$

with the initial conditions $\hat{x}_{1r}(T)$, and $P_{1r}(T)$, given by 0, and $\pi(T)$, respectively.

Now, given knowledge of $\hat{x}_{1r}(t)$ and $\hat{x}_{1f}(t)$ we can form the first-pass smoothed estimate, $\hat{x}_{1s}(t)$, and its associated smoothing error covariance matrix, P_{1s}, as

$$\hat{x}_{1s}(t) = P_{1s}\left\{P_{1f}^{-1}\hat{x}_{1f}(t) + P_{1r}^{-1}\hat{x}_{1r}(t)\right\} \quad , \tag{A.12}$$

with $$P_{1s}^{-1} = P_{1f}^{-1} + P_{1r}^{-1} - \pi^{-1} \quad . \tag{A.13}$$

We next demonstrate the continuity of P_{1s} and $\hat{x}_{1s}(\cdot)$. From relation (A.12) we form $P_{1s}(t_\ell-)$ and $P_{1s}(t_\ell+)$ as

$$P_{1s}^{-1}(t_\ell-) = P_{1f}^{-1}(t_\ell-) + P_{1r}^{-1}(t_\ell-) - \pi^{-1}(t_\ell) \quad , \tag{A.14}$$

and $$P_{1s}(t_\ell+) = P_{1f}^{-1}(t_\ell+) + P_{1r}^{-1}(t_\ell+) - \pi^{-1}(t_\ell) \quad . \tag{A.15}$$

Substituting relation (A.5) for $P_{1f}^{-1}(t_\ell+)$ on the right-hand side of equation (A.15), and using (A.9) to replace $P_{1r}^{-1}(t_\ell-)$ on the right-hand side of equation (A.14), we can verify the following identities:

$$\begin{aligned} P_{1s}^{-1}(t_\ell-) &\equiv P_{1s}^{-1}(t_\ell+) \\ &= P_{1f}^{-1}(t_\ell-) + P_{1r}^{-1}(t_\ell+) + H_1'R_1^{-1}H_1 - \pi^{-1}(t_\ell) \quad . \end{aligned} \tag{A.16}$$

To prove the continuity of $\hat{x}_{1s}(\cdot)$ we first note from relation (A.12) that $\hat{x}_{1s}(t_\ell-)$ and $\hat{x}_{1s}(t_\ell+)$ are defined by

$$\hat{x}_{1s}(t_{\ell}-) = P_{1s}(t_{\ell}-)\left\{P_{1f}^{-1}(t_{\ell}-)\hat{x}_{1f}(t_{\ell}-) + P_{1r}^{-1}(t_{\ell}-)\hat{x}_{1r}(t_{\ell}-)\right\} , \tag{A.17}$$

$$\text{and} \quad \hat{x}_{1s}(t_{\ell}+) = P_{1s}(t_{\ell}+)\left\{P_{1f}^{-1}(t_{\ell}+)\hat{x}_{1f}(t_{\ell}+) + P_{1r}^{-1}(t_{\ell}+)\hat{x}_{1r}(t_{\ell}+)\right\} . \tag{A.18}$$

We now observe that the estimate updating relations at $t=t_{\ell}$, described by equations (A.4) and (A.8), can be rewritten as

$$P_{1f}^{-1}(t_{\ell}+)\hat{x}_{1f}(t_{\ell}+) = P_{1f}^{-1}(t_{\ell}-)\hat{x}_{1f}(t_{\ell}-) + H_1'R_1^{-1}y_1(\ell) , \tag{A.19}$$

$$\text{and} \quad P_{1r}^{-1}(t_{\ell}-)\hat{x}_{1r}(t_{\ell}-) = P_{1r}^{-1}(t_{\ell}+)\hat{x}_{1r}(t_{\ell}+) + H_1'R_1^{-1}y_1(\ell) . \tag{A.20}$$

Substituting (A.19) for $P_{1f}^{-1}(t_{\ell}+)\hat{x}_{1f}(t_{\ell}+)$ on the right-hand side of equation (A.18), using (A.20) to replace $P_{1r}^{-1}(t_{\ell}-)\hat{x}_{1r}(t_{\ell}-)$ on the right-hand side of equation (A.17), and noting relation (A.16), we can verify the following identities:

$$\begin{aligned}\hat{x}_{1s}(t_{\ell}-) &\equiv \hat{x}_{1s}(t_{\ell}+) \\ &= P_{1s}(t_{\ell})\left\{P_{1f}^{-1}(t_{\ell}-)\hat{x}_{1f}(t_{\ell}-) + P_{1r}^{-1}(t_{\ell}+)\hat{x}_{1r}(t_{\ell}+)\right. \\ &\qquad \left. + H_1'R_1^{-1}y_1(\ell)\right\} . \end{aligned} \tag{A.21}$$

Appendix 5B

Derivation of Equations for the Evolution of $\hat{x}_f(\cdot)$, $P_f(\cdot)$, $\hat{x}_r(\cdot)$, and $P_r(\cdot)$

We now sketch the construction of the two-pass forward and reverse filtered estimates and their associated error covariance matrices. In the case of first-pass filtering based on the discrete measurements

$$y_1(\ell) = H_1 x(t_\ell) + D_1 v_1(\ell) \quad , \tag{B.1}$$

and a continuous state model, no measurements are available between discrete measurement times, and hence the operation of filtering for times $t \in (t_\ell, t_{\ell+1})$ reduces to prediction. However, for the two-pass filtering problem, continuous second-pass measurements

$$dy_2(t) = H_2 x(t)dt + D_2 dv_2(t) \quad , \tag{B.2}$$

are available between the discrete first-pass measurement times, and hence for intermediate times the two-pass filtered estimate is constructed by standard Kalman filtering equations. Therefore, for $t_\ell < t < t_{\ell+1}$ $\hat{x}_f(\cdot)$ evolves according to

$$d\hat{x}_f(t) = (A - P_f H_2' R_2^{-1} H_2)\hat{x}_f(t)dt + P_f H_2' R_2^{-1} dy_2(t) \ , \qquad (B.3)$$

where P_f satisfies

$$\dot{P}_f = A P_f + P_f A' + Q - P_f H_2' R_2^{-1} H_2 P_f \ , \qquad (B.4)$$

with the initial conditions $\hat{x}_f(0)$ and $P_f(0)$ given by 0 and $\pi(0)$, respectively. Reasoning similarly, the two-pass reverse filtered estimate for $t_\ell < t \leq t_{\ell+1}$ evolves according to

$$-d\hat{x}_r(t) = (-A - Q\pi^{-1} - P_r H_2' R_2^{-1} H_2)\hat{x}_r(t)dt + P_r H_2' R_2^{-1} dy_2(t), \qquad (B.5)$$

where P_r satisfies

$$-\dot{P}_r = (-A - Q\pi^{-1})P_r + P_r\left(-A - Q\pi^{-1}\right)' + Q - P_r H_2' R_2^{-1} H_2 P_r \ , \qquad (B.6)$$

with the initial conditions $\hat{x}_r(T), P_r(T)$ given by $0, \pi(T)$, respectively.

We now show that the two-pass forward and reverse filtered estimate, and filtering error covariance, updating equations at the discrete first-pass measurement times, t_i, assume the same form as those for the corresponding first-pass

quantities with $\hat{x}_{1f}(\cdot)$, $\hat{x}_{1r}(\cdot)$, P_{1f}, and P_{1r} replaced by $\hat{x}_f(\cdot)$, $\hat{x}_r(\cdot)$, P_f, and P_r, respectively. We will focus on the derivation of the two-pass forward filtering update equations at $t = t_\ell$, since the reverse filtering update equations are exactly analogous. We first note that $\hat{x}_f(t_\ell+)$ is defined by

$$\hat{x}_f(t_\ell+) = E\left[x(t_\ell)\middle| Y^-_{1,\ell+1} \vee Y^-_{2t_\ell}\right] . \tag{B.7}$$

We can express the Hilbert space spanned by the two-pass data up to time $t = t_\ell+$ as

$$Y^-_{1,\ell+1} \vee Y^-_{2t_\ell} = H(y_1(\ell)) \vee \left(Y^-_{1,\ell} \vee Y^-_{2t_\ell}\right) , \tag{B.8}$$

or alternatively by the following orthogonal decomposition:

$$Y^-_{1,\ell+1} \vee Y^-_{2t_\ell} = H\left(y_1(\ell) - E\left[y_1(\ell)\middle| Y^-_{1,\ell} \vee Y^-_{2t_\ell}\right]\right) \oplus \left(Y^-_{1,\ell} \vee Y^-_{2t_\ell}\right). \tag{B.9}$$

Now, by employing the definition of $y_1(\ell)$ and $\hat{x}_f(t_\ell-)$, we can show that

$$y_1(\ell) - E\left[y_1(\ell)\middle| Y^-_{1,\ell} \vee Y^-_{2t_\ell}\right] = H_1\tilde{x}_f(t_\ell-) + D_1v_1(\ell), \tag{B.10}$$

where $\tilde{x}_f(t_\ell-)$ denotes the two-pass filtering error at $t = t_\ell-$. Therefore, by employing the orthogonal decomposition of relation (B.9) to form $\hat{x}_f(t_\ell+)$ as defined by (B.7), and taking into account relation (B.10), we obtain the following relation:

$$\hat{x}_f(t_\ell+) = E[x(t_\ell)|H(H_1\tilde{x}_f(t_\ell-) + D_1 v_1(\ell))] + \hat{x}_f(t_\ell-) \quad . \quad \text{(B.11)}$$

Noting that

$$x(t_\ell) = \hat{x}_f(t_\ell-) + \tilde{x}_f(t_\ell-) \quad , \quad \text{(B.12)}$$

where $\hat{x}_f(t_\ell-) \perp \tilde{x}_f(t_\ell-)$ and $v_1(\ell)$, relation (B.11) is rewritten as

$$\hat{x}_f(t_\ell+) = E[\tilde{x}_f(t_\ell-)|H(H_1\tilde{x}_f(t_\ell-) + D_1 v_1(\ell))] + \hat{x}_f(t_\ell-). \quad \text{(B.13)}$$

Subtracting both sides of relation (B.13) from $x(t_\ell)$ we obtain the identity

$$\tilde{x}_f(t_\ell+) = \tilde{x}_f(t_\ell-) - E[\tilde{x}_f(t_\ell-)|H(H_1\tilde{x}_f(t_\ell-) + D_1 v_1(\ell))]. \quad \text{(B.14)}$$

Hence, by using (B.13) and (B.14) we obtain the following relations for updating $\hat{x}_f(\cdot)$ and P_f at $t = t_\ell$:

$$\hat{x}_f(t_\ell+) = \hat{x}_f(t_\ell-) + P_f(t_\ell-)H_1'\left(H_1P_f(t_\ell-)H_1' + R_1\right)^{-1}\left[y_1(\ell) - H_1\hat{x}_f(t_\ell-)\right], \tag{B.15}$$

and

$$P_f(t_\ell+) = P_f(t_\ell-) - P_f(t_\ell-)H_1'\left(H_1P_f(t_\ell-)H_1' + R_1\right)^{-1}H_1P_f(t_\ell-). \tag{B.16}$$

By using matrix identities [2], we can show that equations (B.15) - (B.16) are expressable by the alternate forms

$$\hat{x}_f(t_\ell+) = (I - P_f(t_\ell+)H_1'R_1^{-1}H_1)\hat{x}_f(t_\ell-) + P_{1f}(t_\ell+)H_1'R_1^{-1}y_1(\ell), \tag{B.17}$$

and

$$P_f^{-1}(t_\ell+) = P_f^{-1}(t_\ell-) + H_1'R_1^{-1}H_1 \quad . \tag{B.18}$$

The formulas for updating $\hat{x}_r(\cdot)$ and P_r at $t = t_\ell$ are completely analogous to (B.17) - (B.18).

Appendix 5C

Explicit Representation of the Smoothing Error Process following from the Innovations Form of the Smoothed Estimate

In this Appendix we derive an explicit innovations type formula for the smoothed estimate $\hat{x}_{1s}(t)$ based on the discrete measurements

$$y_1(\ell) = H_1 x(t_\ell) + D_1 v_1(\ell) \quad , \tag{C.1}$$

and a continuous state model. This expression for $\hat{x}_{1s}(t)$ yields a representation for $\tilde{x}_{1s}(t)$ that we will employ in Appendix 5D for checking Markovian realizations of the first-pass smoothing error process. We define the first-pass innovations process as

$$\nu_1(i) = y_1(i) - E[y_1(i) | Y_{1,i}^{-}] \quad . \tag{C.2}$$

Letting $\tilde{x}_{1f}(\cdot)$ denote the filtering error process, relation (C.2) may be expressed as

$$\nu_1(i) = H_1 \tilde{x}_{1f}(t_i-) + D_1 v_1(i) \quad . \tag{C.3}$$

The innovations solution for $\hat{x}_{1s}(t)$, as defined for $t_\ell < t \le t_{\ell+1}$, is based on the following orthogonal decomposition of the first-pass observations space Y_1:

$$Y_1 = Y_{1,\ell+1}^{-} \oplus \boldsymbol{\nu}_{1,\ell+1}^{+} \quad . \tag{C.4}$$

Hence, forming $\hat{x}_{1s}(t)$ by using the decomposition for Y_1 in (C.4), using the fact that $x(t) = \hat{x}_{1f}(t) + \tilde{x}_{1f}(t)$, where $\hat{x}_{1f}(t)$ is orthogonal to future values of $\tilde{x}_{1f}(\cdot)$, and utilizing relation (C.3) to express $\nu_1(i)$, we obtain the following expression for $\hat{x}_{1s}(t)$:

$$\hat{x}_{1s}(t) = \hat{x}_{1f}(t) + \sum_{j=1}^{N-\ell} E[\tilde{x}_{1f}(t)\tilde{x}_{1f}'(t_{\ell+j}-)]H_1' P_{\nu_1}^{-1}(\ell+j)\nu_1(\ell+j) \quad , \tag{C.5}$$

where

$$P_{\nu_1}(i) \triangleq E[\nu_1(i)\nu_1'(i)] = H_1' P_{1f}(t_i-)H_1 + R_1 \quad . \tag{C.6}$$

We now note that since the $\tilde{x}_{1f}(t_i-)$'s can be identified as the one-step ahead prediction errors following from a discrete state model for the $x(t_i)$'s, and observation equation (C.1), we may employ the results of Appendix 2A to express the evolution of these prediction errors as follows:

$$\tilde{x}_{1f}(t_{\ell+1}-) = \Phi_A(t_{\ell+1},t_\ell)\left(I - P_{1f}(t_\ell+)H_1'R_1^{-1}H_1\right)\tilde{x}_{1f}(t_\ell-)$$

$$+ w_\ell - \Phi_A(t_{\ell+1},t_\ell)P_{1f}(t_\ell+)H_1'R_1^{-1}D_1v_1(\ell) \quad , \tag{C.7}$$

where $$w_\ell \triangleq \int_{\tau=t_\ell}^{t_{\ell+1}} \Phi_A(t_{\ell+1},\tau)B\,du(\tau) \quad . \tag{C.8}$$

Defining the discrete transition matrix $\Omega(i,j)$ associated with the dynamical equation (C.7) as

$$\Omega(i,j) = \begin{cases} I & i = j \\ \prod_{i_1=j}^{i-1} \Phi_A(t_{i_1+1},t_{i_1})(I - P_{1f}(t_{i_1}+)H_1'R_1^{-1}H_1) & i > j \end{cases} \quad , \tag{C.9}$$

and noting that from equations of Appendix 5A for the evolution of the first-pass filtered estimate between measurements

$$d\tilde{x}_{1f}(\tau) = A(\tau)\tilde{x}_{1f}(\tau)d\tau + B(\tau)du(\tau) \quad , \tag{C.10}$$

and hence

$$\tilde{x}_{1f}(t_{\ell+1}-) = \Phi_A(t_{\ell+1},t)\tilde{x}_{1f}(t) + \int_{\tau'=t}^{t_{\ell+1}} \Phi_A(t_{\ell+1},\tau')B(\tau')du(\tau'), \tag{C.11}$$

we can employ relations (C.7) - (C.11) to compute $E[\tilde{x}_{1f}(t)\tilde{x}'_{1f}(t_{\ell+j}-)]$ as

$$E[\tilde{x}_{1f}(t)\tilde{x}'_{1f}(t_{\ell+j}-)] = P_{1f}(t-)\Phi'_A(t_{\ell+1},t)\Omega'(\ell+j,\ell+1). \quad (C.12)$$

In relation (C.12), $P_{1f}(t-)$ denotes the left continuous version of $P_{1f}(\cdot)$. Hence, relations (C.5) and (C.12) allow us to express $\tilde{x}_{1s}(t)$ for $t_\ell < t \leq t_{\ell+1}$, where $\ell = 0,\ldots,N-1$, as

$$\tilde{x}_{1s}(t) = \tilde{x}_{1f}(t-) - P_{1f}(t-)\Phi'_A(t_{\ell+1},t)\sum_{j=1}^{N-\ell}\Omega'(\ell+j,\ell+1)H'_1P^{-1}_{\nu_1}(\ell+j)\nu_1(\ell+j). \quad (C.13)$$

For $t_N < t \leq T$ the smoothed estimate is identical with the filtered estimate and hence

$$\tilde{x}_{1s}(t) = \tilde{x}_{1f}(t) \ . \quad (C.14)$$

Relations (C.13) - (C.14) taken together represent the smoothing error process for any $t \in [0,T]$.

Appendix 5D

Proof of an Identity for the Projection of the Increments of the Process Noise onto the Hilbert Space Spanned by Future Values of the Smoothing Errors

In this Appendix we prove the following identity:

$$E[du(t)|\tilde{\chi}_{1t}^{+}] = B'P_{1f}^{-1}(t-)\tilde{x}_{1s}(t)dt \ , \qquad (D.1)$$

where $\tilde{\chi}_{1t}^{+}$ denotes the Hilbert space spanned by future values of the first-pass smoothing errors, associated with smoothed estimates based on the discrete measurements

$$y_1(\ell) = H_1 x(t_\ell) + D_1 v_1(\ell), \quad \text{for } \ell = 1,\ldots,N \ , \qquad (D.2)$$

and a continuous state model. We will prove (D.1) by checking the orthogonality condition

$$E\left[\left(du(t) - B'P_{1f}^{-1}(t-)\tilde{x}_{1s}(t)dt\right)\tilde{x}_{1s}'(\tau)\right] = 0 \ , \qquad (D.3)$$

for all $t \in [0,T]$, and $t \leq \tau \leq T$.

Before beginning the systematic verification of (D.3), we summarize some results that follow from Appendix 5C, and

Section 5.2, for the representation of the smoothing errors, $\tilde{x}_{1s}(\cdot)$, and the evolution of the first-pass filtering errors, $\tilde{x}_{1f}(\cdot)$. In Appendix 5C we showed that for $t_\ell < t \le t_{\ell+1}$, $\ell = 0,\ldots,N-1$,

$$\tilde{x}_{1s}(t) = \tilde{x}_{1f}(t-) - P_{1f}(t-)\Phi_A'(t_{\ell+1},t)\sum_{j=1}^{N-\ell}\Omega'(\ell+j,\ell+1)H_1'P_{\nu_1}^{-1}(\ell+j)\nu_1(\ell+j), \tag{D.4}$$

where

$$\nu_1(\ell+j) = H_1\hat{x}_f(t_{\ell+j}-) + D_1v_1(\ell+j) , \tag{D.5}$$

$$P_{\nu_1}(\ell+j) = H_1P_{1f}(t_{\ell+j}-)H_1' + R_1 , \tag{D.6}$$

and

$$\Omega(i,j) = \begin{cases} I & i = j \\ \prod_{i_1=j}^{i-1}\Phi_A(t_{i_1+1},t_{i_1})\left(I - P_{1f}(t_{i_1}+)H_1'R_1^{-1}H_1\right) & i > j \end{cases} . \tag{D.7}$$

For $T \ge t > t_N$, smoothing errors and filtering errors are equivalent, so that

$$\hat{x}_{1s}(t) = \hat{x}_{1f}(t) \quad . \tag{D.8}$$

To describe the evolution of the first-pass filtering errors, we first note that between discrete measurements the $\tilde{x}_{1f}(\cdot)$ are essentially prediction errors and satisfy the equation

$$d\tilde{x}_{1f}(t) = A\tilde{x}_{1f}(t)dt + B\,du(t) \quad . \tag{D.9}$$

By using relations of Appendix 5A for updating $\hat{x}_{1f}(\cdot)$ at $t = t_\ell$ we can obtain the following equation relating $\tilde{x}_{1f}(t_\ell+)$ and $\tilde{x}_{1f}(t_\ell-)$:

$$\tilde{x}_{1f}(t_\ell+) = \left(I - P_{1f}(t_\ell+)H_1'R_1^{-1}H_1\right)\tilde{x}_{1f}(t_\ell-) - P_{1f}(t_\ell+)H_1'R_1^{-1}D_1v_1(\ell). \tag{D.10}$$

Finally, we note that we showed in Appendix 5C that the $\tilde{x}_{1f}(t_i-)$'s evolve as

$$\tilde{x}_{1f}(t_{\ell+1}-) = \Phi_A(t_{\ell+1},t_\ell)\left(I - P_{1f}(t_\ell+)H_1'R_1^{-1}H_1\right)\tilde{x}_{1f}(t_\ell-) + w_\ell - \Phi_A(t_{\ell+1},t_\ell)P_{1f}(t_\ell+)H_1'R_1^{-1}D_1v_1(\ell) \quad , \tag{D.11}$$

where $$w_\ell \triangleq \int_{\tau'=t_\ell}^{t_{\ell+1}} \Phi_A(t_{\ell+1},\tau')B\,du(\tau') \quad . \tag{D.12}$$

We first verify relation (D.3) for $0 \le t \le t_N$ by assuming that $t_\ell < t \le t_{\ell+1}$, where we set $t_0 \triangleq 0$. For this case, $\tilde{x}_{1s}(t)$ is represented by relation (D.4). We now proceed to check (D.3) for τ in the range $t \le \tau \le t_{\ell+1}$, $t_{\ell+i} < \tau \le t_{\ell+i+1}$ where $1 \le i \le N-i-1$, and finally for $t_N < \tau \le T$. For $t \le \tau \le t_{\ell+1}$ we can represent $\tilde{x}_{1s}(\tau)$ by the following equation of the same form as (D.4):

$$\tilde{x}_{1s}(\tau) = \tilde{x}_{1f}(\tau-) - P_{1f}(\tau-)\Phi_A'(t_{\ell+1},\tau)\sum_{j=1}^{N-\ell}\Omega'(\ell+j,\ell+1)H_1'P_{\nu_1}^{-1}(\ell+j)\nu_1(\ell+j). \tag{D.13}$$

We will proceed to use the representation (D.13) to form $E[du(t)\tilde{x}_{1s}'(\tau)]$. Now, by using the fact that from (D.9)

$$\tilde{x}_{1f}(\tau-) = \Phi_A(\tau,t_\ell)\tilde{x}_{1f}(t_\ell+) + \int_{\tau'=t_\ell}^{\tau}\Phi_A(\tau,\tau')B\,du(\tau'), \tag{D.14}$$

and that $du(t) \perp \tilde{x}_{1f}(t_\ell+)$, we can compute $E[du(t)\tilde{x}_{1f}'(\tau-)]$ as

$$E[du(t)\tilde{x}_{1f}'(\tau-)] = B'\Phi_A'(\tau,t)dt \quad . \tag{D.15}$$

Then, by using the definition for $\nu_1(\cdot)$ in (D.5), and the fact that $du(t) \perp v_1(\ell+j)$, $j = 1,\ldots,N-\ell$, we can compute

$E[du(t)\nu_1'(\ell+j)]$ as

$$E[du(t)\nu_1'(\ell+j)] = E[du(t)\tilde{x}_{1f}'(t_{\ell+j}-)]H_1' \quad . \tag{D.16}$$

But by using the definition (D.12) of w_ℓ to show that

$$E[du(t)w_\ell'] = B'\Phi_A'(t_{\ell+1},t)dt \quad , \tag{D.17}$$

and equation (D.11) for the evolution of the $\tilde{x}_{1f}(t_{\ell+j}-)$'s, we can show that (D.16) becomes

$$E[du(t)\nu_1'(\ell+j)] = B'\Phi_A'(t_{\ell+1},t)\Omega'(\ell+j,\ell+1)dt \quad . \tag{D.18}$$

We may now use relations (D.15) and (D.18) to form $E[du(t)\tilde{x}_s'(\tau)]$ as

$$E[du(t)\tilde{x}_s'(\tau)] = \left[B'\Phi_A'(\tau,t) - \sum_{j=1}^{N-\ell} B'\Phi_A'(t_{\ell+1},t)\Omega'(\ell+j,\ell+1) \cdot H_1'P_{\nu_1}^{-1}(\ell+j)H_1\Omega(\ell+j,\ell+1)\Phi_A(t_{\ell+1},\tau)P_{1f}(\tau-)\right]dt. \tag{D.19}$$

To complete the verification of (D.3) for $t \le \tau \le t_{\ell+1}$, we use the representation for $\tilde{x}_{1s}(t)$, given by equation (D.13),

and the expression for $\tilde{x}_{1s}(t)$ given by (D.4), to compute $E[\tilde{x}_{1s}(t)\tilde{x}'_{1s}(\tau)]$. Noting from (D.9) that $E[\tilde{x}_{1f}(t-)\tilde{x}'_{1f}(\tau-)]$ is given by

$$E[\tilde{x}_{1f}(t-)\tilde{x}'_{1f}(\tau-)] = P_{1f}(t-)\Phi'_A(\tau,t) \ , \tag{D.20}$$

and observing that by the use of relations (D.9), (D.11) $E[\tilde{x}_{1f}(t-)\nu'_1(\ell+j)]$ can be expressed as

$$E[\tilde{x}_{1f}(t-)\nu'_1(\ell+j)] = P_{1f}(t-)\Phi'_A(t_{\ell+1},t)\Omega'(\ell+j,\ell+1)H'_1, \tag{D.21}$$

and similarly that $E[\nu_1(\ell+j)\tilde{x}'_{1f}(\tau-)]$ can be computed as

$$E[\nu_1(\ell+j)\tilde{x}'_{1f}(\tau-)] = H_1\Omega(\ell+j,\ell+1)\Phi_A(t_{\ell+1},\tau)P_{1f}(\tau-) \ , \tag{D.22}$$

We can employ relations (D.20) - (D.22) to express $E[\tilde{x}_{1s}(t)\tilde{x}'_{1s}(\tau)]$ as

$$\begin{aligned} E[\tilde{x}_{1s}(t)\tilde{x}'_{1s}(\tau)] &= P_{1f}(t-)\Phi'_A(\tau,t) \\ &\quad - \sum_{i=1}^{N-\ell} P_{1f}(t-)\Phi'_A(t_{\ell+1},t)\Omega'(\ell+i,\ell+1)H'_1 \\ &\quad \cdot P^{-1}_{\nu_1}(\ell+i)H_1\Omega(\ell+i,\ell+1)\Phi_A(t_{\ell+1},\tau)P_{1f}(\tau-) \ . \end{aligned} \tag{D.23}$$

Substituting relations (D.19) and (D.23) into (D.3) validates the desired orthogonality condition for $t_\ell < t \leq t_{\ell+1}$ and $t \leq \tau \leq t_{\ell+1}$.

We next check relation (D.3) for $t_\ell < t \leq t_{\ell+1}$ and $t_{\ell+i} \leq \tau \leq t_{\ell+i+1}$, where $i = 1,\ldots,N-\ell-1$. In direct analogy with relation (D.4), we can express $\tilde{x}_{1s}(\tau)$ for $t_{\ell+i} < \tau \leq t_{\ell+i+1}$ as

$$\tilde{x}_{1s}(\tau) = \tilde{x}_{1f}(\tau-) - P_{1f}(\tau-)\Phi_A'(t_{\ell+i+1},\tau)\sum_{j=1}^{N-\ell-i}\Omega'(\ell+i+j,\ell+i+1)H_1'P_{\nu_1}^{-1}(\ell+i+j)\nu_1(\ell+i+j). \tag{D.24}$$

We first form $E[du(t)\tilde{x}_{1s}'(\tau)]$ by noting from relation (D.18) that

$$E[du(t)\nu_1'(\ell+i+j)] = B'\Phi_A'(t_{\ell+1},t)\Omega'(\ell+i+j,\ell+1)\,dt\ , \tag{D.25}$$

and by computing $E[du(t)\tilde{x}_{1f}'(\tau-)]$. From (D.9) we can express $\tilde{x}_{1f}(\tau-)$ as

$$\tilde{x}_{1f}(\tau-) = \Phi_A(\tau,t_{\ell+i})\tilde{x}_{1f}(t_{\ell+i}+) + \int_{\tau'=t_{\ell+i}}^{\tau}\Phi_A(\tau,\tau')B\,du(\tau')\ , \tag{D.26}$$

and $\tilde{x}_{1f}(t_{\ell+1}-)$ as

$$\tilde{x}_{1f}(t_{\ell+1}-) = \Phi_A(t_{\ell+1},t)\tilde{x}_{1f}(t) + \int_{\tau'=t}^{t_{\ell+1}} \Phi_A(t_{\ell+1},\tau')B\,du(\tau'), \quad (D.27)$$

By using (D.26) - (D.27) in conjunction with relation (D.10) to relate $\tilde{x}_{1f}(t_{\ell+i}+)$ to $\tilde{x}_{1f}(t_{\ell+i}-)$, and equation (D.11) to relate $\tilde{x}_{1f}(t_{\ell+i}-)$ to $\tilde{x}_{1f}(t_{\ell+1}-)$, we can show that $E[du(t)\tilde{x}'_{1f}(\tau-)]$ is given by

$$E[du(t)\tilde{x}'_{1f}(\tau-)] = B'\Phi'_A(t_{\ell+1},t)\Omega'(\ell+i,\ell+1)\left(I - P_{1f}(t_{\ell+i}+)H'_1R_1^{-1}H_1\right)' \cdot \Phi'_A(\tau,t_{\ell+i})dt \ . \quad (D.28)$$

Hence, by using relations (D.25), (D.28) we can form $E[du(t)\tilde{x}'_s(\tau)]$ from relation (D.24) as

$$E[du(t)\tilde{x}'_{1s}(\tau)] = \Bigg[B'\Phi'_A(t_{\ell+1},t)\Omega'(\ell+i,\ell+1) \cdot \left(I - P_{1f}(t_{\ell+i}+)H'_1R_1^{-1}H_1\right)'\Phi'_A(\tau,t_{\ell+i}) - \sum_{j=i}^{N-\ell-i} B'\Phi'_A(t_{\ell+1},t)\Omega'(\ell+i+j,\ell+1)H'_1P_{\nu_1}^{-1}(\ell+i+j)H_1 \cdot \Omega(\ell+i+j,\ell+i+1)\Phi_A(t_{\ell+i+1},\tau)P_{1f}(\tau-)\Bigg]dt \ . \quad (D.29)$$

We complete the verification of relation (D.3) for $t_\ell < t \le t_{\ell+1}$ and $t_{\ell+i} < \tau \le t_{\ell+i+1}$, $i = 1,\ldots,N-\ell-1$, by computing $E[\tilde{x}_{1s}(t)\tilde{x}'_{1s}(\tau)]$. We use the representation for $\tilde{x}_{1s}(t)$, of (D.4), and equation (D.24) to represent $\tilde{x}_{1s}(\tau)$. We first note from relation (D.21) that

$$E[\tilde{x}_{1f}(t-)\nu'_1(\ell+i+j)] = P_{1f}(t-)\Phi'_A(t_{\ell+1},t)\Omega'(\ell+i+j,\ell+1)H'_1 \quad , \qquad (D.30)$$

for $j = 1,\ldots,N-\ell-i$. In addition, we observe that

$$E[\nu_1(\ell+j)\tilde{x}'_{1f}(\tau-)] = 0 \quad , \qquad (D.31)$$

for $j = 1,\ldots,i$, by the orthogonality property satisfied by filtering errors. However, for $j = i+1,\ldots,N-\ell$, by a similar argument to that resulting in relation (D.30), we can show that

$$E[\nu_1(\ell+j)\tilde{x}'_{1f}(\tau-)] = H_1\Omega(\ell+j,\ell+i+1)\Phi_A(t_{\ell+i+1},\tau)P_{1f}(\tau-). \qquad (D.32)$$

Finally, by employing relations (D.26) - (D.27) and (D.10) - (D.11) to express $\tilde{x}_{1f}(\tau-)$ as a function of $\tilde{x}_{1f}(t-)$, we can show that

$$E[\tilde{x}_{1f}(t-)\tilde{x}'_{1f}(\tau-)] = P_{1f}(t-)\Phi'_A(t_{\ell+1},t)\Omega'(\ell+i,\ell+1)$$
$$\cdot \left(I - P_{1f}(t_{\ell+i}+)H'_1R_1^{-1}H_1\right)' \Phi'_A(\tau,t_{\ell+i}). \quad (D.33)$$

We now may use relations (D.30) - (D.33) together with the mutual orthogonality of the $\nu_1(i)$'s to compute $E[\tilde{x}_{1s}(t)\tilde{x}'_{1s}(\tau)]$ as

$$E[\tilde{x}_{1s}(t)\tilde{x}'_{1s}(\tau)] = P_{1f}(t-)\Phi'_A(t_{\ell+1},t)\Omega'(\ell+i,\ell+1)$$
$$\cdot \left(I - P_{1f}(t_{\ell+i}+)H'_1R_1^{-1}H_1\right)' \Phi'_A(\tau,t_{\ell+i})$$
$$- \sum_{j=1}^{N-\ell-i} P_{1f}(t-)\Phi'_A(t_{\ell+1},t)\Omega'(\ell+i+j,\ell+1)H'_1$$
$$\cdot P_{\nu_1}^{-1}(\ell+i+j)H_1\Omega(\ell+i+j,\ell+i+1)\Phi_A(t_{\ell+i+1},\tau)P_{1f}(\tau-). \quad (D.34)$$

Substituting relations (D.29) and (D.34) into relation (D.3) results in the verification of the desired orthogonality condition for $t_\ell < t \le t_{\ell+1}$ and $t_{\ell+i} < \tau \le t_{\ell+i+1}$.

We finally verify relation (5.29) for $t_\ell < t \le t_{\ell+1}$ and $t_N < \tau \le T$. For $\tau > t_N$, the smoothing error, $\tilde{x}_{1s}(\tau)$, is the same as the filtering error, $\tilde{x}_{1f}(\tau)$, i.e.,

$$\tilde{x}_{1s}(\tau) = \tilde{x}_{1f}(\tau) \ . \quad (D.35)$$

Hence, we compute $E[du(t)\tilde{x}'_{1s}(\tau)]$, using the same argument that resulted in relation (D.28), as

$$E[du(t)\tilde{x}'_{1s}(\tau)] = B'\Phi'_A(t_{\ell+1},t)\Omega'(N,\ell+1)\left(I - P_{1f}(t_N+)H'_1R_1^{-1}H_1\right)'\Phi'_A(\tau,t_N)dt. \tag{D.36}$$

Using relation (D.4) to represent $\tilde{x}_{1s}(t)$, and equation (D.35) to represent $\tilde{x}_{1s}(\tau)$, noting relation (D.33) and the fact that $\tilde{x}_{1f}(\tau) \perp \nu_1(i)$, $i = 1,\ldots,N$, we can compute $E[\tilde{x}_{1s}(t)\tilde{x}'_{1s}(\tau)]$ as

$$E[\tilde{x}_{1s}(t)\tilde{x}'_{1s}(\tau)] = P_{1f}(t-)\Phi'_A(t_{\ell+1},t)\Omega'(N,\ell+1) \cdot \left(I - P_{1f}(t_N+)H'_1R_1^{-1}H_1\right)'\Phi'_A(\tau,t_N) \ . \tag{D.37}$$

Substituting relations (D.36) - (D.37) into (D.3) verifies the desired orthogonality condition for $t_\ell < t \le t_{\ell+1}$ and $t_N < \tau \le T$.

We conclude our verification of (D.3) by considering the case when $t_N < t \le T$ and $t \le \tau \le T$. Now, both $\tilde{x}_{1s}(t)$ and $\tilde{x}_{1s}(\tau)$ are identical with $\tilde{x}_{1f}(t)$ and $\tilde{x}_{1f}(\tau)$, respectively. Hence, we may use the $\tilde{x}_{1f}(\cdot)$ dynamics (D.9) to show that

$$E[du(t)\tilde{x}'_{1s}(\tau)] = B'\Phi'_A(\tau,t)dt \ , \tag{D.38}$$

and $$E[\tilde{x}_{ls}(t)\tilde{x}'_{ls}(\tau)] = P_{lf}(t-)\Phi'_A(\tau,t) \quad . \tag{D.39}$$

Relations (D.38) and (D.39), when substituted into relation (D.3), complete our check on the desired orthogonality condition which verifies the identity (D.1) for the projection of du(t) onto the space spanned by future values of the smoothing errors, $\tilde{\chi}^+_t$.

Appendix 5E

Centralized Map-Updating when First-Pass Data is Continuous, and Second-Pass Data is Discrete

In this Appendix we consider a version of the map-updating problem for which the first-pass measurements are modelled by

$$dy_1(t) = H_1 x(t)dt + D_1 dv_1(t) \quad , \tag{E.1}$$

and hence we define

$$Y_1 \triangleq H(dy_1(\tau) \quad 0 \leq \tau \leq T) \ . \tag{E.2}$$

The second-pass measurements will be described by

$$y_2(i) = H_2 x(t_i) + D_2 v_2(i) \ , \tag{E.3}$$

so that we define

$$Y_2 \triangleq H(y_2(i) \quad i = 1,\ldots,N) \ . \tag{E.4}$$

The quantities $dv_1(\cdot)$ and $v_2(\cdot)$ are taken to be a standard Wiener process, and a standard discrete white noise process,

respectively. As before, we assume $dv_1(\cdot)$ and $v_2(\cdot)$ to be uncorrelated. In this case, the desired map-updating procedure follows from the following orthogonal decomposition of the Hilbert space spanned by the two data passes:

$$Y_1 \vee Y_2 = Y_1 \oplus \tilde{Y}_2 \ , \tag{E.5}$$

where $$\tilde{Y}_2 \triangleq H(\tilde{y}_2(i) \quad i = 1,\ldots,N) \ , \tag{E.6}$$

and $$\tilde{y}_2(i) \triangleq y_2(i) - E[y_2(i)|Y_1] \ . \tag{E.7}$$

By using the decomposition (E.5), we can express the two-data pass smoothed estimate as

$$\hat{x}_s(t) = \hat{x}_{1s}(t) + E[\tilde{x}_{1s}(t)|\tilde{Y}_2] \ . \tag{E.8}$$

We now note that from equation (E.3) and definition (E.7), $\tilde{y}_2(i)$ can be formed as

$$\tilde{y}_2(i) = H_2\tilde{x}_{1s}(t_i) + D_2v_2(i) \ . \tag{E.9}$$

Hence, given the following forward and reverse Markovian realizations of $\tilde{x}_{1s}(\cdot)$:

$$d\tilde{x}_{1s}(t) = \left(A + Q(P_{1f}^{-1} - P_{1s}^{-1})\right)\tilde{x}_{1s}(t)dt + B\,d\tilde{u}_{1f}(t) \quad , \qquad (E.10)$$

and $$d\tilde{x}_{1s}(t) = \left(A + QP_{1f}^{-1}\right)\tilde{x}_{1s}(t)dt + B\,d\tilde{u}_{1r}(t) \quad , \qquad (E.11)$$

the problem of forming $E[\tilde{x}_{1s}(t)|\tilde{Y}_2]$ is the same type of continuous model, discrete measurement smoothing problem which we solved in Section 5.2 to generate the first-pass smoothed estimates, $\hat{x}_{1s}(\cdot)$, through relations (5.10) - (5.23).

We now follow the approach of Section 4.2 and specify forward and reverse filtered estimates of the smoothing error process, in order to form $E[\tilde{x}_{1s}(t)|\tilde{Y}_2]$. We define $\hat{\tilde{x}}_f(t), \hat{\tilde{x}}_r(t)$ for $t_\ell < t < t_{\ell+1}$ by

$$\hat{\tilde{x}}_f(t) = E[\tilde{x}_{1s}(t)|\tilde{Y}_{2,\ell+1}^{-}] \quad , \qquad (E.12)$$

and $$\hat{\tilde{x}}_r(t) = E[\tilde{x}_{1s}(t)|\tilde{Y}_{2,\ell+1}^{+}] \quad . \qquad (E.13)$$

We let P_{fs} and P_{rs} denote the error covariance matrices associated with the estimates $\hat{\tilde{x}}_f(t)$ and $\hat{\tilde{x}}_r(t)$, respectively. Then, noting from relation (E.8) that

$$\tilde{x}_s(t) = \tilde{x}_{1s}(t) - E[\tilde{x}_{1s}(t)|\tilde{Y}_2] \quad , \qquad (E.14)$$

we may express $E[\tilde{x}_{1s}(t)|\tilde{Y}_2]$ as

$$E[\tilde{x}_{1s}(t)|\tilde{Y}_2] = P_s\left\{P_{fs}^{-1}\hat{\tilde{x}}_f(t) + P_{rs}^{-1}\hat{\tilde{x}}_r(t)\right\} \quad . \tag{E.15}$$

By employing the forward realization (E.10) for $\tilde{x}_{1s}(\cdot)$, we obtain the following equations for the evolution of $\hat{\tilde{x}}_f(t), P_{fs}$ for $t_\ell < t < t_{\ell+1}$:

$$d\hat{\tilde{x}}_f(t) = \left(A + Q(P_{1f}^{-1} - P_{1s}^{-1})\right)\hat{\tilde{x}}_f(t)dt \quad , \tag{E.16}$$

and

$$\dot{P}_{fs} = \left(A + Q(P_{1f}^{-1} - P_{1s}^{-1})\right)P_{fs} + P_{fs}\left(A + Q(P_{1f}^{-1} - P_{1s}^{-1})\right)' + Q, \tag{E.17}$$

where the initial conditions $\hat{\tilde{x}}_f(0)$, $P_{fs}(0)$ are given as $0, P_{1s}(0)$, respectively, and the following updating relations are satisfied at $t = t_\ell$:

$$\hat{\tilde{x}}_f(t_\ell+) = \left(I - P_{fs}(t_\ell+)H_2'R_2H_2\right)\hat{\tilde{x}}_f(t_\ell-) + P_{fs}(t_\ell+)H_2'R_2^{-1}\tilde{y}_2(\ell) \quad , \tag{E.18}$$

and

$$P_{fs}^{-1}(t_\ell+) = P_{fs}^{-1}(t_\ell-) + H_2'R_2^{-1}H_2 \quad . \tag{E.19}$$

Similarly, we may employ the backward realization (E.11) of $\tilde{x}_{1s}(\cdot)$ to obtain the following backward equations for the

evolution of $\hat{\tilde{x}}_r(t)$ and P_{rs} for $t_\ell < t < t_{\ell+1}$:

$$-d\hat{\tilde{x}}_r(t) = -\left(A + QP_{1f}^{-1}\right)\hat{\tilde{x}}_r(t)dt \ , \tag{E.20}$$

$$\text{and} \quad -\dot{P}_{rs} = -\left(A + QP_{1f}^{-1}\right)P_{rs} - P_{rs}\left(A + QP_{1f}^{-1}\right)' + Q \ , \tag{E.21}$$

where the initial conditions $\hat{\tilde{x}}_r(T), P_{rs}(T)$ are given by $0, P_{1s}(T)$, respectively, and the following updating relations are satisfied at $t = t_{\ell+1}$:

$$\hat{\tilde{x}}_r(t_{\ell+1}-) = \left(I - P_{rs}(t_{\ell+1}-)H_2'R_2^{-1}H_2\right)\hat{\tilde{x}}_r(t_{\ell+1}+) + P_{rs}(t_{\ell+1}-)H_2'R_2^{-1}\tilde{y}_2(\ell+1) \ , \tag{E.22}$$

$$\text{and} \qquad P_{rs}^{-1}(t_{\ell+1}-) = P_{rs}^{-1}(t_{\ell+1}+) + H_2'R_2^{-1}H_2 \ . \tag{E.23}$$

We now note that in Section 5.2 first-pass data was specified as discrete and the second-pass data as continuous measurements, while in this appendix the reverse situation applies. In either case, the problem of forming the two-pass smoothed estimates from two-pass forward and reverse filtered estimates is essentially the same. To compute $\hat{x}_f(\cdot)$, P_f, $\hat{x}_r(\cdot)$, P_r, and 0_0, we need only change the notation of Appendix 5B, or of Section 5.2, to reflect the fact that first-pass

measurements are now continuous, and the second-pass measurements discrete. In addition, we can show in a similar manner as we did in Section 5.2, and Appendix 4A, that the identities

$$P_f^{-1} = P_{1f}^{-1} + P_{fs}^{-1} - P_{1s}^{-1} \quad , \tag{E.24}$$

and

$$O_0 = P_{rs}^{-1} - P_{1f}^{-1} \quad , \tag{E.25}$$

still hold.

If we next define $\gamma_f(t)$ and $\gamma_r(t)$ as

$$\gamma_f(t) \triangleq P_{fs}^{-1} \hat{\hat{x}}_f(t) \quad , \tag{E.26}$$

and

$$\gamma_r(t) \triangleq P_{rs}^{-1} \hat{\hat{x}}_r(t) \quad , \tag{E.27}$$

we may use equations (E.16) - (E.27) to obtain the following relations for the evolution of $\gamma_f(\cdot)$ and $\gamma_r(\cdot)$ for $t_\ell < t < t_{\ell+1}$:

$$d\gamma_f(t) = - (A' + P_f^{-1}Q)\gamma_f(t)dt \quad , \tag{E.28}$$

and

$$-d\gamma_r(t) = (A' - O_0 Q)\gamma_r(t)dt \quad , \tag{E.29}$$

where the initial conditions for $\gamma_f(0), \gamma_r(T)$ are both zero, and the following updating equations are satisfied at $t = t_\ell$:

$$\gamma_f(t_\ell+) = \gamma_f(t_\ell-) + H_2' R_2^{-1} \tilde{y}_2(\ell) \quad , \tag{E.30}$$

and

$$\gamma_r(t_\ell-) = \gamma_r(t_\ell+) + H_2' R_2^{-1} \tilde{y}_2(\ell) \quad . \tag{E.31}$$

Thus, we may alternatively compute $E[\tilde{x}_{1s}(t)|\tilde{Y}_2]$ as

$$E[\tilde{x}_{1s}(t)|\tilde{Y}_2] = P_s[\gamma_f(t) + \gamma_r(t)] \quad . \tag{E.32}$$

Hence, the solution to the centralized map-updating problem when the first-pass data is continuous, and the second-pass data is discrete, is obtained by substituting relation (E.32) into equation (E.8), where $\gamma_f(\cdot)$ and $\gamma_r(\cdot)$ evolve according to relations (E.28) - (E.31). The off-line quantities P_f and O_0 are computed by the same equations as those specified in Section 5.2, with the notation changed to reflect the fact that the first-pass data is now continuous, and the second-pass data discrete.

Chapter 6

The Map-Centralization Problem

6.1 Introduction

In Chapters 4 and 5 we considered one-dimensional formulations of the Centralized Map-Updating and Centralized Map-Combining Problems, i.e., data passes were modelled as either continuous or discrete measurements of some underlying state process over a fixed interval, and maps were identified as smoothed estimates of the state. In this chapter, we first demonstrate how we may capture a particular class of two-dimensional centralized map-updating and map-combining problems by the framework of Chapters 4 and 5, and then in Chapter 7 we present specific examples of these problems.

In both the Geodetic and Meteorological Application areas, discussed in Section 1.2, we typically have a variety of sensors that traverse a given spatial region, making measurements of some underlying random field along certain paths. As the data from different surveys is accumulated, we can conceive of three types of data assimilation problems that are of practical importance:

Centralized Map-Updating

In this problem we have a centralized facility that produces a map of the random field over a given region based on all survey data available. The map-updating problem is then one of updating an existing map in order to incorporate new survey data. As we will see, the results in the preceding chapters provide us with the essential elements required to solve this problem.

Centralized Map-Combining

In this problem we have several maps of the same region produced from different surveys. The combining problem is one of combining these maps to produce an overall map. Using the ideas of Section 4.2 we can show that the solution to this problem can be derived as a consequence of map-updating results.

Map-Centralization

In this problem we have several maps, produced from different surveys, where the maps may not be over identical regions. Thus, local surveys might be used to produce local maps. The map-centralization problem is one of combining these local maps to produce an overall global map of the entire region of interest. In this chapter we will discuss in detail the solution of this problem when all of the processing done for the local maps is "consistent", i.e., where the random field models used in doing the local processing are exactly

interpretable as the restriction of the global field model. We will also comment briefly on the case in which the local models are inconsistent. This may typically happen if the local processing is based on a simplified, approximate model that is obtained by neglecting, or approximating, some of the correlations that exist in the actual global model.

Throughout our discussion in this chapter we limit ourselves to the case in which there are exactly two measurement surveys. The extension to more surveys is immediate although somewhat cumbersome notationally. To motivate and illustrate our approach, consider the case of an M-parallel line measurement geometry, as illustrated in Fig. 6.1. Note that this figure illustrates the fact that we can have duplicate survey tracks. Thus in this case each survey consists of five tracks, but $M = 7$, indicating that there are only seven distinct tracks. While our present discussion will rely heavily on the parallel nature of the tracks, our method extends to essentially general measurement geometries for discrete-space fields. This is illustrated in Chapter 7, where the technical issue that arises in considering the more general track geometries in continuous space is also discussed briefly.

Returning to the case of M parallel paths, we can directly obtain one-dimensional versions of the three problems described

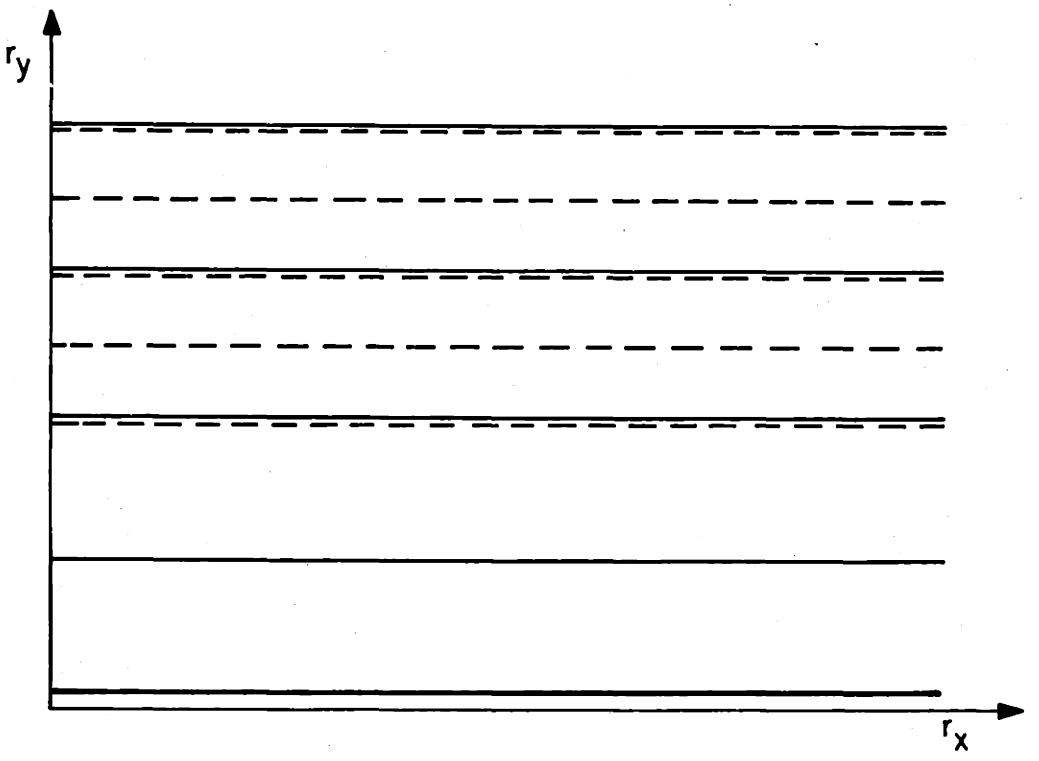

note:

First-Pass Data Tracks ——— (5 Tracks of Data)

Second-Pass Data Tracks - - - (5 Tracks of Data)

(Total of M=7 Measurement Tracks between Two-Surveys-3 of the Second-Pass Tracks are over the same Lines of the First-Pass Measurements.)

Fig. 6.1 Example of an M-Parallel Measurement Track Survey Geometry

previously. Specifically, we will use as our independent variable the quantity t, parameterizing the horizontal distance r_x along the tracks. Suppose that in our overall global map, we would like to estimate the random field along a given set of parallel tracks. That is, suppose that we specify a total of N horizontal tracks, where each track extends spatially from r_x=0 to r_x=R, and has a given r_y coordinate:

$$\left.\begin{aligned} r_1(t) &= \left(r_x^1(t), r_y^1\right) , \\ &\vdots \\ r_N(t) &= \left(r_x^N(t), r_y^N\right) \end{aligned}\right\} \qquad (6.1)$$

where each $r_x^i(t)$ is increasing, and

$$\left.\begin{aligned} r_x^i(0) &= 0 \quad , \\ \text{and} \quad r_x^i(T) &= R \quad . \end{aligned}\right\} \qquad (6.2)$$

Thus, the process we wish to estimate is

$$Z(t) = \begin{pmatrix} f\left(r_x^1(t), r_y^1\right) \\ \vdots \\ f\left(r_x^N(t), r_y^N\right) \end{pmatrix} , \qquad (6.3)$$

where $f(\cdot,\cdot)$ denotes some R^n valued random field defined on the (r_x,r_y) plane.

We will assume that $Z(t)$ can be viewed as being generated by a finite dimensional linear system driven by white noise

$$d\xi(t) = A(t)\xi(t)dt + B(t)du(t) \ , \tag{6.4}$$

with

$$Z(t) = L(t)\xi(t) \quad . \tag{6.5}$$

We will call $\xi(\cdot)$ the global state process, since through (6.5) it is used to represent the field over the global region of interest. In Chapter 7 we will show how to construct models for $Z(t)$ of the above form when $f(\cdot,\cdot)$ is a scalar, stationary field with a separable correlation function, and all $r_x^i(t) = t$ (i.e., constant velocity). These conditions are more restrictive than necessary, especially for discrete-space fields. In particular, the constant velocity assumption can be removed without any difficulty, by using the work of Kam [51]. In addition, we note in Chapter 7 that we can also obtain models of the form (6.4) - (6.5) for the case of nonstationary fields with correlation functions expressable as a sum of separable terms, where each term is formed as a product of one-dimensional space-variant corrrelation functions, associated with each coordinate direction. The correlation functions associated

with such fields may be used to approximate those of arbitrary fields. The extensions mentioned above would, however, obscure the concepts we wish to illustrate. In the next chapter, we will see through an example that the most critical assumption, that of parallel tracks, can be relaxed in a discrete-space setting.

In order for the mapping problem to be formulated, we assume that the N trajectories specified for mapping include the M trajectories over which survey data is collected. If not, then the data collected is not simply noisy measurements of linear combinations of $\xi(\cdot)$, and we have not posed the problem correctly. Note also that, in the formulation which we present, it is possible to have $N > M$, which might correspond to the practically important case of interpolating between measurement tracks. We now formulate our measurement equations as follows. Let us define the vector $Z_i(t)$ obtained by selecting the $M_i \leq M$ partitions of $Z(t)$ corresponding to the i-th survey field variables. Hence, we have

$$Z_i(t) = E_i Z(t) \quad , \tag{6.6}$$

where E_i is an $nM_i \times nM$ matrix with $n \times n$ blocks defined as

$$\left(E_i\right)_{n_1,n_2} \triangleq \begin{cases} 1 & \text{if the } n_2\text{-th track is the } n_1\text{-the track of the i-th survey} \\ 0 & \text{otherwise} \end{cases} \quad . \tag{6.7}$$

Then, we assume that the i-th survey measurements are modelled as

$$dy_i(t) = C_i(t)Z_i(t)dt + D_i(t)dv_i(t) \quad , \tag{6.8}$$

where $v_1(\cdot)$ and $v_2(\cdot)$ are standard, mutually independent vector Brownian motion processes, uncorrelated with the process noise $du(\cdot)$, and

$$D_i(t)D_i'(t) = R_i(t) > 0 \quad . \tag{6.9}$$

If we define

$$H_i(t) \triangleq C_i(t)E_iL(t) \quad , \tag{6.10}$$

then our global state model and the two-survey measurement equations may be summarized as

$$\left.\begin{aligned} d\xi(t) &= A(t)\xi(t)dt + Bdu(t) \quad , \\ dy_1(t) &= H_1(t)\xi(t)dt + D_1(t)dv_1(t) \quad , \\ \text{and} \qquad dy_2(t) &= H_2(t)\xi(t)dt + D_2(t)dv_2(t) \quad . \end{aligned}\right\} \tag{6.11}$$

The goal of each of our problems is to estimate the tracks of the field specified by $Z(\cdot)$, but $Z(t) = L(t)\xi(t)$, and, assuming that the model (6.4) - (6.5) is a minimal order stochastic realization of $Z(\cdot)$, the estimation of $Z(\cdot)$ requires the estimation of $\xi(\cdot)$, and consequently we will refer explicitly only to the estimation of $\xi(\cdot)$.

In terms of the state-space model (6.11) we can now define our first two problems explicitly. We let Y_1 and Y_2 denote the Hilbert spaces spanned by the first and second survey measurements, respectively, and define the aggregate, two-data survey space by

$$Y = Y_1 \vee Y_2 \quad . \tag{6.12}$$

Then, we can define the smoothed, global state estimates

$$\hat{\xi}_s(t) \triangleq E[\xi(t)|Y] \quad , \tag{6.13}$$

and $$\hat{\xi}_{is}(t) \triangleq E[\xi(t)|Y_i] \quad , \quad \text{for } i=1,2 \quad . \tag{6.14}$$

The centralized map-updating problem is then to compute $\hat{\xi}_s(\cdot)$ in terms of $\hat{\xi}_{1s}(\cdot)$ and $dy_2(\cdot)$, and the centralized map-combining problem is to compute $\hat{\xi}_s(\cdot)$ in terms of $\hat{\xi}_{1s}(\cdot)$ and $\hat{\xi}_{2s}(\cdot)$. (See Fig. (6.2) - (6.3) for conceptual diagrams of the information flow and processing implied by these two problems.) We can appeal directly to the results of Chapter 4 for the solution of these problems.

The map centralization problem was defined earlier as that of combining local maps, that are produced by processing regional survey data using local field models, in order to obtain a final map over some global region of interest. In our present context, this problem can be stated as follows: assume that local processors employ their own local models for the i-th survey field variables $Z_i(\cdot)$ in order to generate the local maps. To make this precise, we assume that the i-th local processor models $Z_i(t)$ as

$$Z_i(t) = L_i(t)\theta_i(t) \quad , \tag{6.15}$$

where $$d\theta_i(t) = F_i(t)\theta_i(t)dt + G_i(t)du_i(t) \quad , \tag{6.16}$$

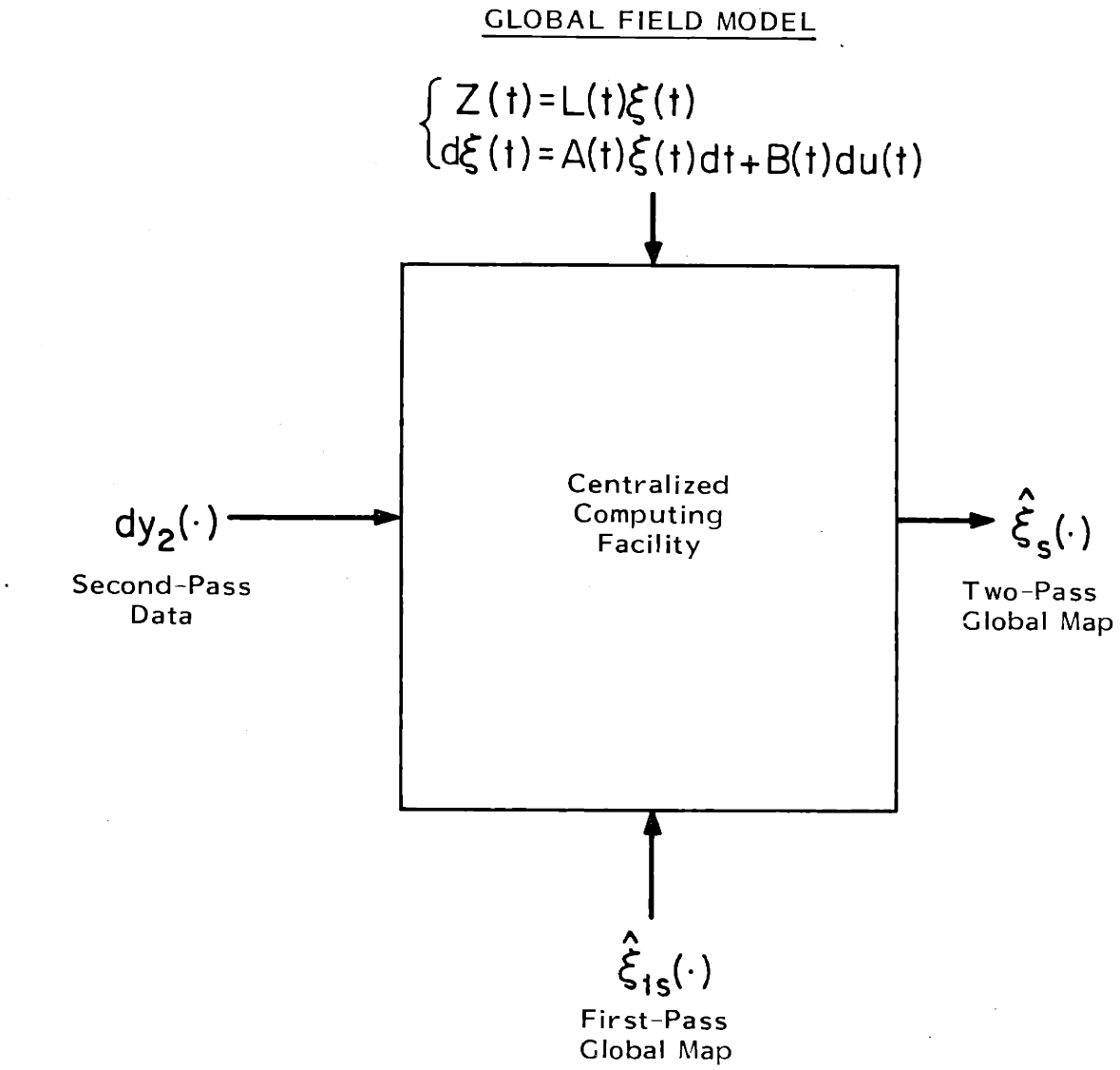

Fig. 6.2 The Centralized Map-Updating Problem for Forming an N-Track Map

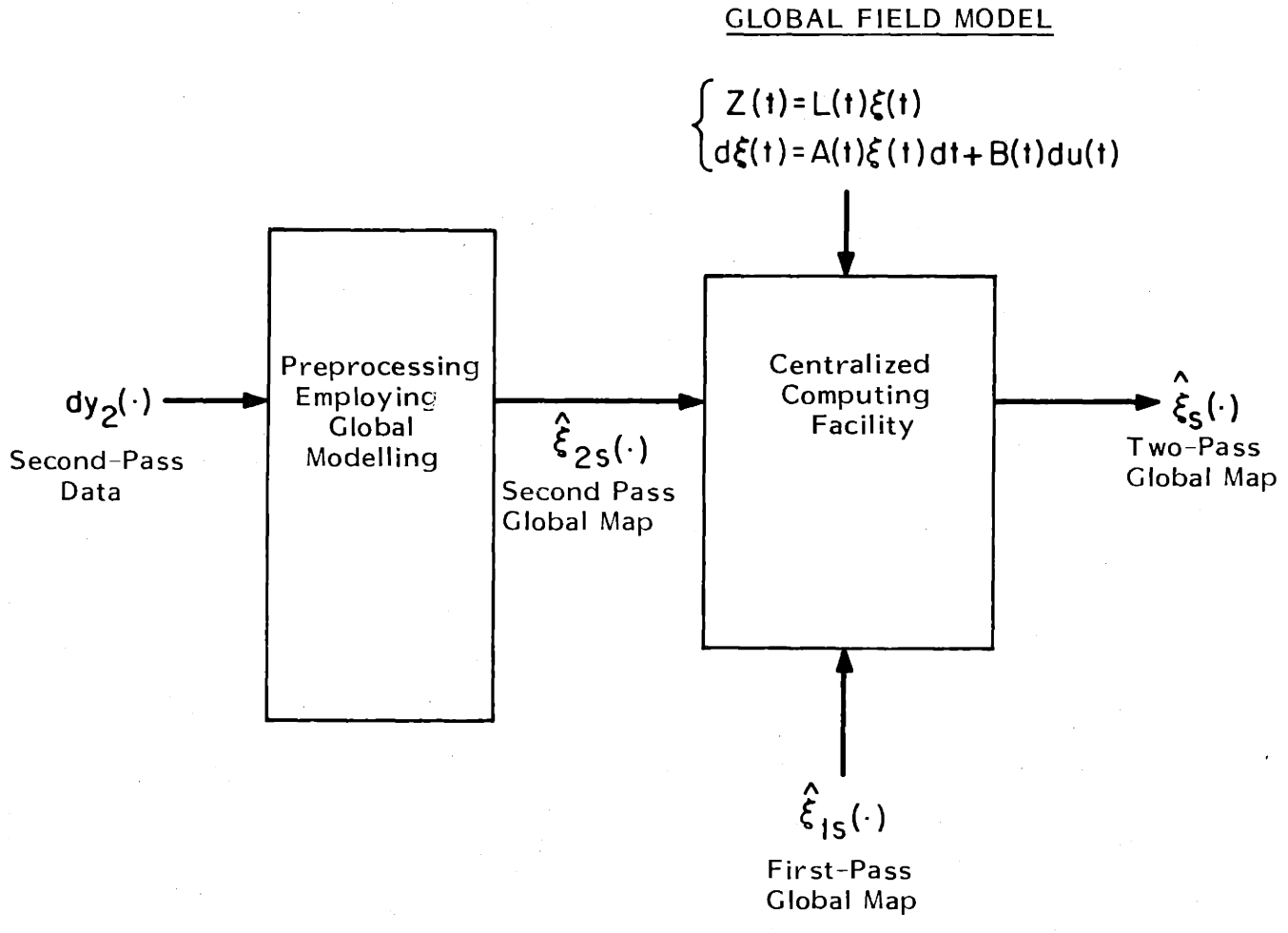

Fig. 6.3 The Centralized Map-Combining Problem for Forming an N-Track Map

and also models the i-th survey measurements in the same manner as the global processor, by

$$dy_i(t) = C_i(t)Z_i(t)dt + D_i(t)dv_i(t) \quad . \tag{6.17}$$

Hence, based on the model for $Z_i(\cdot)$ of (6.15) - (6.16), and the measurement equation (6.17), the i-th local processors compute the smoothed estimates $\hat{\theta}_{is}(\cdot)$, for $i = 1,2$, which define the local maps.

We emphasize here that in general the model (6.15) - (6.16) may not represent an exact realization of the local field variables, $Z_i(\cdot)$, that is consistent with the global model (6.4) - (6.5). In this case the locals maps, $\hat{\theta}_{is}(\cdot)$, represent estimates constructed on the basis of incorrect models, and hence they no longer correspond to conditional expectations. In any case, the <u>map-centralization</u> problem is to compute $\hat{\xi}_s(\cdot)$ in terms of $\hat{\theta}_{1s}(\cdot)$ and $\hat{\theta}_{2s}(\cdot)$. We depict the processing structure for this problem in Fig. 6.4.

It is appropriate to say a few words about the local models. One should think of these models as representing models for portions of the random field, in much the same manner as (6.4) - (6.5) provides a model for the field lines $Z(\cdot)$. For example, for the geometry of Fig. 6.1, the global model might represent a fine grid of lines, while the local

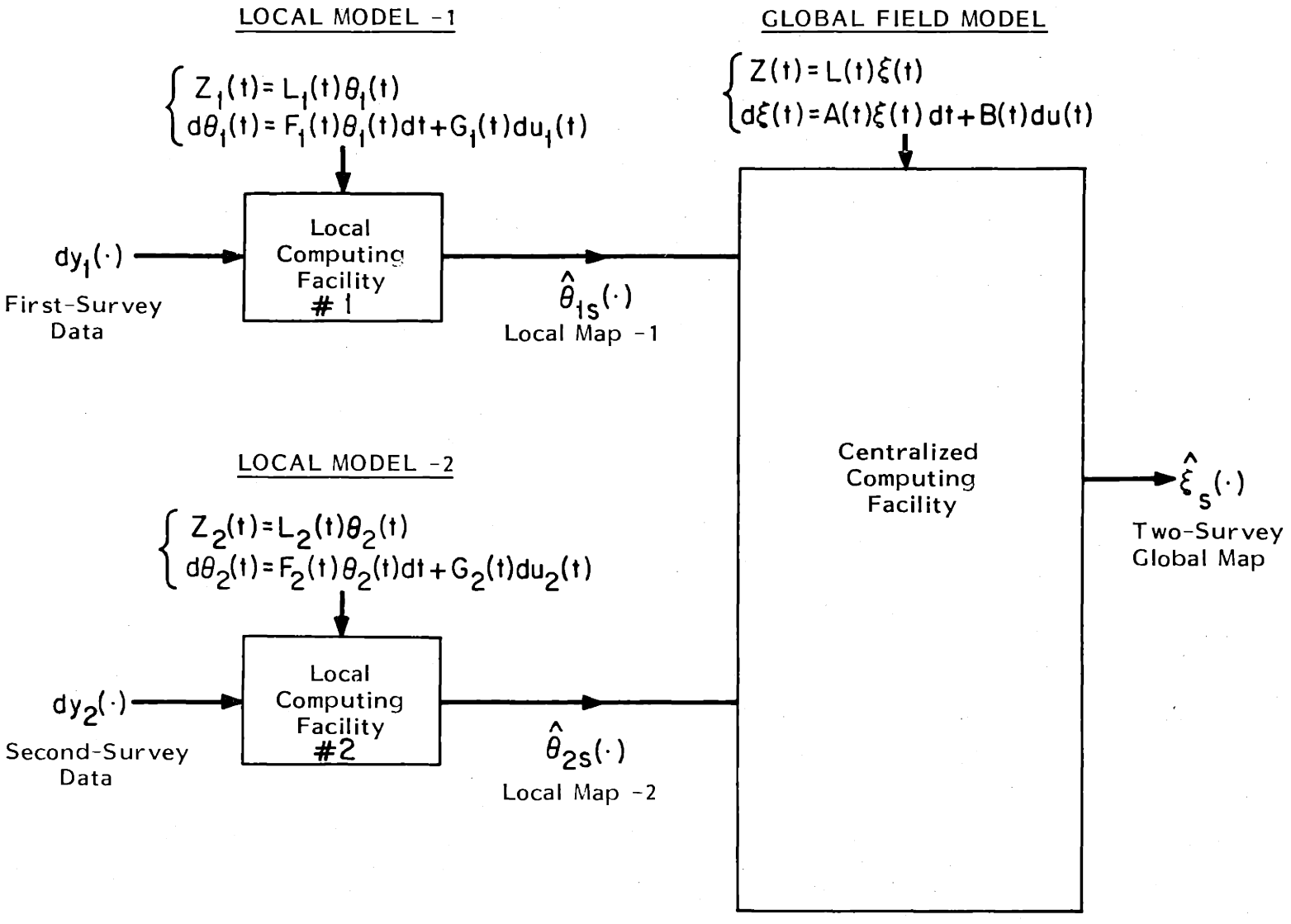

Fig. 6.4 The Map-Centralization Problem for Forming an N-Track Map

model for the first survey might correspond to a coarse grid, that includes $Z_1(\cdot)$, and the second local model might represent a fine grid of only the part of the field covered by the second survey tracks, and hence including $Z_2(\cdot)$. In the next section we solve the map-centralization problem for a case when both the global and local models are exact representations for the field variables $Z(\cdot)$ and $Z_i(\cdot)$, respectively, and the local models correspond to lower dimensional realizations, of the restriction of the global model to the local field variables. In the case for which the local models do not represent exact realizations of the local field variables, and hence are not consistent with the global model, the map-centralization problem reduces to an inversion problem of determining whether we can extract the necessary information from $\hat{\theta}_{1s}(\cdot)$ and $\hat{\theta}_{2s}(\cdot)$ in order to form $\hat{\xi}_s(\cdot)$. We comment briefly on this case in the conclusion of this chapter.

6.2 Map-Centralization when the Local Model is Embedded in the Globally Determined Model for $Z_i(\cdot)$

We now identify a set of relations between global and local models, which allows a solution to the map-centralization problem. We first note that from relations (6.5) - (6.6), and defining $S_i(t)$ as

$$S_i(t) \triangleq E_i L(t) \quad , \tag{6.18}$$

we obtain the following globally determined model for the local field variables $Z_i(\cdot)$:

$$Z_i(t) = S_i(t)\xi(t) \quad , \tag{6.19}$$

where the global state process, $\xi(\cdot)$, is generated by relation (6.4). We let $\pi(\cdot)$ and $\pi_i(\cdot)$ denote the state covariance matrices associated with the global and local models, respectively. In addition, we let q and q_i denote the dimension of the global and local state processes and p and p_i denote the dimensions of the input noises, $du(\cdot)$ and $du_i(\cdot)$, associated with the global and local models, respectively. Finally, we define the equivalent global and local input noise covariance matrices, $Q(t)$ and $Q_i(t)$, by

$$Q(t) \triangleq B(t)B'(t) \quad , \tag{6.20}$$

and $$Q_i(t) \triangleq G_i(t)G_i'(t) \quad . \tag{6.21}$$

We now impose the condition that the local model for $Z_i(\cdot)$ of (6.15) - (6.16) be embedded in the globally determined model for $Z_i(\cdot)$ specified by relations (6.4) and (6.19), in the following sense: we assume that there exists a $q_i \times q$ transformation $T_{i1}(t)$, so that

$$\theta_i(t) = T_{i1}(t)\xi(t) \quad . \tag{6.22}$$

Thus, equations (6.4), (6.15), and (6.22) define an exact model for the i-th survey field variables, $Z_i(\cdot)$, using the global state process.

Relation (6.22) implies that $\theta_i(\cdot)$ and $T_{i1}(\cdot)\xi(\cdot)$ have the same covariance matrices, and hence

$$T_{i1}(0)\pi(0)T_{i1}'(0) = \pi_i(0) \quad , \tag{6.23}$$

and $$T_{i1}(t)Q(t)T_{i1}'(t) = Q_i(t) \quad . \tag{6.24}$$

Another consequence of our assumption is that we must be able to construct a $q \times q$ nonsingular, differentiable transformation

$$T_i(t) \triangleq \begin{pmatrix} T_{i1}(t) \\ \hline\hline T_{i2}(t) \end{pmatrix} \quad , \tag{6.25}$$

so that the transformed process

$$\zeta_i(t) \triangleq \begin{pmatrix} \theta_i(t) \\ \hline\hline \rho_i(t) \end{pmatrix} = T_i(t)\xi(t) \quad , \tag{6.26}$$

has a state representation matching the one of relations (6.19), (6.4). We obtain

$$d\zeta_i(t) = \left(\begin{array}{c|c} F_i(t) & 0 \\ \hline\hline W_i(t) & O_i(t) \end{array}\right) \zeta_i(t)dt + T_i(t)B(t)du(t), \tag{6.27}$$

with $$Z_i(t) = \left(L_i(t) \;\vdots\; 0\right) \zeta_i(t) \quad , \tag{6.28}$$

where the dynamics of $\theta_i(\cdot)$ are decoupled from that of $\rho_i(\cdot)$. Finally, we note that in Appendix 6A we interpret further the consequences of (6.23) - (6.24) and (6.27) - (6.28), for the case of stationary local and global models, on the modelling of the

joint correlation structure of the $Z_i(\cdot)$'s in the spectral domain.

We next outline how we will use the above assumptions to solve the map-centralization problem, i.e., to express $\hat{\xi}_s(\cdot)$ as a linear functional of $\hat{\theta}_{1s}(\cdot)$ and $\hat{\theta}_{2s}(\cdot)$. Our approach will be to show how we may compute $\hat{\xi}_{is}(\cdot)$, the global state smoothed estimates based on the local i-th survey data, as a linear functional of $\hat{\theta}_{is}(\cdot)$, and then use centralized map-combining results to form $\hat{\xi}_s(\cdot)$ in terms of $\hat{\xi}_{1s}(\cdot)$ and $\hat{\xi}_{2s}(\cdot)$. The ability to express $\hat{\xi}_{is}(\cdot)$ in terms of $\hat{\theta}_{is}(\cdot)$ stems from the fact that both global and local processors model the measurement of the local field variables $Z_i(\cdot)$ as in (6.8), and hence through relations (6.26) - (6.28) we can identify the smoothed, transformed global state estimates $\hat{\zeta}_{is}(t)$, defined by

$$\hat{\zeta}_{is}(t) = E[\zeta_i(t)|Y_i] \quad , \tag{6.29}$$

as

$$\hat{\zeta}_{is}(t) = \begin{pmatrix} \hat{\theta}_{is}(t) \\ \text{------} \\ \hat{\rho}_{is}(t) \end{pmatrix} \quad , \tag{6.30}$$

where

$$\hat{\rho}_{is}(t) = E[\rho_i(t)|Y_i] \quad . \tag{6.31}$$

In Fig. 6.5 we diagram the generation of the transformed global state estimates. From the definition (6.26), we may express $\hat{\xi}_{is}(t)$ as

$$\hat{\xi}_{is}(t) = T_i^{-1}(t)\hat{\zeta}_{is}(t) \quad , \tag{6.32}$$

and hence to express $\hat{\xi}_{is}(\cdot)$ as a linear functional of $\hat{\theta}_{is}(\cdot)$ we show in what follows how to compute $\hat{\rho}_{is}(\cdot)$ in terms of $\hat{\theta}_{is}(\cdot)$. The processing embodied in our solution to the map-centralization problem is pictured in Fig. 6.6, where we use the notation $\Xi_i(\hat{\theta}_{is}(\cdot))$ to denote the operation of forming $\hat{\rho}_{is}(\cdot)$ from $\hat{\theta}_{is}(\cdot)$. Again, in what follows we will display inside boxes: (1) the relations that describe our algorithm for calculating $\hat{\rho}_{is}(\cdot)$ from $\hat{\theta}_{is}(\cdot)$; (2) the final equations for the formation of $\hat{\zeta}_{is}(\cdot)$; and (3) the solution of the map-centralization problem via centralized map-combining results.

We now show how the structure of the $\zeta_i(\cdot)$ dynamics allows us to compute $\hat{\rho}_{is}(\cdot)$ as a linear functional of $\hat{\theta}_{is}(\cdot)$. If we define the two input-noise processes, $dw_{i1}(\cdot)$ and $dw_{i2}(\cdot)$, by

$$dw_{i1}(t) = T_{i1}(t)B(t)du(t) \quad , \tag{6.33}$$

and

$$dw_{i2}(t) = T_{i2}(t)B(t)du(t) \quad , \tag{6.34}$$

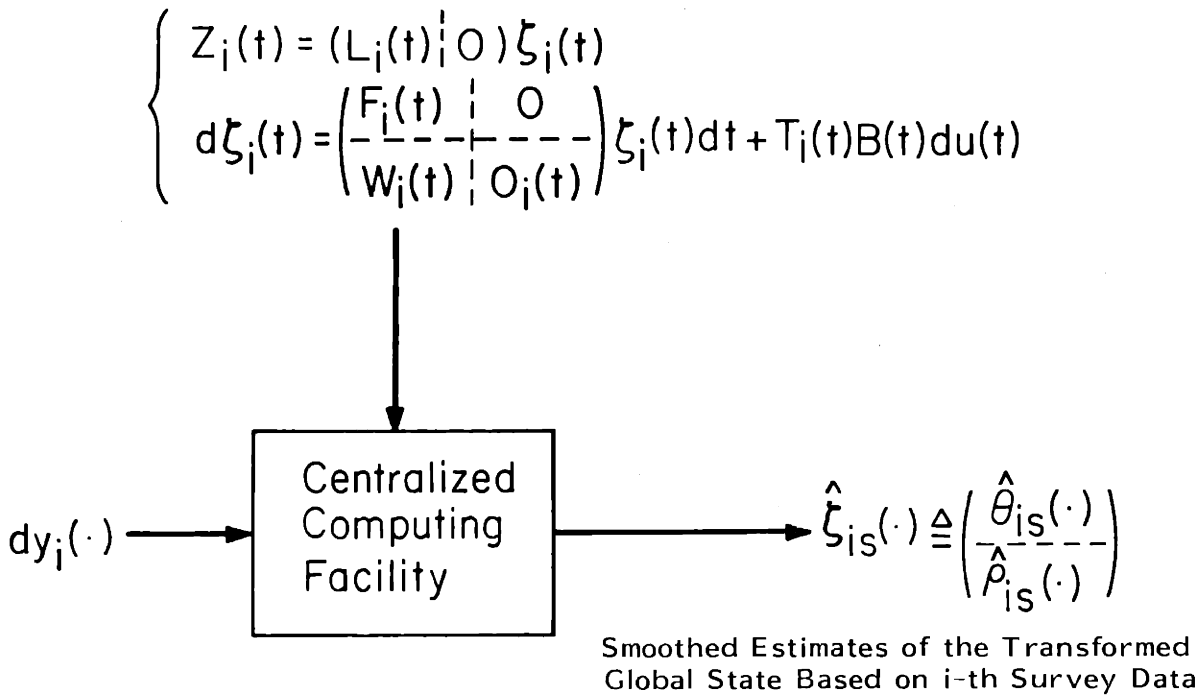

Fig. 6.5 Representation of the Generation of Smoothed, Transformed Global State Estimates based on Local Data

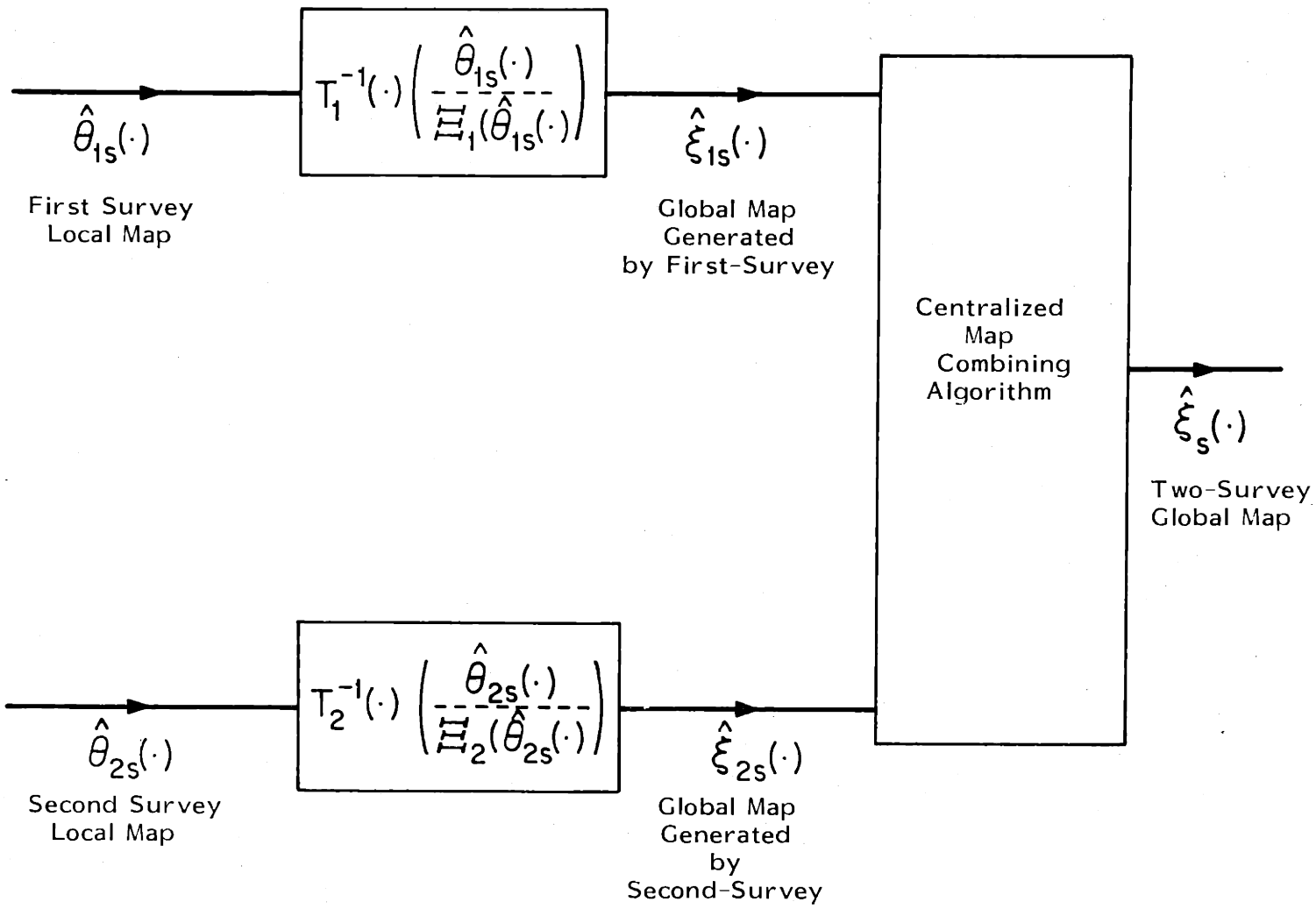

Fig. 6.6 Diagram of Processing Required by the Solution of the Map-Centralization Problem

we may express the dynamics for $\rho_i(\cdot)$ and $\theta_i(\cdot)$ as

$$d\theta_i(t) = F_i(t)\theta_i(t)dt + dw_{i1}(t) \quad , \tag{6.35}$$

and $$d\rho_i(t) = W_i(t)\theta_i(t)dt + O_i(t)\rho_i(t)dt + dw_{i2}(t) \quad , \tag{6.36}$$

(see equation (6.27)). Defining the σ-field, U_{it}^1, by

$$U_{it}^1 \triangleq \sigma\{dw_{i1}(\tau) \quad 0 \le \tau \le t\} \quad , \tag{6.37}$$

we now decompose $dw_{i2}(t)$ with respect to U_{it}^1 as

$$dw_{i2}(t) = E[dw_{i2}(t) | U_{it}^1] + d\tilde{w}_{i2}(t) \quad . \tag{6.38}$$

This decomposition will facilitate the derivation of an equation for the evolution of $\hat{\rho}_{is}(\cdot)$ from relation (6.36). From relations (6.33), (6.34), and the orthogonality of $du(t_1)$ and $du(t_2)$, for $t_1 \neq t_2$, there must exist a matrix, $K_i(t)$, such that

$$E[dw_{i2}(t) | U_{it}^1] = K_i(t)dw_{i1}(t) \quad . \tag{6.39}$$

By imposing the orthogonality condition

$$E\left[(dw_{i2}(t) - K_i(t)dw_{i1}(t))\ dw_{i1}'(\tau)\right] = 0, \text{ for } 0 \le \tau \le t, \tag{6.40}$$

and using relation (6.24), we find that $K_i(t)$ must satisfy the following equation:

$$K_i(t)Q_i(t) = T_{i2}(t)Q(t)T_{i1}'(t) \quad . \tag{6.41}$$

Since any $K_i(t)$ satisfying (6.41) will result in a statistically equivalent value for the conditional mean (6.39), by letting # denote the Moore-Penrose pseudoinverse, we may define $K_i(t)$ as

$$K_i(t) \triangleq [T_{i2}(t)Q(t)T_{i1}'(t)]Q_i^{\#}(t) \quad . \tag{6.42}$$

Then by substituing the relation (6.39) into (6.38), and using relation (6.38) in relation (6.36), we obtain the following equation for the evolution of $\rho_i(\cdot)$:

$$d\rho_i(t) = W_i(t)\theta_i(t)dt + O_i(t)\rho_i(t)dt + K_i(t)dw_{i1}(t) + d\tilde{w}_{i2}(t) \quad . \tag{6.43}$$

Now, taking $E[\cdot|Y_i]$ on both sides of relations (6.43) and (6.35), and using the fact that

$$E[d\tilde{w}_{i2}(t)|Y_i] = 0 \quad , \tag{6.44}$$

since $d\tilde{w}_{i2}(t)$ is orthogonal to $dw_{i1}(\tau)$, $0 \le \tau \le T$, and the observation noise $dv_i(\cdot)$, we obtain the following two relations:

$$d\hat{\theta}_{is}(t) = F_i(t)\hat{\theta}_{is}(t)dt + E[dw_{i1}(t)|Y_i] \ , \tag{6.45}$$

and

$$d\hat{\rho}_{is}(t) = W_i(t)\hat{\theta}_{is}(t)dt + O_i(t)\hat{\rho}_{is}(t)dt + K_i(t)\Big(E[dw_{i1}(t)|Y_i]\Big) . \tag{6.46}$$

Employing relation (6.45) to express $E[dw_{i1}(t)|Y_i]$, and by substitution into relation (6.46), we find the following equation for the evolution of $\hat{\rho}_{is}(\cdot)$:

$$\begin{aligned} d\hat{\rho}_{is}(t) = {} & W_i(t)\hat{\theta}_{is}(t)dt + O_i(t)\hat{\rho}_{is}(t)dt \\ & + K_i(t)[d\hat{\theta}_{is}(t) - F_i(t)\hat{\theta}_{is}(t)dt] \ . \end{aligned} \tag{6.47}$$

Relation (6.47) now yields the desired relations for computing $\hat{\rho}_{is}(\cdot)$ as a linear functional of $\hat{\theta}_{is}(\cdot)$. Let us define $\eta_i(t)$ as

$$\eta_i(t) \triangleq \hat{o}_{is}(t) - K_i(t)\hat{\theta}_{is}(t) \ . \tag{6.48}$$

Then, by employing relations (6.47) - (6.48), we can show that $\eta_i(\cdot)$ evolves according to the equation

$$d\eta_i(t) = \left(W_i(t) + O_i(t)K_i(t) - K_i(t)F_i(t) - \dot{K}_i(t)\right)\hat{\theta}_{is}(t)dt + O_i(t)\eta_i(t)dt \quad . \tag{6.49}$$

Hence, by expressing $\hat{\rho}_{is}(t)$ from relation (6.48) as

$$\hat{\rho}_{is}(t) = K_i(t)\hat{\theta}_{is}(t) + \eta_i(t) \quad , \tag{6.50}$$

and by using equation (6.49) to compute $\eta_i(\cdot)$, we obtain the desired algorithm for computing $\hat{\rho}_{is}(\cdot)$. To complete the algorithm, we need the initial condition, $\eta_i(0)$. Therefore, from definition (6.48), we need to understand how to compute $\hat{\rho}_{is}(0)$.

We now demonstrate how we may determine $\hat{\rho}_{is}(0)$. Let us assume that the transformed global state, $\zeta_i(t)$, has an associated state covariance matrix $\Sigma_i(t)$ that may be represented in the partitioned form

$$\Sigma_i(t) \triangleq \left(\begin{array}{c|c} \pi_i(t) & \Sigma_{i12}(t) \\ \hline \Sigma'_{i12}(t) & \Sigma_{i2}(t) \end{array}\right) \quad , \tag{6.51}$$

where $\pi_i(\cdot)$ and $\Sigma_{i2}(\cdot)$ denote covariance matrices associated with $\theta_i(\cdot)$ and $\rho_i(\cdot)$, respectively. We show first that we may represent $\rho_i(0)$ as

$$\rho_i(0) = \tilde{\rho}_i(0) + \Sigma'_{i12}(0)\pi_i^{-1}(0)\theta_i(0) \quad , \tag{6.52}$$

where $\tilde{\rho}_i(0)$ is orthogonal to $\theta_i(\cdot)$. To prove (6.52) we can verify that

$$E\left[\left(\rho_i(0) - \Sigma'_{i12}(0)\pi_i^{-1}(0)\theta_i(0)\right)\theta'_i(\tau)\right] = 0 \quad , \tag{6.53}$$

for $\tau \geq 0$, by using the following representation for $\theta_i(\tau)$:

$$\theta_i(\tau) = \Phi_{F_i}(\tau,0)\theta_i(0) + \int_{\tau'=0}^{\tau} \Phi_{F_i}(\tau,\tau')dw_{i1}(\tau') \quad , \tag{6.54}$$

where $\Phi_{F_i}(\cdot,\cdot)$ denotes the transition matrix associated with $F_i(\cdot)$. Now, since $\tilde{\rho}_i(0)$ is orthogonal to both $\theta_i(\cdot)$ and $dv_i(\cdot)$,

$$E[\tilde{\rho}_i(0)|Y_i] = 0 \quad , \tag{6.55}$$

and by taking $E[\cdot|Y_i]$ of both sides of relation (6.52), we obtain the following relation for $\hat{\rho}_{is}(0)$:

$$\hat{\rho}_{is}(0) = \Sigma'_{i12}(0)\pi_i^{-1}(0)\hat{\theta}_{is}(0) \quad . \tag{6.56}$$

Hence, from relation (6.48), the initial condition for $\eta_i(\cdot)$ is specified by

$$\eta_i(0) = \left[\Sigma'_{i12}(0)\pi_i^{-1}(0) - K_i(0)\right]\hat{\theta}_{is}(0) \ . \tag{6.57}$$

Through relations (6.49) - (6.50) and (6.57) we have shown how $\hat{\rho}_{is}(\cdot)$ may be computed as a linear functional of $\hat{\theta}_{is}(\cdot)$. Hence, by noting relations (6.30) - (6.32) and (6.50), the locally determined global state estimate, $\hat{\xi}_{is}(t)$, may be expressed as

$$\hat{\xi}_{is}(t) = T_i^{-1}(t)\left(\frac{\hat{\theta}_{is}(t)}{K_i(t)\hat{\theta}_{is}(t) + \eta_i(t)}\right) , \tag{6.58}$$

where $\eta_i(\cdot)$ is computed from the differential equation (6.49) with initial condition (6.57).

We finally use the centralized map-combining algorithm of Chapter 4 in order to state the solution of the map-centralization problem. Noting that (6.11) specifies the first and second survey measurements of the underlying global state process $\xi(\cdot)$, we let Γ_f and Γ_r denote the two-pass, forward and reverse, global state filtering dynamics matrices. We similarly let P_f and P_r denote the two-pass forward and reverse, global state filtering error covariance matrices. Then, by applying the results of Section 4.3, and suppressing the time

dependence of the $H_i(\cdot)$'s and $R_i(\cdot)$'s, we may express the two-pass, smoothed global state estimate as

$$\boxed{\hat{\xi}_s(t) = \hat{\xi}_{1s}(t) + \hat{\xi}_{2s}(t) + P_s\left\{P_f^{-1}\theta_f(t) + P_r^{-1}\theta_r(t)\right\},} \tag{6.59}$$

where

$$\boxed{d\theta_f(t) = \Gamma_f\theta_f(t)dt - P_fH_1'R_1^{-1}H_1\hat{\xi}_{2s}(t)dt - P_fH_2'R_2^{-1}H_2\hat{\xi}_{1s}(t)dt\ ,} \tag{6.60}$$

with $$\boxed{\theta_f(0) = 0\ ,} \tag{6.61}$$

and

$$\boxed{-d\theta_r(t) = \Gamma_r\theta_r(t)dt - P_rH_1'R_1^{-1}H_1\hat{\xi}_{2s}(t)dt - P_rH_2'R_2^{-1}H_2\hat{\xi}_{1s}(t)dt\ ,} \tag{6.62}$$

with $$\boxed{\theta_r(T) = 0\ ,} \tag{6.63}$$

and $$\boxed{P_s^{-1} = P_f^{-1} + P_r^{-1} - \pi^{-1}\ .} \tag{6.64}$$

Hence, through relations (6.49), (6.57), (6.58), and (6.59) - (6.64) we have specified the solution of the map-centralization problem.

In Appendix 6B we present a second approach to solving the map-centralization problem, that is similar to the approach of Appendix 4C for solving the centralized map-updating problem. The starting point for the derivation of the map-centralization algorithm of Appendix 6B is the Wall two-filter form of the global state two-pass smoothed estimate:

$$\hat{\xi}_s(t) = P_s\left\{P_f^{-1}\hat{\xi}_f(t) + P_r^{-1}\hat{\xi}_r(t)\right\} \quad . \tag{6.65}$$

We employ relations (6.23) - (6.24) and (6.27) - (6.28), and identities satisfied by filtered and smoothed estimates to express $\hat{\xi}_f(t)$ as

$$\hat{\xi}_f(t) = \Xi_f(\hat{\theta}_{if}(t), \hat{\theta}_{is}(\tau) \quad 0 \leq \tau \leq t, \; i = 1,2) \; , \tag{6.66}$$

where the notation $\Xi_f(\cdot)$ denotes some linear functional, and $\hat{\theta}_{if}(t)$ denotes the forward filtered estimate for $\theta_i(\cdot)$ based on the i-th survey data. We then similarly obtain a representation for $\hat{\xi}_r(t)$ as

$$\hat{\xi}_r(t) = \Xi_r(\hat{\theta}_{ir}(t), \hat{\theta}_{is}(\tau) \quad t \leq \tau \leq T, \; i = 1,2) \; , \tag{6.67}$$

where $\Xi_r(\cdot)$ denotes a linear functional, and $\hat{\theta}_{ir}(t)$ denotes the reverse filtered estimate for $\theta_i(t)$ based on the i-th

survey data. By substituting the representations for $\hat{\xi}_f(t)$ and $\hat{\xi}_r(t)$ of relations (6.66) and (6.67) into equation (6.65), with a little manipulation we obtain an expression for $\hat{\xi}_s(t)$ as a linear functional of the local maps, $\hat{\theta}_{is}(\tau)$, $0 \leq \tau \leq T$, $i = 1,2$. The map-centralization algorithm of Appendix 6B requires less on-line computation than that in the text, in the sense that we do not need to first form the locally determined global maps, i.e., the $\hat{\xi}_{is}(\cdot)$'s, in order to compute the two-pass global map, $\hat{\xi}_s(\cdot)$.

6.3 Conclusion

In Section 6.2, we solved the map-centralization problem when the local model for the i-th survey field variables is embedded in the globally determined local model. We presented our first approach to the solution of this problem, since on a conceptual level, the role played by the embedding relations (6.23) - (6.24) and (6.27) - (6.28), in obtaining a solution, is clearer than in the second algebraic approach of Appendix 6B. The fact that the measurements of the local field variables $Z_i(\cdot)$ are modelled the same at a local and global level, and the fact that the local model for $Z_i(\cdot)$ is contained in the restriction of the global model to $Z_i(\cdot)$, allows us to identify the local map $\hat{\theta}_{is}(\cdot)$ as a subvector of the transformed global map, $\hat{\zeta}_{is}(\cdot)$, and to ultimately compute $\hat{\xi}_{is}(\cdot)$ as a linear functional of $\hat{\theta}_{is}(\cdot)$. We then used centralized map-combining results to form the two-survey global map, $\hat{\xi}_s(\cdot)$.

To investigate the solution of the map-centralization problem in the case when local and global modelling are inconsistent, i.e., local models may only be approximate, we can use an algebraic approach analogous to that in Appendix 6B, i.e., we look for algebraic conditions under which we can obtain representations for $\hat{\xi}_f(t)$ and $\hat{\xi}_r(t)$ of the form in relations (6.66) - (6.67), such that when these representations are substituted into equation (6.65), we ultimately express $\hat{\xi}_s(t)$ as

a linear functional of the local maps. Such an approach to the general map-centralization problem is followed in [50].

Finally, we note that the results presented in this chapter have a wide range of applications outside of mapping problems for random fields, wherever decentralized estimation structures arise. By this we mean situations such as in multiple target tracking, where we may have lower level processors with restricted sets of information, that communicate their estimates to some centralized, upper level processor for the purpose of combining the lower level estimates.

Appendix 6A

Spectral Domain Interpretation of the Embedding Relations of the Local and Global Models in the Stationary Case

We now assume that the global model for $Z(\cdot)$ and the local models for the $Z_i(\cdot)$ are time-invariant, and interpret the consequences of relations (6.27) - (6.28) and (6.24) on the modelling of the joint correlation structure of the $Z_i(\cdot)$'s in the spectral domain. The case of stationary models for $Z(\cdot)$ and the $Z_i(\cdot)$'s could, as an example, correspond to the case of a parallel track measurement geometry through a stationary random field. We define the transfer function associated with the local model for $Z_i(\cdot)$ by

$$H_i(s) \stackrel{\Delta}{=} L_i(sI - F_i)^{-1}G_i \quad . \tag{A.1}$$

We next note that the relation (6.24), together with the definitions of Q and Q_i, imply the existence of an orthogonal matrix Ψ_i, such that

$$T_{i1}B = (B_i \,\vdots\, 0)\Psi_i \quad . \tag{A.2}$$

Hence, letting $H_{gi}(s)$ denote the transfer function associated with the globally determined model for Z_i of (6.27) - (6.28), and employing equations (A.1) - (A.2) we find that

$$H_{gi}(s) = (H_i(s) \mid 0)\Psi_i \quad . \tag{A.3}$$

Assuming that $H_i(s)$ is a minimal column order spectral factor of $S_{Z_i}(s)$, i.e., a transfer function requiring a minimum number of independent white noise inputs to realize the power spectral density, $S_{Z_i}(s)$, then since in general $p \geq p_i$, $H_{gi}(s)$ represents a nonminimal spectral factor. The restriction inherent in relation (A.3) is seen by noting that in general, a nonminimal spectral factor $H_{gi}(s)$ is related to a minimal spectral factor $H_i(s)$ by

$$H_{gi}(s) = (H_i(s) \mid 0)\psi_i(s) \quad , \tag{A.4}$$

where $\psi_i(s)$ is a para-unitary rational matrix satisfying

$$\psi_i(s)\psi_i'(-s) = I \quad . \tag{A.5}$$

In addition, we note that if we assume that the global model for $Z(\cdot)$, and the local model for $Z_i(\cdot)$, are both controllable and observable, then when $q_i < q$, the relation (A.3)

implies the existence of a transformation T_i such that relations (6.27) - (6.28) and (6.24) hold. This follows since $q_i < q$ and relation (A.3) imply that relations (6.19) and (6.4) do not form an irreducible realization for $H_{gi}(s)$. Hence, since we assumed that the global model was controllable, we must conclude that the model for $Z_i(\cdot)$ described by relations (6.19),(6.4) is not observable and therefore a T_i effecting a reduction of the form (6.27) - (6.28) must exist, with (6.24) holding.

Finally, we observe the consequences of relation (A.3) on the modelling of the joint correlation structure between $Z_1(\cdot)$ and $Z_2(\cdot)$. If we let the first p_1 rows and p_2 columns of the $p \times p$ matrix $[\Psi_1 \Psi_2']$ be denoted by C_{12}, then relation (A.3) implies that the cross power spectral density between $Z_1(\cdot)$ and $Z_2(\cdot)$ can be represented as

$$S_{Z_1 Z_2}(s) = H_1(s) C_{12} H_2'(-s) \quad . \tag{A.6}$$

Appendix 6B

An Algebraic Approach to Map-Centralization when the Local Field Models are Embedded in the Global Model

In this Appendix we derive an alternative solution to the map-centralization problem. The route that we follow is similar to the algebraic solution to the centralized map-updating problem presented in Appendix 4C. We know that the global two-pass smoothed estimate $\hat{\xi}_s(t)$ can be expressed as

$$\hat{\xi}_s(t) = P_s\left\{P_f^{-1}\hat{\xi}_f(t) + P_r^{-1}\hat{\xi}_r(t)\right\} \quad , \tag{B.1}$$

where $$P_s^{-1} = P_f^{-1} + P_r^{-1} - \pi^{-1} \quad . \tag{B.2}$$

Then, by following the same steps employed in the solution of the centralized map-updating problem in Appendix 4C, and by exploiting the properties of $T_i(\cdot)$ embodied in relations (6.23) - (6.24) and (6.27) - (6.28), we can express (B.1) as a function of quantities depending only on the local maps, $\hat{\theta}_{is}(\cdot)$, $i = 1,2$. We proceed to show first how $\hat{\xi}_f(t)$ may be represented as a linear functional of the local filtered and

smoothed estimates, $\hat{\theta}_{if}(\cdot),\hat{\theta}_{is}(\cdot)$. Obtaining a similar representation for $\hat{\xi}_r(t)$, and the substitution of both representations into (B.1), yields the desired map-centralization procedure. For the sake of notational simplicity, we will suppress the time arguments for system and covariance matrices, in what follows.

First, we note from relations (6.4), (6.8), and (6.18), that if we define the two-pass forward filter dynamics matrix Γ_f by

$$\Gamma_f \triangleq A - P_f \sum_{i=1}^{2} S_i' C_i' R_i^{-1} C_i S_i \quad , \tag{B.3}$$

then $\hat{\xi}_f(\cdot)$ is generated by the standard Kalman filtering equations

$$d\hat{\xi}_f(t) = \Gamma_f \hat{\xi}_f(t)dt + P_f \sum_{i=1}^{2} S_i' C_i' R_i^{-1} dy_i(t) \quad , \tag{B.4}$$

with $$\hat{\xi}_f(0) = 0 \quad . \tag{B.5}$$

We now use the fact that relation (6.28) implies that

$$S_i T_i^{-1} = (L_i \mid 0) \quad , \tag{B.6}$$

or alternatively that

$$S_i' = T_i' \begin{pmatrix} L_i' \\ \hline 0 \end{pmatrix} \quad . \tag{B.7}$$

By substituting relation (B.7) into (B.4), the two-pass filtering equation may be rewritten as

$$d\hat{\xi}_f(t) = \Gamma_f \hat{\xi}_f(t)dt + P_f \sum_{i=1}^{2} T_i' \begin{pmatrix} \left[L_i' C_i' R_i^{-1} dy_i(t)\right] \\ \hline 0 \end{pmatrix} \quad . \tag{B.8}$$

Now, arguing as in Appendix 4C, and letting P_{if} denote the error covariance associated with the i-th survey, local forward filtered estimate $\hat{\theta}_{if}(\cdot)$, of $\theta_i(\cdot)$, we can express the term in brackets in relation (B.8) as

$$\left[L_i' C_i' R_i^{-1} dy_i(t)\right] = P_{if}^{-1}\left\{d\hat{\theta}_{if}(t) - (F_i - P_{if}L_i'C_i'R_i^{-1}C_iL_i)\hat{\theta}_{if}(t)dt\right\} \quad . \tag{B.9}$$

We now recall that in Appendix 4C we employed a particular block diagram equivalence expressed in Fig. C.2 to eliminate derivative terms appearing as inputs. In our present case we would like to eliminate the $d\hat{\theta}_{if}(t)$ terms that appear by substituting relation (B.9) into the two-pass filtering equation (B.8). We can achieve the same result as for the block diagram

manipulation suggested in Fig. C.2 by defining the new quantity $r_f(t)$ as

$$r_f(t) \triangleq \hat{\xi}_f(t) - \sum_{i=1}^{2} P_f T_i' \begin{pmatrix} P_{if}^{-1}\hat{\theta}_{if}(t) \\ \hline 0 \end{pmatrix} \tag{B.10}$$

By employing relations (C.8) - (C.10) and the equations for the evolution of $P_{if}(\cdot)$, we can derive the following equation satisfied by $r_f(\cdot)$:

$$\begin{aligned} dr_f(t) = {} & \Gamma_f r_f(t)dt \\ & + P_f \sum_{i=1}^{2} \left\{ T_i' \begin{pmatrix} F_i' P_{if}^{-1}\hat{\theta}_{if}(t) \\ \hline 0 \end{pmatrix} - A' T_i' \begin{pmatrix} P_{if}^{-1}\hat{\theta}_{if}(t) \\ \hline 0 \end{pmatrix} - \dot{T}_i' \begin{pmatrix} P_{if}^{-1}\hat{\theta}_{if}(t) \\ \hline 0 \end{pmatrix} \right\} dt \\ & + \sum_{i=1}^{2} \left\{ - Q T_i' \begin{pmatrix} P_{if}^{-1}\hat{\theta}_{if}(t) \\ \hline 0 \end{pmatrix} + P_f T_i' \begin{pmatrix} P_{if}^{-1} Q_i P_{if}^{-1}\hat{\theta}_{if}(t) \\ \hline 0 \end{pmatrix} \right\} dt, \end{aligned} \tag{B.11}$$

with $$r_f(0) = 0 \quad . \tag{B.12}$$

We now exploit the consequences of relations (6.24), (6.27), and (6.38) - (6.42) to simplify relation (B.11). The relation (6.27) implies that

$$T_i A T_i^{-1} + \dot{T}_i T_i^{-1} = \left(\begin{array}{c|c} F_i & 0 \\ \hline W_i & O_i \end{array}\right) , \tag{B.13}$$

or equivalently that

$$A' T_i' = T_i' \left(\begin{array}{c|c} F_i' & W_i' \\ \hline 0 & O_i' \end{array}\right) - \dot{T}_i' . \tag{B.14}$$

Employing relation (B.14) eliminates the first summation on the right-hand side of relation (B.11). In addition, relations (6.24) and (6.41) imply that

$$T_i Q T_i' = \left(\begin{array}{c|c} Q_i & Q_i K_i' \\ \hline K_i Q_i & T_{i2} Q T_{i2}' \end{array}\right) , \tag{B.15}$$

or equivalently

$$Q T_i' = T_i^{-1} \left(\begin{array}{c|c} Q_i & Q_i K_i' \\ \hline K_i Q_i & T_{i2} Q T_{i2}' \end{array}\right) , \tag{B.16}$$

where K_i is defined by relation (6.42). Using relation (B.16) in the second summation of relation (B.11) we obtain the following equation satisfied by $r_f(\cdot)$:

$$dr_f(t) = \Gamma_f(t) r_f(t) dt + \sum_{i=1}^{2} \Omega_{fi} [Q_i P_{if}^{-1} \hat{\theta}_{if}(t) dt] \quad , \tag{B.17}$$

where

$$\Omega_{fi} \triangleq P_f T_i' \begin{pmatrix} P_{if}^{-1} \\ \hline 0 \end{pmatrix} - T_i^{-1} \begin{pmatrix} I \\ \hline K_i \end{pmatrix} \quad . \tag{B.18}$$

At this point, we make use of an identity in Appendix 4C to express the term inside brackets in the summation of relation (B.17) as

$$[Q_i P_{if}^{-1} \hat{\theta}_{if}(t) dt] = \left[P_{is} \left(F_i' - \pi_i^{-1} Q_i + P_{ir}^{-1} Q_i \right) P_{is}^{-1} + \dot{P}_{is} P_{is}^{-1} \right] \hat{\theta}_{is}(t) dt$$

$$- d\hat{\theta}_{is}(t), \tag{B.19}$$

where P_{is} and P_{ir} denote the local, i-th survey smoothing error covariance matrix and the local, i-th survey reverse filtering error covariance matrix associated with $\hat{\theta}_{is}(\cdot), \hat{\theta}_{ir}(\cdot)$, respectively, and π_i denotes the a-priori state covariance associated with $\theta_i(\cdot)$. We then substitute relation (B.19) into (B.17) and use the same technique as before to eliminate the derivative terms, $d\hat{\theta}_{is}(t)$, by defining the new quantity

$$\alpha_f(t) = r_f(t) + \sum_{i=1}^{2} \Omega_{fi} \hat{\theta}_{is}(t) \quad . \tag{B.20}$$

Employing relations (B.17) - (B.20), we obtain the following equation satisfied by $\alpha_f(\cdot)$:

$$\boxed{d\alpha_f(t) = \Gamma_f \alpha_f(t)dt + \sum_{i=1}^{2} \omega_{fi} \hat{\theta}_{is}(t)dt \quad ,} \tag{B.21}$$

where

$$\boxed{\omega_{fi} \triangleq -\Gamma_f \Omega_{fi} + \Omega_{fi}\left(P_{is}\left(-F_i' - \pi_i^{-1}Q_i + P_{ir}^{-1}Q_i\right)P_{is}^{-1} + \dot{P}_{is}P_{is}^{-1}\right) + \dot{\Omega}_{fi},} \tag{B.22}$$

and

$$\boxed{\alpha_f(0) = 0 \quad .} \tag{B.23}$$

By making use of equations for the evolution of P_f, P_{if}, P_{ir}, and P_{is} we can express ω_{fi} explicitly from relation (B.22) as

$$\begin{aligned}\omega_{fi} = {} & (P_f A' + Q)T_i'\begin{pmatrix} P_{if}^{-1} \\ \hline 0 \end{pmatrix} + \Gamma_f T_i^{-1}\begin{pmatrix} I \\ \hline K_i \end{pmatrix} \\ & + P_f T_i'\begin{pmatrix} -F_i' P_{if}^{-1} + L_i' C_i' R_i^{-1} C_i L_i \\ \hline 0 \end{pmatrix} \\ & - T_i^{-1}\begin{pmatrix} I \\ \hline K_i \end{pmatrix}\left(F_i + Q_i P_{if}^{-1}\right) \\ & + P_f \dot{T}_i'\begin{pmatrix} P_{if}^{-1} \\ \hline 0 \end{pmatrix} - T_i^{-1}\begin{pmatrix} I \\ \hline \dot{K}_i \end{pmatrix} + T_i^{-1}\dot{T}_i T_i^{-1}\begin{pmatrix} I \\ \hline K_i \end{pmatrix} \quad .\end{aligned} \tag{B.24}$$

Hence, by using the relations (B.10), (B.20), and (B.21) - (B.24), we can express the global state two-pass filtered estimate, $\hat{\xi}_f(t)$, as

$$\hat{\xi}_f(t) = \alpha_f(t) + \sum_{i=1}^{2} P_f T_i' \begin{pmatrix} P_{if}^{-1}\hat{\theta}_{if}(t) \\ \hline 0 \end{pmatrix} - \sum_{i=1}^{2} \Omega_{fi}\hat{\theta}_{is}(t) \ . \qquad \text{(B.25)}$$

Without going into the details here, we can follow the same procedure for the two-pass global state reverse filtered estimate, $\hat{\xi}_r(t)$. The result is that we may express $\hat{\xi}_r(t)$ as

$$\hat{\xi}_r(t) = \alpha_r(t) + \sum_{i=1}^{2} P_r T_i' \begin{pmatrix} P_{ir}^{-1}\hat{\theta}_{ir}(t) \\ \hline 0 \end{pmatrix} - \sum_{i=1}^{2} \Omega_{ri}\hat{\theta}_{is}(t) \ , \qquad \text{(B.26)}$$

where

$$\Omega_{ri} \triangleq \left(P_r\pi^{-1} - I\right)T_i^{-1}\begin{pmatrix} I \\ \hline K_i \end{pmatrix} + P_r T_i' \begin{pmatrix} P_{ir}^{-1} - \pi_i^{-1} \\ \hline 0 \end{pmatrix} \ . \qquad \text{(B.27)}$$

Letting

$$\Gamma_r \triangleq -A - Q\pi^{-1} - P_r \sum_{i=1}^{2} S_i' C_i' R_i^{-1} C_i S_i \ , \qquad \text{(B.28)}$$

we find that $\alpha_r(\cdot)$ satisfies the backward equation

$$\boxed{-d\alpha_r(t) = \Gamma_r \alpha_r(t)dt + \sum_{i=1}^{2} \omega_{ri}\hat{\theta}_{is}(t)dt \ ,} \qquad \text{(B.29)}$$

with $\boxed{\alpha_r(T) = 0 \quad ,}$ (B.30)

and $\boxed{\omega_{ri} \triangleq - \Gamma_r \Omega_{ri} + \Omega_{ri}\left(-F_i - Q_i(\pi_i^{-1} - P_{ir}^{-1})\right) - \dot{\Omega}_{ri} \ .}$ (B.31)

By employing equations for the evolution of the appropriate covariance matrices, and using relation (B.31), we may express ω_{ri} explicitly as

$$\boxed{\begin{aligned}
\omega_{ri} = {} & \left[(P_r\pi^{-1} - I)A - P_r \sum_{i=1}^{2} S_i' C_i' R_i^{-1} C_i S_i\right] T_i^{-1} \begin{pmatrix} I \\ \hline K_i \end{pmatrix} \\
& + \left[Q - P_r(A' + \pi^{-1}Q)\right] T_i' \begin{pmatrix} P_{ir}^{-1} - \pi_i^{-1} \\ \hline 0 \end{pmatrix} \\
& + P_r T_i' \begin{pmatrix} F_i'(P_{ir}^{-1} - \pi_i^{-1}) + L_i' C_i' R_i^{-1} C_i L_i \\ \hline 0 \end{pmatrix} \\
& + (P_r\pi^{-1} - I) T_i^{-1} \begin{pmatrix} I \\ \hline K_i \end{pmatrix} \left(-F_i + Q_i(P_{ir}^{-1} - \pi_i^{-1})\right) \\
& - (P_r\pi^{-1} - I) T_i^{-1} \begin{pmatrix} I \\ \hline \dot{K}_i \end{pmatrix} + (P_r\pi^{-1} - I) T_i^{-1} \dot{T}_i T_i^{-1} \begin{pmatrix} I \\ \hline K_i \end{pmatrix} \\
& - P_r \dot{T}_i' \begin{pmatrix} P_{ir}^{-1} - \pi_i^{-1} \\ \hline 0 \end{pmatrix} \ .
\end{aligned}}$$ (B.32)

Finally, by employing relations (B.25) and (B.26) in equation (B.1), for the global state two-pass smoothed estimate, we obtain the following solution to the map-centralization problem:

$$\hat{\xi}_s(t) = P_s\left\{P_f^{-1}\alpha_f(t) + P_r^{-1}\alpha_r(t)\right\} + \sum_{i=1}^{2} T_i^{-1}\begin{pmatrix} I \\ --- \\ K_i \end{pmatrix}\hat{\theta}_{is}(t). \tag{B.33}$$

Chapter 7

Spatial Examples of the Centralized Map-Updating, Map-Combining, and Map-Centralization Problems

7.1 Introduction

In Chapters 4 - 6 we posed and solved the centralized map-updating problem, the centralized map-combining problem, and a special case of the map-centralization problem in a setting where we identify maps with smoothed estimates of some state process generated by a finite dimensional linear model of the form in relation (2.1). In this chapter we illustrate how we can solve some specific spatial examples of these problems by employing the essentially one-dimensional framework of Chapters 4 - 6. In Section 7.2, we first present the solution to all three problems in a continuous space setting for the case of an M-parallel measurement track geometry through a stationary, two-dimensional, scalar random field with a separable correlation function. In Section 7.3, under the same field assumptions, we consider a discrete space example of the map-updating problem for the case where we have two non-parallel measurement tracks.

7.2 Centralized Map-Updating, Centralized Map-Combining, and Map-Centralization for a M-Parallel Measurement Track Geometry through a Stationary, Separable, Two-Dimensional Scalar Random Field

We assume that we have M sensors which follow the trajectories $r_i^*(t)$ defined by

$$r_i^*(t) \triangleq (t, r_y^i) \quad , \tag{7.1}$$

through a stationary, two-dimensional scalar random field, $f(\cdot,\cdot,\omega)$, with a correlation function $R(\tau_1,\tau_2)$ defined by

$$R(\tau_1,\tau_2) = \varphi(\tau_1)\psi(\tau_2) \quad , \tag{7.2}$$

where $\varphi(\cdot)$ and $\psi(\cdot)$ are assumed to be one-dimensional correlation functions realizable by some finite dimensional systems. Powell and Silverman [90] have assumed correlation models of this form to model scalar image intensity random fields. We will show from relations (7.1) - (7.2), following the approach in [90], that the aggregate M-track field vector Z(t) defined by

$$Z(t) \triangleq \begin{pmatrix} f(t,r_y^1) \\ \vdots \\ f(t,r_y^M) \end{pmatrix} \quad , \tag{7.3}$$

has a finite dimensional Markovian representation. We then formulate the centralized map-updating and map-combining problems, relying directly on the results of Chapter 4 for their solution.

From relations (7.2) - (7.3) we can show that the one-dimensional correlation function associated with the aggregate M-track field vector process, Z(t), assumes the form

$$R_Z(\tau) = \begin{pmatrix} \varphi(\tau) & & \\ & \ddots & \\ & & \varphi(\tau) \end{pmatrix} H \quad , \tag{7.4}$$

where H is a M x M matrix with the i,j-th element H_{ij} defined by

$$H_{ij} \triangleq \psi\left(r_y^i - r_y^j\right) \ . \tag{7.5}$$

Since H is a symmetric, positive semi-definite matrix, it may be represented as a product of lower and upper triangular factors as

$$H = \bar{L}\,\bar{L}' \quad , \tag{7.6}$$

where

$$\bar{L} \triangleq \begin{pmatrix} \bar{\ell}_{1,1} & & 0 \\ & \ddots & \\ \bar{\ell}_{M,1} & & \bar{\ell}_{M,M} \end{pmatrix}. \tag{7.7}$$

Hence, by employing relation (7.5), and by noting that $\bar{L}$ commutes with the diagonal matrix whose entries are specified by $\varphi_x(\tau)$, the correlation function $R_Z(\tau)$ for the aggregate M-track field vector process $Z(t)$ may be expressed as

$$R_Z(\tau) = \bar{L} \begin{pmatrix} \varphi(\tau) & & \\ & \ddots & \\ & & \varphi(\tau) \end{pmatrix} \bar{L}' \quad . \tag{7.8}$$

We next use our assumption that $\varphi(\cdot)$ corresponds to a correlation function generated by a finite dimensional system, and relation (7.8) to determine our desired Markovian representation for $Z(\cdot)$. Letting $\mathcal{L}\{\cdot\}$ denote the bilateral Laplace transform, we define $S(s)$ as

$$S(s) = \mathcal{L}\{\varphi(\cdot)\} \quad . \tag{7.9}$$

Assuming that $S(s)$ is strictly proper and rational, i.e., that $S(\infty) = 0$, we can determine a strictly proper rational spectral

factor h(s) with no poles in the right half place such that

$$S(s) = h(s)h(-s) \quad . \tag{7.10}$$

For the purpose of realizing Z(t) we will need M copies of an irreducible state-space realization for h(s) of the form

$$d\gamma_i(t) = F_x\gamma_i(t)dt + G_x dw_i(t) \quad , \tag{7.11}$$

$$\eta_i(t) = h_x\gamma_i(t), \quad \text{for } i = 1,\ldots,M \ , \tag{7.12}$$

where $w_i(\cdot)$ is a standard scalar Brownian motion process and

$$E[\gamma_i(0)\gamma_i'(0)] = \pi_x \quad , \tag{7.13}$$

with π_x being the unique positive definite solution to the equation

$$F_x\pi_x + \pi_x F_x' + G_x G_x' = 0. \tag{7.14}$$

Finally, we employ relations (7.11) - (7.14) and (7.8) to obtain a Markovian representation for the aggregate field vector process Z(t) of the form given by relations (6.4) - (6.5) with

$$\xi(t) \triangleq \begin{pmatrix} \gamma_1(t) \\ \hline \\ \hline \gamma_M(t) \end{pmatrix} , \tag{7.15}$$

$$du(t) \triangleq \begin{pmatrix} dw_1(t) \\ \vdots \\ dw_M(t) \end{pmatrix} , \tag{7.16}$$

$$A(t) \triangleq \begin{pmatrix} F_x & & \\ & \ddots & \\ & & F_x \end{pmatrix} , \tag{7.17}$$

$$B(t) \triangleq \begin{pmatrix} G_x & & \\ & \ddots & \\ & & G_x \end{pmatrix} , \tag{7.18}$$

$$L(t) = \begin{pmatrix} \bar{\ell}_{1,1} h_x & & \\ \vdots & \ddots & \\ \bar{\ell}_{M,1} h_x & \cdots & \bar{\ell}_{M,M} h_x \end{pmatrix} , \tag{7.19}$$

and

$$E[\xi(0)\xi'(0)] = \pi(0) = \begin{pmatrix} \pi_x & & & \\ & \pi_x & & \\ & & \ddots & \\ & & & \pi_x \end{pmatrix} ; \qquad (7.20)$$

Having specified a finite-dimensional Markovian representation for the aggregate field vector process Z(t), of the form in relations (6.4) - (6.5), we can model the physical field variables of the i-th sensor survey, $Z_i(t)$, as

$$Z_i(t) = E_i L(t)\, \xi(t) \quad , \qquad (7.21)$$

where

$$E_i = (\underbrace{0 \ldots \quad 0\ 1}_{\text{i-th}}\ 0 \ldots 0) \quad . \qquad (7.22)$$

We assume that the i-th survey measurements are modelled as

$$dy_i(t) = c_i(t)Z_i(t)dt + d_i(t)dv_i(t) \ , \qquad (7.23)$$

where $$d_i^2(t) = r_i(t) > 0 \quad . \tag{7.24}$$

The $v_i(\cdot)$'s are taken to be standard, mutually independent Brownian motion processes. We note here that by setting $c_{i_k}(t) = 0$, $0 \le t \le T$, for some set of i_k's, we can describe the case in which we have measurements only over some subset of the total number of tracks on which it is desired to map the field. If we next define the j-pass smoothed estimate of the global state, $\hat{\xi}_s^{(j)}(t)$, as

$$\hat{\xi}_s^{(j)}(t) = E\left[\xi(t) \middle| \bigvee_{i=1}^{j} Y_i\right] \quad , \tag{7.25}$$

and the i-th survey estimate of the global state, $\hat{\xi}_{is}(t)$, as

$$\hat{\xi}_{is}(t) = E[\xi(t)|Y_i] \quad , \tag{7.26}$$

we can use some simple generalizations of the centralized map-updating and map-combining results of Chapter 4 in order to express $\hat{\xi}_s^{(j)}(t)$ as a linear functional of $\hat{\xi}_s^{(j-1)}(\cdot)$ and $dy_j(\cdot)$, or as a linear functional of the $\hat{\xi}_{is}(\cdot)$'s for $i = 1,\ldots,j$, respectively.

We next pose and solve a version of the map-centralization problem of the type discussed in Section 6.2, where the local i-th track field model is embedded in, and thus consistent with,

the global M-track field model. We suppose that the physical field variables along the i-th measurement trajectory are modelled separately, with a correlation function, $R_{Z_i}(\tau)$, consistent with relation (7.2), and specified by

$$R_{Z_i}(\tau) = \varphi(\tau)\psi(0) \quad . \tag{7.27}$$

Noting from relations (7.4) - (7.6) that

$$\bar{\ell}^{-2}_{1,1} = \psi(0) \quad , \tag{7.28}$$

and using the relations (7.11) - (7.12) to specify a finite dimensional Markovian realization of a process with correlation function $\varphi(\tau)$, we obtain the following representation for $Z_i(t)$:

$$Z_i(t) = L_i(t)\,\theta_i(t) \quad , \tag{7.29}$$

where $$d\theta_i(t) = F_x\theta_i(t)dt + G_x du_i(t) \quad , \tag{7.30}$$

$$L_i(t) = \bar{\ell}_{1,1}\, h_x \quad , \tag{7.31}$$

and $$E[\theta_i(0)\theta_i'(0)] = \pi_x \quad . \tag{7.32}$$

By consistency with relation (7.23), we assume also that the i-th survey, field variable measurements are modelled locally as

$$dy_i(t) = c_i(t)Z_i(t)dt + d_i(t)dv_i(t) \ . \qquad (7.33)$$

Then, letting $\hat{\theta}_{is}(t)$ denote the smoothed estimate for $\theta_i(t)$ based on the model of relations (7.29) - (7.32), and the measurement equation (7.33), we define the map-centralization problem as that of computing the global state, aggregate M-pass smoothed estimate, $\hat{\xi}_s(t)$, a linear functional of the $\hat{\theta}_{is}(\cdot)$'s, for $i = 1,\ldots,M$.

By construction, the global model for the i-th survey field variables $Z_i(\cdot)$ is statistically equivalent to the local model for $Z_i(\cdot)$ determined by (7.29) - (7.32). We next demonstrate that we can find some transformations T_i that cast the map-centralization problem of this section in the exact form of that in Section 6.2. We note that the global model represents $Z_i(t)$ as

$$Z_i(t) = (\bar{\ell}_{i,1}h_x \ \vdots \ \bar{\ell}_{i,i}h_x \ \vdots \ 0 \ldots \ 0)\begin{pmatrix} \gamma_1(t) \\ \vdots \\ \gamma_M(t) \end{pmatrix} \ , \qquad (7.34)$$

and the local model represents $Z_i(t)$ as

$$Z_i(t) = \bar{\ell}_{1,1} h_x \theta_i(t) \quad , \tag{7.35}$$

where the $\gamma_i(\cdot)$'s and $\theta_i(\cdot)$'s are statistically equivalent, and modelled by (7.11) and (7.30), respectively. We would like to determine a transformation T_i so that the model for $Z_i(\cdot)$ of (7.34) can be represented in terms of the transformed state variables

$$\zeta_i(t) = T_i \xi(t) \quad , \tag{7.36}$$

in the same form as (7.35). We first note that relation (7.34) can be expressed as

$$Z_i(t) = \bar{\ell}_{1,1} h_x \zeta_{i1}(t) \ , \tag{7.37}$$

where

$$\zeta_{i1}(t) = \sum_{j=1}^{i} \frac{\bar{\ell}_{i,j}}{\bar{\ell}_{1,1}} \gamma_j(t) \ . \tag{7.38}$$

As a consequence of the factorization of the H matrix (see relation (7.5)) into the product of the lower and upper triangular factors $\bar{L}$ and $\bar{L}'$, we can show that

$$\sum_{j=1}^{i} \left(\frac{\bar{\ell}_{i,j}}{\bar{\ell}_{1,1}} \right)^2 = 1 \quad , \tag{7.39}$$

and therefore from (7.38) we can verify that $\zeta_{i1}(\cdot)$ is statistically equivalent to $\theta_i(\cdot)$. Hence, we can identify $\zeta_{i1}(\cdot)$ as the first component vector of the transformed state process $\zeta_i(\cdot)$, composed of $\zeta_{ij}(\cdot)$ for $j = 1,\ldots,M$. This motivates the following construction for T_i. We note that from relation (7.39) and a theorem in [61], we can find a matrix σ_*^i such that the $M \times M$ matrix σ^i defined by

$$\sigma^i \triangleq \begin{pmatrix} \frac{\bar{\ell}_{i,1}}{\bar{\ell}_{1,1}} & \cdots & \frac{\bar{\ell}_{i,i}}{\bar{\ell}_{1,1}} & 0 & \cdots & 0 \\ \hline & & \sigma_*^i & & & \end{pmatrix}, \tag{7.40}$$

is an orthogonal matrix. Then, by letting $\sigma^i_{\ell_1,\ell_2}$ denote the (ℓ_1,ℓ_2)-th element of σ^i, we define T_i as

$$T_i \triangleq \begin{pmatrix} \sigma^i_{1,1} I & \cdots & \sigma^i_{1,M} I \\ \vdots & & \\ \sigma^i_{M,1} I & \cdots & \sigma^i_{M,M} I \end{pmatrix} . \tag{7.41}$$

The above choice for T_i effectively decouples the dynamics of $\zeta_{i1}(\cdot)$ from $\zeta_{ij}(\cdot)$, for $j \geq 2$, and results in a global model for $Z_i(\cdot)$ of the form in (7.35).

Rather than assuming an explicit form for T_i as in (7.41), and using the map-centralization results of Chapter 6, we find by following the steps of the algebraic approach to map-centralization of Appendix 6B that due to the simple diagonal structure of the system matrices associated with the global field model, it is unnecessary to calculate the T_i's in order to derive an algorithm for forming $\hat{\xi}_s(\cdot)$ as a linear functional of the $\hat{\theta}_{is}(\cdot)$'s. Hence, letting $\Gamma_f(t)$ and $\Gamma_r(t)$ denote the aggregate M-pass global state forward and reverse filter dynamics matrices, and letting $P_f(t)$ and $P_r(t)$ denote the aggregate M-pass global state forward and reverse filtering error covariance matrices, and by employing the following notations:

$$\hat{\theta}_{\ell}(t) \triangleq \begin{pmatrix} \hat{\theta}_{1s}(t) \\ \\ \hat{\theta}_{Ms}(t) \end{pmatrix} , \tag{7.42}$$

$$H_I \triangleq \begin{pmatrix} I & \frac{\bar{\ell}_{2,1}}{\bar{\ell}_{1,1}} I & \cdots & \frac{\bar{\ell}_{M,1}}{\bar{\ell}_{1,1}} I \\ & & & \\ & & & \frac{\bar{\ell}_{M,M}}{\bar{\ell}_{1,1}} I \end{pmatrix} , \tag{7.43}$$

$$H_M(t) \triangleq \begin{pmatrix} \bar{\ell}_{1,1}^2 \frac{c_1^2(t)}{r_1(t)}[G_x G_x'] & \cdots & \bar{\ell}_{1,1}\bar{\ell}_{M,1} \frac{c_M^2(t)}{r_M(t)}[G_x G_x'] \\ & \vdots & \\ \bar{\ell}_{1,1}\bar{\ell}_{M,M} \frac{c_M^2(t)}{r_M(t)}[G_x G_x'] & & \end{pmatrix}, \quad (7.44)$$

and

$$D_M(t) \triangleq \begin{pmatrix} \frac{c_1^2(t)}{r_1(t)} & 0 & \cdots & 0 \\ & \ddots & & 0 \\ 0 & & \ddots & \\ \vdots & & & \frac{c_M^2(t)}{r_M(t)} \\ 0 & \cdots & 0 & \end{pmatrix}, \quad (7.45)$$

by manipulations analogous to those of Appendix 6B, we derive the following algorithm for computing $\hat{\xi}_s(t)$ as a linear functional of $\hat{\theta}_\ell(\cdot)$:

$$\hat{\xi}_s(t) = P_s(t)\left\{P_f^{-1}(t)\alpha_f(t) + P_r^{-1}(t)\alpha_r(t)\right\} + H_I\theta_\ell(t) \ , \quad (7.46)$$

where $$P_s^{-1}(t) = P_f^{-1}(t) + P_r^{-1}(t) - \pi^{-1} \ , \quad (7.47)$$

$$d\alpha_f(t) = \Gamma_f(t)\alpha_f(t)dt + P_f(t)\left[H_M(t) - \left\{L'(t)D_M(t)L(t)\right\}H_I\right]\hat{\theta}_\ell(t)dt, \quad (7.48)$$

$$-d\alpha_r(t) = \Gamma_r(t)\alpha_r(t)dt + P_r(t)\left[H_M(t) - \left\{L'(t)D_M(t)L(t)\right\}H_I\right]\hat{\theta}_{\ell}(t)dt, \tag{7.49}$$

and $$\alpha_f(0) = \alpha_r(T) = 0 \ . \tag{7.50}$$

In this section we have solved the centralized map-updating, centralized map-combining, and map-centralization problems for the case of a measurement geometry constituted of M parallel lines through a stationary, scalar, separable two-dimensional random field. We note here that we can extend the technique of this section for obtaining a finite dimensional Markovian representation of the aggregate field vector process $Z(\cdot)$ to the case when the field has correlation function

$$R(\tau_1,\tau_2) = \sum_{i=1}^{N} \varphi_i(\tau_1)\psi_i(\tau_2) \ , \tag{7.51}$$

where the $\varphi_i(\cdot)$'s and $\psi_i(\cdot)$'s represent correlation functions realizable by finite dimensional systems. In a similar manner, we can obtain some finite dimensional realizations for $Z(\cdot)$ in the case of a space variant random field with correlation function

$$R(t_1,y_1,t_2,y_2) = E[f(t_1,y_1,\omega)f(t_2,y_2,\omega)] \ , \tag{7.52}$$

defined by

$$R(t_1,y_1,t_2,y_2) = \sum_{i=1}^{N} \varphi_i(t_1,t_2)\psi_i(y_1,y_2) \quad , \tag{7.53}$$

where the $\varphi_i(t_1,t_2)$'s and $\psi_i(y_1,y_2)$'s represent one-dimensional correlation functions realizable by finite dimensional systems. Hence, in both of the above cases, we can obtain finite dimensional Markovian representations of $Z(\cdot)$, which we may employ to obtain solutions to the centralized map-updating or centralized map-combining problems.

For the case of more general measurement geometries, i.e., nonparallel measurement tracks and a field correlation function of the form in relations (7.2) or (7.51), the aggregate field vector process $Z(\cdot)$ does not have an exact finite dimensional Markovian representation. Even for the case where we have parallel measurement trajectories, not aligned with the directions of separability of the field, $Z(\cdot)$ will not have a finite dimensional realization. In these cases, we may either employ an approximate finite dimensional representation of $Z(\cdot)$ and then use the results of Chapter 4 to obtain approximate solutions to the centralized map-updating and centralized map-combining problems, or we could attempt to develop analogous centralized map-updating and map-combining solutions for the case when $Z(t)$ has some infinite dimensional state space

representation. In the following section, we demonstrate how the need for infinite dimensional representations for $Z(\cdot)$ does not arise in a discrete space setting. To do so, we will solve an example of the map-updating problem for the case of a non-parallel line measurement geometry through a scalar random field with a separate correlation function.

7.3 Discrete Space Map-Updating for the Case of Two Nonparallel Measurement Tracks through a Stationary, Separable, Two-Dimensional Scalar Random Field

In this section we consider a discrete space map-updating problem corresponding to a measurement geometry with non-parallel measurement tracks through a scalar, separable, stationary, random field. As will become clear, our approach can be applied to a large class of discrete space mapping problems. We view this as an important contribution, and as an important indicator of the significance of the results of this part of the thesis.

Let $f(i,j)$ denote the values of the field for $i = 1,\ldots,T$, $j = 1,\ldots,M$, and assume that the process is zero-mean, with a correlation function $R(i,j)$ defined by

$$R(i,j) = \left[\sigma_x^2 \alpha_x^{|i|}\right]\left[\sigma_y^2 \alpha_y^{|j|}\right] \quad . \tag{7.54}$$

We let $y_1(t)$ and $y_2(t)$ denote the first and second pass measurements defined by

$$y_1(t) = f(t,M) + n_1(t) \quad , \tag{7.55}$$

and

$$y_2(t) = f(t,q-t+1) + n_2(t) \quad , \tag{7.56}$$

where $n_1(\cdot)$ and $n_2(\cdot)$ are independent, discrete white noise sequences with

$$E[n_1^2(t)] = \sigma_{1n}^2 \quad , \tag{7.57}$$

and

$$E[n_2^2(t)] = \sigma_{2n}^2 \quad . \tag{7.58}$$

The measurement geometry defined by relations (7.55) - (7.56) is pictured in Fig. 7.1. We assume that $q-T+1<M$, i.e., that we have two full passes of measurements over the region of interest for the field, $f(i,j)$ for $i = 1,\ldots,T$, $j = 1,\ldots,M$ (as opposed to having the second pass just touch a corner of the region of interest).

We next derive a finite dimensional state space representation for the evolution of the field quantities $f(\cdot,\cdot)$ over the region of interest, as we advance from left to right in Fig. 7.1, one column at a time. We then employ this representation to model the first and second pass measurements of relations (7.55) - (7.56) as linear observations of some underlying state process. We will find that since our first pass proceeds along a direction of separability of the field, the first-pass measurements are described by a stationary model. The second-pass measurements are not made along a direction of separability of the field, and hence are described by a

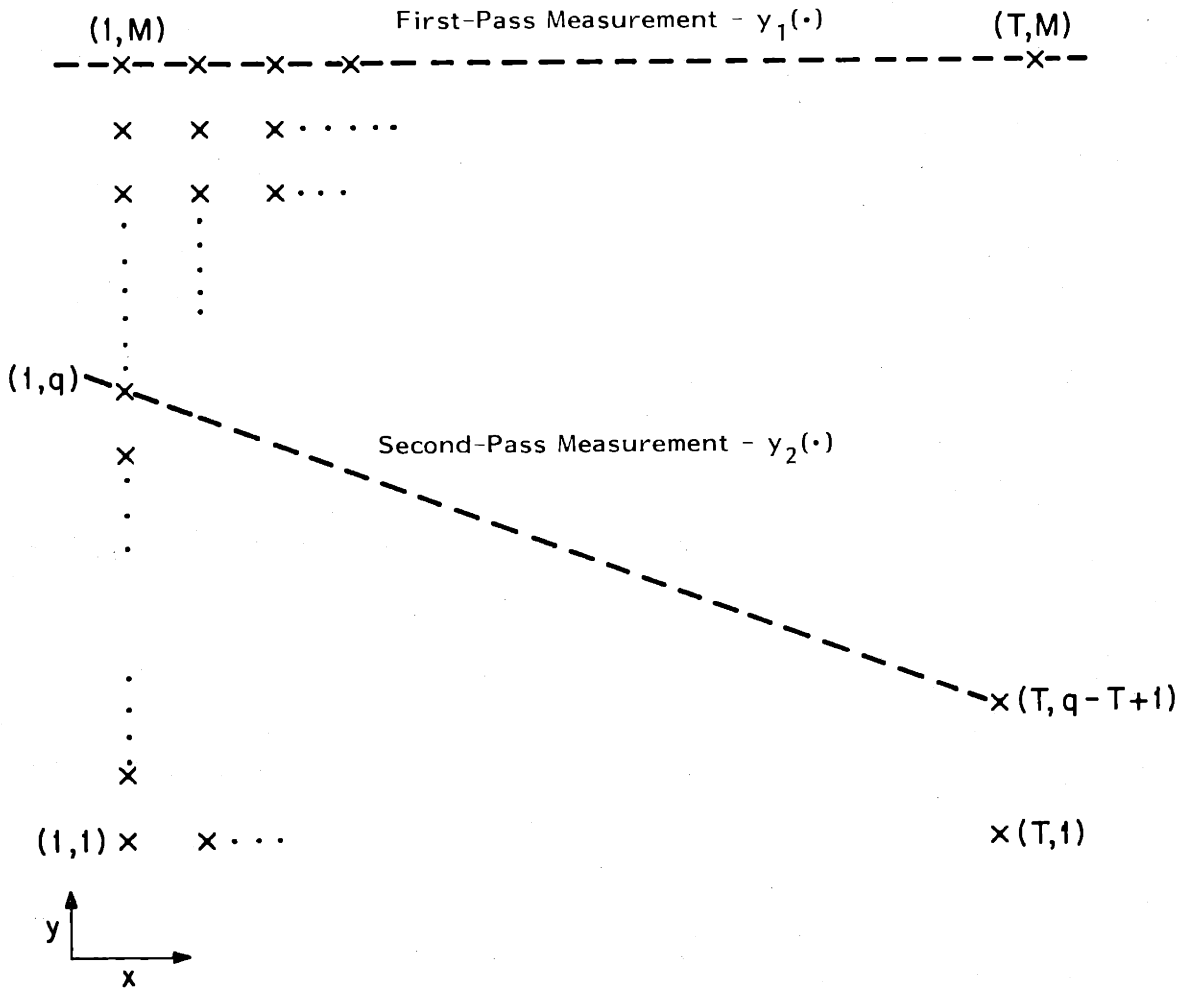

Fig. 7.1 Measurement Geometry for a Discrete-Space Map-Updating Example

nonstationary model, but with the same underlying state process (i.e., the space variations will appear only in the measurement equation). We finally cast the map-updating problem of this section in the framework of the discrete time centralized map-updating problem solved in Appendix 4E.

We now define the aggregate field vector process $Z(t)$ as

$$Z(t) \triangleq \begin{pmatrix} f(t,M) \\ \vdots \\ f(t,1) \end{pmatrix} \quad , \tag{7.59}$$

and derive a finite dimensional Markovian representation for $Z(\cdot)$ by using the field correlation function of relation (7.54) in a completely analogous manner to our analysis in Section 7.2. We can express the correlation function of the $Z(\cdot)$ process as

$$R_Z(i) = L \begin{pmatrix} \sigma_x^2 \alpha_x^{|i|} & & \\ & \ddots & \\ & & \sigma_x^2 \alpha_x^{|i|} \end{pmatrix} L' \quad , \tag{7.60}$$

where the (i,j)-th element of L, $[L]_{i,j}$ is defined as

$$[L]_{i,j} = \begin{cases} \sigma_y \alpha_y^{i-1} & j = 1 \\ \sigma_y \alpha_y^{i-j} \sqrt{1 - \alpha_y^2} & 1 < j \leq i \\ 0 & \text{otherwise} \end{cases} \quad . \tag{7.61}$$

From relations (7.60) - (7.61) we can motivate a representation for Z(t) of the form

$$Z(t) = L\,\xi(t) \quad , \tag{7.62}$$

with

$$\xi(t+1) = A(t)\xi(t) + B(t)u(t) \quad , \tag{7.63}$$

where

$$A(t) \triangleq \begin{pmatrix} \alpha_x & & \\ & \ddots & \\ & & \alpha_x \end{pmatrix} \quad , \tag{7.64}$$

$$B(t) \triangleq \begin{pmatrix} \sigma_x\sqrt{1-\alpha_x^2} & & \\ & \ddots & \\ & & \sigma_x\sqrt{1-\alpha_x^2} \end{pmatrix} \quad , \tag{7.65}$$

$$\xi(t) \triangleq \begin{pmatrix} \gamma_1(t) \\ \vdots \\ \gamma_M(t) \end{pmatrix} \quad , \tag{7.66}$$

$$E[\xi(0)\xi'(0)] = \begin{pmatrix} \sigma_x^2 & & \\ & \ddots & \\ & & \sigma_x^2 \end{pmatrix} \quad , \tag{7.67}$$

and

$$u(t) \triangleq \begin{pmatrix} w_1(t) \\ \vdots \\ w_M(t) \end{pmatrix} \quad , \tag{7.68}$$

where the $w_i(\cdot)$'s are standard, independent discrete white noise sequences.

By employing relations (7.59) and (7.62) - (7.68), we can represent the first and second pass data defined by relations (7.55) - (7.56) as

$$y_1(t) = E_1(t)\, L\, \xi(t) + n_1(t) \quad , \tag{7.69}$$

and $$y_2(t) = E_2(t)\, L\, \xi(t) + n_2(t) \quad , \tag{7.70}$$

where $$E_1(t) \triangleq (1\ 0\ .\ .\ .\ 0\ 0\ ..\ 0) \ , \tag{7.71}$$

and $$E_2(t) \triangleq (\underbrace{0\ \ldots\ 1}_{q'+t-1}\ 0\ ..\ 0) \ , \tag{7.72}$$

where $q' = M-q+1$. Relations (7.69) - (7.70) show that the only space variant modelling occurs in the description of the second pass measurements. We now define $H_1(t)$ and $H_2(t)$ by

$$H_1(t) = E_1(t)L \equiv (\sigma_y \quad 0 \ldots \qquad\qquad 0 \ldots \qquad 0), \tag{7.73}$$

and

$$H_2(t) = E_2(t)L \equiv (\underbrace{\sigma_y\alpha_y^{q'+t-2} \mid \sigma_y\alpha_y^{q'+t-3}\sqrt{1-\alpha_y^2} \mid \ldots \mid \sigma_y\sqrt{1-\alpha_y^2}}_{q'+t-1} \mid 0 \ldots 0). \tag{7.74}$$

Consequently, the two measurement passes can be modelled as

$$y_1(t) = H_1(t)\xi(t) + n_1(t) , \tag{7.75}$$

and

$$y_2(t) = H_2(t)\xi(t) + n_2(t) . \tag{7.76}$$

By employing the Markovian representation for $\xi(\cdot)$ defined by relations (7.62) - (7.68), and the observation equations of relations (7.75) - (7.76), we can define the map-updating problem as that of computing the two-pass smoothed estimates of $\xi(\cdot)$, $\hat{\xi}_s(\cdot)$, as a linear functional of the first-pass smoothed estimates, $\hat{\xi}_{1s}(\cdot)$, and new data $y_2(\cdot)$. To solve this problem we can apply the results of Appendix 4E on the solution to the discrete time centralized map-updating problem. In Appendix 7A we perform a detailed investigation of the structure of the map-updating algorithm for our current problem, by drawing on results in Appendix 4E. We outline the results of Appendix 7A in what follows. From Appendix 4E the two-pass smoothed

estimate of the global state $\xi(t)$, $\hat{\xi}_s(t)$, can be expressed as

$$\hat{\xi}_s(t) = \hat{\xi}_{1s}(t) + P_s(t)\left\{P_{fs}^{-1}(t)\hat{\hat{\xi}}_f(t) + P_{rps}^{-1}(t)\hat{\hat{\xi}}_{rp}(t)\right\}, \quad (7.77)$$

where $P_s(t)$ denotes the two-pass, state smoothing error covariance matrix, and where $\hat{\hat{\xi}}_f(t)$, $\hat{\hat{\xi}}_{rp}(t)$ and $P_{fs}(t)$, $P_{rps}(t)$ denote, respectively, the forward filtered and reverse predicted estimates of the first-pass smoothing error process, $\tilde{\xi}_{1s}(t)$, and their corresponding error covariance matrices, based on the observations $\tilde{y}_2(t')$ defined by

$$\tilde{y}_2(t') = y_2(t') - H_2(t')\hat{\xi}_{1s}(t'). \quad (7.78)$$

We now note that for the problem of this section the global state $\xi(t)$ was defined by

$$\xi(t) = \begin{pmatrix} \gamma_1(t) \\ \vdots \\ \gamma_M(t) \end{pmatrix}, \quad (7.79)$$

where each of the $\gamma_i(\cdot)$'s evolved as a one-dimensional discrete time Markov process. We will use the following notation to refer to the components of $\hat{\xi}_{1s}(t)$ and $\tilde{\xi}_{1s}(t)$:

$$\hat{\xi}_{1s}(t) = \begin{pmatrix} \hat{\gamma}_{1s1}(t) \\ \vdots \\ \hat{\gamma}_{1sM}(t) \end{pmatrix} , \tag{7.80}$$

and

$$\tilde{\xi}_{1s}(t) = \begin{pmatrix} \tilde{\gamma}_{1s1}(t) \\ \vdots \\ \tilde{\gamma}_{1sM}(t) \end{pmatrix} . \tag{7.81}$$

We note here that since the $\gamma_i(\cdot)$'s are all statistically independent, and the first-pass measurements defined by (7.73), (7.75) only provide information about $\gamma_1(\cdot)$, we can express the first-pass smoothed global state estimates by

$$\hat{\xi}_{1s}(t) = \begin{pmatrix} \hat{\gamma}_{1s1}(t) \\ 0 \\ \vdots \\ 0 \end{pmatrix} . \tag{7.82}$$

In Appendix 7A we show that the correction term added to the old map, in the map-updating equation (7.77), only results in changes for the estimates of the components $\gamma_i(\cdot)$, for $i = 1,\ldots,q'+T-1$. This is a consequence of the fact that while our first-pass measurements provide information about $\gamma_1(\cdot)$,

our second-pass data for the field on the slanted line, is modelled in (7.73), (7.75) as a functional of the $\gamma_i(\cdot)$'s for $i = 1,\ldots,q'+T-1$. Hence, we have corrections to the old map, $\hat{\xi}_{1s}(\cdot)$, corresponding to components of the global state that can be used to represent the field above or on the second-pass measurement trajectory. This is a direct result of the specific state realization for $Z(\cdot)$ that we have chosen. This suggests that it may be fruitful to examine the question of what realizations lead to the most efficient updating algorithms for specific measurement geometries. Finally from relation (7.62), we form the two data pass field map as

$$\hat{Z}_s(t) = L\,\hat{\xi}_s(t) \quad . \tag{7.83}$$

We conclude this section by noting that the approach to map-updating outlined here is not limited to fields with separable correlation functions. We may also consider stationary fields with correlation functions analogous to (7.51), and space variant fields with correlation functions like that of (7.53). Woods and Radewan in [88] show that by assuming the knowledge of a specific type of two-dimensional, autoregressive representation of a general, stationary random field, and by making suitable assumptions on the boundary conditions over the region

of interest, we can at least derive approximate finite dimensional Markovian representations for the process $Z(t)$ of relation (7.59), and hence may cast the map-updating problem in the framework of Appendix 4E.

7.4 Conclusion

In this Chapter we have provided some concrete spatial examples of the centralized map-updating, centralized map-combining, and map-centralization problems. In Section 7.2 we presented a specific case of these problems in a continuous space setting for a M parallel line measurement geometry through a stationary, separable, scalar random field. The difficulty in constructing two-dimensional, continuous-space, examples of the centralized map-updating, map-combining, and map-centralization problems, with non-trivial measurement geometries, i.e., nonparallel measurement trajectories, stems from the fact that the aggregate field vector process $Z(\cdot)$ may have no exact finite dimensional representation. Hence, this motivates the need for future work in developing analogous map-updating and map-combining algorithms when we assume that $Z(\cdot)$ has some infinite dimensional model. We note that in this case our Hilbert space approach should at least provide representations for the solutions of these problems.

In Section 7.3 we presented a discrete space example of the map-updating problem for a non-trivial measurement geometry, constituted of two nonparallel lines through a scalar, stationary and separable random field. We can easily extend our analysis to the case of fields with correlation functions

analogous to (7.51), (7.53). We argue finally that the work of Woods and Radewan [87] - [88], and the results of Appendix 4E , provide the basis for considering map-updating problems for arbitrary measurement geometries through general scalar, and ultimately vector, stationary random fields. Hence, we have succeeded in developing a computationally efficient mathematical framework for a very wide class of map-updating problems, for which the updating operation is no more difficult than that of map formation.

Appendix 7A

Detailed Solution of the Map-Updating Problem of Section 7.3

In this Appendix we apply the results of Appendix 4E to solving the discrete grid map-updating problem specified in Section 7.3. We find that the two-pass smoothed estimate of the global state $\xi(t)$, $\hat{\xi}_s(t)$, can be expressed as

$$\hat{\xi}_s(t) = \hat{\xi}_{1s}(t) + P_s(t)\left\{P_{fs}^{-1}(t)\hat{\tilde{\xi}}_f(t) + P_{rps}^{-1}(t)\hat{\tilde{\xi}}_{rp}(t)\right\} . \quad (A.1)$$

Here $P_s(t)$ denotes the two-pass state smoothing error covariance matrix. The estimates $\hat{\tilde{\xi}}_f(t)$, $\hat{\tilde{\xi}}_{rp}(t)$, with associated error covariance matrices $P_{fs}(t)$, $P_{rps}(t)$, denote forward filtered and reverse predicted estimates of the first-pass smoothing error process $\tilde{\xi}_{1s}(t)$ based on the observations $\tilde{y}_2(t')$ defined by

$$\tilde{y}_2(t') = y_2(t') - H_2(t')\hat{\xi}_{1s}(t') \quad . \quad (A.2)$$

In this Appendix we employ relations (E.30) - (E.37) of Appendix 4E to detail the evolution of the filtered estimates

$\hat{\tilde{\xi}}_f(t)$, $\hat{\tilde{\xi}}_{rp}(t)$ and of their corresponding error covariance matrices, $P_{fs}(t)$ and $P_{rps}(t)$.

In order to form the equations for the evolution of $\hat{\tilde{\xi}}_f(\cdot)$ and $\hat{\tilde{\xi}}_{rp}(\cdot)$, we must first calculate the first-pass forward filtering, and one-step ahead prediction error covariance matrices, $P_{1f}(\cdot)$ and $P_{1fp}(\cdot)$, defined by relations (E.21) - (E.23) of Appendix 4E, and the reverse filtering, and reverse prediction error covariances matrices, $P_{1b}(\cdot)$ and $P_{1bp}(\cdot)$, associated with the estimation of the adjoint state process, and determined by relations (E.16) - (E.18) of Appendix 4E. Hence, assuming that our underlying state process is defined by relations (7.63) - (7.68), and the first-pass measurements modelled by relation (7.75), we may show that $P_{1f}(t)$, $P_{1fp}(t+1)$, $P_{1bp}(t)$, and $P_{1b}(t-1)$ assume the following forms:

$$P_{1f}(t) = \text{diag}\left(p_{1f}(t), \sigma_x^2, \ldots, \sigma_x^2\right) \quad , \tag{A.3}$$

$$P_{1fp}(t+1) = \text{diag}\left(\alpha_x^2 p_{1f}(t) + \sigma_x^2(1-\alpha_x^2),\ \sigma_x^2, \ldots, \sigma_x^2\right) \ , \tag{A.4}$$

$$P_{1b}(t-1) = \text{diag}\left(p_{1b}(t-1),\ 0, \ldots, 0\right) \ , \tag{A.5}$$

$$P_{1bp}(t) = \text{diag}\left(\alpha_x^2 p_{1b}(t+1) + \frac{\sigma_y^2}{\sigma_{1n}^2},\ 0, \ldots, 0\right) \ , \tag{A.6}$$

where

$$p_{1f}(t) = \left[\alpha_x^2 p_{1f}(t-1) + \sigma_x^2(1-\sigma_x^2)\right]\left\{1 - \frac{\sigma_y^2\left[\alpha_x^2 p_{1f}(t-1) + \sigma_x^2(1-\alpha_x^2)\right]}{\left[\sigma_y^2\left[\alpha_x^2 p_{1f}(t-1) + \sigma_x^2(1-\alpha_x^2)\right] + \sigma_{1n}^2\right]}\right\},$$

(A.7)

with $$p_{1f}(0) = \sigma_x^2 \quad , \tag{A.8}$$

and

$$p_{1b}(t) = \left[\alpha_x^2 p_{1b}(t+1) + \frac{\sigma_y^2}{\sigma_{1n}^2}\right]\left\{1 - \frac{\sigma_x^2(1-\alpha_x^2)\left[\alpha_x^2 p_{1b}(t+1) + \frac{\sigma_y^2}{\sigma_{1n}^2}\right]}{\left[\sigma_x^2(1-\alpha_x^2)\left[\alpha_x^2 p_{1b}(t+1) + \frac{\sigma_y^2}{\sigma_{1n}^2}\right] + 1\right]}\right\},$$

(A.9)

with $$p_{1b}(T) = 0 \quad . \tag{A.10}$$

From equation (E.38), Appendix 4E, we may express the first-pass smoothing error covariance matrix as

$$P_{1s}(t+1) = \text{diag}\left(p_{1s}(t+1),\ \sigma_x^2,\ \ldots,\ \sigma_x^2\right) \ , \tag{A.11}$$

where

$$p_{1s}(t+1) = \left[\frac{1}{\left[\alpha_x^2 p_{1f}(t) + \sigma_x^2(1-\alpha_x^2)\right]} + \left[\alpha_x^2 p_{1b}(t+1) + \frac{\sigma_y^2}{\sigma_{1n}^2} \right] \right]^{-1} . \quad (A.12)$$

Relations (A.4) - (A.12) are a reflection of the fact that the first-pass measurements only give us information about the first component, $\gamma_1(\cdot)$, of the global state vector, $\xi(\cdot)$. Since the $\gamma_i(\cdot)$'s are all statistically independent, using the notation (7.80) we find that

$$\hat{\xi}_{1s}(t) = \begin{pmatrix} \hat{\gamma}_{1s1}(t) \\ 0 \\ \vdots \\ 0 \end{pmatrix} . \quad (A.13)$$

Before detailing the computation of the correction term to the old map, embedded in the map-updating equation (A.1), we make some general comments on the structure which we expect those corrections to assume, based on the form of the second-pass measurements. We first recall that the second-pass data is modelled as

$$y_2(t) = H_2(t)\xi(t) + n_2(t) \quad , \quad (A.14)$$

where

$$H_2(t) = \Big(\underbrace{\sigma_y\alpha_y^{q'+t-2} \;\; \sigma_y\alpha_y^{q'+t-3}\sqrt{1-\alpha_y^2} \;\; .. \;\; \sigma_y\sqrt{1-\alpha_y^2}}_{q'+t-1} \;\; 0 \;\; .. \;\; 0\Big). \quad (A.15)$$

Relations (A.14) - (A.15) imply that $y_2(t)$ provides us with information about $\gamma_i(t)$ for $i = 1,\ldots,q'+t-1$. Hence, as t varies from 1 to T, the $y_2(\cdot)$ data measures the $\gamma_i(\cdot)$'s for $i = 1,\ldots,q'+T-1$, and therefore the map-updating procedure can only be expected to provide new information for those components of $\xi(\cdot)$.

We now use relations (E.30) - (E.33) to derive equations for the evolution of $P_{fps}(t)$, $P_{fs}(t)$, and $\hat{\tilde{\xi}}_f(t)$. Let us define the matrices $A_{lfs}(t-1)$, $Q_{lfs}(t-1)$ as

$$A_{lfs}(t-1) \triangleq \text{diag}\Big(\alpha_x\big[1 - \sigma_x^2(1-\alpha_x^2)P_{lb}(t-1)\big], \; \alpha_x, \; \ldots, \; \alpha_x\Big), \quad (A.16)$$

and

$$Q_{lfs}(t-1) = \text{diag}\Big(\sigma_x^2(1-\alpha_x^2)\big[1 - \sigma_x^2(1-\alpha_x^2)P_{lb}(t-1)\big], \; \sigma_x^2(1-\alpha_x^2), \; \ldots, \sigma_x^2(1-\alpha_x^2)\Big). \quad (A.17)$$

In addition, we define the matrix $H_0(t)$ as

$$H_0(t) \triangleq H_2'(t)H_2(t) \quad , \tag{A.18}$$

where $H_0(t)$ assumes the form

$$H_0(t) = \left(\begin{array}{ccc|c} \sigma_y^2\alpha_y^{2(q'+t-2)} & & \sigma_y^2\alpha_y^{q'+t-2\sqrt{1-\alpha_y^2}} & \\ \vdots & & \vdots & 0 \\ \sigma_y^2\alpha_y^{q'+t-2\sqrt{1-\alpha_y^2}} & \cdots & \sigma_y^2(1-\alpha_y^2) & \\ \hline 0 & & & 0 \end{array}\right) \begin{array}{l} \} q'+t-1 \\ \\ \\ \end{array}$$

$$\underbrace{\qquad\qquad\qquad\qquad}_{q'+t-1} \tag{A.19}$$

Using the above notations we find that

$$P_{fps}(t) = A_{1fs}(t-1)P_{fs}(t-1)A_{1fs}(t-1) + Q_{1fs}(t-1) \quad , \tag{A.20}$$

$$P_{fs}(t) = P_{fps}(t) - \frac{1}{\sigma_{f\nu}^2(t)} P_{fps}(t)H_0(t)P_{fps}(t) \quad , \tag{A.21}$$

where $$\sigma_{f\nu}^2(t) \triangleq H_2(t)P_{fps}(t)H_2'(t) + \sigma_{2n}^2 \quad , \tag{A.22}$$

and finally

$$\hat{\tilde{\xi}}_f(t) = \left[I - \frac{1}{\sigma_{2n}^2} P_{fs}(t) H_0(t) \right] A_{1fs}(t-1) \tilde{\xi}_f(t-1)$$

$$+ \frac{1}{\sigma_{2n}^2} P_{fs}(t) H_2'(t) \left[y_2(t) - \sigma_y \alpha_y^{q'+t-2} \hat{\gamma}_{1s1}(t) \right] , \qquad (A.23)$$

with the initial conditions

$$P_{fs}(0) = P_{1s}(0) , \qquad (A.24)$$

and $$\tilde{\xi}_f(0) = 0 \quad . \qquad (A.25)$$

From relations (A.20) - (A.21), and the initial condition (A.24), we can show that the structure of $P_{fs}(t)$ is similar to that of $H_0(t)$, pictured in (A.19), except that $P_{fs}(t)$ will have non-zero diagonal, σ_x^2, terms for the q'+t to M-th rows. Hence, taking into account the form of $P_{fs}(\cdot)$ and $H_2'(\cdot)$ appearing in relation (A.23) for the evolution of $\tilde{\xi}_f(\cdot)$, we can conclude that by observing $y_2(t')$ for $t' = 1,\ldots,t$, we obtain new information on $\gamma_i(t)$ only for $i = 1,\ldots,q'+t-1$, consistent with our earlier discussion.

We next use relations (E.34) - (E.37) of Appendix 4E to derive backward equations for the evolution of $P_{rps}(\cdot)$, $P_{rs}(\cdot)$, and $\hat{\tilde{\xi}}_{rp}(\cdot)$. Let us define the matrices $A_{1rs}(t+1)$, $Q_{1rs}(t+1)$ by

$$A_{1rs}(t+1) \triangleq \text{diag}\left(\alpha_x^{-1}\left(1 - \frac{\sigma_x^2(1-\alpha_x^2)}{\alpha_x^2 P_{1f}(t) + \sigma_x^2(1-\alpha_x^2)}\right),\ \alpha_x,\ \ldots\ \alpha_x\right) , \tag{A.26}$$

$$Q_{1rs}(t+1) \triangleq \text{diag}\left(\frac{\sigma_x^2(1-\alpha_x^2)}{\alpha_x^2}\left(1 - \frac{\sigma_x^2(1-\alpha_x^2)}{\alpha_x^2 P_{1f}(t) + \sigma_x^2(1-\alpha_x^2)}\right),\ \sigma_x^2(1-\alpha_x^2),\ \ldots\ \sigma_x^2(1-\alpha_x^2)\right) . \tag{A.27}$$

Then, we find that

$$P_{rps}(t) = A_{1rs}(t+1)P_{rs}(t+1)A_{1rs}(t+1) + Q_{1rs}(t+1) , \tag{A.28}$$

$$P_{rs}(t+1) = P_{rps}(t+1) - \frac{1}{\sigma_{r\nu}^2(t+1)} P_{rps}(t+1)H_0(t+1)P_{rps}(t+1) , \tag{A.29}$$

with $$\sigma_{r\nu}^2(t+1) \triangleq H_2(t+1)P_{rps}(t+1)H_2'(t+1) + \sigma_{2n}^2 , \tag{A.30}$$

and finally

$$\hat{\tilde{\xi}}_{rp}(t) = A_{1rs}(t+1)\left\{\left[I - \frac{1}{\sigma_{2n}^2} P_{rs}(t+1)H_0(t+1)\right]\hat{\tilde{\xi}}_{rp}(t+1)\right.$$

$$+\frac{1}{\sigma_{2n}^2} P_{rs}(t+1)H_s'(t+1)$$

$$\left.\cdot\left[y_2(t+1) - \sigma_y \alpha_y^{q'+t-1}\hat{\gamma}_{1s1}(t+1)\right]\right\}, \quad (A.31)$$

with initial conditions

$$P_{rps}(T) = P_{1s}(T) \quad , \quad (A.32)$$

and

$$\tilde{\xi}_{rp}(T) = 0 \quad . \quad (A.33)$$

From examining relations (A.28) - (A.33) we can conclude that observing $y_2(t')$ for $t+1 \leq t' \leq T$ provides us with new information about $\gamma_i(t)$ for $i = 1, \ldots, q+T-1$. Hence, when we combine $\hat{\tilde{\xi}}_f(t)$ and $\hat{\tilde{\xi}}_{rp}(t)$ to obtain the correction term in the map-updating procedure (A.1), we obtain new information on $\gamma_i(t)$ for $i = 1, \ldots, q+T-1$. We finally note that the error covariance matrix associated with the two measurement pass map is specified by

$$P_s^{-1}(t) = P_{fs}^{-1}(t) + P_{rps}^{-1}(t) - P_{ls}^{-1}(t) \ , \qquad (A.34)$$

where $P_{fs}(\cdot)$ is generated by relations (A.20) - (A.22), $P_{rps}(\cdot)$ is determined by equations (A.28) - (A.30), and $P_{ls}(\cdot)$ is defined by (A.11).

Chapter 8

One-Dimensional Approaches for Terrain Masking Analysis

8.1 Introduction

In the work of Chapters 8 - 9, we focus on developing analytical approaches for characterizing the effect of terrain in masking a radar's observation of some object. We note that for the case of a radar sited on a hill of known height, in a region where we have perfect knowledge of the terrain elevations, the problem of deciding whether an object is masked or unmasked with respect to the radar, is purely deterministic. However, in actual practice, we may have many radars sited in a given region, with unknown locations, and hence, for the purpose of studying the effect of radar location on object visibility, it is reasonable to adopt the perspective of viewing the terrain as a spatial random process.

The idea of modeling the terrain as a random field has appeared often in the analysis of the scattering of electromagnetic radiation off the earth's surface. Hayre and Moore in [107] assumed that the terrain may be described as an isotropic, stationary, Gaussian random field with an exponential correlation function, and derived theoretical scattering results that match well with experimental results.

Cohen, in [108], demonstrated that ground elevations could be modelled as Gaussian, and fitted an exponential correlation function to experimentally derived terrain correlations. In [109], Carlson and Bair showed that realistic digital terrain surfaces could be generated by assuming an isotropic terrain correlation function corresponding to a sum of two exponential terms.

Most existing work on characterizing the terrain masking effect has been of an empirical nature [110]. For example, one measure of terrain masking is the average fraction of the circumference of a disk of radius r about the radar, at which an object, at some given additional height, is masked or unmasked. To derive an average value for the fractional blockage of the circumference of the disk, given that the radar is located at some specified height, and the terrain is of a given type, i.e., smooth, hilly, or mountainous, we would need to first obtain terrain elevation data from a collection of sites. We would then compute for each site the fractional blockage of the circumference of each disk of radius r, and then average the values that we obtain over all the sites. This is a time-consuming and costly procedure, and it may be difficult to find enough

sites to derive a good estimate for the average fractional blockage of the circumference. Hence, it is of interest to develop less costly and more powerful analytical methods for understanding and quantifying the masking effect, allowing us to display the interplay between radar siting height, terrain type, object range and altitude, and the object visibility to the radar.

Before introducing the mathematical formulations that we will employ to investigate the masking effect, we make some preliminary observations about radars. For our purposes, a radar is essentially an antenna that transmits and receives electromagnetic radiation. The antenna pattern associated with the radar determines the distribution of the electromagnetic energy directed outwards. Let us denote the radar elevation angle φ as the angle with respect to the horizontal at which the maximal amount of energy is directed. To simplify the complex problem in propagation physics determined by attempting to analyze the values of the electromagnetic field at a given location, we will use an approximation that becomes valid for high frequencies, or for radars with highly directive antennas. We imagine that all the energy from the radar propagates along a line determined by the radar elevation angle, and we call this path, the line of sight [111].

In addition, we note that there are two main classes of radars, search radars and tracking radars. In our idealized view, a search radar maintains a fixed elevation angle and rotates around, scanning the horizon for incoming objects. Tracking radars, on the other hand, are designed to adjust their orientation to follow an object. We will present two different terrain masking formulations which are appropriate for the mode of operation of search radars and tracking radars, respectively.

In Figure 8.1 we present two one-dimensional geometries, which capture the masking effect, and make sense for tracking and search radars, respectively. We note that all our terrain heights will be specified with respect to some mean terrain elevation. In each masking geometry, $\xi(\ell)$ denotes the terrain height at range ℓ, $\eta(\ell)$, the line of sight, and h_R, the height of the radar antenna mounted at an altitude $\xi(0) = X_1$. In the terrain-following geometry, h_0 denotes the additional height above the terrain at which some object is imagined to be following the terrain perfectly. The two geometries of Figure 8.1 differ in how the line-of-sight curve, $\eta(\cdot)$, is determined. In either case, the line of sight $\eta(\ell)$ will be parameterized by a parabolic curve of the

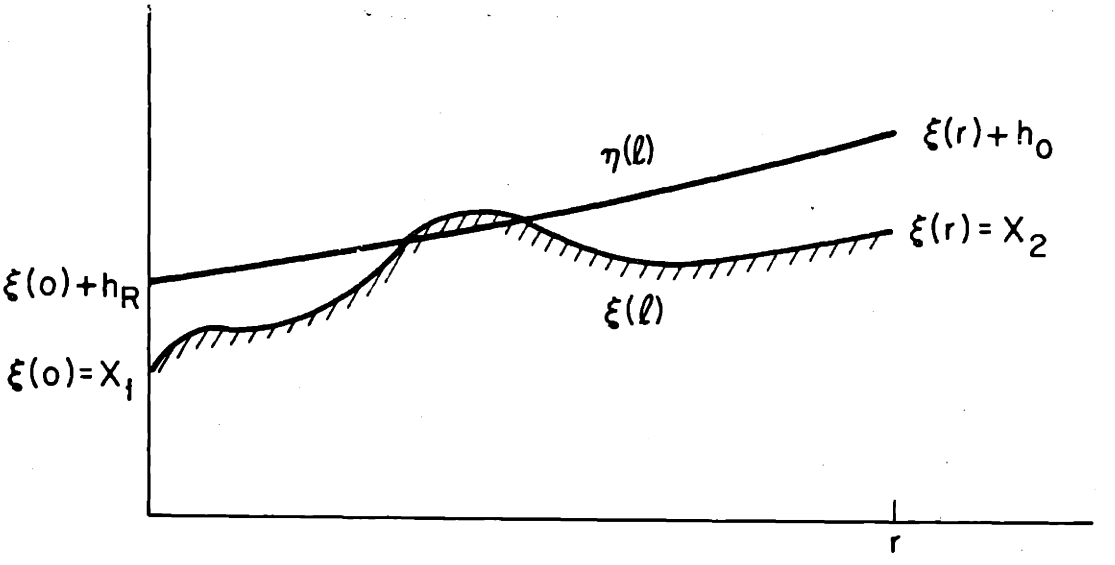

TERRAIN-FOLLOWING GEOMETRY

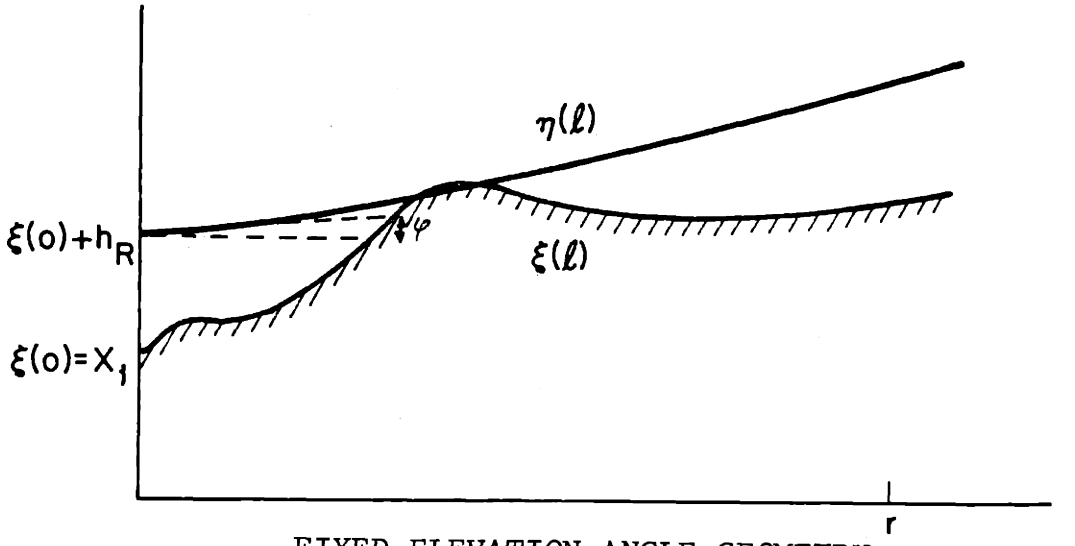

FIXED ELEVATION ANGLE GEOMETRY

Fig. 8.1 One-Dimensional Masking Geometries

form

$$\eta(\ell) = S\ell + \frac{\ell^2}{2R_e} + X_1 + h_R, \tag{8.1}$$

where S denotes the slope of the L.O.S. at the radar and R_e is the earth's radius in kilometers. The description (8.1) implies that

$$\eta(0) = X_1 + h_R, \tag{8.2}$$

i.e., the curve begins at the radar antenna, and

$$\eta''(0) = \frac{1}{R_e} . \tag{8.3}$$

Equation (8.3) is a reflection of the fact that since in our masking geometry, we assume a flat earth, we must curve the line of sight to approximately account for the effect of the earth's curvature. When the range from the radar, r, is sufficiently small, we may neglect the quadratic term in (8.1).

In the case of the terrain-following masking geometry, we imagine that the radar is tracking an object that follows the terrain perfectly at some additional height, h_0. Hence, we require the line of sight to pass both through the antenna and the terrain-following object. This geometry

was conceived to analyze the interaction between the terrain statistics, the radar site elevation, X_1, the terrain following height, h_0, the antenna mounting height, h_R, and the object visibility to the radar. Letting the terrain altitude, $\xi(r)$, at the range r of the object being tracked, be equal to X_2, then by imposing the condition

$$\eta(r) = X_2 + h_0, \tag{8.4}$$

we obtain the following equation for the slope parameter S of equation (8.1):

$$S \equiv S(X_1,X_2) = \frac{(X_2 + h_0) - (X_1 + h_R)}{r} - \frac{r}{2R_e} . \tag{8.5}$$

Hence, if we view the <u>range</u>, r, and the <u>radar site altitude</u>, $\xi(0) = X_1$ as <u>fixed</u>, then the slope parameter $S(X_1,X_2)$ is a random variable depending on $\xi(r) = X_2$, and the terrain following geometry is defined by the following L.O.S.:

$$\underline{\text{Terrain Following Geometry L.O.S.}} \qquad \eta(\ell) = S(X_1,X_2)\ell + \frac{\ell^2}{2R_e} + X_1 + h_R \tag{8.6}$$

In the second one-dimensional masking geometry of Figure 8.1, we focus our attention on a single line-of-sight curve, $\eta(\cdot)$, by fixing the slope parameter S as

$$S = \tan\varphi \quad , \tag{8.7}$$

where φ denotes the radar elevation angle. Hence, the fixed elevation angle geometry is defined by the following L.O.S.:

$$\underline{\text{Fixed Elevation Angle Geometry L.O.S.}} \tag{8.8}$$

$$\eta(\ell) = \tan\varphi\ell + \frac{\ell^2}{2R_e} + X_1 + h_R$$

The fixed elevation angle geometry allows us to characterize the effect of terrain statistics, radar site elevation, X_1, and antenna mounting height, h_R, on a fixed line of sight's visibility over some range r, and hence, relates to what a radar operating in the search mode can see over that range. The fact that S is a constant, facilitates the analysis of various measures of visibility associated with the line of sight.

Our analysis will center on three different statistical measures of the masking effect produced by blockages of the line of sight by the terrain, as defined in either the terrain-following or fixed elevation angle geometries. We let $p_c(r|X_1)$ denote the probability that the terrain curve, $\xi(.)$, crosses the line-of-sight curve, $\eta(.)$, at least once over the range $[0,r]$, given that $\xi(0) = X_1$. We then define $\overline{n}_c(r|X_1)$ and $\overline{f}_c(r|X_1)$ as the average number of crossings

between the terrain process and the line-of-sight curve over the range [0,r], and the average fraction of the interval [0,r] that the terrain lies above the line of sight, respectively, given that $\xi(0) = X_1$. We note that the corresponding random variables, $n_c(r)$ and $f_c(r)$ [which are associated with one particular sample path of $\xi(\cdot)$], are related in that both are equal to zero, or greater than zero, simultaneously.

The problems of analyzing $\bar{n}_c(r|X_1)$, $\bar{f}_c(r|X_1)$, and $p_c(r|X_1)$ fall into the general category of level and curve crossing problems for random processes. Hence, we briefly outline the development of work in that area. For a comprehensive survey, the reader should consult the article of Lindsey and Blake [113]. Kac [116] and Rice [114] were the first authors to derive expressions for the average number of crossings per unit time of a given level, for certain restricted classes of processes, that were later shown by Bendat [115] to hold for Gaussian, stationary processes having finite second moments of their power spectral densities. Then, Leadbetter [117] derived expressions for the average number of crossings over a fixed interval between a stationary, Gaussian, process and a fixed deterministic curve, as well as results for the average fraction of the interval that the process spends above the curve.

The results for average frequencies of crossings of a given curve or level are relatively weak, in the sense that they are obtained as first moments of certain random variables. Exact results on containment probabilities, i.e., the probability that a given stationary, Gaussian process stays above a given level or curve are available only for special cases. In [120] Slepian derived upper and lower bounds, and exact results for some special cases, of the probability that a zero mean, Gaussian, stationary process stays non-negative over an interval. Gallager and Helstrom [119] proposed an upper bound for the probability that a Gaussian, stationary process stays above a given fixed curve over an interval.

Deeper results, such as the exact calculation of the probability that a process crosses a given level over some time, given that it starts at a specified value, have been obtained by imposing the additional mathematical structure that the process is Markov. The early work in this area of Darling and Siegert [124] - [125] considered the case of one-dimensional Markov processes, and formulated the derivation of the probability density for the time until the first crossing of a given level, called the first-passage time density, as the solution of either integral equations, or as the

solution to certain Fokker-Planck type partial differential equations. Mehr and McFadden in [123] considered the derivation of first-passage time densities for the case of one-dimensional, conditionally Markov processes, i.e., those processes which are Markov after having been conditioned on starting at a specified value. These authors derived a technique for transforming any curve crossing problem involving a conditionally Markov process to another curve crossing problem involving the standard Weiner process. Finally, Fortet [122] examined the problem of formulating the calculation of the probability that a one-dimensional diffusion process crosses a given fixed curve at least once over an interval, given some starting point, as the solution to an integral equation and a boundary value problem.

Continuing work turned to the extension of techniques for formulating the computation of crossing probabilities to the case of vector Markov processes. In [126] Darling and Siegert presented a general method for computing as the solution of an integral equation, or certain Fokker Planck type partial differential equations, the characteristic function associated with the density of given integral functional of a vector Markov process. In [127] Helstrom used a similar technique

to derive integral equations satisfied by the moment generating function associated with the discrete probability distribution for the number of zero crossings of one component of a stationary, vector Markov process. Finally, Dynkin [132] used the general theory of Markov processes to formulate the problem of computing the containment probability that a given vector Markov process stays inside some region over a period ot time, as the solution of a Fokker-Planck type boundary value problem. In [131], Friedland, et al., give a complete review of bounding techniques for containment probabilities connected with vector Markov processes.

Hence, from the above discussion, the difficulty involved in analyzing level or curve crossing problems varies with the assumptions we are willing to make about the underlying process. In our analysis, we will start with weak assumptions, and make stronger requirements as we progress. Therefore, in what follows, we will first assume that the terrain is modelled as a stationary, Gaussian random process, and draw on the work [112] - [118] on frequencies of curve and level crossings, in order to analyze $\bar{n}_c(r|X_1)$ and $\bar{f}_c(r|X_1)$. We then shift our perspective, by assuming that the terrain may be modelled as the output of a vector Markov process, and use the theory of first-passage times for vector Markov

processes to formulate the exact calculation of $p_c(r|X_1)$.

The presentation of the one-dimensional terrain masking problems in this chapter are organized as follows. In Sections 8.2.1 - 8.2.2, we first analyze $\bar{n}_c(r|X_1)$ and $\bar{f}_c(r|X_1)$ for the terrain-following geometry, when the terrain is modelled by a Gaussian, stationary, random process. We present specific numerical results in Section 8.2.3 for a case where the terrain correlation function is generated by a second-order Markov process. Next, we consider the analysis of the crossing probability, $p_c(r|X_1)$, first in Section 8.3.1 - 8.3.2 for the fixed radar elevation angle geometry and later in Section 8.3.2 for the terrain-following geometry, assuming that the terrain may be modelled as the output of a vector Markov process. In Section 8.3.1, we derive upper and lower bounds on the crossing probability for the fixed elevation angle masking geometry in the case when the terrain is modelled by a one-dimensional Markov process - the Ornstein-Uhlenbeck process, and present the results of specific numerical evaluations of these bounds.

8.2 Analysis of $\bar{n}_c(r|X_1)$, $\bar{f}_c(r|X_1)$ for the Terrain-Following Geometry

Before proceeding to outline the details of the calculation of the mean values $\bar{n}_c(r|X_1)$ and $\bar{f}_c(r|X_1)$, it is necessary to summarize the assumptions that will be made about the random process $\xi(\ell)$, which models the terrain height. We assume that $\xi(\ell)$ is a separable, stationary, Gaussian random process with zero mean, and with correlation function

$$R(\tau) \triangleq E[\xi(x+\tau)\xi(x)] \quad . \tag{8.9}$$

We will denote the spectral distribution function corresponding to $R(\tau)$ by $F(\lambda)$, i.e.,

$$R(\tau) = \int_{-\infty}^{+\infty} e^{i\tau\lambda} dF(\lambda) \quad . \tag{8.10}$$

For the calculation of $\bar{n}_c(r|X_1)$ we will make the additional assumption that the sample functions of $\xi(\ell)$ have first derivatives that are everywhere continuous with probability one. Hunt, in [133], proves that the following are conditions sufficient to guarantee the existence of a process $\bar{\xi}(\ell)$, equivalent to $\xi(\ell)$, with continuously differentiable sample paths:

$$\int_{-\infty}^{+\infty} \lambda^2 \left[\left| \log(1+|\lambda|) \right| \right]^{1+\varepsilon} dF(\lambda) < \infty, \tag{8.11}$$

for some $\varepsilon > 0$, or in the correlation domain,

$$R(\tau) = 1 - \frac{\lambda_2 \tau^2}{2} + 0\left\{\tau^2 \left|\log|\tau|\right|^{-(1+\varepsilon)}\right\} \quad \text{as } \tau \to 0, \tag{8.12}$$

where λ_2 denotes the second moment associated with the spectral distribution function $F(\lambda)$, i.e.,

$$\lambda_2 \triangleq \int_{-\infty}^{+\infty} \lambda^2 dF(\lambda) \tag{8.13}$$

Finally, we remark that while the calculations of this section are directed at a one-dimensional model for the terrain, the results are applicable to the case of a stationary, Gaussian, two-dimensional random field. In this case, we fix our attention on an object approaching the radar along a single ray. Given a two-dimensional correlation function for the terrain field, $R(.,.)$, we can easily calculate the correlation function for the process along any straight line path, and use that result as an input for the calculations described here.

8.2.1 Computation of $\bar{n}_c(r|X_1)$

Prior to analyzing $\bar{n}_c(r|X_1)$, we first note the connection between this quantity and the crossing probability $p_c(r|X_1)$. Let us define the probability of visibility of the object to the radar, given $\xi(0) = X_1$, as

$$p_v(r|X_1) = 1 - p_c(r|X_1) \quad . \tag{8.14}$$

Now, since $\xi(\cdot)$ is modelled as a Gaussian random process, the probability of exact tangencies between the terrain and the line of sight curves is zero [121]. For the terrain following masking geometry, since the line of sight is constrained to be above the terrain at the radar location and at the range r, the crossings between $\xi(\cdot)$ and $\eta(\cdot)$ occur in pairs, as in Figure 8.1. Therefore, since the crossing probability, $p_c(r|X_1)$, is equivalent to the probability that $n_c(r) \geq 2$, given $\xi(0) = X_1$, we may use $\bar{n}_c(r|X_1)$ in forming the simplest Chebyshev upper bound on $p_c(r|X_1)$

$$p_c(r|X_1) \leq \frac{n_c(r|X_1)}{2} \quad , \tag{8.15}$$

or equivalently,

$$p_v(r|X_1) \geq 1 - \frac{\bar{n}_c(r|X_1)}{2} \quad . \tag{8.16}$$

In Appendix 8A we show how the bounding technique of Gallager and Helstrom [119] can be used to obtain a lower bound on $p_c(r|X_1)$.

We now proceed to describe the calculation of $\bar{n}_c(r|X_1)$. The approach is adapted from that of Leadbetter in [118], who rigorously defines the calculation of the expected number of crossings between a random process satisfying the previous assumptions with an arbitrary, continuously differentiable deterministic curve. Our problem is more complex, since the two curves that we are considering are random and statistically related. This follows from the fact that the line of sight, defined by relation (8.6) is determined by $\xi(0)$ and $\xi(r)$, which are both random variables, and are correlated with intermediate terrain heights, $\xi(\ell)$, for $0 < \ell < r$. The calculation of $\bar{n}_c(r|X_1)$ follows from an explicit expression for the number of crossings between the terrain and line of sight curves out to some range r. This expression follows from the fact that for a given deterministic function f(t) which is continuously differentiable, and such that f(t) and f'(t) are not simultaneously zero, the number of zero crossings $n_z(r)$ over the interval [0,r] can be expressed as

$$n_z(r) = \int_0^r \delta\Big(f(t)\Big)\ |f'(t)|\ dt \quad . \tag{8.17}$$

Since equation (8.17) involves the distribution $\delta(\cdot)$, it is a formal relation that follows from the scaling property of delta functions [145]. The $f'(t)$ term serves to normalize the impulse so that each time the integration in (8.17) passes through a zero-crossing, we obtain a new contribution of plus one. Hence, to obtain an expression for $n_c(r)$, we identify $f(t)$ in equation (8.17) with the difference between the line of sight, $\eta(\ell)$, and the terrain, $\xi(\ell)$. By introducing the notation $\eta(X_1,X_2,\ell)$ and $\eta'(X_1,X_2,\ell)$ to emphasize the dependence of the line of sight and line of sight derivative curves on the terminal elevations of the terrain $\xi(0) = X_1$ and $\xi(r) = X_2$, we can express $n_c(r)$ as

$$n_c(r) = \int_{\ell=0}^{r} \delta\Big(\eta(X_1,X_2,\ell) - \xi(\ell)\Big)\Big|\eta'(X_1,X_2,\ell) - \xi'(\ell)\Big|d\ell. \tag{8.18}$$

We determine $\eta(X_1,X_2,\ell)$ and $\eta'(X_1,X_2,\ell)$ from relation (8.6).

To calculate $\bar{n}_c(r|X_1)$, we first consider the calculation of $\bar{n}_c(r|X_1,X_2)$, the expected value of $n_c(r)$ given $\xi(0) = X_1$ and $\xi(r) = X_2$. We then form $\bar{n}_c(r|X_1)$ by averaging

$\bar{n}_c(r|X_1,X_2)$ over the conditional density for $\xi(r) = X_2$ given $\xi(0) = X_1$, $q(X_2|X_1)$, as

$$\bar{n}_c(r|X_1) = \int_{X_2=-\infty}^{+\infty} \bar{n}_c(r|X_1,X_2)\, q(X_2|X_1)\, dX_2 \quad . \tag{8.19}$$

For the sake of emphasis, we will display inside boxes the final relations that define $n_c(r|X_1)$. By using our Gaussian assumption, we can express the conditional density for $\xi(r)$ given $\xi(0) = X_1$ as

$$\boxed{q(X_2|X_1) = \frac{1}{\sqrt{2\pi\sigma_r^2}} \exp\left\{-\frac{1}{2\sigma_r^2}\left(X_2 - \frac{R(r)}{R(0)}X_1\right)^2\right\}} \quad , \tag{8.20}$$

where

$$\boxed{\sigma_r^2 \triangleq R(0)\left[1 - \left(\frac{R(r)}{R(0)}\right)^2\right]} \quad . \tag{8.21}$$

We now focus on evaluating $\bar{n}_c(r|X_1,X_2)$ the conditional expectation of $n_c(r)$ given $\xi(0) = X_1$ and $\xi(r) = X_2$. By examining relation (8.18) for $n_c(r)$, we see that computing $\bar{n}_c(r|X_1,X_2)$ requires the conditional density for $\xi(\ell)$ and $\dot{\xi}(\ell)$ given $\xi(0) = X_1$ and $\xi(r) = X_2$, $p(\cdot,\cdot|X_1,X_2)$. The impulse in relation (8.18) acts to sample the $\xi(\ell)$ variable in the conditional density at $\eta(X_1,X_2,\ell)$. Hence, letting X_3

denote the variable $\dot{\xi}(\ell)$, $\bar{n}_c(r|X_1,X_2)$ is determined as

$$n_c(r|X_1,X_2) = \int_{\ell=0}^{r} \int_{X_3=-\infty}^{+\infty} p\left(\eta(X_1,X_2,\ell),X_3|X_1,X_2\right) |\eta'(X_1,X_2,\ell) - X_3| dX_3 d\ell \quad . \tag{8.22}$$

We next use our Gaussian assumption to first form the conditional density for $[\xi(\ell),\xi'(\ell)]$ given $[\xi(0),\xi(r)]$, and then evaluate the inner integral of relation (8.22) in terms of

$$Q[x] = \frac{1}{\sqrt{2\pi}} \int_{t=x}^{\infty} e^{-t^2/2} dt \quad . \tag{8.23}$$

We note that for two zero mean random vectors Z_1,Z_2 whose joint distribution is Gaussian, the conditional density for Z_1 given Z_2 is specified by the conditional mean and conditional covariance for Z_1 given Z_2 as follows:

$$m_{Z_1|Z_2} = \Lambda_{12}\Lambda_{22}^{-1}Z_2 \quad , \tag{8.24}$$

and

$$\Lambda_{Z_1|Z_2} = \Lambda_{11} - \Lambda_{12}\Lambda_{22}^{-1}\Lambda'_{12} \quad , \tag{8.25}$$

where Λ_{11} and Λ_{22} are the covariance matrices associated with the random vectors Z_1 and Z_2, respectively, and

$$\Lambda_{12} = E[Z_1 Z_2'] \quad . \tag{8.26}$$

We now identify Z_1 and Z_2 as

$$Z_1 \triangleq \begin{pmatrix} \xi(\ell) \\ \dot{\xi}(\ell) \end{pmatrix} \quad , \tag{8.27}$$

and

$$Z_2 \triangleq \begin{pmatrix} \xi(0) \\ \xi(r) \end{pmatrix} \quad . \tag{8.28}$$

If we use the fact that for $\xi(\ell)$ a stationary, Gaussian random process with continuously differentiable sample paths, $\xi(\ell)$ and $\dot{\xi}(\ell)$ are independent random variables,* and

$$E[\xi(x)\dot{\xi}(y)] = -\dot{R}(x-y) \quad , \tag{8.29}$$

we can express the covariance matrices, $\Lambda_{11}, \Lambda_{12}$, and Λ_{22} as follows:

*Independence follows from the fact that $\dot{R}(0) = 0$.

$$\Lambda_{11} = \begin{pmatrix} R(0) & 0 \\ 0 & -\ddot{R}(0) \end{pmatrix} , \tag{8.30}$$

$$\Lambda_{12} = \begin{pmatrix} R(\ell) & R(r-\ell) \\ -\dot{R}(-\ell) & -\dot{R}(r-\ell) \end{pmatrix} , \tag{8.31}$$

and

$$\Lambda_{22} = \begin{pmatrix} R(0) & R(r) \\ R(r) & R(0) \end{pmatrix} . \tag{8.32}$$

If we use the identities (8.24) - (8.25), we find that

$$m_{Z_1|Z_2} = \beta(\ell) Z_2 , \tag{8.33}$$

where $\beta(\ell)$ is a matrix defined by

$$\beta(\ell) \triangleq \left(\begin{array}{c|c} \dfrac{R(0)R(\ell) - R(r)R(r-\ell)}{R^2(0) - R^2(r)} & \dfrac{R(0)R(r-\ell) - R(r)R(\ell)}{R^2(0) - R^2(r)} \\ \hline \dfrac{\dot{R}(r)\dot{R}(r-\ell) - R(0)\ddot{R}(-\ell)}{R^2(0) - R^2(r)} & \dfrac{\dot{R}(r)\dot{R}(-\ell) - R(0)\ddot{R}(r-\ell)}{R^2(0) - R^2(r)} \end{array} \right) , \tag{8.34}$$

and that

$$\Lambda_{Z_1|Z_2} = \left(\begin{array}{c|c} R(0) + \dfrac{\left[\begin{array}{l} 2R(r)R(\ell)R(r-\ell) \\ -R(0)[R^2(\ell) \\ \qquad +R^2(r-\ell)] \end{array}\right]}{R^2(0) - R^2(r)} & \dfrac{\left[\begin{array}{l} R(0)R(\ell)\dot{R}(-\ell) \\ -R(r)R(r-\ell)\dot{R}(-\ell) \\ +R(0)R(r-\ell)\dot{R}(r-\ell) \\ -R(r)R(\ell)\dot{R}(r-\ell) \end{array}\right]}{R^2(0) - R^2(r)} \\ \hline \dfrac{\left[\begin{array}{l} R(0)R(\ell)\dot{R}(-\ell) \\ -R(r)R(r-\ell)\dot{R}(-\ell) \\ +R(0)R(r-\ell)\dot{R}(r-\ell) \\ -R(r)R(\ell)\dot{R}(r-\ell) \end{array}\right]}{R^2(0) - R^2(r)} & -\ddot{R}(0) + \dfrac{\left[\begin{array}{l} 2R(r)\dot{R}(r-\ell)\dot{R}(-\ell) \\ -R(0)[\dot{R}^2(-\ell) \\ \qquad +\dot{R}^2(r-\ell)] \end{array}\right]}{R^2(0) - R^2(r)} \end{array}\right) . \tag{8.35}$$

In the analysis that follows we will let

$$\Delta_{12}(\ell) \triangleq \det\left(\Lambda_{Z_1|Z_2}\right) , \tag{8.36}$$

and

$$\Sigma(\ell) \triangleq \Lambda_{Z_1|Z_2}^{-1} . \tag{8.37}$$

Then, by employing relations (8.33) - (8.37), we may express $p(Z_1|Z_2)$ as

$$p(Z_1|Z_2) = \frac{1}{2\pi \Delta_{12}^{\frac{1}{2}}(\ell)} \exp\left\{-\frac{1}{2}(Z_1 - \beta(\ell)Z_2)' \sum(\ell)[Z_1 - \beta(\ell)Z_2]\right\} . \tag{8.38}$$

Now, by setting

$$Z_1 = \begin{pmatrix} \theta_1 \\ \theta_2 \end{pmatrix}, \tag{8.39}$$

and

$$Z_2 = \begin{pmatrix} X_1 \\ X_2 \end{pmatrix}, \tag{8.40}$$

we may express the conditional density of relation (8.38) as

$$\begin{aligned} p(\theta_1,\theta_2|X_1,X_2) = c(\theta_1,X_1,X_2,\ell)\exp\Bigg\{-\frac{1}{2}\Bigg[\Big\{ & 2\sum_{12}(\ell)[\theta_1 - \beta_{11}(\ell)X_1 - \\ & - \beta_{12}(\ell)X_2] \\ & - 2\sum_{22}(\ell)[B_{21}(\ell)X_1 \\ & + \beta_{22}(\ell)X_2]\Big\}\theta_2 \\ & + \sum_{22}(\ell)\theta_2^2\Bigg]\Bigg\} \end{aligned} \tag{8.41}$$

where

$$c(\theta_1,X_1,X_2,\ell) \triangleq \frac{1}{2\pi\,\Delta_{12}^{\frac{1}{2}}(\ell)} \exp\Bigg\{-\frac{1}{2}\Big[\,\Sigma_{11}(\ell)[\theta_1-\beta_{11}(\ell)X_1-\beta_{12}(\ell)X_2]^2 - 2\,\Sigma_{12}(\ell)[\theta_1-\beta_{11}(\ell)X_1-\beta_{12}(\ell)X_2] \cdot [\beta_{21}(\ell)X_1+\beta_{22}(\ell)X_2] + \Sigma_{22}(\ell)[\beta_{21}(\ell)X_1+\beta_{22}(\ell)X_2]^2\Big]\Bigg\} . \tag{8.42}$$

Now, by completing the square of the exponent in the θ_2 variable, in relation (8.42), we can evaluate the inner integral over the X_3 variable of relation (8.22). Letting

$$\alpha(X_1,X_2,\ell) \triangleq 2\,\Sigma_{12}(\ell)[\eta(X_1,X_2,\ell) - \beta_{11}(\ell)X_1 - \beta_{12}(\ell)X_2] - 2\,\Sigma_{22}(\ell)[\beta_{21}(\ell)X_1 + \beta_{22}(\ell)X_2] \quad , \tag{8.43}$$

and

$$\gamma(X_1,X_2,\ell) \triangleq -\frac{\alpha(X_1,X_2,\ell)}{2\,\Sigma_{22}(\ell)} \quad , \tag{8.44}$$

we can express $\bar{n}_c(r|X_1,X_2)$ from relation (8.22) as

$$\bar{n}_c(r|X_1,X_2) = \int_0^r K(X_1,X_2,\ell)\,d\ell \quad , \tag{8.45}$$

$$K(X_1,X_2,\ell) \triangleq c(\eta(X_1,X_2,\ell),X_1,X_2,\ell)\ \exp\left\{\frac{\alpha^2(X_1,X_2,\ell)}{8\ \Sigma_{22}(\ell)}\right\}$$

$$\cdot\left[\frac{[\eta'(X_1,X_2,\ell)-\gamma(X_1,X_2,\ell)]}{\Sigma_{22}^{\frac{1}{2}}(\ell)}\sqrt{2\pi}\right.$$

$$\cdot\left\{1\ -\ 2Q\left[\frac{\eta'(X_1,X_2,\ell)-\gamma(X_1,X_2,\ell)}{\Sigma_{22}^{\frac{1}{2}}(\ell)}\right]\right\}$$

$$\left.+\ \frac{2\ \exp\left\{-\ \frac{1}{2}\ \frac{[\eta'(X_1,X_2,\ell)-\gamma(X_1,X_2,\ell)]^2}{\Sigma_{22}^{-1}(\ell)}\right\}}{\Sigma_{22}(\ell)}\right], \qquad (8.46)$$

and $c(\theta_1,X_1,X_2,\ell)$, $\alpha(X_1,X_2,\ell)$, and $\gamma(X_1,X_2,\ell)$ are defined by relations (8.42) - (8.44), respectively.

Finally, by combining equations (8.19) and (8.45), we can express the conditional expectation of $n_c(r)$, given $\xi(0) = X_1$, as

$$\bar{n}_c(r|X_1) = \int_{X_2=-\infty}^{+\infty}\int_{\ell=0}^{r} K(X_1,X_2,\ell)q(X_2|X_1)d\ell dX_2\ , \qquad (8.47)$$

where $K(X_1,X_2,\ell)$ is determined by relations (8.42) - (8.44) and (8.46), and $q(X_2|X_1)$ is defined by relations (8.20) - (8.21). The integral of equation (8.47) may be evaluated numerically for specific $R(\cdot)$, r, and X_1 by using standard techniques of approximate multiple integration. We present the results of some sample calculations in Section 8.2.3.

Before proceeding to the analysis of $\bar{f}_c(r|X_1)$, we describe several alternative uses for $\bar{n}_c(r|X_1)$. We first note that the terrain following geometry may also be employed to represent the problem of line-of-sight communication in hilly terrain between spatially separated outposts. In this case, $\bar{n}_c(r|X_1,X_2)/2$ provides us with an upper bound on the probability of not being able to communicate, given that our installations are sited at heights X_1 and X_2, and separated by a range r. Finally, as we mentioned earlier, we can define $n_c(e)$ at some point in the plane $e = (x,y)$, as the number of crossings between the terrain and the terrain-following line-of-sight curves obtained by focusing attention on a one-dimensional slice of the terrain determined by the ray connecting e and the origin. Hence, we can use the result of our previous calculation (8.47) to define $\bar{n}_c(e|X_1)$. Now consider some curve in the plane, C, or some region, A. We can define the fraction of the length m_C, of the curve C, or the fraction of the area m_A, of the region A, that an object

which traverses the curve C, or region A, is masked or unmasked with respect to the radar as

$$f_b(C) \triangleq \frac{\int_C \chi_{(n_c(e)\geq 2)}\,de}{m_C} \quad , \tag{8.48}$$

and

$$f_b(A) \triangleq \frac{\int_A \chi_{(n_c(e)\geq 2)}\,de}{m_A} \quad , \tag{8.49}$$

where

$$\chi_{(n_c(e)\geq 2)} \triangleq \begin{cases} 1 & n_c(e) \geq 2 \\ 0 & \text{otherwise} \end{cases} \quad . \tag{8.50}$$

Then, we may employ our calculation of $\bar{n}_c(e|X_1)$ to derive the following upper bounds on the mean values of $f_b(C)$ and $f_b(A)$, conditioned on a given radar siting height:

$$\bar{f}_b(C|X_1) \leq \frac{\int_C \bar{n}_c(e|X_1)\,de}{2m_C} \quad , \tag{8.51}$$

and

$$\bar{f}_b(A|X_1) \leq \frac{\int_A \bar{n}_c(e|X_1)\,de}{2m_A} \quad . \tag{8.52}$$

If we let C denote the circumference of a disk of radius r

about the radar, we obtain from (8.51) an upper bound on the average fractional blockage of that circumference. Alternatively, if we let C denote some trajectory directed at the radar, then $\bar{f}_b(C|X_1)$ will give us an upper bound on the average fraction of the length of that trajectory over which the object will be visible to the radar. In addition, we may use relation (8.52) to obtain an upper bound on the average fraction of a given region not covered by the radar or, alternatively, an upper bound on the fraction of an area not reachable by some communications installation.

As a final comment, we note that in the case when the event of an excursion of the terrain above the line-of-sight is of low probability, we expect that $\bar{n}_c(r|X_1)/2$ will be a reasonably tight upper bound for $p_c(r|X_1)$. Hence, we can conclude that in this case, the bounds (8.51) - (8.52) will be useful.

8.2.2 Computation of $\bar{f}_c(r|X_1)$

While $\bar{n}_c(r|X_1)$ gives us information about the number of excursions of the terrain above the line-of-sight, the quantity $f_c(r)$ tells us about the length of those excursions. As in the case of $\bar{n}_c(r|X_1)$, the analysis of $\bar{f}_c(r|X_1)$ follows from an explicit expression for $f_c(r)$, the fraction of the range r that the terrain blocks the line of sight, as a function of $\xi(\ell)$, $0 \le \ell \le r$. Letting $U_{-1}(\cdot)$ denote the unit step function, then $f_c(r)$ may be expressed as

$$f_c(r) = \frac{1}{r}\int_0^r U_{-1}[\xi(\ell) - \eta(X_1,X_2,\ell)]d\ell \qquad (8.53)$$

We proceed as in the case of $\bar{n}_c(r|X_1)$ by first forming $\bar{f}_c(r|X_1,X_2)$, the expected value of $f_c(r)$ conditioned on $\xi(0) = X_1, \xi(r) = X_2$, and then by computing $\bar{f}_c(r|X_1)$, the expected value of $f_c(r)$ conditioned on $\xi(0) = X_1$, by averaging over X_2 as

$$\bar{f}_c(r|X_1) = \int_{X_2=-\infty}^{+\infty} \bar{f}_c(r|X_1,X_2)q(X_2|X_1)dX_2 \ . \qquad (8.54)$$

To calculate $\bar{f}_c(r|X_1,X_2)$, we note that the integrand in the definition of $f_c(r)$ is 1 when $\xi(\ell) > \eta(X_1,X_2,\ell)$, and zero otherwise. Hence, we form $\bar{f}_c(r|X_1,X_2)$ as

$$\bar{f}_c(r|X_1,X_2) = \frac{1}{r}\int_0^r \Pr\left\{\xi(\ell) > \eta(X_1,X_2,\ell)\,|\,\xi(0)=X_1,\xi(r)=X_2\right\}d\ell. \quad (8.55)$$

By employing our Gaussian assumption on the terrain process, we need only compute the conditional mean and variance of $\xi(\ell)$ given $\xi(0)=X_1$, $\xi(r)=X_2$ to form $\bar{f}_c(r|X_1,X_2)$ as

$$\bar{f}_c(r|X_1,X_2) = \frac{1}{r}\int_0^r Q\left[\frac{\left(\eta(X_1,X_2,\ell) - E[\xi(\ell)\,|\,\xi(0)=X_1,\xi(r)=X_2]\right)}{\left[\mathrm{Var}[\xi(\ell)\,|\,\xi(0)=X_1,\xi(r)=X_2]^{\frac{1}{2}}\right]}\right] d\ell \ . \quad (8.56)$$

Using the standard relations (8.24) - (8.25) for the conditional statistics of Gaussian random vectors, we find that

$$E[\xi(\ell)\,|\,\xi(0)=X_1,\xi(r)=X_2] = \beta_1(\ell)X_1 + \beta_2(\ell)X_2 \ , \quad (8.57)$$

where

$$\beta_1(\ell) \triangleq \frac{R(0)R(\ell) - R(r)R(r-\ell)}{R^2(0) - R^2(r)} \ , \quad (8.58)$$

and

$$\beta_2(\ell) \triangleq \frac{R(0)R(r-\ell) - R(r)R(\ell)}{R^2(0) - R^2(r)} \ , \quad (8.59)$$

and, finally,

$$\mathrm{Var}[\xi(\ell)\,|\,\xi(0)=X_1,\xi(r)=X_2] =$$

$$R(0) - \left\{\frac{R(0)[R^2(\ell)+R^2(r-\ell)] - 2R(r)R(\ell)R(r-\ell)}{R^2(0) - R^2(r)}\right\} \tag{8.60}$$

We finally note some possible uses for $\bar{f}_c(r|X_1)$. We first observe that $\bar{f}_c(r|X_1)$, from relations (8.54) - (8.55), essentially corresponds to the average value for the probability of the terrain exceeding the line of sight, over the range r. Hence, $\bar{f}_c(r|X_1)$ allows us to examine the average likelihood of terrain excursions above the line of sight, as a function of range. In addition, we note that there is great current interest in being able to determine the power received from the radar, by some object at a given range and terrain-following height. The solution to this problem by employing standard electromagnetic theory is extremely complex and costly from a computational point of view. We speculate that one may be able to model the average power received as a function of the average fraction of the range over which the line of sight is blocked.

In summary, we note that in Sections 8.2.1 - 8.2.2 we formulated the computation of $\bar{n}_c(r|X_1)$ and $\bar{f}_c(r|X_1)$ when the terrain was modelled as a stationary, Gaussian, random process. The assumption of stationarity was not really necessary for our analysis. The only necessary requirement is the non-singularity of the conditional densities that appear in the calculation of $\bar{n}_c(r|X_1)$ and $\bar{f}_c(r|X_1)$.

8.2.3 Numerical Results for $\bar{n}_c(r|X_1)$, $\bar{f}_c(r|X_1)$ when the Terrain Correlation Function Corresponds to that of Some Second Order Markov Process

In this subsection we present the results of numerical calculations of $\bar{n}_c(r|X_1)$ and $\bar{f}_c(r|X_1)$ when the terrain correlation function is taken as

$$R(\tau) = \sigma^2 \exp\left\{- |\tau| \frac{\delta_2}{\tau_c}\right\}\left[1 + |\tau| \frac{\delta_2}{\tau_c}\right] \quad , \tag{8.61}$$

where δ_2 is a constant chosen so that

$$R(\pm \tau_c) = e^{-1} R(0) \quad . \tag{8.62}$$

Hence, τ_c denotes the correlation length associated with the terrain model (8.61).

In Figs. 8.2 - 8.3, 8.4 - 8.5, and 8.6 - 8.7 we display $\bar{n}_c(r|X_1)/2$ and $\bar{f}_c(r|X_1)$, respectively, for three different terrain models of the form (8.61). In Figs. 8.2 - 8.3 we depict results for a case when

$$\left.\begin{aligned} &\sigma = 10 \text{ m} \quad , \\ \text{and} \quad &\tau_c = 8 \text{ km} \quad , \end{aligned}\right\} \tag{8.63}$$

corresponding to a smooth terrain of the type found in the Great Plains. In Figs. 8.4 - 8.5 we display results for the

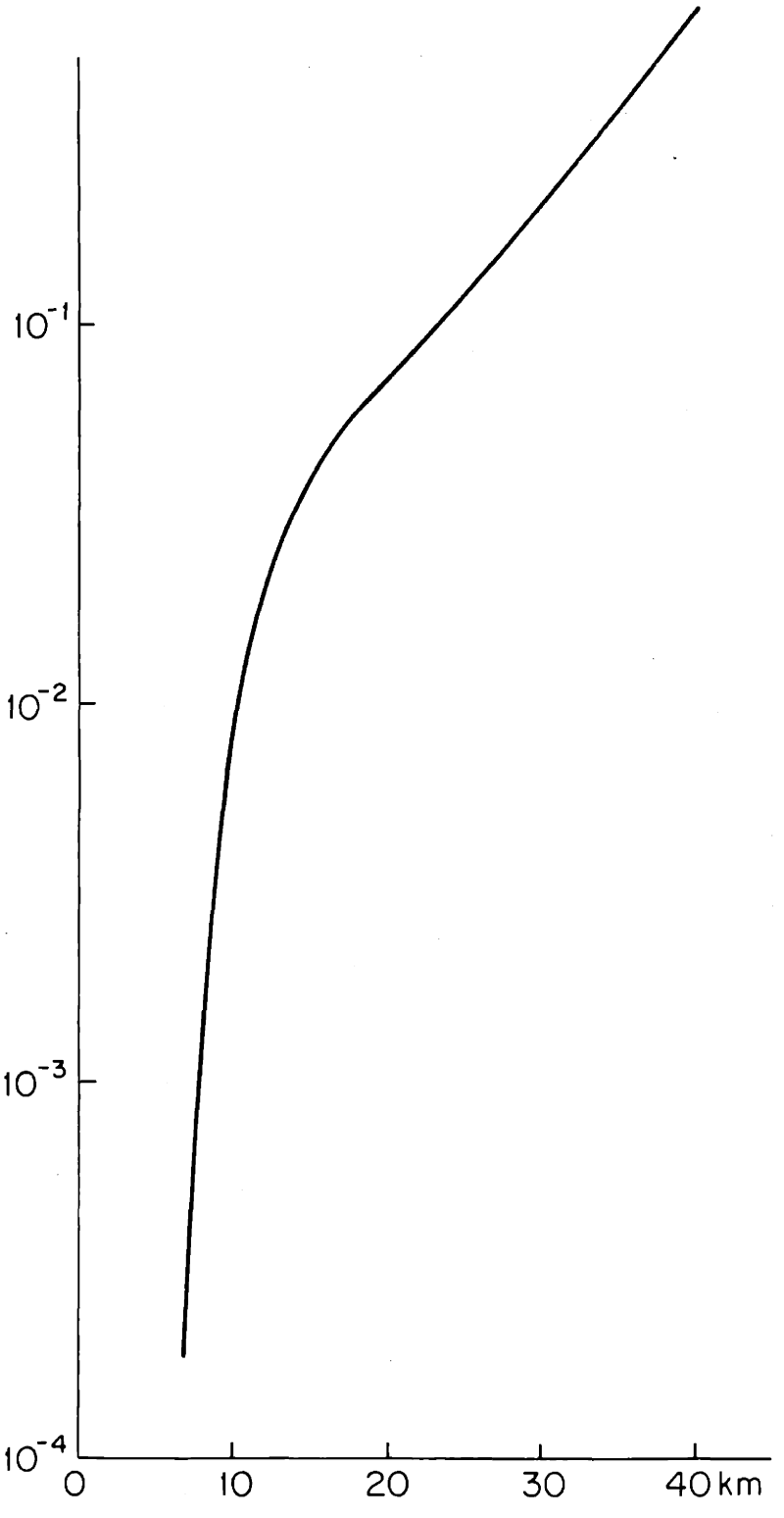

Fig. 8.2 Graph of $\bar{n}_c(r|X_1)/2$ vs. r for a Smooth Terrain Example

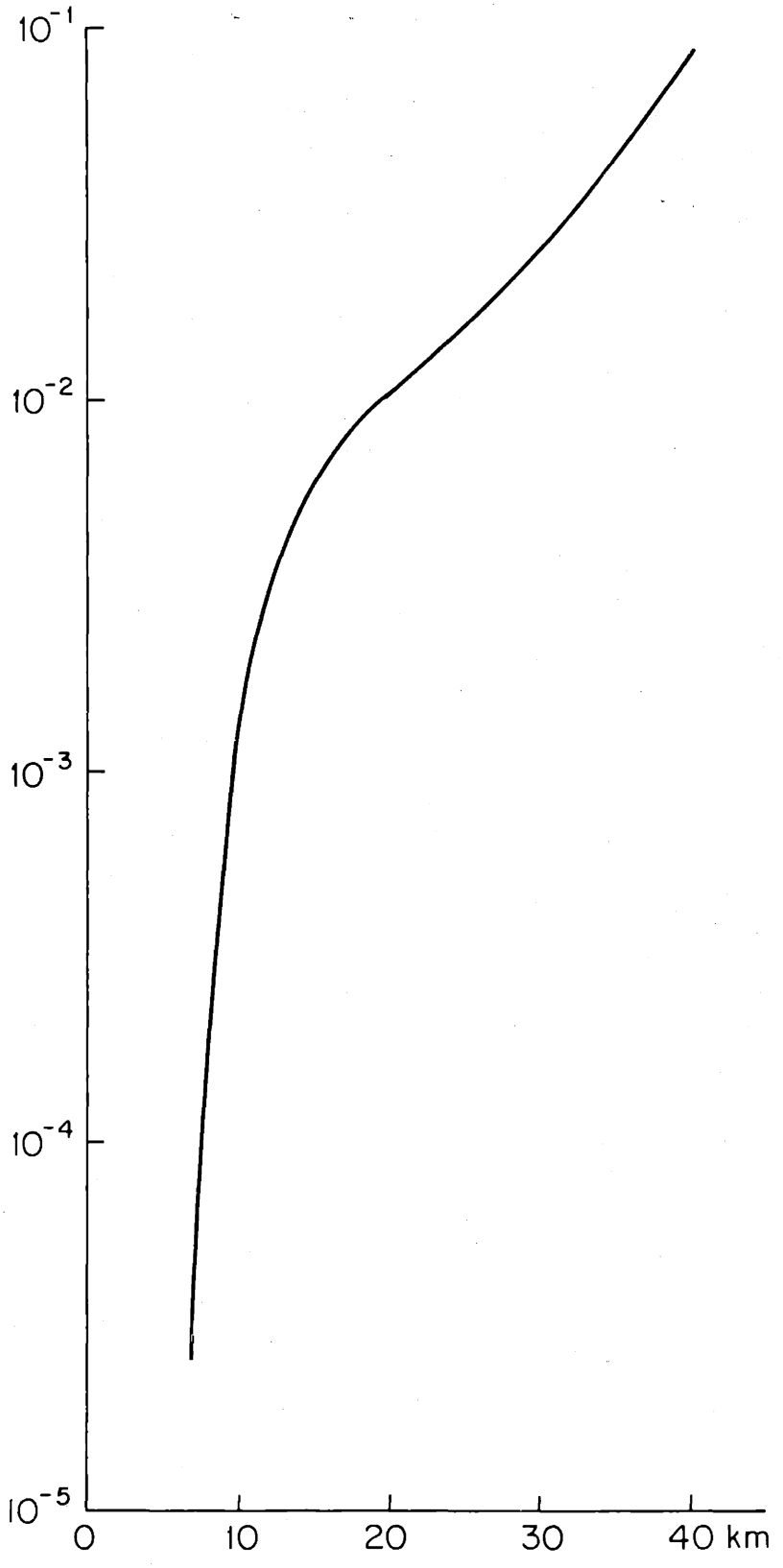

Fig. 8.3 Graph of $\bar{f}_c(r|X_1)$ vs. r for a Smooth Terrain Example

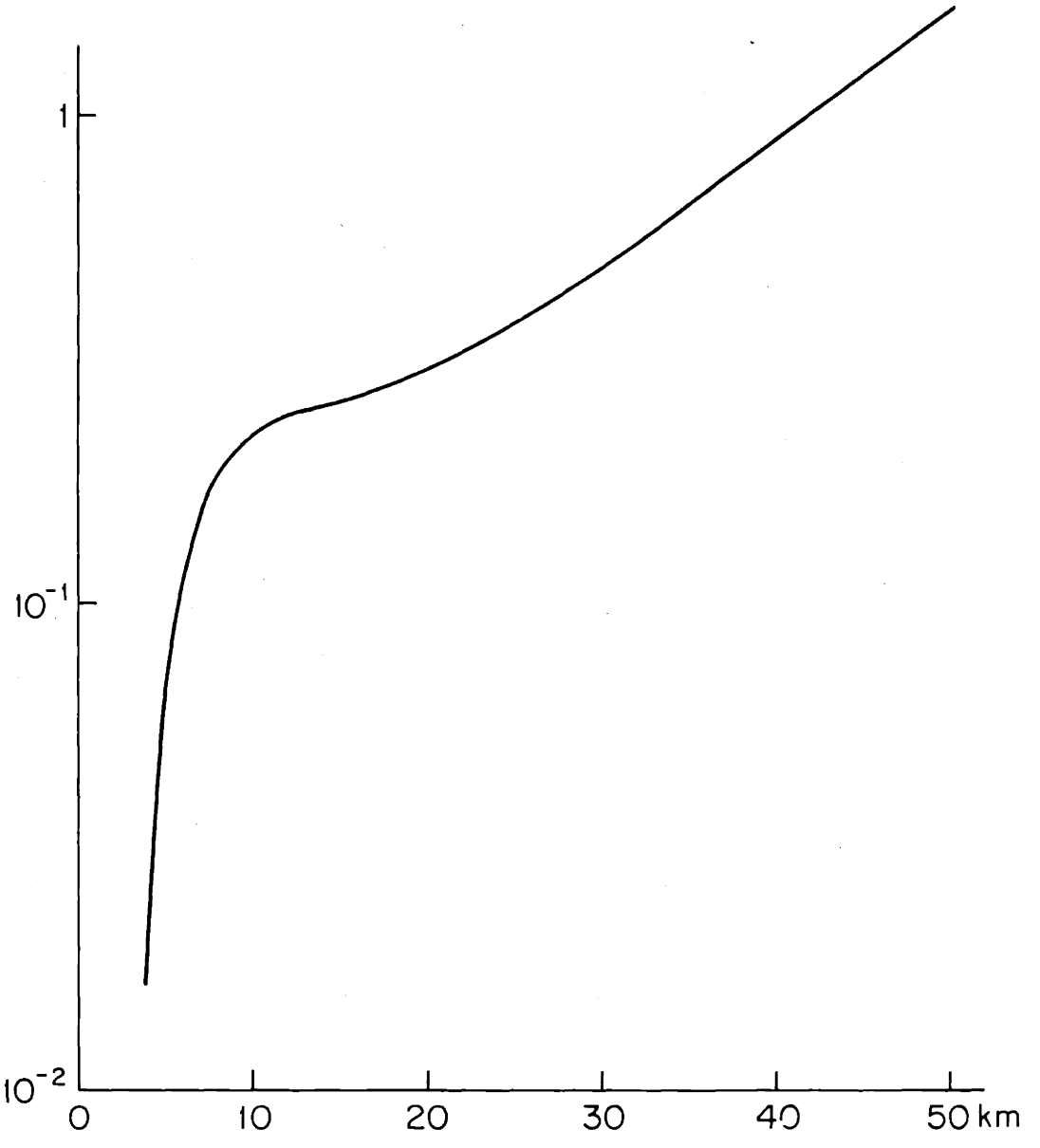

Fig. 8.4 Graph of $\bar{n}_c(r|X_1)/2$ vs. r for a Rolling Terrain Example

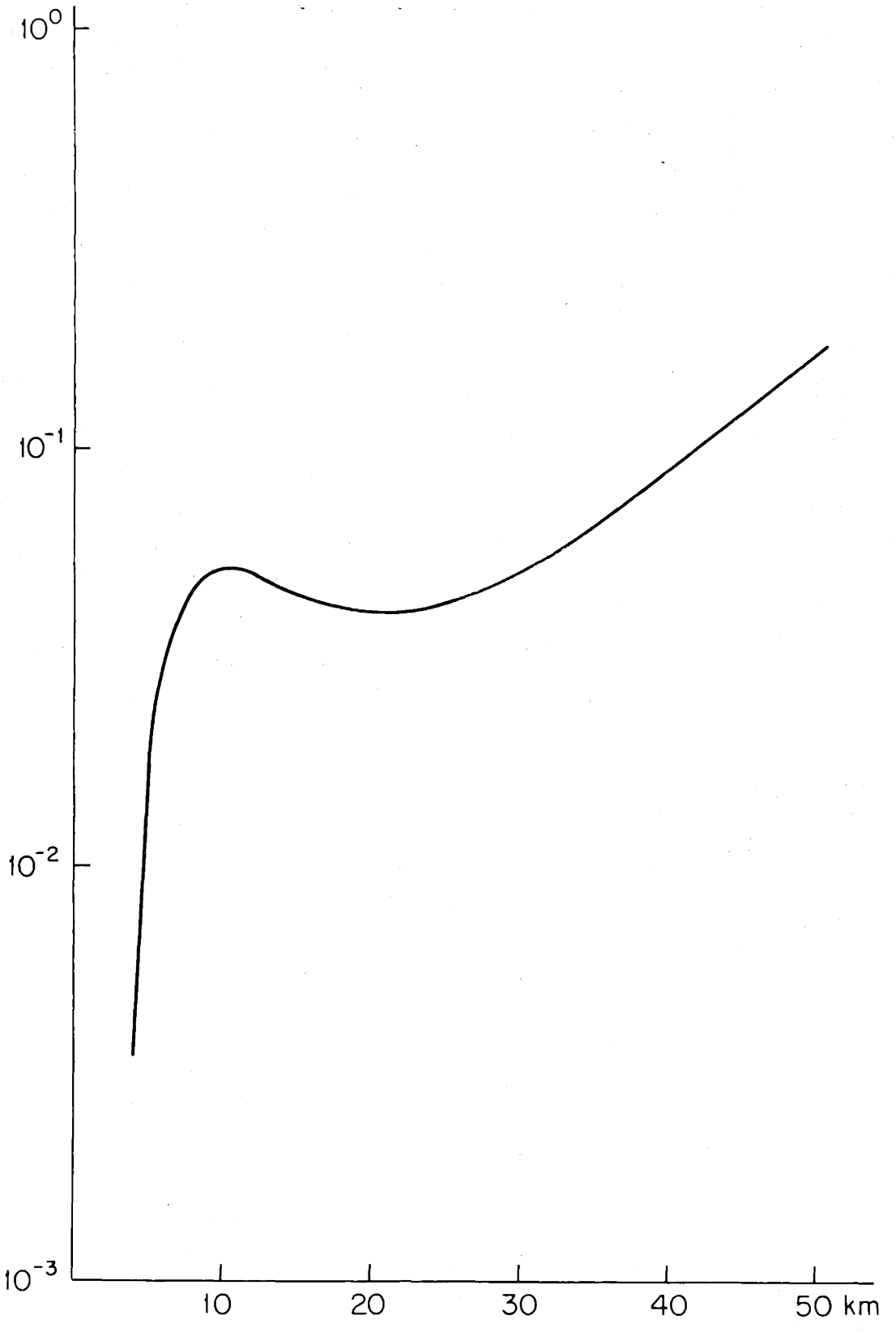

Fig. 8.5 Graph of $\bar{f}_c(r|X_1)$ vs. r for a Rolling Terrain Example

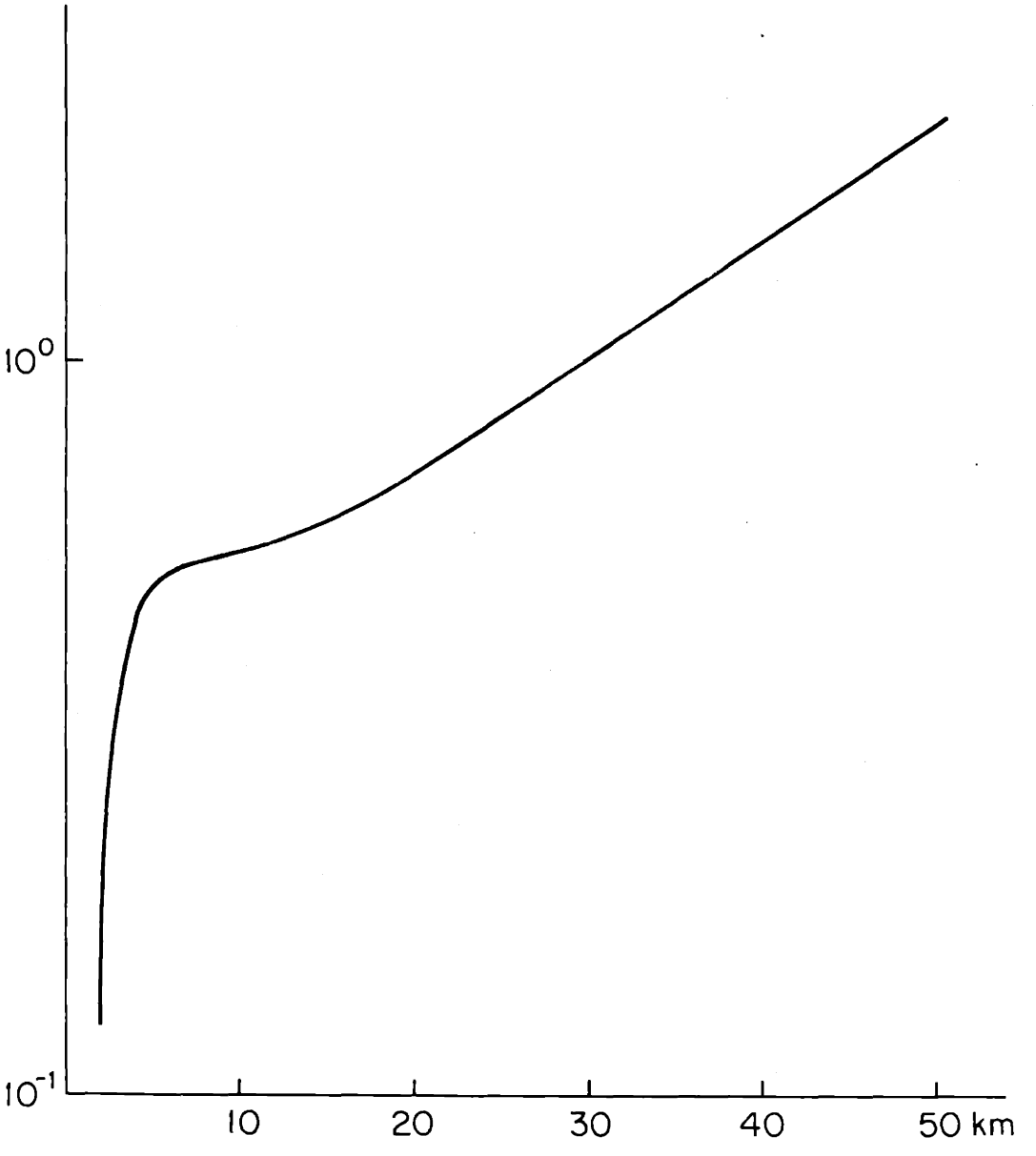

Fig. 8.6 Graph of $\bar{n}_c(r|X_1)/2$ vs. r for a Rough Terrain Example

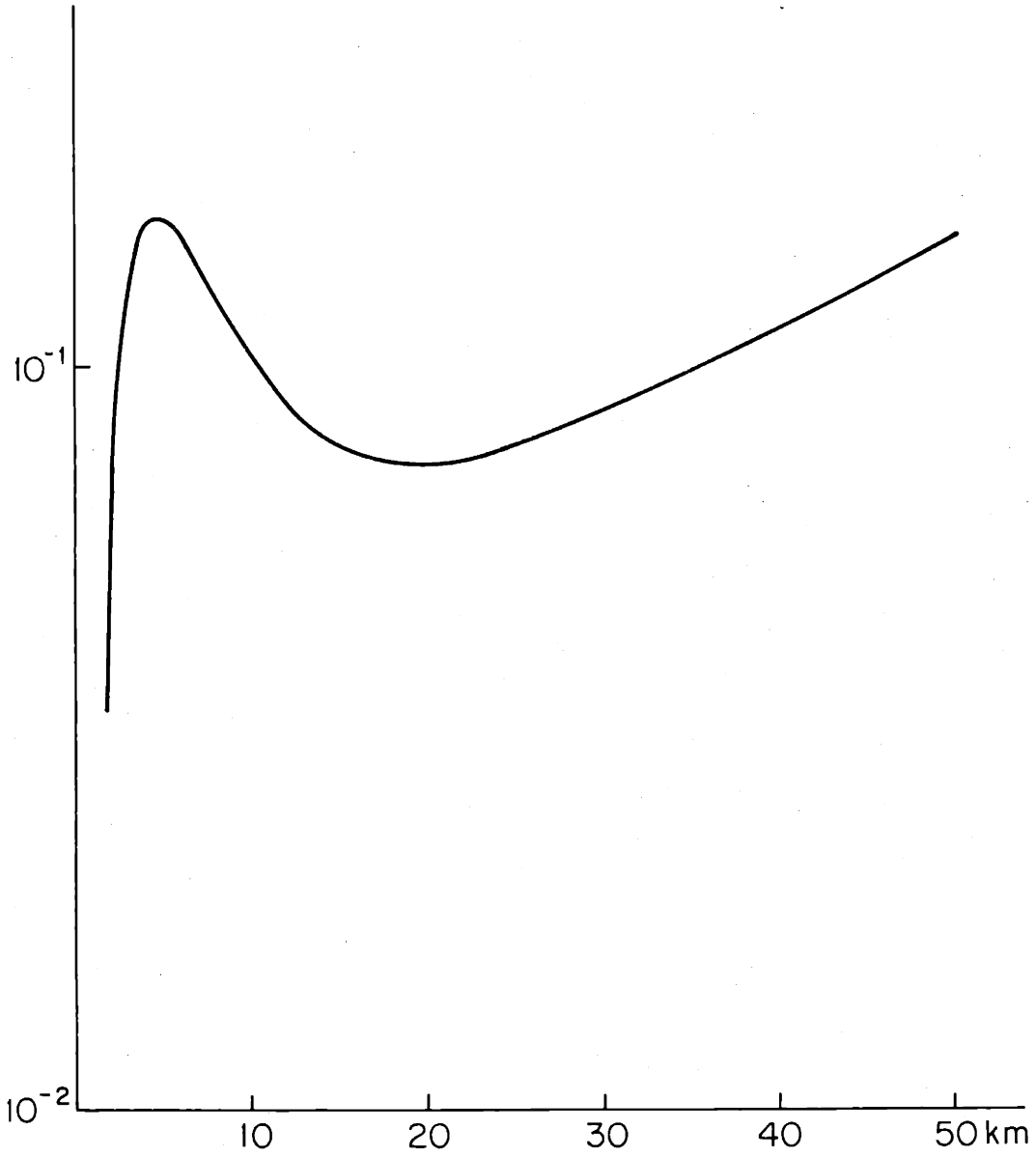

Fig. 8.7 Graph of $\bar{f}_c(r|X_1)$ vs. r for a Rough Terrain Example

case when

$$\left.\begin{aligned} &\sigma = 20 \text{ m} \quad , \\ \text{and} \qquad &\tau_c = 6 \text{ km} \quad , \end{aligned}\right\} \tag{8.64}$$

representing a rolling terrain similar to relatively benign east coast land forms. Finally, in Figs. 8.6 - 8.7 we include results for a rough terrain example for which

$$\left.\begin{aligned} &\sigma = 40 \text{ m} \quad , \\ \text{and} \qquad &\tau_c = 4 \text{ km} \quad , \end{aligned}\right\} \tag{8.65}$$

representing land like that in foothills. In each case we let the radar siting elevation be determined by

$$X_1 = 3.1\,\sigma \quad , \tag{8.66}$$

and set

$$\left.\begin{aligned} &h_R = 10 \text{ m} \quad , \\ \text{and} \qquad &h_0 = 30 \text{ m} \quad . \end{aligned}\right\} \tag{8.67}$$

Relation (8.66) implies that for each example, the radar is sited at an elevation of the same size relative to the magnitude of terrain fluctuations.

We plot $\bar{n}_c(r|X_1)/2$ in Figs. 8.2, 8.4, and 8.6, since as mentioned earlier, this quantity provides an upper bound on the crossing probability, $p_c(r|X_1)$. We expect that this upper bound is tight only over some limited range about the radar, over which such crossings will be low probability events. For larger ranges at which $\bar{n}_c(r|X_1)/2$ exceeds one, we can interpret this quantity as the average number of upcrossings of the terrain curve, above the line-of-sight curve. One can conclude from comparing Figs. 8.2, 8.4, and 8.6 that as we vary the terrain type considered from smooth to rough, it is not sufficient to simply site the radar at a location of the same size relative to terrain fluctuations in order to maintain the same value for our upper bound on the masking probability at a given range, $\bar{n}_c(r|X_1)/2$. This is seen from the fact that in each of our cases, $X_1 = 3.1\sigma$, but due to the increasing variability of the terrains with shorter correlation lengths, there is an increase in $\bar{n}_c(r|X_1)/2$ from Figs. 8.2, 8.4, to 8.6.

We note that while from Figs. 8.2, 8.4, and 8.6 $\bar{n}_c(r|X_1)$ is an increasing function of the range r, from Figs. 8.5 and 8.7, $\bar{f}_c(r|X_1)$ exhibits non-monotonic behavior as the range increases. This is a consequence of the variation of the line-of-sight curve as a function of range. We recall that the terrain-following line-of-sight curve is specified by

$$\eta(\ell) = S\left(\xi(0),\xi(r)\right)\ell + \frac{\ell^2}{2R_e} + \xi(0) + h_R \quad , \tag{8.68}$$

where $$S\left(\xi(0),\xi(r)\right) \triangleq \frac{(h_0 - h_R) + (\xi(r) - \xi(0))}{r} - \frac{r}{2R_e} . \tag{8.69}$$

We observe from (8.68) - (8.69) that conditioning on $\xi(0) = X_1$, $S(\xi(0),\xi(r))$, and thus $\eta(\ell)$, are random variables through their dependence on $\xi(r)$. We can explain the behavior of $\bar{f}_c(r|X_1)$ by examining the behavior of what we will term the average line of sight, $\bar{\eta}(\ell)$, defined by

$$\bar{\eta}(\ell) \triangleq \bar{S}(r)\ell + \frac{\ell^2}{2R_e} + \xi(0) + h_R \quad , \tag{8.70}$$

where $$\bar{S}(r) \triangleq E\left[S\left(\xi(0),\xi(r)\right) | \xi(0)=X_1\right] \quad . \tag{8.71}$$

We now argue that intervals over which $\bar{f}_c(r|X_1)$ is increasing roughly correspond to intervals over which $\bar{S}(r)$ decreases, and conversely that intervals for which $\bar{f}_c(r|X_1)$ decreases roughly correspond to intervals over which $\bar{S}(r)$ increases. The basis for this statement, for a particular terrain sample function, is depicted in Fig. 8.8. We note that as we move from range r_1 to r_2, the radar elevation angle decreases, and hence $S(\xi(0),\xi(r))$ decreases, while the region over which the line of sight is blocked increases from B_1 to B_2, suggesting that $f_c(r_1) < f_c(r_2)$.

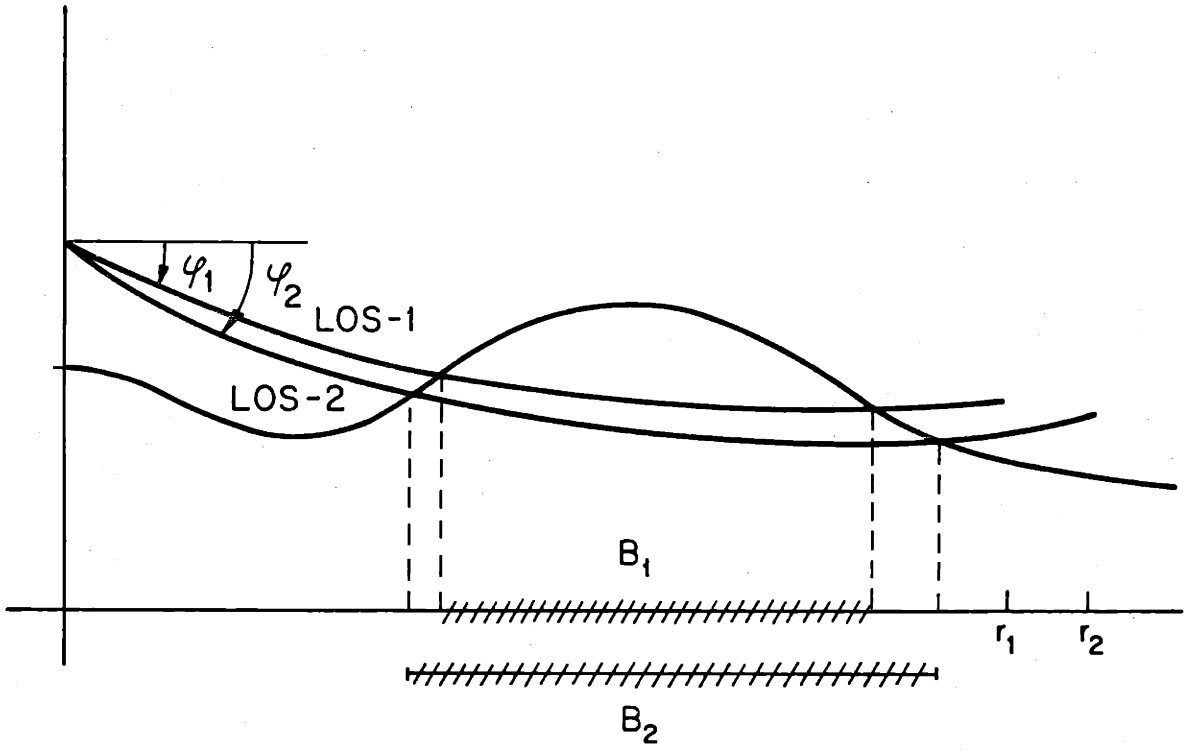

Fig. 8.8 A Depiction of the Change in the Region over which the LOS is Blocked, from Range r_1, to r_2

From the preceding argument, to show that the behavior of $\bar{f}_c(r|X_1)$ in Figs. 8.5, 8.7 is reasonable, we need only demonstrate that it is possible for $\bar{S}(\cdot)$ to initially decrease, then increase, and ultimately decrease. For very small ranges of r, we expect that $E[\xi(r)|\xi(0)] \cong \xi(0)$ and hence

$$\bar{S}(r) \cong \frac{h_0 - h_R}{r} - \frac{r}{2R_e} \quad . \tag{8.72}$$

For small enough r, the first term in (8.72) represents the dominant effect in describing the variation of $\bar{S}(\cdot)$. Hence when $h_0 - h_R > 0$, the case of interest, we expect $\bar{S}(\cdot)$ to be decreasing. We next note that as r becomes larger than several multiplies of the correlation distance, $E[\xi(r)|\xi(0)] \cong 0$, and hence

$$\bar{S}(r) \cong \frac{(h_0 - h_R) - X_1}{r} - \frac{r}{2R_e} \quad . \tag{8.73}$$

For an intermediate range r, and $(h_0 - h_R) < X_1$, we expect the first term in (8.73) to describe the behavior of $\bar{S}(\cdot)$. Hence, relation (8.73) predicts that in this case $\bar{S}(\cdot)$ is increasing. Finally, we note that as r becomes sufficiently large

$$\bar{S}(r) \cong - \frac{r}{2R_e} \quad , \tag{8.74}$$

i.e., the effect of the earth's curvature dominates and thus $\bar{S}(\cdot)$ decreases with increasing range.

We have just argued heuristically why $\bar{f}_c(r|X_1)$ does not vary monotonically as a function of range. The reason why we have not observed similar behavior for $\bar{n}_c(r|X_1)$ is suggested by Fig. 8.8, i.e., it is possible to have sizable variations in $f_c(\cdot)$ without any change in $n_c(\cdot)$. Hence, for the intermediate values of the range r for which $\bar{S}(r)$ is described by (8.73), the derivative of $\bar{n}_c(r|X_1)$ appears to decrease, but $\bar{n}_c(r|X_1)$ itself never decreases.

In this section we have demonstrated that both $\bar{n}_c(r|X_1)$ and $\bar{f}_c(r|X_1)$ may be used to quantify variations in the masking effect with changes in radar siting elevation, and terrain statistical parameters. Together with the lower bound on $p_c(r|X_1)$ of Appendix 8A, we have up to now developed three new analytical tools for characterizing terrain masking.

8.3 Analysis of the Line-of-Sight Crossing Probability

In the current section, we introduce the new assumption, not used in the preceding analysis, that either the terrain itself is a Markov process, or more generally that the terrain can be modelled as one component of a vector Markov process, in order to consider the calculation of the line-of-sight crossing probability $p_c(r|X_1)$, i.e., the probability that the terrain process crosses the line-of-sight curve at least once over some range r given that the radar is located at an elevation $\xi(0) = X_1$.

We begin by examining the calculation of $p_c(r|X_1)$ for the more mathematically tractable fixed radar elevation angle geometry of Fig. 8.1. This mathematical simplification is a consequence of the fact that unlike in the case of the terrain-following geometry, once we condition on a specified radar siting height, the fixed elevation angle line of sight becomes a deterministic function. We first assume that the terrain itself is a one-dimensional Markov process. We will follow an approach originally introduced by Fortet [122] for computing the crossing probability between some general curve Γ and a one-dimensional Markov process. In this context, the crossing probability is obtained as the solution to an integral equation. By solving this integral equation for the crossing probability for a special choice of curves Γ and of the

underlying diffusion process, and by using a technique suggested by Mehr & McFadden [123], we obtain upper and lower bounds for $p_c(r|X_1)$ when the terrain is modelled as the Ornstein-Uhlenbeck process. We finally use some results from the theory of exit times for general vector Markov processes [128] - [132] to formulate the calculation of $p_c(r|X_1)$ in the general case where the terrain is taken to be one component of a vector Markov process. We then show how the same approach may be applied for computing $p_c(r|X_1)$ for the terrain-following geometry.

8.3.1 Analysis of $p_c(r|X_1)$ for the Fixed Elevation Angle Geometry when the Terrain is a One-Dimensional Markov Process

We begin by deriving the integral equation of Fortet [122], for the crossing probability between a one-dimensional diffusion process, denoted by $\zeta(t)$, and a general curve, Γ, specified by $f(t)$. We denote by $P(\tau,y;t,x)$ the transition probability density, i.e., the probability that $\zeta(\tau)=y$ given that $\zeta(t)=x$. Then we define $P_\Gamma(\tau;t,x)$ as the probability that $\zeta(t')=f(t')$ at least once for $t<t'\leq\tau$ given that $\zeta(t)=x$. We assume that $x<f(t)$ and denote by $[z_0,z_1]$ some interval contained in $[f(\tau),\infty]$. We can express the probability that $\zeta(\tau)\in[z_0,z_1]$ given that $\zeta(t)=x$ in the two different ways specified by the right and left-hand sides of the following equality:

$$\int_{z_0}^{z_1} P(\tau,y;t,x)dy = \int_{t'=t}^{\tau}\int_{z_0}^{z_1} P(\tau,y;t',f(t'))dy\, d_{t'}(P_\Gamma(t';t,x)) \tag{8.75}$$

The right-hand side of relation (8.75) performs some averaging over all possible intermediate times t', $t<t'\leq\tau$, at which a curve crossing between $\zeta(\cdot)$ and $f(\cdot)$ occurs. Since $[z_0,z_1]$ is an arbitrary interval contained in $[f(\tau),\infty]$, by changing the order of integration on the right-hand side of relation (8.75), we can prove the following identity:

$$P(\tau,y;t,x) = \int_{t'=t}^{\tau} P(\tau,y;t',f(t'))d_{t'}(P_{\Gamma}(t';t,x)) \ , \tag{8.76}$$

for all $y > f(\tau)$. Assuming that $P_{\Gamma}(t';t,x)$ has a bounded partial derivative with respect to the t' variable, i.e., $P_{\Gamma}(t';t,x)$ may be expressed as

$$P_{\Gamma}(t';t,x) = \int_{t''=t}^{t'} \psi_{\Gamma}(t'';t,x)dt'' \ , \tag{8.77}$$

then the integral equation (8.76) may be reformulated as

$$\boxed{P(\tau,y;t,x) = \int_{t'=t}^{\tau} P(\tau,y;t',f(t'))\psi_{\Gamma}(t';t,x)dt' \ .} \tag{8.78}$$

Equation (8.78) gives us an integral equation for $\psi_{\Gamma}(\cdot;t,x)$, allowing us ultimately to compute the crossing probability through (8.77). We note that in the simple case when our curve $f(\cdot) = a$ and our transition probabilities are stationary, i.e., $P(\tau,y;t,x)$ is only a function of the time difference τ-t, we may integrate y from a to ∞ on both sides of relation (8.78) in order to obtain a convolution equation, which may be solved by using transforms [124].

We now assume, for purposes of simplicity, that the terrain process, $\xi(\cdot)$, is modelled by the Ornstein-Uhlenbeck process, i.e., that the correlation function $R(\tau)$ is specified by

$$R(\tau) = \sigma^2 \, e^{-\alpha|\tau|} \quad . \tag{8.79}$$

We also assume that for the fixed radar elevation angle geometry, the line-of-sight curve $\eta(\ell)$, defined by relation (8.8), may be approximated as

$$\eta(\ell) = \tan\varphi \, \ell + X_1 + h_R \quad . \tag{8.80}$$

Then, we can employ the relation (8.79) to write the transition density, $P(t_2,\xi_2;t_1,\xi_1)$, as

$$P(t_2,\xi_2;t_1,\xi_1) = \frac{1}{\sqrt{2\pi\sigma^2\left(1 - e^{-2\alpha(t_2-t_1)}\right)}} \exp\left\{\frac{-\left(\xi_2 - e^{-\alpha(t_2-t_1)}\xi_1\right)^2}{2\sigma^2\left(1 - e^{-2\alpha(t_2-t_1)}\right)}\right\} \tag{8.81}$$

Finally, we may now substitute $\eta(\cdot)$ for $f(\cdot)$ and use $P(\cdot,\cdot;\cdot,\cdot)$ defined by relation (8.81) to formulate, from equation (8.78), an integral equation for $\psi_{LOS}(t';0,X_1)$, $0 \le t' \le r$. In terms of

$\psi_{LOS}(t';0,X_1)$, we compute the desired crossing probability from relation (8.77) as

$$p_c(r|X_1) = \int_{t'=0}^{r} \psi_{LOS}(t';0,X_1)dt' \quad . \tag{8.82}$$

Since the integral equation (8.78) obtained by identifying $\eta(\cdot)$ with $f(\cdot)$ and determining $P(\cdot,\cdot;\cdot,\cdot)$ from relation (8.81) admits no explicit analytical solution, we use an idea suggested by Mehr and McFadden [123] to reduce our original curve crossing problem between the terrain and line of sight to a new curve crossing problem involving the standard Wiener process, $w(\cdot)$. We then use solutions of the integral equation (8.78) for the case when Γ is a straight line and $\zeta(\cdot) = w(\cdot)$ to obtain some upper and lower bounds for $p_c(r|X_1)$.

The technique of Mehr and Mcfadden is to obtain a representation for the process $\zeta(\cdot)$, conditioned on $\zeta(0) = X$, in terms of the standard Wiener process. The ability to obtain such a representation rests on the fact that any one-dimensional zero mean Gauss-Markov process, $\tilde{\zeta}(\cdot)$, has a correlation function

$$\tilde{R}(t_1,t_2) = \begin{cases} g_1(t_2)g_2(t_1) & t_1 \geq t_2 \\ \\ g_1(t_1)g_2(t_2) & t_1 < t_2 \end{cases} , \tag{8.83}$$

and thus can be represented as

$$\tilde{\zeta}(t) = g_2(t)w\left(\frac{g_1(t)}{g_2(t)}\right) \quad . \tag{8.84}$$

Hence, if we define $\tilde{\zeta}(t)$ as

$$\tilde{\zeta}(t) = \zeta(t) - E[\zeta(t)|\zeta(0)=X] \quad , \tag{8.85}$$

and can show that $\tilde{\zeta}(\cdot)$ has a correlation function of the form (8.83), we can represent $\zeta(t)$, given that $\zeta(0) = X$, as

$$\zeta(t) = E[\zeta(t)|\zeta(0)=X] + g_2(t)w\left(\frac{g_1(t)}{g_2(t)}\right) \quad . \tag{8.86}$$

Now, assuming that the terrain $\xi(\cdot)$ is modelled by the Ornstein-Uhlenbeck process, with correlation function defined by relation (8.79), we can show that the conditional mean for $\xi(t)$ is given by

$$E[\xi(t)|\xi(0)=X_1] = X_1 e^{-\alpha t} \quad , \tag{8.87}$$

and that the correlation function of the zero mean process $\tilde{\xi}(t)$, defined by

$$\tilde{\xi}(t) = \xi(t) - X_1 e^{-\alpha t} \quad , \tag{8.88}$$

is given as

$$\tilde{R}(t_1,t_2) = \begin{cases} \sigma^2\left(1 - e^{-2\alpha t_2}\right)e^{\alpha t_2}\, e^{-\alpha t_1} & t_1 \geq t_2 \\ \sigma^2\left(1 - e^{-2\alpha t_1}\right)e^{\alpha t_1}\, e^{-\alpha t_2} & t_1 < t_2 \end{cases} \quad . \tag{8.89}$$

Hence, from relations (8.83) - (8.86), we can represent $\xi(t)$, conditioned on $\xi(0) = X_1$, as

$$\xi(t) = X_1 e^{-\alpha t} + \sigma\, e^{-\alpha t}\, w(e^{2\alpha t} - 1) \quad . \tag{8.90}$$

By employing the above representation for $\xi(t)$, we now show that our original curve crossing problem between $\xi(\cdot)$ and the line of sight $\eta(\cdot)$, determined by equation (8.80), is equivalent to a curve crossing problem between the standard Wiener process, $w(\cdot)$, and a new curve, which we call $\eta^*(\cdot)$. If we define the transformed time variable s by

$$s \triangleq e^{2\alpha t} - 1 \quad , \tag{8.91}$$

and hence

$$t = \frac{\mathrm{Ln}(s+1)}{2\alpha} \quad , \tag{8.92}$$

we see that crossings between $\xi(\cdot)$ and $\eta(\cdot)$ are equivalent to crossings between w(s) and $\eta^*(s)$, defined by

$$\eta^*(s) \triangleq \frac{\tan\varphi}{2\alpha\sigma}\mathrm{Ln}(s+1)(s+1)^{\frac{1}{2}} + \frac{(h_R + X_1)}{\sigma}(s+1)^{\frac{1}{2}} - \frac{X_1}{\sigma} \; . \tag{8.93}$$

Our original curve crossing problem in the t variable on the interval [0,r] has been mapped into a new curve crossing problem in the s variable on $[0, e^{2\alpha r}-1]$.

We now use properties of the curve $\eta^*(\cdot)$ to motivate the construction of upper and lower bounds to the crossing probability, $p_c(r|X_1)$. When the radar elevation angle φ is positive, a case of practical interest for a radar not sited at a high elevation relative to the size of terrain fluctuations, from relation (8.93) we may prove that $\eta^*(s)$ is an increasing, convex function of s. Hence, $\eta^*(s)$ must lie below the family of tangent lines specified in Fig. 8.9 by $L_u(s')$, for $0 < s' \leq e^{2\alpha r}-1$. In addition, convexity requires that $\eta^*(s)$ lie above the chord L_ℓ connecting $\eta^*(0)$ and $\eta^*(e^{2\alpha r}-1)$. Now let $P_{L_u(s')}(e^{2\alpha r}-1;0,0)$, and $P_{L_\ell}(e^{2\alpha r}-1;0,0)$ denote the solutions of the integral equation

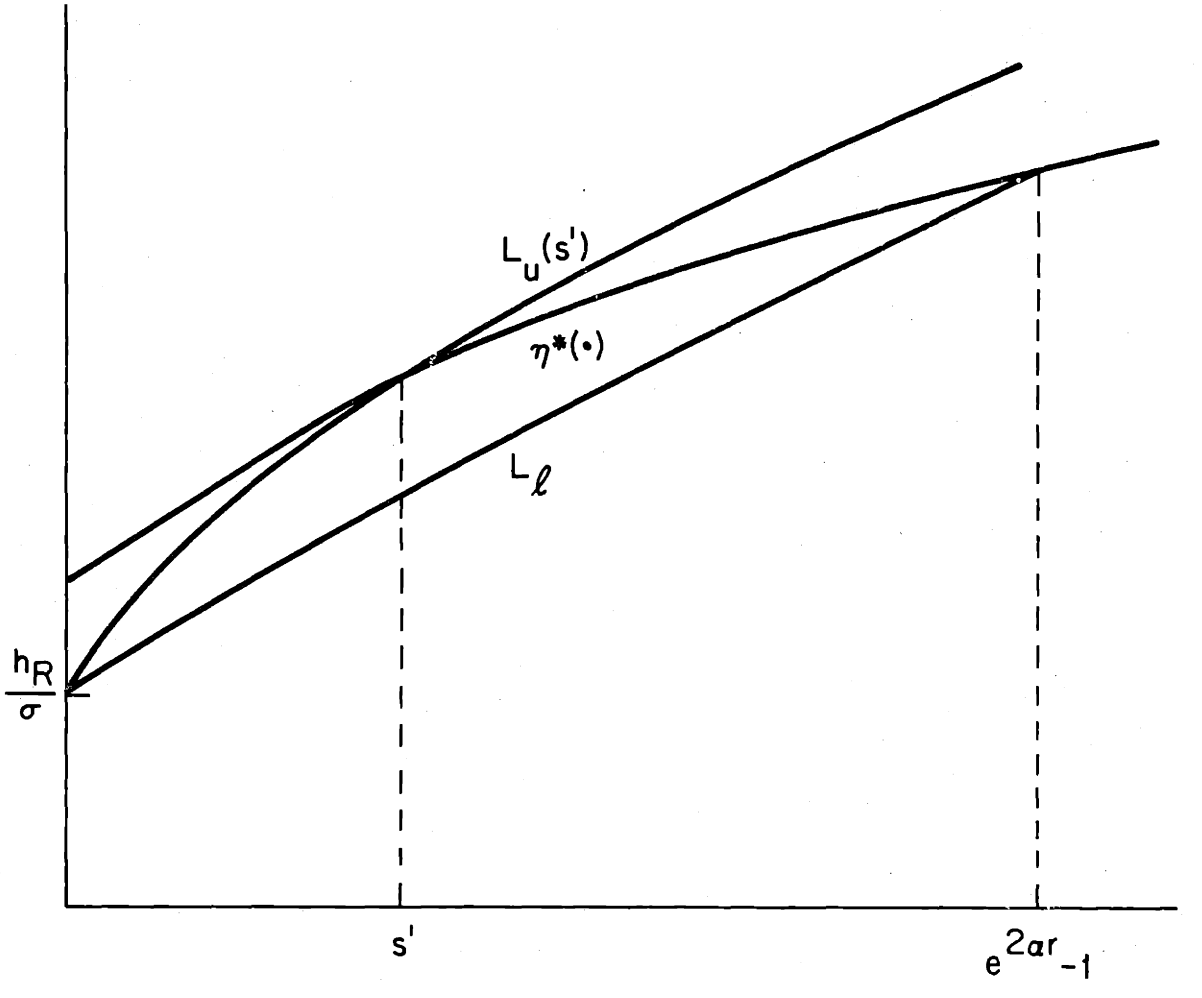

Fig. 8.9 Upper and Lower Bounding Lines for the $\eta^*(\cdot)$ Curve

(8.76), for the crossing probability over the interval $[0,e^{2\alpha r}-1]$, between the standard Wiener process $w(\cdot)$ and the lines $L_u(s')$ and L_ℓ, respectively, then Fig. 8.9 implies the following upper and lower bounds for $p_c(r|X_1)$:

$$\sup_{0 \le s' \le e^{2\alpha r}-1} \left\{ P_{L_u(s')}(e^{2\alpha r}-1;0,0) \right\} \le p_c(r|X_1) \le P_{L_\ell}(e^{2\alpha r}-1;0,0). \quad (8.94)$$

Relation (8.94) indicates that we may obtain upper and lower bounds for $p_c(r|X_1)$ by solving the integral equation (8.76) for the curve crossing probability, $P_{L(b,c)}(t;0,0)$, between the standard Wiener process $w(\cdot)$, and the line with intercept b and slope c, over some time interval $[0,t]$. We may solve for $P_{L(b,c)}(t;0,0)$ by employing the approach suggested in relations (8.77) - (8.78), i.e., we compute $P_{L(b,c)}(t;0,0)$ as

$$P_{L(b,c)}(t;0,0) = \int_0^t \psi_{L(b,c)}(t';0,0)dt' \quad , \quad (8.95)$$

where $\psi_{L(b,c)}(t';0,0)$ satisfies an integral equation of the form specified by relation (8.78). We can verify [123] that $\psi_{L(b,c)}(t';0,0)$ is given by

$$\psi_{L(b,c)}(t';0,0) = \frac{|b|}{\sqrt{2\pi}\, t'^{3/2}} \exp\left\{ -\frac{1}{2} \frac{(ct'+b)^2}{t'} \right\}. \quad (8.96)$$

Finally, we note that the lines $L_u(s')$ are parameterized by letting

$$c_u(s') \triangleq \frac{d}{ds}\,\eta^*(s)\Big|_{s=s'} , \tag{8.97}$$

and $$b_u(s') \triangleq \eta^*(s') - c_u(s')s' , \tag{8.98}$$

and L_ℓ is parameterized by setting

$$c_\ell \triangleq \frac{\eta^*(e^{2\alpha r}-1) - \eta^*(0)}{e^{2\alpha r} - 1} , \tag{8.99}$$

and $$b_\ell \triangleq \eta^*(0) \quad . \tag{8.100}$$

Hence, by evaluating numerically integrals of the form (8.95), with L(b,c) determined by relations (8.97) - (8.100), we can determine the upper and lower bounds to $p_c(r|X_1)$ specified by relation (8.94). Since the upper and lower bounding lines $L_u(s')$ and L_ℓ will approximate the curve $\eta^*(\cdot)$ best for small r, it is reasonable to conclude that our upper and lower bounds on $p_c(r|X_1)$ will be tight over some restricted range of r's.

In Figs. 8.10 and 8.11 we present the results of specific calculations of the upper and lower bounds to $p_c(r|X_1)$ of relation (8.94). The two curves correspond to a smooth ($\sigma = 10$ m, $\alpha^{-1} = 10$ km) and rough terrain ($\sigma = 30$ m, $\alpha^{-1} = 3$ km)

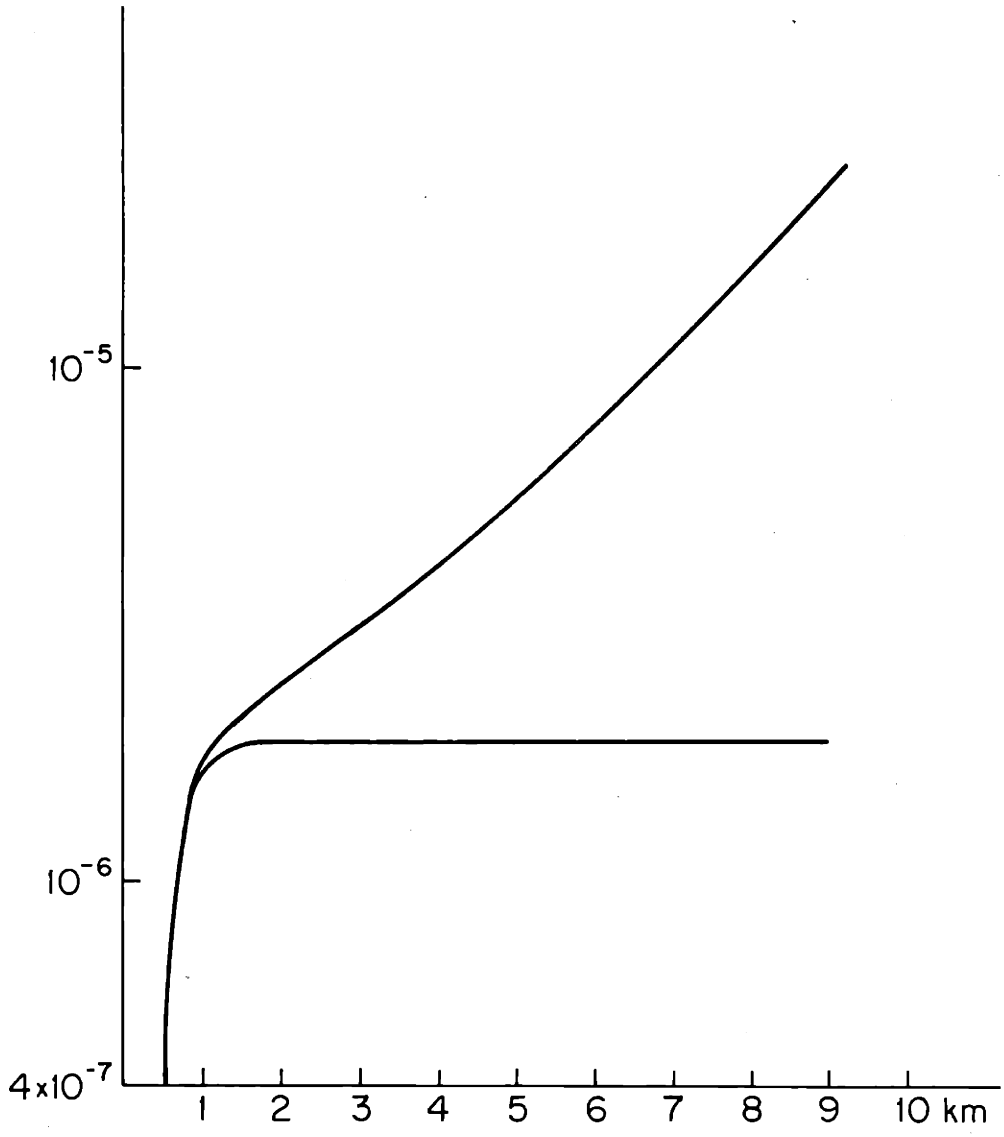

Fig. 8.10 Graph of Upper and Lower Bounds to $p_c(r|X_1)$ vs. r, for a Smooth Terrain Example

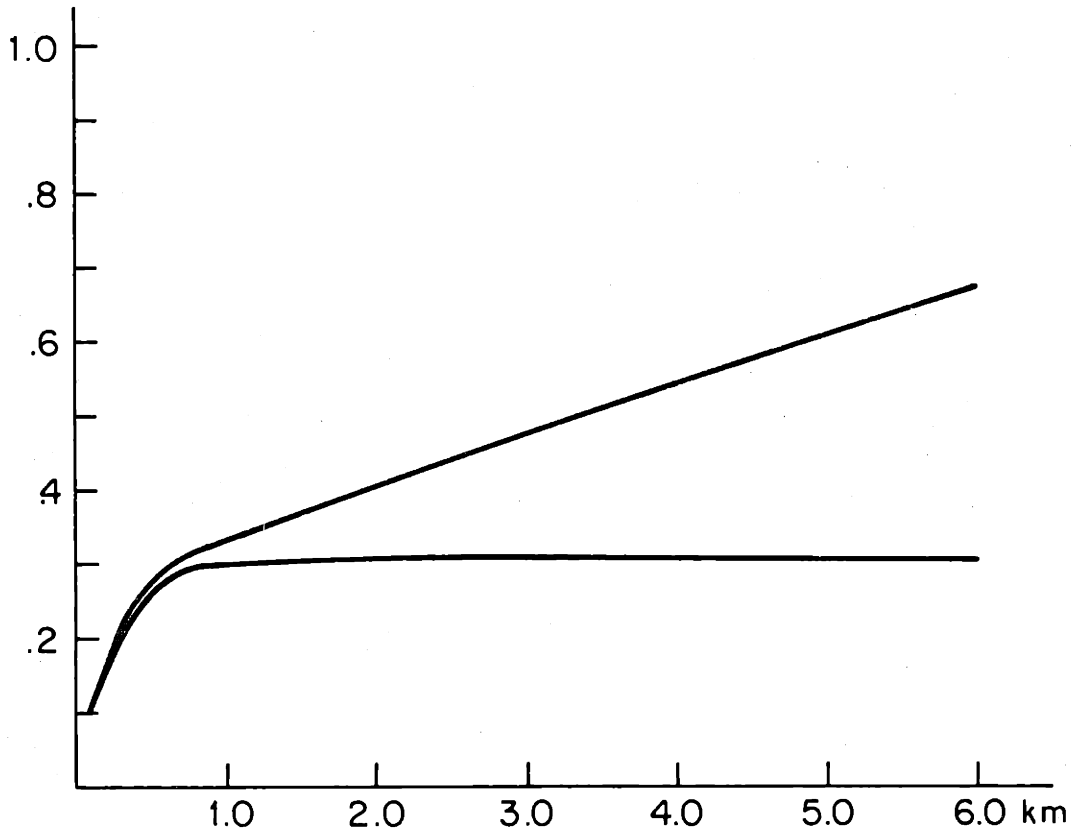

Fig. 8.11 Graph of Upper and Lower Bounds to $p_c(r|X_1)$ vs. r, for a Rough Terrain Example

example, respectively, where the radar siting height is chosen as $X_1 = 2.3\sigma$ in each case. Hence for the same radar elevation, relative to the size of the terrain standard deviation σ, and the same radar elevation angle of $\varphi = .01$ radians, the crossing probabilities of Fig. 8.10 are a factor of 10^{-5} smaller than those of Fig. 8.11. In both cases, as predicted, the upper and lower bounds on $p_c(r|X_1)$ are tight over a limited range. Hence, in future work it is worth investigating the use of the lower bound on $p_c(r|X_1)$ of Appendix 8A, or the use of the alternative bounding techniques of [131].

8.3.2 Computation of $p_c(r|X_1)$ when the Terrain is Modelled as the Output of a Vector Gauss-Markov Process

In this section we assume that $\xi(t)$ may be modelled by

$$\xi(t) = \theta_1(t) \quad , \tag{8.101}$$

where $\theta(t)$ represents a vector Gauss-Markov process, evolving in R^n, according to the following stochastic differential equation:

$$d\theta(t) = A\,\theta(t)\,dt + B\,du(t) \quad , \tag{8.102}$$

with $$\theta(0) = \theta_0 \quad , \tag{8.103}$$

and where $u(\cdot)$ is a standard p-dimensional Wiener process. We rely on results from the theory of exit times for general vector Markov processes, of the diffusion type, to pose the calculation of $p_c(r|\theta_0)$, the probability of a crossing between the terrain and line-of-sight curves over the range $[0,r]$ given $\theta(0) = \theta_0$. This problem will be considered for the fixed radar elevation angle geometry, and the solution that is obtained will be in the form of a particular n-dimensional boundary value problem. We then employ results on pinned, vector Markov processes to

similarly pose the calculation of $p_c(r|\theta_0,\theta_r)$, the probability of a crossing between the terrain and line-of-sight curves given $\theta(0) = \theta_0$ and $\theta(r) = \theta_r$, for the terrain following masking geometry. The desired crossing probability, $p_c(r|X_1)$, can then be derived from either $p_c(r|\theta_0)$ or $p_c(r|\theta_0,\theta_r)$ by appropriate averaging operations.

Calculation of the Crossing Probability for the Fixed Elevation Angle Geometry

We prove in Appendix 8B a result from the theory of exit times for vector Markov processes, of the diffusion type, that we will employ to formulate the calculation of $p_c(r|\theta_0)$ for the fixed elevation angle geometry. Let x(t) be an n-vector Markov process described by the stochastic differential equation

$$dx(t) = a(t,x(t))dt + g(t,x(t))du(t) \ , \tag{8.104}$$

with $$x(0) = x_0 \ . \tag{8.105}$$

We note that a(t,x(t)) specifies an n-vector while g(t,x(t)) denotes an n x p matrix. Let D denote some not necessarily bounded region in R^n and ∂D denote the boundary of that region. Then we define τ as the first time the process x(t) hits the boundary ∂D. If x(t) fails to collide with ∂D in any finite time, we will say that $\tau = \infty$. Finally, letting $\varphi(x,t)$ denote

some scalar function of the n-vector x and time t, twice differentiable in x, we define the Kolmogorov operator $\mathcal{L}$ by

$$\mathcal{L}\varphi(x,t) = \varphi_x'(x,t)a(t,x) + \frac{1}{2}\mathrm{tr}\left\{g(t,x)g'(t,x)\varphi_{xx}(x,t)\right\}, \quad (8.106)$$

where $\varphi_x'(x,t)$ denotes the gradient vector, and $\varphi_{xx}(x,t)$ denotes the Hessian matrix. The result that we prove in Appendix 8B is that, if we assume that the solution of the boundary value problem

$$\mathcal{L}U(x,t) = U_t(x,t), \quad \text{for } x \in D, \quad (8.107)$$

$$\text{with} \quad U(x,0) = 0, \quad \text{for } x \in D, \quad (8.108)$$

$$\text{and} \quad U(x,t) = 1, \quad \text{for } x \in \partial D, \quad (8.109)$$

is well defined, then we have

$$U(x_0,t) = \Pr\left\{\tau \le t \mid x(0)=x_0\right\}. \quad (8.110)$$

We now demonstrate how we may employ the boundary value formulation described by relations (8.107) - (8.110) to pose the computation of the crossing probability, $p_c(r|\theta_0)$, for the

fixed elevation angle geometry, when the terrain is modelled as the first component of the vector Markov process defined by relations (8.102) - (8.103). We are able to apply the relations (8.107) - (8.110) by defining a new vector Markov process $\sigma(t)$, given by

$$\sigma(t) \triangleq \begin{pmatrix} \gamma(t) \\ \theta_2(t) \\ \vdots \\ \theta_n(t) \end{pmatrix} , \tag{8.111}$$

where $\gamma(t)$ denotes the difference between the line-of-sight curve, and the terrain process, i.e.,

$$\gamma(t) \triangleq \eta(t) - \theta_1(t) \quad . \tag{8.112}$$

Then, by using (8.112) and the fact that

$$d\gamma(t) = \dot{\eta}(t)dt - d\theta_1(t) \quad , \tag{8.113}$$

we can show that $\sigma(t)$ obeys the following stochastic differential equation:

$$d\sigma(t) = F(t,\sigma(t))dt + J\, du(t) \, , \tag{8.114}$$

where if a_{ij} and b_{ij} denote the (i,j)-th elements of the matrices A and B, respectively, in (8.102), we have

$$F_1(t,\sigma(t)) \triangleq \dot{\eta}(t) - a_{11}(\eta(t) - \sigma_1(t)) - \sum_{j=2}^{n} a_{1j}\sigma_j(t) \ , \tag{8.115}$$

$$F_i(t,\sigma(t)) \triangleq a_{i1}(\eta(t) - \sigma_1(t)) + \sum_{j=2}^{n} a_{ij}\sigma_j(t), \text{ for } n \geq i \geq 2, \tag{8.116}$$

and J is defined as

$$J \triangleq \begin{pmatrix} -b_{11} & \cdots & -b_{1p} \\ b_{21} & \cdots & b_{2p} \\ b_{n1} & \cdots & b_{np} \end{pmatrix} \ . \tag{8.117}$$

Hence, we can describe our original curve crossing problem as an exit time problem in the space of the σ_i's, where

$$D \triangleq \{\sigma: \sigma_1 > 0\} \ , \tag{8.118}$$

and

$$\partial D \triangleq \{\sigma: \sigma_1 = 0\} \ . \tag{8.119}$$

We now note from relations (8.112) and (8.8) that $\sigma(0)$ is determined as

$$\sigma(0) = \begin{pmatrix} \gamma_0 \\ \theta_{02} \\ \vdots \\ \theta_{0n} \end{pmatrix} \triangleq \sigma_0 \quad , \tag{8.120}$$

where $\gamma_0 = h_R > 0$, and hence $\sigma(0) \in D$.

Hence, by solving a boundary value problem of the type defined by relations (8.107) - (8.109), where D and ∂D are determined by equations (8.118) - (8.119) and the appropriate $a(t,\cdot)$ and $g(t,\cdot)$ are determined by relations (8.115) - (8.117), respectively, we can express the crossing probability, $p_c(r|\theta_0)$, as

$$p_c(r|\theta_0) = U(\sigma_0, r) \quad . \tag{8.121}$$

We note here that the dependence of the crossing probability on the radar siting height, θ_{01}, is derived from the fact that the line-of-sight curve $\eta(t)$, which appears in relations (8.115) - (8.116), is defined as

$$\eta(t) = S\,t + \frac{t^2}{2R_e} + \theta_{01} + \gamma_0 \quad , \tag{8.122}$$

where $S = \tan\varphi$. Finally, given the assumption that $\theta(0)$ is a Gaussian random variable with zero mean and covariance matrix,

$\pi(0)$, we can form the conditional density for $(\theta_{02},\ldots,\theta_{0n})$ given θ_{01} and compute $p_c(r|X_1)$ as

$$p_c(r|X_1) = \int_{-\infty}^{+\infty}\cdots\int_{-\infty}^{+\infty} p_c(r|X_1,\theta_{02},\ldots,\theta_{0n})p(\theta_{02},\ldots,\theta_{0n}|\theta_{01}=X_1) \cdot d\theta_{02},\ldots,d\theta_{0n}. \tag{8.123}$$

Formulation of the Calculation of the Crossing Probability for the Fixed Elevation Angle Geometry when the Terrain is the Ornstein-Uhlenbeck Process

For illustrative purposes, we now formulate the problem of computing the crossing probability, $p_c(r|X_1)$, for the case when the terrain is modelled by the Ornstein-Uhlenbeck process with correlation function (8.79). In this case, we can show that $\xi(t)$ may be modelled by $\theta_1(t)$, where

$$d\theta_1(t) = -\alpha\,\theta_1(t)\,dt + \sqrt{2\alpha}\,\sigma\,du_1(t) \quad , \tag{8.124}$$

with $$\theta_1(0) = X_1 \quad . \tag{8.125}$$

Hence, from relations (8.112) and (8.115) we find that the difference between the terrain and line of sight, $\sigma_1(t)$, can be modelled as

$$d\sigma_1(t) = \left[S + \frac{t}{R_e} + \alpha \left\{ St + \frac{t^2}{2R_e} + X_1 + \sigma_1(0) - \sigma_1(t) \right\} \right] dt - \sqrt{2\alpha}\,\sigma\, du_1(t), \tag{8.126}$$

with $$\sigma_1(0) = h_R \ . \tag{8.127}$$

Then if we let $U(t,\sigma_1)$ denote the solution to the boundary value problem given by

$$\frac{\partial}{\partial t} U(t,\sigma_1) = \left[S + \frac{t}{R_e} + \alpha \left\{ St + \frac{t^2}{2R_e} + X_1 \right\} \right] \frac{\partial}{\partial \sigma_1} U(t,\sigma_1) + \sigma^2 \alpha \frac{\partial^2}{\partial \sigma_1^2} U(t,\sigma_1), \tag{8.128}$$

for $\sigma_1 > 0$, and where

$$U(\sigma_1,0) = 0 \quad , \quad \sigma_1 > 0 \quad , \tag{8.129}$$

and $$U(0,t) = 1 \quad , \tag{8.130}$$

the crossing probability $p_c(r|X_1)$ is given by

$$p_c(r|X_1) = U(r,h_R) \ . \tag{8.131}$$

Calculation of the Crossing Probability for the Terrain-Following Masking Geometry

Through relations (8.114) - (8.119) we demonstrated that we can pose the problem of computing the crossing probability, $p_c(r|\theta_0)$, for the fixed elevation angle geometry, as the solution to a boundary value problem of the form defined by equations (8.107) - (8.109). We now show, by deriving a result on pinned vector Markov processes, that we may use a similar procedure to compute the crossing probability for the terrain-following masking geometry. More specifically, we show how to pose the calculation of $p_c(r|\theta_0,\theta_r)$, the probability of at least one crossing between the terrain and line of sight, as defined by relation (8.6), over the range r, and conditioned on $\theta(0) = \theta_0$, $\theta(r) = \theta_r$.

As in [53], we will first use a martingale decomposition of the process noise du(t) to derive a Markovian realization for $\theta(\cdot)$, conditioned on $\theta(0) = \theta_0$, $\theta(r) = \theta_r$. This conditional realization for $\theta(\cdot)$ is called a pinned Markov process. Our new pinned realization for $\theta(\cdot)$ is then the state-space model that can be used to define a boundary value problem whose solution yields the crossing probability, $p_c(r|\theta_0,\theta_r)$. We finally formulate the boundary value problem for the crossing probability in the case when the terrain is modelled by the Ornstein-Uhlenbeck process.

The pinned model for $\theta(\cdot)$ follows from decomposing $du(t)$ with respect to the σ-field $\mathcal{P}_t$, where

$$\mathcal{P}_t \triangleq \sigma\left\{\chi_t^-, \theta(r)\right\} \quad , \tag{8.132}$$

and $$\chi_t^- = \sigma\{\theta(\tau) \quad 0 \le \tau \le t\} \quad . \tag{8.133}$$

We use the fact that by writing out the solution to (8.102) as

$$\theta(r) = \Phi_A(r,t)\theta(t) + \int_{\tau=t}^{r} \Phi_A(r,\tau)\, B\, du(\tau) \quad , \tag{8.134}$$

we may express $\mathcal{P}_t$ as

$$\mathcal{P}_t = \sigma\left\{\chi_t^-, \tilde{\theta}(r,t)\right\} \quad , \tag{8.135}$$

where $$\tilde{\theta}(r,t) \triangleq \theta(r) - \Phi_A(r,t)\theta(t) \quad . \tag{8.136}$$

We now use the fact that χ_t^- and the σ-field generated by $\tilde{\theta}(r,t)$ are independent, and $du(t)$ is independent of χ_t^-, to express $Bdu(t)$ as

$$Bdu(t) = BE[du(t)|\tilde{\theta}(r,t)] + Bd\tilde{u}(t) \quad , \tag{8.137}$$

where $d\tilde{u}(\cdot)$ is a standard Wiener process. Letting $\pi(r,t)$ denote the covariance matrix associated with $\tilde{\theta}(r,t)$, then $\pi(r,t)$ is determined as

$$\pi(r,t) = \int_{\tau=t}^{r} \Phi_A(r,\tau)BB'\Phi_A'(r,\tau)d\tau \quad . \tag{8.138}$$

Hence, from relations (2.128) - (2.130) we can express $Bdu(t)$ as

$$Bdu(t)=BB'\Phi_A'(r,t)\pi^{-1}(r,t)[\theta(r) - \Phi_A(r,t)\theta(t)]dt + Bd\tilde{u}(t). \tag{8.139}$$

and the pinned model for $\theta(\cdot)$ assumes the form

$$d\theta(t) = \Big\{\Big[A - BB'\Phi_A'(r,t)\pi^{-1}(r,t)\Phi_A(r,t)\Big]\theta(t) + BB'\Phi_A'(r,t)\pi^{-1}(r,t)\theta(r)\Big\}dt + Bd\tilde{u}(t). \tag{8.140}$$

Relation (8.140) now plays the same role as our original model of relation (8.111), i.e., we employ equation (8.140) to determine a vector Markov process model for $\sigma(t)$, defined by relation (2.102). Then the problem of computing $p_c(r|\theta_0,\theta_r)$ for the terrain-following geometry is posed as the problem of computing the collision probability for the $\sigma(t)$ process, starting at some initial condition defined by relation (2.120),

and inside a region D determined by relation (2.118), to hit ∂D specified by relation (2.119). Hence, we employ the boundary value formulation of relations (2.107) - (2.110) to compute the desired collision probability.

Formulation of the Crossing Probability Calculation for the Terrain-Following Geometry, when the Terrain is the Ornstein-Uhlenbeck Process

We finally illustrate how to formulate the calculation of $p_c(r|X_1,X_2)$ for the terrain-following geometry, when the terrain is modelled by the Ornstein-Uhlenbeck process. By using equations (8.124) - (8.125) and (8.140) we obtain the following pinned model for the terrain process:

$$d\theta_1(t) = \left\{\left[-\alpha - \alpha\,\mathrm{sech}[\alpha(r-t)]\, e^{-\alpha(r-t)}\right]\theta_1(t) + \alpha\,\mathrm{sech}[\alpha(r-t)]\,X_2\right\}dt + \sqrt{2\alpha}\,\sigma\, d\tilde{u}_1(t) \quad , \tag{8.141}$$

where $$\theta_1(r) = X_2 \ . \tag{8.142}$$

Hence, by employing relations (8.141) and (8.112) - (8.113), letting $S(X_1,X_2)$ be defined by (8.5), and noting the expression (8.1) for the line-of-sight curve, we obtain the following stochastic differential equation for the evolution of $\sigma_1(t)$, the difference between the line of sight and the terrain:

$$d\sigma_1(t) = \left\{ S(X_1,X_2) + \frac{t}{R_e} + \left[\alpha + \alpha\,\mathrm{sech}[\alpha(r-t)]e^{-\alpha(r-t)}\right] \right.$$

$$\cdot \left[S(X_1,X_2)t + \frac{t^2}{2R_e} + X_1 + \sigma_1(0) - \sigma_1(t) \right]$$

$$\left. - \alpha\,\mathrm{sech}[\alpha(r-t)]X_2 \right\} dt$$

$$- \sqrt{2\alpha}\,\sigma\, d\tilde{u}_1(t) \quad . \tag{8.143}$$

Finally, if $U(t,\sigma_1)$ denotes the solution to the boundary value problem defined by

$$\frac{\partial}{\partial t}U(t,\sigma_1) = \left\{ S(X_1,X_2) + \frac{t}{R_e} + \left[\alpha + \alpha\,\mathrm{sech}[\alpha(r-t)]e^{-\alpha(r-t)}\right] \right.$$

$$\cdot \left[S(X_1,X_2)t + \frac{t^2}{2R_e} + X_1 \right]$$

$$\left. - \alpha\,\mathrm{sech}[\alpha(r-t)]X_2 \right\} \frac{\partial}{\partial\sigma_1} U(t,\sigma_1)$$

$$+ \sigma^2\alpha \frac{\partial^2}{\partial\sigma_1^2} U(t,\sigma_1) \quad , \tag{8.144}$$

for $\sigma_1 > 0$, and where

$$U(\sigma_1,0) = 0 \quad , \ \sigma_1 > 0 \quad , \tag{8.145}$$

and

$$U(0,t) = 1 \quad , \tag{8.146}$$

the crossing probability, $p_c(r|X_1,X_2)$, is given by

$$p_c(r|X_1,X_2) = U(r,h_R) \quad . \tag{8.147}$$

We may then compute $p_c(r|X_1)$ by averaging $p_c(r|X_1,X_2)$ over the transition density for $\theta(r) = X_2$, given $\theta(0) = X_1$, determined by equation (8.81).

8.4 Conclusion

In this chapter we have defined and computed three different measures of the masking effect, $\bar{n}_c(r|X_1)$, $\bar{f}_c(r|X_1)$, and $p_c(r|X_1)$ for two different one-dimensional masking geometries. In Sections 8.2.1 - 8.2.2 we analyzed $\bar{n}_c(r|X_1)$ and $\bar{f}_c(r|X_1)$ for the terrain-following geometry when the terrain was modelled as a stationary, Gaussian random process. In a completely analogous manner we could analyze these quantities for the fixed elevation angle geometry. In Section 8.2.3 we presented specific results of the computation of $\bar{n}_c(r|X_1)$ and $\bar{f}_c(r|X_1)$, requiring the evaluation of two-dimensional multiple integrals, for a terrain correlation function corresponding to a second order Markov process. The inequality (8.15) shows that $\bar{n}_c(r|X_1)$ can be used to obtain an upper bound on the crossing probability, $p_c(r|X_1)$. A lower bound on $p_c(r|X_1)$ can also be derived and the corresponding analysis is sketched in Appendix 8A.

In Section 8.3 we altered our perspective by making the further assumption that the terrain itself is represented by a Markov process, or more generally that the terrain is obtained as one component of a vector Markov process. In Section 8.3.1 we examined the case when the terrain was modelled as a one-dimensional Markov process and derived an integral equation for the solution of the crossing probability. We considered

the special case when the terrain was the Ornstein-Uhlenbeck process and for the fixed elevation angle geometry we derived and computed some upper and lower bounds on the crossing probability, $p_c(r|X_1)$. These bounds require the evaluation of one-dimensional integrals. Then, in Section 8.3.2, we showed how to formulate the exact computation of the crossing probability, $p_c(r|X_1)$, for both of the two masking geometries, when the terrain is modelled as one component of a vector Markov process. In the case of the fixed elevation angle geometry, the calculation of $p_c(r|\theta_0)$, where

$$\theta_0 = \begin{pmatrix} \theta_{01} \\ \vdots \\ \theta_{0n} \end{pmatrix} \quad , \tag{8.148}$$

necessitates the solution of an n-dimensional, parabolic boundary value problem. Hence, the numerical solution of $p_c(r|\theta_0)$ for sufficiently small n, and the subsequent calculation of $p_c(r|X_1)$, is a possible area for further research. The technique presented in Section 8.3.2 for forming $p_c(r|X_1)$ in the case of the terrain-following masking geometry is probably computationally infeasible, since it requires the solution of an infinite number of parabolic boundary value problems, i.e., we must calculate $p_c(r|\theta_0,\theta_r)$ for all θ_r's and then average

over θ_r to obtain $p_c(r|\theta_0)$, and finally $p_c(r|X_1)$. However, the method presented for computing $p_c(r|X_1)$, for the terrain-following geometry, may have some use in motivating the calculation of suitable upper and lower bounds (see [131] for a discussion of such bounding techniques).

Appendix 8A

Lower Bound on $p_c(r|X_1)$ for the Terrain-Following Geometry

In this Appendix, we use a bounding technique of Helstrom and Gallager [119] to obtain a lower bound on $p_c(r|X_1)$.

We obtain an upper bound on $p_v(r|X_1,X_2)$, the probability that the line of sight remains unblocked over the range r given $\xi(0) = X_1$, $\xi(r) = X_2$ and hence, equivalently, a lower bound on $p_c(r|X_1,X_2)$, the probability of at least one crossing between the terrain and line of sight over the range r, given $\xi(0) = X_1$, $\xi(r) = X_2$. We then use the lower bound on $p_c(r|X_1,X_2)$ to form a lower bound on $p_c(r|X_1)$ by using the identity

$$p_c(r|X_1) = \int_{X_2=-\infty}^{+\infty} p_c(r|X_1,X_2)q(X_2|X_1)dX_2 \quad , \tag{A.1}$$

where $q(\cdot|\cdot)$ denotes the density for $\xi(r)$ conditioned on $\xi(0)$, and is defined by (8.20) - (8.21).

To obtain an upper bound on $p_v(r|X_1,X_2)$, we note that the event of the terrain remaining below the line of sight over the range r given $\xi(0) = X_1$, $\xi(r) = X_2$ is contained in the event that

$$\int_{\tau=0}^{r} \lambda(\tau)[\eta(X_1,X_2,\tau) - \xi(\tau)]d\tau > 0 \quad , \tag{A.2}$$

for all non-negative functions $\lambda(\cdot)$, given $\xi(0) = X_1$, $\xi(r) = X_2$. Hence, by optimizing over the choice of $\lambda(\cdot)$, we obtain the bound

$$p_v(r|X_1,X_2) \leq \min_{\lambda(\cdot)\geq 0}\left[\Pr\left\{\int_{\tau=0}^{r}\lambda(\tau)[\eta(X_1,X_2,\tau) - \xi(\tau)]d\tau > 0 \,\middle|\, \begin{matrix}\xi(0)=X_1,\\ \xi(r)=X_2\end{matrix}\right\}\right]. \tag{A.3}$$

We then define the random variable $\mathcal{Z}$ as

$$\mathcal{Z} = \int_{\tau=0}^{r}\lambda(\tau)\xi(\tau)d\tau \quad , \tag{A.4}$$

to facilitate the evaluation of the probability on the right-hand side of relation (A.3). We note that $\mathcal{Z}$ is a zero mean, Gaussian random variable with

$$E[\mathcal{Z}|\xi(0)=X_1,\xi(r)=X_2] = \int_{\tau=0}^{r}\lambda(\tau)E[\xi(\tau)|\xi(0)=X_1,\xi(r)=X_2]d\tau, \tag{A.5}$$

$$E[\mathcal{Z}^2|\xi(0)=X_1,\xi(r)=X_2] = \int_{\tau_1=0}^{r}\int_{\tau_2=0}^{r}\lambda(\tau_1)\lambda(\tau_2) \cdot E[\xi(\tau_1)\xi(\tau_2)|\xi(0)=X_1,\xi(r)=X_2]d\tau_1 d\tau_2, \tag{A.6}$$

and

$$\mathrm{Var}[\mathcal{Z}^2 | \xi(0)=X_1, \xi(r)=X_2] \triangleq E[\mathcal{Z}^2 | \xi(0)=X_1, \xi(r)=X_2] - \left[E[\mathcal{Z} | \xi(0)=X_1, \xi(r)=X_2]\right]^2. \tag{A.7}$$

Now, by employing the bound in relation (A.3) on $p_v(r|X_1,X_2)$, the relation between $p_v(r|X_1,X_2)$ and $p_c(r|X_1,X_2)$, and (A.4) - (A.7), we obtain the following lower bound on $p_c(r|X_1,X_2)$:

$$p_c(r|X_1,X_2) \geq \max_{\lambda(\cdot)\geq 0} \left\{ Q\left[\frac{\int_{\tau=0}^{r} \lambda(\tau)\eta(X_1,X_2,\tau)\,d\tau - E[\mathcal{Z} | \xi(0)=X_1, \xi(r)=X_2]}{\mathrm{Var}[\mathcal{Z} | \xi(0)=X_1, \xi(r)=X_2]^{\frac{1}{2}}} \right] \right\}. \tag{A.8}$$

Here $Q[\cdot]$ is defined by relation (8.23). Substituting (A.8) into equation (A.1) provides the desired lower bound on $p_c(r|X_1)$.

Appendix 8B

Proof of the Boundary Value Formulation for the Computation of the Crossing Probability

In this Appendix we prove relation (8.110) by applying the Ito-differential rule [48] to the function $U(\tilde{x},\tilde{t}-t)$, where $U(\cdot,t)$ denotes the solution to the boundary value problem determined by equations (8.107) - (8.109). We first note that for a function $\varphi(\tilde{x},t)$, the Ito-differential rule implies that

$$\varphi(\tilde{x}(t),t) - \varphi(x_0,0) = \int_{t'=0}^{t} [\varphi_t(\tilde{x}(t'),t') + \mathcal{L}\varphi(x(t'),t')]dt' + \int_{t'=0}^{t} \varphi'_x(x(t'),t')g(t',x(t'))du(t'). \quad (B.1)$$

Now, by letting

$$\varphi(x,t) \equiv U(x,\tilde{t}-t) , \quad (B.2)$$

we obtain from relation (B.1) that

$$U(x(t),\tilde{t}-t) - U(x_0,\tilde{t}) = \int_{t'=0}^{t} [\mathcal{L}U(x(t'),\tilde{t}-t') - U_t(x(t'),\tilde{t}-t')]dt' + \int_{t'=0}^{t} U'_x(x(t'),\tilde{t}-t')g(t',x(t'))du(t') . \quad (B.3)$$

We recall now that τ denotes the Markov time defined by the first time the process $x(\cdot)$ hits the boundary of the region $D-\partial D$. By defining the Markov time $\tilde{\tau}$ as

$$\tilde{\tau} = \min\{\tilde{t},\tau\} \ , \tag{B.4}$$

letting $t=\tilde{\tau}$ in relation (B.4), and taking the expectation of both sides of equation (B.3) conditioned on $x(0)=x_0$, we will show that we obtain relation (8.110) for the collision probability. Setting $t=\tilde{\tau}$ in relation (B.3), we find that

$$U(x(\tilde{\tau}),\tilde{t}-\tilde{\tau}) - U(x_0,\tilde{t}) = \int_{t'=0}^{\tilde{\tau}} [\mathcal{A}U(x(t'),\tilde{t}-t') - U_t(x(t'),\tilde{t}-t')]dt' + \int_{t'=0}^{\tilde{\tau}} U'_x(x(t'),\tilde{t}-t')g(t',x(t'))du(t'). \tag{B.5}$$

We note now that for $0 \le t' \le \tilde{\tau}$, we have $x(t') \in D$, and therefore from relation (8.107), the integrand of the integral with respect to time in relation (B.5) must vanish. In addition, we note that the process $\mu(t)$ defined by the stochastic integral

$$\mu(t) \triangleq \int_{t'=0}^{t} U'_x(x(t'),\tilde{t}-t')g(t',x(t'))du(t'), \tag{B.6}$$

is a martingale with respect to the increasing family of σ fields $\mathcal{I}_t$, defined by

$$\mathcal{I}_t = \sigma\{x_0, du(t') \quad 0 \le t' \le t\} \quad . \tag{B.7}$$

Hence, since τ is a Markov time with respect to $\mathcal{I}_t$, $\mu[\min(t,\tau)]$ is a martingale with respect to $\mathcal{I}_t$ [48]. By invoking the martingale property for $\mu[\min(t,\tau)]$ we find that

$$E\left[\mu[\min(t,\tau)] \,|\, \mathcal{I}_0\right] = \mu(0) = 0 \quad . \tag{B.8}$$

Hence, by letting $t = \tilde{t}$ in relation (B.8), we have demonstrated that the expectation of the second term on the right-hand side of relation (B.5), conditioned on $x(0) = x_0$, is zero. Therefore, by taking the expectation of both sides of relation (B.5), conditioned on $x(0) = x_0$, we finally obtain the equation

$$E[U(x(\tilde{\tau}), \tilde{t}-\tilde{\tau}) \,|\, x(0)=x_0] = U(x_0, \tilde{t}) \quad . \tag{B.9}$$

We now demonstrate that

$$\chi(\tau \le \tilde{t}) = U(x(\tilde{\tau}), \tilde{t}-\tilde{\tau}) \quad , \tag{B.10}$$

where $\chi(\tau \leq \tilde{t})$ denotes the characteristic function associated with the event that a collision of $x(t)$ with ∂D occurs at some time in the interval $[0,\tilde{t}]$, i.e.,

$$\chi(\tau \leq \tilde{t}) \triangleq \begin{cases} 1 & \tau \leq \tilde{t} \\ 0 & \text{otherwise} \end{cases} . \tag{B.11}$$

For $\tau > \tilde{t}$, $\tilde{\tau} = \tilde{t}$, and

$$U(x(\tilde{\tau}),\tilde{t}-\tilde{\tau}) = U(x(\tilde{t}),0) = 0 \quad . \tag{B.12}$$

The second equality in (B.12) follows from the fact that $x(\tilde{t}) \in D$ and the initial condition imposed by equation (8.108). But for $\tau \leq \tilde{t}$, $\tilde{\tau} = \tau$ and

$$U(x(\tilde{\tau}),\tilde{t}-\tilde{\tau}) = U(x(\tau),\tilde{t}-\tau) = 1 \quad . \tag{B.13}$$

The second equality in relation (B.13) follows from the fact that $x(\tau) \in \partial D$ and the boundary condition imposed by equation (8.109). Hence, we have succeeded in verifying relation (B.10). By employing equation (B.10) in (B.9), the relation (8.110) for the collision probability immediately follows.

Chapter 9

Two-Dimensional Approaches to Terrain-Masking Analysis

9.1 Introduction

In the preceding chapter we introduced three different measures of the masking effect for two one-dimensional masking geometries:

- $\bar{n}_c(r|X_1)$ - The average number of crossings between the terrain and line of sight over a range r,
- $\bar{f}_c(r|X_1)$ - The average fraction of the range r that the terrain exceeds the line of sight, and
- $p_c(r|X_1)$ - The probability of at least one crossing between the terrain and the line of sight over the range r.

These three measures of the masking effect of the random terrain are each conditioned on the height X_1 of the radar location.

In this chapter, we consider the generalization of $\bar{n}_c(r|X_1)$ and $\bar{f}_c(r|X_1)$ for a two-dimensional masking geometry that is analogous to the one-dimensional fixed elevation angle geometry. We do not attempt to generalize the terrain-following masking geometry to two dimensions since that would require the specification of a trajectory for the terrain-following object, and consequently, would be a one-dimensional problem.

We now define a two-dimensional masking geometry that generalizes the one-dimensional fixed elevation angle geometry of the preceding chapter. We will then determine some generalizations of $\bar{n}_c(r|X_1)$ and $\bar{f}_c(r|X_1)$ for this two-dimensional problem. Throughout this chapter we will assume that the two-dimensional terrain process, $\xi(x,y)$, is a stationary, zero-mean, Gaussian random field with correlation function, $R(x,y)$. When necessary, we will impose some additional regularity conditions on the field. We denote the polar coordinates corresponding to (x,y) by (ρ,θ), and then given that $\xi(0,0) = X_1$, we imagine generating a surface of sight $\eta(x,y)$ by rotating the one-dimensional line-of-sight curve, defined by relation (8.8) through a complete revolution about the z axis, i.e.,

$$\eta(x,y) \triangleq X_1 + h_R + q(x,y) \quad , \tag{9.1}$$

where

$$q(x,y) \triangleq \tan\varphi\,\rho + \frac{\rho^2}{2R_e} \equiv \Phi(\rho) \quad . \tag{9.2}$$

Relation (9.1) defines a cone-like surface of sight, where the shape of the cone is specified by the function $q(x,y)$ defined by equation (9.2). We picture this surface of sight and the terrain surface in Fig. 9.1. We note that the idea of a surface of sight is especially appropriate for search radars, which essentially scan the horizon, looking out at some fixed radar

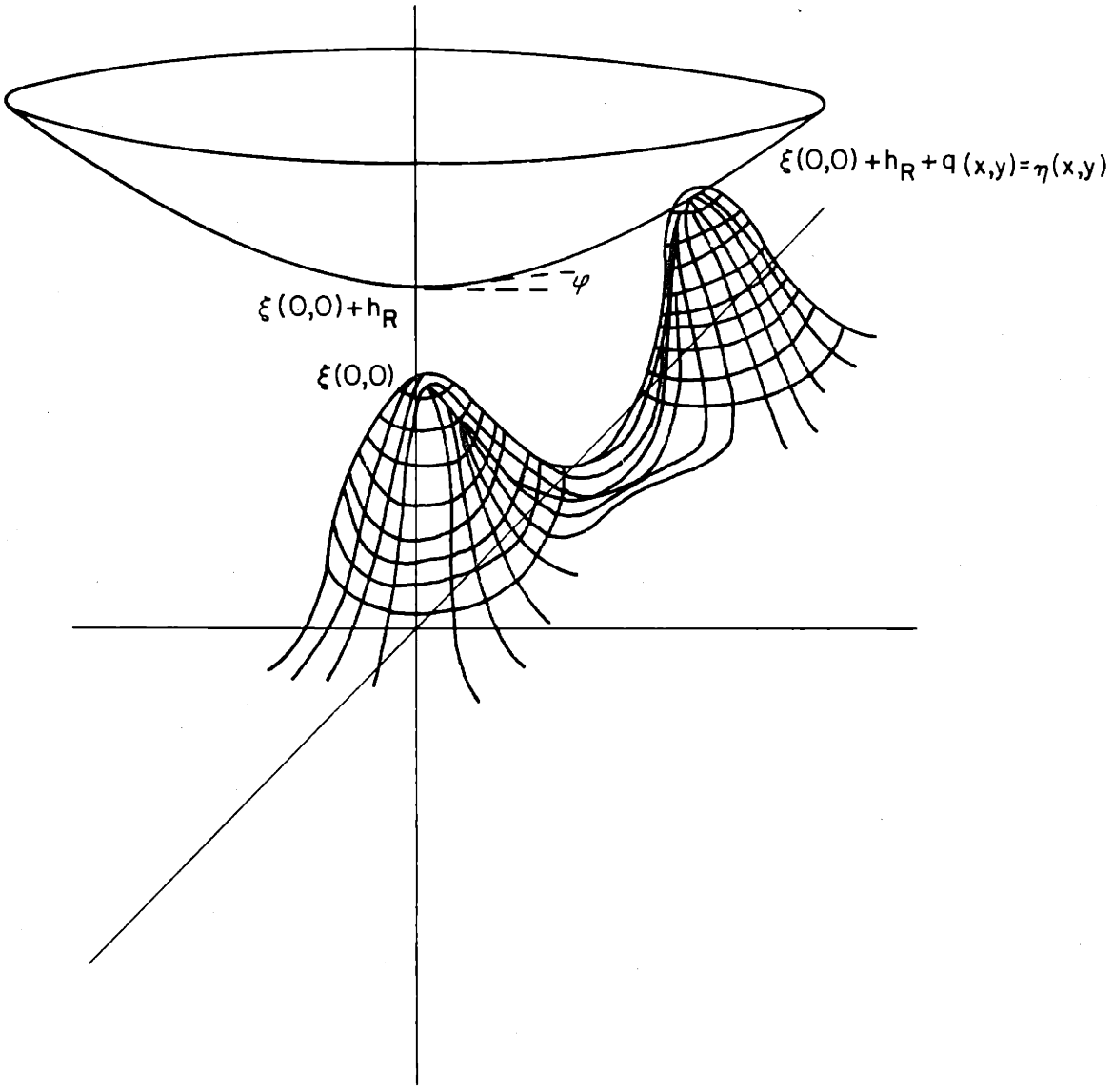

Fig. 9.1 Two-Dimensional Generalization of the Fixed Elevation Angle Geometry

elevation angle. We will call excursion sets the regions in the (x,y) plane where the terrain surface pokes through the surface of sight.

We next let D_r denote the disk of radius r about the radar, i.e.,

$$D_r \triangleq \{(x,y): \quad 0 \leq \rho \leq r\} \quad . \tag{9.3}$$

We then define the excursion set E_r as the set of points in the (x,y) plane, belonging to D_r, where the terrain surface exceeds the surface of sight, i.e.,

$$E_r \triangleq \{(x,y): \ (x,y) \in D_r \quad \text{and} \quad \xi(x,y) \geq \eta(x,y)\} \ . \tag{9.4}$$

Hence, the set E_r pictured in Fig. 9.2, denotes the collection of regions in the (x,y) plane, within a range r of the radar, that the terrain blocks the surface of sight. To generalize $f_c(r)$ to the two-dimensional case, we define $f_c(r)$ as the ratio of the Lesbegue measure of E_r, $m(E_r)$, to the area of the disk D_r, i.e.,

$$f_c(r) = \frac{m(E_r)}{\pi r^2} \quad . \tag{9.5}$$

Therefore, we obtain the following definition of $f_c(r|X_1)$:

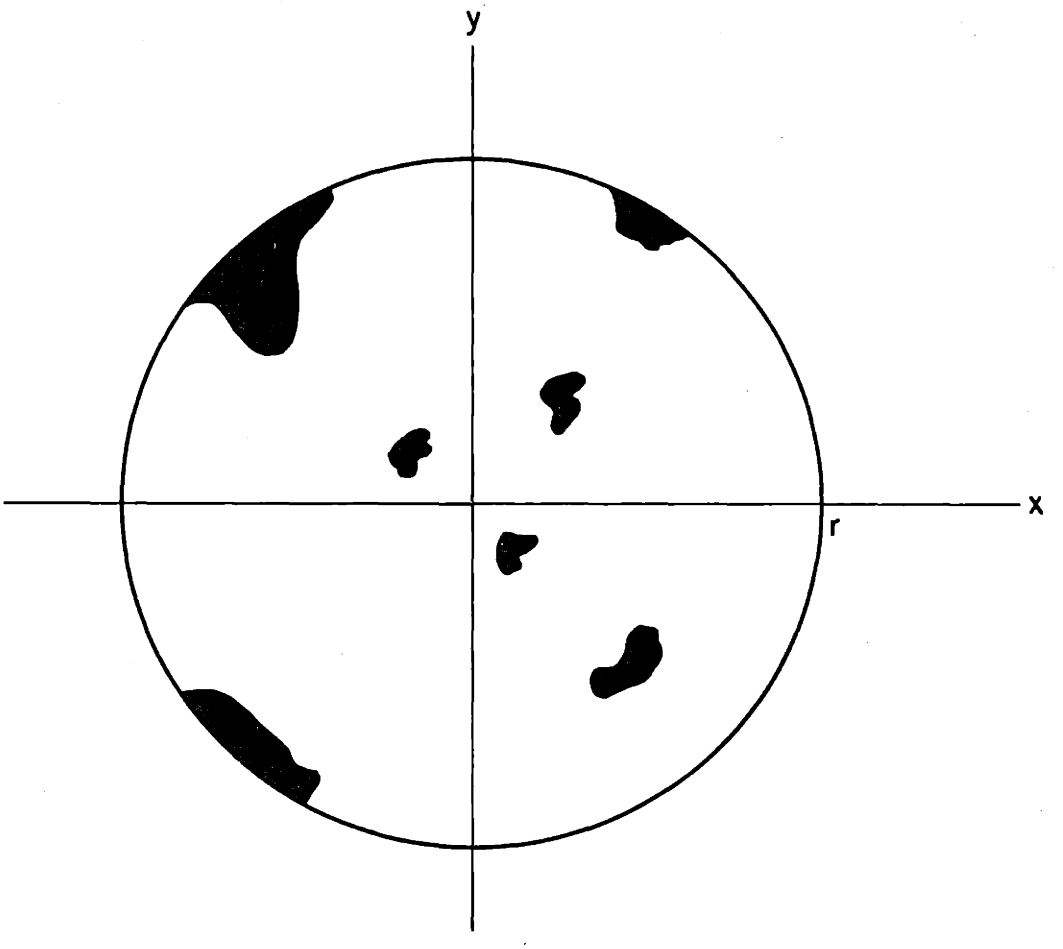

Fig. 9.2 Typical Excursion Set E_r

$$f_c(r|X_1) \triangleq E\left[\frac{m(E_r)}{2\pi r^2}\middle|\xi(0,0)=X_1\right] . \tag{9.6}$$

We now determine an appropriate generalization of $n_c(r)$ to the two-dimensional masking geometry considered here. In one dimension, $n_c(r)$ is related to the number of upcrossings of the terrain curve above the line-of-sight curve. In the case of the one-dimensional fixed elevation angle geometry, when $n_c(r)$ is even, the number of upcrossings is simply $n_c(r)/2$; when $n_c(r)$ is odd, the number of upcrossings is $(n_c(r)-1)/2+1$. Hence, we need to generalize the notion of upcrossings to a random field. In Fig. 9.2 we depict a typical excursion set E_r. For a random field whose sample functions are sufficiently regular (we will define below what we mean by regularity), E_r consists of a finite number of separate pieces, or <u>connected components</u>. By letting $N(E_r)$ denote the number of connected components in E_r we obtain a random variable that generalizes the notion of upcrossings to a two-dimensional setting. Thus, we will let $\bar{N}(E_r|X_1)$, defined by

$$\bar{N}(E_r|X_1) \triangleq E[N(E_r)|\xi(0,0)=X_1] , \tag{9.7}$$

denote the two-dimensional counterpart to $\bar{n}_c(r|X_1)$.

The study of quantities such as $N(E_r)$ and $f_c(r)$ fall into the general family of level and surface crossing problems for random fields. Hence, we briefly outline the work in this area. Longuet Higgins [136], motivated by the study of the statistics of the sea surface, was one of the first authors to analyze a variety of different geometrical characteristics for a two-dimensional, Gaussian, stationary random field. By employing the one-dimensional zero-counting techniques of Kac [116] and Rice [114], and their generalizations, he computed quantities such as the average number of zero crossings along a line, the average length per unit area of contours generated by some fixed level of the field, and the average number density of two-dimensional relative maxima, minima, and saddle points.

Next, Belyaev [137] studied the sets of critical points of a general n-dimensional random field in a rigorous mathematical setting. Let $f(x_1,\ldots,x_k)$ denote some scalar function of k variables, then the critical points are defined as those $a \in R^k$ such that

$$\frac{\partial f}{\partial x_i}(a) = 0 \ , \text{ for } i = 1,\ldots,k \quad . \tag{9.8}$$

Critical points, or alternatively stationary points, are classified as being non-degenerate if the Hessian matrix h(a), whose entries $h_{ij}(a)$ are defined as

$$h_{ij}(a) = \frac{\partial^2 f}{\partial x_i \partial x_j}(a) \quad , \tag{9.9}$$

is nonsingular, and are called degenerate otherwise. The physical signficance of a function $f(x_1,\ldots,x_k)$ having non-degenerate critical points stems from the fact that it has been shown [144] that in this case each critical point is isolated, i.e., we can construct a neighborhood around each stationary point within which there exist no other critical points. In addition, by choosing a small enough neighborhood around a nondegenerate stationary point, we can describe the behavior of $f(x_1,\ldots,x_k)$ by the quadratic function

$$f(a) + \sum_{i,j} h_{ij}\, x_i x_j \quad . \tag{9.10}$$

As an example of a degenerate critical point, consider the one-dimensional function $f(x) = x^3$ at $x = 0$. The behavior of x^3 may not be adequately described by a quadratic function, in any neighborhood of zero. Belyaev [137] derived general conditions on the joint probability density of the second-order derivatives of a given random field, so that with probability one the critical points are all non-degenerate and finite in number over a given bounded region. He also derived conditions on the joint density of the field and its first derivatives to exclude the finite

probability of the tangency of the field to some level. Then, for k-dimensional fields which satisfy the type of regularity conditions that we have described, Belyaev expressed the average number density of relative maxima, minima, and saddle points above some level as some multidimensional integrals.

Other work in the area of random fields level and surface-crossings problems has concentrated on generalizing the idea of upcrossings to a multidimensional setting, and ultimately in obtaining methods for computing the frequency of such upcrossings. We earlier suggested the use of $N(E_r)$, the number of connected components in the excursion set of the terrain surface above the surface of sight, as our generalization of the notion of upcrossings for a random field. Let us similarly define $N(A_u)$ as the number of connected components in the excursion set of some field $f(x,y)$, above the level u, and contained in the region A. Unfortunately, no work has yet demonstrated that $N(A_u)$ is amenable to statistical analysis, i.e., no one has been able to derive the statistics of $N(A_u)$ by employing finite-dimensional distributions of the field such as the joint density for the field and its first and second order derivatives. Therefore, work has centered on deriving excursion measures that are related to $N(A_u)$.

Drawing on ideas from integral geometry and differential topology, Adler and Hasofer [142] have proposed an excursion

characteristic $\chi(A_u)$ that is defined as follows. Allowing s to denote a point in the plane and f(s) the corresponding field value, let us define the set functions $\chi_+(A_u)$ and $\chi_-(A_u)$ by

$$\left.\begin{aligned} \chi_+(A_u) &\triangleq \begin{cases} \text{the number of } s \in A \\ \text{so that} \\ f(s) = u,\ f_x(s) = 0 \\ f_{yy}(s) > 0,\ f_{xy}(s) < 0 \end{cases} , \\ \text{and} \\ \chi_-(A_u) &\triangleq \begin{cases} \text{the number of } s \in A \\ \text{so that} \\ f(s) = u,\ f_x(s) = 0 \\ f_{yy}(s) > 0,\ f_{xy}(s) > 0 \end{cases} . \end{aligned}\right\} \tag{9.11}$$

Then, $\chi(A_u)$ is defined as

$$\chi(A_u) \triangleq \chi_+(A_u) - \chi_-(A_u) \quad . \tag{9.12}$$

The definitions in (9.11) imply that the mean values of $\chi_+(A_u)$ and $\chi_-(A_u)$ may be calculated using the joint density for f(s), $f_x(s)$, $f_{yy}(s)$, and $f_{xy}(s)$, and by employing counting techniques similar to those used in the computation of the frequencies of one-dimensional level crossings. Adler and Hasofer show that $\chi(A_u)$ corresponds exactly to $N(A_u)$ when the following two conditions are satisfied:

(1) Individual connected components of A_u are homeomorphic to the unit disk, and

(2) No excursions occur on the boundary of A.

Condition (2) is self-explanatory. In condition (1), a set homeomorphic to the unit disk is one that has a smooth boundary and no holes. This excludes doughnut-shaped sets of the form depicted in Fig. 9.3, i.e., the counting technique of Adler and Hasofer will not count excursion sets that are "crater"-like. For a complete discussion of $\chi(A_u)$, and an exhaustive presentation of existing results connected with the random fields level-crossing problem, we refer the reader to Adler's book [143].

For our problem, we expect that, in general, neither of the two conditions required for Adler and Hasofer's excursion characteristic to correspond to $N(E_r)$ will be satisfied. This motivates us to follow an approach introduced by Nosko [140] which consists of obtaining an upper bound to $N(E_r)$. The construction will be detailed later. This will allow us to obtain an upper bound for $\bar{N}(E_r|X_1)$, $\bar{U}(E_r|X_1)$, where

$$\bar{U}(E_r|X_1) = E[U(E_r)|\xi(0,0)=X_1]. \tag{9.13}$$

We note finally that if we let $p_c(r|X_1)$ denote the probability of the terrain surface crossing the surface of sight at least once over the disk of radius $r\text{-}D_r$, given that the radar is sited at a height X_1, then by a reasoning analagous to the one of Chapter 8, i.e., by employing the simplest Chebyshev inequality, we obtain the following upper bound:

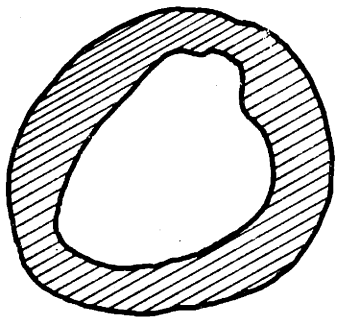

Fig. 9.3 Example of an Excursion Set not Homeomorphic to the Unit Disk

$$p_c(r|X_1) \leq \bar{N}(E_r|X_1) \leq \bar{U}(E_r|X_1) \quad . \tag{9.14}$$

In Appendix 9a we describe the construction of a lower bound on $p_c(r|X_1)$.

In the following chapter we first present, in Section 9.2, the construction of $U(E_r)$ and the analysis of $\bar{U}(E_r|X_1)$. Then, in Section 9.3, we conclude the chapter with the analysis of $\bar{f}_c(r|X_1)$.

9.2 Construction of $U(E_r)$ and Analysis of $\bar{U}(E_r|X_1)$

Nosko, in [140], has employed the Morse inequalities of differential topology to obtain some upper and lower bounds on the number of connected components in the excursion set of a field above some fixed level and contained in some two-dimensional domain D with a closed smooth boundary Γ: $x = x(t)$, $y = y(t)$, where $x(\cdot)$ and $y(\cdot)$ belong to C^3. The Morse inequalities effectively relate the topological structure of the excursion set, over some bounded region D, with the number of critical points, of different types, of the field $f(\cdot)$ and the function $f_\Gamma(t)$ defined on the interior of D and the boundary Γ, respectively. We will only make use here of the upper bound, which may be motivated without any knowledge of the Morse inequalities. The lower bound, which requires the Morse inequalities, may be analyzed in a similar manner to the analysis of the upper bound. We first reformulate the surface crossing problem involving the terrain and surface of sight as a level-crossing problem, then state the upper bound, $U(E_r)$, on $N(E_r)$, and finally discuss the regularity conditions underlying the analysis of $U(E_r)$. The remainder of the section will then be devoted to the calculation of $\bar{U}(E_r|X_1)$.

To reformulate the surface-crossing problem as a level-crossing problem, we define the following inhomogenous random field:

$$\Delta(x,y) \triangleq \xi(x,y) - X_1 - q(x,y) \quad , \tag{9.15}$$

where $q(x,y)$ is defined by relation (9.2) and $\xi(0,0) = X_1$. We can redefine the excursion set E_r as

$$E_r \triangleq \{(x,y): \quad (x,y) \in D_r \quad \text{and} \quad \Delta(x,y) \geq h_R\} \quad . \tag{9.16}$$

We define $\Delta(x,y)$ on the boundary of D_r - ∂D_r by $\Delta(\theta)$, where

$$\Delta(\theta) = \xi(r\cos\theta,\ r\sin\theta) - X_1 - \Phi(r) \quad , \tag{9.17}$$

and $\Phi(r)$ is defined by relation (9.2). Now we let $N_2(A)$ and $N_1(B)$ denote two set functions defined for $A \in D_r$ and $B \in \partial D_r$ that count the number of two-dimensional relative maxima of $\Delta(x,y)$ in A and the number of one-dimensional relative maxima of $\Delta(\theta)$ in B, respectively. Then Nosko's upper bound, $U(E_r)$, on the number of connected components in E_r is defined by

$$U(E_r) = N_2(E_r) + N_1(E_r \cap \partial D_r) \quad . \tag{9.18}$$

The motivation behind the bound (9.18) lies in the fact that $[\Delta(x,y) - h_R]$ represents the difference between the terrain field and the surface of sight. For every connected component of E_r that lies in the interior of D_r, we can associate at least one two-dimensional relative maximum of $[\Delta(x,y) - h_R]$ or, equivalently, at least one two-dimensional relative maximum of $\Delta(x,y)$. This follows from Fig. 9.4, where we display a connected component of E_r inside D_r with two associated relative maxima. Hence, the first term in relation (9.18) provides an upper bound for the number of connected components of E_r that lie in the interior of D_r. The second term results from the contribution of connected components of E_r that intersect the boundary ∂D_r of D_r. For such connected components of E_r overlapping onto ∂D_r, we may have no associated two-dimensional relative maximum of $[\Delta(x,y) - h_R]$, but we will always have at least one one-dimensional relative maximum associated with $\Delta(\theta) - h_R$ or, equivalently, a one-dimensional relative maximum of $\Delta(\theta)$. This case is pictured in Fig. 9.5.

To compute the conditional means of $N_2(E_r)$ and $N_1(E_r \cap \partial D_r)$ we can use some counting techniques analogous to that used in the analysis of $n_c(r)$. For these counting techniques to be meaningful, the random field, $\Delta(x,y)$, must satisfy certain regularity conditions. For the analysis of $N_2(E_r)$ to be well-defined, we need the following two conditions to be satisfied:

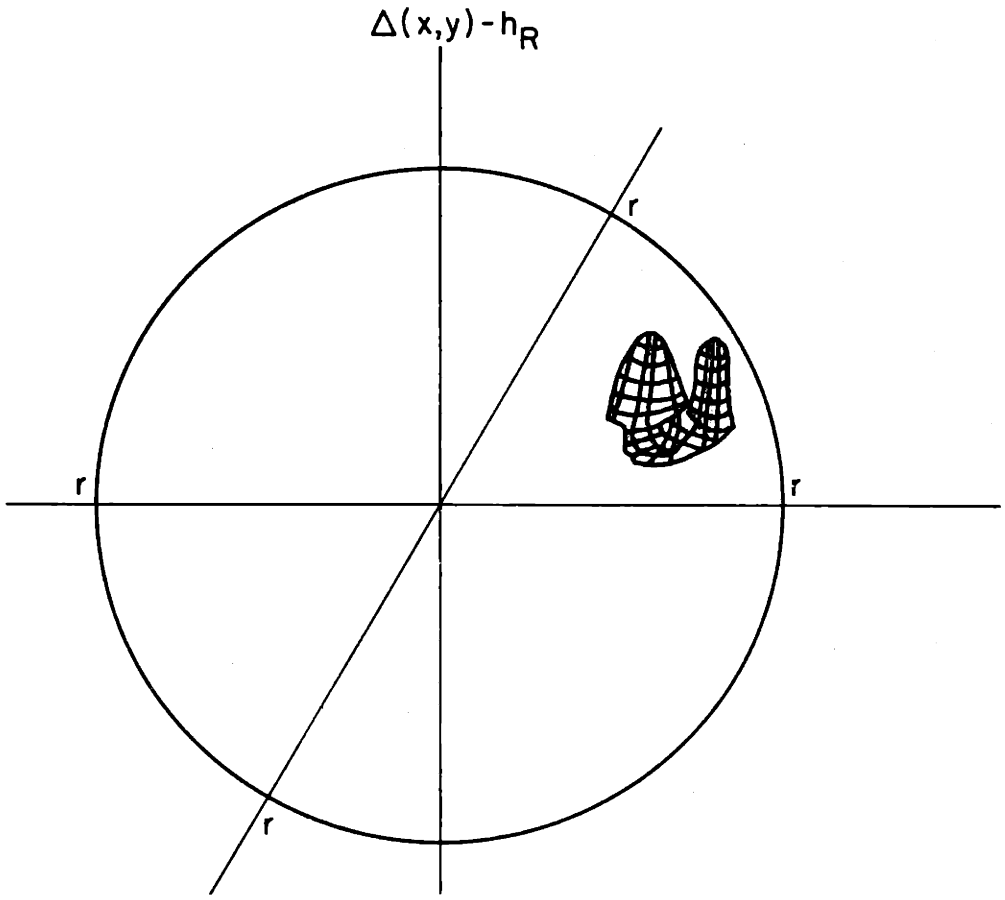

Fig. 9.4 Example of a Connected Component of E_r Contained in the Interior of D_r

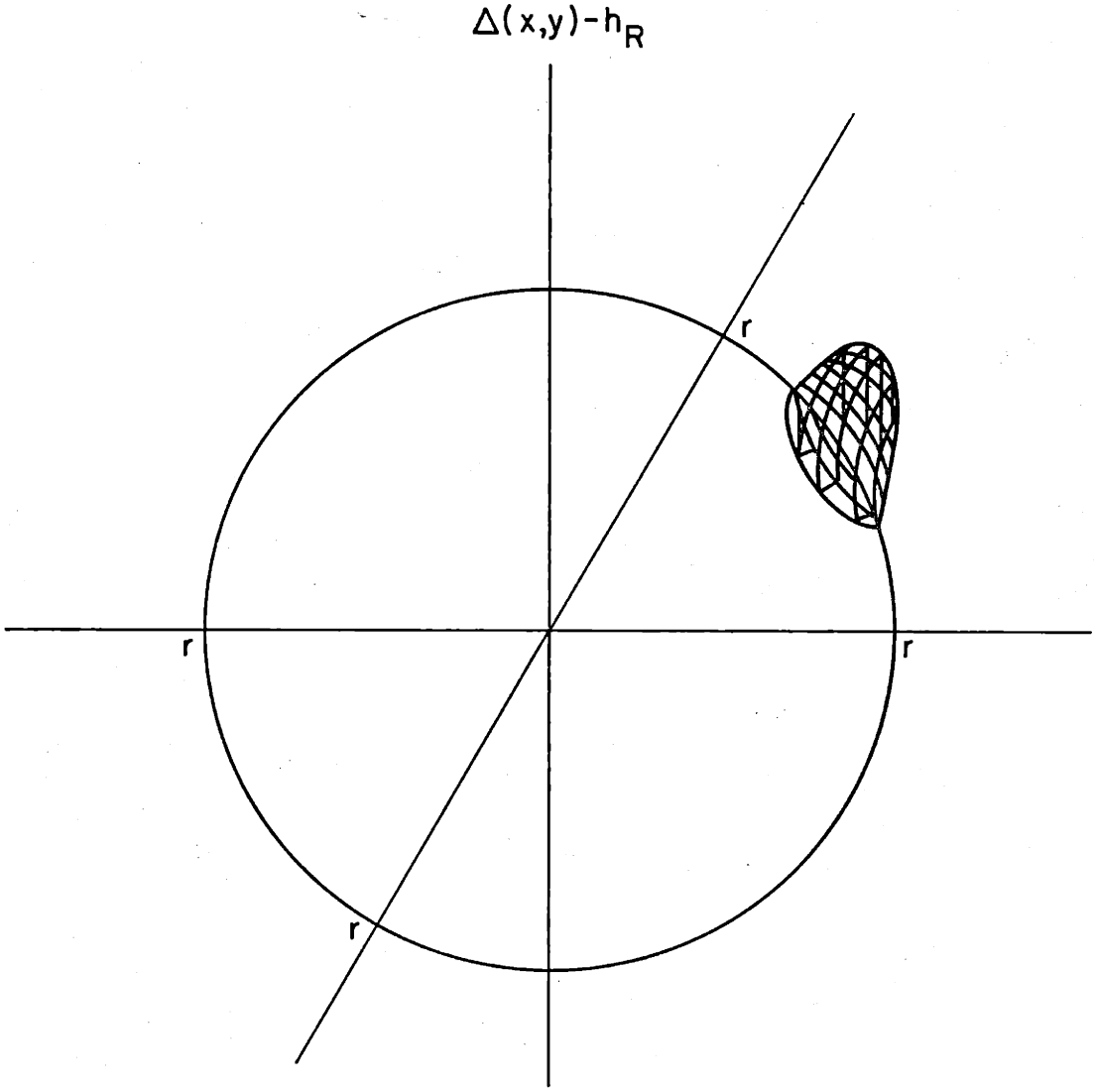

Fig. 9.5 Example of a Connected Component of E_r Overlapping ∂D_r

(1) $\Delta(\cdot,\cdot)$ has no two-dimensional relative maximum at some height $\geq h_R$, with finite non-zero probability, and

(2) The relative maxima of $\Delta(\cdot,\cdot)$ are non-degenerate.

Condition (1) excludes the non-zero probability of the tangency of the field $\Delta(\cdot,\cdot)$ to some level. With respect to Condition (2), we defined the non-degeneracy of a critical point earlier as requiring the nonsingularity of the Hessian matrix, hence implying that stationary points are isolated and that the behavior of the field in their vicinity may essentially be described by a quadratic function of the form (9.10).

For the analysis of $N_1(E_r \cap \partial D_r)$ to be well-defined, we need the following two conditions to be satisfied:

(1) The function $\Delta(\theta)$ defined on ∂D_r has no relative maximum at some height $\geq h_R$, with finite non-zero probability, and

(2) The relative maxima of $\Delta(\theta)$ are non-degenerate.

Condition (1) again excludes the non-zero probability of the tangency of the process to some level. Condition (2) requires that the second derivative not vanish at relative maxima of $\Delta(\theta)$. We now introduce the following notation in order to state a sufficient condition under which the desired regularity conditions on $\Delta(x,y)$ inside D_r, and $\Delta(\theta)$ on ∂D_r, will be satisfied. Let

$$s \triangleq (x,y) \quad , \tag{9.19}$$

and define

$$\left.\begin{aligned} z_1(s) &= \xi(x,y) \quad , \\ z_2(s) &= \xi_x(x,y) \quad , \\ z_3(s) &= \xi_y(x,y) \quad , \\ z_4(s) &= \xi_{xx}(x,y) \quad , \\ z_5(s) &= \xi_{xy}(x,y) \quad , \\ \text{and} \quad z_6(s) &= \xi_{yy}(x,y) \quad . \end{aligned}\right\} \tag{9.20}$$

We will let $\underline{z}(s)$ denote the column vector containing the $z_i(s)$'s. By using arguments from Adler [143] and Belyaev [137], we can show that the desired regularity conditions will be satisfied if the conditional density $p_2(\underline{z}(s)|X_1)$ of $\underline{z}(s)$ given $\xi(0,0) = X_1$ is nonsingular for each $s \neq (0,0)$, i.e., we want to require that the covariance matrix $\Lambda(s)$, defined by

$$\Lambda(s) = E\Big[(\underline{z}(s) - E[\underline{z}(s)|\xi(0,0)=X_1]) \cdot (\underline{z}(s) - E[\underline{z}(s)|\xi(0,0)=X_1])' \,|\, \xi(0,0)=X_1\Big], \tag{9.21}$$

be positive definite for each $s \neq (0,0)$.

We finally note that the application of the Morse inequalities in [140] requires that the sample functions of the random field be three times continuously differentiable with probability

one, while our analysis of the upper bound $U(E_r)$ only requires the mean square differentiability of the field to second order, and the nonsingularity of the conditional density $p_2(\vec{z}(s)|X_1)$.

Having defined the regularity conditions that need to be satisfied by the terrain $\xi(x,y)$, we now turn to the analysis of the mean of $U(E_r)$ conditioned on $\xi(0,0) = X_1$, $\bar{U}(E_r|X_1)$. From equation (9.18), we can express $\bar{U}(E_r|X_1)$ as

$$U(E_r|X_1) = E[N_2(E_r)|\xi(0,0)=X_1] + E[N_1(E_r \cap \partial D_r)|\xi(0,0)=X_1] \; . \tag{9.22}$$

Hence, we must focus our attention on the analysis of the two quantities on the right-hand side of (9.22). The earlier work of Longuet Higgins [136] and Belyaev [138] computed the average number density of maxima and minima, above a given level, for a stationary field. We use the generalization of the one-dimensional zero-counting techniques of Kac [116], Rice [114], and Leadbetter [118] for counting relative maxima in the case of the nonhomogenous random field $-\Delta(x,y)$. We employ essentially the same method to analyze the number of relative maxima in $E_r \cap \partial D_r$ of the nonstationary process, $\Delta(\theta)$.

We begin with the analysis of the mean of $N_2(E_r)$, conditioned on $\xi(0,0) = X_1$, by first enumerating the necessary

conditions that a two-dimensional relative maxima of $\Delta(x,y)$ in E_r must satisfy. We obtain the following six conditions:

$$(1)\quad \Delta(x,y) \geq h_R \quad , \tag{9.23}$$

$$(2)\quad \Delta_x(x,y) = 0 \quad , \tag{9.24}$$

$$(3)\quad \Delta_y(x,y) = 0 \quad , \tag{9.25}$$

$$(4)\quad \Delta_{xx}(x,y) \leq 0 \quad , \tag{9.26}$$

$$(5)\quad \Delta_{yy}(x,y) \leq 0 \quad , \tag{9.27}$$

and

$$(6)\quad \Delta_{xx}(x,y)\Delta_{yy}(x,y) - [\Delta_{xy}(x,y)]^2 > 0 \; . \tag{9.28}$$

By employing the definition of $\Delta(x,y)$, and the notation defined by (9.20), the relations (9.23) - (9.28) may be reformulated in terms of conditions on the terrain process and its partial derivatives up to second order as follows:

$$(1)\quad z_1(s) \geq X_1 + h_R + q(s) \quad , \tag{9.29}$$

$$(2)\quad z_2(s) = q_x(s) \quad , \tag{9.30}$$

$$(3)\quad z_3(s) = q_y(s) \quad , \tag{9.31}$$

$$(4)\quad z_4(s) \leq q_{xx}(s) \quad , \tag{9.32}$$

$$(5)\quad z_6(s) \leq q_{yy}(s) \quad , \tag{9.33}$$

and

$$(6)\quad [z_4(s)z_6(s) - z_5^2(s)] - [q_{yy}(s)z_4(s) - 2q_{xy}(s)z_5(s) + q_{xx}(s)z_6(s) + q_{xy}^2(s) - q_{xx}(s)q_{yy}(s)] > 0 \; . \tag{9.34}$$

We will use the notation $\Omega(s)$ to denote the set of $[z_1(s), z_4(s), z_5(s), z_6(s)]$ four-tuples such that the above relations (1) and (4) - (6) are satisfied.

By using an analogous technique to that employed for expressing $n_c(r)$ in our one-dimensional masking analysis, we can now express $N_2(E_r)$. At each point $s \in D_r$, we define the characteristic function $\chi_2(s)$ by

$$\chi_2(s) \triangleq \begin{cases} 1 & \text{if } [z_1(s), z_4(s), z_5(s), z_6(s)] \in \Omega(s) \\ 0 & \text{otherwise} \end{cases} , \qquad (9.35)$$

Now let $\delta(x,y)$ denote the two-dimensional delta function. Then we can formally express $N_2(E_r)$ by the following integral over D_r:

$$N_2(E_r) = \int_{s \in D_r} \chi_2(s) \delta\Big(z_2(s) - q_x(s), z_3(s) - q_y(s)\Big) J(s)\, ds , \qquad (9.36)$$

where

$$\begin{aligned} J(s) \triangleq [z_4(s)z_6(s) - z_5^2(s)] - [q_{yy}(s)z_4(s) - 2q_{xy}(s)z_5(s) \\ + q_{xx}(s)z_6(s) + q_{xy}^2(s) \\ - q_{xx}(s)q_{yy}(s)] . \end{aligned} \qquad (9.37)$$

The Jacobian term, J(s), serves to normalize the two-dimensional impulse function so as to count a new unit contribution every time the integration domain includes a new two-dimensional relative maximum of $\Delta(x,y)$.

Now, by employing relation (9.36) and the joint density for $\underline{z}(s)$ conditioned on $\xi(0,0) = X_1$, we can express the conditional mean of $N_2(E_r)$ given $\xi(0,0) = X_1$ as

$$E[N_2(E_r)|\xi(0,0)=X_1] = \int_{s\epsilon D_r} \int_{[z_1(s),z_4(s),z_5(s),z_6(s)]\epsilon\Omega(s)} \cdot p_2\left(z_1(s),q_x(s),q_y(s),z_4(s),z_5(s)z_6(s)|X_1\right) \cdot J(s)dz_1(s)dz_4(s)dz_5(s)dz_6(s)\,ds\,. \quad (9.38)$$

In Appendix 9B we derive $p_2(\underline{z}(s)|X_1)$, and define and partially evaluate the inner integration over the region $\Omega(s)$ in (9.38).

We next make some observations on the behavior of $E[N_2(E_r)|\xi(0,0)=X_1]$ as a function of range. Since $N_2(E_r)$ is a strictly increasing function of range, we can expect $E[N_2(E_r)|\xi(0,0)=X_1]$ to behave similarly. In addition, since from (9.1) - (9.2) the surface of sight elevation increases indefinitely, for sufficiently large ranges, it is reasonable to conclude that with high probability, the excursions of the terrain above the surface of sight will be contained inside

some finite disk. Therefore, we expect that $E[N_2(E_r)|\xi(0,0)=X_1]$ will approach some limiting value as r becomes large.

Relation (9.38) represents the contribution to the upper bound $\bar{U}(E_r|X_1)$ of the connected components of E_r that lie in the interior of the disk D_r. We now proceed to analyze the contribution to $\bar{U}(E_r|X_1)$ that is derived from connected components of E_r that lie on the boundary of $D_r - \partial D_r$. To do so, we formulate the computation of the mean of $N_1(E_r \cap \partial D_r)$ given $\xi(0,0) = X_1$.

Our analysis of the conditional mean of $N_1(E_r \cap \partial D_r)$ follows from the following explicit representation:

$$N_1(E_r \cap \partial D_r) = \int_0^{2\pi} \delta[\dot{\Delta}(\theta)] |\ddot{\Delta}(\theta)| \chi_1(\theta)\, d\theta \quad , \tag{9.39}$$

where

$$\chi_1(\theta) \triangleq \begin{cases} 1 & \ddot{\Delta}(\theta) \le 0,\ \Delta(\theta) \ge h_R \\ 0 & \text{otherwise} \end{cases} \quad . \tag{9.40}$$

The integral in relation (9.39) counts zero crossings of $\dot{\Delta}(\cdot)$ that occur when $\ddot{\Delta}(\theta) \le 0$ and $\Delta(\theta) \ge h_R$, i.e., it counts one-dimensional relative maxima of $\Delta(\theta)$ contained in $E_r \cap \partial D_r$. Assuming that we have the joint density for $\Delta(\theta)$, $\dot{\Delta}(\theta)$, and $\ddot{\Delta}(\theta)$ conditioned on $\xi(0,0) = X_1$, $p_1(\zeta_1(\theta), \zeta_2(\theta), \zeta_3(\theta)|X_1)$, where

$$\zeta_1(\theta) \triangleq \Delta(\theta) \quad , \tag{9.41}$$

$$\zeta_2(\theta) \triangleq \dot{\Delta}(\theta) \quad , \tag{9.42}$$

and $$\zeta_3(\theta) \triangleq \ddot{\Delta}(\theta) \quad , \tag{9.43}$$

we may compute the conditional mean for $N_1(E_r \cap \partial D_r)$ from relations (9.39) - (9.40) as

$$E[N_1(E_r \cap \partial D_r) | \xi(0,0)=X_1] = \int_{\theta=0}^{2\pi} \int_{\zeta_1(\theta)=h_R}^{\infty} \int_{\zeta_3(\theta)=-\infty}^{0} p_1(\zeta_2(\theta),0,\zeta_3(\theta)|X_1)|\zeta_3(\theta)| \, d\zeta_3(\theta) d\zeta_1(\theta) d\theta \quad . \tag{9.44}$$

In Appendix 9C, we show how to compute the conditional density for $\Delta(\theta)$, $\dot{\Delta}(\theta)$, and $\ddot{\Delta}(\theta)$, and then employ this density to evaluate the integration over $\zeta_3(\theta)$ in relation (9.44).

We now make some observations on the behavior we expect from $E[N_1(E_r \cap \partial D_r) | \xi(0,0)=X_1]$ as a function of range. Since along a fixed radial direction the probability of the terrain exceeding the surface of sight, conditioned on $\xi(0,0)=X_1$, is negligible both very near and far from the radar, it is reasonable to conclude that there is some range at which this probability becomes a maximum. Hence, we can expect that both

$N_1(E_r \cap \partial D_r)$ and $E[N_1(E_r \cap \partial D_r) | \xi(0,0)=X_1]$ initially increase, reach a maximum value, and then decrease to zero for sufficiently large ranges. The conditional mean, $E[N_1(E_r \cap \partial D_r) | \xi(0,0)=X_1]$, converges to zero for large r, despite the fact that the circumference of D_r varies ~r, due to the fact that for large enough r, the probability of the terrain exceeding the surface of sight will vary as

$$\sim \frac{c}{X_1 + h_R + \Phi(r)} \exp\left(-(X_1 + h_R + \Phi(r))^2\right).$$

At this point we have completed our analysis of both the interior and boundary contributions to $\bar{U}(E_r | X_1)$, the upper bound on the mean number of connected components in the excursion set E_r. The computation of the conditional mean of $N_2(E_r)$, as specified by relation (9.38) and in Appendix 9B, requires the numerical evaluation of a five-dimensional multiple integral. This may be accomplished by equidistributional sampling techniques [146]. In addition, the computation of the conditional mean of $N_1(E_r \cap \partial D_r)$, as defined by relation (9.44) and in Appendix 9C, requires the numerical evaluation of a two-dimensional integral.

Finally, we note that asymptotic results [143] on the structure of excursion sets above high levels, showing that in this case individual connected components in the excursion set may

be associated with single relative maxima above the given level, suggest strongly that when excursions of the terrain surface above the surface of sight are of sufficiently low probability, the quantity $\bar{U}(E_r|X_1)$ will be a tight upper bound for the crossing probability, $p_c(r|X_1)$. Since as we mentioned earlier, $E[N_1(E_r \cap \partial D_r)|\xi(0,0)=X_1]$ becomes negligible for sufficiently large ranges, $\bar{U}(E_r|X_1)$ converges to the same limiting value as $E[N_2(E_r)|\xi(0,0)=X_1]$, which may then be interpreted as an upper bound on the probability of at least one excursion of the terrain above the surface of sight.

In addition, we observe that $p_c(r|X_1)$ may alternatively be interpreted as the probability that an observation post or a communications installation, at an elevation X_1, looking out or directing its transmissions, respectively, at some fixed angle with respect to the horizontal, is not able to cover a surrounding circular region of radius r. Hence, $\bar{U}(E_r|X_1)$ may find uses in these other application areas as a criterion for evaluating the effect of varying site elevation, X_1.

9.3 Analysis of $\bar{f}_c(r|X_1)$

While our analysis of $\bar{U}(E_r|X_1)$ gives us information about the average number of times the terrain surface crosses the surface of sight, the analysis of $\bar{f}_c(r|X_1)$ informs us of the average fraction of the disk of radius r, D_r, that the terrain blocks the surface of sight. The analysis of the conditional mean of $f_c(r)$ follows from the following explicit representation:

$$f_c(r) = \frac{1}{\pi r^2} \int_{\theta=0}^{2\pi} \int_{\rho=0}^{r} U_{-1}\Big(\xi(\rho\cos\theta, \rho\sin\theta) - [X_1 + h_R + \Phi(\rho)]\Big)\rho d\rho d\theta, \tag{9.45}$$

where $U_{-1}(\cdot)$ denotes the unit step function. We note here that if we knew that terrain following objects are only likely to approach the radar from particular angles, we could modify our definition of $f_c(r)$ in equation (9.45) by restricting the integration over θ to reflect this case.

From relation (9.45), we can express $\bar{f}_c(r|X_1)$ as

$$\bar{f}_c(r|X_1) = \frac{1}{\pi r^2} \int_{\theta=0}^{2\pi} \int_{\rho=0}^{r} \Pr\Big(\xi(\rho\cos\theta, \rho\sin\theta) > [X_1 + h_R + \Phi(\rho)] \,|\, \xi(0,0)=X_1\Big)\rho d\rho d\theta. \tag{9.46}$$

The probability in the integrand of relation (9.46) may be computed from the conditional mean and variance of

$\xi(\rho\cos\theta,\rho\sin\theta)$, which are defined by

$$E[\xi(\rho\cos\theta,\rho\sin\theta)\,|\,\xi(0,0)=X_1] = R(\rho\cos\theta,\rho\sin\theta)\frac{X_1}{\sigma^2}\,, \qquad (9.47)$$

and

$$\mathrm{Var}[\xi(\rho\cos\theta,\rho\sin\theta)\,|\,\xi(0,0)=X_1] = \sigma^2\left[1 - \left(\frac{R(\rho\cos\theta,\rho\sin\theta)}{\sigma^2}\right)^2\right]. \qquad (9.48)$$

Hence, by employing the $Q[\cdot]$ function defined by relation (8.23), and equations (9.46) - (9.48), we may express $\bar{f}_c(r|X_1)$ as

$$\bar{f}_c(r|X_1) = \frac{1}{\pi r^2}\int_{\theta=0}^{2\pi}\int_{\rho=0}^{r} Q\left[\frac{X_1 + h_R + \Phi(\rho) - R(\rho\cos\theta,\rho\sin\theta)\frac{X_1}{\sigma^2}}{\left[\sigma^2 - \frac{R^2(\rho\cos\theta,\rho\sin\theta)}{\sigma^2}\right]^{\frac{1}{2}}}\right]\rho\,d\rho\,d\theta. \qquad (9.49)$$

Finally, from relation (9.49) we note that $\bar{f}_c(r|X_1)$ essentially corresponds to the average value of the probability of the terrain exceeding the surface of sight, over the region D_r, and conditioned on the radar being located at a height X_1. Since with high probability the excursions of the terrain above the surface of sight will be contained in a disk of finite radius, we expect $\bar{f}_c(r|X_1)$ to initially increase, reach a maximum value, and then decrease as a function of range.

9.4 Conclusions

In this chapter we analyzed two measures of the masking effect for a two-dimensional generalization of the fixed radar elevation angle masking geometry. In Section 9.2 we analyzed $\bar{U}(E_r|X_1)$, the conditional mean for a given radar siting height X_1, of an upper bound on the number of connected components in the excursion set of the terrain surface above the surface of sight, over a disk of radius r. The calculation of $\bar{U}(E_r|X_1)$ requires the numerical evaluation of both a five- and a two-dimensional multiple integral. The computation of $\bar{U}(E_r|X_1)$ provides us with an upper bound on the two-dimensional analog of the crossing probability, $p_c(r|X_1)$. Some further work might focus on the evaluation of the lower bound on $p_c(r|X_1)$, whose analysis is sketched in Appendix 9A, and the numerical calculation of $E[N_1(E_r \cap \partial D_r)|\xi(0,0)=X_1]$, $E[N_2(E_r)|\xi(0,0)=X_1]$, and $\bar{U}(E_r|X_1)$.

Finally, in Section 9.3, we analyzed $\bar{f}_c(r|X_1)$, the conditional mean for a given radar siting height X_1, of the fraction of the disk of radius r that the terrain exceeds the line-of-sight surface. The calculation of $\bar{f}_c(r|X_1)$ requires the numerical evaluation of a two-dimensional multiple integral, and is worth pursuing in continuing work.

Appendix 9A

Lower Bound on $p_c(r|X_1)$ for the Two-Dimensional Fixed Elevation Angle Geometry

In this Appendix, we sketch the analysis of a lower bound for $p_c(r|X_1)$, motivated by the bounding technique of Helstrom and Gallager [119], which we employed in obtaining the lower bound on $p_c(r|X_1)$ for the terrain-following geometry in Appendix 8A. We first define the probability that the terrain stays below the surface of sight over the disk of radius r, given the radar is sited on a hill of height X_1, as

$$p_v(r|X_1) = 1 - p_c(r|X_1) \ . \tag{A.1}$$

We will use the notation $\lambda(\rho,\theta)$, $\eta(\rho,\theta,X_1)$, and $\xi(\rho,\theta)$ to denote the values of some two-dimensional function $\lambda(\cdot,\cdot)$, the surface of sight, and of the terrain process, respectively, at some polar coordinate location (ρ,θ). Then we note that the event that the terrain stays below the surface of sight over the disk of radius r is contained in the event that

$$\int_{\rho=0}^{r} \int_{\theta=0}^{2\pi} \lambda(\rho,\theta)[\eta(\rho,\theta,X_1) - \xi(\rho,\theta)]\rho d\theta d\rho \geq 0 \ , \tag{A.2}$$

for all non-negative functions, $\lambda(\cdot,\cdot)$. Hence, we obtain the following upper bound on $p_v(r|X_1)$:

$$p_v(r|X_1) \le \min_{\lambda(\cdot,\cdot)\ge 0} \left\{ \Pr\left[\int_{\rho=0}^{r} \int_{\theta=0}^{2\pi} \lambda(\rho,\theta)[\eta(\rho,\theta,X_1) - \xi(\rho,\theta)] \cdot \rho d\theta d\rho \ge 0 \,\middle|\, \xi(0,0)=X_1 \right] \right\}. \tag{A.3}$$

We next define the zero mean, Gaussian random variable $\not{z}$ as

$$\not{z} \triangleq \int_{\rho=0}^{r} \int_{\theta=0}^{2\pi} \lambda(\rho,\theta)\xi(\rho,\theta)\rho d\theta d\rho \quad , \tag{A.4}$$

to facilitate the analysis of the right-hand side of equation (A.3). From relation (A.4) we determine

$$E[\not{z}|\xi(0,0)=X_1] = \int_{\rho=0}^{r} \int_{\theta=0}^{2\pi} \lambda(\rho,\theta)E[\xi(\rho,\theta)|\xi(0,0)=X_1]\rho d\theta d\rho \quad , \tag{A.5}$$

$$E[\not{z}^2|\xi(0,0)=X_1] = \int_{\rho_1=0}^{r} \int_{\theta_1=0}^{2\pi} \int_{\rho_2=0}^{r} \int_{\theta_2=0}^{2\pi} \lambda(\rho_1,\theta_1)\lambda(\rho_2,\theta_2)\rho_1\rho_2 \cdot E[\xi(\rho_1,\theta_1)\xi(\rho_2,\theta_2)|\xi(0,0)=X_1]d\theta_2 d\rho_2 d\theta_1 d\rho_1 \quad , \tag{A.6}$$

and

$$\mathrm{Var}[\mathcal{Z}|\xi(0,0)=X_1] = E[\mathcal{Z}^2|\xi(0,0)=X_1] - \left[E[\mathcal{Z}|\xi(0,0)=X_1]\right]^2 . \quad (A.7)$$

Finally, combining the relations (A.1) and (A.3) - (A.7), we obtain the following lower bound on $p_c(r|X_1)$:

$$p_c(r|X_1) \geq \max_{\lambda(\cdot,\cdot)\geq 0} \left\{ Q\left[\frac{\int_{\rho=0}^{r} \int_{\theta=0}^{2\pi} \lambda(\rho,\theta)\eta(\rho,\theta,X_1)\rho d\theta d\rho - E[\mathcal{Z}|\xi(0,0)=X_1]}{\left[\mathrm{Var}[\mathcal{Z}|\xi(0,0)=X_1]\right]^{\frac{1}{2}}} \right] \right\}, \quad (A.8)$$

where $Q[\cdot]$ is defined by (8.23).

Appendix 9B

Evaluation of $E[N_2(E_r) | \xi(0,0)=X_1]$

In this appendix we show how to form the joint density for the $z_i(s)$'s, defined by relations (9.20), conditioned on $\xi(0,0) = X_1$. We also show how we can define and partially evaluate the inner integration over $\Omega(s)$ in relation (9.38).

If we let $\underline{z}(s)$ denote the vector of $z_i(s)$'s, $i = 1,\ldots,6$, and let

$$\sigma^2 \triangleq R(0,0) \quad , \tag{B.1}$$

then the conditional density for $\underline{z}(s)$ given $\xi(0,0) = X_1$ is specified by the conditional mean

$$E[\underline{z}(s) | \xi(0,0)=X_1] = \beta(s)\, X_1 \quad , \tag{B.2}$$

where

$$\beta(s) \triangleq E\left[\underline{z}(s)\xi(0,0)\right]\frac{1}{\sigma^2} \quad , \tag{B.3}$$

and the conditional covariance

$$E[(\underline{z}(s) - \beta(s)X_1)(\underline{z}(s) - \beta(s)X_1)' | \xi(0,0)=X_1] = \Lambda(s) \quad , \tag{B.4}$$

where

$$\Lambda(s) \triangleq E[\underline{z}(s)\underline{z}'(s)] - \frac{E[\underline{z}(s)\xi(0,0)]\,E[\xi(0,0)\underline{z}'(s)]}{\sigma^2} . \quad (B.5)$$

To compute the correlation terms in $\beta(s)$ and $\Lambda(s)$ we use the fact that

$$E\left[\left[\frac{\partial^{p+q}}{\partial x^p \partial y^q}\,\xi(x,y)\Big|_{(x_1,y_1)}\right]\left[\frac{\partial^{p'+q'}}{\partial x^{p'} \partial y^{q'}}\,\xi(x,y)\Big|_{(x_2,y_2)}\right]\right] =$$

$$(-1)^{p'+q'}\,\frac{\partial^{p+p'+q+q'}}{\partial x^{p+p'} \partial y^{q+q'}}\,R(x,y)\Big|_{(x_1-x_2,\,y_1-y_2)} , \quad (B.6)$$

and that when $(x_1,y_1) = (x_2,y_2)$, and $p+q-p'-q'$ is an odd number, the right-hand side of the relation (B.6) vanishes [136]. We will now adopt the following shorthand notation for partial derivatives of $R(\cdot,\cdot)$ at a point s in the plane:

$$\frac{\partial^{p+q}}{\partial x^p \partial y^q}\,R(s) \triangleq R_{p,q}(s) \quad (B.7)$$

Hence, we form the elements of $\beta(s)$ as

$$\beta(s) \triangleq \begin{pmatrix} R_{0,0}(s)/\sigma^2 \\ R_{1,0}(s)/\sigma^2 \\ R_{0,2}(s)/\sigma^2 \\ R_{2,0}(s)/\sigma^2 \\ R_{1,1}(s)/\sigma^2 \\ R_{0,2}(s)/\sigma^2 \end{pmatrix} . \tag{B.8}$$

The upper triangular entries of the conditional covariance matrix $\Lambda(s)$ are defined by the following relations:

$$\Lambda_{11}(s) = \sigma^2\left[1 - \left(\frac{R_{0,0}(s)}{\sigma^2}\right)^2\right], \tag{B.9}$$

$$\Lambda_{12}(s) = -\frac{R_{0,0}(s)R_{1,0}(s)}{\sigma^2}, \tag{B.10}$$

$$\Lambda_{13}(s) = -\frac{R_{2,0}(s)R_{0,1}(s)}{\sigma^2}, \tag{B.11}$$

$$\Lambda_{14}(s) = R_{2,0}(0,0) - \frac{R_{0,0}(s)R_{2,0}(s)}{\sigma^2}, \tag{B.12}$$

$$\Lambda_{15}(s) = R_{1,1}(0,0) - \frac{R_{0,0}(s)R_{1,1}(s)}{\sigma^2}, \tag{B.13}$$

$$\Lambda_{16}(s) = R_{0,2}(0,0) - \frac{R_{0,0}(s)R_{0,2}(s)}{\sigma^2}, \tag{B.14}$$

$$\Lambda_{22}(s) = -R_{2,0}(0,0) - \frac{R_{1,0}^2(s)}{\sigma^2}, \tag{B.15}$$

$$\Lambda_{23}(s) = -R_{1,1}(0,0) - \frac{R_{1,0}(s)R_{0,1}(s)}{\sigma^2} , \tag{B.16}$$

$$\Lambda_{24}(s) = - \frac{R_{1,0}(s)R_{2,0}(s)}{\sigma^2} , \tag{B.17}$$

$$\Lambda_{25}(s) = - \frac{R_{1,0}(s)R_{1,1}(s)}{\sigma^2} , \tag{B.18}$$

$$\Lambda_{26}(s) = - \frac{R_{1,0}(s)R_{0,2}(s)}{\sigma^2} , \tag{B.19}$$

$$\Lambda_{33}(s) = -R_{0,2}(0,0) - \frac{R_{0,1}^2(s)}{\sigma^2} , \tag{B.20}$$

$$\Lambda_{34}(s) = - \frac{R_{0,1}(s)R_{2,0}(s)}{\sigma^2} , \tag{B.21}$$

$$\Lambda_{35}(s) = - \frac{R_{0,1}(s)R_{1,1}(s)}{\sigma^2} , \tag{B.22}$$

$$\Lambda_{36}(s) = - \frac{R_{0,1}(s)R_{0,2}(s)}{\sigma^2} , \tag{B.23}$$

$$\Lambda_{44}(s) = R_{4,0}(0,0) - \frac{R_{2,0}^2(s)}{\sigma^2} , \tag{B.24}$$

$$\Lambda_{45}(s) = R_{3,1}(0,0) - \frac{R_{2,0}(s)R_{1,1}(s)}{\sigma^2} , \tag{B.25}$$

$$\Lambda_{46}(s) = R_{2,2}(0,0) - \frac{R_{2,0}(s)R_{0,2}(s)}{\sigma^2} , \tag{B.26}$$

$$\Lambda_{55}(s) = R_{2,2}(0,0) - \frac{R_{1,1}^2(s)}{\sigma^2} \quad , \tag{B.27}$$

$$\Lambda_{56}(s) = R_{1,3}(0,0) - \frac{R_{1,1}(s)R_{0,2}(s)}{\sigma^2} \quad , \tag{B.28}$$

and

$$\Lambda_{66}(s) = R_{0,4}(0,0) - \frac{R_{0,2}^2(s)}{\sigma^2} \quad . \tag{B.29}$$

Finally, by defining

$$\sum(s) = \Lambda^{-1}(s) \quad , \tag{B.30}$$

and

$$d(s) = \det\{\Lambda(s)\} \quad , \tag{B.31}$$

we can express the joint density for $\underline{z}(s)$ conditioned on $\xi(0,0) = X_1$ as

$$p_2\left(z_1(s), z_2(s), z_3(s), z_4(s), z_5(s), z_6(s) \mid X_1\right) = \frac{\exp\left\{-\frac{1}{2}\sum_{i,j}\left[z_i(s) - \beta_i(s)X_1\right]\left[z_j(s) - \beta_j(s)X_1\right]\sum_{ij}(s)\right\}}{(2\pi)^3\, d^{\frac{1}{2}}(s)} \quad . \tag{B.32}$$

We note that the conditional density for $\underline{z}(s)$ given $\xi(0,0) = X_1$ appears in relation (9.38) with the $z_2(s)$ and $z_3(s)$ variables sampled at $q_x(s)$ and $q_y(s)$, respectively. Hence, for notational convenience in the analysis that follows, we define three sets of indices corresponding to the zeroth, first, and second-order partial derivatives of the terrain process:

$$I_0 = \{1\} \quad , \tag{B.33}$$

$$I_1 \triangleq \{2,3\} \quad , \tag{B.34}$$

and

$$I_2 \triangleq \{4,5,6\} \quad . \tag{B.35}$$

We also define the union of I_2 and I_0 as

$$I_{20} \triangleq I_0 \cup I_2 \quad . \tag{B.36}$$

Then, we may express the conditional density of the $z_i(s)$'s, with $z_2(s)$ and $z_3(s)$ sampled at $q_x(s)$ and $q_y(s)$ as

$$p_2\left(z_1(s), q_x(s), q_y(s), z_4(s), z_6(s) \mid X_1\right) = \frac{\Xi(s)}{(2\pi)^3 \, d^{\frac{1}{2}}(s)} \exp\left\{-\frac{1}{2}\left(\sum_{(i,j)\in I_{20}^2} [z_i(s)-\beta_i(s)X_1][z_j(s)-\beta_j(s)X_1] \sum_{ij}(s) + \sum_{\ell \in I_{20}} \gamma_\ell(s)[z_\ell(s)-\beta_\ell(s)X_1]\right)\right\} \quad , \tag{B.37}$$

where

$$\Xi(s) \triangleq \exp\left\{-\frac{1}{2}\left(\sum_{(i,j)\in I_1^2} [z_i(s)-\beta_i(s)X_1] \cdot [z_j(s)-\beta_j(s)X_1] \sum_{ij}(s)\right)\right\} \Bigg|_{\substack{z_2(s)=q_x(s) \\ z_3(s)=q_y(s)}} \quad , \tag{B.38}$$

and

$$\gamma_{\ell}(s) \triangleq \sum_{m \in I_1} 2[z_m(s) - \beta(s)X_1] \sum_{\ell m}(s) \Bigg|_{\substack{z_2(s)=q_x(s) \\ z_3(s)=q_y(s)}} , \qquad (B.39)$$

for $\ell \in I_2$.

If we now denote

$$a_i(s) = z_i(s) - \beta_i(s)X_1 , \qquad (B.40)$$

for $i \in I_{20}$, and substitute relations (B.37) and (B.40) into (9.38), we obtain the following expression for the conditional mean of $N_2(E_r)$ given $\xi(0,0) = X_1$:

$$E[N_2(E_r) | \xi(0,0)=X_1] = \int_{s \in D_r} \frac{\Xi(s)}{(2\pi)^3 d^{\frac{1}{2}}(s)} \int_{[a_1(s),a_4(s),a_5(s),a_6(s)] \in \Omega'(s)}$$

$$\cdot \exp\left\{-\frac{1}{2}\left(\sum_{(i,j) \in I_{20}^2} a_i(s)a_j(s) \sum_{ij}(s) + \sum_{\ell \in I_{20}} \gamma_{\ell}(s)a(s)\right)\right\}$$

$$\cdot J(s)da_1(s)da_4(s)da_5(s)da_6(s)ds , \qquad (B.41)$$

where

$$\Omega'(s) \triangleq \left\{ \begin{array}{l} a_1(s) \geq c_1(s) \\ a_4(s) < c_6(s),\ a_6(s) < c_4(s) \\ a_4(s)a_6(s)-a_5^2(s) > c_4(s)a_4(s)+c_5(s)a_5(s) \\ \qquad\qquad +c_6(s)a_6(s)+c_7(s) \end{array} \right\}, \tag{B.42}$$

$$J(s) = a_4(s)a_6(s)-a_5^2(s)-c_4(s)a_4(s)-c_5(s)a_5(s)-c_6(s)a_6(s)-c_7(s), \tag{B.43}$$

and where the $c_i(s)$'s are defined by

$$\begin{aligned} c_1(s) &\triangleq X_1 + h_R + q(s) - \beta_1(s)X_1 \ , \\ c_4(s) &\triangleq q_{yy}(s) - \beta_6(s)X_1 \ , \\ c_5(s) &\triangleq -2q_{xy}(s) + 2\beta_5(s)X_1 \ , \\ c_6(s) &\triangleq q_{xx}(s) - \beta_4(s)X_1 \ , \\ c_7(s) &\triangleq q_{xy}^2(s) - q_{xx}(s)q_{yy}(s) + q_{yy}(s)\beta_4(s)X_1 - 2q_{xy}(s)\beta_5(s)X_1 \\ &\quad + q_{xx}(s)\beta_6(s)X_1 + [\beta_5^2(s) - \beta_4(s)\beta_6(s)]X_1^2 \ . \end{aligned} \tag{B.44}$$

We note from the definition of $\Omega'(s)$ that we can evaluate the integral in relation (B.41) with respect to the $a_1(s)$ variable. To do so we can complete the square of the exponent in $a_1(s)$, and use the Gaussian integral defined by relation (8.23). By doing so, we obtain the following expression:

$$E[N_2(E_r)\,|\,\xi(0,0)=X_1] = \int_{s\in D_r} \frac{\Xi(s)}{(2\pi)^{5/2}\left[d(s)\,\Sigma_{11}(s)\right]^{1/2}}$$

$$\int_{[a_4(s),a_5(s),a_6(s)]\in\Omega_r'(s)} Q\left[\frac{c_1(s)-b(s)}{\Sigma_{11}^{-1/2}(s)}\right]$$

$$\exp\left\{-\frac{1}{2}\left[\sum_{(i,j)\in I_2^2} a_i(s)a_j(s)\,\Sigma_{ij}(s) + \sum_{\ell\in I_2}\gamma_\ell(s)a_\ell(s) - \Sigma_{11}(s)b^2(s)\right]\right\}$$

$$J(s)da_4(s)da_5(s)da_6(s)ds \quad , \qquad \text{(B.45)}$$

where

$$b(s) \triangleq \frac{-\left[\sum_{j\in I_2} a_j(s)\,\Sigma_{1j}(s) + \gamma_1(s)/2\right]}{\Sigma_{11}(s)} \quad , \qquad \text{(B.46)}$$

and

$$\Omega_r'(s) \triangleq \left\{ \begin{array}{l} a_4(s) < c_6(s) \quad a_6(s) < c_4(s) \\ \\ a_4(s)a_6(s) - a_5^2(s) > c_4(s)a_4(s) + c_5(s)a_5(s) \\ \qquad\qquad + c_6(s)a_6(s) + c_7(s) \end{array} \right\} . \qquad \text{(B.47)}$$

We conclude our analysis of the mean value of $N_2(E_r)$, conditioned on $\xi(0,0) = X_1$, by finding an expression for the inner integration over the region $\Omega'_r(s)$, determined by relation (B.47). The structure of $\Omega'_r(s)$ becomes more apparent if we make the change of variables

$$a_4(s) = a'_4(s) + c_6(s) \ , \tag{B.48}$$

and

$$a_6(s) = a'_6(s) + c_4(s) \ . \tag{B.49}$$

Then, $\Omega'_r(s)$ is mapped into the new region $\Omega''_r(s)$, defined in terms of the $[a'_4(s), a_5(s), a'_6(s)]$ variables as

$$\Omega''_r(s) \triangleq \left\{ \begin{array}{l} a'_4(s) < 0 \ , \ a'_6(s) < 0 \\ \\ -a_5^2(s) - c_5(s) a_5(s) + [a'_4(s) a'_6(s) - c_4(s) c_6(s) - c_7(s)] > 0 \end{array} \right\} . \tag{B.50}$$

If we first think of $a'_4(s)$ and $a'_6(s)$ as fixed, then the third constraint in relation (B.50), through the solution of the quadratic equation in $a_5(s)$, determines the range of admissible values for $a_5(s)$, i.e., $a_5(s)$ varies from $r_-[a'_4(s), a'_6(s)]$ to $r_+[a'_4(s), a'_6(s)]$, with

$$r_{\pm}[a_4'(s),a_6'(s)] \triangleq -\frac{c_5(s)}{2} \pm \sqrt{a_4'(s)a_6'(s) - c^*(s)} \quad , \tag{B.51}$$

where

$$c^*(s) \triangleq c_4(s)c_6(s) + c_7(s) - \frac{c_5^2(s)}{4} \quad . \tag{B.52}$$

In addition, for $r_{\pm}[a_4'(s),a_6'(s)]$ to represent a real number, we must impose the constraint that the discriminant of the related quadratic equation be non-negative, i.e.,

$$a_4'(s)a_6'(s) \geq c^*(s) \quad . \tag{B.53}$$

Hence, by relations (B.51) - (B.53) we may redefine the region $\Omega_r''(s)$ as

$$\Omega_r''(s) \equiv \Big\{[a_4'(s),a_5(s),a_6'(s)]: \quad a_4'(s) < 0,\ a_6'(s) < 0,$$
$$a_4'(s)a_6'(s) \geq c^*(s),$$
$$r_-[a_4'(s),a_6'(s)] < a_5(s) < r_+[a_4'(s), a_6'(s)]\Big\} \tag{B.54}$$

This expression for $\Omega_r''(s)$ can be used to define the inner integration in relation (B.45) more concretely. Let $\psi[a_4(s),a_5(s),a_6(s)]$ be defined as

$$\psi[a_4(s),a_5(s),a_6(s)] \triangleq Q\left[\frac{c_1(s) - b(s)}{\sum_{11}^{-1/2}(s)}\right] \cdot \exp\left\{-\frac{1}{2}\left(\sum_{(i,j)\in I_2^2} a_i(s)a_j(s)\sum_{ij}(s) + \sum_{\ell\in I_2}\gamma_\ell(s)a_\ell(s) - \sum_{11}(s)b^2(s)\right)\right\} J(s) \quad , \quad (B.55)$$

and then letting I(s) be determined as

$$I(s) \triangleq \begin{cases} \displaystyle\int_{a_4'(s)=-\infty}^{0} \int_{a_6'(s)=-\infty}^{\frac{c^*(s)}{a_4'(s)}} \int_{a_5(s)=r_-[a_4'(s),a_6'(s)]}^{r_+[a_4'(s),a_6'(s)]} \cdot \psi[a_4'(s)+c_6(s),a_5(s),a_6'(s)+c_4(s)]\, da_5(s)da_6'(s)da_4'(s) \\ \qquad\qquad \text{for } c^*(s) > 0 \\ \displaystyle\int_{a_4'(s)=-\infty}^{0} \int_{a_6'(s)=-\infty}^{0} \int_{a_5(s)=r_-[a_4'(s),a_6'(s)]}^{r_+[a_4'(s),a_6'(s)]} \cdot \psi[a_4'(s)+c_6(s),a_5(s),a_6'(s)+c_4(s)]\, da_5(s)da_6'(s)da_4'(s) \\ \qquad\qquad \text{for } c^*(s) \le 0 \quad , \end{cases} \quad (B.56)$$

we can express the mean of $N_2(E_r)$ given $\xi(0,0) = X_1$ as

$$E[N_2(E_r) | \xi(0,0)=X_1] = \int_{s\epsilon D_r} \frac{\Xi(s)\, I(s)}{(2\pi)^{5/2} \left[d(s) \sum_{11}(s) \right]^{1/2}} \, ds. \quad (B.57)$$

We finally note that the integrand in (B.57) may be interpreted as the average number density of relative maxima for the field $\Delta(x,y)$, defined by (9.15), above the level h_R. Since $\Delta(x,y)$ is an inhomogenous field, i.e., its mean value is a function of the location, the average number density of relative maxima above h_R is also a function of s. This is reasonable since we expect that excursions at $\Delta(\cdot,\cdot)$ above h_R, or equivalently of the terrain above the surface of sight, will occur with very low probability both near and far from the radar location.

The expression (B.57) was obtained by using the same type of counting technique, involving two-dimensional delta functions, as has been employed [136] to compute the average number density of relative maxima above some level for a homogenous field. It is not surprising that the integral (B.47) cannot, in general, be evaluated in closed form. Even for the problem of computing the average number density of relative maxima above the level $-\infty$, for a homogenous field, the result can only be expressed in terms of elliptic integrals, which must be evaluated numerically.

Appendix 9C

Evaluation of $E[N_1(E_r \cap \partial D_r) | \xi(0,0)=X_1]$

In this Appendix we compute the joint density of $\Delta(\theta)$, $\dot{\Delta}(\theta)$ and $\ddot{\Delta}(\theta)$ conditioned on $\xi(0,0) = X_1$, and use the result to evaluate the integral over $\zeta_3(\theta)$ in relation (9.44). We first note that we may express $\Delta(\theta)$, $\dot{\Delta}(\theta)$, and $\ddot{\Delta}(\theta)$ in terms of $\xi(s_\theta)$, $\xi_x(s_\theta)$, $\xi_y(s_\theta)$, $\xi_{xx}(s_\theta)$, $\xi_{xy}(s_\theta)$, and $\xi_{yy}(s_\theta)$, where

$$s_\theta \stackrel{\Delta}{=} (r\cos\theta, r\sin\theta) \quad . \tag{C.1}$$

From relation (9.17), we can express $\Delta(\theta)$, $\dot{\Delta}(\theta)$, and $\ddot{\Delta}(\theta)$ as

$$\Delta(\theta) = \xi(s_\theta) - X_1 - \Phi(r) \quad , \tag{C.2}$$

$$\dot{\Delta}(\theta) = - r\sin\theta\ \xi_x(s_\theta) + r\cos\theta\ \xi_y(s_\theta) \ , \tag{C.3}$$

and

$$\ddot{\Delta}(\theta) = r^2\sin^2\theta\ \xi_{xx}(s_\theta) - r^2\sin 2\theta\, \xi_{xy}(s_\theta) + r^2\cos^2\theta\ \xi_{yy}(s_\theta)$$
$$- r\cos\theta\ \xi_x(s_\theta) - r\sin\theta\ \xi_y(s_\theta) \quad . \tag{C.4}$$

From relations (C.2) - (C.4) we can see that the random variables $\Delta(\theta)$, $\dot{\Delta}(\theta)$, $\ddot{\Delta}(\theta)$, and $\xi(0,0)$ are jointly Gaussian. Hence, we may use the standard formulae for jointly Gaussian random vectors to form the density for $\Delta(\theta)$, $\dot{\Delta}(\theta)$, and $\ddot{\Delta}(\theta)$ conditioned on $\xi(0,0) = X_1$.

We next derive the conditional density for $\Delta(\theta)$, $\dot{\Delta}(\theta)$, and $\ddot{\Delta}(\theta)$. Letting

$$\zeta(\theta) \triangleq \begin{pmatrix} \Delta(\theta) \\ \dot{\Delta}(\theta) \\ \ddot{\Delta}(\theta) \end{pmatrix} , \tag{C.5}$$

and $$\tilde{\zeta}(\theta) \triangleq \zeta(\theta) - E[\zeta(\theta)] , \tag{C.6}$$

the desired conditional density is specified by the conditional mean

$$E[\zeta(\theta)|\xi(0,0)=X_1] = E[\tilde{\zeta}(\theta)\xi(0,0)]\frac{X_1}{\sigma^2} + \begin{pmatrix} -X_1-\Phi(r) \\ 0 \\ 0 \end{pmatrix} \equiv \begin{pmatrix} m_1(\theta) \\ m_2(\theta) \\ m_3(\theta) \end{pmatrix} , \tag{C.7}$$

and the conditional covariance matrix

$$\lambda(\theta) = E[\tilde{\zeta}(\theta)\tilde{\zeta}'(\theta)] - \frac{E[\tilde{\zeta}(\theta)\xi(0,0)]E[\xi(0,0)\tilde{\zeta}'(\theta)]}{\sigma^2} . \tag{C.8}$$

Hence, by employing the correlation relations and notation of Appendix 9B, we can show that the $m_i(\theta)$'s, $i = 1,\ldots,3$, and the upper triangular part of the $\lambda(\theta)$ matrix are specified as

$$m_1(\theta) = [R_{0,0}(s_\theta)] \frac{X_1}{\sigma^2} - X_1 - \Phi(r) , \tag{C.9}$$

$$m_2(\theta) = [- r \sin\theta \; R_{1,0}(s_\theta) + r \cos\theta \; R_{0,1}(s_\theta)] \frac{X_1}{\sigma^2} , \tag{C.10}$$

$$m_3(\theta) = [r^2\sin^2\theta\ R_{2,0}(s_\theta) - r^2\sin 2\theta\, R_{1,1}(s_\theta) + r^2\cos^2\theta\ R_{0,2}(s_\theta) - r\cos\theta\ R_{1,0}(s_\theta) - r\sin\theta\ R_{0,1}(s_\theta)]\ \frac{X_1}{\sigma^2}\ , \qquad (C.11)$$

$$\lambda_{11}(\theta) = \sigma^2\left(1 - \left(\frac{R_{0,0}(s_\theta)}{\sigma^2}\right)^2\right)\ , \qquad (C.12)$$

$$\lambda_{12}(\theta) = \frac{-[R_{0,0}(s_\theta)][-r\sin\theta\ R_{1,0}(s_\theta) + r\cos\theta\ R_{0,1}(s_\theta)]}{\sigma^2}\ , \qquad (C.13)$$

$$\lambda_{13}(\theta) = [r^2\sin^2\theta\ R_{2,0}(0,0) - r^2\sin 2\theta\ R_{1,1}(0,0) + r^2\cos^2\theta\, R_{0,2}(0,0)] - \frac{-[R_{0,0}(s_\theta)]\left[\begin{array}{l} r^2\sin^2\theta\ R_{2,0}(s_\theta) - r^2\sin 2\theta\, R_{1,1}(s_\theta) \\ + r^2\cos^2\theta\ R_{0,2}(s_\theta) - r\cos\theta\ R_{1,0}(s_\theta) \\ - r\sin\theta\ R_{0,1}(s_\theta) \end{array}\right]}{\sigma^2}\ , \qquad (C.14)$$

$$\lambda_{22}(\theta) = [-r^2\sin^2\theta\ R_{2,0}(0,0) + r^2\sin 2\theta\, R_{1,1}(0,0) - r^2\cos^2\theta\ R_{0,2}(0,0)] - \frac{[-r\sin\theta\ R_{1,0}(s_\theta) + r\cos\theta\ R_{0,1}(s_\theta)]^2}{\sigma^2}\ , \qquad (C.15)$$

$$\lambda_{23}(\theta) = [- r^2 \sin\theta \cos\theta \; R_{2,0}(0,0) + r^2(\cos^2\theta - \sin^2\theta)R_{1,1}(0,0) + r^2 \sin\theta \cos\theta \; R_{0,2}(0,0)]$$

$$- \frac{\begin{bmatrix} - r \sin\theta \; R_{1,0}(s_\theta) \\ + r \cos\theta \; R_{0,1}(s_\theta) \end{bmatrix} \begin{bmatrix} r^2\sin^2\theta \, R_{2,0}(s_\theta) - r^2 \sin 2\theta \, R_{1,1}(s_\theta) \\ + r^2\cos^2\theta \, R_{0,2}(s_\theta) - r \cos\theta \, R_{1,0}(s_\theta) \\ - r \sin\theta \, R_{0,1}(s_\theta) \end{bmatrix}}{\sigma^2} ,$$

(C.16)

and

$$\lambda_{33}(\theta) = [r^4\sin^4\theta \; R_{4,0}(0,0) - 2r^4\sin^2\theta \sin 2\theta \; R_{3,1}(0,0) + 6r^4\sin^2\theta\cos^2\theta \, R_{2,2}(0,0) - 2r^4\cos^2\theta \sin 2\theta \; R_{1,3}(0,0) + r^4\cos^4\theta \; R_{0,4}(0,0) - r^2\cos^2\theta \; R_{2,0}(0,0) - 2r^2\cos\theta \sin\theta \, R_{1,1}(0,0) - r^2\sin^2\theta \; R_{0,2}(0,0)]$$

$$- \frac{\begin{bmatrix} r^2\sin^2\theta \; R_{2,0}(s_\theta) - r^2\sin 2\theta \, R_{1,1}(s_\theta) + r^2\cos^2\theta \; R_{0,2}(s_\theta) \\ - r \cos\theta \; R_{1,0}(s_\theta) - r \sin\theta \; R_{0,1}(s_\theta) \end{bmatrix}^2}{\sigma^2} .$$

(C.17)

Finally, by letting

$$e(\theta) \triangleq \det\{\lambda(\theta)\} \quad , \qquad \text{(C.18)}$$

and $$\alpha(\theta) = \lambda^{-1}(\theta) \quad , \tag{C.19}$$

we can determine the conditional density $p_1\left(\zeta_1(\theta),\zeta_2(\theta),\zeta_3(\theta)\,|\,X_1\right)$ as

$$p_1\left(\zeta_1(\theta),\zeta_2(\theta),\zeta_3(\theta)\,|\,X_1\right) = \frac{1}{(2\pi)^{3/2}e^{1/2}(\theta)} \cdot \exp\left\{-\frac{1}{2}\sum_{i,j}[\zeta_i(\theta)-m_i(\theta)][\zeta_j(\theta)-m_j(\theta)]\alpha_{ij}(\theta)\right\} . \tag{C.20}$$

Now, by employing relation (C.20) for the conditional density of $\Delta(\theta)$, $\dot{\Delta}(\theta)$, and $\ddot{\Delta}(\theta)$, and computing the square of the exponent in $[\zeta_1(\theta) - m_1(\theta)]$, we can evaluate the integral over $\zeta_1(\theta)$ in relation (9.44), and derive the following formula for the conditional mean of $N_1(E_r \cap \partial D_r)$:

$$E[N_1(E_r \cap \partial D_r)\,|\,\xi(0,0)=X_1] = \int_{\theta=0}^{2\pi} \frac{1}{2\pi[\alpha_{11}(\theta)e(\theta)]^{1/2}} \cdot \int_{\zeta_3(\theta)=-\infty}^{0} c[\zeta_3(\theta)]\,|\zeta_3(\theta)| \cdot Q\left[\frac{h_R - m_1(\theta) - v(\theta)}{\alpha_{11}^{-1/2}(\theta)}\right] d\zeta_3(\theta)d\theta \ , \tag{C.21}$$

where

$$v(\theta) \triangleq \frac{m_2(\theta)\alpha_{21}(\theta) - [\zeta_3(\theta) - m_3(\theta)]\alpha_{13}(\theta)}{\alpha_{11}(\theta)}, \tag{C.22}$$

and

$$c[\zeta_3(\theta)] \triangleq \exp\left\{-\frac{1}{2}\left[m_2^2(\theta)\alpha_{22}(\theta) - \alpha_{11}(\theta)v^2(\theta) + [\zeta_3(\theta)-m_3(\theta)]^2\alpha_{33}(\theta) - 2m_2(\theta)\alpha_{23}(\theta)[\zeta_3(\theta)-m_3(\theta)]\right]\right\} \tag{C.23}$$

Finally, we note that to derive relation (C.21) we employed the one-dimensional zero counting technique of Kac [116], Rice [114], and Leadbetter [118] to count zeroes of $\dot{\Delta}(\theta)$ corresponding to relative maxima of $\Delta(\cdot)$, above the level h_R. The process $\Delta(\theta)$ is in general non-stationary, and hence the average number density along ∂D_r, of such relative maxima, varies as a function of θ.

Chapter 10

Subproblems Connecting Terrain-Masking Analysis and Mapping Problems

10.1 Introduction

In Chapters 4 - 5 we derived several processing schemes that were employed in Chapter 7 for the mapping of random fields. The ultimate use of such a map dictates the size of map errors that are allowable. Hence, for each field of application, such as in making geodetic, meteorological, or topographic surveys, it is important to understand how to design measurement schemes, i.e., to assess how many measurement passes we need to make with a given sensor or sensors in order to obtain a final map that will meet our accuracy requirements. In this chapter, we connect the two major areas discussed in this thesis, the map-updating and the terrain-modelling, masking analysis problem areas, by addressing the issue of how accurate the map of a terrain should be, in the context of two different applications.

In Section 10.2 we consider the problem of using terrain map information in a terrain-following vehicle. Earlier, in our description of the one-dimensional terrain-following masking geometry, we assumed that an object, under observation

from the radar, is able to follow the terrain exactly at some additional height h_0. This assumption breaks down due to the finite response time of any real system, physical limitations on control inputs to the system, and inaccuracies in our knowledge of the terrain. Another effect at work which negates the perfect terrain-following assumption is the fact that due to errors in the inertial navigation system, the terrain-following vehicle does not have exact knowledge of its position. Typically this last effect is at least partially dealt with by the correlation of map information with some vehicle sensor measurements. We will not consider this aspect further in our analysis here, although its inclusion is certainly of importance in assessing map accuracy requirements. Consider Fig. 10.1 as a typical record of the altitude of a terrain-following vehicle. We let h_c denote the desired clearance level which the vehicle control system is designed to maintain, and h_v denotes a larger clearance above which, from our earlier masking analysis, we can show that the probability of the object being visible to some radar is unacceptably high. Then, due to imperfect terrain following, we can imagine the following two types of undesirable events: the vehicle exceeds a clearance of h_v, or the vehicle crashes. Assuming that the terrain-following control system has been properly designed, these will be low probability events. Hence, we can reasonably think of the

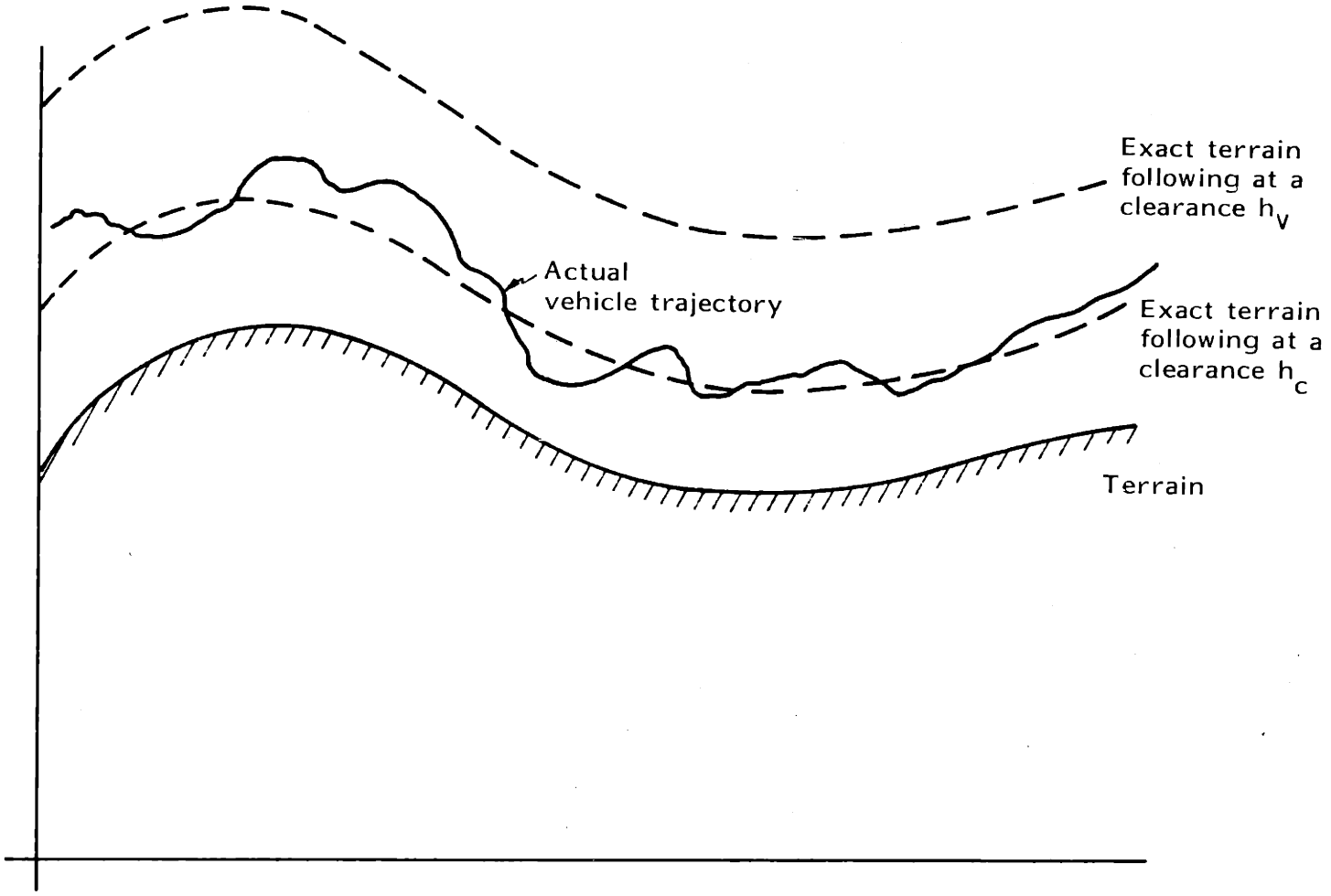

Fig. 10.1 Record of the Altitude of a Terrain-Following Vehicle

average number of crossings, per unit distance, between the vehicle trajectory and either the curve determined by adding h_v onto the terrain, or with the terrain itself, as specifying upper bounds on the probability, per unit distance, of either exceeding the clearance h_v, or crashing, respectively. Therefore, in Section 10.2 we assume a simplified model of the vehicle dynamics, and of the terrain-following control law, and we analyze the steady state frequency of crossings between the vehicle trajectory and either the level h_v above the terrain, or the terrain itself. We perform our analysis under varying assumptions of the control system's knowledge of the terrain process. We consider three cases: when the vehicle has perfect terrain knowledge, when the vehicle has a stored map of the terrain available, and finally, when an on-board processor combines an old map, in a causal manner, with new measurements obtained from some vehicle sensor. Thus, for the terrain-following application, the frequencies of curve crossings that we compute become the criteria by which to evaluate the adequacy or inadequacy of a given terrain map.

In Section 10.3 we consider a second application, where one is given some map information to determine the visibility or invisibility of some object at a given range and height above the terrain. We use the terrain-following masking geometry, and we assume that some map $\hat{\xi}_s(\cdot)$ of the terrain is

given in order to decide whether an object at range r, and terrain-following height h_0, is masked or unmasked with respect to the radar. We then sketch the analysis of an upper bound for the probability of making a wrong decision on the basis of map information. This upper bound becomes a criterion by which to measure the adequacy or inadequacy of a terrain map for detecting a low flying object.

10.2 Analysis of the Effect of Terrain Information on the Steady State Frequency of Crossings between a Terrain-Following Vehicle's Trajectory, and either the Terrain Curve, or the h_v Clearance Level

In this section, we present a simple model for the vertical dynamics and control system associated with a terrain-following vehicle, allowing us to analyze the effect of varying terrain information on the crossing frequency between the vehicle trajectory and either the terrain curve or the h_v clearance level. The same type of analysis may be carried out more generally for the case when the vehicle dynamics and control law may be described by some linear, finite-dimensional, time-invariant state equations.

We will assume that the terrain may be modelled as a stationary random process with a state-space representation of the form

$$\xi(\ell) = h\, x(\ell) \quad , \tag{10.1}$$

where

$$dx(\ell) = A\, x(\ell) d\ell + B\, du(\ell) \ , \tag{10.2}$$

A is a stability matrix, and ℓ denotes spatial distance along a specified trajectory. In addition, for the purpose of simplicity, we imagine that our terrain map is formed based on an infinite-length record of old survey data along the extension

of the line of travel of the vehicle, i.e., if we define

$$dm_1(\ell) = H_1 x(\ell) d\ell + D_1 dv_1(\ell) \quad , \tag{10.3}$$

where $v_1(\cdot)$ is a standard vector Wiener process, and

$$D_1 D_1' = R_1 > 0 \quad , \tag{10.4}$$

and let

$$M_1 \triangleq H(dm_1(\tau) \quad -\infty \leq \tau \leq +\infty) \quad , \tag{10.5}$$

then our terrain map $\hat{\xi}_{1s}(\ell)$ is formed as

$$\hat{\xi}_{1s}(\ell) = h\, \hat{x}_{1s}(\ell) \quad , \tag{10.6}$$

where $$\hat{x}_{1s}(\ell) = E[x(\ell) | M_1] \quad . \tag{10.7}$$

Relations (10.1) - (10.7) imply that the map error process, $\tilde{\xi}_{1s}(\cdot)$, will be stationary. We note that the first case which we analyze, where the terrain-following control system has inexact knowledge of the terrain, is defined by assuming the vehicle uses the map $\hat{\xi}_{1s}(\cdot)$, specified by (10.1) - (10.7).

In addition, the second case for which the vehicle has imperfect terrain information, and for which we will compute the two crossing frequencies, is that in which the terrain-following control system employs an estimate for the terrain derived from causally combining terrain map information with measurements of

some vehicle sensor. The centralized map-updating problem formulation provides a natural framework for the formation of such a terrain estimate. From the work of Kam [51], on estimation of a random field, using data from a sensor that traverses the field with some positive, not necessarily constant velocity, we can assume that we may equivalently model the measurements of our vehicle sensor in the spatial domain as

$$dm_2(\ell) = H_2 x(\ell) d\ell + D_2 dv_2(\ell) \quad , \tag{10.8}$$

where $v_2(\cdot)$ and $v_1(\cdot)$ are independent, and

$$D_2 D_2' = R_2 > 0 \quad , \tag{10.9}$$

and

$$M_{2\ell}^{-} \triangleq H[dm_2(\tau) \quad -\infty \leq \tau \leq \ell] \quad . \tag{10.10}$$

We assume data available on the semi-infinite interval for the purpose of simplicity. Then, we can view the on-board processor as forming the state estimate

$$\hat{x}_{fs}(\ell) = E[x(\ell) | M_1 \vee M_{2\ell}^{-}] \quad , \tag{10.11}$$

where the subscript "fs" will denote the noncausal use of our

original survey data M_1, and the causal use of the vehicle sensor data $\bar{M}_{2\ell}$. Hence, in this case the terrain-following control system employs the terrain estimate

$$\hat{\xi}_{fs}(\ell) = h\, \hat{x}_{fs}(\ell) \quad . \tag{10.12}$$

By making the orthogonal decomposition

$$M_1 \vee \bar{M}_{2\ell} = M_1 \oplus \tilde{\bar{M}}_{2\ell} \quad , \tag{10.13}$$

where

$$\tilde{\bar{M}}_{2\ell} = H[dy_2(\tau) - H_2\, \hat{x}_{1s}(\tau)d\tau \quad -\infty \le \tau \le \ell] \quad , \tag{10.14}$$

we can express $\hat{x}_{fs}(\ell)$ of (10.11) as

$$\hat{x}_{fs}(\ell) = \hat{x}_{1s}(\ell) + E[\tilde{x}_{1s}(\ell) | \tilde{\bar{M}}_{2\ell}] \quad . \tag{10.15}$$

The second term in relation (10.15) corresponds to a filtered estimate for the map error $\tilde{x}_{1s}(\ell)$, based on the $\tilde{\bar{M}}_{2\ell}$ measurements, i.e., the part of the vehicle sensor measurements not predictable from the old survey data. If we employ the notation and results of Section 4.2, we find that

$$\hat{\tilde{x}}_f(\ell) \triangleq E[\tilde{x}_{1s}(\ell) | \tilde{\bar{M}}_{2\ell}] \quad , \tag{10.16}$$

where

$$d\hat{\tilde{x}}_f(\ell) = \Gamma_{fs}\hat{\tilde{x}}_f(\ell)d\ell + P_{fs}H_2'R_2^{-1}[dm_2(\ell) - H_2\,\hat{x}_{1s}(\ell)\,d\ell] \ , \quad (10.17)$$

and

$$\Gamma_{fs} \triangleq A + BB'\left(P_{1f}^{-1} - P_{1s}^{-1}\right) - P_{fs}H_2'R_2^{-1}H_2 \ , \quad (10.18)$$

and where P_{fs} denotes the steady state filtering error covariance matrix associated with the estimation of $\tilde{x}_{1s}(\ell)$ from $\tilde{M}_{2\ell}^{-}$, and P_{1f}, P_{1s} denote the steady state first pass filtering and smoothing error covariance matrices, respectively. Hence, we may define P_{fs} as the unique positive definite solution of the algebraic Ricatti equation

$$0 = \left[A + BB'\left(P_{1f}^{-1} - P_{1s}^{-1}\right)\right]P_{fs} + P_{fs}\left[A + BB'\left(P_{1f}^{-1} - P_{1s}^{-1}\right)\right]'$$
$$+ BB' - P_{fs}H_2'R_2^{-1}H_2P_{fs} \ . \quad (10.19)$$

We may compute $\left(P_{1f}^{-1} - P_{1s}^{-1}\right)$ by recognizing from Appendix 2G that

$$-O_{01} = P_{1f}^{-1} - P_{1s}^{-1} \ , \quad (10.20)$$

where O_{01} satifies the equation

$$0 = A'O_{01} + O_{01}A + H_1'R_1^{-1}H_1 - O_{01}BB'O_{01} \quad . \tag{10.21}$$

Finally, we note that as in the case of $\hat{\xi}_{ls}(\cdot)$, the error process $\tilde{\xi}_{fs}(\cdot)$ associated with the terrain estimate $\hat{\xi}_{fs}(\cdot)$ in (10.12), will be a stationary process.

At this point, we will use the notation $\hat{\xi}(\cdot)$ to denote three types of varying amounts of terrain information employed by the terrain-following control system. When

$$\hat{\xi}(\cdot) = \xi(\cdot) \quad , \tag{10.22}$$

we will assume perfect knowledge of the terrain. When

$$\hat{\xi}(\cdot) = \hat{\xi}_{ls}(\cdot) \quad , \tag{10.23}$$

we will assume that the vehicle employs a map of the terrain defined by relations (10.6) - (10.7). Finally, when

$$\hat{\xi}(\cdot) = \hat{\xi}_{fs}(\cdot) \quad , \tag{10.24}$$

we assume that a processor causally combines the terrain map information with measurements from an on-board sensor, to obtain a terrain estimate defined by relations (10.12) and (10.15) - (10.18).

Having defined explicitly the three cases of varying terrain information, for which we will analyze the average frequency of crossings between the vehicle trajectory and either the terrain curve or the h_v clearance level, we next present our simple model for the vertical vehicle dynamics, and the terrain-following control system. We assume that the vehicle moves in a horizontal direction with some constant velocity, v, and knows its position perfectly. Letting m denote the vehicle mass, C and K denote proportionality constants, h_c specify the desired terrain-following clearance, and y(t) denote the vehicle height relative to the terrain mean elevation, then we assume that y(t) obeys the equation

$$m\ddot{y}(t) = -mg - C\dot{y}(t) + K\,e(t) \quad , \tag{10.25}$$

where e(t) is an error signal defined by

$$e(t) = \hat{\xi}(vt) + h_c - y(t) \quad . \tag{10.26}$$

We first emphasize that (10.25) and (10.26) were adopted for the sake of simplicity. The important point in our analysis is not the structure of the terrain-following control system, or our model for the vehicle dynamics, but the method which we present for evaluating the effect of varying terrain

information. The term $C\dot{y}$ is meant to correspond to some retarding force on the vehicle, proportional to the velocity. The term $K\,e(t)$ represents the force exerted on the vehicle by the control system, in response to the error signal $e(t)$. We note that the control law (10.26) is the simplest one, resulting in a finite steady state tracking error [40] of the desired clearance level h_c, for a flat terrain, i.e., $\xi(\cdot)$ = constant.

Now, defining the spatial variable s by

$$s \triangleq vt \quad , \tag{10.27}$$

letting

$$Y(s) = y\left(\frac{s}{v}\right) \quad , \tag{10.28}$$

and defining the constants

$$\alpha \triangleq \frac{C}{m} \quad , \tag{10.29}$$

and

$$\beta \triangleq \frac{K}{m} \quad , \tag{10.30}$$

by employing equations (10.25) - (10.26) we obtain the following spatial dynamics for $Y(\cdot)$:

$$\boxed{v^2 Y''(s) + \alpha v Y'(s) + \beta Y(s) = [\beta h_c - g] + \beta \hat{\xi}(s).} \quad (10.31)$$

We will employ equation (10.31) to compute, in the steady state, for our three choices of $\hat{\xi}(\cdot)$, the frequency of curve crossings per unit distance between $Y(s)$ and $\xi(s)$ and between $Y(s)$ and $\xi(s)+h_v$.

From (10.31) we can argue that in the steady state, $Y(s)$ may be represented as

$$Y(s) = \left[h_c - \frac{g}{\beta}\right] + \gamma(s) \quad , \quad (10.32)$$

where $\gamma(s)$ is the output of a system with transfer function $H(j\omega)$ defined by

$$H(j\omega) \triangleq \frac{\beta}{v^2(j\omega)^2 + v\alpha(j\omega) + \beta} \quad , \quad (10.33)$$

and input, $\hat{\xi}(s)$. Let us now define the process $\not{z}(s)$ as the difference between the terrain height at location s, $\xi(s)$, and the vehicle height at location s, $Y(s)$, i.e.,

$$\not{z}(s) \triangleq Y(s) - \xi(s) \quad . \quad (10.34)$$

Then, the vehicle trajectory crosses the terrain curve or the h_v clearance level when $\bar{z}(s) = 0$ or $\bar{z}(s) = h_v$, respectively, or equivalently, by substituting (10.32) into (10.34), whenever the zero-mean process $\delta(s)$ defined by

$$\boxed{\delta(s) \triangleq \gamma(s) - \xi(s) \ ,} \tag{10.35}$$

crosses the levels $\left[-h_c + \frac{g}{\beta}\right]$ or $\left[h_v - h_c + \frac{g}{\beta}\right]$, respectively. Under the three cases for $\hat{\xi}(s)$ defined by relations (10.22) - (10.24), the process $\delta(\cdot)$ will be stationary, and we may use results on the frequency of level crossings for stationary random processes [117] to express the average number of crossings per unit distance between $\delta(\cdot)$ and the level a as

$$\boxed{N_a(\hat{\xi}) = \frac{1}{\pi}\left(-\frac{R_\delta''(0)}{R_\delta(0)}\right)^{\frac{1}{2}} \exp\left\{-\frac{a^2}{2R_\delta(0)}\right\} \ ,} \tag{10.36}$$

where

$$\boxed{R_\delta(\tau) = E[\delta(s+\tau)\delta(s)] \ .} \tag{10.37}$$

Hence, we evaluate $N_a(\hat{\xi})$ for $a = \left[-h_c + \frac{g}{\beta}\right]$ or $a = \left[h_v - h_c + \frac{g}{\beta}\right]$ in order to compute the desired crossing frequencies.

In the remainder of this section, we investigate the calculation of $R_\delta(0)$ and $R''_\delta(0)$. If we define the correlation function, $R_\gamma(\tau)$, and the cross-correlation function, $R_{\gamma\xi}(\tau)$, by

$$R_\gamma(\tau) = E[\gamma(s+\tau)\gamma(s)] \quad , \tag{10.38}$$

and

$$R_{\gamma\xi}(\tau) = E[\gamma(s+\tau)\xi(s)] \quad , \tag{10.39}$$

then by employing relation (10.35), we may show that

$$\boxed{R_\delta(0) = R_\gamma(0) + R_\xi(0) - 2R_{\gamma\xi}(0) \quad ,} \tag{10.40}$$

and

$$\boxed{R''_\delta(0) = R''_\gamma(0) + R''_\xi(0) - 2R''_{\gamma\xi}(0) \quad .} \tag{10.41}$$

Assuming that the terrain correlation function, $R_\xi(\tau)$, is known, and is consistent with the state space model of relations (10.1) - (10.2), we need only determine $R_\gamma(0), R''_\gamma(0)$ and $R_{\gamma\xi}(0), R''_{\gamma\xi}(0)$ to calculate $R_\delta(0), R''_\delta(0)$ from equations (10.40) - (10.41). Defining the power spectral densities corresponding to $R_\gamma(\cdot)$ and $R_{\gamma\xi}(\cdot)$ by

$$S_\gamma(\omega) = \mathcal{F}\{R_\gamma(\cdot)\} \quad , \tag{10.42}$$

and

$$S_{\gamma\xi}(\omega) = \mathcal{F}\{R_{\gamma\xi}(\cdot)\} \tag{10.43}$$

where $\mathcal{F}\{\cdot\}$ denotes the Fourier transform, we can define the desired quantities by the following frequency domain integrals:

$$R_{\gamma}(0) = \frac{1}{2\pi}\int_{-\infty}^{+\infty} S_{\gamma}(\omega)\,d\omega \quad , \tag{10.44}$$

$$R''_{\gamma}(0) = -\frac{1}{2\pi}\int_{-\infty}^{+\infty} \omega^2 S_{\gamma}(\omega)\,d\omega \quad , \tag{10.45}$$

$$R_{\gamma\xi}(0) = \frac{1}{2\pi}\int_{-\infty}^{+\infty} \mathrm{Re}\{S_{\gamma\xi}(\omega)\}d\omega \quad , \tag{10.46}$$

and

$$R''_{\gamma\xi}(0) = -\frac{1}{2\pi}\int_{-\infty}^{+\infty} \omega^2\,\mathrm{Re}\{S_{\gamma\xi}(\omega)\}d\omega \quad . \tag{10.47}$$

In Fig. 10.2 we describe the input-output relationship between $\hat{\xi}(\cdot)$ and $\gamma(\cdot)$, where the transfer function $H(j\omega)$ is defined by equation (10.33). Hence, we can express $S_{\gamma}(\omega)$ and $S_{\gamma\xi}(\omega)$ as

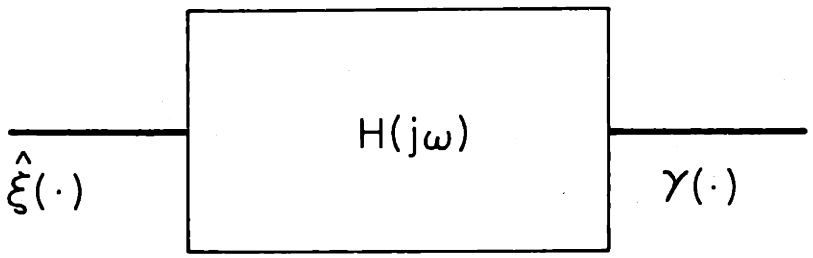

Fig. 10.2 Diagram of the Input-Output Relationship between $\gamma(\cdot)$ and $\hat{\xi}(\cdot)$

$$S_{\gamma}(\omega) = S_{\hat{\xi}}(\omega)\,|H(j\omega)|^2 \quad , \tag{10.48}$$

and

$$S_{\gamma\xi}(\omega) = H(j\omega)S_{\hat{\xi}\xi}(\omega) \quad . \tag{10.49}$$

This shows that we need only to form $S_{\hat{\xi}}(\omega)$ and $S_{\hat{\xi}\xi}(\omega)$, in each of our three cases for $\hat{\xi}(\cdot)$, in order to perform the calculations defined by relations (10.44) - (10.47). When $\hat{\xi}(\cdot) = \xi(\cdot)$, the case of perfect terrain knowledge, we have

$$S_{\hat{\xi}}(\omega) = S_{\xi}(\omega) \quad , \tag{10.50}$$

and

$$S_{\hat{\xi}\xi}(\omega) = S_{\xi}(\omega) \quad . \tag{10.51}$$

For the case when $\hat{\xi}(\cdot) = \hat{\xi}_{1s}(\cdot)$, we can use orthogonality properties satisfied by the smoothing errors, $\tilde{\xi}_{1s}(\cdot)$, to show that

$$S_{\hat{\xi}}(\omega) = S_{\xi}(\omega) - S_{\tilde{\xi}_{1s}}(\omega) \quad , \tag{10.52}$$

and

$$S_{\hat{\xi}\xi}(\omega) = S_{\xi}(\omega) - S_{\tilde{\xi}_{1s}}(\omega) \quad . \tag{10.53}$$

Finally, for the case when $\hat{\xi}(\cdot) = \hat{\xi}_{fs}(\cdot)$, if we define

$$F(\omega) \triangleq \mathcal{F}\left\{R_{\xi\tilde{\xi}_{fs}}(|\tau|)\right\} \quad , \tag{10.54}$$

and

$$G(\omega) \triangleq \mathcal{F}\{g(\tau)\} \quad , \tag{10.55}$$

where

$$g(\tau) = \begin{cases} R_{\tilde{\xi}_{fs}}(\tau) & \tau \geq 0 \\ R_{\xi\tilde{\xi}_{fs}}(-\tau) & \tau < 0 \end{cases} \quad , \tag{10.56}$$

we may employ orthogonality properties satisfied by $\tilde{\xi}_{fs}(\cdot)$ to show that

$$\boxed{S_{\hat{\xi}}(\omega) = S_{\xi}(\omega) - F(\omega) \quad ,} \tag{10.57}$$

and

$$\boxed{S_{\hat{\xi}\xi}(\omega) = S_{\xi}(\omega) - G(\omega) \quad .} \tag{10.58}$$

The quantities $S_{\tilde{\xi}_s}(\omega)$, $F(\omega)$, and $G(\omega)$ that appear in relations (10.52) - (10.53) and (10.57) - (10.58) reflect the impact of errors in the terrain estimates, $\hat{\xi}_{ls}(\cdot)$ and $\hat{\xi}_{fs}(\cdot)$, on the calculations of $S_{\hat{\xi}}(\omega)$ and $S_{\hat{\xi}\xi}(\omega)$, and hence ultimately on the calculation of the desired crossing frequencies between

the vehicle trajectory and the terrain curve, or between the vehicle trajectory and the h_v clearance level. We next show that using a block diagram representation for the estimates $\hat{x}_{ls}(\cdot)$ and $\hat{x}_{fs}(\cdot)$, it is possible to form $S_{\hat{\xi}}(\omega)$ and $S_{\hat{\xi}\hat{\xi}}(\omega)$ directly. To obtain such a block diagram representation for $\hat{x}_{ls}(\cdot)$ and $\hat{x}_{fs}(\cdot)$, it is more convenient to work with a white noise formulation of the estimation problems defining them. Hence, we will imagine that the state process $x(\cdot)$ is modelled by

$$\frac{dx}{d\ell} = A\ x(\ell) + w(\ell) \quad , \tag{10.59}$$

where

$$E[w(\ell_1)w'(\ell_2)] = Q\ \delta(\ell_1 - \ell_2), \tag{10.60}$$

and

$$Q \triangleq BB' \quad . \tag{10.61}$$

Similarly, we assume that the old survey measurements, $z_1(\ell)$, and the vehicle sensor measurements, $z_2(\ell)$, are specified by

$$z_1(\ell) = H_1 x(\ell) + n_1(\ell) \quad , \tag{10.62}$$

and

$$z_2(\ell) = H_2 x(\ell) + n_2(\ell) \quad , \tag{10.63}$$

where

$$E[n_1(\ell_1)n_1'(\ell_2)] = R_1\ \delta(\ell_1 - \ell_2) \quad , \tag{10.64}$$

$$E[n_2(\ell_1)n_2'(\ell_2)] = R_2\ \delta(\ell_1 - \ell_2) \quad , \tag{10.65}$$

and $n_1(\cdot), n_2(\cdot)$ are uncorrelated. In this setting we note that $\hat{x}_{1s}(\ell)$ is derived as the output of a system with input $z_1(\cdot)$, and with an associated nonrealizable transfer function $H_{sm}(j\omega)$ defined by

$$H_{sm}(j\omega) \triangleq S_x(j\omega)H_1'\left[H_1 S_x(j\omega)H_1' + R_1\right]^{-1} \quad , \tag{10.66}$$

where

$$S_x(j\omega) = (j\omega I - A)^{-1}\ Q(-j\omega I - A')^{-1} \quad . \tag{10.67}$$

We next note that in our white noise formulation, $\hat{x}_{fs}(\ell)$ is represented from equations (10.15) and (10.17) as

$$\hat{x}_{fs}(\ell) = \hat{x}_{1s}(\ell) + \hat{\tilde{x}}_f(\ell) \quad , \tag{10.68}$$

where

$$\frac{d\hat{\tilde{x}}_f(\ell)}{d\ell} = \Gamma_{fs}\hat{\tilde{x}}_f(\ell) + P_{fs}H_2'R_2^{-1}H_2\tilde{x}_{1s}(\ell) + P_{fs}H_2'R_2^{-1}n_2(\ell) \quad . \tag{10.69}$$

By using (10.66) and (10.68) - (10.69) we obtain the block diagram of Fig. 10.3 for representing $\hat{x}_{ls}(\cdot)$ and $\hat{x}_{fs}(\cdot)$, and their associated errors, $\tilde{x}_{ls}(\cdot)$ and $\tilde{x}_{fs}(\cdot)$. From Fig. 10.3 we can express the transfer functions from w to $\hat{x}_{ls}$ and from n_1 to $\hat{x}_{ls}$, denoted by $H_{\hat{x}_{ls},w}(j\omega)$ and $H_{\hat{x}_{ls},n_1}(j\omega)$, respectively, as

$$H_{\hat{x}_{ls},w}(j\omega) \triangleq H_{sm}(j\omega)H_1(j\omega I - A)^{-1} \quad , \tag{10.70}$$

and

$$H_{\hat{x}_{ls},n_1}(j\omega) \triangleq H_{sm}(j\omega) \quad . \tag{10.71}$$

Hence, we may express the power spectral densities $S_{\hat{x}_{ls}}(\omega)$ and $S_{\hat{x}_{ls}\,x}(\omega)$ as

$$S_{\hat{x}_{ls}}(\omega) = H_{\hat{x}_{ls},w}(j\omega)\, Q\, H'_{\hat{x}_{ls},w}(-j\omega) + H_{\hat{x}_{ls},n_1}(j\omega)\, R_1\, H'_{\hat{x}_{ls},n_1}(-j\omega), \tag{10.72}$$

and

$$S_{\hat{x}_{ls}\,x}(\omega) = H_{\hat{x}_{ls},w}(j\omega)\, Q(-j\omega I - A')^{-1} \quad . \tag{10.73}$$

Similarly, we may express the transfer functions from w to $\hat{x}_{fs}$, n_1 to $\hat{x}_{fs}$, and n_2 to $\hat{x}_{fs}$, denoted by the notations $H_{\hat{x}_{fs},w}(j\omega)$, $H_{\hat{x}_{fs},n_1}(j\omega)$, and $H_{\hat{x}_{fs},n_2}(j\omega)$, respectively, as

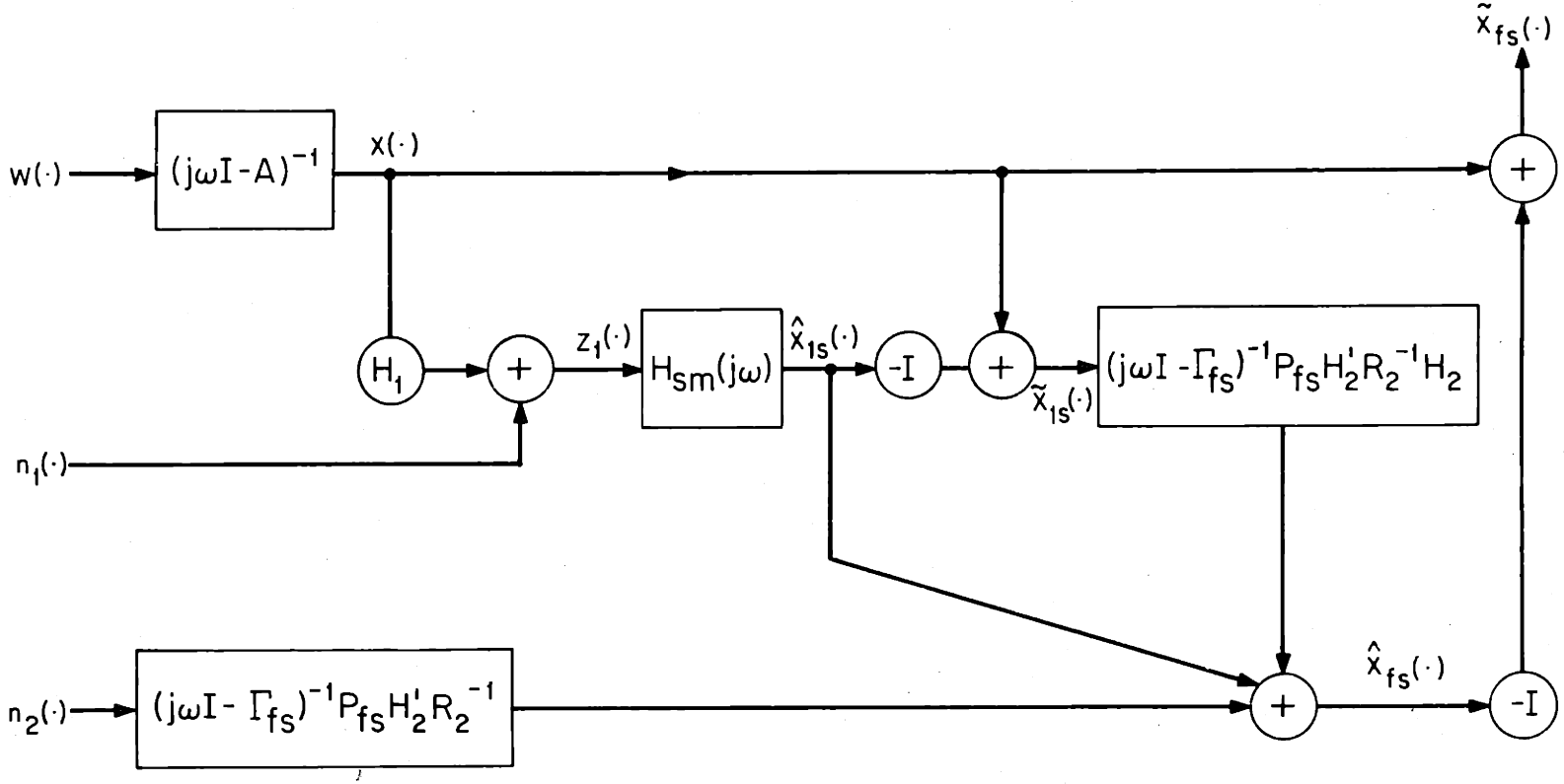

Fig. 10.3 Block Diagram Representation for $\hat{x}_{1s}(\cdot)$, $\hat{x}_{fs}(\cdot)$, $\tilde{x}_{1s}(\cdot)$, and $\tilde{x}_{fs}(\cdot)$

$$H_{\hat{x}_{fs},w}(j\omega) = \left[(j\omega I - \Gamma_{fs})^{-1} P_{fs} H_2' R_2^{-1} H_2\right](j\omega I - A)^{-1}$$

$$+ \left\{I - \left[(j\omega I - \Gamma_{fs})^{-1} P_{fs} H_2' R_2^{-1} H_2\right]\right\} H_{sm}(j\omega) H_1 (j\omega I - A)^{-1}, \tag{10.74}$$

$$H_{\hat{x}_{fs},n_1}(j\omega) = \left\{I - \left[(j\omega I - \Gamma_{fs})^{-1} P_{fs} H_2' R_2^{-1} H_2\right]\right\} H_{sm}(j\omega) \ , \tag{10.75}$$

and

$$H_{\hat{x}_{fs},n_2}(j\omega) = (j\omega I - \Gamma_{fs})^{-1} P_{fs} H_2' R_2^{-1} \ . \tag{10.76}$$

Therefore, we compute the power spectral densities $S_{\hat{x}_{fs}}(\omega)$ and $S_{\hat{x}_{fs}\,x}(\omega)$ as

$$S_{\hat{x}_{fs}}(\omega) = H_{\hat{x}_{fs},w}(j\omega)\, Q\, H'_{\hat{x}_{fs},w}(-j\omega) + H_{\hat{x}_{fs},n_1}(j\omega)\, R_1\, H'_{\hat{x}_{fs},n_1}(-j\omega)$$

$$+ H_{\hat{x}_{fs},n_2}(j\omega)\, R_2\, H'_{\hat{x}_{fs},n_2}(-j\omega) \ , \tag{10.77}$$

and

$$S_{\hat{x}_{fs}\,x}(j\omega) = H_{\hat{x}_{fs},w}(j\omega)\, Q(-j\omega I - A')^{-1} \ . \tag{10.78}$$

Finally, we note that given our expressions for $S_{\hat{x}_{ls}}(\omega)$, $S_{\hat{x}_{ls}x}(\omega)$, $S_{\hat{x}_{fs}}(\omega)$, and $S_{\hat{x}_{fs}x}(\omega)$ we can compute $S_{\hat{\xi}}(\omega)$ and $S_{\hat{\xi}\xi}(\omega)$ by using (10.6) and (10.12).

In conclusion, we note that by employing the expressions for $S_{\hat{\xi}}(\omega)$ and $S_{\hat{\xi}\xi}(\omega)$ derived from relations (10.72) - (10.73) and (10.77) - (10.78) to define $S_{\gamma}(\omega)$ and $S_{\gamma\xi}(\omega)$, and to evaluate the integrals of relations (10.44) - (10.47) for $R_{\gamma}(0)$, $R''_{\gamma}(0)$, $R_{\gamma\xi}(0)$, and $R''_{\gamma\xi}(0)$, we may ultimately compute $R_{\delta}(0)$ and $R''_{\delta}(0)$, for use in expression (10.36) for the frequency of level crossings of the $\delta(\cdot)$ process. We earlier showed that crossings between $\delta(\cdot)$ and the levels $\left[-h_c + \frac{g}{\beta}\right]$ and $\left[h_v - h_c + \frac{g}{\beta}\right]$ are equivalent to crossings between the vehicle trajectory and the terrain curve or between the vehicle trajectory and the h_v clearance level, respectively. We note that the analysis presented here for the simple vehicle dynamics model (10.25), and control law (10.26), is only a first step, providing the basis for the evaluation of more sophisticated terrain-following controllers, i.e., such as control laws that use information on future values of the terrain height, to anticipate hills. We can check the consistency of the results we have obtained by noting that when the horizontal velocity v approaches zero, $\gamma(\cdot)$ approaches $\hat{\xi}(\cdot)$, so that in the case for which we have a good map of the terrain, i.e., $\hat{\xi}(\cdot) \cong \xi(\cdot)$, we can expect that

the variance of $\delta(\cdot)$, $R_\delta(0)$, will be small. Therefore, by choosing a appropriately in evaluating (10.36), we can verify that in this case the frequencies of crossings between the vehicle trajectory and either the terrain curve or the h_v clearance level, will be small.

10.3 The Use of Terrain Map Information in Deciding whether a Terrain-Following Object is Masked or Unmasked with respect to a Radar

In Chapter 8 we considered three different measures of the masking effect created by a terrain, on radar observations, for some one-dimensional terrain-masking geometries. Let us imagine that we have a map of the terrain, $\hat{\xi}_s(\cdot)$, which is defined by equations (10.6) - (10.7), i.e., a set of smoothed estimates determined by assuming a terrain model of the form in equations (10.1) - (10.2), and a measurement equation, (10.3). Assuming the idealized formulation of the terrain-following masking geometry, we consider the use of the map, $\hat{\xi}_s(\cdot)$, to decide whether an object at range r and height h_0 is masked or unmasked with respect to the radar. In this section, we sketch the construction of an upper bound on the probability of making a wrong decision concerning object visibility or invisibility with respect to the radar, based on map information. This upper bound can then be used as a criterion by which to evaluate the adequacy of a given map, resulting in a possible savings of resources, by allowing one to make an intelligent decision as to whether more measurements are needed to obtain an improved map.

We first examine the use of the terrain map, $\hat{\xi}_s(\cdot)$, to determine whether the object is masked or unmasked with respect to the radar. We recall from Section 8.2.1 that one of our

measures of the masking effect, whose conditional mean was analyzed for the terrain-following masking geometry, was $n_c(r)$, the number of crossings between the terrain curve and line-of-sight curve, over the range r. We can express $n_c(r)$ explicitly as

$$n_c(r) = \int_{\ell_1=0}^{r} \delta\Big(\eta(\ell_1) - \xi(\ell_1)\Big)\,|\dot{\eta}(\ell_1) - \dot{\xi}(\ell_1)|\,d\ell_1 \quad , \qquad (10.79)$$

where

$$\eta(\ell_1) \triangleq \eta\big(\xi(0), \xi(r), \ell_1\big) \quad , \qquad (10.80)$$

represents the line-of-sight curve (8.6). Hence, when $n_c(r) > 0$, the object is masked with respect to the radar; and when $n_c(r) = 0$, the object is visible to the radar. We can describe the use of a map, $\hat{\xi}_s(\cdot)$, to determine object visibility or invisibility in an analogous manner by forming $\hat{n}_c(r)$ as

$$\hat{n}_c(r) = \int_{\ell_2=0}^{r} \delta\Big(\hat{\eta}(\ell_2) - \hat{\xi}_s(\ell_2)\Big)\,|\dot{\hat{\eta}}(\ell_2) - \dot{\hat{\xi}}_s(\ell_2)|\,d\ell_2 \quad , \qquad (10.81)$$

where

$$\hat{\eta}(\ell_2) \triangleq \hat{\eta}\big(\hat{\xi}_s(0), \hat{\xi}_s(r), \ell_2\big) \quad . \qquad (10.82)$$

Then, we decide that the object is visible when $\hat{n}_c(r) = 0$, and that it is invisible when $\hat{n}_c(r) > 0$.

We next define two mutually exclusive events, which we term E_1 and E_2, which together define the event of making a wrong decision as to object visibility based on map information. We let

$$E_1 \triangleq \left\{[n_c(r) > 0] \cap [\hat{n}_c(r) = 0]\right\} \quad , \tag{10.83}$$

and

$$E_2 \triangleq \left\{[n_c(r) = 0] \cap [\hat{n}_c(r) > 0]\right\} \quad . \tag{10.84}$$

The event E_1 denotes the case when we decide that the object is visible, when it is actually masked, and similarly E_2 denotes the case when we decide that the object is masked, when in reality it is visible to the radar. We will determine an event E_3 such that

$$E_1 \cup E_2 \in E_3 \quad , \tag{10.85}$$

and hence

$$\Pr\{E_1 \cup E_2\} \leq \Pr\{E_3\} \quad . \tag{10.86}$$

If we define the random variable $\Delta_c(r)$ by

$$\Delta_c(r) = n_c(r) - \hat{n}_c(r) \ , \tag{10.87}$$

then a suitable choice for E_3 is defined by

$$E_3 \triangleq \left\{\Delta_c^2(r) > 0\right\} \ . \tag{10.88}$$

Since both $n_c(r)$ and $\hat{n}_c(r)$ assume only even-numbered values with probability 1, the smallest nonzero value assumed by $\Delta_c^2(r)$ is 4. Hence, by employing the simplest Chebyshev inequality to upper bound $\Pr\{E_3\}$, we obtain the following upper bound on $\Pr\{E_1 \cup E_2\}$:

$$\boxed{\Pr\left\{E_1 \cup E_2\right\} \leq \frac{1}{4} E\left[\Delta_c^2(r)\right] \ .} \tag{10.89}$$

We note that in the case when $\Pr\{|\Delta_c(r)| > 2\}$ is negligible, we expect the bound (10.89) is quite tight.

In the remainder of this section, we compute $E\left[\Delta_c^2(r)\right]$. From equation (10.87) we can express the second moment of $\Delta_c(r)$ as

$$E\left[\Delta_c^2(r)\right] = E\left[n_c^2(r)\right] + E\left[\hat{n}_c^2(r)\right] - 2E\left[n_c(r)\hat{n}_c(r)\right] \ . \tag{10.90}$$

To evaluate $E\left[n_c^2(r)\right]$ we employ the explicit representation of

equations (10.79) - (10.80), and the joint density for $[\xi(0), \xi(r), \xi(\ell_1), \dot{\xi}(\ell_1), \xi(\ell_2), \dot{\xi}(\ell_2)]$, $p(\cdot,\cdot,\cdot,\cdot,\cdot,\cdot)$, as follows:

$$E\left[n_c^2(r)\right] = \int_{\ell_1=0}^{r} \int_{\ell_2=0}^{r} \int_{(\zeta_1,\zeta_2,\zeta_4,\zeta_6)} p(\zeta_1,\zeta_2,\eta(\ell_1),\zeta_4,\eta(\ell_2),\zeta_6)$$

$$\cdot\ |\zeta_4 - \dot{\eta}(\ell_1)|\,|\zeta_6 - \dot{\eta}(\ell_2)|\, d\zeta_1 d\zeta_2 d\zeta_4 d\zeta_6 d\ell_2 d\ell_1 . \qquad (10.91)$$

To evaluate $E\left[\hat{n}_c^2(r)\right]$ we similarly employ the explicit representation of equations (10.81) - (10.82), and the joint density for $[\hat{\xi}_s(0), \hat{\xi}_s(r), \hat{\xi}_s(\ell_1), \dot{\hat{\xi}}_s(\ell_1), \hat{\xi}_s(\ell_2), \dot{\hat{\xi}}_s(\ell_2)]$, $\hat{p}(\cdot,\cdot,\cdot,\cdot,\cdot,\cdot)$, as follows:

$$E\left[\hat{n}_c^2(r)\right] = \int_{\ell_1=0}^{r} \int_{\ell_2=0}^{r} \int_{(\zeta_1,\zeta_2,\zeta_4,\zeta_6)} \hat{p}(\zeta_1,\zeta_2,\hat{\eta}(\ell_1),\zeta_4,\hat{\eta}(\ell_2),\zeta_6)$$

$$\cdot\ |\zeta_4 - \dot{\hat{\eta}}(\ell_1)|\,|\zeta_6 - \dot{\hat{\eta}}(\ell_2)|\, d\zeta_1 d\zeta_2 d\zeta_4 d\zeta_6 d\ell_2 d\ell_1 . \qquad (10.92)$$

Finally, to form $E[n_c(r)\hat{n}_c(r)]$ we employ explicit representations for both $n_c(r)$ and $\hat{n}_c(r)$, and the joint density for $[\xi(0), \xi(r), \xi(\ell_1), \dot{\xi}(\ell_1), \hat{\xi}_s(0), \hat{\xi}_s(r), \hat{\xi}_s(\ell_2), \dot{\hat{\xi}}_s(\ell_2)]$, $\hat{p}(\cdot,\cdot,\cdot,\cdot,\cdot,\cdot,\cdot,\cdot)$, as follows:

$$E[n_c(r)\hat{n}_c(r)] = \int_{\ell_1=0}^{r} \int_{\ell_2=0}^{r} \int_{(\zeta_1,\zeta_2,\zeta_4,\zeta_5,\zeta_6,\zeta_8)}$$

$$\cdot \hat{p}(\zeta_1,\zeta_2,\eta(\ell_1),\zeta_4,\zeta_5,\zeta_6,\hat{\eta}(\ell_2),\zeta_8)$$

$$\cdot |\zeta_4 - \dot{\eta}(\ell_1)||\zeta_8 - \dot{\hat{\eta}}(\ell_2)| d\zeta_1 d\zeta_2 d\zeta_4 d\zeta_5 d\zeta_6 d\zeta_8 d\ell_2 d\ell_1. \quad (10.93)$$

We finally note that as in the formation of the conditional mean of $n_c(r)$, we can explicitly evaluate the integration over (ζ_4,ζ_6) in relations (10.91) - (10.92) and (ζ_4,ζ_8) in equation (10.93). In this manner, the evaluation of $E\left[n_c^2(r)\right]$ and $E\left[\hat{n}_c^2(r)\right]$ can be reduced to a four-dimensional multiple integral, and the calculation of $E[n_c(r)\hat{n}_c(r)]$ may be reduced to a six-dimensional multiple integral. Such integrals may be evaluated numerically by the method of equidistributional sampling [146].

We now note that to form the joint densities required to evaluate the integrals of equations (10.91) - (10.93), we use the assumption that both the terrain, $\xi(\cdot)$, and the terrain map, $\hat{\xi}_s(\cdot)$, are zero-mean, at least mean-square differentiable, Guassian random processes. In the case when the terrain model and terrain map are determined as in relations (10.1) - (10.7), both the terrain, $\xi(\cdot)$, and the map errors, $\tilde{\xi}_s(\cdot)$, are

stationary processes. Hence, to evaluate the joint density, $p(\cdot,\cdot,\cdot,\cdot,\cdot,\cdot)$, for $[\xi(0),\xi(r),\xi(\ell_1),\dot{\xi}(\ell_1),\xi(\ell_2),\dot{\xi}(\ell_2)]$ we employ the correlation relations:

$$E[\xi(s_1)\xi(s_2)] = R_{\xi}(s_2 - s_1) \ , \tag{10.94}$$

$$E[\xi(s_1)\dot{\xi}(s_2)] = \dot{R}_{\xi}(s_2 - s_1) \ , \tag{10.95}$$

and $$E[\dot{\xi}(s_1)\dot{\xi}(s_2)] = -\ddot{R}_{\xi}(s_2 - s_1) \ . \tag{10.96}$$

To evaluate the joint density, $\hat{p}(\cdot,\cdot,\cdot,\cdot,\cdot,\cdot)$, for $[\hat{\xi}_s(0),\hat{\xi}_s(r),\hat{\xi}_s(\ell_1),\dot{\hat{\xi}}_s(\ell_1),\hat{\xi}_s(\ell_2),\dot{\hat{\xi}}_s(\ell_2)]$, we employ the orthogonality properties satisfied by smoothed estimates to derive the correlation relations:

$$E[\hat{\xi}_s(s_1)\hat{\xi}_s(s_2)] = R_{\xi}(s_2 - s_1) - R_{\tilde{\xi}_s}(s_2 - s_1) \ , \tag{10.97}$$

$$E[\hat{\xi}_s(s_1)\dot{\hat{\xi}}_s(s_2)] = \dot{R}_{\xi}(s_2 - s_1) - \dot{R}_{\tilde{\xi}_s}(s_2 - s_1) \ , \tag{10.98}$$

$$E[\dot{\hat{\xi}}_s(s_1)\dot{\hat{\xi}}_s(s_2)] = -\ddot{R}_{\xi}(s_2 - s_1) + \ddot{R}_{\tilde{\xi}_s}(s_2 - s_1) \ . \tag{10.99}$$

Finally, to evaluate the joint density, $\hat{p}(\cdot,\cdot,\cdot,\cdot,\cdot,\cdot,\cdot,\cdot)$, for $[\xi(0),\xi(r),\xi(\ell_1),\dot{\xi}(\ell_1),\hat{\xi}_s(0),\hat{\xi}_s(r),\hat{\xi}_s(\ell_2),\dot{\hat{\xi}}_s(\ell_2)]$, we again use orthogonality properties satisfied by smoothed

estimates to show that

$$E[\xi(s_1)\hat{\xi}_s(s_2)] = R_\xi(s_2 - s_1) - R_{\tilde{\xi}_s}(s_2 - s_1) \ , \qquad (10.100)$$

$$E[\dot{\xi}(s_1)\hat{\xi}_s(s_2)] = -\dot{R}_\xi(s_2 - s_1) + \dot{R}_{\tilde{\xi}_s}(s_2 - s_1) \ , \qquad (10.101)$$

$$E[\xi(s_1)\dot{\hat{\xi}}_s(s_2)] = \dot{R}_\xi(s_2 - s_1) - \dot{R}_{\tilde{\xi}_s}(s_2 - s_1) \ , \qquad (10.102)$$

and $$E[\dot{\xi}(s_1)\dot{\hat{\xi}}_s(s_2)] = -\ddot{R}_\xi(s_2 - s_1) + \ddot{R}_{\tilde{\xi}_s}(s_2 - s_1) \ . \qquad (10.103)$$

Hence, the statistics of our map errors have some impact on the upper bound in relation (10.89) for the probability of making a wrong decision as to object visibility, based on map information, through the $R_{\tilde{\xi}_s}(\cdot)$ terms in equations (10.97) - (10.103).

10.4 Conclusion

In this chapter we considered two specific applications for terrain mapping results: we studied the use of a map by a terrain-following vehicle as well as the use of a map by a radar station to decide whether a terrain-following object is masked or unmasked with respect to a radar. In each case, we proposed and sketched the analysis of some criteria by which to judge the adequacy or inadequacy of the maps accuracy. In the case of the terrain-following vehicle, we suggested two criteria: either the frequency of crossings between the vehicle trajectory and the terrain curve (crashes), or the frequency of times the vehicle exceeds the h_v clearance level. For the case of using map information to determine object visibility, the criterion we presented is an upper bound on the probability of making a wrong decision. Through the analysis of each criterion, we displayed the impact of map error statistics.

The problem formulations of this chapter represent first approaches to evaluating the effect of terrain map errors in the context of two distinct map usages. By employing similar approaches, we can analyze the effect of map errors in many other applications. As another example, consider the use of a map of the gravitational field as part of an inertial navigation system, such as a ship or submarine. In this case, the

map errors become inputs to the navigation system, and result in errors in the position that is computed. If we let $(\Delta_x(t), \Delta_y(t))$ denote the vector corresponding to the two-dimensional position error, we can employ results of Belyaev [135] on crossings between vector processes and the boundaries of general regions, to compute the average frequency of exits for the error vector, from some disk of a specified radius. This exit frequency then becomes a logical criterion by which to evaluate the adequacy of a given gravitational map.

Chapter 11

Conclusions and Suggestions for Future Work

In this thesis we have considered two specific classes of problems involving spatially-distributed random processes. In Chapters 2 - 7, we employed Hilbert space decomposition ideas to obtain efficient algorithms for solving a wide class of spatial data assimilation problems. In Chapters 8 - 9 we developed a novel, practical application of level and curve crossing results for random processes, and random fields, in characterizing the masking effect produced by terrain on a radars observations. Furthermore, in Chapter 10 we presented some significant first steps in addressing the issue of how accurate a terrain map need be for two important applications. These problems also provide a natural bridge between the two parts of this thesis. We summarize the major contributions of this work as follows:

(1) The presentation of a unified Hilbert space perspective on the Innovations, Hamiltonian, Rauch-Tung-Striebel, Mayne-Fraser, Wall, and Weinert and Desai's solution to the linear

fixed interval smoothing problem in both continuous and discrete time.

(2) The development of a simple, first-principles derivation of forward and reverse Markovian realizations of the smoothing error process in both continuous and discrete time, by employing martingale decompositions of the process noise. We also demonstrate clearly how the structure of the backward model for the smoothing errors is completely determined by the form of the backward model for the filtering errors.

(3) The utilization of our results on smoothing error dynamics to obtain simple solutions of problems of centralized map-updating and map-combining in continuous-time, discrete-time, and mixed cases (in which some measurements are continuous and others are discrete).

(4) The formulation of the map-centralization problem, i.e., the problem of forming a global field map over some region based on local maps over sub-regions, constructed on the basis of local models. We presented a solution to this problem in the case when the local and global modelling are consistent.

(5) The solution of a discrete-space example of the centralized map-updating problem for a non-trivial measurement geometry, i.e., the case of non-parallel measurement tracks, thereby demonstrating the applicability of our map-updating formalism to the case of arbitrary survey geometries through a discrete-space stationary random field.

(6) The development of both one and two dimensional analytical approaches for characterizing the masking effect of terrain on a radar's observations, and hence quantifying the interplay between terrain blockages of the line of sight, radar siting height, and terrain statistics.

(7) The formulation of two different problems in which one must assess the impact of map errors on a procedure that uses these maps for some purpose. Specifically, we examined the effect of map errors on the ability of a terrain-following vehicle to follow the terrain accurately enough, and we also analyzed the errors that can result from using a terrain map to decide if an object will be masked by the terrain at a given range. We provided analysis of a simple model

for the first problem, and a thorough analysis for the latter. These results provide useful tools for the assessment of the adequacy of given maps for these applications.

It is our belief that the significance of this thesis lies not only in the problems we have solved, but also in the additional problems it has uncovered. One area open to additional inquiry is the solution of continuous space map-updating and map-combining problems for the case of non-parallel measurement geometries, or even the case of parallel measurement paths through a separable field, where the trajectories are not aligned with the directions of separability of the field. In this case, the aggregate field vector defined by sampling the field on the measurement trajectories, as well as other lines on which field estimates are desired, does not have a finite-dimensional realization, and hence the map-updating and map-combining problems become infinite dimensional estimation problems. While the results that we have developed do not apply to this case, the approach we have taken does shed light on the structure of the solution and on what must be done. In particular, it will be necessary not only to develop the appropriate stochastic realization for our aggregate field vector process, but also to obtain dynamic models for the resulting

smoothing errors. These models would then provide the key to obtaining the desired solution, much as the results of Chapter 3 did for us.

Another important area for further work is the consideration of map-updating and map-combining problems for the case of fields that are not static, i.e., fields that evolve with time. In this case we would need some model for the time variations of the field. In a discrete-space, discrete-time setting we could conceive of the field as satisfying some stochastic partial difference equation in two space variables, as well as one time variable. Here, we must confront the problem of efficiently updating an old map to take into account the passage of time, as well as the presence of new data. The solution of mapping problems for such non-static fields would have applications to numerical weather prediction [101] and cloud-tracking [106].

A third area for continuing work is in the study of the map-centralization problem in the general case when local and global modelling are inconsistent. Some initial steps have been taken in [50] for solving this problem, but the complete understanding of this problem appears to be connected with questions concerning the invertibility of the smoothed estimates, which have not yet been resolved.

In our characterization of the effect of terrain in masking a radar's observations, through the analysis of $\bar{n}_c(r|X_1)$, $\bar{f}_c(r|X_1)$, or $p_c(r|X_1)$, we developed quantitative means for evaluating the effect on these quantities of our statistical description of the terrain, i.e., such as the terrain correlation function. Our approach requires, however, the complete field description. That is, we have not yet addressed the question, either through analysis or experimentation, of whether one can determine a finite set of terrain parameters, such as the standard deviation, correlation length, or various integral moments of the power spectral density, that will allow us to quantify the masking effect. One approach to this problem might be to investigate the sensitivity of $\bar{n}_c(r|X_1)$, $\bar{f}_c(r|X_1)$, or $p_c(r|X_1)$ to changes in the exact form of the terrain correlation function, while fixing quantities such as the correlation length, and the terrain standard deviation, etc.

As we have noted above, the analysis of the various characterizations of the masking effect which we have considered, require the assumption of some statistical terrain model. We frequently used the assumption that the terrain could be modelled as a Gaussian random field with a specified correlation function. We would like to understand for what types of terrain, and over what areas, such stationary models

are valid. Hence, more work needs to be done on terrain modelling in order to be able to work with statistical descriptions that reflect the characteristics of real terrain. In addition, in the case where we have constructed a terrain map by processing terrain elevation measurements on the basis of some statistical terrain model, we can view the terrain as being modelled as the map plus some map error process. The statistics of the map errors will be determined by the terrain survey geometry, and measurement relations, and the original terrain model. In the above case, we would like to consider the analysis of our different characterizations of the masking effect, conditioned on the knowledge of the terrain map and the underlying terrain model on which the construction of the map is based.

Computational examples of some of the quantities we have analyzed remain to be completed. It would be interesting to consider the exact calculation of the crossing probability, $p_c(r|X_1)$, in the case when the terrain is modelled as the output of a vector Markov process, by using the boundary value formulation of Chapter 8. We could then compare the results that we obtain with empirical values for $p_c(r|X_1)$ derived from digitized terrain data. Also, we have yet to compute the lower bound on $p_c(r|X_1)$ of Appendix 8A, or the two-dimensional measures of terrain masking which we analyzed in Chapter 9.

The work of Chapters 8 - 9 focused on the analysis of statistical measures of masking with respect to a single radar. Suppose we have two radars contained in a disk of radius r, at vector locations s_1 and s_2. We would like to understand how to bound or calculate $p_c(r,\theta;s_1,s_2|H_1,H_2)$, the probability that an object at range r, and azimuth θ, is masked with respect to <u>both</u> radars at locations s_1,s_2, which are sited at elevations H_1,H_2, respectively. Given $p_c(r,\theta;s_1,s_2|H_1,H_2)$, or some upper bound, and a probability density $p_a(\theta)$ for the direction of approach of an incoming object, we could consider the problem of optimally placing two radars inside the disk of radius r, so as to minimize the total probability, $p_m(r)$, that an object at range r will not be detected by either radar. We would compute $p_m(r)$ as

$$p_m(r) = \int_0^{2\pi} p_c(r,\theta;s_1,s_2|H_1,H_2)p_a(\theta)d\theta \quad . \tag{11.1}$$

Finally, we note that it would of interest to extend the analysis of Chapter 10 for the steady state crossing frequencies between some terrain-following vehicle's trajectory and the terrain itself, or the h_v clearance level, to the case of more realistic models for the vehicle dynamics, and more sophisticated terrain-following control laws. In addition, we would

like to simplify further our integral expression for the upper bound on the probability of making a wrong decision, as to whether an object is masked or unmasked, based on map information. Problems such as these that we have considered in Chapter 10 represent merely a first attempt to develop user-oriented analysis tools for evaluating the effect of map errors in various applications. The examination of other problems of this type is a very promising and important direction for future work.

References

Linear Filtering, Smoothing, and Scattering Theory

[1] Jazwinski, A, Stochastic Processes and Filtering Theory, Academic Press, NY, c. 1970.

[2] Gelb, A. (ed.), Applied Optimal Estimation, The M.I.T. Press, Cambridge, MA, c. 1974.

[3] Davis, M.H.A., Linear Estimation and Stochastic Control, Chapman and Hall, London, c. 1977.

[4] Anderson, B. and Moore, J., Optimal Filtering, Prentice-Hall, Inc., Englewood Cliffs, NJ, c. 1979.

[5] Meyer, P.A., "Sur un Probleme de Filtration," University of Strasbourg Seminaire de Probabilites, pp. 223 - 247, 1971/1972.

[6] Meditch, J.S., "On Optimal Linear Smoothing Theory," Information and Control, V. 10, pp. 598 - 615, 1967.

[7] Meditch, J.S., "A Survey of Data Smoothing for Linear and Nonlinear Dynamic Systems," Automatica, V. 9, pp. 151 - 162, 1973.

[8] Kolmogorov, A.N., "Interpolation und Extrapolation von Stationaren Zufalligen Folgen," Bull. Acad. Sci. USSR., Ser. Math, V. 5, pp. 3 - 14, 1941.

[9] Rauch, H.E., "Linear Estimation of Sampled Stochastic Processes with Random Parameters," Tech. Report 2108-1, Stanford Electronics Laboratory, Stanford University, Stanford, CA, 1962.

[10] Rauch, H.E., "Solutions to the Linear Smoothing Problem," IEEE Trans. Aut. Control, AC-8, pp. 371 - 372, 1963.

[11] Rauch, H.E., et al., "Maximum Likelihood Estimates of Linear Dynamic Systems," AIAA J., V. 3, pp. 1445 - 1450, 1965.

[12] Bryson, A.E. and Frazier, M., "Smoothing for Linear and Nonlinear Dynamic Systems," TDR 63-119, Aero. Sys. Div., Wright-Patterson Air Force Base, OH, pp. 353 - 364, 1963.

[13] Masani, P. and Wiener, N., "Nonlinear Prediction," Proc. of the 4-th Berkeley Symposium on Mathematical Statistics and Probability, V. 2, pp. 403 - 419, 1961.

[14] Masani, P., "Wiener's Contributions to Generalized Harmonic Analysis, Prediction Theory, and Filtering Theory," Bull. Am. Math. Soc., V. 72, pp. 73 - 125, 1966.

[15] Wold, H., A Study in the Analysis of Stationary Time Series, Almquist and Wiksell, Uppsala, Sweden, 1938.

[16] Cox, H., "On the Estimation of State Variables and Parameters for Noisy Dynamic Systems," IEEE Trans. Aut. Control, AC-9, pp. 5 - 12, 1964.

[17] Mayne, D.Q., "A Solution to the Smoothing Problem for Linear Dynamic Systems," Automatica, V. 4, pp. 73 - 92, 1964.

[18] Fraser, D.C., "A New Technique for the Optimal Smoothing of Data," Sc.D. Dissertation, Dept. of Aero. and Astro., M.I.T., Cambridge, MA, 1967.

[19] Fraser, D.C. and Potter, J.E., "The Optimum Linear Smoother as a Combination of Two Optimum Linear Filters," IEEE Trans. Aut. Control, AC-14, pp. 387 - 390, 1969.

[20] Kailath, T., "A Note on Least Squares Estimation by the Innovations Method," SIAM J. Control, V. 10, pp. 477 - 486, 1972.

[21] Kailath, T., "Supplement to A Survey of Data Smoothing," Automatica, V. 11, pp. 109 - 111, 1975.

[22] Kailath, T., "An Innovations Approach to Least-Squares Estimation, Part I: Linear Filtering in Additive White Noise," IEEE Trans. Aut. Control, AC-13, pp. 646 - 655, 1968.

[23] Kailath, T. and Frost, P., "An Innovations Approach to Least-Squares Estimation, Part II: Linear Smoothing in Additive White Noise," IEEE Trans. on Aut. Control, AC-13, pp. 655 - 660, 1968.

[24] Kailath, T. and Geesey, R., "An Innovations Approach to Least-Squares Estimation, Part IV: Recursive Estimation Given the Covariance Function," IEEE Trans. Aut. Control, AC-16, pp. 720 - 727, 1971.

[25] Zachrisson, L.E., "On Optimal Smoothing of Continuous-Time Kalman Processes," Information Sciences, V. 1, pp. 143 - 172, 1969.

[26] Laniotis, D.G., "Optimal Linear Smoothing: Continuous Data Case," Int. J. Control, V. 17, pp. 921 - 930, 1973.

[27] Bucy, R., Filtering for Stochastic Processes with Applications to Guidance, John Wiley, NY, c. 1968.

[28] Redheffer, R., "On the Relation of Transmission-Line Theory to Scattering and Transfer," J. Math. Phys., V. XLI, pp. 1 - 41, 1962.

[29] Ljung, L., et al., "Scattering Theory and Linear Least Squares Estimation, Part I: Continuous Time Problems," Proc. of IEEE, V. 64, pp. 131 - 139, 1976.

[30] Friedlander, B., et al., "Scattering Theory and Linear Least Squares Estimation, Part II: Discrete Time Problems," J. of the Franklin Institute, V. 301, pp. 71 - 82, 1976.

[31] Verghese, G., et al., "Scattering Theory and Linear Least-Squares Estimation, Part III: The Estimates," IEEE Trans. on Aut. Control, AC-25, pp. 794 - 802, 1980.

[32] Friedlander, B., "A Scattering Theory Framework for Discrete Time Smoothing," Conference on Information Systems and Sciences, John Hopkins, March 1977.

[33] Ljung, L. and Kailath, T., "A Unified Approach to Smoothing Formulas," Automatica, V. 12, pp. 147 - 157, 1976.

[34] Mason, "Feedback Theory, Further Properties of Signal Flow Graphs," Proc. of I.R.E., V. 44, pp. 920 - 926, 1956.

[35] Ljung, L. and Kailath, T., "Backward Markovian Models for Second-Order Stochastic Processes," IEEE Trans. on Inf. Theory, IT-22, pp. 483 - 491, 1976.

[36] Verghese, G. and Kailath, T., "A Further Note on Backward Markovian Models," IEEE Trans. on Inf. Theory, IT-25, pp. 121 - 124, 1979.

[37] Sidhu, G.S. and Desai, U.B., "New Smoothing Algorithms Based on Reversed-Time Lumped Models," IEEE Trans. Aut. Control, AC-21, pp. 538 - 541, 1976.

[38] Wall, J., et al., "On the Fixed Interval Smoothing Problem," Stochastics, V. 5, pp. 1 - 41, 1981.

[39] Varaiya, P., Notes on Optimization, Van Nostrand Reinhold Company, NY, c. 1972.

[40] Kwakernaak, H. and Sivan, R., Linear Optimal Control Systems, Wiley-Interscience, NY, c. 1972.

[41] Chen, Introduction to Linear System Theory, Holt, Rinehart and Winston, Inc., NY, c. 1970.

[42] Silverman, L. and Meadows, H.E., "Controllability and Observability of Time-Variable Linear Systems," SIAM J. Contr., V. 5, pp. 64 - 73, 1967.

[43] Wong, E., "Recent Progress in Stochastic Processes - A Survey," IEEE Trans. on Inf. Theory, IT-19, pp. 262 - 273.

[44] Wong, E., "Representation of Martingales, Quadratic Variation and Applications," SIAM J. Control, V. 9, pp. 621 - 632, 1971.

[45] Fisk, D.L., "Sample Quadratic Variation of Sample Continuous Second Order Martingales," Z. Whrscheinlichkeitstheorie und Verw. Gebiete, V. 6, pp. 273 - 278, 1966.

[46] Fisk, D.L., "Quasi-Martingales," Trans. Amer. Math. Soc., V. 120, pp. 369 - 389, 1965.

[47] Segal, A., "Stochastic Processes in Estimation Theory," IEEE Trans. on Inf. Theory, IT-22, pp. 275 - 286, 1976.

[48] Lipster, R.S. and Shiryayev, A.N., Statistics of Random Processes I, General Theory, Springer-Verlag, NY, c. 1974.

[49] Weinert, H.L. and Desai, U.B., "On Complementary Models and Fixed-Interval Smoothing." (To appear in IEEE Trans. on Automatic Control, August 1981.)

[50] Willsky, A., et al., "Combining and Updating of Local Estimates and Regional Maps Along Sets of One-Dimensional Tracks." (Submitted to IEEE Trans. on Aut. Control.)

[51] Kam, P.Y., "Modelling and Estimation of Space-Time Stochastic Processes," Ph.D. Thesis, Dept. of E.E. and Computer Sciences, M.I.T., 1975.

[52] Levy, B., et al., "A Scattering Framework for Decentralized Estimation Problems," LIDS-P-1075, March 1981.

[53] Castannon, D., et al., "Some Methods for the Modelling of Shipping Lanes in Surveillance Theory," LIDS-P-913, May 1979.

[54] Willsky, A. and Sandell, R., "The Stochastic Analysis of Dynamic Systems Moving Through Random Fields," (Submitted to IEEE Trans. on Aut. Control.)

[55] Willsky, A., Digital Signal Processing and Control and Estimation Theory, Points of Tangency, Areas of Intersection, and Parallel Directions, The M.I.T. Press, Cambridge, MA, c. 1979.

[56] Cole, R., Theory of Ordinary Differential Equations, Appleton-Century-Croft, NY, c. 1968.

[57] Cramer, H., "On the Structure of Purely Nondeterministic Stochastic Processes," Ark. Mat., V. 4, pp. 2 - 3 and 249 - 266, 1961.

[58] Hida, T., "Canonical Representations of Gaussian Processes and their Applications," Mem. Coll. Kyoto University, V. A-XXXIII, pp. 109 - 155, 1960.

[59] Kallianpur, G. and Mandrekar, V., "Multiplicity and Representation Theory for Purely Non-deterministic Stochastic Processes," Theory Prob. Appl. (USSR), V. 10, pp. 553 - 580, 1965.

[60] McKean, H.P., "Brownian Motion with a Several Dimensional Time," Theory Prob. Appl. (USSR), V. 8, pp. 335 - 354, 1963.

[61] Newcomb, R.W. and Anderson, B.D.O., "On the Generation of All Spectral Factors," IEEE Trans. on Inf. Theory, IT-14, pp. 512 - 513, 1968.

[62] Davis, M.C., "Factoring the Spectral Matrix," IEEE Trans. Aut. Control, AC-8, pp. 296 - 305, 1963.

[63] Youla, D.C., "On the Factorization of Rational Matrices," IRE Trans. Inf. Theory, IT-7, pp. 172 - 189, 1961.

[64] Anderson, B.D.O., "The Inverse Problem of Stationary Covariance Generation," J. of Statistical Physics, V. 1, pp. 133 - 147, 1969.

[65] Brandenburg, L.H., "Shaping Filter Models for Nonstationary Random Processes," Ph.D. Dissertation, Columbia University, NY, 1968.

[66] Anderson, B.D.O., et al., "Spectral Factorization of Time Varying Covariance Functions," IEEE Trans. Inf. Theory, IT-15, pp. 550 - 557, 1969.

[67] Anderson, B.D.O. and Moylan, P., "Spectral Factorization of a Finite-Dimensional Nonstationary Matrix Covariance," IEEE Trans. on Aut. Control, AC-19, pp. 680 - 692, 1974.

[68] Stear, E.B., "Shaping Filters for Stochastic Processes," in Modern Control Systems Theory, McGraw-Hill, NY, c. 1965.

[69] Kailath, T. and Geesey, R., "An Innovations Approach to Least Squares Estimation, Part V: Innovations Representations and Recursive Estimation in Colored Noise," IEEE Trans. on Aut. Control, AC-18, pp. 435 - 453, 1973.

[70] Halyo, N. and McAlpine, G., "On the Spectral Factorization of Nonstationary Vector Random Processes," IEEE Trans on Aut. Control, AC-19, pp. 674 - 678, 1974.

[71] Akaike, H., "Stochastic Theory of Minimal Realization," IEEE Trans. on Aut. Control, AC-19, pp. 667 - 673, 1974.

[72] Faurre, P., "Realizations Markoviennes de Processus Stationaires," IRIA Rep. No. 13, 1973.

[73] Ruckebusch, G., "Representations Markoviennes de Processus Gaussiens Stationaires," These de 3eme Cycle, Lab. de Calcul. des Probabilites, Universite de Paris VI, Mai 1975.

[74] Ruckebusch, G., "Theorie Geometrique de la Representation Markovienne," These de Doctorat D'etat es Sciences Mathematiques Probabilites, Universite Pierre et Marie Curie, 1980.

[75] Clerget, M., "Systemes Lineaires Positifs Non Stationaires," IRIA Rep. No. 65, 1974.

[76] Germain, F., "Algoritmes de Calcul de Realisations Markoviennes Cas Singuliers et Stabilite," IRIA Rep. No. 66, 1974.

[77] Picci, G., "Stochastic Realization of Gaussian Processes," Proc. of the IEEE, V. 64, 1976.

[78] Lindquist, A. and Picci, G., "A State-Space Theory for Stationary Stochastic Processes," Proc. 21st Midwest Symposium on Circuits and Systems, 1978.

[79] Lindquist, A., et al., "On Minimal Splitting Subspaces and Markovian Representations," Math Syst. Theory, V. 12, pp. 271 - 279, 1979.

[80] Lindquist, A. and Picci, G., "On the Structure of Minimal Splitting Subspaces in Stochastic Realization Theory," Proc. 1977 Conf. Decision and Control, New Orleans, Dec. 1977.

[81] Lindquist, A. and Picci, G., "Realization Theory for Multivariate Gaussian Processes, I: State Space Construction," 4-th Int. Symposium on the Math. Theory of Networks and Systems, Delft, Holland, July 1979.

[82] Lindquist, A. and Picci, G., "On the Stochastic Realization Problem," SIAM J. Control and Optimization, V. 17, pp. 365 - 389, 1979.

[83] Badawi, F., et al., "A Stochastic Realization Approach to the Smoothing Problem," IEEE Trans. on Aut. Control, AC-24, pp. 878 - 887, 1979.

[84] Badawi, F., "Structures and Algorithms in Stochastic Realization Theory and the Smoothing Problem," Ph.D. Thesis, Dept. of Mathematics, Univ. of Kentucky, Lexington, KY, Jan. 1980.

[85] Pavon, M., "Stochastic Realization and Invariant Directions of the Matrix Ricatti Equation," SIAM J. Control, V. 18, pp. 155 - 180, 1979.

[86] Finesso, L. and Picci, G., "On the Structure of Minimal Spectral Factors," (Submitted to IEEE Trans. on Aut. Control.)

Image Processing, Meteorological, and Geodetic References

[87] Ekstrom, M. and Woods, J., "Two-Dimensional Spectral Factorization with Applications in Recursive Digital Filtering," IEEE Trans. Acoust., Speech, Signal Processing, ASSP-24, pp. 115 - 128, 1976.

[88] Woods, J. and Radewan, C., "Kalman Filtering in Two Dimensions," IEEE Trans. Inf. Theory, IT-23, pp. 473 - 482, 1977.

[89] Nahi, N., "The Role of Recursive Estimation in Statistical Image Enhancement," IEEE Proc., V. 60, pp. 872 - 877, 1972.

[90] Powell, S. and Silverman, L., "Modeling of Two-Dimensional Covariance Functions with Application to Image Restoration," IEEE Trans. on Aut. Control, AC-19, pp. 8 - 12, 1974.

[91] Murphy, M. and Silverman, L., "Image Model Representation and Line by Line Recursive Restoration," IEEE Trans. on Aut. Control, AC-23, pp. 809 - 816, 1978.

[92] Attasi, S., "Modelling and Recursive Estimation for Double Indexed Sequences," in System Identification: Advances and Case Studies, Academic Press, NY, c. 1976.

[93] Wong, E., "Recursive Causal Linear Filtering for Two-Dimensional Random Fields," IEEE Trans. on Inf. Theory, IT-24, pp. 50 - 59, 1978.

[94] Ogier, R. and Wong, E., "Recursive Linear Smoothing of Two-Dimensional Random Fields," IEEE Trans. on Inf. Theory, IT-27, pp. 77 - 83, 1981.

[95] Nash, R. and Jordan, S., "Statistical Geodesy, An Engineering Perspective," Proc. of IEEE, V. 66, pp. 532 - 550, 1978.

[96] Heiskanen, W.A. and Moritz, H., Physical Geodesy, W.H. Freeman, San Francisco, CA, c. 1967.

[97] Jordan, S.K., "Self-Consistent Statistical Models for the Gravity Anomaly, Vertical Deflections, and Undulation of the Geoid," J. Geophys. Res., V. 77, pp. 3660 - 3670, 1972.

[98] Heller, W.G., "A New Self-Consistent Statistical Gravity Field Model," Fall Annual Meeting, Amer. Geophys., Univ. San Francisco, CA, Dec. 1976.

[99] Jordan, S., "Moving-Base Gravity Gradiometer Surveys and Interpretation," Geophys., Feb. 1978.

[100] Brammer, R., "Resolution of Short Wavelength Variations in the Geoid by GEOS-3 Radar Altimetry," presented at Spring Annual Meeting, Amer. Geophys., U. Washington, DC, May 1977.

[101] Haltner, Numerical Weather Prediction, Wiley, NY, c. 1971.

[102] Holton, J.R., An Introduction to Dynamic Meteorology, Academic Press, NY, c. 1972.

[103] Staelin, D.H., "Passive Remote Sensing of Microwave Wavelengths," Proc. IEEE, V. 57, pp. 427 - 439, 1969.

[104] Ledsham, W. and Staelin, D.H., "An Extended Kalman-Bucy Filter for Atmospheric Temperature Retrieval Using a Passive Microwave Sounder," J. Applied Meteorology, V. 17, pp. 1023 - 1033, 1978.

[105] Smith, W.L., et al., "A Regression Method for Obtaining Real-Time Temperature and Geopotential Height Profiles from Satellite Spectrometer Measurements and its Application to NIMBUS 3 "SIRS" Observations," Mon. Wea. Rev., V. 98, pp. 582 - 603, 1970.

[106] Smith, E.A. and Phillips, D.R., "Automated Cloud Tracking Using Precisely Aligned Digital ATS Pictures," IEEE Trans. Comp., C-21, pp. 715 - 729, 1972.

[107] Hayne, H. and Moore, R., "Theoretical Scattering for Near Vertical Incidence from Contour Maps," J. of Research of the National Bureau of Standards, D. Radio Propagation, V. 65D, pp. 427 - 432, 1961.

[108] Cohen, R., "Some Analytical and Practical Aspects of Wiener's Theory of Prediction," Thesis for MS.E.E., M.I.T, Cambridge, MA, May 1948.

[109] Carlson, G. and Bair, G., "Simple Generation of One-Parameter Pseudoterrain Surfaces," IEEE Trans. on Aerospace and Electronic Systems, V. 5, pp. 735 - 737, 1979.

[110] Beebe, J.L., et al., "Terrain Effects on the Detection of Low Altitude Penetrators by Soviet Radars," Memorandum 2-7923-0000-006, Boeing, Dec. 1970.

[111] Melling, N.P., "On the Validity of Simple Terrain Masking Models in the Assessment of Low Altitude Detection," Memorandum RM-1696, General Research Corp., Santa Barbara, CA, April 1973.

Geometric Characterizations of Random Processes (Level and Curve Crossings, First Passage Times, etc.)

[112] Cramer, H. and Leadbetter, M.R., Stationary and Related Stochastic Processes, John Wiley & Sons, Inc., NY, c. 1967.

[113] Blake, I.F. and Lindsey, W., "Level-Crossing Problems for Random Processes," IEEE Trans. on Inf. Theory, IT-19, 1973.

[114] Rice, S.O., "The Mathematical Analysis of Random Noise," Bell Syst. Tech. J., V. 23, pp. 282 - 332, 1944; V. 24, pp. 46 - 156, 1945.

[115] Bendat, J.S., Principles and Applications of Random Noise Theory, John Wiley & Sons, Inc., NY, c. 1958.

[116] Kac, M., "On the Average Number of Real Roots of a Random Algebraic Equation," Bull. Amer. Math. Soc., V. 49, pp. 314 - 319, 1943.

[117] Leadbetter, M.R., "On Crossings of Levels and Curves by a Wide Class of Stochastic Processes," Ann. Math. Statist., V. 37, pp. 260 - 267, 1966.

[118] Leadbetter, M.R., "On Crossings of Arbitrary Curves by Certain Gaussian Processes," Proc. Amer. Math. Soc., V. 16, pp. 60 - 68, 1965.

[119] Gallager, R. and Helstrom, C., "A Bound on the Probability that a Gaussian Process Exceeds a Given Function," IEEE Trans. on Inf. Theory, V. 15, pp. 163 - 166, 1969.

[120] Slepian, D., "The One-Sided Barrier Problem for Gaussian Noise," Bell Syst. Tech. J., V. 41, pp. 463 - 501, 1962.

[121] Ylvisaker, N.D., "A Note on the Absence of Tangencies in Gaussian Sample Paths," Ann. Math. Statist., V. 39, pp. 261 - 262, 1968.

[122] Fortet, R., "Les Fonctions Aleatoires du Type de Markoff Associees a Certaines Equations Lineares Aux Derivees Partialles du Type Parabolic," J. Math Pures Appl., V. 22, pp. 177 - 243, 1943.

[123] Mehr, C.B. and McFadden, J.A., "Certain Properties of Gaussian Processes and their First Passage Times," J. Roy. Statist. Soc. (B), pp. 505 - 522, 1965.

[124] Siegert, A., "On the First Passage Time Probability Problem," Physical Review, V. 81, pp. 617 - 623, 1951.

[125] Darling, D.A. and Siegert, A., "The First Passage Problem for a Continuous Markov Process," Ann. Math. Statist., V. 24, pp. 624 - 639, 1953.

[126] Darling, D.A. and Siegert, A., "A Systematic Approach to a Class of Problems in the Theory of Noise and other Random Phenomena, Parts I and II," IRE Trans. on Inf. Theory, IT-3, pp. 32 - 43, 1957.

[127] Helstrom, C., "The Distribution of the Number of Crossings of a Gaussian Stochastic Process," IRE Trans. on Inf. Theory, IT-3, pp. 232 - 237, 1957.

[128] Helstrom, C., "Markov Processes and their Application," in Communication Theory, Balakrishnan (ed.), McGraw-Hill, NY, c. 1968.

[129] Lindsey, W.C., Synchronization Systems in Communication and Control, Prentice-Hall, Englewood Cliffs, NJ, c. 1972.

[130] Friedman, A., Stochastic Differential Equations and Applications, V. 1 - 2, Academic Press, NY, c. 1975.

[131] Friedland, B., et al., "Stability Problems in Randomly-Excited Dynamic Systems," JACC, Seattle, WA, Aug. 1966.

[132] Dynkin, E.B., Markov Processes, V. 1 - 2, Academic Press, NY, c. 1965.

[133] Hunt, G.A., "Random Fourier Transforms," Trans. Amer. Math. Soc., V. 71, pp. 38 - 69, 1951.

[134] Belyaev, Y., "Continuity and Holder's Conditions for Sample Functions of Stationary Gaussian Processes," Proc. Fourth Berkeley Symp. Math. Statist. Prob., V. 2, pp. 23 - 24, 1961.

[135] Belyaev, Y., "On the Number of Exits Across the Boundary of a Region by a Vector Stochastic Process," Theory Prob. Appl., V. 13, pp. 320 - 324, 1968.

[136] Longuet-Higgins, M.S., "The Statistical Analysis of a Random Moving Surface," Phil. Trans. A, V. 249, pp. 321 - 387, 1957.

[137] Belyaev, Y., "Point Processes and First Passage Problems," Proc. of Sixth Berkeley Symposium, Math. Statist. Prob., V. 3, pp. 1 - 17, 1972.

[138] Belyaev, Y., "Bursts and Shines of Random Fields," Soviet Math Dokl., V. 8, pp. 1107 - 1109, 1967.

[139] Nosko, V.P., "The Characteristics of Excursions of Gaussian Homogeneous Fields Above a High Level," Proc. USSR-Japan Symp. on Probability, Novosibirsk, 1969.

[140] Nosko, V.P., "On the Possibility of Using the Morse Inequalities for the Estimation of the Number of Excursions of a Random Field in a Domain," Theor. Probability Appl., V. 18, pp. 821 - 822, 1973.

[141] Adler, R. and Hasofer, A., "Level Crossings for Random Fields," The Annals of Probability, V. 4, pp. 1 - 12, 1976.

[142] Adler, R., "Excursions Above a Fixed Level by n-Dimensional Random Fields," J. Appl. Prob., V. 13, pp. 276 - 289, 1976.

[143] Adler, R., The Geometry of Random Fields, John Wiley & Sons, NY, c. 1981.

[144] Pollack, A. and Guillemin, V., Differential Topology, Prentice-Hall, Englewood Cliffs, NJ, c. 1974.

[145] Papoulis, A., The Fourier Integral and its Applications, McGraw-Hill, NY, c. 1962.

[146] Davis, P. and Rabinowitz, P., Methods of Numerical Integration, Academic Press, NY, c. 1975.

Biographical Note

Martin G. Bello was born on October 7, 1953, in Brookline, Massachusetts. He graduated from Needham High School in May, 1971 and subsequently spent his undergraduate years at Cornell University. In his junior and senior years, he became a member of the honor societies Tau Beta Pi and Eta Kappa Nu, respectively. He graduated in May of 1975, with a B.S. in Electrical Engineering, receiving the Sibley Prize for academic excellence, and being ranked third in the Engineering School.

In September of 1975 he entered Graduate School at M.I.T. as a research assistant. In February of 1977 he was awarded the M.S. degree for his thesis, "The Estimation of Delay Gradients for Purposes of Routing in Data-Communications Networks", and concurrently he became a member of Sigma Xi.

His professional experience includes the following: work as a scientific programmer at Signatron, Inc., during the summers of 1969 - 1971, work involving the analysis and simulation of communication systems at CNR, Inc. during the summers of 1973 - 1975, and work during the summer of 1978 at TASC, involving the analysis and computation of power spectral densities associated with smoothing and filtering errors.

During his graduate years at M.I.T. he spent the first two years as a Research Assistant, a year as a Teaching Assistant for an introductory course on random processes, and the last several years as a Research Assistant sponsored by Lincoln Laboratory.